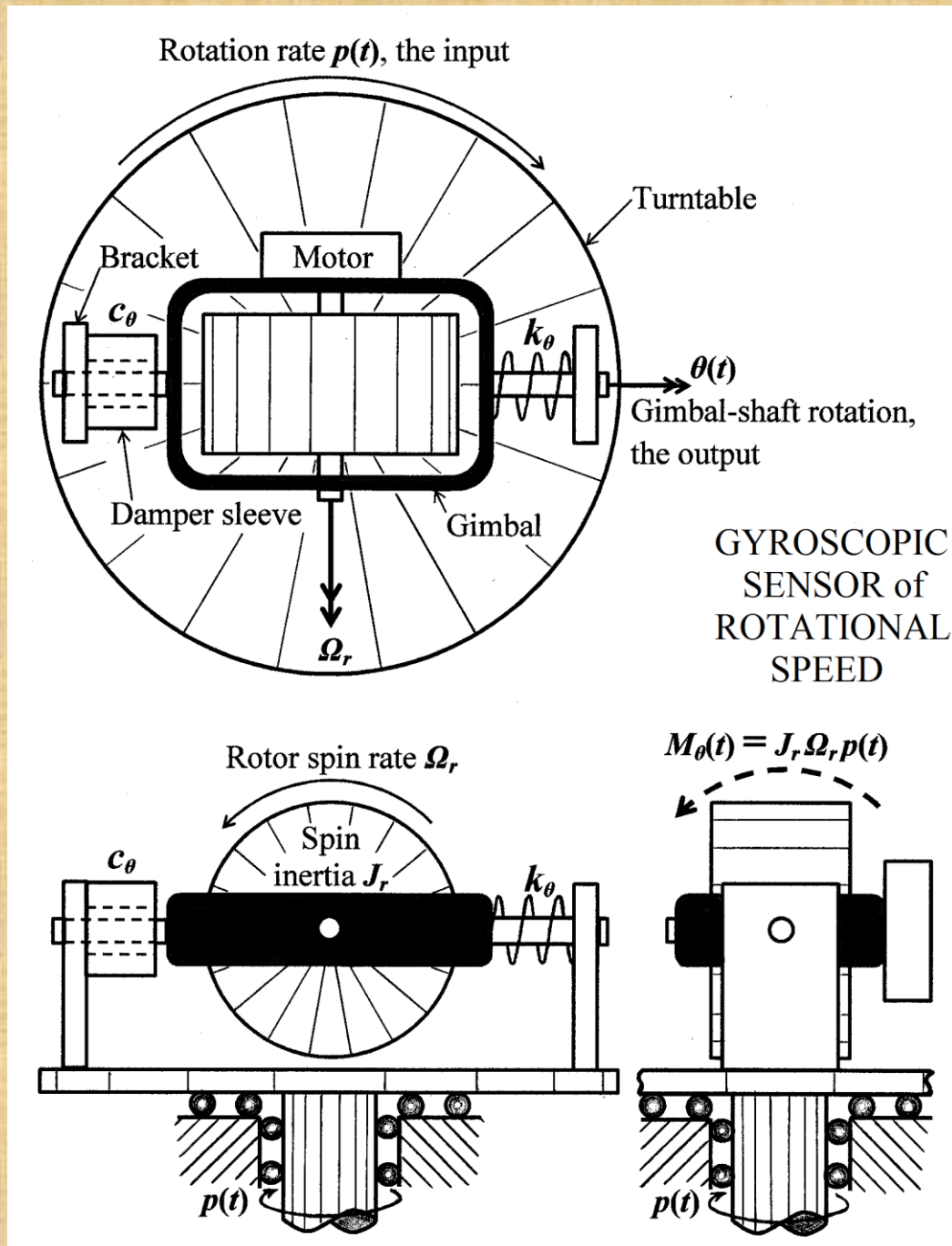


Introduction to Linear, Time-Invariant, Dynamic Systems for Students of Engineering

William L. Hallauer, Jr.



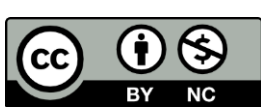
INTRODUCTION TO LINEAR, TIME-INVARIANT, DYNAMIC SYSTEMS FOR STUDENTS OF ENGINEERING

William L. Hallauer, Jr.

Permission of the author is granted for reproduction in any form of this book or any part of this book, provided that there is appropriate attribution, for example, by a citation in the References section of a technical article, and provided that the reproduction is not made for the purpose of charging a fee to users (*e.g.*, students in a class) beyond the cost of reproduction.

However, plagiarism from this book is prohibited, and any use of the material in this book to produce profit or income beyond the cost of reproduction is prohibited.

© 2016 by William L. Hallauer, Jr.



Introduction to Linear, Time-Invariant, Dynamic Systems for Students of Engineering is licensed under a Creative Commons Attribution-NonCommercial 4.0 International License. For details of use requirements, please see <https://creativecommons.org/licenses/by-nc/4.0/>.

Trademark Notice: Product or corporate names printed herein may be trademarks or registered trademarks. They are printed only for unique identification and for explanation, without intent to infringe.

INTRODUCTION TO LINEAR, TIME-INVARIANT DYNAMIC SYSTEMS FOR STUDENTS OF ENGINEERING

William L. Hallauer, Jr.

AUTHOR'S PREFACE

I taught many times the college undergraduate, junior-level, one-semester course entitled “AOE 3034, Vehicle Vibration and Control” in the Department of Aerospace and Ocean Engineering (AOE) at Virginia Polytechnic Institute and State University (VPI & SU). I was dissatisfied using commercially available textbooks for AOE 3034, so I began writing my own course notes, and those notes grew into this book. Although this project began with preparation of informal handout notes, the completed book is a formal college engineering textbook, complete with homework problems at the end of each chapter, a detailed Table of Contents, a list of References, and a detailed Index. I hope that this book will be understandable and enlightening for students of engineering system dynamics, a valuable teaching resource for course instructors, and a useful reference for self-study and review.

The content of this book is based primarily on topics that the faculty of AOE and VPI & SU elected to include in AOE 3034 during the 1990s and early 2000s. The concise course description is: “Free and forced motions of first-order systems. Free and forced motions of second-order systems, both undamped and damped. Frequency and time responses. Introduction to control, transfer functions, block diagrams, and closed-loop system characteristics. Higher-order systems.” A more detailed course description is provided by the following list of *primary learning objectives*, which were developed to satisfy requirements of the agency that accredits engineering college degrees in the United States:

At the completion of AOE 3034, the student should be able to:

1. Solve first-, second-, and higher-order, linear, time-invariant (LTI) ordinary differential equations (ODEs) with forcing, using both time-domain and Laplace-transform methods.
2. Solve for the frequency response of an LTI system to periodic sinusoidal excitation and plot this response in standard form (log magnitude and phase versus frequency).
3. Explain the role of the “time constant” in the response of a first-order LTI system, and the roles of “natural frequency”, “damping ratio”, and “resonance” in the response of a second-order LTI system.

4. Derive and analyze mathematical models (ODEs) for low-order mechanical systems, both translational and rotational systems, that are composed of inertial elements, spring elements, and damping devices.
5. Derive and analyze mathematical models (ODEs) for low-order electrical systems (circuits) composed of resistors, capacitors, inductors, and operational amplifiers.
6. Derive (from ODEs) and manipulate Laplace transfer functions and block diagrams representing output-to-input relationships of discrete elements and of systems.
7. Define and evaluate “stability” for an LTI system.
8. Explain “proportional”, “integral”, and “derivative” types of feedback control for single-input, single-output (SISO), LTI systems.
9. Sketch the locus of characteristic values, as a control parameter varies, for a feedback-controlled SISO, LTI system.
10. Use MATLAB¹ as a tool to study the time and frequency responses of LTI systems.

Rather than summarizing the contents of this book chapter by chapter, I invite the reader of this preface to peruse the detailed Table of Contents. However, the book’s general organization is the following: Chapters 1-10 deal primarily with the ODEs and behaviors of first-order and second-order dynamic systems; Chapters 11 and 12 touch on the ODEs and behaviors of mechanical systems having two degrees of freedom, *i.e.*, fourth-order systems; Chapters 13 and 14 introduce classical feedback control, motivating the concept with what I believe is a unique approach based on the standard ODE of a second-order dynamic system; Chapter 15 presents the basic features of proportional, integral, and derivative types of classical control; and Chapters 16 and 17 discuss methods for analyzing the stability of classical control systems. The principal parts of Chapters 1-16 are focused on the ten primary learning objectives listed above. I added Chapter 17 on frequency-response stability analysis because I feel that an introduction to classical control theory and design is incomplete without that subject, even though it was not included in AOE 3034.

The general minimum prerequisite for studying this book is the intellectual maturity of a junior-level (third-year) college student in an accredited four-year engineering curriculum. More specifically, a reader of this book should already have passed standard first courses in engineering dynamics and ODEs. It will be helpful if, but probably is not

¹ MATLAB ® is a registered trademark of The MathWorks, Inc. MATLAB is widely available to engineers in practice and to engineering colleges. Furthermore, MATLAB-like software that uses command-line language similar to MATLAB’s, and functions similarly to MATLAB in many respects, is available for download from the Internet, for example, GNU Octave (<http://www.gnu.org/software/octave/>).

mandatory that, the reader has studied basic electrical circuits, perhaps in an introductory college physics course. It is necessary that the reader has studied basic computer programming. MATLAB computer programs and commands appear throughout this book, so the reader should be able to understand MATLAB commands. However, MATLAB commands are generally clearly expressed in standard English and standard arithmetic notation, so a person who has done any computer programming, even if that was not with MATLAB, probably can follow the computer commands and command sequences in this book. Familiarity with matrix notation and matrix arithmetic operations also will be helpful, especially for Chapters 11 and 12. My students who took at the same time AOE 3034 and a mathematics course on operational methods (primarily Laplace transforms) often found that the combination of those courses was unusually complementary and beneficial to their comprehension of the material.

A mathematical second-order system is represented in this book primarily by a single second-order ODE, not in the *state-space* form by a pair of coupled first-order ODEs. Similarly, a two-degrees-of-freedom (fourth-order) system is represented in Chapters 11 and 12 by a pair of coupled second-order ODEs, not in the state-space form by four coupled first-order ODEs. A reader who can understand the mathematics and dynamics of relatively simple systems expressed here in classical second-order form probably will have little trouble making the transition in more advanced literature to the general state-space representation of higher order systems.

This book deals mostly with specific idealized models of basic physical systems, such as mass-damper-spring mechanisms and single-loop electrical circuits. The emphases are on fundamental ODEs and fundamental system response characteristics. I have chosen, therefore, not to burden the reader with *bond graph* modeling, the general and powerful, but complicated, modern tool for analysis of dynamic systems. However, the material in this book is an appropriate preparation for the bond graph approach presented in, for example, *System Dynamics: Modeling, Simulation, and Control of Mechatronic Systems*, 5th edition, by Dean C. Karnopp, Donald L. Margolis, and Ronald C. Rosenberg, published by John Wiley & Sons, 2012.

I intended originally that Chapters 1-16 of the course notes (before they grew into a book) could be covered in a normally-paced course of three fifty-minute lessons per week in a standard college semester of fourteen weeks duration. Even so, instructors of AOE 3034, including myself, had difficulty squeezing all of that content into forty-two lessons. Furthermore, in the process of converting the course notes into a complete textbook, I added material that is relevant and interesting (to me, at least) in many complete “new” sections to the ends of Chapters 1², 7, 8, 10, 14, and 16. And, as mentioned above, I also added a complete “new” Chapter 17. Consequently, I doubt that even the

² I added Section 1-10, which deals with mass-spring systems, after working with several graduate students whose research subjects were design, analysis, and testing of aerodynamic sensors that include mechanical components. These graduate students had not recently reviewed elementary system dynamics, and so were unfamiliar with fundamental concepts such as natural frequency and resonance. I decided, therefore, to make Chapter 1 a succinct summary of basic mechanical-system dynamics (excluding feedback control), suitable for quick review by graduate students or any engineers who specialize in other areas but need to understand at least the most basic of this book’s lessons.

most demanding course instructor can, while still treating the students fairly, cover this entire book in a three-credit, one-semester course. Therefore, instructors who wish to use this as a one-semester course textbook should decide in advance which parts of the book are essential to the course and which parts they cannot cover in the time allotted for the course. If, for example, it is essential to cover all of Chapters 13-17 on classical control, an instructor might elect to skip some or all of the “new” sections in Chapters 1, 7, 8, and 10, and to skip Chapters 11 and 12 on systems with two degrees of freedom, but to cover most everything else in the book. Sections 6-4, 6-5, and 8-11 deal primarily with computational methods for calculating approximate time-response solutions of first- and second-order ODEs; the contents of these sections are nicely compatible with the chapters in which they reside; but they are not essential to the reader’s understanding of system dynamics, so they can be omitted from course coverage without great loss. On the other hand, I discourage the omission of Chapter 5 on basic electrical systems, not only because I believe the material is important to most engineers, but also because such systems provide many examples and homework problems later in the book.

The homework problems at the ends of chapters are very important to the learning objectives of this book. I wrote each problem statement while at the same time preparing the solution, in order to help make the statements as clear, correct, and unambiguous as possible. In many cases, I stated a result, such as a Laplace transform, in a chapter’s text but left as a homework problem the proof or other development of that result. When teaching a lesson from the course notes that grew into this book, I would often not lecture on the material of the reading that I had assigned for the lesson. Instead, I would assume that the students had, in fact, completed and understood the assigned reading, summarize the main results of that reading and ask if there were questions about it, then, after responding to any questions, spend most remaining lesson time discussing some of the related homework problems.

A major focus of this book is computer calculation of system characteristics and responses and display of the results graphically, with use of MATLAB commands and programs. However, the book employs, for the most part, basic MATLAB commands and operations (aside from array operations), such as those on hand calculators; there is very little use of advanced MATLAB operations and functions, because these can produce results without the user having to understand the processes of production. For this introductory material, I think it is important that the computer and software function as a “super calculator”, which relieves the user of the drudgery of calculations, especially complex and/or repetitive calculations, but still requires the user to understand the process well enough to be able to design and program the calculations and graphical displays.

Since 1967 with the publication of *Dynamics of Physical Systems* by Robert H. Cannon, Jr., most textbooks on introductory system dynamics have included very few, if any, applications specifically relevant to aerospace engineering. Therefore, I have tried to include in this book at least some relevant examples and homework problems. These include rolling dynamics of flight vehicles in Chapter 3, spacecraft actuators in Chapters 3, 10, and 12, aerospace motion sensors in Chapters 9 and 10, aeroelasticity in Chapters

Author's Preface

11 and 12, attitude control of spacecraft and aircraft in Chapters 14-16, and an analysis of aeroelastic flutter in the final homework problem of Chapter 16.

I favor illustrating and validating theory, whenever possible, with measured data. I also favor using measured data to identify system dynamic characteristics based on mathematical models (*e.g.*, time constants and natural frequencies), and system basic properties (*e.g.*, mass, stiffness, and damping). Accordingly, I included quite a lot of material in this book about identification of first- and second-order systems, especially in Chapters 9 and 10. Photographs of instructional laboratory structures and motion data measured from those structures are included, for examples, in Section 7-6 on distributed-parameter structures, and in homework Problems 7.10 and 12.5. Other applications of real and simulated experimental data appear in several homework problems.

I welcome feedback about this book from anyone who reads it. Please send your comments to my VPI & SU email address, whallaue@vt.edu. I will be grateful to learn of any errors that readers detect and report to me. I retain all of the source word-processor files, so I am able to correct errors and replace any defective file with the corrected version. I regard the basic organization of the book as fixed, so that, except to correct major, serious errors, I will not revise the chapters and appendices so extensively as to disrupt the original page numbering, equation numbering, Table of Contents, and Index. I am ready and willing, however, to add files that supplement chapter and appendix contents, when such additions will improve the book. In particular, I would welcome new examples and homework problems that are clearly relevant to aerospace engineering, while still being compatible with the introductory level of the book. If you send to me any such educational and motivational gem and if I decide that it satisfies my criteria, then I will be most pleased to add it as a supplementary file and to acknowledge your contribution.

Acknowledgments

I am grateful to my colleagues who developed the course content of AOE 3034, and/or who joined me in teaching sections of AOE 3034, and/or who used early versions of my AOE 3034 course notes from which this book grew: Scott Bland, Eugene Cliff, Rafael Haftka, Rakesh Kapania, Frederick Lutze, and Craig Woolsey. Professor Kapania, in particular, suggested topics to include, used the early versions in his teaching, and encouraged me to finish and publish the book.

With this book, I have aspired to approach the high quality, if not the breadth and depth, of *Dynamics of Physical Systems (DPS)*, which was written by Robert H. Cannon, Jr., published first in hardback by McGraw-Hill in 1967, and subsequently re-published in paperback by Dover. I have been instructed, guided, and inspired by *DPS*, so the attentive reader of this book will observe throughout more citations of *DPS* than of any other reference. *DPS* was designed to serve many different university courses, from sophomore level to advanced graduate level, so its length is three to four times that of this book. I highly recommend *DPS* as a complement to this book and as a source of additional material both at and beyond this book's level. Professor Cannon's book is a clearly

Author's Preface

written and beautifully illustrated textbook of basic and more advanced theory of system dynamics and of interesting applications to many fields, classical aerospace engineering in particular. *DPS* is surely one of the two or three finest textbooks I have encountered in my entire career as student, practicing engineer, and instructor.³

I thank The MathWorks, Inc. for developing MATLAB, and for distributing it broadly to the engineering and educational communities, and, in particular, for making MATLAB available to me as an essential instructional resource in AOE 3034 and other courses, and as a tool in research as well. One of the principal differences between this book and *Dynamics of Physical Systems* is the emphasis I have been enabled by modern personal computers and MATLAB to place on computer calculation of numerical system characteristics and response solutions, in both the instructional content and the homework problems. Professor Cannon had no such luxuries: when *Dynamics of Physical Systems* was published, the primary calculator used by engineering students was still the slide rule, the concept of a small personal computer was just the hopeful dream of a few visionaries, and undergraduates generally had little or no access to mainframe computers and peripheral equipment for printing and plotting. In order to calculate and graph the system characteristics and responses that can be produced now so easily with MATLAB, students then who did have access to mainframe computers would need to write a program in an inflexible language such as FORTRAN or BASIC, then enter the program onto cards with keypunch machines at a computer center, one line of program per card, then submit the card deck of the complete program to a computer operator, then wait, sometimes several days, for the card deck to reach the front of the queue and be run on the mainframe computer to produce printed and/or plotted output, then find and debug errors in the programming that prevented correct execution, then repeat the whole process as many times as was required until the program would finally succeed and deliver the desired results.

William L. Hallauer, Jr.
June 2, 2016
whallaue@vt.edu

³ There is considerable irony in my admiration now for *Dynamics of Physical Systems*. As a college junior at Stanford University during the Winter Quarter of 1964, I was enrolled in the course Engineering 104, Dynamic Response. The required course reference was part of a preliminary, pre-publication version of *Dynamics of Physical Systems*, which had apparently been chosen by someone other than the instructor who was assigned to teach the course. That version was an extremely rough draft full of typographical errors and other mistakes, with figures that seemed to have been sketched in great haste, and it was badly reproduced. My memory is that we students and the instructor tolerated it, but only barely. The quality of *Dynamics of Physical Systems* improved tremendously between that time and the formal publication in 1967.

**INTRODUCTION TO
LINEAR, TIME-INVARIANT DYNAMIC SYSTEMS
FOR STUDENTS OF ENGINEERING**

© 2016 by William L. Hallauer, Jr.

TABLE OF CONTENTS

<u>Section</u>	<u>Title</u>	<u>Page</u>
Chapter 1	Introduction; examples of 1st and 2nd order systems; example analysis and MATLAB¹ graphing	
1-1	Introduction	1-1
1-2	Linear, time-invariant (LTI) systems and ordinary differential equations (ODEs)	1-1
1-3	The mass-damper system: example of 1 st order, linear, time-invariant (LTI) system and ordinary differential equation (ODE)	1-3
1-4	A short discussion of engineering models	1-5
1-5	The mass-damper system (continued): example of solving the 1 st order, LTI ODE for time-history response, given a pulse excitation and an initial condition (IC)	1-6
1-6	The mass-damper system (continued): numerical/graphical evaluation of time-history response using MATLAB	1-9
1-7	Some notes regarding good engineering graphical practice, with reference to Figure 1-2	1-10
1-8	Plausibility checks of system response equations and calculations	1-11
1-9	The mass-damper-spring system: example of 2 nd order LTI system and ODE	1-12
1-10	The mass-damper-spring system: example of solving a 2 nd order LTI ODE for time response	1-13
1-11	Homework problems for Chapter 1	1-18

¹ MATLAB ® is a registered trademark of The MathWorks, Inc.

Table of Contents

<u>Section</u>	<u>Title</u>	<u>Page</u>
Chapter 2 Complex numbers and arithmetic; Laplace transforms; partial-fraction expansion		
2-1	Review of complex numbers and arithmetic	2-1
2-2	Introduction to application of Laplace transforms	2-5
2-3	More about partial-fraction expansion	2-11
2-4	Additional useful functions and Laplace transforms: step, sine, cosine, definite integral	2-12
2-5	Homework problems for Chapter 2	2-15
Chapter 3 Mechanical units; low-order mechanical systems; simple transient responses of 1st order systems		
3-1	Common mechanical units	3-1
3-2	Calculation of mass from measured weight	3-2
3-3	Reaction wheel: a rotational 1 st order system	3-3
3-4	Simple transient responses of 1 st order systems, 1 st order time constant and settling time	3-4
3-5	Aileron-induced rolling of an airplane or missile	3-8
3-6	Translational spring and viscous damper (dashpot)	3-11
3-7	More examples of damped mechanical systems	3-13
3-8	Homework problems for Chapter 3	3-17

Table of Contents

<u>Section</u>	<u>Title</u>	<u>Page</u>
Chapter Frequency response of 1st order systems; transfer function;		
4	general method for derivation of frequency response	
4-1	Definition of frequency response	4-1
4-2	Response of a 1 st order system to a suddenly applied cosine, $\cos\omega t$	4-1
4-3	Frequency response of the 1 st order damper-spring system	4-4
4-4	Period, frequency, and phase of periodic signals	4-8
4-5	Easy derivation of the complex frequency-response function for standard stable 1 st order systems	4-10
4-6	Transfer function, general definition	4-11
4-7	Frequency-response function from transfer function, general derivation	4-12
4-8	Homework problems for Chapter 4	4-15
Chapter 5 Basic electrical components and circuits		
5-1	Introduction	5-1
5-2	Passive components: resistor, capacitor, and inductor	5-1
5-3	Operational amplifier (op-amp) and op-amp circuits	5-9
5-4	<i>RC</i> band-pass filter	5-12
5-5	Homework problems for Chapter 5	5-13
Chapter General time response of 1st order systems by application of		
6	the convolution integral	
6-1	The convolution transform and its inverse, the convolution integral	6-1

Table of Contents

<u>Section</u>	<u>Title</u>	<u>Page</u>
6-2	General solution of the standard stable 1 st order ODE + IC by application of the convolution integral	6-2
6-3	Examples of 1 st order system response	6-3
6-4	General solution of the standard 1 st order problem: an alternate derivation	6-6
6-5	Numerical algorithm for the general solution of the standard 1 st order problem	6-7
6-6	Homework problems for Chapter 6	6-11

Chapter 7 Undamped 2nd order systems: general time response; undamped vibration

7-1	Standard form for undamped 2 nd order systems; natural frequency ω_n	7-1
7-2	General solution for output $x(t)$ of undamped 2 nd order systems	7-3
7-3	Simple IC response and step response of undamped 2 nd order systems	7-4
7-4	Discussion of the physical applicability of step-response solutions	7-6
7-5	Dynamic motion of a mechanical system relative to a non-trivial static equilibrium position; dynamic free-body diagram	7-7
7-6	Introduction to vibrations of distributed-parameter systems	7-9
7-7	Homework problems for Chapter 7	7-17

Chapter 8 Pulse inputs; Dirac delta function; impulse response; initial-value theorem; convolution sum

8-1	Flat pulse	8-1
-----	------------	-----

Table of Contents

Section	Title	Page
8-2	Impulse-momentum theorem for a mass particle translating in one direction	8-2
8-3	Flat impulse	8-3
8-4	Dirac delta function, ideal impulse	8-3
8-5	Ideal impulse response of a standard stable 1 st order system	8-5
8-6	Derivation of the initial-value theorem	8-7
8-7	Ideal impulse response of an undamped 2 nd order system	8-9
8-8	Ideal impulse response vs. real response of systems	8-10
8-9	Unit-step-response function and unit-impulse-response function (IRF)	8-12
8-10	The convolution integral as a superposition of ideal impulse responses	8-14
8-11	Approximate numerical solutions for 1 st and 2 nd order LTI systems based on the convolution sum	8-15
8-12	Homework problems for Chapter 8	8-28

Chapter 9 Damped 2nd order systems: general time response

9-1	Homogeneous solutions for damped 2 nd order systems; viscous damping ratio ζ	9-1
9-2	Standard form of ODE for damped 2 nd order systems	9-3
9-3	General solution for output $x(t)$ of underdamped 2 nd order systems	9-6
9-4	Initial-condition transient response of underdamped 2 nd order systems	9-8
9-5	Calculation of viscous damping ratio ζ from free-vibration response	9-9
9-6	Step response of underdamped 2 nd order systems	9-12
9-7	Ideal impulse response of underdamped 2 nd order systems	9-13

Table of Contents

Section	Title	Page
9-8	Step-response specifications for underdamped systems	9-14
9-9	Identification of a mass-damper-spring system from measured response to a short force pulse	9-18
9-10	Deriving response equations for overdamped 2 nd order systems	9-20
9-11	Homework problems for Chapter 9	9-23

Chapter 10 2nd order systems: frequency response; beating response to suddenly applied sinusoidal (SAS) excitation

10-1	Frequency response of undamped 2 nd order systems; resonance	10-1
10-2	Frequency response of damped 2 nd order systems	10-2
10-3	Frequency response of mass-damper-spring systems, and system identification by sinusoidal vibration testing	10-7
10-4	Frequency-response function of an <i>RC</i> band-pass filter	10-10
10-5	Common frequency-response functions for electrical and mechanical-structural systems	10-11
10-6	Beating response of 2 nd order systems to suddenly applied sinusoidal excitation	10-14
10-7	Homework problems for Chapter 10	10-19

Chapter 11 Mechanical systems with rigid-body plane translation and rotation

11-1	Equations of motion for a rigid body in general plane motion	11-1
11-2	Equation of motion for a rigid body in pure plane rotation	11-3
11-3	Examples of equations of motion for rigid bodies in plane motion	11-5

Table of Contents

Section	Title	Page
11-4	Homework problems for Chapter 11	11-13
Chapter 12	Vibration modes of undamped mechanical systems with two degrees of freedom	
12-1	Introduction: undamped mass-spring system	12-1
12-2	Undamped two-mass-two-spring system	12-2
12-3	Vibration modes of an undamped 2-DOF typical-section model of a wing	12-9
12-4	Homework problems for Chapter 12	12-13
Chapter 13	Laplace block diagrams, and additional background material for the study of feedback-control systems	
13-1	Laplace block diagrams for an <i>RC</i> band-pass filter	13-1
13-2	Laplace block diagram with feedback branches for an <i>m-c-k</i> system with base excitation	13-2
13-3	Forced response of an <i>m-c-k</i> system with base excitation	13-4
13-4	Homework problems for Chapter 13	13-7
Chapter 14	Introduction to feedback control: output operations for control of rotational position	
14-1	Initial definitions and terminology	14-1
14-2	More definitions, and examples of open-loop control systems	14-2
14-3	Closed-loop control of rotor position using position feedback	14-6

Table of Contents

Section	Title	Page
14-4	Transfer function of a single closed loop	14-9
14-5	Closed-loop control of rotor position using position feedback plus rate feedback	14-11
14-6	Comments regarding classical control theory and modern control theory	14-17
14-7	Homework problems for Chapter 14	14-18

Chapter 15 Input-error operations: proportional, integral, and derivative types of control

15-1	Initial definitions; proportional-integral-derivative (PID) control	15-1
15-2	Examples of proportional (P) and proportional-integral (PI) control	15-2
15-3	Derivation of the final-value theorem	15-12
15-4	Example of proportional-derivative (PD) control	15-13
15-5	Homework problems for Chapter 15	15-16

Chapter 16 Introduction to system stability: time-response criteria

16-1	General time-response stability criterion for linear, time-invariant systems	16-1
16-2	Stable and unstable PD-controlled-rotor systems	16-6
16-3	Routh's stability criteria	16-12
16-4	Loci of roots for 2 nd order systems	16-18
16-5	Loci of roots for 3 rd order systems	16-22
16-6	Open-loop transfer functions and loci of roots	16-31

Table of Contents

<u>Section</u>	<u>Title</u>	<u>Page</u>
16-7	Homework problems for Chapter 16	16-34

Chapter Introduction to system stability: frequency-response criteria 17

17-1	Gain margins, phase margins, and Bode diagrams	17-1
17-2	Nyquist plots	17-9
17-3	The practical effects of an open-loop transfer-function pole at $s = 0 + j0$	17-12
17-4	The Nyquist stability criterion	17-15
17-5	Homework problems for Chapter 17	17-23

References Refs-1

Appendix A: Table and derivations of Laplace transform pairs

A-1	Table of Laplace transform pairs used in this book	A-1
A-2	Laplace transform of a ratio of two polynomials, with only simple poles	A-4
A-3	Derivation of the Laplace transform of a definite integral	A-5
A-4	Applications of the Laplace transform of a definite integral	A-6
A-5	Derivation of the Laplace transform of the convolution integral	A-7

Table of Contents

<u>Section</u>	<u>Title</u>	<u>Page</u>
Appendix B: Notes on work, energy, and power in mechanical systems and electrical circuits		
B-1	Definitions of work and power	B-1
B-2	Mechanical work, energy, and power (complementary to Chapter 3)	B-2
B-3	Work, energy, and power in electrical circuits (complementary to Chapter 5)	B-4
B-4	Analogies between an $m-c-k$ mechanical system and an LRC electrical circuit	B-8
B-5	Hysteresis and dissipation of mechanical energy by damping	B-9
Index for all Chapters and Appendices		Index-1

Chapter 1 Introduction; examples of 1st and 2nd order systems, time-response analysis and graphing with MATLAB¹

© 2016 by William L. Hallauer, Jr.

1-1 Introduction

The subject of this book is the *dynamic behavior* of *physical systems*, with some emphasis on simple mechanical and electrical systems representative of or analogous to those often encountered in aerospace and mechanical engineering. A *system*, as defined in this book, is a combination of two or more simple physical *elements* or *components*, these being connected together in such a way that they all influence the dynamic behavior of the entire system. An *element* or *component*, as defined in this book, is usually a discrete object, such as a mechanical spring or an electrical resistor. This object usually produces a discrete effect, such as a motion-induced force or a voltage drop. *Dynamic behavior* is the variation in time of some physical response quantity of the system, for example, the position of a mass, or the voltage at some location in an electrical circuit.

The general subject of this book is relevant to courses that are offered in most engineering colleges for students who major in aerospace engineering, mechanical engineering, engineering mechanics, ocean engineering or naval architecture, electrical engineering, and chemical engineering. Many of the specific topics addressed within chapters and in homework problems following chapters are relevant especially to the study and practice of aerospace engineering.

1-2 Linear, time-invariant (LTI) systems and ordinary differential equations (ODEs)

We consider physical systems that can be modeled with reasonable engineering fidelity as *linear, time-invariant* (LTI) systems. Such a system is represented mathematically by an *ordinary differential equation* (ODE), or by a set of coupled ODEs, for which the single independent variable is time, denoted as t . These ODEs are linear, and they have constant coefficients, so we describe them as linear, time-invariant (LTI), the same as the systems they represent.² For example, suppose we denote a dependent variable as $x(t)$, here a general symbol representing some physical dynamic *response* quantity for which we want to solve. Then an LTI ODE that models an LTI physical system might have the form

$$\frac{dx}{dt} - a x = b u(t) \quad (1-1)$$

¹ MATLAB ® is a registered trademark of The MathWorks, Inc.

² LTI ODEs are also sometimes described as *linear, constant-coefficient*, or LCC.

in which a and b are constant multiplying coefficients, and known function $u(t)$ is the *excitation* and is independent of the response.³ In the study of systems, an independent excitation $u(t)$ is often called an *input*, and a dependent response $x(t)$ is often called an *output*.

Hereafter, we will usually employ the common shorthand dot notation for denoting derivatives with respect to time: $\frac{dx}{dt} \equiv \dot{x}$, $\frac{d^2x}{dt^2} \equiv \ddot{x}$, etc., so that Eq. (1-1) can be written more simply as $\dot{x} - ax = bu(t)$.

The *linearity* of Eq. (1-1) is manifested by the linear appearance of $x(t)$ and all of its derivatives in the ODE. The following are some similar ODEs that are not linear (they are *nonlinear*) for obvious reasons: $\dot{x} - ax^2 = bu(t)$; $\sin(\dot{x}) - ax = bu(t)$; $\sqrt{\dot{x}} - a \tan(x) = bu(t)$. Linear ODEs are almost always easier to solve (at least in closed form, i.e., as equations involving standard functions) than nonlinear ODEs. Moreover, the important *principle of superposition* applies to linear ODEs, but not to nonlinear ODEs. An example of the application of this principle is: let the response to input $u_1(t)$ be $x_1(t)$, and let the response to another input $u_2(t)$ be $x_2(t)$; if a third input is the sum of multiplied terms $u_3(t) = c_1 u_1(t) + c_2 u_2(t)$, in which c_1 and c_2 are constants, then the response to $u_3(t)$ is $x_3(t) = c_1 x_1(t) + c_2 x_2(t)$. This result is easy to derive just by multiplying two ODEs such as (1-1) by the constants, then adding the multiplied ODEs. The principle of superposition allows us to solve accurately for the responses of linear systems to any physically realistic inputs. (See Section 8-10 for a derivation of system response to an arbitrary physically realistic input by direct application of superposition.)

The *time invariance* of Eq. (1-1) is manifested by the constant coefficients of $x(t)$ and all of its derivatives in the ODE. ODEs with time-invariant coefficients model the behavior of systems assumed to have physical properties that either remain constant in time or vary so slowly and/or slightly that the variation is negligible for engineering purposes. But many practically important systems have time-varying physical properties. For example, a vehicle such as a space shuttle between liftoff and achievement of orbital position has rapidly varying (decreasing) mass as propellant is burned and external fuel tanks and boosters are released. The following is a linear equation somewhat similar to Eq.(1-1), but with an obviously time-varying coefficient: $\dot{x} - 3(1 - e^{-2t})x = bu(t)$. The study of systems with time-varying physical properties is generally more complicated, not fundamental, so only time-invariant systems and ODEs are considered in this book.

The form of Eq. (1-1), $\dot{x} - ax = bu(t)$, is widely regarded as **the standard form** for a 1st order LTI ODE, and we will use it as such in this book. Beginning in the next section, we will study idealized physical systems whose dynamic behaviors are described by equations that are directly analogous to Eq. (1-1). We will express the mathematical

³ Some synonyms for *excitation* in this book are *stimulus*, *stimulation*, and *forcing function* for systems in general, and *command* and *disturbance* specifically for controlled systems.

constants a and b in terms of specific physical constants. Also, the roles of input $u(t)$ and output $x(t)$ in Eq. (1-1) will be assumed by some specific physical quantities, such as force, velocity, voltage, etc., and we will denote them with relevant symbols [often different than $u(t)$ and $x(t)$] when appropriate.

Although only 1st order ODEs are discussed in this section, we certainly will encounter and study systems and ODEs of 2nd and higher orders.

1-3 The mass-damper system: example of 1st order LTI system and ODE

Consider a rigid body of mass m that is constrained to sliding translation $x(t)$ in only one direction, Fig. 1-1. The mass is subjected to an externally applied, arbitrary

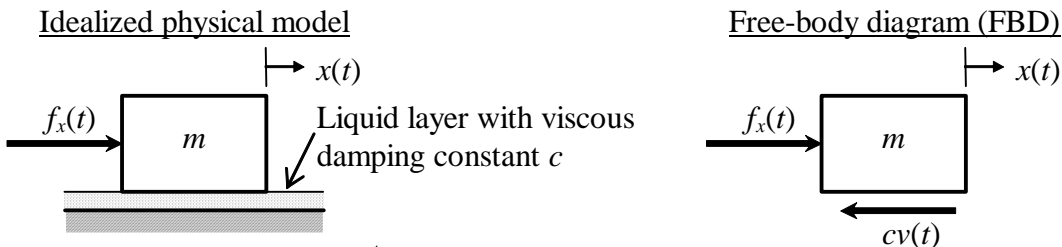


Figure 1-1 1st order mass-damper mechanical system

force $f_x(t)$, and it can slide on a thin, viscous liquid layer such as water or oil. The viscous force acting on the mass due to sliding on the liquid layer is opposite to the direction of velocity, $v(t) \equiv \dot{x}(t)$, and we assume that the magnitude of viscous force is proportional to velocity with constant of proportionality c , called the *viscous damping constant*. Mass m and viscous damping constant c are positive physical quantities. All of the forces acting on the mass are as shown on the *free-body diagram* (FBD) of Fig. 1-1.

Next, we use (from your engineering dynamics course) the FBD of Fig. 1-1 and Newton's 2nd law of motion (after English physicist and mathematician Isaac Newton, 1642-1727) for translation in a single direction, to write the equation of motion for the mass:

$$\Sigma (\text{Forces})_x = \text{mass} \times (\text{acceleration})_x, \text{ where } (\text{acceleration})_x = \frac{dv}{dt} = \dot{v};$$

$$f_x(t) - cv = m\dot{v}.$$

As is customary in writing ODEs, we collect all terms involving the dependent variable and its derivatives on the left-hand side, and put all independent input functions on the right-hand side:

$$m\dot{v} + cv = f_x(t) \quad (1-2)$$

ODE (1-2) is clearly linear in the single dependent variable, velocity $v(t)$, and time-invariant, assuming that m and c are constants. The highest derivative of $v(t)$ in the ODE is the first derivative, so this is called a 1st order ODE, and the mass-damper system is called a 1st order system. If $f_x(t)$ is defined explicitly, and if we also know some *initial condition* (IC) of the velocity, $v_0 \equiv v(t_0)$ at time $t = t_0$, then we can, at least in principle, solve ODE (1-2) for velocity $v(t)$ at all times $t > t_0$. (In this book, we will usually define the initial time as $t_0 = 0$ second.)

Equation (1-2) expressed in the form of the standard 1st order LTI ODE (1-1) becomes $\dot{v} - av = bf_x(t)$, where $a = -c/m$ and $b = 1/m$. Since m and c are positive physical constants, a is clearly negative. This negative polarity is characteristic of most physical systems that we will study; we shall see that it has an important influence on the general nature of the transient response of systems.

Note that after solving for velocity $v(t)$, we can solve by direct integration another ODE for position $x(t)$, provided that we know the initial position $x_0 \equiv x(t_0)$ at time $t = t_0$. One systematic method for finding $x(t)$ is based upon the derivative definition:

$$\text{ODE: } \dot{x}(t) \equiv \frac{dx(t)}{dt} = v(t)$$

The following shows careful definite integration of both sides of the ODE, using τ as the “dummy” variable of integration to distinguish it from the upper limit, time t :

$$\begin{aligned} \int_{\tau=t_0}^{\tau=t} \frac{dx(\tau)}{d\tau} d\tau &= \int_{\tau=t_0}^{\tau=t} v(\tau) d\tau \quad \Rightarrow \quad x(t) - x(t_0) = \int_{\tau=t_0}^{\tau=t} v(\tau) d\tau \\ &\Rightarrow \quad x(t) = x_0 + \int_{\tau=t_0}^{\tau=t} v(\tau) d\tau \end{aligned} \tag{1-3}$$

Another popular method of solution is to find the antiderivative (indefinite integral) of the ODE and add a constant of integration C , which then must be determined in terms of the initial condition:

$$\begin{aligned} x(t) &= \int v(t) dt + C \quad \Rightarrow \quad x(t_0) = \left[\int v(t) dt \right]_{t=t_0} + C \quad \Rightarrow \quad C = x_0 - \left[\int v(t) dt \right]_{t=t_0} \\ &\Rightarrow \quad x(t) = x_0 + \int v(t) dt - \left[\int v(t) dt \right]_{t=t_0} \end{aligned} \tag{1-4}$$

1-4 A short discussion of engineering models

The mass-damper of Fig. 1-1 can be used to represent approximately (*i.e.*, to *model*) some actual physical systems. One such system is a surface ship moving over the water under its own propulsion or being pushed/pulled by a tugboat. Another is an automobile hydroplaning on a wet road. You can probably think of other similar real systems. However, it is important for us, as engineers, to recognize that the mass-damper system is not the actual system, but only an approximate idealized physical model of the actual system. We are able to derive from this idealized physical model the solvable *mathematical model*, which consists of ODE (1-2) and known values for $f_x(t)$ and v_0 . The actual physical system, on the other hand, might be so complicated that it cannot be characterized mathematically with absolute precision. For example, the ideal viscous damping model used in the derivation of ODE (1-2) is almost certainly not an exact representation of the liquid drag forces acting on either a surface ship or a hydroplaning car.

The same general observation applies for almost any idealized physical model and associated mathematical model developed for engineering purposes: the physical model is, at best, a reasonably accurate approximation of the actual physical system. The fidelity of a model usually depends on a number of factors, including system complexity, uncertainties, the costs of modeling and mathematical/computational solutions, time constraints, modeling skills of the engineer, *etc.*

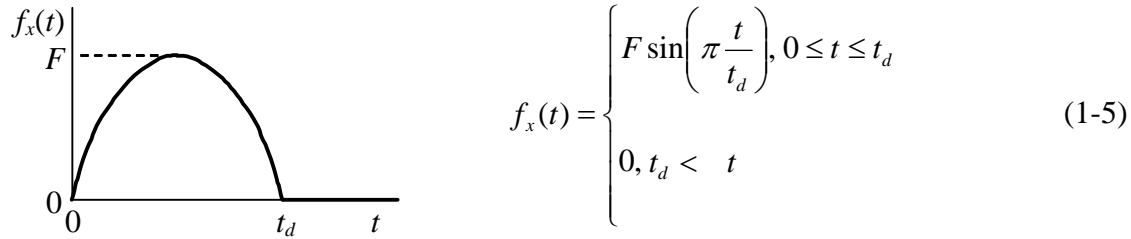
But a reasonably accurate approximate model often suffices for engineering purposes. Engineering systems are usually designed conservatively, with redundancies and factors of safety to compensate for severe overloads, unexpected material flaws, operator error, and the many other unpredictable influences that can arise in the functioning of a system. As engineers, we almost never require 100% accuracy; we are usually satisfied if our mathematical/computational predictions of system behavior are qualitatively correct and are quantitatively within around $\pm 10\%$ (in a general sense) of the actual behavior.

The main point of this discussion is to emphasize that any idealized physical model used for engineering analysis and design is only an approximation of an actual physical system. Moreover, the primary subjects of this book are the fundamental dynamic characteristics of idealized physical models, because a great deal of practical experience has shown that these are also the characteristics of many real engineering systems. Therefore, this book does not consider in depth the development of idealized physical models to represent actual systems; rather, we shall focus on deriving mathematical models (mostly ODEs) that describe idealized physical models, and on solving the mathematical equations and exploring the characteristics of the solutions.

The process of developing idealized physical models to represent real systems involves both science (theory and experimental data) and “art” (experience and intuition); you probably will encounter this process in laboratory and design courses, and later in your professional practice of engineering.

1-5 The mass-damper system (continued): example of solving the 1st order LTI ODE for time response, given a pulse excitation and an IC

An input of limited duration, typically called a *pulse*, is a very common type of excitation imposed onto systems. For example, when a hammer strikes a nail, the force imposed on the nail by the hammer is a pulse. A real pulse such as hammer impact force is often modeled as a *half-sine pulse*. Let the force acting on the mass in Fig. 1-1 be the half-sine pulse described by the following figure and Eq. (1-5):



In Eq. (1-5) for $f_x(t)$, t_d denotes the pulse duration. The notation will be more manageable in this problem if we express the time-varying sinusoid in the form $\sin \omega t$, where ω denotes the *circular frequency* of oscillation, in radians per second. In this case, clearly the circular frequency is expressed in terms of the pulse duration as $\omega = \pi/t_d$. Let's specify that the initial velocity of the mass at time $t = 0$ is some known value v_0 . The mathematical statement of the problem for finding the velocity time-history is:

ODE: $m \dot{v} + c v = f_x(t)$ (1-2, repeated)

IC: $v(0) = v_0$

Find: $v(t)$ for all $t > 0$.

To solve this problem in closed form, we will use a method with which you should be familiar from your previous study of ODEs. First, we find the *homogeneous* (also called *complementary*) solution $v_h(t)$, which is the solution of the homogeneous ODE, the version of Eq. (1-2) with zero right-hand side:

$$m \dot{v}_h + c v_h = 0 \quad (1-6)$$

A homogeneous LTI ODE always has solutions in time-linear powers of $e = 2.71828\dots$ (the base of natural logarithms), with some initially unknown constant coefficients:

$$v_h(t) = C e^{\lambda t}, \text{ in which constants } C \text{ and } \lambda \text{ are unknown at this stage.}$$

To find λ , we substitute the solution into the homogeneous ODE (1-6):

$$mC\lambda e^{\lambda t} + cC e^{\lambda t} = (m\lambda + c)C e^{\lambda t} = 0$$

If $C e^{\lambda t} = 0$, we get the useless trivial solution $v_h(t) = 0$, so a useful solution requires that $m\lambda + c = 0$, which is known as the *characteristic equation* of the ODE. Solution of this equation gives the so-called *characteristic value*, $\lambda = -c/m$, leading to:

$$v_h(t) = C e^{-(c/m)t} \quad (1-7)$$

Note that we still have not solved for constant C . We can find C only after we have determined a *particular* solution, also known as the *non-homogeneous* solution because it is a solution that satisfies the complete ODE (1-2) for the given right-hand side $f_x(t)$. For this problem, we will need two particular solutions, because $f_x(t)$ is defined differently over two different intervals of time, Eq. (1-5). First, we find a particular solution $v_p(t)$ valid over the pulse duration, $0 \leq t \leq t_d$, for which the ODE is:

$$m\dot{v}_p + cv_p = F \sin \omega t, \text{ where } \omega = \pi/t_d \quad (1-8)$$

To find a particular $v_p(t)$ that satisfies ODE (1-8), we apply the *method of undetermined coefficients*, which entails making an educated guess of the functional character of the solution, using multiplicative coefficients that will be determined by substituting the candidate solution back into ODE (1-8). The right-hand-side sine function of ODE (1-8) has a finite set of derivatives: the derivative of a sine is a cosine, the derivative of a cosine is a sine, *etc.* Therefore, we assume a form of solution consisting of a linear sum of the function and all of its derivatives:

$$v_p(t) = P_1 \sin \omega t + P_2 \cos \omega t, \text{ with coefficients } P_1 \text{ and } P_2 \text{ undetermined at this stage.}$$

Substitute this candidate solution back into ODE (1-8):

$$m\omega(P_1 \cos \omega t - P_2 \sin \omega t) + c(P_1 \sin \omega t + P_2 \cos \omega t) = F \sin \omega t$$

Collect terms that multiply $\sin \omega t$ and $\cos \omega t$ on both sides of the equation:

$$(-m\omega P_2 + cP_1)\sin \omega t + (m\omega P_1 + cP_2)\cos \omega t = (F)\sin \omega t + (0)\cos \omega t$$

Functions $\sin \omega t$ and $\cos \omega t$ are *linearly independent* of each other, which requires that the left-hand-side and right-hand-side terms multiplying $\sin \omega t$ must equal each other, and the same for the terms multiplying $\cos \omega t$, leading to two algebraic equations for the coefficients P_1 and P_2 :

$$cP_1 - m\omega P_2 = F \quad \text{and} \quad m\omega P_1 + cP_2 = 0$$

The second equation gives $P_2 = -(m\omega/c)P_1$, and substituting this into the first equation to eliminate P_2 leads to:

$$P_1 = \frac{cF}{(m\omega)^2 + c^2} \quad \text{and} \quad P_2 = \frac{-m\omega}{c} P_1 \quad (1-9)$$

Rather than write out messy algebraic formulas for all the coefficients in this problem, it is convenient to express all others in terms of P_1 , as is P_2 in Eq. (1-9).

To obtain the complete solution for the pulse duration, $0 \leq t \leq t_d$, we now combine the homogeneous and particular solutions:

$$v(t) = v_h(t) + v_p(t) = C e^{-(c/m)t} + P_1 \sin \omega t + P_2 \cos \omega t, \text{ for } 0 \leq t \leq t_d \quad (1-10)$$

Coefficient C in Eq. (1-10) is still not known; but now, finally, we can apply the initial condition (IC) to determine C :

$$v(0) = v_0 = C(1) + P_1(0) + P_2(1) \quad \Rightarrow \quad C = v_0 - P_2 = v_0 + (m\omega/c)P_1 \quad (1-11)$$

Equations (1-9) through (1-11) describe the velocity response during the pulse duration, $0 \leq t \leq t_d$, so we still need to find the post-pulse response, for $t_d < t$. To do so, we should recognize two facts: (1) $f_x(t) = 0$ for $t_d < t$; and (2) velocity $v(t)$ cannot suddenly change at $t = t_d$ (because acceleration cannot be infinite), rather, velocity must equal Eq. (1-10) evaluated at $t = t_d$. Fact 1 means that the ODE for $t_d < t$ is homogeneous; hence, the particular solution is zero, and we have only a homogeneous solution, but now with a different coefficient, D , than before:

$$v(t) = D e^{-(c/m)t}, \text{ for } t_d < t \quad (1-12)$$

To find D , we use Fact 2, which essentially is the IC for $t_d < t$, and Eq. (1-10):

$$D e^{-(c/m)t_d} = v(t_d) = C e^{-(c/m)t_d} + P_1 \sin \omega t_d + P_2 \cos \omega t_d \quad (1-13)$$

$$\Rightarrow D = v(t_d) e^{(c/m)t_d}$$

$$\Rightarrow v(t) = v(t_d) e^{-\frac{c}{m}(t-t_d)}, \text{ for } t_d < t \quad (1-14)$$

Equation (1-14), with Eq. (1-13) for $v(t_d)$, combined with Eq. (1-9) and Eq. (1-11) for coefficients P_1 , P_2 and C , represents the response for $t_d < t$. Because mass m and vis-

cous damping constant c are positive physical quantities, Eq. (1-14) is a pure exponential decay, which approaches zero as $t \rightarrow \infty$.

1-6 The mass-damper system (continued): numerical/graphical evaluation of time response using MATLAB

For the mass-damper response solution developed in the previous section, consider the following numerical case, with all quantities expressed in SI units: $m = 5 \text{ kg}$, $c = 2 \text{ N}\cdot\text{sec}/\text{m}$, $F = 18 \text{ N}$, $t_d = 7.5 \text{ sec}$, $v_0 = 3.3 \text{ m/sec}$. A MATLAB script M-file, named MATLABdemol1.m, to calculate and graph the response from 0 to 25 seconds is given below. The MATLAB commands are supplemented with explanatory comments, so you should be able to follow and understand the M-file without much difficulty. Writing comments in this manner is good practice for your own programs; comments added while you are writing a computer program are especially helpful if you need to revise or refer back to the program long after you have forgotten the details.

MATLAB script:

```
%MATLABdemol1.m
%Mass-damper system response to IC + half-sine pulse forcing
m=5;c=2; %system mass & viscous damping coefficient, SI units
F=18;td=7.5; %half-sine pulse, amplitude (N), pulse duration (sec)
vo=3.3; %initial velocity (m/sec)
w=pi/td; %circular frequency of half-sine pulse (rad/sec)
t1=0:0.05:td; %time instants for forced response
f1=F*sin(w*t1); %force pulse
P1=c*F/((w*m)^2+c^2);P2=P1*(-w*m/c);C=vo-P2; %constants
v1=C*exp(-c/m*t1)+P1*sin(w*t1)+P2*cos(w*t1);%time series of forced velocity
nt1end=length(t1);v2o=v1(nt1end);%initial velocity for post-pulse response
t2=td:0.1:25; %time instants for post-pulse unforced response
v2=v2o*exp(-c/m*(t2-td));%time series of post-pulse unforced velocity
f2=zeros(1,length(t2)); %null force after pulse
plot(t1,f1/10,'k',t1,v1,'k',t2,f2,'k',t2,v2,'k'),grid,xlabel('Time t (sec)')
ylabel('Force f_x(t) (daN), and Velocity v(t) (m/sec)')
title('Response of mass-damper system to IC + half-sine pulse forcing')
```

To execute in MATLAB an M-file that is stored on a folder (directory) of your computer's hard disk, you must have added that folder to the so-called MATLABpath. In Versions 6 and higher of MATLAB, you can add the folder to the MATLABpath by specifying the folder as the "Current Directory" in the formatting toolbar above the MATLAB command window. The command line below executes the script M-file.

MATLAB command:

```
>> MATLABdemol1
```

The resulting MATLAB (Versions 6 and higher) graph, Fig. 1-2, is on the next page. The graph was edited in the MATLAB figure window, mainly to reduce the size and to add curve labels and arrows.

Note that the unit of force “daN” on Fig. 1-2 is a deka-newton, which means 10 newtons. All of the mechanical units used in this book are described in Chapter 3.

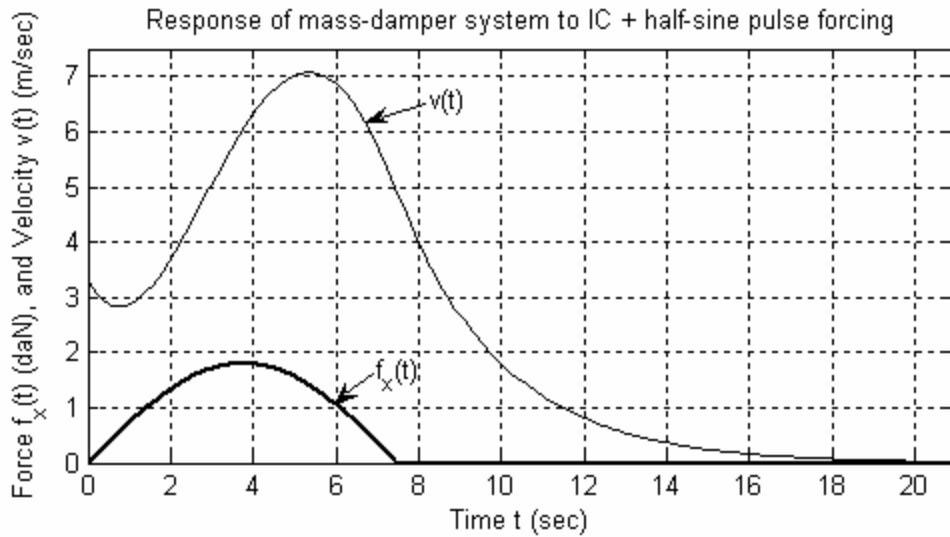


Figure 1-2 Excitation and response of a mass-damper system

1-7 Some notes regarding good engineering graphical practice, with reference to Figure 1-2

- * Always label both axes, and always include the units of physical quantities.
- * Always write an explanatory one-line title. Such a short title cannot explain everything about the graph, but any title you use will almost certainly help the reader to understand the graph.
- * It is usually good practice to add grids to a graph. Grids help the reader to perceive values correctly. For example, the grids on Fig. 1-2 show clearly that the peak velocity response is just above 7 m/sec at a little after 5 sec.
- * The commands in the script file that specify the densities of computed points are, first, $t1=0:0.05:td$ while the pulse acts and, second, $t2=td:0.1:25$ following the pulse. For example, the first line directs MATLAB to compute the response at 0.05-sec intervals; then $plot(...,t1,v1,'k',...)$ directs MATLAB to plot small points for those instants, and to connect each two adjacent points with a straight line. If you use high point densities, then the overall plotted line will capture all important features of the response (extreme values, for example), and will appear to be a smooth curve. Indeed, the overall line should look like a smooth curve, because it represents a continuous physical response; neither the response itself nor its low-order derivatives should be discontinuous. On the other hand, if you use low point densities, then you might miss important features of the response, and the overall line will be unnaturally piecewise linear, with kinks (slope dis-

continuities). To visualize an extreme example of low point density, suppose that for the mass-damper system you were to compute and plot the velocity response at 4-sec intervals; the velocity graph in Fig. 1-2 would consist only of straight lines connecting the computed points at 0, 4, 8, 12, 16, and 20 seconds, which would badly represent the actual response. So always specify high point density on graphs of continuous physical response. You might not know initially what point density you should use, especially if you are analyzing an unfamiliar system. But try some plausible point density. If your plotted response curve appears unnaturally kinky, then increase the point density appropriately and run the M-file again. It will cost you nothing more than the little time required to edit and re-run the M-file (or any other graphing computer program).

1-8 Plausibility checks of system response equations and calculations

We all make mistakes in the process of analyzing engineering problems. Most common are mistakes in arithmetic, algebra, calculus, theory, and calculation algorithms (usually computer programming). Also, sometimes we simply use incorrect data. It seems that there are countless ways to make mistakes. Therefore, it is important always to check your mathematical, numerical, and computational operations and results in every way possible. An important type of check for any problem with physical results is the *plausibility check*, known more colloquially as *reality check* and *sanity test*. Essentially you examine the results to determine if they are physically plausible (believable, credible, reasonable). Do the results make sense physically? A classic example of implausible result that often appears on exam papers in structures courses is the structural deformation on the order of 10^3 or 10^6 inches, when it ought to be on the order of 10^{-3} inches.

To illustrate a plausibility check, let's examine Fig. 1-2 for the velocity response of the mass-damper system to an initial condition and half-sine pulse excitation. First, the specified initial velocity is $v_0 = 3.3$ m/sec, and the response curve at time $t = 0$ correctly reflects that initial condition. Next, for about the first half-second of response, the velocity decreases due to viscous drag force cv . But then, as the applied force $f_x(t)$ increases, the velocity dips to a local minimum and subsequently increases. Applied force $f_x(t)$ peaks at $t = \frac{1}{2}t_d = 3.75$ sec, and the graph shows that the slope of the velocity curve, acceleration \dot{v} , is maximum at about the same time. The velocity itself peaks at a bit past 5 sec. Because velocity is the integral of acceleration (area under the acceleration curve), this lag of the velocity peak behind the force pulse peak is quite plausible. After the velocity peaks, it decreases monotonically toward zero as the applied force decreases to zero at $t = t_d = 7.50$ sec and remains at zero thereafter. So the entire response, as depicted graphically, is physically plausible.

Plausibility of a calculated response does not guarantee that it is correct, although it is reassuring. On the other hand, implausibility of a calculated response almost certainly guarantees that it is wrong. The primary justification for conducting a plausibility check is to catch incorrect engineering predictions before they cause trouble (which can vary from point loss on homework or exams, to a major disaster, the unpredicted failure of an engineering system).

1-9 The mass-damper-spring system: example of 2nd order LTI system and ODE

Consider a rigid body of mass m that is constrained to sliding translation $x(t)$ in only one direction, Fig. 1-3. The mass is subjected to an externally applied, arbitrary

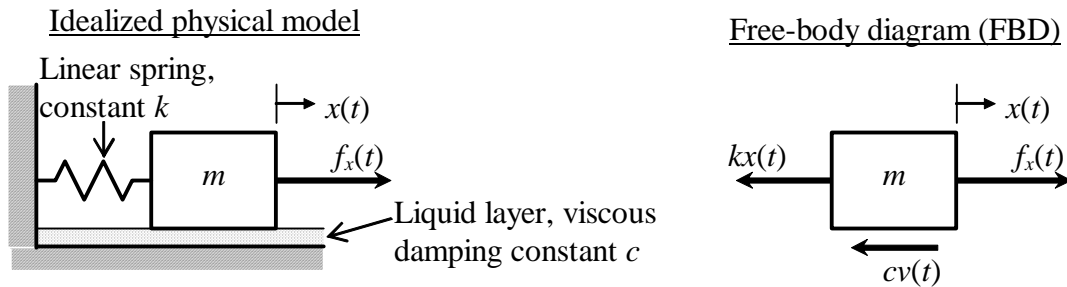


Figure 1-3 2nd order mass-damper-spring mechanical system

force $f_x(t)$, and it slides on a thin, viscous, liquid layer that has linear viscous damping constant c . Additionally, the mass is restrained by a *linear spring*. The force exerted by the spring on the mass is proportional to translation $x(t)$ relative to the undeformed state of the spring, the constant of proportionality being k . Parameters m , c , and k are positive physical quantities. All of the horizontal forces acting on the mass are shown on the FBD of Fig. 1-3.

From the FBD of Fig. 1-3 and Newton's 2nd law for translation in a single direction, we write the equation of motion for the mass:

$$\Sigma (\text{Forces})_x = \text{mass} \times (\text{acceleration})_x, \text{ where } (\text{acceleration})_x = \dot{v} = \ddot{x};$$

$$f_x(t) - cv - kx = m\dot{v}.$$

Re-arrange this equation, and add the relationship between $x(t)$ and $v(t)$, $\dot{x} = v$:

$$m\dot{v} + cv + kx = f_x(t) \quad (1-15a)$$

$$\dot{x} - v = 0 \quad (1-15b)$$

Equations (1-15a) and (1-15b) are a pair of 1st order ODEs in the dependent variables $v(t)$ and $x(t)$. The two ODEs are said to be *coupled*, because each equation contains both dependent variables and neither equation can be solved independently of the other. Such a pair of coupled 1st order ODEs is called a 2nd order set of ODEs.

Solving 1st order ODE (1-2) in the single dependent variable $v(t)$ for all times $t > t_0$ requires knowledge of a single IC, which we previously expressed as $v_0 = v(t_0)$. Similarly, solving the coupled pair of 1st order ODEs, Eqs. (1-15a) and (1-15b), in dependent variables $v(t)$ and $x(t)$ for all times $t > t_0$, requires a known IC for each of the dependent variables:

$$v_0 \equiv v(t_0) = \dot{x}(t_0) \text{ and } x_0 = x(t_0) \quad (1-16)$$

In this book, the mathematical problem is expressed in a form different from Eqs. (1-15a) and (1-15b): we eliminate v from (1-15a) by substituting for it from (1-15b) with $v = \dot{x}$ and the associated derivative $\dot{v} = \ddot{x}$, which gives⁴

$$m \ddot{x} + c \dot{x} + k x = f_x(t) \quad (1-17)$$

ODE (1-17) is clearly linear in the single dependent variable, position $x(t)$, and time-invariant, assuming that m , c , and k are constants. The highest derivative of $x(t)$ in the ODE is the second derivative, so this is a 2nd order ODE, and the mass-damper-spring mechanical system is called a 2nd order system. If $f_x(t)$ is defined explicitly, and if we also know ICs (1-16) for both the velocity $\dot{x}(t_0)$ and the position $x(t_0)$, then we can, at least in principle, solve ODE (1-17) for position $x(t)$ at all times $t > t_0$. We shall study the response of 2nd order systems in considerable detail, beginning in Chapter 7, for which the following section is a preview.

1-10 The mass-spring system: example of solving a 2nd order LTI ODE for time response

Suppose that we have a system of the type depicted on Fig. 1-3 for which the damping force, $c\dot{x}$ in Eq. (1-17), is negligibly small in comparison with inertial force $m\ddot{x}$ and structural force kx . Figure 1-4

is a photograph of a real system⁵ with so little damping that, under some circumstances, we may neglect the damping force. The mass carriage of this system rides back and forth on low-friction linear ball bearings, which are enclosed underneath the carriage and not visible in the photograph. The entire length of this system, from the left (fixed) end of the spring, to the rightmost edge of the mass carriage is 8½ inches (21.6 cm), and each of the three light-colored metal slabs attached to the carriage has mass of ½ kilogram.

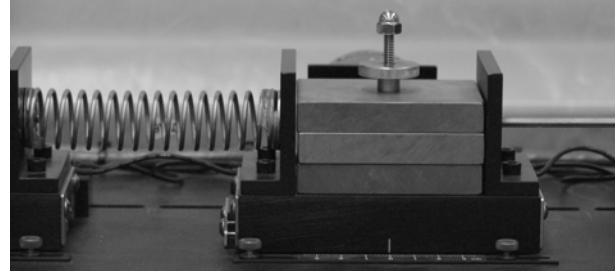


Figure 1-4 Laboratory mass-spring system

If we may neglect the damping force in a system such as that of Fig. 1-4, then the term $c\dot{x}$ drops out of Eq. (1-17), and we are left with the simpler 2nd order ODE,

⁴ An alternative derivation of ODE (1-17) is presented in Appendix B, Section B-2. The rate of change of system energy is equated with the power supplied to the system.

⁵ This is part of a Model 210a Rectilinear Plant designed and fabricated by Educational Control Products of Bell Canyon, California, USA.

$$m \ddot{x} + k x = f_x(t) \quad (1-18)$$

If we know ICs (1-16) and excitation force $f_x(t)$, then we can solve Eq. (1-18) for $x(t)$. For future reference, note that mass quantity m and spring stiffness constant k are intrinsically positive values. Also, observe that $f_x(t)$ may be applied to the system of Fig. 1-4 through the link visible at the right-hand side of the mass carriage.

It will be instructive to determine a time response for this 2nd order mass-spring ($m-k$) system, by applying the standard ODE solution procedure described in Section 1-5. We shall find the complete algebraic solution as the sum of homogeneous and particular solutions, $x(t) = x_h(t) + x_p(t)$. Suppose that at time $t = 0$ the spring is undeformed and the mass is at rest, so that ICs (1-16) are

$$\dot{x}(0) = 0 \text{ and } x(0) = 0 \quad (1-19)$$

Suppose also that the excitation is a force pulse described by the equation $f_x(t) = F_m(t/t_m)e^{(1-t/t_m)}$; by applying calculus to this function, you can easily prove that it rises from zero at $t = 0$ to the maximum value F_m at time $t = t_m$, and, thereafter, it gradually drops back to zero (see Fig. 1-5). In dynamics, a linear function of time such as t/t_m is often called a “ramp” function; since our excitation consists of a declining exponential function multiplied by a ramp function, we call this excitation a “ramped exponential” force pulse.

The homogeneous ODE associated with Eq. (1-18) is $m \ddot{x}_h + k x_h = 0$. We cast this equation into a familiar form by dividing through by mass m and defining the positive quantity $\omega_n^2 = k/m$, giving the ODE

$$\ddot{x}_h + \omega_n^2 x_h = 0 \quad (1-20)$$

The positive root $\omega_n = \sqrt{k/m}$ is called the *natural frequency* of this $m-k$ system, and ω_n has physical significance that will be discussed below with the final solution. You might remember from your previous study of ODEs, or you can easily verify by substitution into Eq. (1-20), that the solution can be expressed as

$$x_h(t) = C_1 \sin \omega_n t + C_2 \cos \omega_n t \quad (1-21)$$

Constants C_1 and C_2 are unknown at this point in the solution process.

With excitation by the ramped exponential pulse defined above, any particular solution $x_p(t)$ must satisfy the non-homogeneous ODE

$$m \ddot{x}_p + k x_p = F_m(t/t_m) e^{(1-t/t_m)} \quad (1-22)$$

To find a particular $x_p(t)$ that satisfies ODE (1-22), we apply the method of undetermined coefficients, just as in Section 1-5. It is easy to show by successive differentiations that all derivatives with respect to time of the function $(t/t_m)e^{(1-t/t_m)}$ produce only constant multiples of $(t/t_m)e^{(1-t/t_m)}$ itself, and of $e^{(1-t/t_m)}$. Therefore, we seek a particular solution that consists of a linear sum of these two functions:

$$x_p(t) = P_1(t/t_m)e^{(1-t/t_m)} + P_2 e^{(1-t/t_m)} \quad (1-23)$$

We determine constants P_1 and P_2 by substituting Eq. (1-23) into Eq. (1-22), equating the coefficients of $(t/t_m)e^{(1-t/t_m)}$ and $e^{(1-t/t_m)}$ on the two sides of the resulting algebraic equation, and then solving for P_1 and P_2 [homework Problem 1.10(a)]. This process produces the results

$$P_1 = \frac{F_m}{m/t_m^2 + k} \quad \text{and} \quad P_2 = \frac{2m/t_m^2}{m/t_m^2 + k} P_1 \quad (1-24)$$

The complete (but not yet final) solution is

$$x(t) = x_h(t) + x_p(t) = C_1 \sin \omega_n t + C_2 \cos \omega_n t + P_1(t/t_m)e^{(1-t/t_m)} + P_2 e^{(1-t/t_m)} \quad (1-25)$$

We now can determine the remaining unknown constants by substituting Eq. (1-25) into ICs (1-19), $\dot{x}(0) = 0$ and $x(0) = 0$, and solving algebraically for constants C_1 and C_2 [homework Problem 1.10(b)]. The results are

$$C_1 = \frac{P_2 - P_1}{\omega_n t_m} e^1, \text{ with } \omega_n = \sqrt{\frac{k}{m}} \quad \text{and} \quad C_2 = -P_2 e^1 \quad (1-26)$$

The complete and final solution is Eq. (1-25), with constants C_1 , C_2 , P_1 , and P_2 defined in terms of the basic parameters m , k , F_m , and t_m by Eqs. (1-24) and (1-26). Let's calculate and plot a time response for the system of Fig. 1-4. The total mass of the carriage plus the three ½-kilogram attached metal slabs is $m = 2.20$ kg, and the stiffness of the spring is $k = 770$ N/m. Suppose that the ramped exponential force pulse has maximum value $F_m = 6$ N at the instant $t_m = 1/12$ sec. The MATLAB command lines on the next page calculate and print out the frequency quantity $f_n = \omega_n / 2\pi$, and they calculate and plot the time response over the interval $0 \leq t \leq 2$ sec. Note that it was not necessary to assemble these command lines into a formal M-file; rather, the lines were composed in a text-editing program, then the entire group of lines was copied together and pasted onto the prompt “>>” on the MATLAB command window. Also, since solution Eq. (1-25)

includes the product of two functions of time in the term $(t/t_m)e^{(1-t/t_m)}$, it is necessary to implement this product using MATLAB array multiplication (.*) in the operation prod=tt.*efun.

```
>> %Mass-spring response: rest ICs; ramped exponential pulse input
m=2.20;k=770; %system mass and stiffness, SI units
wn=sqrt(k/m);fn=wn/2/pi;
disp('Natural frequency (cycles/sec) fn ='),disp(fn)
Fm=6.0;tm=1/12; %excitation parameters
t=0:.005:2; %time sequence for excitation/response
tt=t(tm);efun=exp(1-tt);prod=tt.*efun;f=Fm*prod; %excitation
a1=m/tm^2;a2=a1+k;P1=Fm/a2;P2=2*a1*P1/a2; %P constants
C1=(P2-P1)*exp(1)/wn/tm;C2=-P2*exp(1); %C constants
wt=wn*t;x=C1*sin(wt)+C2*cos(wt)+P1*prod+P2*efun; %response
plot(t,100*f/k,'k.',t,100*x,'k'),grid,xlabel('Time t [sec]'),...
ylabel('Translations reference f_x(t)/k and actual x(t) [cm]'),...
title('Response of mass-spring system to ramped exponential pulse')

Natural frequency (cycles/sec) fn =
2.9775
```

Figure 1-5 is the MATLAB graph produced by the sequence of commands above. The graph was edited in the MATLAB figure window, mainly to reduce the size and to add the legend.

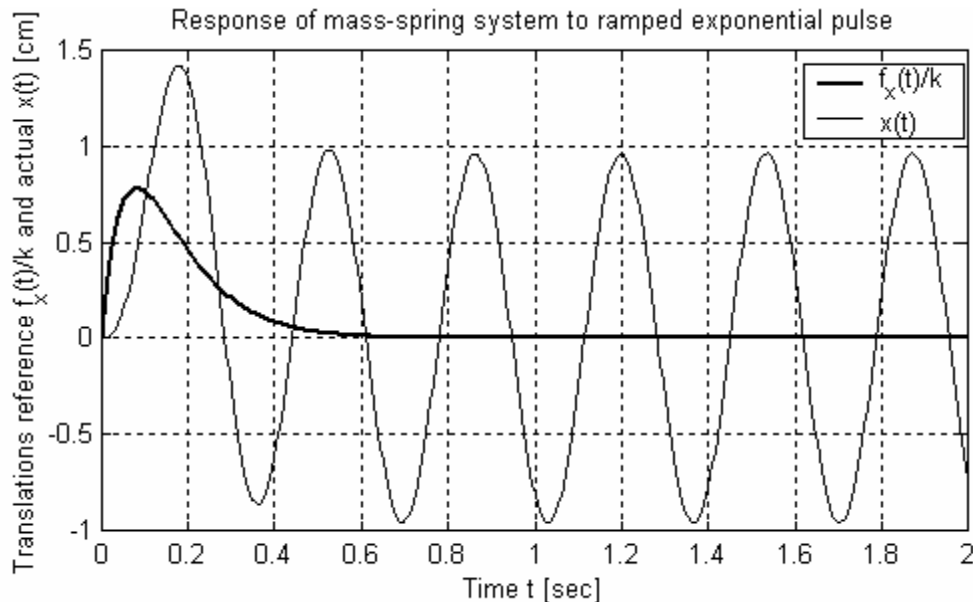


Figure 1-5 Excitation and response of a mass-spring system

The reference quantity $f_x(t)/k$ plotted on Fig. 1-5 represents the excitation force, but divided by k , so that it has the units of translation. You can see from the basic ODE (1-18), $m\ddot{x} + kx = f_x(t)$, that the plotted quantity physically represents the spring deformation that dynamic excitation $f_x(t)$ would produce if mass m were zero or negligible.

Because this reference quantity is calculated by neglect of the entire dynamic inertial force, $m \ddot{x}$, it is often called the *pseudo-static* response.

Observe on Fig. 1-5 that the actual dynamic translation $x(t)$ of the mass greatly overshoots the pseudo-static translation initially (with peak response of about +1.4 cm at about 0.18 sec), and that the actual response persists as significant *vibration* after the pulse excitation has died away. These are important dynamic characteristics of many systems that we encounter in engineering practice. In reality, all mechanical systems that consist of purely passive masses and passive structural members have some degree of positive damping; but, if the damping forces are low in comparison with inertial and structural forces, then these real systems will respond to excitation similarly, at least in a qualitative sense, to the “actual” response of Fig. 1-5. For example, the real system of Fig. 1-4 is positively but lightly damped; in response to the given force pulse, this system would experience just about the same initial response and overshoot as shown on Fig. 1-5, but the vibration would die away gradually, and motion would cease completely after three or four seconds.

The terms in Eq. (1-25) that primarily represent vibration are the sinusoidal functions $\sin \omega_n t$ and $\cos \omega_n t$, with the angle (in radians) argument of these periodic functions being $\theta(t) = \omega_n t$. The *period* of such a function is the time required for the function to complete a full cycle and begin repeating itself. In this case, let’s denote that period as T_n and observe that its natural physical units are seconds/cycle. The associated *frequency* f_n , in the units cycles/second,⁶ is obviously just the inverse of the period, $f_n = 1/T_n$. Thus, the angle (in radians) argument of the periodic sinusoidal functions can be written in the following equivalent forms: $\theta(t) = \omega_n t = 2\pi(t/T_n) = 2\pi f_n t$. The important relationship between *circular* natural frequency ω_n , in radians/second, and *cyclic* natural frequency f_n , in cycles/second, is $f_n = \omega_n/2\pi$. For the values of mass m and stiffness k used in the MATLAB calculations above, the printed-out value of f_n is 2.98 cycles per second, and this is the frequency that is most obvious in Fig. 1-5; for example, as closely as we can detect by eye, almost exactly three complete cycles of vibration occur between $t = 0.7$ sec and $t = 1.7$ sec.

⁶ More commonly in modern terminology, a cycle/second is designated as a *hertz*, with the abbreviation Hz.

1-11 Homework problems for Chapter 1

1.1(a) Super hero Dynamaman is cruising along at 126 km/hr when the Dynamobile suddenly encounters wet pavement and begins hydroplaning. Naturally, Dynamobile is headed straight for a thick, solid steel barrier and will crash if it can't stop. Also naturally, Dynamobile is equipped not only with conventional brakes (useless against hydroplaning) but also with jet reverse thrusters that can provide emergency braking in the form of a half-sine pulse. Dynamaman hits the panic button, which activates all sensors and the onboard computer. The sensors instantly detect initial velocity $v_0 = 35.0$ m/sec, Dynamobile total mass $m = 1,500$ kg, and hydroplaning viscous damping constant $c = 7.70$ N-sec/m. The computer calculates that a possible disaster-avoidance action is to deploy the maximum available braking thrust amplitude of $F = -7,200$ N (-7.2 kN) in a half-sine pulse extending over 10.0 sec [$f_x(t) = F \sin(0.100\pi t)$ for $0 \leq t \leq 10.0$ sec]. Your task is to demonstrate the effectiveness of this braking thrust by making a MATLAB graph that shows the velocity of Dynamobile over 15 seconds (the 10-sec braking period plus another 5 seconds of coasting). Be sure to use good engineering graphical practice: provide grids, a title, appropriate labels, and high point density. Submit your MATLAB script as well as your graph.

(b) Consider the same scenario as in part (a), but with the following different data: $v_0 = 40.0$ m/sec, $m = 1,700$ kg, $c = 130$ N-sec/m, with braking force amplitude $F = -30,000$ N (-30.0 kN) in the pulse $f_x(t) = F \sin(0.250\pi t)$ for $0 \leq t \leq 4.00$ sec. Make a MATLAB graph that shows the velocity of Dynamobile over 8 seconds (the 4-sec braking period plus another 4 seconds of coasting).

(c) Consider the same scenario as in part (a), but with the following different data: $v_0 = 60.0$ m/sec, $m = 1,700$ kg, $c = 1,100$ N-sec/m, with braking force amplitude $F = -120,000$ N (-120 kN) in the pulse $f_x(t) = F \sin(\pi t)$ for $0 \leq t \leq 1.00$ sec. Make a MATLAB graph that shows the velocity of Dynamobile over 3 seconds (the 1-sec braking period plus another 2 seconds of coasting).

1.2 Consider again the hydroplaning Dynamobile of Problem 1.1 with total mass m , hydroplaning viscous damping constant c , and initial velocity $v(0) \equiv v_0$.

(a) Integrate $\dot{x} = v(t)$ given in Eq. (1-10) to derive an algebraic equation for position $x(t)$ while the braking pulse is active. In order to keep the equation algebraically simple (relatively, anyway), leave it in terms of constants C , P_1 , and P_2 (don't write those constants in terms of m , c , v_0 , F , and t_d). Make sure that your $x(t)$ equation gives the initial position as zero, $x(0) = 0$, by either (i) carefully evaluating the definite integral of $v(t)$ between the limits 0 and t [see Eq. (1-3)], or (ii) taking the antiderivative of the $v(t)$ equation and adding an appropriate constant of integration [see Eq. (1-4)]. Using the numerical data of Problem 1.1 [part (a) or (b) or (c), whichever you solved before], calculate the distance traveled by Dynamobile at the end of the braking (pulse) period. (Com-

ment: in reality, to prevent collision with the barrier, wouldn't you need to know Dynamobile's initial distance from the barrier as well as its initial velocity?)

(b) Differentiate $v(t)$ given in Eq. (1-10) to derive an algebraic equation for acceleration $a(t) = \dot{v}$ while the braking pulse is active. In order to keep the equation algebraically simple, leave it in terms of constants C , P_1 , and P_2 . Using the numerical data of Problem 1.1 [part (a) or (b) or (c), whichever you solved before], make a MATLAB graph that shows the acceleration in G 's of Dynamobile over the braking (pulse) period. To calculate acceleration in G 's, divide acceleration in m/sec² by the nominal SI acceleration of gravity, $g = 9.807$ m/sec². [Comment: we presume that Dynaman would not survive the collision if there were no braking, but, in fact, would he survive the deceleration (perhaps many G 's) required to prevent the collision?]

1.3 Consider again the hydroplaning Dynamobile of Problems 1.1 and 1.2. Suppose that all parameters are known except F , the pulse magnitude. Now we want to find the optimum pulse magnitude, $F \equiv F_{opt}$, defined here as the value that will bring Dynamobile to a dead stop at the end of the pulse duration, $v(t_d) = 0$.

(a) Use Eqs. (1-9)-(1-11) for $v(t)$ to derive an algebraic equation for F_{opt} in terms of the parameters m , c , v_0 , and t_d . Next, evaluate your equation numerically for $m = 1,700$ kg, $c = 130$ N/m/sec, $v_0 = 40.0$ m/sec, and $t_d = 4.00$ sec. (answer: $F_{opt} = -22.87$ kN)

(b) Use the algebraic equation for position $x(t)$ from Problem 1.2(a), and the value $F \equiv F_{opt}$ from Problem 1.3(a) to calculate how far Dynamobile would travel after activation of thrust braking before coming to a dead stop. (answer: $x(t_d) = 75.18$ m)

1.4 Consider a mass-damper system with a cosine forcing function, as described by the 1st order, LTI ODE $m\dot{v} + cv = F \cos \omega t$, in which velocity $v(t)$ is the dependent variable, and the known constant parameters are mass m , viscous damping constant c , force amplitude F , and circular frequency of forcing ω . Use the method of undetermined coefficients to derive an algebraic equation (in terms of the given constants) for the particular solution $v_p(t)$ of this ODE and forcing function.

1.5 The “standard” 1st order ODE is $\dot{x} - ax = bu(t)$.

(a) Suppose that $u(t) = U \sin \omega t$, $t > 0$, where U is a constant amplitude, and that $x(0) = 0$. Derive the following solution of the standard 1st order ODE:

$$x(t) = \frac{-abU}{\omega^2 + a^2} \left(-\frac{\omega}{a} e^{at} + \sin \omega t + \frac{\omega}{a} \cos \omega t \right), t \geq 0$$

- (b) Suppose that $u(t) = U \cos \omega t$, $t > 0$, where U is a constant amplitude, and that $x(0) = 0$. Derive the following solution of the standard 1st order ODE:

$$x(t) = \frac{-abU}{\omega^2 + a^2} \left(-e^{at} - \frac{\omega}{a} \sin \omega t + \cos \omega t \right), t \geq 0$$

1.6 Symbolic software such as Mathematica⁷ and MATLAB (the Symbolic Math Toolbox) can solve some ODEs, including those discussed in Chapter 1. For an introduction to this type of solution, solve Problem 1.5(a) in MATLAB. Begin with the following MATLAB commands:

```
>> syms a b U w t
>> x=dsolve('Dx-a*x=b*U*sin(w*t)', 'x(0)=0')
```

The MATLAB response will probably be a long, algebraically undisciplined equation for $x(t)$. In order to express the equation in a more economical form, type the command

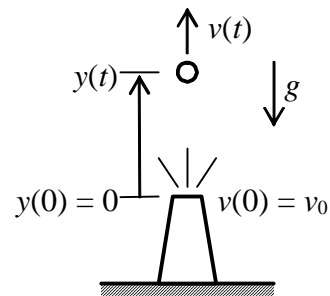
```
>> x=simple(x)
```

The simplified equation will still be in rather awkward computer notation, so, to express the equation in a more conventional form, type the command:

```
>> pretty(x)
```

A few words of warning about symbolic software are appropriate. For more complex ODEs, symbolic software might give algebraic solutions that are correct, but are expressed in an unfamiliar form, or in an algebraic form that must be simplified by hand in order to be useful. For this reason and others, engineers often regard symbolic software as useful mainly for providing checks on mathematical results that have been derived the old-fashioned way, by hand.

- 1.7** Imagine a spherical cannon ball having the diameter d and mass m of a regulation baseball, but with a very smooth surface (not somewhat rough, like a baseball's stitched cowhide cover). Suppose that we launch this ball vertically upward from sea level against Earth's gravity, with known launch (muzzle) vertical velocity v_0 being sufficiently low that the acceleration of gravity g remains essentially constant over the entire ascent and descent of the ball. Denote the varying altitude (vertical position) of the ball as $y(t)$, positive upwards, so the ball's velocity is $v(t) = \dot{y}(t)$.



- (a) First, let's idealize the aerodynamic drag force as being linearly viscous with damping constant c , $D_1 = cv$ (subscript 1 denotes this mathematical model of drag as

⁷ Mathematica ® is a registered trademark of Wolfram Research, Inc.

proportional to the 1st power of velocity, v^1). Draw and label an appropriate free-body diagram (FBD), showing the direction of drag force, by convention in analysis of aerodynamics, as being opposite to the direction of velocity $v(t)$. Using your FBD, apply Newton's 2nd law to derive the ODE of motion, $m\dot{v} + cv = -mg$.⁸

(b) Solve the ODE of part (a) to determine an equation for velocity $v(t)$, $t \geq 0$, given the known IC, $v(0) = v_0$. First, observe that the homogeneous ODE is the same as Eq. (1-6), so that Eq. (1-7) is the homogeneous solution. Next, find the simplest possible particular solution, v_p , a constant. Next, enforce the initial condition to determine the unknown constant of the homogeneous solution. From your $v(t)$ equation, show that $v_p = v_{t1}$, the constant *terminal velocity* of the ball's descent for drag D_1 . Also, derive an equation for the instant of time t_{z1} when velocity is zero, which, of course, corresponds to the peak altitude, y_{\max_1} of the ball. (*Partial answers:* $v_{t1} = -mg/c$; $t_{z1} = (m/c)\ln(1-v_0/v_{t1})$, in which \ln denotes the natural logarithm, *i.e.*, the logarithm to base e .)

1.7(c) Integrate $v(t)$ of part (b) to derive an equation for the ball's altitude, $y(t)$, $t \geq 0$; define the launch point to be the reference position, *i.e.*, set the IC as $y(0) = 0$. (*Answer:* $y(t) = (m/c)(v_0 - v_{t1})(1 - e^{-(c/m)t}) + v_{t1}t$.)

(d) Next, let's consider the mathematical model for the aerodynamic drag force that is generally considered most appropriate for a smooth ball: $D_2 = \pm \bar{q} S C_D$, with the plus sign for ascent ($v \geq 0$), and the minus sign for descent ($v < 0$). The terms in this equation are: $\bar{q} = \frac{1}{2}\rho v^2$, the dynamic pressure, with sea-level air density $\rho = 0.002377$ slug/ft³ = 0.002377 lb-sec²/ft⁴; $S = \pi d^2/4$, the ball's projected area, with baseball diameter about $d = 2.90$ inches; and C_D , the dimensionless drag coefficient, which is about $C_D = 0.50$ for the smooth ball, provided its airspeed is less than about 140 mph (miles/hour). Write two 1st order ODEs for $v(t)$ with drag model D_2 , one ODE applying to ascent, the other to descent. Explain what it is about these ODEs that makes them nonlinear. Do not attempt to solve these ODEs in general, but use the appropriately simplified form of the descent ODE to find an algebraic equation for v_{t2} , the constant *terminal velocity* of the ball's descent for drag D_2 ; and then calculate the value of v_{t2} in mph. Use the average weight of baseballs, $mg = 5\frac{1}{8}$ ounces, with $g = 32.17$ ft/sec². Note: 60 mph = 88 ft/sec, 1 foot = 12 inches, and 1 lb = 16 ounces. (*Partial answer:* $v_{t2} = -74.91$ mph. It might seem counterintuitive that the terminal velocity of a stitched baseball is -95 mph, a much greater speed than that of an otherwise equivalent smooth ball; see Adair, 1994, pages 5-12.⁹)

⁸ In Appendix B, Section B-2, this ODE is derived by an alternative method using energy and power.

⁹ Literature references such as this are described in detail in the References section following Chapter 17.

(e) Let's attempt to establish some sort of "equivalent" linear mathematical model relative to the nonlinear model of part (d). The only comparable results that we have determined for this purpose are the equations for terminal velocity. Therefore, calculate an "equivalent" linear viscous damping constant c by equating $v_{t1} = v_{t2}$. Suppose that $v_0 = 110$ mph, the average speed at which a baseball rebounds from a bat on the ball's way to a 400-foot major league home run. Calculate the total ascent time t_{z1} (in seconds) and the peak altitude $y(t_{z1}) \equiv y_{\max_1}$ (in feet), quantities that are defined in parts (b) and (c). It happens that both nonlinear ODEs of part (d) can be solved in terms of standard mathematical functions.¹⁰ In particular, solution of the nonlinear ODE for ascent leads to the equation for total ascent time, $t_{z2} = [(-v_{t2})/g]\tan^{-1}[v_0/(-v_{t2})]$, and the equation for peak altitude, $y(t_{z2}) \equiv y_{\max_2} = (v_{t2}^2/g)\ln\sqrt{1+(v_0/v_{t2})^2}$. Calculate t_{z2} and y_{\max_2} , and compare them, respectively, with t_{z1} and y_{\max_1} ; note, however, that we cannot infer from this limited comparison the general quality of the "equivalent" linear model relative to the nonlinear model. (*Partial answers:* $c = 2.955 \times 10^{-3}$ lb-sec/ft; $y_{\max_1} = 210.7$ ft; $t_{z2} = 3.299$ sec)

1.8 The ODE solution procedure illustrated in Section 1-5 for a 1st order ODE can be used to solve any LTI ODE or system of LTI ODEs. Consider, for example, the 2nd order ODE (1-17) for a mass-damper-spring system, $m\ddot{x} + c\dot{x} + kx = f_x(t)$. The physical parameters m , c , and k are known constants.

(a) Seek a homogeneous solution in the form $x_h(t) = C e^{\lambda t}$ as follows. First, show that the characteristic equation is a quadratic polynomial in the unknown λ . Next, solve the polynomial equation and show in detail that there are two characteristic values (roots),

$$\lambda_{1,2} = -\frac{c}{2m} \pm \sqrt{\left(\frac{c}{2m}\right)^2 - \frac{k}{m}}$$
. Assume that $\left(\frac{c}{2m}\right)^2 > \frac{k}{m}$. Therefore, the general homogeneous solution must have the form $x_h(t) = C_1 e^{\lambda_1 t} + C_2 e^{\lambda_2 t}$, with two initially unknown constants.

(b) Suppose that the excitation force has the sinusoidal form $f_x(t) = F \sin \omega t$, in which force amplitude F and circular frequency ω (in radians/second) are considered to be known. Seek a particular solution by using the method of undetermined coefficients. First, express the solution as $x_p(t) = P_1 \sin \omega t + P_2 \cos \omega t$. Now, substitute this $x_p(t)$ into the non-homogeneous ODE to find algebraic equations for P_1 and P_2 in terms of the constants that m , c , k , F , and ω . (*Partial answer:* $P_2 = \frac{-c\omega}{(k-m\omega^2)^2 + (c\omega)^2} F$)

¹⁰ For examples of these solutions, see: an ascent solution in Greenwood, 1965, Problem 3-4 on pages 128 and 503; and a descent solution in Sommerfeld, 1964, pages 21-22.

- (c) Express the complete solution as $x(t) = x_h(t) + x_p(t)$. Suppose that the mass m is initially at rest with ICs: initial position $x(0) = 0$ and initial velocity $\dot{x}(0) = 0$. Use these ICs to write two linear equations with unknowns C_1 and C_2 . Solve for C_1 and C_2 ; show that they can be written as $C_1 = \frac{P_2\lambda_2 - P_1\omega}{\lambda_1 - \lambda_2}$ and $C_2 = \frac{P_1\omega - P_2\lambda_1}{\lambda_1 - \lambda_2}$.

Note that a reasonably efficient algebraic equation for the final result $x(t)$ is derived by defining constants C_1 and C_2 in terms of the previously defined λ_i and P_i , rather than writing them in terms of all the basic parameters, m , c , k , F , and ω .

1.9 Solve Problem 1.8 in MATLAB. Begin with the following MATLAB commands:

```
>> syms x t m c k F w
>> x=dsolve('D2x+c/m*Dx+k/m*x=F/m*sin(w*t)', 'x(0)=0', 'Dx(0)=0')
```

The MATLAB response will probably be an equation for $x(t)$ of truly breathtaking length. You can try simplification operations such as `x=simple(x)` and `pretty(x)` and the `subexpr` command, but they will not necessarily lead to a more useful equation for $x(t)$. At some point, you might decide that, rather than continuing to flail away at the symbolic software, your time is used more efficiently if you just solve by hand and define intermediate symbols in terms of the basic parameters, as is done in Problem 1.8.

1.10 This problem relates to the details of the mass-spring-system ODE solution presented in Section 1-10.

- (a) Substitute the assumed particular solution Eq. (1-23) into non-homogeneous ODE (1-22), then carry out the process in all algebraic detail to verify Eqs. (1-24) for P_1 and P_2 .
- (b) Substitute ICs (1-19), $\dot{x}(0) = 0$ and $x(0) = 0$ into complete solution Eq. (1-25), then carry out the process in all algebraic detail to verify Eqs. (1-26) for C_1 and C_2 .

1.11 Consider a mass-spring system with an “exponential step” forcing function, as described by the 2nd order LTI ODE $m\ddot{x} + kx = f_x(t) = F(1 - e^{-t/t_c})$, in which position $x(t)$ is the dependent variable, and the known constant parameters are mass m , spring stiffness constant k , force amplitude F , and *time constant* t_c . The time constant is the time required for the “exponential unit-step” function, $1 - e^{-t/t_c}$, to rise from 0 at $t = 0$ to the value $1 - e^{-1} = 0.6321$, on its way to the asymptotic value 1 as $t \rightarrow \infty$.

- (a) Use the method of undetermined coefficients to derive an algebraic equation (in terms of the given constants) for the particular solution $x_p(t)$ of this ODE and forcing function.

- (b) Let the ICs for this $m\text{-}k$ system be $\dot{x}(0) = 0$ and $x(0) = 0$. Use the result of part (a) and whatever else is required to derive in all detail the following complete algebraic solution for $x(t)$, $t \geq 0$, in which $\omega_n = \sqrt{k/m}$:

$$x(t) = \frac{F}{k} \left\{ 1 - \frac{1}{1 + (1/\omega_n t_c)^2} \left[e^{-t/t_c} + (1/\omega_n t_c) \sin \omega_n t + (1/\omega_n t_c)^2 \cos \omega_n t \right] \right\}$$

- 1.11 (c)** Consider the specific numerical case of mass $m = 8.03$ kg, spring stiffness constant $k = 317$ N/m, and force amplitude $F = 4.50$ N. Calculate the circular natural frequency ω_n and the cyclic natural frequency f_n . Let excitation time constant $t_c = 1/\omega_n$, a much shorter interval than the $m\text{-}k$ system's natural period $T_n = 2\pi/\omega_n$. Compose and run a MATLAB program that does the following: calculate the actual dynamic response $x(t)$ and the pseudo-static response $f_x(t)/k$ over the time interval $0 \leq t \leq 2.5$ sec; plot both $x(t)$ and $f_x(t)/k$ on the same graph in units of either centimeters or millimeters. Explain in a sentence or two what feature of your plot of $x(t)$ demonstrates and conforms with your calculation of f_n .

- 1.12** Consider a mass-spring system with a sinusoidal forcing function, as described by the 2nd order LTI ODE $m\ddot{x} + kx = f_x(t) = F \sin \omega t$, in which position $x(t)$ is the dependent variable, and the known constant parameters are mass m , spring stiffness constant k , force amplitude F , and excitation frequency ω .

- (a) Use the method of undetermined coefficients to derive an algebraic equation (in terms of the given constants) for the particular solution $x_p(t)$ of this ODE and forcing function, a solution that is valid provided $\omega^2 \neq k/m$.

- (b) Let the ICs for this $m\text{-}k$ system be $\dot{x}(0) = 0$ and $x(0) = 0$. Use the result of part (a) and whatever else is required to derive in all detail the following complete algebraic solution for $x(t)$, $t \geq 0$, in which $\omega_n = \sqrt{k/m}$:

$$x(t) = \frac{F}{k} \frac{1}{1 - (\omega/\omega_n)^2} [\sin \omega t - (\omega/\omega_n) \sin \omega_n t], \text{ valid for } \omega \neq \omega_n$$

- (c) Consider the specific numerical case of mass $m = 0.230$ lb-sec²/inch (which weighs about 88.8 lb), spring stiffness constant $k = 227$ lb/inch, and force amplitude $F = 45.0$ lb. Calculate the circular natural frequency ω_n and the cyclic natural frequency f_n . For excitation frequency $\omega = 1.2\omega_n$, compose and run a MATLAB program that does the following: calculate the actual dynamic response $x(t)$ and the pseudo-static response $f_x(t)/k$ over the time interval $0 \leq t \leq 2$ sec; plot both $x(t)$ and $f_x(t)/k$ on the same graph. Your $x(t)$ plot should exhibit the phenomenon of *beating*, which is analyzed more completely in Section 10-6.

(d) The $x(t)$ equation derived in part (b) is not valid if excitation frequency ω equals natural frequency ω_n , but note that in this case the $x(t)$ equation has the indeterminate form 0/0, so that we can apply l'Hospital's rule (which is described in any calculus textbook) to find the limit-case response solution. Define $\beta = \omega/\omega_n$, so that $\omega t = \beta\omega_n t$. Now, hold ω_n constant and take the limit as $\beta \rightarrow 1$ of the $x(t)$ equation in order to determine the correct response $x(t)$ equation for the case $\omega = \omega_n$.

Chapter 2 Complex numbers and arithmetic; Laplace transforms; partial-fraction expansion

© 2016 by William L. Hallauer, Jr.

2-1 Review of complex numbers and arithmetic

We will find many uses in system dynamics for analysis with complex numbers and variables. It is instructive first to imagine how complex numbers might have been developed historically. It seems likely that they appeared first in solutions for roots of polynomial equations. To see how, let's examine the 2nd degree polynomial, the standard quadratic equation, and its solutions. The quadratic equation is

$$az^2 + bz + c = 0 \quad (2-1)$$

where z is the unknown and a , b , and c are known constants. The standard solution for roots z is

$$z = -\frac{b}{2a} \pm \frac{1}{2a} \sqrt{b^2 - 4ac} \quad (2-2)$$

Provided that $b^2 - 4ac \geq 0$, solution (2-2) can be calculated easily. But suppose the constants have values such that $b^2 - 4ac < 0$, so that Eq. (2-2) indicates the square root of a negative number. That must have seemed strange to early mathematicians. Nevertheless, (2-2) is the correct solution regardless of the sign of $b^2 - 4ac$, which you can verify simply by substituting (2-2) back into (2-1). So it was necessary to recognize the existence of the square root of a negative number and to invent notation and terminology for describing such a number.

For $b^2 - 4ac < 0$, we can write

$$\sqrt{b^2 - 4ac} = \sqrt{(-1)(4ac - b^2)} = \sqrt{-1} \times \sqrt{4ac - b^2} \equiv j\sqrt{4ac - b^2}$$

in which we define the *unit imaginary number* as $j \equiv \sqrt{-1}$. Perhaps early mathematicians used the adjective “imaginary” because such a number seemed unreal to them. With this definition, we can write (2-2) in the form

$$z = -\frac{b}{2a} \pm j \frac{1}{2a} \sqrt{4ac - b^2}$$

This is called a *complex number*, which is the sum of a normal, or *real* number and an imaginary number (j times a real number being a general imaginary number).

If x and y are reals, then any complex number can be written in the *rectangular* form:

$$z = x + j y, \text{ with real part } x \equiv \text{Re}(z), \text{ and imaginary part } y \equiv \text{Im}(z) \quad (2-3)$$

This form is called “rectangular” because it expresses the complex number in terms of its rectangular, or Cartesian components, x and y . Equation (2-3) is similar mathematically to a two-dimensional vector \mathbf{v} expressed in terms of Cartesian components and unit vectors $\mathbf{1}_x$ and $\mathbf{1}_y$: $\mathbf{v} = v_x \mathbf{1}_x + v_y \mathbf{1}_y$. Therefore, we can represent a complex number $z = x + j y$ graphically in the Cartesian form similar to that used for two-dimensional vectors, as shown in Fig. 2-1.

From Fig. 2-1, we can infer another useful way to represent a complex number. By defining the *magnitude* (*length, absolute value, modulus*) of z as the positive number

$$r = \sqrt{x^2 + y^2} \quad (2-4)$$

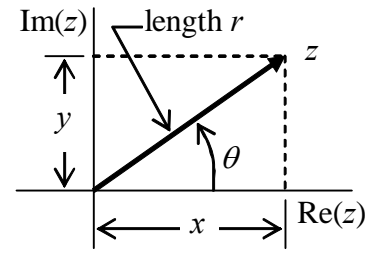


Figure 2-1

we can write

$$z = x + j y = r \left(\frac{x}{r} + j \frac{y}{r} \right) = r (\cos \theta + j \sin \theta) \quad (2-5)$$

In Eq. (2-5), we employ the standard trigonometric functions of angle θ originating on the positive real axis and defined positive in the counterclockwise (CCW) sense, Fig. 2-1. Angle θ is often called the *argument* of z . The general definition is

$$\theta = \tan^{-1} \left(\frac{y}{x} \right) \quad (2-6)$$

It is necessary to recognize Eq. (2-6) as the *four-quadrant inverse tangent* (or *arctangent*). For example, if y is positive and x is negative, then (2-6) should give angle θ in the second quadrant, $90^\circ < \theta < 180^\circ$; or, if both y and x are negative, then (2-6) should give angle θ in the 3rd quadrant, $-180^\circ < \theta < -90^\circ$ (which also can be written as $180^\circ < \theta < 270^\circ$). Unfortunately, the \tan^{-1} or *arctan* function on hand calculators does not calculate the four-quadrant inverse tangent, but only considers the sign of the quotient y/x , and produces a θ value in the 1st or 4th quadrants, $-90^\circ < \theta < +90^\circ$. So, if you are evaluating (2-6) on your hand calculator, you need to account for the signs of both y and x , and you need to modify appropriately the answer given by your calculator. If you are evaluating (2-6) in MATLAB, then you should use MATLAB’s four-quadrant inverse tangent function, `atan2(y,x)`.

Chapter 2 Complex numbers and arithmetic; Laplace transforms; partial-fraction expansion

Equation (2-5) is just an intermediate result. To achieve the desired final form, we rewrite (2-5) using the well-known Taylor power series expansions for sine, cosine and exponential functions:

$$\begin{aligned} z &= r(\cos \theta + j \sin \theta) = r \left[\left(1 - \frac{\theta^2}{2!} + \frac{\theta^4}{4!} - \dots \right) + j \left(\theta - \frac{\theta^3}{3!} + \frac{\theta^5}{5!} - \dots \right) \right] \\ z &= r(\cos \theta + j \sin \theta) = r \left(1 + (j\theta) + \frac{(j\theta)^2}{2!} + \frac{(j\theta)^3}{3!} + \frac{(j\theta)^4}{4!} + \frac{(j\theta)^5}{5!} + \dots \right) \equiv r e^{j\theta} \\ z &= r e^{j\theta} \end{aligned} \quad (2-7)$$

The important result

$$\cos \theta + j \sin \theta = e^{j\theta} \quad (2-8)$$

is known as *Euler's equation* (after Leonhard Euler, 1707-1783, Swiss mathematician and physicist). See homework Problem 2.1 for other equations closely related to Eq. (2-8).

A complex number in the form $z = r e^{j\theta}$ is called the *polar* form because it employs polar coordinates r and θ . We can visualize the complex exponential term $e^{j\theta}$ itself as a clock hand in the complex plane, Fig. 2-1; the clock hand has unit length, and it is rotated CCW by angle θ from the 3 o'clock position. Similarly, the full complex number $z = r e^{j\theta}$ represents a clock hand of length r that is rotated CCW by angle θ from the 3 o'clock position, so the notation $z = r\angle\theta$ is often used, where the symbol \angle stands for “angle.”

We will occasionally need to convert a complex number from rectangular form into polar form using Eqs. (2-4) and (2-6). The MATLAB functions `abs` and `angle` are especially useful for this task, as is illustrated in Complex-arithmetic Example 2 below.

We also will need to use complex arithmetic, so let's review (from your mathematics courses) some of the basics, supposing that we have two complex numbers z and w expressed in both rectangular and polar forms:

$$z = x + jy = r e^{j\theta} \quad \text{and} \quad w = u + jv = q e^{j\phi}, \quad \text{where } x, y, r, \theta, u, v, q, \text{ and } \phi \text{ all are real.}$$

Addition or subtraction, rectangular: $z \pm w = (x \pm u) + j(y \pm v)$.

Addition or subtraction, polar: $r e^{j\theta} \pm q e^{j\phi} \equiv Z \equiv R e^{j\Theta}$.

$$Z = r \cos \theta + q \cos \phi \pm j(r \sin \theta + q \sin \phi)$$

$$R = \sqrt{[\operatorname{Re}(Z)]^2 + [\operatorname{Im}(Z)]^2} = \sqrt{r^2 + q^2 + 2rq \cos(\theta - \phi)}$$

$$\Theta = \tan^{-1} [\operatorname{Im}(Z)/\operatorname{Re}(Z)] = \tan^{-1} [\pm(r \sin \theta + q \sin \phi)/(r \cos \theta + q \cos \phi)]$$

Multiplication, rectangular: $z \times w = xu + j(xv + yu) + j^2(yv) = (xu - yv) + j(xv + yu)$.

Multiplication, polar: $z \times w = rq e^{j(\theta+\phi)}$.

The *complex conjugate* of $z = x + jy = r e^{j\theta}$ is defined as $\bar{z} = x - jy = r e^{-j\theta}$, so that the product of a complex number and its conjugate is real, and equal to the square of the magnitude: $z \bar{z} = x^2 + j(-xy + yx) - j^2 y^2 = x^2 + y^2 = r^2$, or more easily in polar form, $z \bar{z} = r e^{j\theta} \times r e^{-j\theta} = r^2 e^{j(\theta-\theta)} = r^2$. Suppose that we have the quotient of two complex numbers z by w , both in rectangular form, and we wish to cast the result into standard rectangular form; it is common practice first to multiply both denominator and numerator by the conjugate of the denominator, thus forming a real denominator:

$$\text{Division, rectangular: } \frac{z}{w} = \frac{x + jy}{u + jv} = \frac{(x + jy)(u - jv)}{(u + jv)(u - jv)} = \frac{xu + yv}{u^2 + v^2} + j \frac{-xv + yu}{u^2 + v^2}$$

$$\text{Division, polar, } \frac{z}{w} = \frac{r}{q} e^{j(\theta-\phi)}$$

Complex-arithmetic Example 1 Cast the following complex fraction into standard rectangular form, then convert it into polar form:

$$z = \frac{3 - j4}{1 + j2} = \frac{(3 - j4)(1 - j2)}{(1 + j2)(1 - j2)} = \frac{3 - 8 + j(-6 - 4)}{5} = -1 - j2$$

$$r = \sqrt{(-1)^2 + (-2)^2} = 2.236, \quad \theta = \tan^{-1} \left(\frac{-2}{-1} \right) = -116.6^\circ \times \frac{\pi \text{ rad}}{180^\circ} = -2.034 \text{ rad}$$

$$\Rightarrow z = \frac{3 - j4}{1 + j2} = -1 - j2 = 2.236 e^{j(-116.6^\circ)} \equiv 2.236 \angle (-2.034 \text{ rad})$$

Note that when you take $\tan^{-1}(2)$ on your hand calculator, it gives 63.43° . Because you are really trying to find $\tan^{-1}(-2/-1)$, you must recognize that the correct angle is in the 3rd quadrant and, therefore, add $+180^\circ$ or -180° to the calculator's solution in order to obtain the correct result, $+243.4^\circ$ or -116.6° .

Complex-arithmetic Example 2 Cast the following complex fraction into standard rectangular form, then convert it into polar form:

$$z = \frac{(3-j2)(4+j)}{2-j3} - 7+j4 = \frac{(14-j5)(2+j3)}{(2-j3)(2+j3)} - 7+j4 = \frac{43+j32}{13} - 7+j4$$

$$z = \left(\frac{43}{13} - 7 \right) + j \left(\frac{32}{13} + 4 \right) = -3.692 + j 6.462$$

$$r = \sqrt{(-3.692)^2 + (6.462)^2} = 7.442, \quad \theta = \tan^{-1} \left(\frac{6.462}{-3.692} \right) = -60.255^\circ + 180^\circ = 119.7^\circ$$

$$\Rightarrow z = \frac{(3-j2)(4+j)}{2-j3} - 7+j4 = -3.692 + j 6.462 = 7.442 e^{j119.7^\circ}$$

A solution of Complex-arithmetic Example 2 in terms of MATLAB operations follows:

```
>> z=(3-2j)*(4+j)/(2-3j)-7+4j
z =
-3.6923 + 6.4615i
>> r=abs(z),theta=angle(z)
r =
7.4421
theta =
2.0899
>> thetadeg=theta*pi
thetadeg =
119.7449
```

Note that MATLAB prefers, and gives results in terms of the unit imaginary number denoted as i , but it recognizes our notation of j . Note also that the radian is MATLAB's default unit for angles: if you want a MATLAB angle result in degrees, you must convert from radians; also, if you wish to calculate a trigonometric function of an angle, you must express that angle in radians.

2-2 Introduction to application of Laplace transforms

The *Laplace transform* (after French mathematician and celestial mechanician Pierre Simon Laplace, 1749-1827) is a mathematical tool primarily for solving ODEs, but with other important applications in system dynamics that we will study later. In Laplace

transformation, we deal with a *complex variable* denoted as s , which is usually expressed in terms of its real and imaginary parts as

$$s = \sigma + j\omega \quad (2-9)$$

in which σ and ω both are real. We define a complex function of s , $F(s)$. The type of function that we will encounter often takes the form of a ratio of two polynomials:

$$F(s) \equiv \frac{Num(s)}{Den(s)} = \frac{b_1 s^m + b_2 s^{m-1} + \dots + b_{m+1}}{a_1 s^n + a_2 s^{n-1} + \dots + a_{n+1}} = \frac{b_1(s - z_1)(s - z_2) \cdots (s - z_m)}{a_1(s - p_1)(s - p_2) \cdots (s - p_n)} \quad (2-10)$$

In the first polynomial form of Eq. (2-10), a_1, \dots, a_{n+1} and b_1, \dots, b_{m+1} are real constants (with the symbols and numbering system keyed to MATLAB notation); numerator $Num(s)$ is an m^{th} degree polynomial in s , and denominator $Den(s)$ is an n^{th} degree polynomial in s , with $m \leq n$ in general. In the second polynomial form, with factored $Num(s)$ and $Den(s)$, complex constants z_1, z_2, \dots, z_m are called *zeros* of $F(s)$ because $F(s)$ is zero if s equals any one of them, and complex constants p_1, p_2, \dots, p_n are called *poles* of $F(s)$ because $F(s)$ is infinite if s equals any one of them. If $m < n$, $F(s)$ in Eq. (2-10) also goes to zero as $s \rightarrow \infty$.

Solving a simple ODE problem with Laplace transforms is a gentle introduction to the subject. Consider the 1st order LTI ODE written in standard form: $\dot{x} - ax = bu(t)$, Eq. (1-1). Let's solve this ODE with a known IC, $x(0) = x_0$, and with a specific exponential input function, $u(t) = U e^{-wt}$, U being a dimensional magnitude; in any physically realistic problem, constant w would be a real number, but for generality here we allow it to be a complex number. So the complete problem statement is:

$$\dot{x} - ax = bU e^{-wt}, x(0) = x_0, \text{ solve for } x(t), t > 0 \quad (2-11)$$

To begin the solution, we multiply the ODE by a complex exponential, e^{-st} , then take the definite integral over time from $t = 0$ to $t = \infty$ of the entire multiplied ODE:

$$\int_{t=0}^{t=\infty} e^{-st} (\dot{x} - ax = bU e^{-wt}) dt \Rightarrow \int_{t=0}^{t=\infty} e^{-st} \dot{x} dt - a \int_{t=0}^{t=\infty} e^{-st} x dt = bU \int_{t=0}^{t=\infty} e^{-st} e^{-wt} dt \quad (2-12)$$

In (2-12), s is a complex variable that must have values for which the integrals exist. Based upon (2-12), we define the *forward Laplace transform* of dependent variable $x(t)$ ¹:

¹ In Section 8-4 we develop a more general definition, Eq. (8-12), in order to accommodate the ideal unit-impulse function, which is important in linear-system theory and applications.

$$L[x(t)] \equiv X(s) \equiv \int_{t=0}^{t=\infty} e^{-st} x(t) dt \quad (2-13)$$

In (2-13), the function x of time t is *transformed* by the definite integration into a function X of Laplace variable s . Also, the ODE of (2-11) is transformed into (2-12), which, as we will find, becomes an easily solvable algebraic equation in the unknown $X(s)$. After we solve that algebraic equation for $X(s)$, then we will reverse the process to find the original unknown $x(t)$ by applying the *inverse Laplace transform*, denoted as $L^{-1}[X(s)] \equiv x(t)$. For any Laplace-transformable function $f(t)$, and its transform $F(s)$, the companion equations $L[f(t)] = F(s)$ and $L^{-1}[F(s)] = f(t)$ are called a *Laplace transform pair*.

In order to transform Eq. (2-12) into an algebraic equation, let's carefully consider each integration in (2-12), beginning with that on the right-hand side:

$$\begin{aligned} \int_{t=0}^{t=\infty} e^{-st} e^{-wt} dt &= \int_{t=0}^{t=\infty} e^{-(s+w)t} dt = \frac{1}{-(s+w)} \int_{t=0}^{t=\infty} dt [e^{-(s+w)t}] = \frac{1}{-(s+w)} [e^{-(s+w)t}]_{t=0}^{t=\infty} \\ &= \frac{1}{-(s+w)} [e^{-(s+w)\infty} - 1] = \frac{1}{s+w} \end{aligned}$$

An important step in this derivation involves the complex exponential, with use of Eqs. (2-3) and (2-8): $e^z = e^{(x+jy)} = e^x(\cos y + j \sin y)$. Since $\sin y$ and $\cos y$ vary periodically as y varies, the only way for e^z to $\rightarrow 0 + j0$ for all values of y is for $x \rightarrow -\infty$. Thus, in the last step of the integration, we assume that $\operatorname{Re}(s+w) > 0$, or $\operatorname{Re}(s) > -\operatorname{Re}(w)$, so that $e^{-(s+w)\infty} = 0 + j0$. The integration above establishes the following Laplace transform pair, which is one of the most important of all pairs for applications:

$$L[e^{-wt}] = \frac{1}{s+w} \quad \text{and} \quad L^{-1}\left[\frac{1}{s+w}\right] = e^{-wt} \quad (2-14)$$

For your convenience, transform pair (2-14) and all other fundamental Laplace transform pairs used in this book are tabulated in Appendix A at the end of the book. Appendix A also includes some of the longer but less instructive transform derivations, should you wish to study them.

Next, let's evaluate the first term on the left-hand side of (2-12) by the standard method of *integration by parts* in the form $\int_{t=0}^{t=\infty} u dv = [uv]_{t=0}^{t=\infty} - \int_{t=0}^{t=\infty} v du$:

Chapter 2 Complex numbers and arithmetic; Laplace transforms; partial-fraction expansion

$$\int_{t=0}^{t=\infty} e^{-st} \overset{u}{\overbrace{\dot{x}}} dt = \left[e^{-st} x(t) \right]_{t=0}^{t=\infty} - \int_{t=0}^{t=\infty} x(t) \times (-s) e^{-st} dt = \left[e^{-s \times \infty} x(\infty) - e^{-0} x(0) \right] + s X(s)$$

$$= -x(0) + s X(s) \quad (2-15a)$$

To obtain this result, we assume that $e^{-(s \times \infty)} x(\infty) = 0$, which generally means $\text{Re}(s) > 0$. This result is the important general Laplace transform of the first derivative of any transformable function $f(t)$:

$$L[\dot{f}(t)] = s F(s) - f(0) \quad (2-15b)$$

Equation (2-15b) is the basis for derivation of the Laplace transform of a derivative of any order n , which we will use later (Ogata², 1998, pp. 25-26):

$$L\left[\frac{d^n}{dt^n} f(t)\right] = s^n F(s) - s^{n-1} f(0) - s^{n-2} \dot{f}(0) - \cdots - {}^{(n-1)} \ddot{f}(0) \quad (2-16)$$

For example, the Laplace transform of the 2nd derivative is (homework Problem 2.7):

$$L[\ddot{f}(t)] = s^2 F(s) - s f(0) - \dot{f}(0) \quad (2-17)$$

Proceeding with the solution of ODE + IC (2-11), we now substitute Eqs. (2-13), (2-14), and (2-15a) back into (2-12) to obtain an algebraic equation for transform $X(s)$, which is easily solved:

$$s X(s) - x(0) - a X(s) = \frac{bU}{s+w} \Rightarrow (s-a) X(s) = x_0 + \frac{bU}{s+w}$$

$$\Rightarrow X(s) = \frac{1}{(s-a)} x_0 + \frac{bU}{(s-a)(s+w)} \quad (2-18)$$

To solve for the ultimate unknown $x(t)$, we now need to find the inverse transform of $X(s)$ in (2-18). Using (2-14) easily gives us the inverse of the first term on the right-hand side:

$$L^{-1}\left[\left(\frac{1}{s-a}\right)x_0\right] = x_0 L^{-1}\left[\frac{1}{s-a}\right] = x_0 e^{at} \quad (2-19)$$

² Literature sources such as this are described in detail in the References section following Chapter 17.

Inverting the second term on the right-hand side of (2-18) is a greater challenge, which requires us to use *partial-fraction expansion* in order to expand that term into two simpler terms, each of which has the easily invertible form of a constant divided by a single factor of the form $(s - p)$. We first write the troublesome term as two simpler fractions with unknown constant numerators, C_1 and C_2 , which are called *residues* of the partial-fraction expansion. (A more detailed justification for this form is derived in the next section.):

$$\frac{1}{(s-a)(s+w)} = \frac{C_1}{s-a} + \frac{C_2}{s+w} \Rightarrow \frac{C_1}{s-a} + \frac{C_2}{s+w} = \frac{1}{(s-a)(s+w)} \quad (2-20)$$

There are two common methods for finding C_1 and C_2 , which we shall call the “labor-saving” method and the “brute-force” method.

Consider first the labor-saving method. Let’s go in great detail through the steps required to find C_1 , for example. First, multiply both sides of Eq. (2-20) by $s - a$, the denominator of the C_1 term:

$$(s-a)\left(\frac{C_1}{s-a} + \frac{C_2}{s+w}\right) = C_1 + (s-a)\left(\frac{C_2}{s+w}\right) = (s-a)\left(\frac{1}{(s-a)(s+w)}\right)$$

Isolate C_1 on the left-hand side:

$$C_1 = -(s-a)\left(\frac{C_2}{s+w}\right) + (s-a)\left(\frac{1}{(s-a)(s+w)}\right)$$

Now, in order to eliminate the C_2 term on the right-hand side, set $s = a$. Note that this does not eliminate the second right-hand-side term because $(s-a)$ is in both the denominator and the numerator.

$$C_1 = \left[-(s-a)\left(\frac{C_2}{s+w}\right) + (s-a)\left(\frac{1}{(s-a)(s+w)}\right) \right]_{s=a} = \left[(s-a)\left(\frac{1}{(s-a)(s+w)}\right) \right]_{s=a}$$

Thus, we obtain the required equation for C_1 :

$$C_1 = \left[(s-a)\left(\frac{1}{(s-a)(s+w)}\right) \right]_{s=a} = \frac{1}{a+w}$$

Now that we see the logic of the labor-saving method, we can dispense with most of the intermediate steps and quickly write the corresponding equation for C_2 directly from Eq. (2-20):

$$C_2 = \left[(s+w) \left(\frac{1}{(s-a)(s+w)} \right) \right]_{s=-w} = \frac{1}{-w-a} = -\frac{1}{a+w}$$

Next, the brute-force method begins with use of the traditional algebraic method for combining the two fractions of Eq. (2-20) into a single fraction:

$$\frac{1}{(s-a)(s+w)} = \frac{C_1}{s-a} + \frac{C_2}{s+w} = \frac{C_1(s+w) + C_2(s-a)}{(s-a)(s+w)} = \frac{s(C_1 + C_2) + (C_1w - C_2a)}{(s-a)(s+w)}$$

Equate coefficients of like powers of s in the numerators:

$$\begin{aligned} s^1: 0 &= C_1 + C_2 \Rightarrow C_2 = -C_1 \\ s^0: 1 &= C_1w - C_2a = C_1(w+a) \Rightarrow C_1 = \frac{1}{a+w} = -C_2 \end{aligned}$$

In this simple problem, the brute-force method is not much more demanding algebraically than the labor-saving method. However, for a slightly more complex original fraction, say, one with three denominator polynomial factors instead of just two, the brute-force method can require orders of magnitude more algebra than the labor-saving method. The point of this discussion: exert the mental energy to understand the labor-saving method, and always use it rather than the brute-force method [see homework Problem 2.9(b)].

Using the partial-fraction expansion developed above, we now express the complete second term on the right-hand side of Eq. (2-18) in the easily invertible form

$$F(s) = \frac{bU}{(s-a)(s+w)} = \frac{bU}{a+w} \left(\frac{1}{s-a} - \frac{1}{s+w} \right)$$

Using the fundamental inverse transform from Eq. (2-14) gives

$$f(t) = \frac{bU}{a+w} (e^{at} - e^{-wt}) \quad (2-21)$$

Finally, combining Eqs. (2-19) and (2-21) gives the inverse of (2-18) and the final desired solution of ODE + IC (2-11):

$$x(t) = x_0 e^{at} + \frac{bU}{a+w} (e^{at} - e^{-wt}), \text{ for } t \geq 0 \quad (2-22)$$

The introduction to Laplace transformation in this section is not mathematically rigorous. The focus in introductory system dynamics is more with applying Laplace transforms than with the detailed theory. It is relevant, however, to comment on the existence of Laplace transforms: a transform generally exists (*i.e.*, the defining integral Eq.

(2-13) can be evaluated, in principle) for any function $f(t)$ for which the product $e^{-at}|f(t)| \rightarrow 0$ as $t \rightarrow \infty$, where a is some finite, positive, real constant (Hildebrand, 1962, Section 2.2). Practically speaking, this means that any physically realizable function, the type of function that we encounter in engineering, has a Laplace transform.

2-3 More about partial-fraction expansion

Let's examine in more detail the justification for the form of the partial-fraction expansion presented in Eq. (2-20). As an example, consider the following sum of three fractional terms:

$$\begin{aligned} F_3(s) &= \sum_{k=1}^3 \frac{C_k}{s - p_k} = \frac{C_1}{s - p_1} + \frac{C_2}{s - p_2} + \frac{C_3}{s - p_3} \\ &= \frac{C_1(s - p_2)(s - p_3) + C_2(s - p_1)(s - p_3) + C_3(s - p_1)(s - p_2)}{(s - p_1)(s - p_2)(s - p_3)} \end{aligned} \quad (2-23)$$

In the combination of the three fractional terms into a single fraction, the denominator is a cubic polynomial ($n = 3$), and the degree of the numerator polynomial is, at most, $m = 2$. Depending upon the values of constants C_k , the degree of the numerator polynomial can be from 0 to 2, so that $0 \leq m < n$.

Next, let's generalize the observation of the previous paragraph by considering a general sum of fractional terms in the form

$$F_n(s) = \sum_{k=1}^n \frac{C_k}{s - p_k} \quad (2-24)$$

If we combine all n of these terms into a single ratio using the traditional algebraic method illustrated in Eq. (2-23), then the result will have the following general form:

$$F_n(s) = \frac{c_1 s^m + c_2 s^{m-1} + \dots + c_{m+1}}{(s - p_1)(s - p_2) \cdots (s - p_n)}$$

The denominator is a polynomial of degree n , and the numerator is a polynomial of, at most, degree $m = (n - 1)$. We therefore can conclude the following: a ratio of polynomials, in which the numerator has a lower degree than that of the denominator, can usually be expanded into the simple partial-fraction form (2-24). In other words, provided that $0 \leq m < n$, we can usually find finite residues C_k in the partial-fraction expansion:

$$F_n(s) = \frac{b_1 s^m + b_2 s^{m-1} + \dots + b_{m+1}}{a_1 s^n + a_2 s^{n-1} + \dots + a_{n+1}} = \frac{b_1 (s - z_1)(s - z_2) \cdots (s - z_m)}{a_1 (s - p_1)(s - p_2) \cdots (s - p_n)} = \sum_{k=1}^n \frac{C_k}{s - p_k} \quad (2-25a)$$

with the residues given by the labor-saving method as³

$$C_k = [(s - p_k) F_n(s)]_{s=p_k}, k = 1, 2, \dots, n \quad (2-25b)$$

Consider, for example, part of the partial-fraction expansion of a quadratic divided by a cubic:

$$F_3(s) = \frac{b_1 s^2 + b_2 s + b_3}{(s - p_1)(s - p_2)(s - p_3)} = \frac{C_1}{s - p_1} + \frac{C_2}{s - p_2} + \frac{C_3}{s - p_3}$$

Using Eq. (2-25b), to determine, for example, residue C_1 gives:

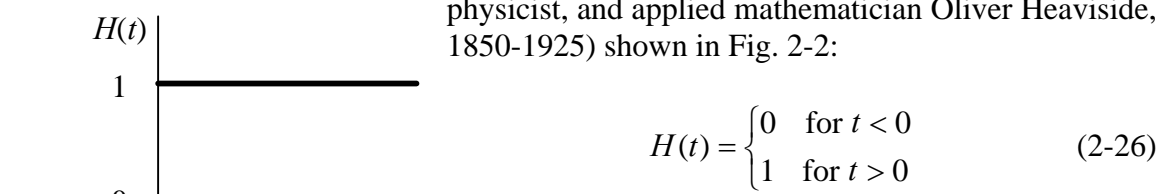
$$C_1 = [(s - p_1) F_3(s)]_{s=p_1} = \frac{b_1 p_1^2 + b_2 p_1 + b_3}{(p_1 - p_2)(p_1 - p_3)}$$

This equation for C_1 reveals an exception to the rule: this equation clearly would not be valid if the denominator polynomial were to have repeated roots, $p_1 = p_2$ or $p_1 = p_3$; in that case, a form different than Eqs. (2-25) would be appropriate (Ogata, 1998, pp. 33-34). That is a special case which we shall address in this book only as the need arises.

Finally, observe that it is easy to check the validity/correctness of a partial-fraction expansion after we have solved for residues C_k . Simply combine the individual fractions into a single ratio, as is illustrated in Eq. (2-23); the resulting ratio should equal the original ratio of polynomials that we expanded into partial fractions.

2-4 Additional useful functions and Laplace transforms: step, sine, cosine, definite integral

We shall describe and transform several different useful mathematical functions. A common feature of most of these functions is that they are defined to have non-zero values only for positive time, *i.e.*, they are zero before $t = 0$. The fundamental function of this type is the basic *Heaviside unit-step function* (after English electrical engineer,



$$H(t) = \begin{cases} 0 & \text{for } t < 0 \\ 1 & \text{for } t > 0 \end{cases} \quad (2-26)$$

Figure 2-2

$H(t)$ is dimensionless, and it is undefined mathematically at the discontinuity at $t = 0$. If we wish to write

³ An interesting alternative form of Eq. (2-25b) is developed in Appendix A, Section A-2.

an equation for a physical input quantity that is applied quickly and remains constant thereafter, we can use $H(t)$ to represent it approximately; for example, a “step” force $f_x(t)$ can be described with the equation $f_x(t) = F \times H(t) \equiv F H(t)$, where F is the dimensional force magnitude. For many physical input quantities, a step function is an idealized approximation; such a quantity increases quickly but continuously, not as a discontinuous pure step, from zero to a constant value. [The notation $H(t)$ used here for the unit-step function is common but not standard; in fact, there is no standard symbol in engineering literature.]

A more general unit-step function describes a step that occurs at some time t_s different than the instant defined to be $t = 0$. This function (Fig. 2-3) is:

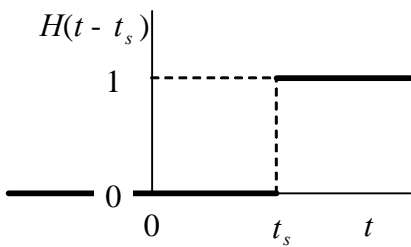


Figure 2-3

If the time of discontinuity is $t_s = 0$, then this more general function becomes the basic function of (2-26).

The Laplace transform of $H(t - t_s)$ is

$$L[H(t - t_s)] = \int_{t=0}^{t=\infty} e^{-st} H(t - t_s) dt = \int_{t=t_s}^{t=\infty} e^{-st} dt = \frac{1}{-s} \int_{t=t_s}^{t=\infty} d(e^{-st}) = -\frac{1}{s} (e^{-s \times \infty} - e^{-st_s})$$

$$L[H(t - t_s)] = \frac{e^{-st_s}}{s} \quad (2-28)$$

Note, in particular, the version of Eq. (2-28) for the basic unit-step function with $t_s = 0$:

$$L[H(t)] = \frac{1}{s} \quad (2-29)$$

We will frequently use sine and cosine functions of time with circular frequency ω , the functions being non-zero only for positive time, $t \geq 0$. Using precise notation, such a sine function, for example, should be denoted $H(t) \times \sin \omega t$; however, with few exceptions, we will consider mostly $t \geq 0$, so we can almost always omit the “ $H(t) \times$ ” part of the equation, with the implicit understanding that the analysis applies only for $t \geq 0$.

Next we derive the Laplace transform of the sine function by expressing the sine in terms of complex exponential functions (homework Problem 2.1) and using the basic forward transform of Eq. (2-14):

Chapter 2 Complex numbers and arithmetic; Laplace transforms; partial-fraction expansion

$$L[\sin \omega t] = L\left[\frac{e^{j\omega t} - e^{-j\omega t}}{2j} \right] = \frac{1}{2j} \left(\frac{1}{s - j\omega} - \frac{1}{s + j\omega} \right) = \frac{1}{2j} \left(\frac{s + j\omega - (s - j\omega)}{(s - j\omega)(s + j\omega)} \right)$$

$$L[\sin \omega t] = \frac{1}{2j} \left(\frac{2j\omega}{s^2 + \omega^2} \right) = \frac{\omega}{s^2 + \omega^2} \quad (2-30)$$

Using a similar process, you can derive (homework Problem 2.10) the following Laplace transform of the cosine function:

$$L[\cos \omega t] = \frac{s}{s^2 + \omega^2} \quad (2-31)$$

Another useful Laplace transform is that of a definite integral. Suppose that a physically realistic function $f(t)$ has Laplace transform $F(s) = L[f(t)]$, and that we need

the transform of the definite integral $\int_{\tau=-\infty}^{\tau=t \geq 0} f(\tau) d\tau$. Note the lower limit of $\tau = -\infty$; we will usually consider $f(t)$ only for $t \geq 0$, but occasionally the integral of $f(t)$ over previous time, $t < 0$, is also needed. The general transform, which is derived in Appendix A, Section A-3, is:

$$L\left[\int_{\tau=-\infty}^{\tau=t \geq 0} f(\tau) d\tau \right] = \frac{1}{s} F(s) + \frac{1}{s} \int_{\tau=-\infty}^{\tau=0} f(\tau) d\tau \quad (2-32)$$

For most applications, we will have $f(t) = 0$ for $t < 0$, for which the simpler transform is:

$$L\left[\int_{\tau=0}^{\tau=t \geq 0} f(\tau) d\tau \right] = \frac{1}{s} F(s) \quad (2-33)$$

If we regard the integral of $f(t)$ as being the first “negative” derivative (antiderivative), then we see that transform (2-32) is logically consistent with transform (2-15b) for a “positive” derivative, with respect to both power of s and the initial value term.

2-5 Homework problems for Chapter 2

2.1 Refer to Euler's equation, Eq. (2-8), which is $e^{j\theta} = \cos\theta + j\sin\theta$. The cosine is an even (symmetric) function, $\cos(-\theta) = \cos\theta$, and the sine is an odd (antisymmetric) function, $\sin(-\theta) = -\sin\theta$, so the conjugate to Euler's equation is

$$e^{-j\theta} = e^{j(-\theta)} = \cos(-\theta) + j\sin(-\theta) = \cos\theta - j\sin\theta$$

(a) Add the conjugate to Euler's equation to prove $\cos\theta = \frac{e^{j\theta} + e^{-j\theta}}{2}$. Subtract the conjugate from Euler's equation to prove $\sin\theta = \frac{e^{j\theta} - e^{-j\theta}}{2j}$.

(b) Use the results of part (a) to prove the trigonometric identities $\cos^2\theta = \frac{1}{2}(1 + \cos 2\theta)$ and $\sin^2\theta = \frac{1}{2}(1 - \cos 2\theta)$. Use these results to prove $\cos^2\theta - \sin^2\theta = \cos 2\theta$.

(c) Use the results of part (a) to prove the identity $\sin\theta \times \cos\theta = \frac{1}{2}\sin 2\theta$.

2.2 Given the following complex numbers:

$$(a) \frac{1}{-0.4 - j0.3} \quad (b) 5j \times (2 - j) \quad (c) \frac{0.7 - j2.4}{0.5 + j1.2} \quad (d) \frac{-10 + j5}{0.6 + j0.8}$$

First, express the complex number in rectangular form, $z = \text{Re}(z) + j \text{Im}(z)$, where $\text{Re}(z)$ and $\text{Im}(z)$ are real numbers. Next, express the complex number in polar form $re^{j\theta}$, that is, calculate by hand and calculator the radius r and the phase angle θ , where θ is in degrees, $-180^\circ \leq \theta < +180^\circ$. You may check your hand calculations by using the `abs` and `angle` commands appropriately in MATLAB.

2.3 Given: two complex numbers expressed in polar form $z_1 = r_1 e^{j\theta_1}$ and $z_2 = r_2 e^{j\theta_2}$, with r_1 , r_2 , θ_1 , and θ_2 all real numbers.

(a) Use complex arithmetic with complex numbers in polar form to show that the conjugate of a product equals the product of conjugates, which is expressed in equation form as $\overline{(z_1 \times z_2)} = \bar{z}_1 \times \bar{z}_2$.

(b) Use complex arithmetic with complex numbers in polar form to show that the conjugate of a quotient equals the quotient of conjugates, which is expressed in equation form as $\overline{(z_1/z_2)} = \bar{z}_1/\bar{z}_2$.

2.4 Express a complex number in rectangular form, $z = x + jy$, and prove the following identity: $z + \bar{z} = 2 \operatorname{Re}(z) = 2x$.

2.5 Given: complex numbers $A = A_r + jA_i$ and $B = B_r + jB_i$ (A_r, A_i, B_r, B_i all real) and complex variable $z = x + jy$ (with real, non-zero values of x and y , which are independent of each other), in the equation $C = Az + B\bar{z}$.

Prove: use complex arithmetic with complex values in rectangular form to show that C can be real, $C = C_r + j0$, only if $B = \bar{A}$. (Note that you can also prove this by applying the results of homework Problems 2.3(a) and 2.4.)

2.6 The following complex function will arise when we study the frequency response of a 2nd order system: $Z(\beta) = \frac{1}{(1 - \beta^2) + j2\zeta\beta}$, in which β is a positive, real, dimensionless forcing frequency (not dimensional frequency ω), and ζ is a positive, real, dimensionless ratio that represents viscous damping.

(a) Convert the $Z(\beta)$ equation above into polar form $Z(\beta) = r(\beta)e^{j\theta(\beta)}$. In particular, carry out the detailed algebraic steps to show that the magnitude and phase angle are

$$r(\beta) = \sqrt{(1 - \beta^2)^2 + (2\zeta\beta)^2} \quad \text{and} \quad \theta(\beta) = \tan^{-1}\left(\frac{-2\zeta\beta}{1 - \beta^2}\right).$$

(b) Calculate values of the magnitude and phase angle for several values of forcing frequency β and for two values of damping ratio ζ (specifics below). Make these calculations with a hand calculator, not with MATLAB or some other computer software (although you may check your hand calculations with computer software). These calculations will give you a small preview of frequency response, and (especially) they should help you to understand the care required when you evaluate the four-quadrant arctangent. Specifically, for each of the damping ratios $\zeta = 0$ and $\zeta = 0.1$ (or another value assigned by your instructor), calculate the quantities in the empty cells of the table below (to at least three significant figures, preferably four, but no more); also, calculate phase angles using the standard engineering convention, $-180^\circ \leq \theta < +180^\circ$, not $0^\circ \leq \theta < +360^\circ$.

Hints for the $\zeta = 0$ case: (1) for the $r(\beta)$ calculations, recognize that the equation requires $r(\beta) > 0$, even if $\beta > 1$; (2) for the $\theta(\beta)$ calculations, imagine that ζ has an extremely small, positive value, say $\zeta = +1 \times 10^{-10}$.

β	$r(\beta)$	$\theta(\beta)$ degrees	$\theta(\beta)$ radians
0			
0.5			
1			
2			
5			

2.7 Prove Eq. (2-17), $L[\ddot{f}(t)] = s^2 F(s) - s f(0) - \dot{f}(0)$: first define $g(t) = \dot{f}(t)$; now use the fundamental equation (2-15b) twice, first as $G(s) = L[\dot{f}] = s F(s) - f(0)$, and then as $L[\dot{g}] = s G(s) - g(0)$.

2.8 Consider the Laplace transform shown below, both in the first form, which is derived directly from an ODE, and in a partial-fraction expansion,

$$F(s) = \left(\frac{1}{s-a} \right) \left(\frac{1}{s-j\omega} + \frac{1}{s+j\omega} \right) = \frac{C_1}{s-a} + \frac{C_2}{s-j\omega} + \frac{C_3}{s+j\omega}$$

in which a and ω are real constants. Find residues C_1 , C_2 , and C_3 in terms of a and ω , and show that C_1 is real. Use the labor-saving method directly, without first completing the products in the form derived from an ODE.

2.9 Find the inverse Laplace transform $f(t)$, $t \geq 0$, for the given function $F(s)$ below. First use partial-fraction expansion to express $F(s)$ as a sum of simple quotients, and then apply the appropriate inverse transformation equations. Also, find the values of any zeros and poles of $F(s)$.

(a) $F(s) = \frac{s+3}{(s+1)(s+5)}$ [Answer: $f(t) = \frac{1}{2}(e^{-t} + e^{-5t})$, $t \geq 0$]

(b) $F(s) = \frac{2(s+1)}{s(s+3)(s+4)}$ [Answer: $f(t) = \frac{1}{6} + \frac{4}{3}e^{-3t} - \frac{3}{2}e^{-4t}$, $t \geq 0$]

2.10 Derive the Laplace transform $L[\cos \omega t] = \frac{s}{s^2 + \omega^2}$. Follow the same procedure, with appropriate changes in details, as the derivation of $L[\sin \omega t]$, Eq. (2-30). Show all steps, just as in the derivation of $L[\sin \omega t]$.

2.11 Solution (2-22) of ODE problem (2-11) was derived by Laplace transformation, a technique that is probably new to you, so you might be a little skeptical. To convince yourself that (2-22) is indeed the correct solution of (2-11), substitute (2-22) back into the ODE and IC of (2-11), and show that the original equations are satisfied. This method can always be used to check the correctness of an ODE solution.

2.12 Consider the standard 1st order ODE $\dot{x} - ax = bu(t)$ with IC $x(0) \equiv x_0$. Use Laplace transformation to solve for $x(t)$ with the $u(t)$ functions given below. It will ease your algebraic burden greatly if you will make liberal use of the identities involving complex numbers proved in homework Problems 2.3 and 2.4. Also, use where appropriate the transforms of $\sin \omega t$ from Eq. (2-30) and $\cos \omega t$ from Eq. (2-31) or homework Problem 2.10.

- (a) Let $u(t) = U \sin \omega t$, $t > 0$, where U is a constant amplitude.

$$[Answer: \quad x(t) = x_0 e^{at} + \frac{bU\omega}{\omega^2 + a^2} \left(e^{at} - \frac{a}{\omega} \sin \omega t - \cos \omega t \right), \quad t \geq 0]$$

- (b) Let $u(t) = U \cos \omega t$, $t > 0$, where U is a constant amplitude.

$$[Answer: \quad x(t) = x_0 e^{at} + \frac{bU}{\omega^2 + a^2} \left(a e^{at} - a \cos \omega t + \omega \sin \omega t \right), \quad t \geq 0]$$

2.13 Suppose that t is a real number representing time, and that ω is imaginary, $\omega = j\mu$, where μ is real. Use the results of homework Problem 2.1 and, from calculus, the definitions of the hyperbolic cosine, $\cosh \mu t$, and the hyperbolic sine, $\sinh \mu t$, to prove the following: $\cos \omega t = \cosh \mu t$, and $\sin \omega t / \omega = \sinh \mu t / \mu$.

2.14 For a mass-spring system with negligible damping, the appropriate ODE is Eq. (1-18), $m \ddot{x} + k x = f_x(t)$. Consider the case of this mass-spring system having imposed initial conditions at time $t = 0$, $x(0) = x_0$ and $\dot{x}(0) = v_0$, and then after $t = 0$ being subjected to constant force F , which we can express mathematically as $f_x(t) = F H(t)$, or equivalently, $f(t) = F$ for $t > 0$. In this application, unit-step function $H(t)$ is used to remind you that the Laplace transform is $L[f_x(t)] = F/s$. (In fact, force F could have been applied even before $t = 0$, but that would be irrelevant because the initial conditions establish the state of the system at $t = 0$, regardless of whatever force acts before $t = 0$.) Your task is to solve the problem by using Laplace transformation.

- (a) First take the Laplace transform of the ODE, accounting for the ICs, and solve for the transform of the output to find

$$L[x(t)] \equiv X(s) = x_0 \frac{s}{s^2 + \omega_n^2} + \frac{v_0}{\omega_n} \frac{\omega_n}{s^2 + \omega_n^2} + \frac{F}{m} \frac{1}{s(s^2 + \omega_n^2)}$$

In this equation, we define the *natural frequency of vibration*, $\omega_n = \sqrt{k/m}$, from Eq. (1-20). (See Section 1-10 for an explanation of the physical significance of ω_n .) Show all of your work leading to your result, as if the correct answer above were not given.

- (b) In order to derive the inverse transform, $L^{-1}[X(s)] = x(t)$, you could, of course, find partial-fraction expansions for each of the three terms in $X(s)$, then use the inverse transform of the fundamental transform pair (2-15b), and, after much algebra, finally derive an acceptable final algebraic equation for $x(t)$. But this would be equivalent to reinventing the wheel, because people have been evaluating exactly the same inverse transforms for the two centuries since Laplace developed the method. To preclude the neces-

sity for starting from scratch every time the same Laplace transform appears, the technical community has assembled tables of Laplace transform pairs in many handbooks and textbooks, in symbolic software, and even on the Internet. Your assignment is to invert $X(s)$ and derive the complete algebraic equation for $x(t)$, $t \geq 0$. You can find explicitly in Section 2-4 two of the three transform pairs in $X(s)$, but you are required to look up the third pair in some source other than Chapter 2.

2.15 Apply MATLAB's `residue` operation to determine the partial-fraction expansion of $F(s) = \frac{3s^3 - 2s^2 + s}{-2s^4 + 3s^3 + 4s^2 + 5s + 6}$. Submit a copy of your MATLAB session, and also

write out the partial-fraction expansion in equation form (as in the example below). The following example illustrates the `residue` operation for the polynomial ratio of Problem 2.9(b), $F(s) = \frac{2(s+1)}{s(s+3)(s+4)} = \frac{2(s+1)}{s^3 + 7s^2 + 12s}$. On the MATLAB command window,

enter as arrays the coefficients of the numerator and denominator polynomials in descending powers of s . Then enter the `residue` command to calculate the residues, poles, and *direct term* (a constant or a term proportional to s raised to some positive power, which appears only if $m \geq n$) of the expansion:

```
>> num=2*[1 1];den=[1 7 12 0]; [resids poles dterm]=residue(num,den)
```

resids =	poles =	dterm =
-1.5000 1.3333 0.1667	-4 -3 0	[]

In equation form, $F(s) = \frac{-1.5}{s - (-4)} + \frac{1.3333}{s - (-3)} + \frac{0.1667}{s - 0} = -\frac{3}{2}\left(\frac{1}{s+4}\right) + \frac{4}{3}\left(\frac{1}{s+3}\right) + \frac{1}{6}\left(\frac{1}{s}\right)$.

Chapter 3 Mechanical units; low-order mechanical systems; simple transient responses of 1st order systems

© 2016 by William L. Hallauer, Jr.

3-1 Common mechanical units

We shall evaluate mechanical systems numerically using three different systems of units that are common in the United States: *International System, SI* (based on kilogram mass, meter, and second; kg-m-sec), *traditional aeronautical* (based on pound force, foot, and second; lb-ft-sec), and *traditional structural* (based on pound force, inch, and second; lb-inch-sec). Table 3-1 summarizes the units of mechanical quantities that arise most often in this book.

Table 3-1 Common units of mechanical quantities

Unit System Quantity \	International System SI (kg-m-sec)	Traditional aero- nautical (lb-ft-sec)	Traditional struc- tural (lb-inch-sec)
Mass (translational inertia), m	kilogram mass (kg)	slug $= \text{lb}\cdot\text{sec}^2/\text{ft}$	$\text{lb}\cdot\text{sec}^2/\text{inch}$
Length, translational motion	meter (m)	foot (ft)	inch (in.)
Time, t	second (sec)	second (sec)	second (sec)
Force, translational action	newton (N) $= \text{kg}\cdot\text{m/sec}^2$	pound force (lb)	pound force (lb)
Translational stiffness constant, k	N/m	lb/ft	lb/inch
Translational damping constant, c	$\text{N}/(\text{m/sec})$ $= \text{N}\cdot\text{sec}/\text{m}$	$\text{lb}/(\text{ft/sec})$ $= \text{lb}\cdot\text{sec}/\text{ft}$	$\text{lb}/(\text{inch/sec})$ $= \text{lb}\cdot\text{sec}/\text{inch}$
Angle, rotational motion	radian (rad), which is dimensionless	radian (rad), which is dimensionless	radian (rad), which is dimensionless
Rotational inertia, J	$\text{kg}\cdot\text{m}^2$	slug-ft ² $= \text{lb}\cdot\text{sec}^2\cdot\text{ft}$	$\text{lb}\cdot\text{sec}^2\cdot\text{inch}$
Moment or torque, rotational action	N-m	lb-ft	lb-inch
Rotational stiffness constant, k_θ	$(\text{N}\cdot\text{m})/\text{rad}$ $= \text{N}\cdot\text{m}$	$(\text{lb}\cdot\text{ft})/\text{rad}$ $= \text{lb}\cdot\text{ft}$	$(\text{lb}\cdot\text{inch})/\text{rad}$ $= \text{lb}\cdot\text{inch}$
Rotational damping constant, c_θ	$(\text{N}\cdot\text{m})/(\text{rad/sec})$ $= \text{N}\cdot\text{m}\cdot\text{sec}$	$(\text{lb}\cdot\text{ft})/(\text{rad/sec})$ $= \text{lb}\cdot\text{ft}\cdot\text{sec}$	$(\text{lb}\cdot\text{inch})/(\text{rad/sec})$ $= \text{lb}\cdot\text{inch}\cdot\text{sec}$

SI is called an *absolute* system of units, and the other two are called *gravitational* systems. Absolute and gravitational systems differ fundamentally in their primary and derived units as defined in the context of Newton's 2nd law. In any absolute system, mass

is a primary unit, along with length, and time, but force is a unit derived from those of mass, length, and time. Thus, the SI force unit, the newton (N), is precisely defined from $F = ma$, as a kilogram-meter/second² (kg-m/s²). In any gravitational unit system, force is considered to be a primary unit, and mass is a derived unit. Thus, from $m = F/a$, the mass unit in the traditional aeronautical system, commonly called a slug, is precisely defined as a pound-second²/foot (lb-sec²/ft). In all of these systems, the *weight* of an object on Earth (in the force units) is defined as the mass times the standard sea-level gravitational acceleration, which is denoted as g , so $W = mg$. Table 3-2 includes the relevant values of g .

Table 3-2 Standard sea-level gravitational acceleration

Unit System Quantity \	International System SI (kg-m-sec)	Traditional aero- nautical (lb-ft-sec)	Traditional struc- tural (lb-inch-sec)
Standard accelera- tion of gravity, g	9.807 m/sec ²	32.17 ft/sec ²	386.1 inch/sec ²

Table 3-3 Prefixes for units

Multiple	Prefix	Letter prefix
10^9	giga	G
10^6	mega	M
10^3	kilo	k
10^2	hecto	h
10	deka	da
10^{-1}	deci	d
10^{-2}	centi	c
10^{-3}	milli	m
10^{-6}	micro	μ
10^{-9}	nano	n

It is often convenient in technical notation to use prefixes that indicate powers of ten. For example, a force of 456,700 N can also be written as 456.7×10^3 N, or in more economical form as 456.7 kN, where kN denotes a kilo-newton = 10^3 N. Table 3-3 includes a standard set of prefixes used in dynamics of mechanical systems. We also use the “e” notation that is becoming standard for input to and output from computer programs. Thus, for examples, the 456.7 kN force can be expressed as 456.7e3 (or e03, e+03, e+003, etc.) N, and a length of 4.321 mm can be expressed as 4.321e-3 (or e-03, e-003, etc.) m.

3-2 Calculation of mass from measured weight

This practically important process is straightforward for the traditional aeronautical and structural unit systems, but we can be confused when working in the SI system if the particular sensor used measures weight in the kilogram force (kg_f) unit. Let’s consider an example: suppose we have a laboratory scale with two different modes of weight measurement, pound force (lb) and kilogram force (kg_f). We place an object on the scale with the display set to the lb mode, and the reading is $W = 15.50$ lb. We next change the display to the kg_f mode, and the reading changes to $W = 7.031$ kg_f. Let’s calculate the mass in the three different unit systems using $m = W/g$.

$$\text{lb-inch-sec system: } m = \frac{15.50 \text{ lb}}{386.1 \text{ inch/sec}^2} = 0.04015 \frac{\text{lb-sec}^2}{\text{inch}} \equiv 4.015 \times 10^{-2} \frac{\text{lb-sec}^2}{\text{inch}}$$

lb-ft-sec system: $m = \frac{15.50 \text{ lb}}{32.17 \text{ ft/sec}^2} = 0.4818 \text{ slug} \equiv 4.818\text{e}-1 \text{ slug} \equiv 4.818 \text{ deci-slug}$

For the SI calculation, we need to recognize that the kg_f is not a consistent SI force unit, even though many weight scales sold and used in the United States have been calibrated in this unit since the 19th century. The only consistent SI force unit is the newton (N). So let's ignore the $W = 7.031 \text{ kg}_f$ reading for now and use, instead, the $W = 15.50 \text{ lb}$ reading in association with the well-known conversion, $1 \text{ lb} = 4.448 \text{ N}$:

$$\text{SI system: } m = \frac{15.50 \text{ lb} \times 4.448 \frac{\text{N}}{\text{lb}}}{9.807 \text{ m/sec}^2} = \frac{68.95 \text{ N}}{9.807 \text{ m/sec}^2} = 7.031 \text{ kg}$$

So, in the SI system, the mass in kg has the same numerical value as the weight in kg_f, which, in the future, will relieve us from having to calculate a conversion. This equality is precisely true only at elevations on Earth where g is exactly 9.807 m/sec^2 , but it is close enough for most engineering calculations using weights measured anywhere on Earth's surface.

3-3 Reaction wheel: a rotational 1st order system

Reaction wheels are used for attitude control of spacecraft. The principal component of a reaction wheel is a rotor, the “wheel,” which is normally either not spinning or spinning at a constant nonzero rotational velocity. When a motor increases or decreases the rotational velocity from the normal value, a control moment is imposed upon the vehicle to which the reaction wheel is attached.

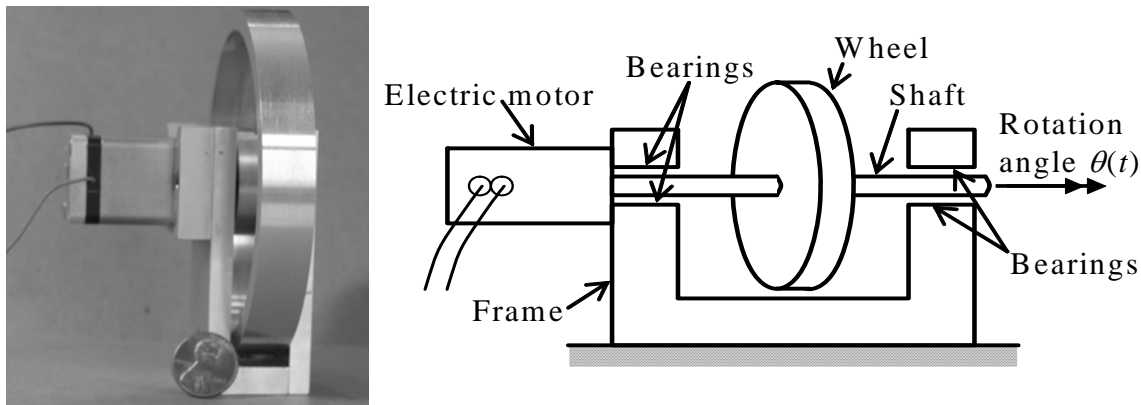


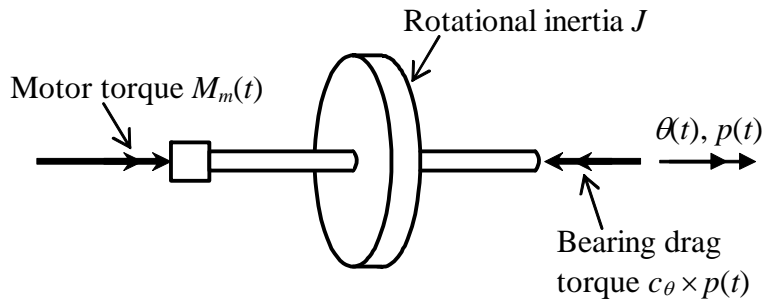
Figure 3-1 Laboratory reaction-wheel assembly: photograph at left, schematic drawing at right

The reaction-wheel assembly drawn in Fig. 3-1 is a small laboratory device used in experimental research. Its basic functioning is the same as that of a flight-qualified reaction-wheel assembly. The rotating members are the wheel, the shaft, and the rotor of the motor. We denote their combined *rotational inertia* about the shaft axis as J , also called *moment of inertia*. The shaft is held in bearings, which are lubricated, but

nevertheless impose a drag moment. The rotation angle of the rotating members is denoted $\theta(t)$, and it is represented graphically in Fig. 3-1 by a double-headed arrow and the *right-hand rule* giving the polarity of rotation. The rotational velocity (angular velocity, spin rate) is denoted $\dot{\theta}(t) \equiv p(t)$, a symbol commonly used for angular velocity in aeronautical applications.

We will idealize the drag moment as having the linear viscous form $c_\theta \times p(t)$, where c_θ is the rotational viscous damping constant, which can be measured on real hardware. Also, we will denote as $M_m(t)$ the torque imposed on the rotating members by the electric motor, this torque being an independent input quantity.

The drawing below is the free-body diagram (FBD) of all moments (torques in this case) acting on the rotating members, with the bearing drag shown as a single torque, even though it is actually distributed over all bearing surfaces:



In order to derive the equation of motion, we write Newton's 2nd law for rotation about the shaft axis, based upon the FBD:

$$\Sigma(\text{Moments})_{\text{about shaft axis}} = (\text{rotational inertia}) \times (\text{rotational acceleration})_{\text{about shaft axis}};$$

$$M_m(t) - c_\theta p = J \dot{p} \Rightarrow J \dot{p} + c_\theta p = M_m(t) \quad (3-1)$$

Converting (3-1) into the standard 1st order form gives

$$\dot{p} - \left(-\frac{c_\theta}{J} \right) p = \frac{1}{J} M_m(t) \Rightarrow \dot{p} - a p = b M_m(t) \quad \text{where } a = -\frac{c_\theta}{J} \text{ and } b = \frac{1}{J} \quad (3-2)$$

3-4 Simple transient responses of 1st order systems, 1st order time constant and settling time

The adjective *transient* applies to system response that is dynamic for a finite time interval (often called the *settling time*), but is essentially static thereafter.

Consider the 1st order problem presented in Chapter 2,

$$\dot{x} - ax = bU e^{-wt}, x(0) = x_0, \text{ solve for } x(t), t > 0 \quad (2-11, \text{ repeated})$$

with solution,

$$x(t) = x_0 e^{at} + \frac{bU}{a+w} (e^{at} - e^{-wt}), \text{ for } t \geq 0 \quad (2-22, \text{ repeated})$$

If we let $w = 0$, then the input term becomes the step function, $U[e^{-wt}]_{w=0} = U H(t) = U$ for $t > 0$, $H(t)$ being the Heaviside unit-step function defined in Section 2-4. So the problem and solution become:

$$\dot{x} - ax = bU, x(0) = x_0, \text{ solve for } x(t), t > 0$$

$$x(t) = \frac{bU}{(-a)} (1 - e^{-(-a)t}) + x_0 e^{-(-a)t}, \text{ for } t \geq 0 \quad (3-3)$$

In Eq. (3-3), we write $a = -(-a)$ because usually $a < 0$ for engineering systems, as in Eq. (3-2). We want to consider two special cases of solution (3-3): (1) pure initial condition response for $U = 0$; and (2) pure step response for $x_0 = 0$.

Stable initial condition (IC) response

$$x(t) = x_0 e^{-(-a)t}, \text{ for } t \geq 0 \quad (3-4)$$

Define the 1st order-system *time constant*,

$$\tau_1 \equiv \frac{1}{(-a)} \quad (3-5)$$

For example, the time constant for the reaction wheel from (3-2) is $\tau_1 \equiv \frac{J}{c_\theta}$. You should satisfy yourself, using Table 3-1 if necessary, that the quantity J/c_θ has the dimension of time (unit of second). With this definition of time constant τ_1 , solution (3-4) becomes:

$$x(t) = x_0 e^{-t/\tau_1} \equiv x_0 \exp(-t/\tau_1), \text{ for } t \geq 0 \quad (3-6)$$

Figure 3-2 is a graph of *exponential decay* indicated in Eq. (3-6).

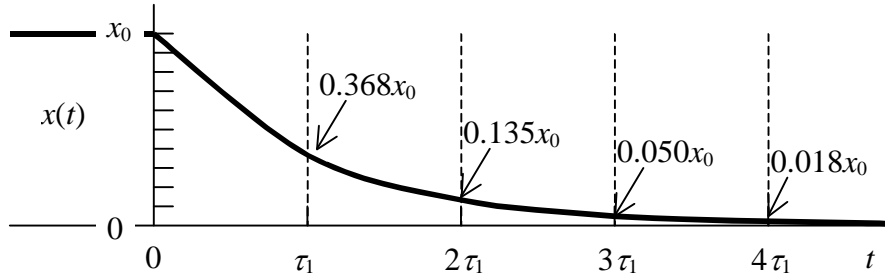


Figure 3-2 1st order initial-condition response

At the *time constant*, $t = \tau_1$, the response has decayed to $e^{-1} = 37\%$ of the initial value. The other time “milestone” to which we shall often refer is $t = 4\tau_1$, which we call the *settling time*, at which time the response has decayed to $e^{-4} = 2\%$ of the initial value. For most practical engineering purposes, this settling time is considered to be the time required for the response essentially to reach its final steady-state value, which is $x = 0$ in this case of IC response. Mathematically, $x \rightarrow 0$ only as $t \rightarrow \infty$.

If the constant a is positive, then we write IC solution (3-4) as $x(t) = x_0 e^{at}$. The mathematical response represented by this solution is unbounded: $x \rightarrow \infty$ as $t \rightarrow \infty$. In reality, no engineering variable will ever become infinite: as the variable becomes large, something in the system will fail or overload, or the system will become nonlinear, or the response will be limited by a governor, *etc.* Even though the actual response will not become infinite, an exponentially increasing linear mathematical response such as this is usually undesirable for practical purposes; an engineering system that exhibits this kind of response is considered to be *unstable*. On the other hand, an engineering system with negative constant a is *stable*.

The time constant τ_1 is such an important quantity for stable 1st order systems that we shall re-cast the standard 1st order system ODE in terms of τ_1 , rather than constant a , using Eq. (3-5). Thus, rather than analyzing Eq. (1-1), $\dot{x} - ax = bu(t)$, hereafter we shall usually consider the following *standard stable form* for 1st order systems:

$$\dot{x} + \frac{1}{\tau_1}x = bu(t) \quad (3-7)$$

Stable step response

In Eq. (3-3), we set $x_0 = 0$ and use time constant definition (3-5) to obtain

$$x(t) = bU\tau_1 \left(1 - e^{-t/\tau_1}\right) \equiv bU\tau_1 [1 - \exp(-t/\tau_1)], \text{ for } t \geq 0 \quad (3-8)$$

Figure 3-3 is a graph of the *exponential rise* to a positive final value that is indicated in Eq. (3-8).

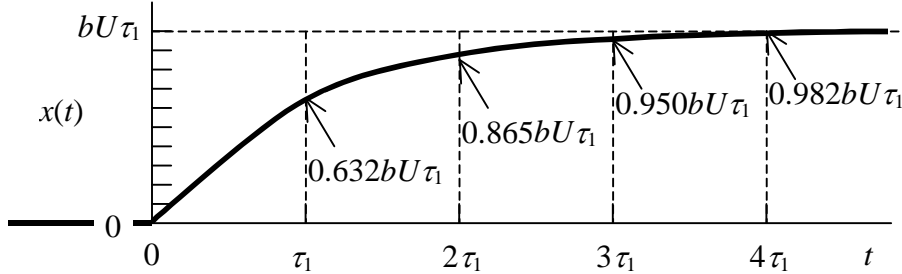


Figure 3-3 1st order step response

The final value of unit-step response is $bU\tau_1$, and it is approached asymptotically as $t \rightarrow \infty$. At the *time constant*, $t = \tau_1$, the response has risen from the IC of zero to $1 - e^{-1} = 63\%$ of the final value. At $t = 4\tau_1$, the *settling time*, the response has risen to $1 - e^{-4} = 98\%$ of the final value.

Step response solutions such as (3-8) are usually an approximation to the actual response since, in reality, a pure, discontinuous step change in a physical input quantity is rarely achievable. Nevertheless, step input is a sufficiently close approximation to many real physical inputs that step response solutions such as (3-8) are close approximations to actual physical responses.

Consider again the reaction wheel of the previous section. Let's denote a step input from the motor as $M_m(t) = M \times H(t)$. Then ODE (3-2) becomes

$$\dot{p} - ap = bM_m(t) = bMH(t) = bM \text{ for } t > 0, \text{ where } a = -\frac{c_\theta}{J} = -\frac{1}{\tau_1} \text{ and } b = \frac{1}{J} \quad (3-9)$$

So the time constant is $\tau_1 = -1/a = J/c_\theta$, and solution (3-8) becomes

$$p(t) = bM\tau_1(1 - e^{-t/\tau_1}) = \frac{1}{J}M \frac{J}{c_\theta}(1 - e^{-t/\tau_1}) = \frac{M}{c_\theta}(1 - e^{-t/\tau_1}) \text{ rad/sec, for } t \geq 0 \quad (3-10)$$

Note that in this case we adapt the “standard” mathematical solution (3-8) to a particular physical problem. This approach is common in system dynamics. In other words, it is not always necessary to solve an ODE for every new physical problem; if a standard ODE solution has already been derived, you may just adapt that standard solution to the physical problem at hand, rather than re-deriving the ODE solution.

3-5 Aileron-induced rolling of an airplane or missile

The principal source for the aerodynamic theory of this section is Nelson, 1989, pages 19-20, 153-156 and 250-260. The aerodynamic rolling moment on an airplane or missile is written in standard aeronautical notation as

$$L(t) = \frac{\partial L}{\partial \delta} \delta(t) + \frac{\partial L}{\partial p} p(t) \equiv L_\delta \delta(t) + L_p p(t) \quad (3-11)$$

(There is a notational ambiguity between moment $L(t)$ and the Laplace transform operator $L[f(t)]$ introduced in Chapter 2; such ambiguities are unavoidable in technical work, so you should become accustomed to them.) The roll (bank) angle (in radians) is $\theta(t)$, defined here as being positive clockwise as seen by an observer behind the vehicle, in other words, rightward rolling (Fig. 3-4). In Eq. (3-11), $\delta(t)$ is the input aileron deflection angle (in radians) to produce rolling, the right aileron being deflected upward and the left aileron being deflected downward to produce a positive roll rate, $p(t) \equiv \dot{\theta}$ (rad/sec).

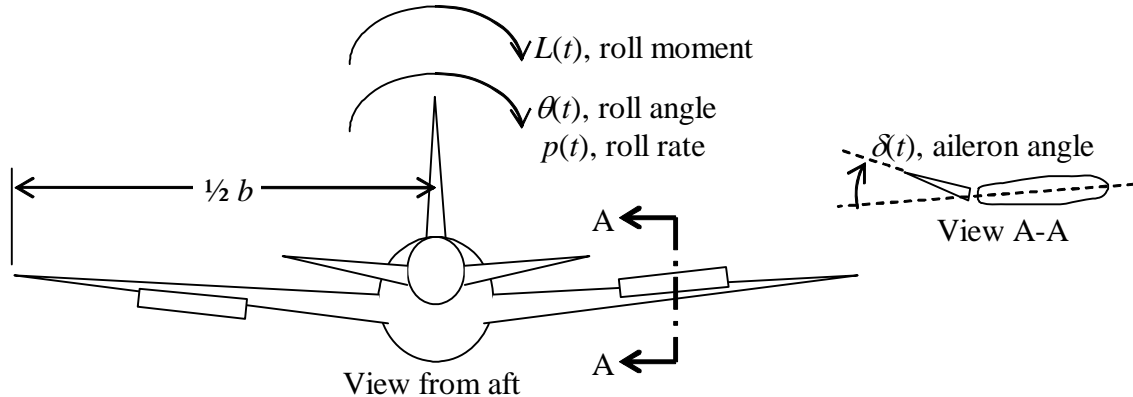


Figure 3-4 Aileron-induced rolling of an airplane

The dimensional aerodynamic derivatives in (3-11) are related to dimensionless coefficients by:

$$L_\delta = \bar{q} S b C_\delta > 0 \quad \left(\frac{\text{lb} \cdot \text{ft}}{\text{rad}} \text{ or } \frac{\text{N} \cdot \text{m}}{\text{rad}} \right) \quad (3-12)$$

$$L_p = \bar{q} S b \frac{b}{2V} C_p = \frac{\bar{q} S b^2}{2V} C_p < 0 \quad \left(\frac{\text{lb} \cdot \text{ft}}{\text{rad/sec}} \text{ or } \frac{\text{N} \cdot \text{m}}{\text{rad/sec}} \right) \quad (3-13)$$

The constants in Eqs. (3-12) and (3-13) are defined as:

$\bar{q} = \frac{1}{2} \rho V^2$ is the free-stream dynamic pressure (lb/ft² or N/m²)

ρ is air density (slug/ft³ or kg/m³)

V is the free-stream airspeed (ft/sec or m/sec)

S is the wing planform area (ft² or m²)

b is the full wing span (ft or m)

$C_\delta > 0$ is the dimensionless aerodynamic stability moment coefficient (rad⁻¹), rolling moment due to aileron deflection (a function of Mach number)

$C_p < 0$ is the dimensionless aerodynamic stability moment coefficient (rad⁻¹), roll damping due to roll rate (a function of Mach number).

The term $b/2V$ in Eq. (3-13), the damping moment due to roll rate, merits some explanation. The clockwise rolling velocity of the right wingtip is $p \times b/2$, so the addi-

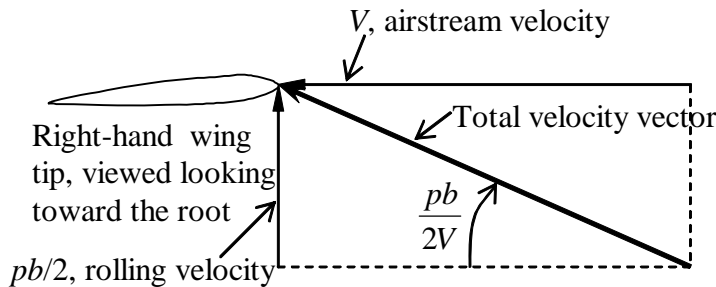


Figure 3-5 Angle of attack induced by rolling velocity

tional angle of attack induced at the wingtip by the roll rate is $\tan^{-1} \left[\frac{pb/2}{V} \right] \approx \frac{pb}{2V}$, a small angle (the magnitude of the angle is exaggerated in Fig. 3-5, just to improve clarity). Thus, $\frac{b}{2V} p(t)$ in Eqs. (3-13) and (3-11) plays the same role as that of $\delta(t)$ in Eqs. (3-12) and (3-11).

Newton's 2nd law equation of motion for rolling is $J\ddot{\theta} \equiv J\dot{p} = L(t)$, in which J (slug-ft² or kg-m²) is the rotational inertia of the vehicle about its rolling axis. This equation is based upon the assumption that the vehicle can only roll (*i.e.*, no coupling with other degrees of freedom such as sideslip and yaw). Substituting Eqs. (3-11)-(3-13) into Newton's law gives:

$$J\dot{p} = L_\delta \delta + L_p p \Rightarrow J\dot{p} - L_p p = L_\delta \delta$$

$$\Rightarrow \dot{p} + \left(\frac{-L_p}{J} \right) p = \left(\frac{-L_p}{J} \right) \left(\frac{L_\delta}{-L_p} \right) \delta(t) = \left(\frac{-L_p}{J} \right) \frac{2V}{b} \left(\frac{C_\delta}{-C_p} \right) \delta(t) \quad (3-14)$$

Writing (3-14) in 1st order standard form (3-7) gives [with b in (3-7) temporarily replaced by B to reduce notational ambiguity]:

$$\dot{p} + \frac{1}{\tau_1} p = B \delta(t) \quad (3-15)$$

in which we have, respectively, time constant τ_1 and constant B :

$$\tau_1 = \frac{J}{-L_p} = \frac{2VJ}{\bar{q}Sb^2(-C_p)} = \frac{4J}{\rho VSb^2(-C_p)} > 0 \quad (3-16)$$

$$B = \left(\frac{-L_p}{J} \right) \frac{2V}{b} \left(\frac{C_\delta}{-C_p} \right) = \frac{1}{\tau_1} \frac{2V}{b} \left(\frac{C_\delta}{-C_p} \right) = \frac{\bar{q}SbC_\delta}{J} > 0 \quad (3-17)$$

Example 3-1: Use the results of this section and the general 1st order step response Eq. (3-8) to calculate rolling response to a $\delta(t) = 2.5^\circ H(t)$ step aileron input for a hypothetical medium-sized civilian transport airplane. The following are representative data: rotational inertia about the rolling axis is $J = 4.0e5$ slug-ft², wing planform area is $S = 1,100$ ft², and wing span is $b = 90$ ft; for flight at 10,000 ft altitude and free-stream airspeed $V = 350$ ft/sec, aerodynamic dimensionless rolling-moment coefficients are $C_\delta = 0.061$ per radian and $C_p = -0.34$ per radian. At 10,000 ft altitude, standard air density is $\rho = 0.001755$ slug/ft³ (Nelson, 1989, p. 248).

$$\bar{q} = \frac{1}{2} \rho V^2 = \frac{1}{2} \times 1.755e-3 \frac{\text{slug}}{\text{ft}^3} \times \left(350 \frac{\text{ft}}{\text{sec}} \right)^2 = 107.5 \frac{\text{lb}}{\text{ft}^2}$$

$$L_p = \frac{\bar{q}Sb^2}{2V} C_p = \frac{107.5 \text{ lb}/\text{ft}^2 \times 1,100 \text{ ft}^2 \times (90 \text{ ft})^2}{2 \times 350 \text{ ft/sec}} \times (-0.34 \text{ rad}^{-1}) = -4.65e5 \frac{\text{lb} \cdot \text{ft}}{\text{rad/sec}}$$

$$\tau_1 = \frac{J}{-L_p} = \frac{4.0e5 \text{ lb} \cdot \text{sec}^2 \cdot \text{ft}}{4.65e5 \text{ lb} \cdot \text{sec} \cdot \text{ft/rad}} = 0.86 \text{ sec}$$

(Comments regarding units: Angle is a dimensionless quantity, so the radian, which is the fundamental metric of angle, is unitless. In the calculation above for L_p , all of the units shown, including radian, balance in the final result to give the correct resulting unit, $\frac{\text{lb} \cdot \text{ft}}{\text{rad/sec}}$; it is important to recognize this unit as opposed, for example, to $\frac{\text{lb} \cdot \text{ft}}{\text{deg/sec}}$,

which would be the case if C_p were given per degree. However, in calculations that produce results which are not angular quantities, such as τ_1 above, the radian must be recognized as unitless, and it should not appear in the units of the final numerical result. This is a general characteristic that can confuse us when we check to make certain that units of numerical answers are correct.)

$$B = \frac{1}{\tau_1} \frac{2V}{b} \left(\frac{C_\delta}{-C_p} \right) = \frac{1}{0.86 \text{ sec}} \times \frac{2 \times 350 \text{ ft/sec}}{90 \text{ ft}} \times \frac{0.061 \text{ rad}^{-1}}{0.34 \text{ rad}^{-1}} = 1.62 \text{ sec}^{-2}$$

From Eq. (3-8), the roll-rate response to the 2.5° step input is

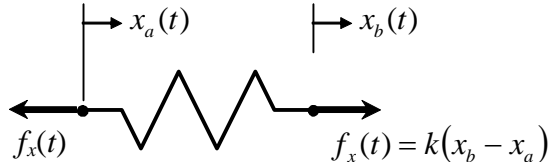
$$p(t) = BU\tau_1 [1 - \exp(-t/\tau_1)] = 1.62 \text{ sec}^{-2} \times 2.5 \text{ deg} \times 0.86 \text{ sec} \times (1 - e^{-t/(0.86 \text{ sec})})$$

$$p(t) = 3.5 [1 - \exp(-1.16t)] \frac{\text{degrees}}{\text{sec}}$$

The time constant is $\tau_1 = 0.86 \text{ sec}$, and the steady-state roll rate of 3.5 deg/sec is essentially achieved in the settling time of $4\tau_1 = 3.44 \text{ sec}$.

3-6 Translational spring and viscous damper (dashpot)

The linear translation spring was introduced in Section 1-9 as the mechanical element connecting a mass to a rigid wall; for that simple case, the end of the spring attached to the wall was stationary. Now, let's consider the more general case in which both ends of the spring can move,



as indicated in Fig. 3.7. The force $f_x(t)$ required to deform the spring by the amount $x_b(t) - x_a(t)$, relative to the undeformed length of the spring, is proportional to the deformation. With the constant of proportionality denoted as k , the more general spring law is

$$f_x(t) = k[x_b(t) - x_a(t)] \quad (3-18)$$

The standard sign convention defines stretching of the spring as positive, $x_b - x_a > 0$, corresponding to tensile force, $f_x(t) > 0$; accordingly, compression is negative in the standard convention. Equation (3-18) clearly accommodates both tension and compression of the spring. Occasionally, however, it is convenient to define compression as positive, as is illustrated in Example 3-4 in the next section.

With the spring end forces equal and opposite as shown in Fig. 3-7, we have neglected the *inertial force* of the spring. Inertial forces are terms such as $m \times a$, mass times acceleration, in Newton's 2nd law. In this case, the inertial force of the spring is $m_s \times \ddot{x}_s$, in which m_s is the mass of the spring, and \ddot{x}_s is acceleration of the spring's center of mass. So neglecting inertial forces means we assume they are negligibly small in comparison with the force of Eq. (3-18). Notice that this does not strictly mean we are neglecting the mass, because even a tiny mass, when multiplied by a large acceleration, can produce a non-negligible inertial force. It is common to neglect the inertial forces of springs, but we should remember when doing so that we are really assuming both the inertias are small and the accelerations are sufficiently slow.

A dashpot (mechanical viscous damper) is a discrete component that resists translational velocity. An idealized linear, viscous damper is represented graphically by a piston-cylinder assembly, Fig. 3-8. This device opposes relative velocity between piston and cylinder. With the forces on the dashpot defined to be positive in tension, as shown

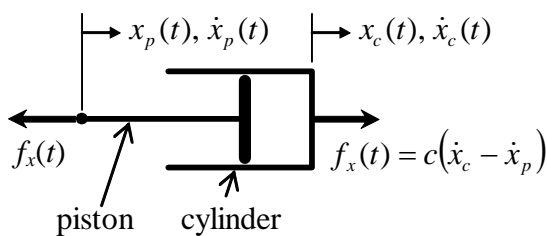


Figure 3-8 Ideal linear, viscous dashpot with damping constant c

on Fig. 3-8, the linear damping law is

$$f_x(t) = c[\dot{x}_c(t) - \dot{x}_p(t)] \quad (3-19)$$

in which c is the damping constant. The damping constant plays the same role for a dashpot here that it plays in Chapter 1 [Fig. 1-1 and Eq. (1-2)] for a block sliding on a viscous liquid film. If we were to

define the forces to be positive in compression, then we would have to reverse the signs in the damping law, Eq. (3-19); it is sometimes appropriate to do so, as in Example 3-4 in the next section.

With the cylinder and piston forces equal and opposite as shown in Fig. 3-8, we have neglected the *inertial forces* of the cylinder and piston. It is common to neglect the inertial forces of dashpots, but we should remember when doing so that we are really assuming that both the inertias are small and the accelerations are sufficiently slow. On the other hand, in Example 3-4 of the next section, inertial forces of a piston-cylinder assembly are not neglected.

The idealized dashpot model of Fig. 3-8 and Eq. (3-19) is convenient for linear mathematical analysis because of its simplicity. It is assumed to resist motion between piston and cylinder by means of the drag force produced by a viscous fluid boundary layer between the two solid objects. We can use the simple dashpot to model approximately real devices such as door dampers and shock absorbers. However, it is not a precise model for most real damping devices. In most real translational dampers, a piston forces fluid through an orifice within a cylinder, and this generates a major portion of the resisting force. Unfortunately for the purposes of linear mathematical analysis, the resisting force is a complex and highly nonlinear function of the relative motion between piston and cylinder.

3-7 More examples of damped mechanical systems

Let's consider next some combinations of dashpots with springs and masses. In each case, we will draw the physical device, draw appropriate free-body diagrams, and then derive the equations of motion. Force $f_x(t)$ is considered to be an independent input quantity in all of these examples.

Example 3-2: Mass-damper-spring system, Fig. 3-9

Newton's 2nd law for translation of the mass: $m \ddot{x} = f_x(t) - c \dot{x} - k x$

$$\Rightarrow \text{ODE: } m \ddot{x} + c \dot{x} + k x = f_x(t) \quad (3-20)$$

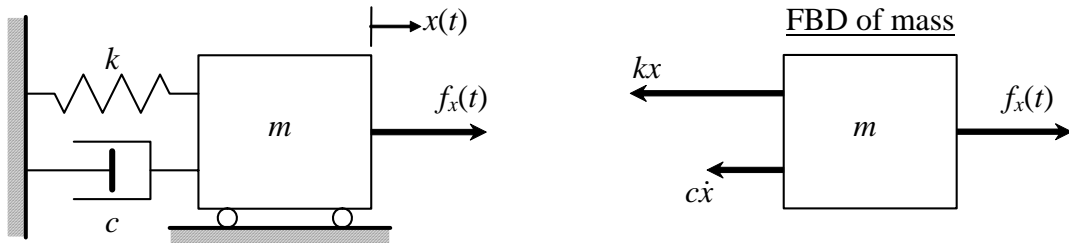


Figure 3-9 Mass-damper-spring system

Example 3-3: Ideal shock strut, parallel damper-spring system, Fig. 3-10

This combination is very similar to the mass-damper-spring system, except the inertial force of the mass (now considered just a rigid link) is assumed to be negligible.

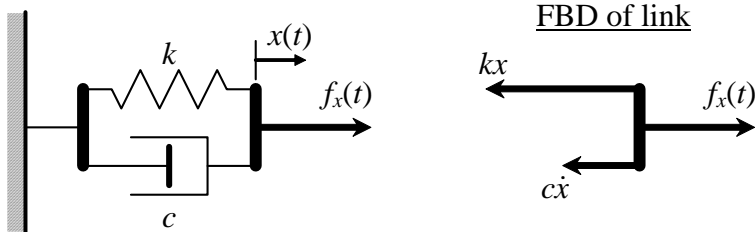


Figure 3-10 Parallel damper-spring system

Newton's 2nd law for translation of the link: $m \ddot{x} \equiv 0 = f_x(t) - c \dot{x} - k x$

$$\Rightarrow \text{ODE: } c \dot{x} + k x = f_x(t) \quad (3-21)$$

Note that Eq. (3-21) is a typical 1st order LTI ODE, but now the unknown quantity is translation (position) $x(t)$ of the rigid link.

Example 3-4: Series combination of mass, dashpot, and spring, Fig. 3-11

For the examples above, it is not necessary to draw separate FBDs of the spring and of the dashpot's piston and cylinder. However, it is necessary to draw separate FBDs for systems such as that of Fig. 3-11, where dashpot and spring are arranged in *series*, not in *parallel*, and, for variety and generality, the inertial forces of the dashpot's piston and cylinder are considered to be significant, not negligible. Take notice of the component interaction forces f_c and f_k ; note especially that piston-cylinder interaction force f_c is shown as an equal and opposite pair, as required by Newton's 3rd law.

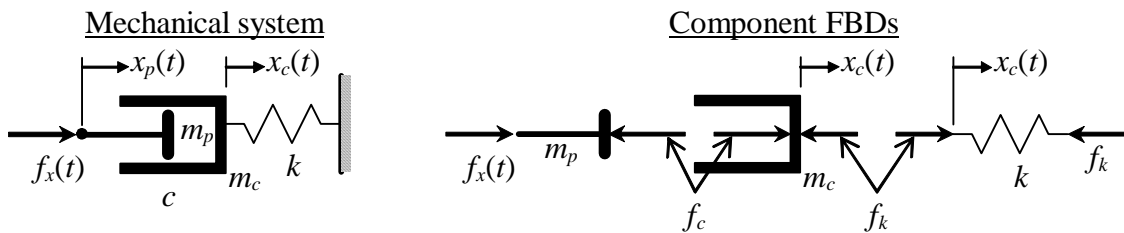


Figure 3-11 Example series mass-dashpot-spring

$$\text{Newton's 2}^{\text{nd}} \text{ law for translation of the dashpot piston: } m_p \ddot{x}_p = f_x(t) - f_c$$

$$\text{Newton's 2}^{\text{nd}} \text{ law for translation of the dashpot cylinder: } m_c \ddot{x}_c = f_c - f_k$$

$$\text{Damper law: } f_c = c(\dot{x}_p - \dot{x}_c)$$

$$\text{Spring law: } f_k = k x_c$$

Combining equations of motion and damper/spring laws gives:

$$m_p \ddot{x}_p + c \dot{x}_p - c \dot{x}_c = f_x(t) \quad (3-22a)$$

$$m_c \ddot{x}_c - c \dot{x}_p + c \dot{x}_c + k x_c = 0 \quad (3-22b)$$

Equations (3-22) are a pair of *coupled* 2nd order ODEs in the two dependent variables $x_p(t)$ and $x_c(t)$. Thus, the system of Fig. 3-11 is a 4th order system. The dynamic response of a particular class of 4th order systems is discussed Chapter 12. However, this book does not address the dynamic response of general 4th order and higher-order systems; that is a subject of more advanced textbooks such as Ogata, 1998, Chapter 10.

Example 3-5: Series damper-spring systems—idealized mechanical filters, Fig. 3-12

For both of the series damper-spring combinations in Fig. 3-12, we specify the known input quantity to be translation $x_i(t)$, which is produced by an idealized motor that is capable of dictating a commanded displacement regardless of the force required. The

output quantity in each case is translation $x_o(t)$. The damper and spring masses are assumed here to be negligible, which cannot be valid for all practical circumstances; therefore, these are idealized, not real, mechanical systems. But these idealized systems are worth studying because they have significant dynamic characteristics that will be the subjects of subsequent parts of this book.

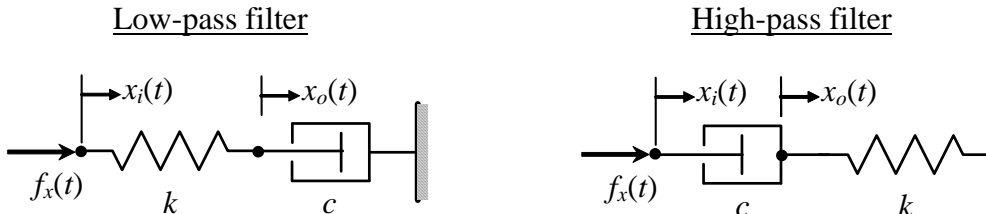
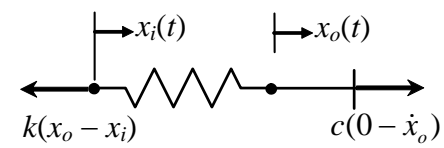


Figure 3-12 Series damper-spring idealized mechanical filters

The governing ODE for the low-pass filter, with spring and damper masses idealized to be negligible, is derived easily from the FBD at right of the series combination consisting of the spring and the damper piston: $k(x_o - x_i) = c(0 - \dot{x}_o)$. Therefore the ODE for the low-pass filter is

$$\dot{x}_o + \frac{1}{\tau_1} x_o = \frac{1}{\tau_1} x_i(t), \quad \tau_1 \equiv \frac{c}{k} \quad (3-23)$$



The mathematical derivation and description of low-pass-filter characteristics will follow in later chapters, but it is appropriate here to describe the practical nature of the low-pass filter with use of the low-pass filter drawing in Fig. 3-12 and physical intuition. Imagine that the input translation $x_i(t)$ is a steady oscillation at a fixed frequency. If that frequency is very low, so that translational velocity is low, then the damper resisting force $c\dot{x}_o$ will be very small and, consequently, both the spring and the damper piston will move slowly back and forth in unison by about the same distance as the input translation, $x_o(t) \approx x_i(t)$. On the other hand, if the frequency of oscillation is very high, then the damper resisting force $c\dot{x}_o$ will be great, so the input oscillatory translation $x_i(t)$ will compress and stretch the spring but the damper piston will act almost like a rigid wall, *i.e.*, $x_o(t) \approx 0$. For frequencies of oscillation between very low and very high, our intuition suggests that the output motion amplitude [the maximum of oscillatory $x_o(t)$] will be between the two extremes of the input motion amplitude and zero motion. The *low-pass filter* is so named because it “passes” through, without much alteration, low-frequency inputs, but it “blocks” high-frequency inputs.

Derivation of the governing ODE for the damper-spring high-pass filter is left for homework Problem 3.7. The result is:

$$\dot{x}_o + \frac{1}{\tau_1} x_o = \dot{x}_i(t), \quad \tau_1 \equiv \frac{c}{k} \quad (3-24)$$

As is done above for the damper-spring low-pass-filter, it is appropriate to describe the practical nature of the high-pass filter with use of the high-pass filter drawing in Fig. 3-12 and physical intuition. Imagine that the input translation $x_i(t)$ is a steady oscillation at a fixed frequency. If that frequency is very low, so that translational velocity is low, then the damper resisting force $c(\dot{x}_i - \dot{x}_o)$ will be very small; consequently, the damper piston will move slowly back and forth within the cylinder by about the same distance as the input translation; but very little force will be imposed upon the cylinder and spring, so the spring will be deformed hardly at all, $x_o(t) \approx 0$. On the other hand, if the frequency of oscillation is very high, then the damper resisting force $c(\dot{x}_i - \dot{x}_o)$ will be great, so the piston and cylinder will appear to become a single rigid body, and most of the input translation will be transmitted through the damper, $x_o(t) \approx x_i(t)$, to compress and stretch the spring. For frequencies of oscillation between very low and very high, our intuition suggests that the output motion amplitude will be between the two extremes of zero motion and the input motion amplitude. The *high-pass filter* is so named because it “blocks” low-frequency inputs, but it “passes” through, without much alteration, high-frequency inputs.

The damper-spring high-pass filter system is said to have *right-hand-side (RHS) dynamics* due to the explicit derivative of the input translation, \dot{x}_i , on the RHS of ODE (3-24). Therefore, Eq. (3-24) does not have the standard stable 1st order form of Eq. (3-7), $\dot{x} + (1/\tau_1)x = bu(t)$, with the input $u(t)$ on the RHS, but none of its derivatives. For standard forms such as Eq. (3-7), many readily available mathematical response solutions exist, *e.g.*, step response Eq. (3-8). But that is not the case for non-standard forms, so the non-standard character might be considered inconvenient. However, there is a process that converts non-standard ODE (3-24) into standard form.¹ We define the difference variable $x_d(t)$:

$$x_d(t) = x_o(t) - x_i(t) \quad (3-25)$$

Differentiating Eq. (3-25) and substituting the result into Eq. (3-24) leads to the following standard-form ODE for $x_d(t)$ plus the auxiliary equation required to retrieve the desired output $x_o(t)$ from solution $x_d(t)$ of the ODE:

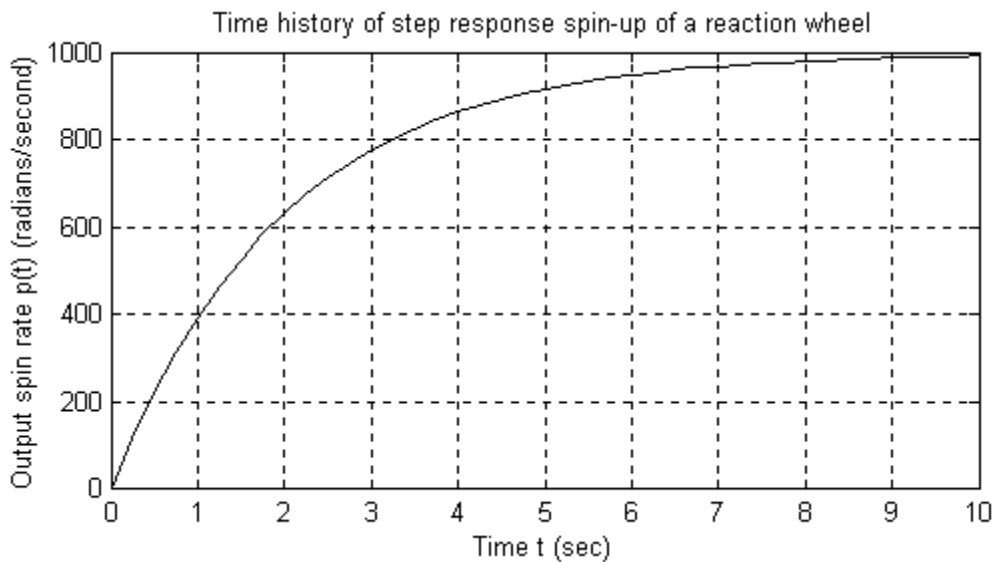
$$\dot{x}_d + \frac{1}{\tau_1} x_d = -\frac{1}{\tau_1} x_i(t), \quad x_o(t) = x_d(t) + x_i(t) \quad (3-26)$$

¹ The process shown here for a 1st order ODE is the simplest form of a more general process that can be applied to system ODEs of any order having RHS dynamics; see the textbook by Brogan, 1974, pages 174-177.

3-8 Homework problems for Chapter 3

3.1 Consider the reaction-wheel assembly described in Section 3-3. The rotor has been carefully machined to have rotational inertia $J = 2.56e-3$ lb-sec²-inch. We wish to determine the viscous damping constant c_θ of the bearings by indirect experimental measurement. We feed electric current into the motor and spin up the rotor to a high speed. Then we shut off the motor, allowing the wheel to spin down freely. With an optical tachometer, we measure the spin-down rotational speed at one instant to be 4,000 revolutions per minute (rpm). Exactly 20.0 seconds later, we measure the speed to be 1,010 rpm. From these data, calculate c_θ in consistent lb-sec-inch units.

3.2 Given: an LTI reaction-wheel assembly, with unknown rotational inertia J and unknown rotational viscous damping constant c_θ associated with drag of the bearings. Your task is to calculate J and c_θ from experimental measurement. Starting with the wheel at rest (motionless), a motor torque in the form of a step is imposed upon the wheel, $M_m(t) = M \times H(t)$, where $M = 1.5$ N-m. The resulting spin rate $p(t)$ of the wheel is measured, in radians/second, and its time history for the first 10 seconds of spin-up is recorded on the following graph.



Use the data from the graph to calculate (with as much precision as possible, given the graphical nature of the data) the values of J and c_θ in consistent SI units.

3.3 The weight of an ocean surface ship is denoted as W , and the acceleration of gravity in consistent units is g . The resistance to low-velocity motion of the ship is modeled as being proportional to velocity, with viscous damping constant c . The ship is initially at rest when, at time $t = 0$, a tugboat begins pushing it with constant force F . Write algebraic equations (in terms of the given parameters, all assumed to be in consistent units) for velocity $v(t)$ and distance traveled $x(t)$.

3.4 Nominal data (Nelson, 1989, p. 260) for the Boeing 747 civilian transport airplane are: rotational inertia about the rolling axis $J = 18.2\text{e}6 \text{ slug}\cdot\text{ft}^2$, wing planform area $S = 5,500 \text{ ft}^2$, and wing span $b = 195.68 \text{ ft}$. For flight at Mach number 0.25 and at sea level altitude, nominal aerodynamic dimensionless coefficients relevant to uncoupled rolling are $C_\delta = 0.0461$ per radian and $C_p = -0.450$ per radian. At sea level, air density is $\rho = 0.002377 \text{ slug}/\text{ft}^3$, and Mach number 0.25 corresponds to free-stream airspeed $V = 279.0 \text{ ft/sec}$.

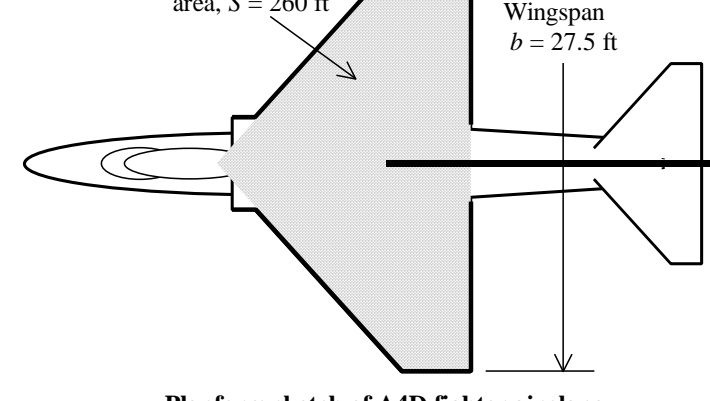
(a) Calculate the dimensional aerodynamic derivatives L_δ (in lb-ft/rad) and L_p (in lb-ft per rad/sec), then calculate the 1st order system time constant τ_1 .

(b) Suppose that the 747 is in level flight with zero initial roll rate, $p(0) = 0$, when the pilot cycles the ailerons through one complete sinusoid with amplitude 10° over a period of 5 seconds: $\delta(t) = 10^\circ \sin(0.4\pi t)$, $0 \leq t \leq 5 \text{ sec}$. Calculate the roll rate p (in degrees per sec) at the end of the 5-second period. Don't develop any new theoretical solutions for this problem; just adapt to this problem the result of Problem 1.5(a). Your intuition might suggest that roll rate is zero at the end of the aileron cycling, since the total aileron "impulse" is zero, but you should find that roll rate is not zero.

3.5 The A-4 Skyhawk was a durable and versatile small (17.5-24.5 klb) fighter-bomber-trainer that first flew in 1954 and was still used in military operations, with updated technology, in the 1990s (Lightbody *et al.*, 1990, pp. 104-111).

The relevant mass and geometry data for one model are: rolling rotational inertia $J = 8,090 \text{ slug}\cdot\text{ft}^2$; wing planform area $S = 260 \text{ ft}^2$; wing span $b = 27.5 \text{ ft}$. A flight test of this airplane is conducted at sea level and Mach number 0.4, for which the air density is $\rho = 0.002377 \text{ slug}/\text{ft}^3$ and the free-stream velocity is $V = 446.6 \text{ ft/sec}$. Starting from straight and level flight, the pilot at time $t = 0 \text{ sec}$ abruptly actuates the ailerons to $+5^\circ$ deflection, producing a step input that rolls the airplane clockwise. The resulting roll rate is sensed by a rate gyroscope, digitized, and recorded. The data are analyzed, and it is found that the following equation fits the data very well: $\dot{\theta}(t) = p(t) = 50.0(1 - e^{-1.667t})$ degrees/sec.

The relevant mass and geometry data for one model are: rolling rotational inertia $J = 8,090 \text{ slug}\cdot\text{ft}^2$; wing planform area $S = 260 \text{ ft}^2$; wing span $b = 27.5 \text{ ft}$. A flight test of this airplane is conducted at sea level and Mach number 0.4, for which the air density is $\rho = 0.002377 \text{ slug}/\text{ft}^3$ and the free-stream velocity is $V = 446.6 \text{ ft/sec}$. Starting from straight and level flight, the pilot at time $t = 0 \text{ sec}$ abruptly actuates the ailerons to $+5^\circ$ deflection, producing a step input that rolls the airplane clockwise. The resulting roll rate is sensed by a rate gyroscope, digitized, and recorded. The data are analyzed, and it is found that the following equation fits the data very well: $\dot{\theta}(t) = p(t) = 50.0(1 - e^{-1.667t})$ degrees/sec.

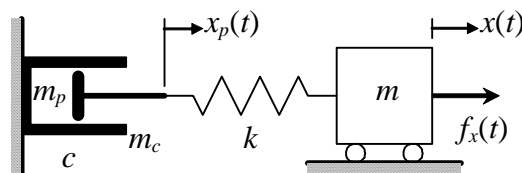


(a) Use the measured roll rate to perform *parameter identification*, specifically to determine values for the two roll aerodynamic stability coefficients C_p and C_δ , both dimensionless. Begin by calculating time constant τ_1 of the response, then use that to calculate aerodynamic derivative L_p , then use that to calculate C_p . Having these values, you can

now use the steady-state roll rate to calculate C_δ . Check the units of your calculations to make certain that your final calculated coefficients are, in fact, dimensionless.

- (b) Given that $\theta(0) = 0$ (level flight), derive an equation for $\theta(t)$ in degrees, $t \geq 0$. Evaluate that equation to calculate the bank angles at $t = \tau_1$ (one time constant) and at $t = 4\tau_1$ (\approx steady-state roll rate).

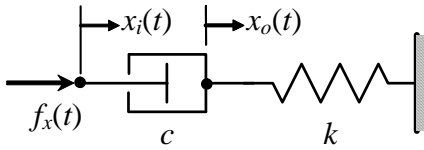
3.6 Sketch (carefully) the appropriate free-body diagrams for the mechanical system drawn below. The dashpot's damping coefficient is c , its cylinder is fixed to the wall, and its piston has mass m_p . Next, use the FBDs and appropriate linear laws for the spring and dashpot to derive the ODEs that describe the motion of this system in terms of dependent variables $x_p(t)$ and $x(t)$. Note that the spring stretch is $x - x_p$, so the tensile force developed in the spring is $k(x - x_p)$. Do not neglect the inertial forces of the dashpot's piston and of the block with mass m , which rolls without friction. Force $f_x(t)$ is an independent input quantity.



Series mass-dashpot-spring system

piston and of the block with mass m , which rolls without friction. Force $f_x(t)$ is an independent input quantity.

3.7 The LTI damper-spring high-pass filter of Fig. 3-12 is repeated below. In this problem, neglect inertial forces of the damper and the spring. Input $x_i(t)$ is translation of the damper piston, generated by some displacement-controlling motor. Output $x_o(t)$ is translation of the damper cylinder and spring end. Sketch an appropriate free-body diagram (or more than one), then write equilibrium equation(s) from which you derive the ODE $\tau_1 \dot{x}_o + x_o = \tau_1 \dot{x}_i$, which has right-hand-side (RHS) dynamics. Express time constant τ_1 in terms of damper constant c and spring constant k . (Hint: recognize that piston force $f_x(t)$ shown is a dependent variable, related to independent input $x_i(t)$ and output $x_o(t)$, but $f_x(t)$ should not appear in the equation of motion.)



Input $x_i(t)$ is translation of the damper piston, generated by some displacement-controlling motor. Output $x_o(t)$ is translation of the damper cylinder and spring end. Sketch an appropriate free-body diagram (or more than one), then write equilibrium equation(s) from which you derive the ODE $\tau_1 \dot{x}_o + x_o = \tau_1 \dot{x}_i$, which has right-hand-side (RHS) dynamics. Express time constant τ_1 in terms of damper constant c and spring constant k . (Hint: recognize that piston force $f_x(t)$ shown is a dependent variable, related to independent input $x_i(t)$ and output $x_o(t)$, but $f_x(t)$ should not appear in the equation of motion.)

Chapter 4 Frequency response of 1st order systems; transfer functions; general method for derivation of frequency response

© 2016 by William L. Hallauer, Jr.

4-1 Definition of frequency response

We now consider system excitation that varies with time sinusoidally, as either $\sin \omega t$ or $\cos \omega t$, and persists for an indefinitely long duration. The frequency of excitation is ω radians/sec, or $\omega/2\pi$ Hz (for hertz, which means cycles/sec, named for German physicist and engineer Heinrich Rudolf Hertz, 1857-1894). After any transients due to initial conditions have decayed away, a stable linear system responds in the same sinusoidal fashion. That is, the *steady-state* response of a stable linear system to sinusoidal excitation also varies sinusoidally, as either $\sin(\omega t + \phi)$ or $\cos(\omega t + \phi)$, where the frequency ω is the same as the excitation frequency, and ϕ is a *phase angle*. This steady-state sinusoidal response is generally called *frequency response*. Although the frequency of response is the same as that of excitation, the magnitude of response can vary greatly for different excitation frequencies; therefore, in order to prevent the overloading of a system, it is important to know the frequencies of excitation to which the system is most sensitive.

Both mathematical and experimental analyses of system frequency response are common in engineering practice. We shall study the basic methods of mathematical analysis. The two primary unknowns in the analysis are the magnitude and phase of response as functions of excitation frequency. We can consider the excitation to vary as either $\sin \omega t$ or $\cos \omega t$; the steady-state frequency response magnitude and phase are the same in either case. For consistency, we will consider primarily $\cos \omega t$ excitation.

4-2 Response of a 1st order system to a suddenly applied cosine, $\cos \omega t$

First, we derive a complete solution in the conventional manner for the original standard 1st order ODE $\dot{x} - ax = bu(t)$ [Eq. (1-1)], with IC $x(0) = x_0$, and with the suddenly applied (at $t = 0$) cosine input $u(t) = U \cos \omega t$, $t > 0$, where U is a constant amplitude [Problem 2.12(b)].

$$\text{ODE + IC: } \dot{x} - ax = bU \cos \omega t = bU \frac{e^{j\omega t} + e^{-j\omega t}}{2}, x(0) = x_0, \text{ find } x(t) \text{ for } t > 0 \quad (4-1)$$

$$\text{Laplace transformation of ODE + IC: } sX(s) - x_0 - aX(s) = \frac{bU}{2} \left(\frac{1}{s - j\omega} + \frac{1}{s + j\omega} \right)$$

Chapter 4 Frequency response of 1st order systems; transfer functions; derivation of freq. response

$$\text{Solve for } X(s): \quad X(s) = \frac{x_0}{s-a} + \frac{bU}{2} \frac{1}{(s-a)} \left(\frac{1}{s-j\omega} + \frac{1}{s+j\omega} \right)$$

Completed partial-fraction expansion (Problem 2.8):

$$X(s) = \frac{x_0}{s-a} + \frac{bU}{2} \frac{1}{a^2 + \omega^2} \left(\frac{2a}{s-a} + \frac{-a-j\omega}{s-j\omega} + \frac{-a+j\omega}{s+j\omega} \right)$$

$$\text{Inverse transform: } x(t) = x_0 e^{at} + \frac{bU}{a^2 + \omega^2} \left[ae^{at} + \frac{1}{2} \left((-a - j\omega)e^{j\omega t} + (-a + j\omega)e^{-j\omega t} \right) \right]$$

$$\Rightarrow x(t) = x_0 e^{at} + \frac{bU}{a^2 + \omega^2} \left[ae^{at} + \frac{1}{2} \left((-a)(e^{j\omega t} + e^{-j\omega t}) + \omega \frac{e^{j\omega t} - e^{-j\omega t}}{j} \right) \right]$$

$$\Rightarrow x(t) = x_0 e^{at} + \frac{bU}{a^2 + \omega^2} \left(ae^{at} - a \cos \omega t + \omega \sin \omega t \right), t \geq 0$$

$$\Rightarrow x(t) = x_0 e^{at} + \left(\frac{b}{-a} \right) \frac{U}{1 + \left(\frac{\omega}{-a} \right)^2} \left[-e^{at} + \cos \omega t + \left(\frac{\omega}{-a} \right) \sin \omega t \right], t \geq 0 \quad (4-2)$$

Next, we adapt solution (4-2) of general 1st order problem (4-1) to the damper-spring system (ideal shock strut) of Fig. 3-9 with suddenly applied cosine force input $f_x(t) = F \cos \omega t$, for which the comparable ODE + IC problem is

$$c\dot{x} + kx = F \cos \omega t, \quad x(0) = x_0, \quad \text{find position } x(t) \text{ for } t > 0 \quad (4-3)$$

Comparing (4-3) with (4-1), we define $U \equiv F$, then the other constants of the standard equation become

$$a = -\frac{k}{c} \equiv -\frac{1}{\tau_1} \Rightarrow \text{time constant } \tau_1 \equiv \frac{1}{-a} = \frac{c}{k} \quad \text{and} \quad b = \frac{1}{c} \quad \text{and} \quad \frac{b}{-a} = \frac{1}{k}$$

$$\Rightarrow x(t) = x_0 e^{-t/\tau_1} + \frac{F}{k} \left(\frac{1}{1 + (\omega \tau_1)^2} \right) \left(-e^{-t/\tau_1} + \cos \omega t + \omega \tau_1 \sin \omega t \right), t \geq 0 \quad (4-4)$$

It is instructive to study the physical nature of response (4-4) in the context of a specific numerical example. Consider an ideal shock strut with the initial condition $x_0 = -2$ m, and with the system parameters $c = 1/\pi$ N/(m/sec) = 0.3183 N-sec/m and $k = 1$ N/m, so that time constant $\tau_1 = 1/\pi$ sec = 0.3183 sec. Let the magnitude of the cosine

Chapter 4 Frequency response of 1st order systems; transfer functions; derivation of freq. response

force be $F = 1.5$ N, and let the *period* of the cosine be $T_p = 1$ sec/cycle. Therefore, the cyclic frequency is $f = 1$ Hz (cycle/sec), and the circular frequency is $\omega = 2\pi$ radians/sec. (Period, frequency, and phase of periodic signals are discussed more generally in Section 4-4.) The numerical solution of Eq. (4-4) with these parameters for time $0 \leq t \leq 3$ sec is calculated and graphed in the following MATLAB operations.

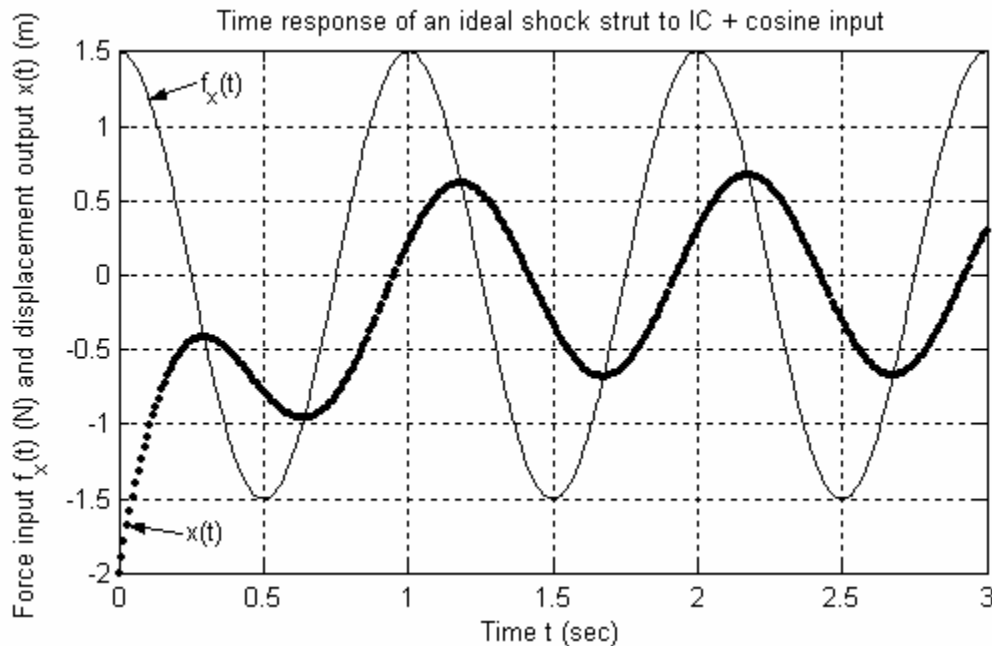
MATLAB M-file script:

```
%MATLABdemo41.m
%Damper-spring ideal shock strut response to IC + cosine forcing
c=1/pi;k=1; %system viscous damping & stiffness constants, SI units
F=1.5;Tp=1; %cosine forcing: amplitude (N), period (sec)
xo=-2; %initial displacement (m)
w=2*pi/Tp; %circular frequency of cosine forcing (rad/sec)
t1=c/k;denom=1+(w*t1)^2;
t=0:0.01:3*Tp; %time instants for forced response
fx=F*cos(w*t);
x=(xo-(F/k)/denom)*exp(-t/t1)+(F/k)/denom*(cos(w*t)+w*t1*sin(w*t));
plot(t,fx,'k',t,x,'k.'),grid,xlabel('Time t (sec)'),...
ylabel('Force input f_x(t) (N) and displacement output x(t) (m)'),...
title('Time response of an ideal shock strut to IC + cosine input')
```

MATLAB command/responses:

```
>> MATLABdemo41
```

The graph of input $f_x(t)$ and response $x(t)$ is below (after figure editing in MATLAB, Version 6 or later, to flatten the aspect ratio and to distinguish the two curves).



Chapter 4 Frequency response of 1st order systems; transfer functions; derivation of freq. response

Let's observe from the graph some important features of the response:

* As calculated above, the time constant of the exponential decay terms in Eq. (4-4) [the two terms involving $\exp(-t/\tau_1)$] is $\tau_1 = 0.3183$ sec, so the settling time for those terms is $4\tau_1 = 1.273$ sec. In other words, the exponential decay terms in $x(t)$ have essentially vanished after about 1.3 sec of response, and this is clear from the graph. Because the exponential decay terms are relatively short-lived, we often refer to them as the “transient” part of the total solution.

* After the exponential decay terms have vanished, only the $\cos \omega t$ and $\sin \omega t$ terms of Eq. (4-4) remain. It appears from the graph that those two terms combine to make a single sinusoid at frequency ω , and that the remaining *steady-state* $x(t)$ sinusoid is displaced in time by a constant *time lag* from the $f_x(t)$ sinusoid. This steady-state sinusoidal response is what we call the frequency response, and we will derive equations that describe it explicitly in the remainder of the chapter.

4-3 Frequency response of the 1st order damper-spring system

To extract the steady-state sinusoidal response $x_{ss}(t)$ from total response equation (4-4), we drop the transient, exponential decay terms:

$$x_{ss}(t) = \frac{F}{k} \left(\frac{1}{1 + (\omega\tau_1)^2} \right) (\cos \omega t + \omega\tau_1 \sin \omega t) \quad (4-5)$$

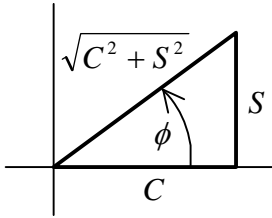
We can write (4-5) in a form that is more physically expressive by using some algebraic manipulation and the general trigonometric identity,

$$\cos \theta \times \cos \phi - \sin \theta \times \sin \phi = \cos(\theta + \phi) \quad (4-6)$$

The algebraic manipulation involves the sinusoidally varying terms of (4-5). For generality, let's assume that each term is multiplied by a general coefficient, C or $-S$, so that those terms can be written and manipulated as

$$C \cos \omega t - S \sin \omega t = \sqrt{C^2 + S^2} \left(\cos \omega t \frac{C}{\sqrt{C^2 + S^2}} - \sin \omega t \frac{S}{\sqrt{C^2 + S^2}} \right)$$

Now we identify the coefficients of $\cos \omega t$ and $\sin \omega t$ inside parentheses as themselves representing trigonometric functions: $\frac{C}{\sqrt{C^2 + S^2}} \equiv \cos \phi$ and $\frac{S}{\sqrt{C^2 + S^2}} \equiv \sin \phi$, where angle ϕ is given by a four-quadrant tangent function,



$$\phi = \tan^{-1}\left(\frac{S}{C}\right) \quad (4-7)$$

These trigonometric relations are illustrated at left on the drawing of a right triangle.

So, with identity (4-6), the trigonometric sum becomes

$$C \cos \omega t - S \sin \omega t = \sqrt{C^2 + S^2} (\cos \omega t \cos \phi - \sin \omega t \sin \phi) = \sqrt{C^2 + S^2} \cos(\omega t + \phi) \quad (4-8)$$

Associating (4-5) with (4-8), we have $C = 1$, $S = -\omega \tau_1$. Therefore, (4-5) becomes

$$x_{ss}(t) = \frac{F}{k} \left(\frac{1}{1 + (\omega \tau_1)^2} \right) \sqrt{1 + (\omega \tau_1)^2} \cos(\omega t + \phi)$$

$$x_{ss}(t) = \frac{F}{k} \frac{1}{\sqrt{1 + (\omega \tau_1)^2}} \cos(\omega t + \phi) = X(\omega) \cos(\omega t + \phi(\omega)), \quad \phi(\omega) = \tan^{-1}\left(\frac{-\omega \tau_1}{1}\right) \quad (4-9)$$

Let's compare the steady-state response (output), $x_{ss}(t)$ of Eq. (4-9), with the excitation (input), $f_x(t) = F \cos \omega t$. The *magnitude* of response, which is a function of excitation frequency ω , is

$$X(\omega) = \frac{F}{k} \frac{1}{\sqrt{1 + (\omega \tau_1)^2}} \quad (4-10)$$

We will often deal with the *magnitude ratio*, defined as the magnitude of response divided by the magnitude of excitation,

$$\frac{X(\omega)}{F} = \frac{1}{k} \frac{1}{\sqrt{1 + (\omega \tau_1)^2}} \quad (4-11)$$

The *phase* (or *phase angle*, since it is an angle in radians or degrees) of response relative to the phase of the excitation is also a function of excitation frequency ω :

$$\phi(\omega) = \tan^{-1}(-\omega \tau_1) \quad (4-12)$$

In general, if phase angle ϕ is positive, $0^\circ < \phi < 180^\circ$, it is called a phase *lead*, because the peaks and zeros of the response occur in time before those of the excitation. If phase angle ϕ is negative, $-180^\circ \leq \phi < 0^\circ$, it is called a phase *lag*, because the peaks and zeros of the response occur in time after those of the excitation. The response is said to be *in-*

Chapter 4 Frequency response of 1st order systems; transfer functions; derivation of freq. response

phase if $\phi = 0^\circ$ exactly, and *out-of-phase* if $\phi = -180^\circ$ exactly. For the standard stable 1st order system considered presently, $\phi(\omega) = \tan^{-1}(-\omega\tau_1)$, which is a phase lag, always negative in the 4th quadrant, $-90^\circ < \phi < 0^\circ$, with $\phi \rightarrow 0^\circ$ for very small ω and $\phi \rightarrow -90^\circ$ for very large ω .

The *frequency-response function* (abbreviated FRF) is considered to consist of both the magnitude ratio, Eq. (4-11) in this case, and the phase angle, Eq. (4-12) in this case. We will see later that both of these functions can be expressed together in a mathematical equation as a single complex function of frequency. It is common in engineering practice to plot these two real functions of frequency ω on a pair of over-and-under graphs in the format of Fig. 4-1, which represents Eqs. (4-11) and (4-12) specifically. This format is a type of *Bode diagram* (after Hendrik Wade Bode, American mathematician, physicist, and control-system engineer, 1905-1982).

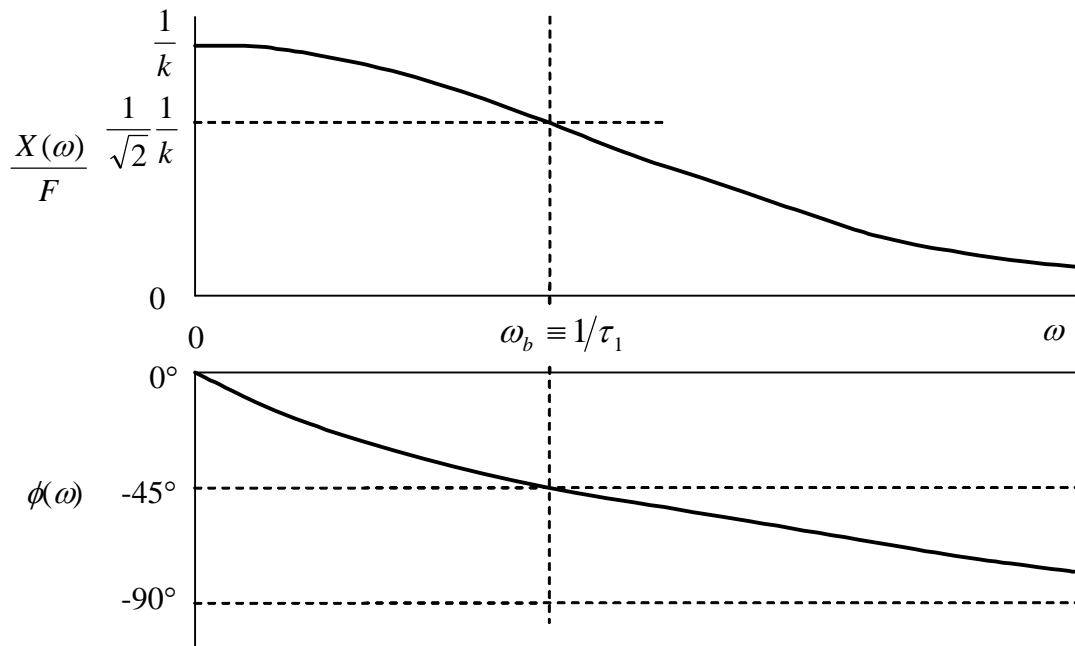


Figure 4-1 Frequency-response function of 1st order damper-spring system

The *break frequency* $\omega_b \equiv 1/\tau_1$ is shown explicitly on Fig. 4-1. There is no obvious “break” in the curves of Fig. 4-1; but a break does indeed exist, the form of which will be revealed in the following discussion.

To represent frequency response over broad bands of frequency, the magnitude ratio and phase are often plotted versus the logarithm of frequency. Moreover, to allow the possibility of very large dynamic ranges of magnitude response, the magnitude ratio itself is often plotted on a logarithmic scale, making the magnitude ratio a log-log graph, where “log” denotes logarithm to the base 10. On such a graph, it is often possible to construct straight-line asymptotes that are useful for describing the variation with frequency of the magnitude. To illustrate this for the 1st order system, we re-write (4-11) as

Chapter 4 Frequency response of 1st order systems; transfer functions; derivation of freq. response

a dimensionless ratio and, for clarity of expression, use the definition $\omega_b \equiv 1/\tau_1$, and then take the logarithm:

$$\frac{X(\omega)}{F/k} = \frac{1}{\sqrt{1+(\omega\tau_1)^2}} = \frac{1}{\sqrt{1+(\omega/\omega_b)^2}} = \frac{1}{\sqrt{1+(f/f_b)^2}} \quad (4-13a)$$

$$\log\left(\frac{X(\omega)}{F/k}\right) = \log\left(\frac{1}{\sqrt{1+(\omega/\omega_b)^2}}\right) = -\frac{1}{2}\log\left[1+\left(\frac{\omega}{\omega_b}\right)^2\right] = -\frac{1}{2}\log\left[1+\left(\frac{f}{f_b}\right)^2\right] \quad (4-13b)$$

In the last versions on the right-hand sides of Eqs. (4-13a and b), we have used $\omega \equiv 2\pi f$ and $\omega_b \equiv 2\pi f_b$ in order to express the equation in terms of cyclic frequency. The *low-frequency asymptote* is the limit of (4-13b) as the frequency $\rightarrow 0$ from above:

$$\lim_{\omega \rightarrow 0} \left[\log\left(\frac{X(\omega)}{F/k}\right) \right] = -\frac{1}{2}\log(1) = 0 \quad (4-14)$$

The *high-frequency asymptote* is the limit of (4-13b) as the frequency $\rightarrow \infty$ from below:

$$\lim_{\omega \rightarrow \infty} \left[\log\left(\frac{X(\omega)}{F/k}\right) \right] = -\frac{1}{2}\log\left[\left(\frac{\omega}{\omega_b}\right)^2\right] = -\log\left(\frac{\omega}{\omega_b}\right) = -\log\left(\frac{f}{f_b}\right) \quad (4-15)$$

Figure 4-2 on the next page is a log-log graph of Eqs. (4-13) that shows the asymptotes (4-14) and (4-15). Notice that on the log-log scale, the low-frequency asymptote is a good approximation for the actual function at frequencies $f < f_b$, and the high-frequency asymptote is a good approximation for the actual function at frequencies $f > f_b$. The intersection of the two asymptotes is called the *break* (or *corner*) because it is a change in slope of the asymptotic approximations to the actual function. The *break* (or *corner*) frequency is denoted f_b . For this 1st order system at $f_b = \omega_b/2\pi = 1/(2\pi\tau_1)$, the magnitude of response is reduced to $1/\sqrt{2}$ of its static ($f=0$) value, and the phase is -45° (see also Fig. 4-1).

The high-frequency asymptote on Fig. 4-2 merits some additional comment. Note that its slope on the log-log scale equals -1 , i.e., the magnitude shrinks one decade (order of magnitude) for each decade increase in the frequency. Frequency response magnitude ratios are often given in *decibels* (dB), especially in acoustics for sound pressure level. A magnitude ratio in *decibels* is defined to be $20 \times \log(\text{magnitude ratio})$. If the magnitude ratio on Fig. 4-2 had been plotted in decibels versus log(frequency), then the slope of the high-frequency asymptote would be -20 ; this is often referred to as a 20 dB/decade roll-off of the magnitude ratio.

Chapter 4 Frequency response of 1st order systems; transfer functions; derivation of freq. response

Another observation worth making, especially from Fig. 4-2, is that the standard 1st order system considered here behaves like a mild *low-pass filter*: the system responds most sensitively to excitation at frequencies below the break frequency, the magnitude of response being about equal to the static response. However, at excitation frequencies above the break frequency, the system responds much less sensitively, and the magnitude of response diminishes progressively as the excitation frequency increases.

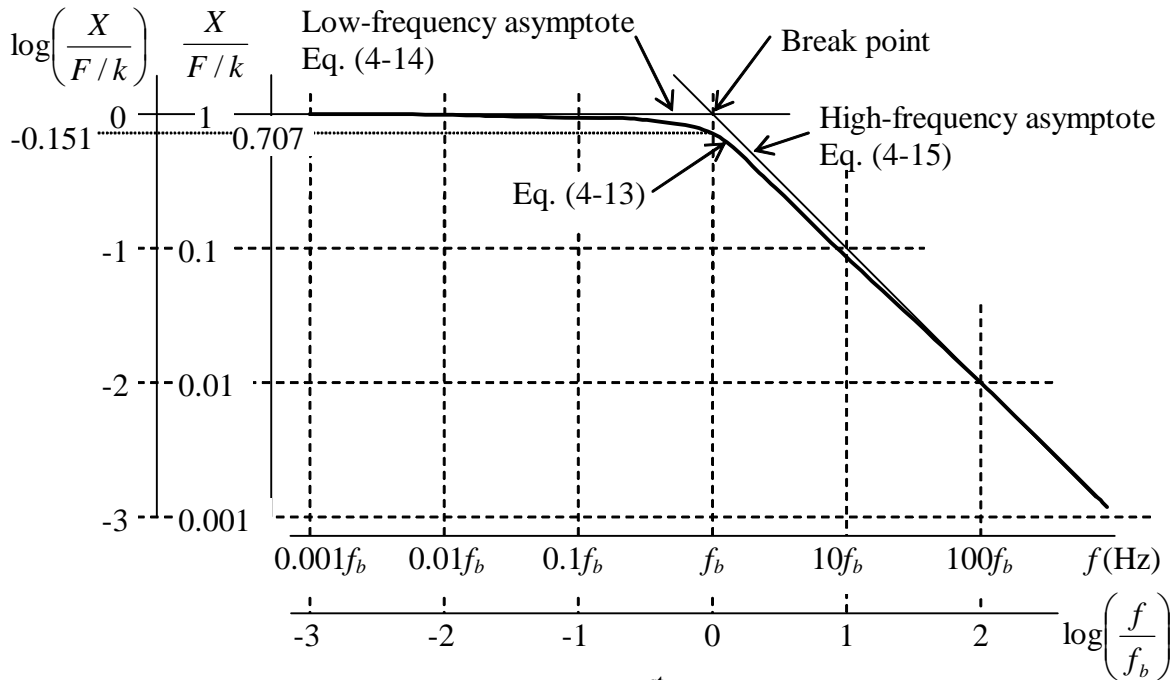


Figure 4-2 Log-log magnitude ratio of 1st order damper-spring system

4-4 Period, frequency, and phase of periodic signals

Let's consider more generally the temporal quantities of periodic signals, represented in our applications by sinusoids. Period T_p is normally measured in seconds per cycle, so the cyclic frequency f in cycles per second is the inverse of period, $f = 1/T_p$. Also, the period is related to the circular frequency ω by $\omega T_p = 2\pi$ radians, so that

$$\text{circular frequency } \omega = \frac{2\pi}{T_p} \equiv 2\pi f \frac{\text{rad}}{\text{sec}}, \text{ and cyclic frequency } f = \frac{\omega}{2\pi} \text{ Hz} \left(\frac{\text{cycles}}{\text{sec}} \right) \quad (4-16)$$

These relationships between period and frequency are worth understanding completely and even memorizing, as we use them a great deal in system dynamics.

It is important also to understand how FRF phase is manifested in time history plots of input and output. This discussion is general, applicable for any LTI system. Suppose that there are plotted on the same graph steady-state sinusoidal time histories of both the input $u(t)$ and the output $x(t)$, as in Fig. 4-3 on the next page. We want to calculate

Chapter 4 Frequency response of 1st order systems; transfer functions; derivation of freq. response

the FRF phase from measurements on the time-history plots. First, find the nearest positive $x(t)$ crest to the left of a reference positive $u(t)$ crest, as shown on Fig. 4-3. Measure the positive time interval T_{lead} in seconds that $x(t)$ leads $u(t)$. (Note that you can measure T_{lead} also by comparing troughs or positive-going or negative-going zeros, as shown on Fig. 4-3.)

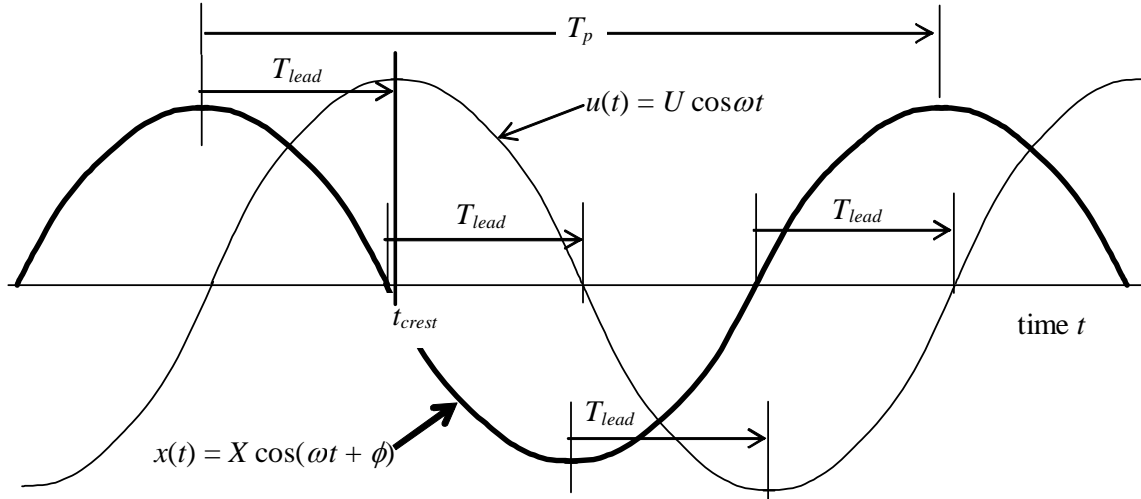


Figure 4-3 Frequency response phase measurement from time-history graphs

Now, referring to the positive crests, let's denote as t_{crest} the instant corresponding to a positive crest of input $u(t)$. Then we see from the drawing that

$$\cos \omega t_{crest} = +1 \Rightarrow \omega t_{crest} = 2\pi n, \text{ where } n \text{ is some integer}$$

$$\cos(\omega[t_{crest} - T_{lead}] + \phi) = +1 \Rightarrow \omega[t_{crest} - T_{lead}] + \phi = 2\pi n$$

Comparing these two equations shows that $\omega[-T_{lead}] + \phi = 0$, which gives the basic equation for phase angle (defined positive as a lead, negative as a lag):

$$\phi = \omega T_{lead} = \frac{2\pi}{T_p} T_{lead} = 2\pi \frac{T_{lead}}{T_p} \text{ rad} \times \frac{360 \text{ deg}}{2\pi \text{ rad}} = 360 \times \frac{T_{lead}}{T_p} \text{ deg} \quad (4-17a)$$

where $T_p (= 2\pi/\omega = 1/f)$ is the period of the input and the steady-state output, as shown on Fig. 4-3.

If you choose to select the nearest positive $x(t)$ crest to the right of a reference $u(t)$ crest, then you are finding time lag T_{lag} , which is a negative lead. In this case, you can find the phase angle, with the correct sign, from

$$\phi = -\omega T_{lag} = -360 \times \frac{T_{lag}}{T_p} \text{ deg} \quad (4-17b)$$

Equations (4-17) give ϕ in the range $0^\circ \leq \phi < 360^\circ$, which is correct but not common. It is not common because the four-quadrant arctangent is conventionally expressed (in MATLAB, for example) in the range $-180^\circ \leq \phi < +180^\circ$. Therefore, if you measure and calculate by the procedure above a phase $\phi \geq +180^\circ$, then it is conventional to replace that ϕ with $(\phi - 360^\circ)$. For example, if you were to measure and calculate the phase $\phi = 262^\circ$, then it would be conventional to express it as a phase lag, $\phi = (262^\circ - 360^\circ) = -98^\circ$, rather than a phase lead of 262° .

4-5 Easy derivation of the complex frequency-response function for standard stable 1st order systems

This section is an example of a much easier method (than that of Sections 4-2 and 4-3) for deriving the frequency-response function of a system. Let's find the frequency response of standard stable 1st order systems. From Eq. (3-7) the standard stable ODE with sinusoidal excitation is

$$\dot{x} + (1/\tau_1)x = bu(t) = bU \cos \omega t$$

We seek steady-state sinusoidal response $x_{ss}(t) = X(\omega) \cos(\omega t + \phi(\omega))$, in which $X(\omega)$ and $\phi(\omega)$ are functions to be found. The first step in the method is to take the general [for arbitrary $u(t)$] Laplace transform, setting the IC to zero:

$$(s + 1/\tau_1)L[x(t)]|_{x_0=0} = bL[u(t)]$$

Next, we form the system general *transfer function*, $TF(s)$, defined as the ratio of the output transform to the input transform, with zero IC:

$$TF(s) \equiv \frac{L[x(t)]|_{x_0=0}}{L[u(t)]} = \frac{b}{s + 1/\tau_1}$$

The Laplace independent variable s is complex in general. However, in order to analyze frequency response, we let s in $TF(s)$ be purely imaginary, $s = j\omega$ (ω being the real circular frequency), producing the complex *frequency-response function* $FRF(\omega)$:

$$TF(s)|_{s=j\omega} \equiv TF(j\omega) \equiv FRF(\omega) = \frac{b}{1/\tau_1 + j\omega} = b\tau_1 \frac{1}{1 + j\omega\tau_1} \quad (4-18a)$$

Next, with use of Eqs. (2-4)-(2-7), we convert $TF(j\omega) \equiv FRF(\omega)$ algebraically into polar form:

Chapter 4 Frequency response of 1st order systems; transfer functions; derivation of freq. response

$$FRF(\omega) = b\tau_1 \frac{1}{1+j\omega\tau_1} \times \frac{1-j\omega\tau_1}{1-j\omega\tau_1} = b\tau_1 \frac{\sqrt{1+(\omega\tau_1)^2}}{1+(\omega\tau_1)^2} \exp\left[j \tan^{-1}\left(\frac{-\omega\tau_1}{1}\right)\right] \quad (4-18b)$$

$$\equiv |FRF(\omega)| e^{j\angle FRF(\omega)} = \frac{b\tau_1}{\sqrt{1+(\omega\tau_1)^2}} e^{j\phi(\omega)}$$

in which phase angle $\phi(\omega) = \tan^{-1}(-\omega\tau_1/1) = \tan^{-1}(-\omega\tau_1)$.

Equations (4-18) define the complex frequency-response function, $FRF(\omega)$, of standard stable 1st order systems. It is proved in Sections 4-6 and 4-7 for LTI systems in general that the real magnitude $|FRF(\omega)|$ of function $FRF(\omega)$ is the magnitude ratio of system frequency response, and the phase angle $\phi(\omega)$ of function $FRF(\omega)$ is the phase angle of system frequency response. For example, let's adapt standard solution (4-18b) to the damper-spring system, for which [from Eq. (4-3)] $b = 1/c$ and $\tau_1 = c/k$. Thus, the magnitude of $FRF(\omega)$ from (4-18b) is

$$|FRF(\omega)| = \frac{X(\omega)}{U} = \frac{b\tau_1}{\sqrt{1+(\omega\tau_1)^2}} = \frac{1}{k} \frac{1}{\sqrt{1+(\omega\tau_1)^2}} \quad (4-19)$$

which is identical to damper-spring system FRF magnitude ratio $X(\omega)/F$ of Eq. (4-11). Also, the phase angle of $FRF(\omega)$ from (4-18b) is

$$\angle FRF(\omega) = \phi(\omega) = \tan^{-1}(-\omega\tau_1) \quad (4-20)$$

which is identical to damper-spring system FRF phase $\phi(\omega)$ of Eq. (4-12). Thus, with $FRF(\omega)$ of Eq. (4-18b), we have obtained here the same final results as before for the damper-spring system, but much more easily.

4-6 Transfer function, general definition

For any LTI, single-input-single-output (SISO) physical system, we denote the input as $u(t)$ and the output as $x(t)$. For an n^{th} order system, in general, the input and output are related by an ODE of the form

$$a_1 \frac{d^n x}{dt^n} + a_2 \frac{d^{n-1} x}{dt^{n-1}} + \dots + a_{n+1} x = b_1 \frac{d^m u}{dt^m} + b_2 \frac{d^{m-1} u}{dt^{m-1}} + \dots + b_{m+1} u \quad (4-21)$$

a_1, \dots, a_{n+1} and b_1, \dots, b_{m+1} are constants (with the numbering system keyed to MATLAB notation), and $m \leq n$. Also, we assume that the system is *stable*, which is defined more precisely in Section 4-7. Taking the Laplace transform of the ODE, with all ICs equal to zero, gives

Chapter 4 Frequency response of 1st order systems; transfer functions; derivation of freq. response

$$(a_1 s^n + a_2 s^{n-1} + \dots + a_{n+1}) L[x(t)]_{ICs=0} = (b_1 s^m + b_2 s^{m-1} + \dots + b_{m+1}) L[u(t)] \quad (4-22)$$

Then, from (4-22), the system *transfer function*, defined to be the ratio of the output transform to the input transform, with zero ICs, is the ratio of two polynomials,

$$TF(s) \equiv \frac{L[x(t)]_{ICs=0}}{L[u(t)]} = \frac{b_1 s^m + b_2 s^{m-1} + \dots + b_{m+1}}{a_1 s^n + a_2 s^{n-1} + \dots + a_{n+1}} \quad (4-23)$$

It is appropriate to state here (without proof) that the transfer function of any physically realizable system has $m \leq n$, i.e., the degree of the numerator polynomial is less than or equal to the degree of the denominator polynomial. The condition $m \leq n$ makes the transfer function *causal*, which means that the current (in time) output of the system is dependent only upon past and present (not future) values of the input. In general, the future values of an input cannot be predicted, so it is logical that a real system and its transfer function must be causal. See Bélanger, 1995, page 440.

Note also from Eq. (4-23) that, if given $TF(s)$ and input $u(t)$, we can express the transform of the output with zero initial conditions as

$$L[x(t)]_{ICs=0} = TF(s) \times L[u(t)] \quad (4-24)$$

4-7 Frequency-response function from transfer function, general derivation

For frequency response of a general LTI SISO stable system, we define the input to be a time-varying cosine, with amplitude U and circular frequency ω ,

$$u(t) = U \cos \omega t = \frac{U}{2} (e^{j\omega t} + e^{-j\omega t}) \quad (4-25)$$

in which we apply the complex exponential form for the cosine that is derived from Euler's equation (Problem 2.1). The Laplace transform of input (4-25) is

$$L[u(t)] = \frac{U}{2} \left(\frac{1}{s - j\omega} + \frac{1}{s + j\omega} \right) \quad (4-26)$$

Substituting (4-23) and (4-26) into (4-24) gives

$$L[x(t)]_{ICs=0} = \left(\frac{b_1 s^m + b_2 s^{m-1} + \dots + b_{m+1}}{a_1 s^n + a_2 s^{n-1} + \dots + a_{n+1}} \right) \frac{U}{2} \left(\frac{1}{s - j\omega} + \frac{1}{s + j\omega} \right) \quad (4-27)$$

By expanding into partial fractions, we will usually be able to cast (4-27) into the form

Chapter 4 Frequency response of 1st order systems; transfer functions; derivation of freq. response

$$L[x(t)]_{|CS=0} = \frac{A}{s - j\omega} + \frac{B}{s + j\omega} + \sum_{k=1}^n \frac{C_k}{s - p_k} \quad (4-28)$$

in which A , B , C_k , and p_k [the poles of $TF(s)$] all are constants. Taking the inverse transform of (4-28) gives

$$x(t) = Ae^{j\omega t} + Be^{-j\omega t} + \sum_{k=1}^n C_k e^{p_k t} \quad (4-29)$$

The first two right-hand-side terms of (4-29) are associated with steady-state forced sinusoidal response, and the third term is associated with response bounded by real exponential functions. The nature of system stability is determined by the poles p_k , in particular, by their real parts. If $\text{Re}[p_k] < 0$ for all $k = 1, 2, \dots, n$, then each of the $e^{p_k t}$ terms is bounded by a decaying exponential, that is, $e^{p_k t} \rightarrow 0$ as $t \rightarrow \infty$. A system for which $\text{Re}[p_k] < 0$ for all k is said to be stable. Therefore, for steady-state sinusoidal response (after all exponentially bounded transients have decayed) of a stable system, only the first two right-hand-side terms of (4-29) remain,

$$x_{ss}(t) = Ae^{j\omega t} + Be^{-j\omega t} \quad (4-30)$$

Our objective now is to find the complex constants A and B in (4-30). The first step is to recognize that $x_{ss}(t)$ must be a real function mathematically; that is, in order to represent actual physical behavior, (4-30) cannot have any imaginary component. From Problem 2.5, we conclude that B must be the complex conjugate of A , *i.e.*, $B = \bar{A}$. Therefore, (4-30) becomes

$$x_{ss}(t) = Ae^{j\omega t} + \bar{A}e^{-j\omega t} \quad (4-31)$$

The Laplace transform of (4-31) is

$$L[x_{ss}(t)] = \frac{A}{s - j\omega} + \frac{\bar{A}}{s + j\omega} \quad (4-32)$$

Recognizing that we seek only constant A for the steady-state sinusoidal response (not any of the C_k constants associated with transient response), we now combine (4-32) and (4-26) into (4-24),

$$L[x_{ss}(t)] = \frac{A}{s - j\omega} + \frac{\bar{A}}{s + j\omega} = TF(s) \frac{U}{2} \left(\frac{1}{s - j\omega} + \frac{1}{s + j\omega} \right) \quad (4-33)$$

Chapter 4 Frequency response of 1st order systems; transfer functions; derivation of freq. response

To find complex constant A and its conjugate, we use the labor-saving method for partial-fraction expansion from Chapter 2,

$$A = \left[(s - j\omega)TF(s) \frac{U}{2} \left(\frac{1}{s - j\omega} + \frac{1}{s + j\omega} \right) \right]_{s=j\omega} = \frac{U}{2} TF(j\omega) \quad (4-34)$$

$$\bar{A} = \left[(s + j\omega)TF(s) \frac{U}{2} \left(\frac{1}{s - j\omega} + \frac{1}{s + j\omega} \right) \right]_{s=-j\omega} = \frac{U}{2} TF(-j\omega) \quad (4-35)$$

Comparing (4-34) and (4-35) shows that

$$TF(-j\omega) = \overline{TF(j\omega)} \quad (4-36)$$

So now we can denote the transfer function terms in general polar form:

$$TF(j\omega) = |TF(j\omega)| e^{j\phi(\omega)}, \text{ where the phase is } \phi(\omega) = \angle[TF(j\omega)] \quad (4-37)$$

$$TF(-j\omega) = |TF(j\omega)| e^{-j\phi(\omega)} \quad (4-38)$$

Substituting (4-37), (4-38), (4-34), and (4-35) back into (4-31) gives

$$x_{ss}(t) = Ae^{j\omega t} + \bar{A}e^{-j\omega t} = \frac{U}{2} |TF(j\omega)| \left\{ e^{j(\omega t + \phi(\omega))} + e^{-j(\omega t + \phi(\omega))} \right\} \quad (4-39)$$

Applying again the formula from Euler's equation that relates the cosine to complex exponentials gives the desired final result,

$$\begin{aligned} x_{ss}(t) &= U |TF(j\omega)| \cos(\omega t + \phi(\omega)) \\ &\equiv X(\omega) \cos(\omega t + \phi(\omega)) \end{aligned} \quad (4-40)$$

in which $X(\omega)$ and $\phi(\omega)$ are, respectively, the amplitude (magnitude) and phase of the steady-state sinusoidal response. Note that $|TF(j\omega)| = X(\omega)/U$, the magnitude ratio.

Therefore, we define the complex frequency-response function $FRF(\omega)$ to be $TF(j\omega)$, (4-37). Expressing $FRF(\omega)$ in polar form gives us the FRF magnitude ratio and phase directly, and relatively easily (without all the work of finding the particular solution of the ODE by the method of undetermined coefficients, or of finding the complete time response by forward and inverse Laplace transformation, etc.):

$$FRF(\omega) \equiv TF(j\omega) = \frac{X(\omega)}{U} e^{j\phi(\omega)} \quad (4-41)$$

This result is general for LTI SISO systems, it is valid for all of the systems considered in this book, and it is widely used in engineering practice.

4-8 Homework problems for Chapter 4

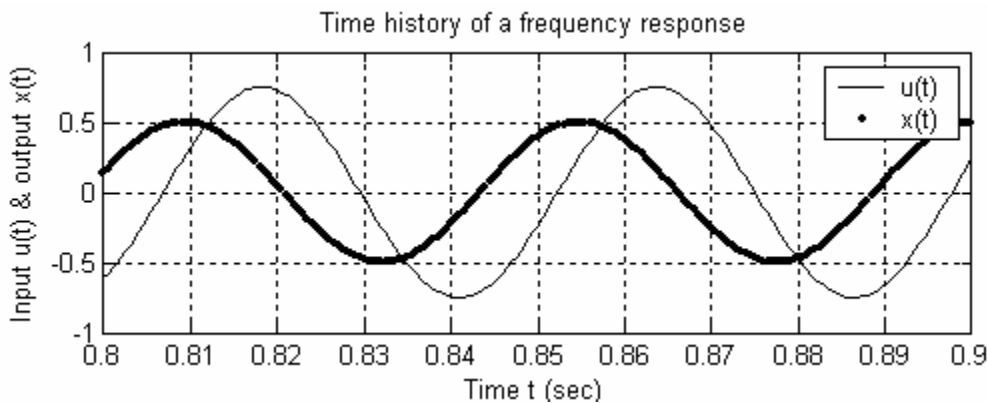
4.1 This problem involves the data and results for the 1st order damper-spring system that is analyzed in Section 4-2 with use of MATLAB program `MATLABdemo41`.

(a) Substitute the damper-spring data and the given values of F and ω into Eqs. (4-10) and (4-12) in order to calculate the magnitude X and phase angle ϕ (in degrees, in the range $-180^\circ \leq \phi < +180^\circ$) of the frequency response.

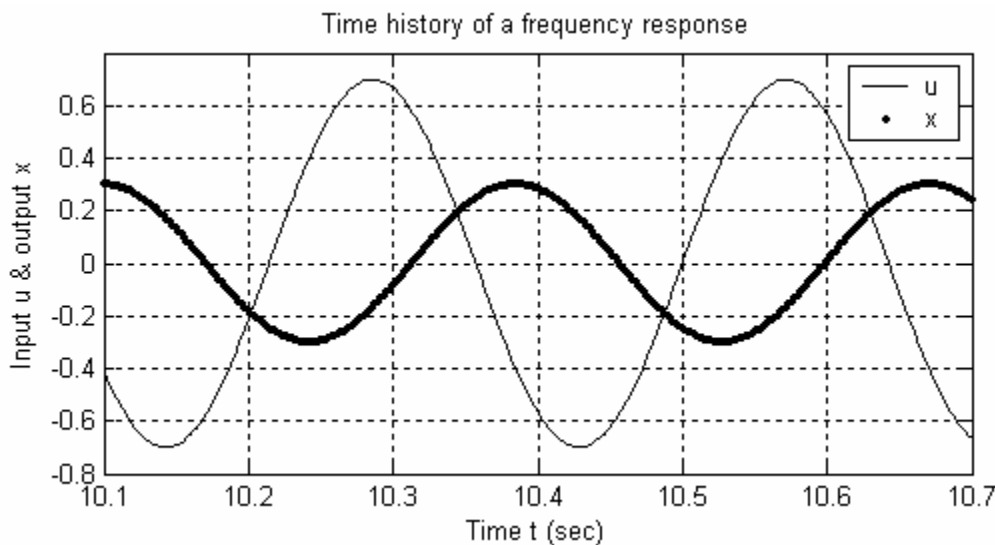
(b) Examine the time history graph generated by MATLAB program `MATLABdemo41`. The purpose of this problem is for you to evaluate that graph as if it were recorded from an experiment. Consider, in particular, the time after about $t = 1.3$ sec, when the output has settled into steady-state sinusoidal response. Measure from the graph the steady-state output magnitude X . Measure whatever information is required from the graph, then calculate phase angle ϕ (in degrees, in the range $-180^\circ \leq \phi < +180^\circ$) of the steady-state state response. These simulated experimental results for X and ϕ should be equal to (or at least close to, since it is not possible to make precise measurements from a graph) the comparable results calculated in part (a) from theoretical formulas.

4.2 An experimental frequency response test is conducted on an LTI system (not necessarily a 1st order system), with input $u(t) = U \cos \omega t$ and output $x(t) = X \cos(\omega t + \phi)$. A simulated graph [(a) or (b) or (c), whichever is assigned] of the steady-state input and output quantities at one particular frequency is shown below or on the next page. Calculate from the graph, with as much accuracy as the data permits, the following values: (i) the sinusoidal period T_p , and then the frequency (in both Hz and rad/sec), (ii) the FRF magnitude ratio X/U (assume consistent physical units), and (iii) the FRF phase ϕ (in degrees, in the range $-180^\circ \leq \phi < +180^\circ$).

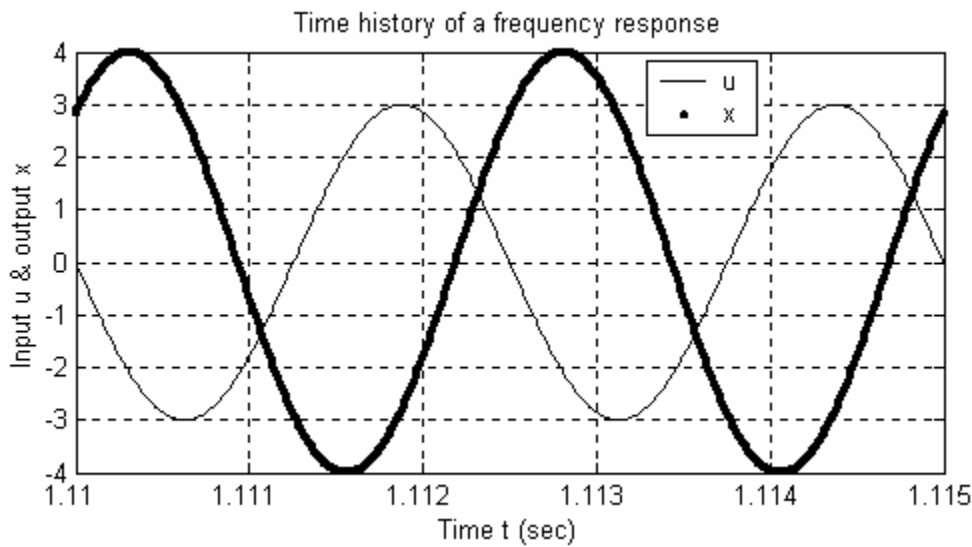
(a)



(b)



(c)



4.3 The governing ODE of the series damper-spring low-pass filter in Fig. 3-12 is Eq. (3-23), $\tau_1 \dot{x}_o + x_o = x_i(t)$. Show that the associated 1st order complex frequency-response function is $FRF(\omega) = TF(j\omega) = 1/(1 + j\omega\tau_1)$. The following MATLAB script graphs from this equation the FRF magnitude ratio and phase in one conventional format (log-log for magnitude ratio, semilog for phase in degrees, magnitude ratio graph directly over phase graph), for the case of time constant $\tau_1 = 0.0145$ sec, with excitation frequencies ranging from 1 Hz to 1,000 Hz. Note that MATLAB does most of the work for you if you start with the complex FRF, and then use MATLAB's capability for performing complex arithmetic. In particular, the MATLAB function `abs` calculates the absolute value (magnitude) of a complex number, and the MATLAB function `angle` calculates the angle in radians of a complex number.

Chapter 4 Frequency response of 1st order systems; transfer functions; derivation of freq. response

```
t1=0.0145; % First-order system time constant (sec)
f=logspace(0,3,200);w=2*pi*f; % 200 pts. 1 Hz-1 kHz evenly spaced on log scale
FRF=1./(1+j*w*t1); % complex FRF; note necessity of array operation ./
magrat=abs(FRF);fazdeg=angle(FRF)*180/pi; % magnitude ratio and phase in deg
subplot(2,1,1),loglog(f,magrat,'k'),grid,ylabel('FRF magnitude ratio'), ...
title('FRF of 1st order system with time constant = 0.0145 sec')
subplot(2,1,2),semilogx(f,fazdeg,'k'),grid, ...
ylabel('FRF phase (deg)'),xlabel('Frequency (Hz)')
```

Run this script on your computer, and submit the graphs that it produces. Additionally, **(a)** calculate the break frequency $f_b = 1/(2\pi\tau_1)$ and show that it matches the break frequency inferred from the MATLAB graphs; **(b)** use complex arithmetic to evaluate by hand (and hand calculator) the complex FRF, $FRF(\omega) = \frac{1}{1 + j\omega\tau_1}$, at frequency $f = 30$ Hz, and show that your hand-calculated magnitude ratio and phase match those of MATLAB. You might have occasion to do more graphing of FRFs, so, for your future reference, make sure that you understand the operations of all the MATLAB commands in the above script.

4.4 The governing ODE of the series damper-spring high-pass filter in Fig. 3-12 is Eq. (3-24), $\dot{x}_o + (1/\tau_1)x_o = \dot{x}_i(t)$ [see also homework Problem 3.7].

- (a)** Show that the associated 1st order high-pass filter complex frequency-response function is $FRF(\omega) = j\omega\tau_1/(1 + j\omega\tau_1)$.
- (b)** For frequency response, we are evaluating the input in the form $x_i(t) = X_i \cos \omega t$ and the output in the form $x_o(t) = X_o \cos(\omega t + \phi)$. Use the FRF of part (a) to show that the equations for FRF magnitude ratio and phase are

$$\frac{X_o(\omega)}{X_i} = \frac{\omega\tau_1}{\sqrt{1 + (\omega\tau_1)^2}}, \quad \phi(\omega) = \frac{\pi}{2} - \tan^{-1}(\omega\tau_1) = \tan^{-1}\left(\frac{1}{\omega\tau_1}\right)$$

Use this magnitude ratio equation to derive equations for the low-frequency and high-frequency asymptotes, and sketch those asymptotes on a log-log graph such as Fig. 4-2. You may use the definition of break frequency, $\omega_b = 1/\tau_1$, so that $\omega\tau_1 = \omega/\omega_b = f/f_b$. This system has the character of a mild *high-pass filter*, so your sketch of the asymptotes should have the appearance appropriate to that name.

- (c)** Let the time constant $\tau_1 = 1$ sec, and consider the excitation frequency range $0.01 \leq \omega \leq 100$ rad/sec ($10^{-2} \leq \omega \leq 10^2$ rad/sec). Adapt the MATLAB program, and use the graphical format provided in homework Problem 4.3 to graph with MATLAB the FRF magnitude ratio and phase (in degrees). As is done in Problem 4.3, program directly the complex FRF, in this case $FRF(\omega) = j\omega\tau_1/(1 + j\omega\tau_1)$, not the equations of part (c).

Chapter 4 Frequency response of 1st order systems; transfer functions; derivation of freq. response

4.5 A standard LTI mass-damper-spring system has the ordinary differential equation of motion $m\ddot{x} + c\dot{x} + kx = f_x(t)$, in which $f_x(t)$ is the input and $x(t)$ is the output.

- (a) Use the ODE to derive the transfer function $TF(s) \equiv L[x(t)]_{ICs=0} / L[f_x(t)]$ for the m - c - k system. This transfer function is an algebraic equation in terms of independent variable s and constants m , c , and k .
- (b) Use transfer function $TF(s)$ to derive the complex frequency-response function $FRF(\omega)$ for the m - c - k system in terms of independent variable frequency ω and constants m , c , and k .
- (c) From $FRF(\omega)$ for the m - c - k system, write equations in terms of independent variable frequency ω and constants m , c , and k for the real magnitude ratio $|FRF(\omega)|$ and the real phase angle $\angle FRF(\omega) = \phi(\omega)$.

Chapter 5 Basic electrical components and circuits

© 2016 by William L. Hallauer, Jr.

5-1 Introduction

Electrical circuits are systems that have many dynamic response characteristics in common with mechanical systems. But electrical variables (voltage, current, charge) and circuits are quite different physically than mechanical variables and systems, and the physical laws and methods for deriving ordinary differential equations that describe behaviors of electrical circuits also are entirely different. This chapter is an introduction to the theory of electrical circuits and basic analog electronics, and to some common but simple practical applications of the theory. The material presented here provides the basis for many examples of system dynamic behavior in later chapters.

Many engineering students in fields other than electrical engineering are exposed to electrical theory only in a required introductory physics course. This presentation is designed for such engineers who, nevertheless, have applications for simple circuits and electronics. For example, almost every engineer who works with electromechanical systems will at some time require at least the background in circuits and electronics that is presented in this chapter. The same is true for almost every engineer who uses sensors of any kind, or is involved with testing of prototypes or products in the laboratory or in the field. Even the process of logically evaluating for possible purchase the capabilities and specifications of modern electronic instrumentation requires more sophistication with circuits and electronics than a student can acquire from an introductory physics course.

5-2 Passive components: resistor, capacitor, and inductor

We denote the electrical potential, the *voltage* in volts (V) SI units, at a point in a circuit as $e(t)$, and the flow of positively charged particles, the *electrical current* in amps (A) SI units, as $i(t)$. These two electrical quantities are the principal variables that will appear in derivations of the ODEs describing the dynamic behavior of circuits.

The circuit drawn in Fig. 5-1 depicts an ideal linear *resistor*, with resistance R ohms (usually denoted by the upper-case omega, Ω) in SI units. The voltage difference

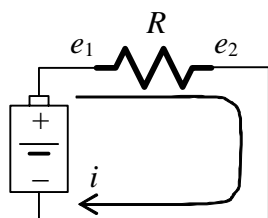


Figure 5-1 Resistor in a simple circuit

(Halliday and Resnick, 1960, Sections 31-2 and 31-3). This relationship is known as

$e_1 - e_2$ between the positive and negative terminals of a battery causes current i to flow through the resistor. The material of the resistor is an electrical conductor, but a poor conductor that provides much more resistance to current flow than a good conductor such as copper wire. This resistance converts part of the electrical energy into heat energy, causing the resistor's temperature to rise slightly. For a standard, commercially produced resistor, the relationship between $e_1 - e_2$ and i is linear, with resistance R defined as the constant of proportionality

Chapter 5 Basic electrical components and circuits

Ohm's law (after German physicist Georg Simon Ohm, 1787-1854), and it is usually expressed in one of the following two forms:

$$e_1 - e_2 = iR \Rightarrow i = \frac{e_1 - e_2}{R} \quad (5-1)$$

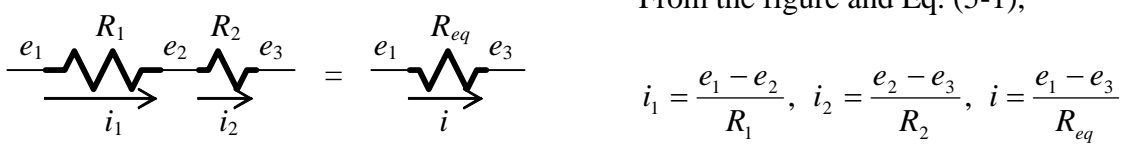
Equation (5-1) applies at each instant, even if the voltages and the current are varying with time.

Note from Ohm's law the unit equivalence $\Omega = V/A$; this relation giving the ohm in terms of the volt and the amp is useful for establishing correct units in calculations. Suppose, for example, that a 10-volt difference is imposed across a $5\text{ k}\Omega$ resistor, typical numbers for instrumentation circuits. Then, from (5-1), the current through the resistor is

$$i = \frac{10\text{ V}}{5 \times 10^3 \text{ V/A}} = 2\text{e-}3 \text{ A} \equiv 2 \text{ mA.}$$

The following two examples serve to introduce a fundamental physical principle for electrical circuits, *Kirchhoff's current law* (abbreviated "KCL", after German physicist Gustav Robert Kirchhoff, 1824-1887), and to illustrate applications of KCL.

Electricity Example 5-1: Given resistors R_1 and R_2 arranged in *series*, as in the figure below, find the equivalent single resistance R_{eq} .



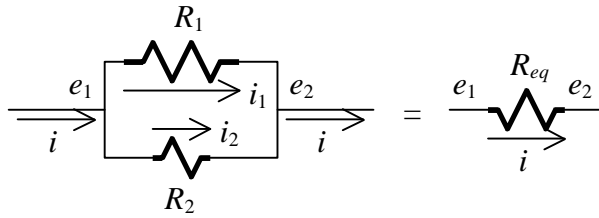
The form of KCL relevant to this situation is: *the quantity of current is continuous in a series arrangement*, so that $i_1 = i_2 \equiv i$. [This *continuity* condition for electrical current is directly analogous to the continuity condition for an incompressible fluid: the volume flow rate (average velocity \times cross-sectional area) remains constant at all points along a flow tube or channel.] The total voltage change is the sum of the individual changes,

$$e_1 - e_3 = (e_1 - e_2) + (e_2 - e_3) = i_1 R_1 + i_2 R_2 = i(R_1 + R_2)$$

$$\Rightarrow i = \frac{e_1 - e_3}{R_1 + R_2} \Rightarrow R_{eq} = R_1 + R_2$$

The resistance of a series combination of resistors is the sum of the individual resistances.

Electricity Example 5-2: Given resistors R_1 and R_2 arranged in *parallel*, as in the figure below, find the equivalent single resistance R_{eq} .



In this case, there are circuit junctions on both sides of the parallel resistors. The more general KCL applicable here is: *the quantity of current leaving a junction equals the quantity of current entering the junction*, so that $i_1 + i_2 = i$.

The voltage difference is the same across each of the parallel resistors, so KCL in terms of voltage differences is

$$\frac{e_1 - e_2}{R_1} + \frac{e_1 - e_2}{R_2} = \frac{e_1 - e_2}{R_{eq}} \Rightarrow \frac{1}{R_1} + \frac{1}{R_2} = \frac{1}{R_{eq}} = \frac{R_1 + R_2}{R_1 R_2} \Rightarrow R_{eq} = \frac{R_1 R_2}{R_1 + R_2}$$

The equivalent (effective) resistance is less than the smaller of the two parallel resistances.

The circuit drawn in Fig. 5-2 depicts a linear *capacitor*, with capacitance C farad (F) in SI units. A voltage generator produces the possibly time-varying voltage difference $e_1 - e_2$ across the capacitor. The graphical symbol representing the capacitor depicts two plates separated by a dielectric (insulating) material. If there is a voltage difference between the plates of such a component, a positive electrical charge $+q$ coulombs (SI unit) appears on one plate, and a negative electrical charge $-q$ coulombs appears on the other plate (Halliday and Resnick, 1960, Section 30-2). The quantity of charge q is proportional to the voltage difference, with capacitance C defined as the constant of proportionality:

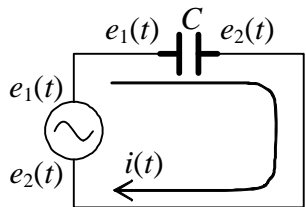


Figure 5-2 Capacitor in a simple circuit

The graphical symbol representing the capacitor depicts two plates separated by a dielectric (insulating) material. If there is a voltage difference between the plates of such a component, a positive electrical charge $+q$ coulombs (SI unit) appears on one plate, and a negative electrical charge $-q$ coulombs appears on the other plate (Halliday and Resnick, 1960, Section 30-2). The quantity of charge q is proportional to the voltage difference, with capacitance C defined as the constant of proportionality:

$$q = C(e_1 - e_2) \quad (5-2)$$

If the voltage difference is constant, then the charge on the plates remains constant, so that there is no flow of charged particles, *i.e.*, no current, which is the variation with time of the charge: $i(t) = \frac{dq}{dt}$. However, if the voltage varies with time, then current flows through the circuit in proportion with the derivative of the voltage difference:

$$i(t) = \frac{dq}{dt} = C \frac{d(e_1 - e_2)}{dt} = C(\dot{e}_1 - \dot{e}_2) \quad (5-3)$$

Conversely, the voltage difference across the capacitor can be expressed in terms of the current by integrating (5-3) from initial time t_0 (when ICs are assumed to be known) to arbitrary time $t > t_0$:

$$\int_{\tau=t_0}^{\tau=t} i(\tau) d\tau = C \int_{\tau=t_0}^{\tau=t} \frac{d(e_1 - e_2)}{d\tau} d\tau = C [(e_1 - e_2)|_t - (e_1 - e_2)|_{t_0}]$$

$$\Rightarrow e_1(t) - e_2(t) = e_1(t_0) - e_2(t_0) + \frac{1}{C} \int_{\tau=t_0}^{\tau=t} i(\tau) d\tau \quad (5-4)$$

Note from Eq. (5-3) the unit equivalence $A = F \times \frac{V}{sec} \Rightarrow F = \frac{A - sec}{V}$; this relation for the farad in terms of the amp, the volt, and the second is useful for clarifying units in calculations. Suppose, for example, that an instrumentation circuit contains a capacitor with $C = 0.25 \mu F = 0.25e-6 F$, a typical value. If, at a particular instant, the voltage across the capacitor is changing at the rate 6,000 V/sec, then the current through the capacitor is, from (5-3), $i = \left(0.25 \times 10^{-6} \frac{A - sec}{V}\right) \times \left(6 \times 10^3 \frac{V}{sec}\right) = 1.5 \times 10^{-3} A \equiv 1.5 \text{ mA}$.

Electricity Example 5-3: 1st order, RC low-pass filter circuit

This is a circuit containing both a resistor and a capacitor. The input voltage signal produced by some source is denoted $e_i(t)$, and the output, filtered signal is denoted $e_o(t)$. Figure 5-3 depicts this filter graphically in both the simple closed-circuit form on

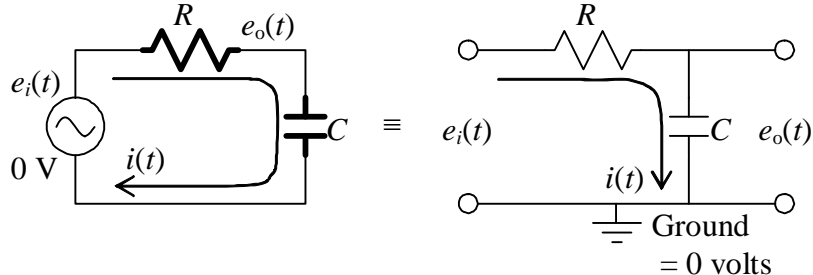


Figure 5-3 RC low-pass filter circuit

the left, and the more modern form on the right, in which the common ground (reference) potential is denoted by a special symbol and is assigned the value zero volts, to which all other circuit voltages are referenced. The input and output terminals are denoted by small circles. Note, in particular, that the output terminals are isolated away from the current-carrying portion of the circuit; this represents the realistic situation in which the filter output voltage is the input to some other circuit that has a very high input resistance, thereby essentially preventing any input current. This downstream circuit could be some measuring instrument (oscilloscope, voltmeter, etc.), or another stage of a larger circuit of which the *RC* circuit is just one part. Note also that this *RC* circuit, and any upstream circuit at its input, and any downstream circuit at its output, all must be referenced to the same ground voltage, which is constant and is the “zero” voltage relative to the other voltages in the circuit; this is an important requirement for practical circuits.

In order to derive the ODE describing the dynamics of this *RC* low-pass filter, we use Eq. (5-1) for current i_R through the resistor, and Eq. (5-3) for current i_C through the capacitor: $i_R = \frac{e_i - e_o}{R}$, $i_C = C(\dot{e}_o - \dot{e}_i) = C\dot{e}_o$. The resistor and capacitor are in series, so Kirchhoff's current law relevant to this situation is $i_C = i_R$:

$$\frac{e_i - e_o}{R} = C\dot{e}_o \Rightarrow \dot{e}_o + \frac{1}{RC}e_o = \frac{1}{RC}e_i \Rightarrow \dot{e}_o + \frac{1}{\tau_1}e_o = \frac{1}{\tau_1}e_i \quad (5-5)$$

in which $\tau_1 \equiv RC$ is the 1st order time constant.

Given ICs on output voltage $e_o(t)$ and given input voltage $e_i(t)$, we can in principle solve Eq. (5-5) for $e_o(t)$ using the mathematical methods discussed previously. In particular, frequency response is the dynamic behavior that is of greatest practical interest for any circuit designed to be a filter. For frequency response, the input voltage is $e_i(t) = E_i \cos \omega t$ and the steady-state sinusoidal output voltage is $e_o(t) = E_o(\omega) \times \cos(\omega t + \phi(\omega))$. Let's find the frequency response simply by adapting a previously derived standard solution. First, we compare Eq. (5-5) with Eq. (3-7), $\dot{x} + (1/\tau_1)x = bu(t)$, which is the standard ODE for stable 1st order systems. If we define $u(t) = U \cos \omega t \equiv e_i(t) \Rightarrow U \equiv E_i$, then the other constant of the standard equation becomes $b = 1/\tau_1$. Therefore, the standard FRF magnitude ratio (4-19) is adapted as

$$\frac{X(\omega)}{U} = \frac{b\tau_1}{\sqrt{1+(\omega\tau_1)^2}} = \frac{E_o(\omega)}{E_i} = \frac{1}{\sqrt{1+(\omega\tau_1)^2}} = \frac{1}{\sqrt{1+(\omega/\omega_b)^2}} \quad (5-5.5)$$

and the standard FRF phase (4-20) is adapted as $\phi(\omega) = \tan^{-1}(-\omega\tau_1) = \tan^{-1}(-\omega/\omega_b)$, in which the break frequency is $\omega_b = 1/\tau_1 = 1/RC = 2\pi f_b$. Figure 5-4 (adapted from Fig. 4-2) is the log-log graph of magnitude ratio versus frequency, which clearly shows the low-pass character of the frequency response.

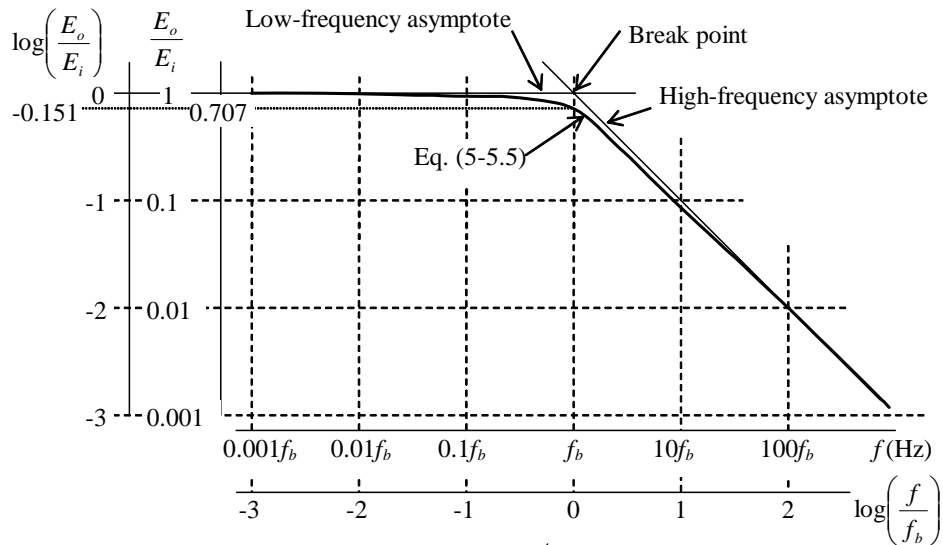
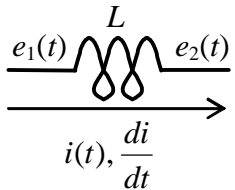


Figure 5-4 Log-log magnitude ratio of 1st order *RC* low-pass filter
5-5

The governing ODE of the mechanical series damper-spring low-pass filter in Fig. 3-12 is Eq. (3-23), $\tau_1 \dot{x}_o + x_o = x_i(t)$ (see also homework Problem 4.3), which has exactly the same form as Eq. (5-5). Accordingly, the electrical low-pass filter is an exact electrical analog of the mechanical low-pass filter, input voltage $e_i(t)$ being directly analogous to input translation $x_i(t)$, output voltage $e_o(t)$ to output translation $x_o(t)$, and electrical time constant $\tau_1 = RC$ to mechanical time constant $\tau_1 = c/k$.

The passive electrical component drawn in Fig. 5-5 represents an ideal linear *inductor*, with inductance L henry (H) in SI units. A time-varying current $i(t)$ is shown



flowing through the inductor. The graphical symbol denoting the inductor depicts a coil of conducting wire. If the current is changing with time in such a coil, then a voltage difference appears across the coil, a voltage difference that opposes the current change (Halliday and Resnick, 1960, Sections 36-1 and 36-3). This voltage difference is called a *self-induced emf* (electromotive force); it is a manifestation of the interaction between

electricity and magnetism that is described by Maxwell's equations of electromagnetism (after Scottish physicist James Clerk Maxwell, 1831-1879). The self-induced emf is proportional to the rate of change of current, with inductance L defined as the constant of proportionality:

$$e_1 - e_2 = L \frac{di}{dt} \quad (5-6)$$

You might find it difficult to perceive how Eq. (5-6) represents physically a voltage difference that opposes current change di/dt . If so, then the following example should illustrate this characteristic more understandably.

Electricity Example 5-4: 1st order LR circuit

Real inductors are not used in instrumentation circuits nearly as often as resistors and capacitors. Moreover, there is no such thing as the ideal inductor instrumentation component of Fig. 5-5. Because an inductor component consists primarily of coiled wire,

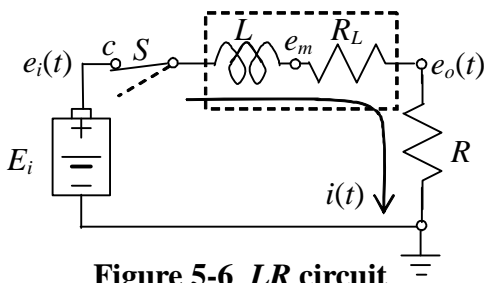


Figure 5-6 LR circuit

and because a considerable length of very fine wire accumulates resistance, a real inductor usually has non-negligible resistance as well as inductance. A common, simple, approximate circuit model for such a real inductor is a series combination of an ideal inductor and a resistor, L and R_L in the circuit of Fig. 5-6. In this circuit, $e_i(t)$ is the input voltage (after switch S is closed to position c), and $e_o(t)$ is the output voltage. R is a resistor placed between the inductor and

ground to permit sensing (by an oscilloscope, for example) of $e_o(t)$, which is directly related to the current by $e_o(t) = R i(t)$.

Next, we derive an ODE governing the dynamic behavior of the *LR* circuit in Fig. 5-6. Observe that the derivative of current, di/dt , appears in Eq. (5-6), unlike Eq. (5-1) for a resistor and Eq. (5-3) for capacitor, in which equations current $i(t)$ appears directly. Because of this, it is usually not convenient to apply Kirchhoff's current law for a circuit containing an inductor. It is usually better for such a circuit to apply *Kirchhoff's voltage law* (abbreviated "KVL"): *the sum of all voltage rises around a circuit loop is zero*. If we proceed around the circuit loop in the direction of defined positive current flow, then the "voltage rise" across any component (including the input voltage generator and every passive component) is defined to be the upstream voltage minus the downstream voltage. To write KVL for this *LR* circuit, we start at the input voltage generator and proceed clockwise:

$$(e_i - 0) + (e_m - e_i) + (e_o - e_m) + (0 - e_o) = 0 \quad (5-7)$$

Kirchhoff's voltage law is a fundamental law of circuits, but note that it also is just an algebraic identity. Next, we substitute Eq. (5-6) and Ohm's law into Eq. (5-7):

$$(e_i - 0) + \left(-L \frac{di}{dt} \right) + (-R_L i) + (-R i) = 0 \Rightarrow L \frac{di}{dt} + (R_L + R)i = e_i(t) \quad (5-8)$$

Equation (5-8) is a stable 1st order LTI ODE solvable for arbitrary input voltage $e_i(t)$. For example, suppose that all ICs = 0 and that the input voltage is a step, $e_i(t) = E_i H(t)$, which is accomplished with use of a battery and a switch, as shown in Fig. 5-6. Comparing (5-8) with standard stable 1st order ODE (3-7), we adapt the standard step-response solution (3-8), with $e_i(t) \equiv u(t)$ so that $E_i \equiv U$, to write the electrical response quantities as

$$i(t) = \frac{E_i}{R_L + R} \left(1 - e^{-t/\tau_1} \right), \quad 0 \leq t \quad \text{in which} \quad \tau_1 = \frac{L}{R_L + R} \quad (5-9a)$$

$$\Rightarrow e_o(t) = R i(t) = \frac{R}{R_L + R} E_i \left(1 - e^{-t/\tau_1} \right) \equiv E_o \left(1 - e^{-t/\tau_1} \right), \quad E_o \equiv \frac{R}{R_L + R} E_i \quad (5-9b)$$

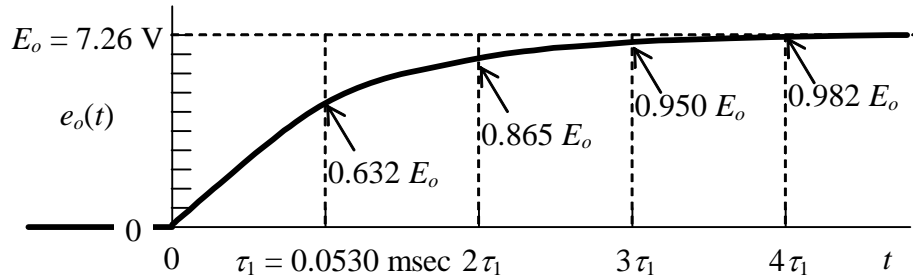
Step response Eqs. (5-9) clearly show the effect of the inductance in opposing and delaying the rise of current flow. If the inductor were not present (*i.e.*, if $L = 0$) in the circuit of Fig. 5-6, then the circuit would be a simple voltage divider (Problem 5.1), and the full step-response output voltage would be achieved instantly, $e_o(t) = E_o H(t)$, instead of rising gradually as in (5-9b).

The response of this circuit illustrates the physical effect of the inductor's self-induced emf, Eq. (5-6). In this circuit, the inductor's upstream voltage is constrained to be the input, $e_i(t)$, so the self-induced emf must act in $e_m(t)$, the voltage at the inductor's downstream terminal. It is helpful to derive from Eqs. (5-7)-(5-9) the equation for that

voltage, $e_m(t) = e_o(t) + R_L i(t) = E_i(1 - e^{-t/\tau_1})$, and the equation for the rate of change of current, $di/dt = (E_i/L)e^{-t/\tau_1}$. At time $t = 0+$ (just after switch S is closed to position c), we have $di/dt(0+) = E_i/L > 0$ but $e_m(0+) = 0$ and $i(0+) = 0$. Thus, at this instant, the inductor holds its downstream voltage at zero and prevents the current from rising instantaneously as a step function, which it would do if the inductor were not present. After time $t = 0+$, the current gradually rises, but at a declining rate, and the current increase is still opposed by the inductor downstream voltage, which also rises at the same declining rate.

From Eq. (5-6), we have the unit equivalence $V = H \times \frac{A}{sec} \Rightarrow H = \frac{V - sec}{A}$;

this relation for the henry is useful for clarifying units in calculations, as shown in the following example. A particular “voice coil” is to be used in an electromagnetic force actuator; this is the type of wire coil found in the speakers of consumer sound systems. We wish to identify experimentally for this coil the parameters L and R_L (based upon the series model of Electricity Example 4) by measuring the step response of the circuit of Fig. 5-6. For this particular circuit, the sensing resistor has $R = 17.5 \Omega$, and the battery voltage is 9.00 V. We close switch S, then record the subsequent time-history graphical response onto the screen of a digital oscilloscope, which stores the data for analysis. The response graph (below) has the appearance of Fig. 3-3, and we measure from it the time



constant $\tau_1 = 0.0530$ msec and the final value of output voltage $E_o = 7.26$ V. From the equations for τ_1 in (5-9a) and E_o in (5-9b), we derive the following equations for the required parameters L and R_L , and then the subsequent calculated values:

$$L = (R_L + R)\tau_1 = \left(\frac{R}{E_o} E_i \right) \tau_1 \\ = \frac{E_i}{E_o} R \tau_1 = \left(\frac{9.00 \text{ V}}{7.26 \text{ V}} \right) \left(17.5 \frac{\text{V}}{\text{A}} \right) (0.0530 \times 10^{-3} \text{ sec}) = 1.15 \times 10^{-3} \frac{\text{V - sec}}{\text{A}} \equiv 1.15 \text{ mH}$$

$$R_L = \frac{R}{E_o} E_i - R = R \left(\frac{E_i}{E_o} - 1 \right) = (17.5 \Omega) \left(\frac{9.00 \text{ V}}{7.26 \text{ V}} - 1 \right) = 4.19 \Omega$$

5-3 Operational amplifier (op-amp) and op-amp circuits

Figure 5-7 is the standard graphical symbol for an operational amplifier (op-amp). An op-amp has a “positive” input port that accepts input voltage e_{ip} , and a “negative” input port that accepts input voltage e_{in} . The symbols e_{ip} and e_{in} are merely labels; they are not meant to restrict the polarities of these input voltages, each of which can be either positive or negative relative to the ground potential.

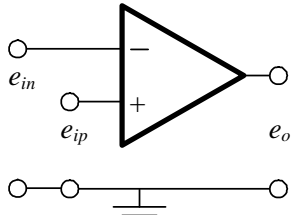


Figure 5-7 Operational amplifier (op-amp)

An op-amp has a single output voltage, labeled e_o on Fig. 5-7. The fundamental ideal output-to-input relationship of an op-amp is (Horowitz and Hill, 1980, Chapter 3)

$$e_o = K(e_{ip} - e_{in}) \quad (5-10)$$

In Eq. (5-10), gain K is a very large positive number, on the order of 10^5 to 10^6 for common, commercially available op-amps. The exact value of K varies gradually with the frequency of signals e_{ip} and e_{in} , but this variation is not important provided that frequency is below a known upper value; as we shall see, a very important characteristic is that K is large, $K \geq O(10^5)$. (This equation is a common mathematical expression meaning “ K is on the order of or greater than 10^5 .”) Another important characteristic of an op-amp is the extremely high resistance of the input ports, on the order of $10^6 \Omega$ to $10^{12} \Omega$. The practical consequence of this high resistance is that essentially zero current can flow through the input ports.

An op-amp is an active device, requiring external power to produce high gain, unlike the simple passive elements (resistor, capacitor, and inductor) of Section 5-2. An energy source (e.g., a ± 15 -volt power supply, or a pair of 9-volt batteries) is usually connected to an op-amp, but this connection is normally not indicated on graphical representations such as Fig. 5-7. An op-amp itself is a complex integrated circuit, full of miniaturized transistors and other electrical components. The physical form of op-amp seen most commonly on circuit boards is approximately the size and similar in appearance to a basement centipede with a black body (actually, more like a 8-legged or 16-legged insect, because it has on each side four or eight metal connectors that look like legs).

Op-amps are not often used in the *open-loop* configuration of Fig. 5-7. Most op-amps can operate linearly according to Eq. (5-10) only over a limited range of $\pm E_{lim}$ on output voltage e_o . The range depends upon the energy source, but typically E_{lim} is on the order of 10 V. If the input voltages e_{ip} and e_{in} are such that (5-10) leads numerically to e_o greater than $+E_{lim}$ or less than $-E_{lim}$, then a real op-amp will limit and stick nonlinearly on either $+E_{lim}$ or $-E_{lim}$, respectively. When this happens, the op-amp is said to be *overloaded* or *saturated*. Since gain K in (5-10) is so high, the input voltage difference $e_{ip} - e_{in}$ clearly must be very small in order for the op-amp to operate in the linear range for which it is primarily designed.

To operate an op-amp in its linear range, we almost always use *feedback*. When there is an electrical connection between the output port and the negative input port, the op-amp is said to be wired in a *closed-loop* manner, with feedback from output to input, specifically in this case, *negative feedback*. This negative feedback acts to make the input voltage difference $e_{ip} - e_{in}$ so small that for practical purposes there is no difference, $e_{ip} \approx e_{in}$.

We can illustrate the practical functioning of an op-amp by analyzing in detail what is probably the most common basic circuit consisting of an op-amp and resistors,

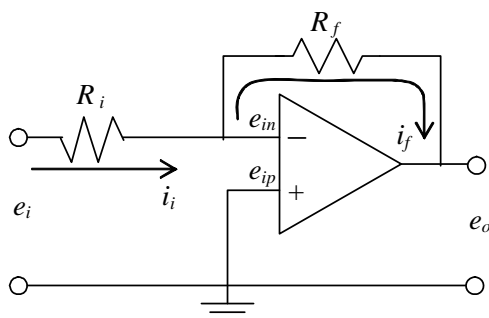


Figure 5-8 Inverting amplifier

the *inverting amplifier* depicted in Fig. 5-8. Note that there is an input resistor R_i , and that there is negative feedback through feedback resistor R_f . These resistances are chosen to be on the order of $10^1\text{-}10^4 \Omega$, at least two orders of magnitude less than the input resistances of the op-amp ports. Note also that the positive input port is grounded, $e_{ip} = 0 \text{ V}$. Hence, from Eq. (5-10),

$$e_o = K(0 - e_{in}) \Rightarrow e_{in} = -\frac{e_o}{K} \quad (5-11)$$

Due to the extremely high resistance of the negative input port relative to R_i and R_f , the current through that port is essentially zero, so Kirchhoff's current law in this case requires the feedback current to equal the input current, $i_i = i_f$. Using Ohm's law to write this condition of current continuity in terms of voltages gives

$$\frac{e_i - e_{in}}{R_i} = \frac{e_{in} - e_o}{R_f} \Rightarrow \frac{e_i - (-e_o/K)}{R_i} = \frac{(-e_o/K) - e_o}{R_f} \quad (5-12)$$

With a little algebra (which you should verify on your own), the solution of Eq. (5-12) for circuit output voltage in terms of input voltage is found to be

$$e_o = -\frac{R_f}{R_i} e_i \frac{1}{1 + \frac{1}{K} \left(1 + \frac{R_f}{R_i} \right)} \quad (5-13a)$$

Let's evaluate the denominator of the large fraction in Eq. (5-13a). In typical applications of this circuit, the resistance ratio R_f/R_i is on the order of 10^2 at most. Therefore, with gain $K = O(10^5)$, the denominator is very, very close to 1: $1 + O(10^{-3}) \approx 1$. (This validates the earlier statement that only the large magnitude of K matters, the exact value being unimportant.) So, the entire large fraction is essentially equal to one, and (5-13a) simplifies considerably to

$$e_o = -\frac{R_f}{R_i} e_i \quad (5-13b)$$

The output voltage equals the input voltage amplified by the ratio R_f/R_i , and the sign is inverted; hence the name *inverting amplifier*.

Note also, from (5-11), that the voltage at the negative input port is negligibly small relative to the output (and input) voltages:

$$e_{in} = -\frac{e_o}{K} \approx 0 = e_{ip} \text{ (the voltage of the grounded port)} \quad (5-14)$$

In other words, the op-amp's high gain drives the voltage e_{in} at the negative input port to be essentially equal to the voltage e_{ip} at the positive input port. Equation (5-14) is just a special case of the simplifying assumption that we can use in general, from Eq. (5-10),

$$e_{ip} - e_{in} = \frac{e_o}{K} \approx 0 \Rightarrow e_{in} = e_{ip} \quad (5-15)$$

In circuit analysis, Eq. (5-15) is considered a useful “rule” or “axiom” rather than just an assumption. In the future (unless directed otherwise, as for a homework or exam problem), you should always apply rule (5-15) right from the very beginning of the derivation for an op-amp circuit with negative feedback, because it simplifies the derivation so much. For example, if we use (5-15) from the beginning for the inverting amplifier, then the derivation becomes two easy steps [using $e_{in} = e_{ip} = 0$ in (5-12)]:

$$\frac{e_i - 0}{R_i} = \frac{0 - e_o}{R_f} \Rightarrow e_o = -\frac{R_f}{R_i} e_i$$

Figure 5-9 depicts an extremely simple, closed-loop op-amp circuit that is useful in practice. The input voltage signal is directed into the positive input port, and this

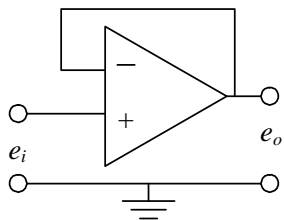


Figure 5-9 Voltage follower

port's high resistance prevents the flow of any current from the input source. Rule (5-15) in combination with the feedback connection states that the output voltage exactly equals the input voltage, $e_o = e_i$. This op-amp circuit functions as a current isolator and voltage transmitter, and it is usually called a *voltage follower*. Its main value is in providing a buffer between two different stages of a more complex circuit: the buffer allows the output voltage of the upstream stage to be the input voltage of the downstream stage, without permitting any current flow between the two stages. Any such interstage

current flow would usually cause malfunctioning of both stages. The application of a voltage follower as a buffer between circuit stages is illustrated in the next section.

5-4 RC band-pass filter

The circuit shown in Fig. 5-10 consists of a low-pass filter stage to the left of the voltage follower, and a high-pass filter stage to the right. [The functioning of a high-pass filter is illustrated in homework Problem 5.4(b)]. As indicated on Fig. 5-10, the currents in the two stages are independent of each other, by virtue of the buffering due to the voltage follower. Therefore, the simple ODEs for each type of 1st order filter are still valid for the two-stage circuit of Fig. 5-10, with mid-circuit voltage $e_m(t)$ being the quantity shared by the two stages, as the output from the low-pass stage and the input to the high-pass stage. These ODEs are Eq. (5-5) for the low-pass filter,

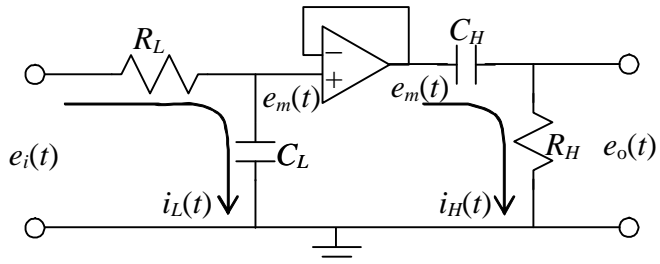


Figure 5-10 RC band-pass filter

and the ODE derived in homework Problem 5.4(a) for the high-pass filter,

$$\tau_H \dot{e}_o + e_o = \tau_H \dot{e}_m, \quad \tau_H = R_H C_H \quad (5-17)$$

An equation such as (5-17) is described as having “right-hand-side (RHS) dynamics” because the right-hand-side includes a derivative of the input (\dot{e}_m in this case), rather than just the undifferentiated input itself.

The combination of these two 1st order circuits turns out to be a 2nd order system, and we shall re-visit this subject in Sections 9-10 and 10-4. We consider the *RC* band-pass filter circuit now because it illustrates (1) application of a voltage follower, and (2) the important physical characteristic of op-amps that is described next.

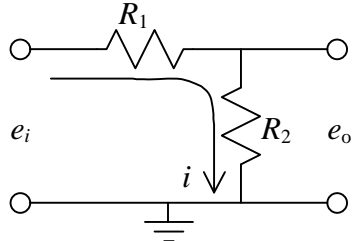
Note in Fig. 5-10 that the feedback wire across the op-amp connects directly to the negative input port; this port has essentially infinite resistance, so there cannot be any current in the feedback wire. But Fig. 5-10 also shows the non-zero, second-stage current $i_H(t)$ downstream of the op-amp; this appears to contradict the claim of zero feedback current in the op-amp, since the graphical representation of the op-amp suggests that the feedback wire is continuous electrically with the downstream circuit. **In fact, the standard graphical representation of an op-amp with negative feedback, such as that in Fig. 5-10, is oversimplified to the point of being misleading. For an actual op-amp (as opposed to the standard graphical representation), the downstream current is not continuous with the feedback current, but instead, is completely independent.** In fact, the current downstream of an op-amp is determined only by the output voltage of the

Chapter 5 Basic electrical components and circuits

op-amp and the downstream electrical components, for example, the second-stage capacitor and resistor in Fig. 5-10. The technical characteristic of an op-amp that permits this independence of currents is very low *output impedance* (Horowitz and Hill, 1980, pages 25, 92-95, and 105). For another example of the independence of feedback and downstream currents, see homework Problem 5.10.

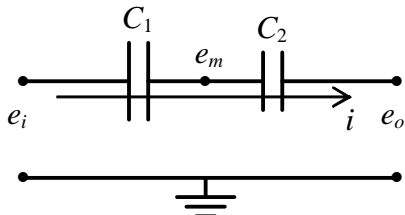
5-5 Homework problems for Chapter 5

- 5.1** The simple series circuit represented graphically below is a *voltage divider*, which is widely used in practical applications. Show that the voltage output-to-input ratio is



$$\frac{e_o}{e_i} = \frac{R_2}{R_1 + R_2}$$

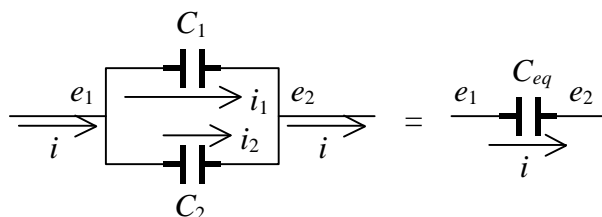
- 5.2** Two capacitors are arranged in series, as shown below.



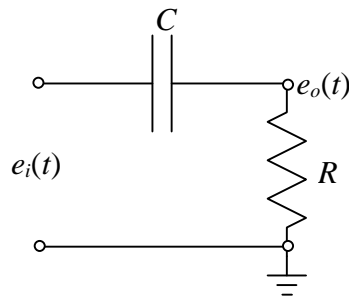
- (a) Use the current-voltage equation for capacitor C_1 to show that $\dot{e}_m = \dot{e}_i - \frac{i}{C_1}$, where the e 's are the voltages indicated on the drawing and i is the current.

- (b) Use the result of part (a) and the capacitor current-voltage equation for capacitor C_2 in order to derive an algebraic formula for the equivalent series capacitance C_{eq} (in terms of C_1 and C_2) in the equation $i = C_{eq}(\dot{e}_i - \dot{e}_o)$.

- 5.3** Given capacitors C_1 and C_2 arranged in parallel, as shown below, find the equivalent single capacitance C_{eq} .



- 5.4** The simple circuit represented graphically below is a 1st order *RC* high-pass filter.



- (a) Use current continuity and the formulas relating current to voltage-difference for resistors and capacitors to derive in all detail the following ODE with right-hand-side (RHS) dynamics, which governs the output voltage $e_o(t)$ in terms of input voltage $e_i(t)$:

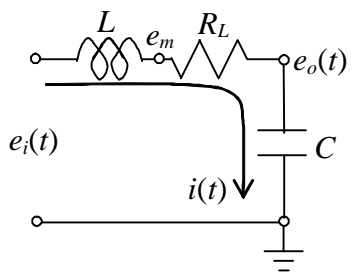
$$\dot{e}_o + \frac{1}{\tau_1} e_o = \dot{e}_i, \tau_1 = RC$$

Explain why this circuit is considered to be an exact electrical analog of the mechanical series damper-spring high-pass filter described in Fig. 3-12 and Eq. (3-24).

(b) For frequency response, the input voltage is $e_i(t) = E_i \cos \omega t$ and the steady-state output voltage is $e_o(t) = E_o \cos(\omega t + \phi)$. Use the governing equation from part (a) to derive the algebraic equations for FRF of the 1st order high-pass filter: the magnitude ratio $E_o(\omega)/E_i$ and the phase $\phi(\omega)$ (in radians) as functions of excitation frequency ω . (partial answer: $E_o(\omega)/E_i = \omega \tau_1 / \sqrt{1 + (\omega \tau_1)^2}$.) Suppose that $R = 40 \text{ k}\Omega$ and $C = 0.25 \mu\text{F}$ (recall that $\mu = 10^{-6}$). Calculate the break frequency $f_b = 1/(2\pi\tau_1)$ in Hz. To get some feeling for the functioning of a high-pass filter, calculate the FRF magnitude ratio $E_o(\omega)/E_i$ for driving frequency ratios $f/f_b = 0.01, 0.1, 1, 10, \text{ and } 100$. (See also homework Problem 4.4.)

(c) Suppose that the input voltage is a ramp, $e_i(t) = e_r(t/t_r)H(t)$, where e_r is a reference voltage and t_r is a reference time such that $e_i(t_r) = e_r$. For IC $e_o(0) = 0$ volt, solve the governing ODE from part (a) for the algebraic equation for $e_o(t)$ in terms of the given algebraic parameters. Note that the derivative of the input voltage in this case is a step function, $\dot{e}_i(t) = (e_r/t_r)H(t)$.

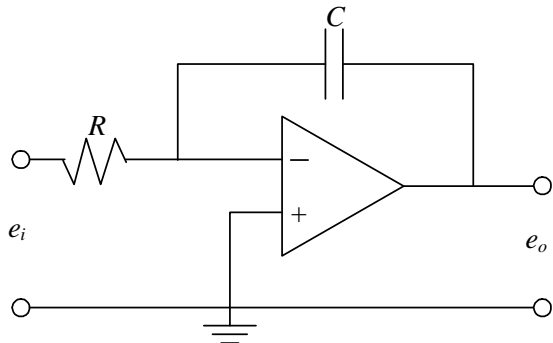
5.5 The circuit drawn below is a series combination of a voltage source $e_i(t)$, a coil



(having both inductance L and resistance R_L), and a capacitor C ; this is known as an *LRC* circuit. The input voltage is applied at time $t = 0$, at which time there is a non-zero voltage on the capacitor, $e_o(0)$. Apply Kirchhoff's voltage law, as in Electricity Example 4, and show that the equation for current $i(t)$ is $L \frac{di}{dt} + R_L i + \frac{1}{C} \int_{\tau=0}^{t} i(\tau) d\tau = e_i(t) - e_o(0)$.

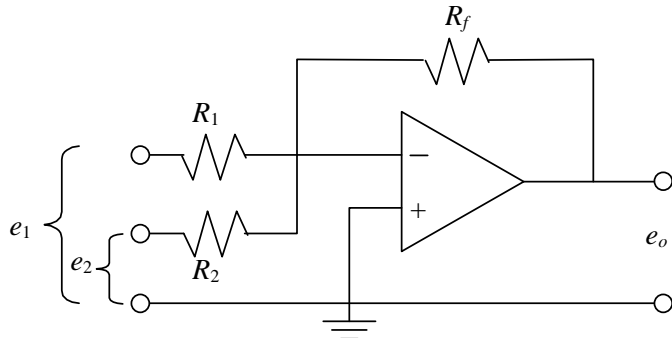
5.6 For the op-amp circuit represented graphically at right, an *integrator*, derive the algebraic equation for the transfer function between input and output voltages, $TF(s) = \frac{L[e_o(t)]}{L[e_i(t)]}$. Assume that

there is no initial charge on the capacitor at time $t = 0$. To simplify the derivation, apply rule (5-15).¹

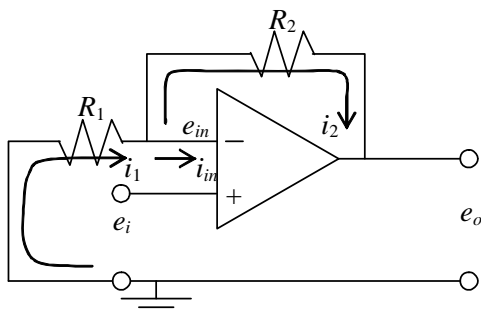


¹ This integrator seems simple on paper, but design of a real integrator that functions properly is difficult, requiring expensive, precision components and many subtle refinements of the basic circuit. Integrators based upon this circuit are essential components of the *electronic analog computer* (EAC), an elegant instrument dating from the 1940s for solving coupled ODEs, but one that has now almost completely been replaced by digital computers. Fifer's 1961 four-volume set is probably the most complete description of all types of analog computers; Peterson's 1967 textbook includes standard instructional material on EACs; and Lang's 2000 article is an interesting, more modern discussion of EACs.

- 5.7** For the op-amp circuit represented graphically below, a *summing inverting amplifier*, derive the algebraic equation for output voltage $e_o(t)$ in terms of resistances R_1 , R_2 , and R_f , and input voltages $e_1(t)$ and $e_2(t)$. To simplify the derivation, apply rule (5-15).

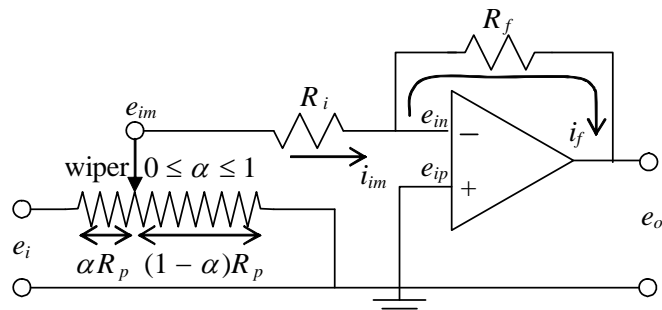


- 5.8 (a)** For the op-amp circuit represented graphically below, a *non-inverting amplifier*, derive the algebraic equation for output voltage $e_o(t)$ in terms of resistances R_1 and R_2 , and input voltage $e_i(t)$. To simplify the derivation, apply rule (5-15).



- (b)** Suppose that $e_i = 1.6$ V, $R_1 = 5$ k Ω , and $R_2 = 15$ k Ω . Determine the values of e_{in} (in V), i_{in} (in millamps, mA), i_1 (in mA), i_2 (in mA), and e_o (in V).

- 5.9** The circuit drawing below shows an inverting amplifier, from Fig. 5-8, and, at the input of the amplifier, a *variable resistor* with a sliding contact, often called a wiper. The maximum useable resistance of the variable resistor is R_p ; however, by moving the wiper along the surface of the resistor (adjusted by turning a dial or a screw), we can connect between e_i and e_{im} any portion αR_p , where $0 \leq \alpha \leq 1$. The purpose of this particular circuit configuration is to allow the gain constant of the amplifier to be adjusted continuously to any value between zero and R_f/R_i , rather than being constrained to the value R_f/R_i of Eq. (5-13b). Your assignment is to derive the following voltage output-to-input equations:



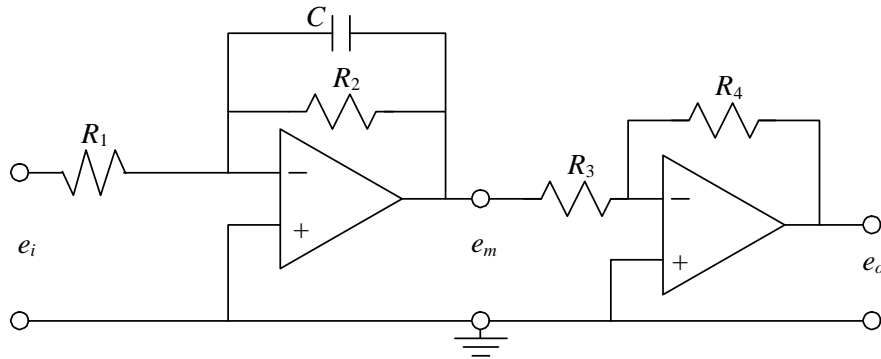
Inverting amplifier with coefficient-setting potentiometer

continuously to any value between zero and R_f/R_i , rather than being constrained to the value R_f/R_i of Eq. (5-13b). Your assignment is to derive the following voltage output-to-input equations:

$$\frac{e_{im}}{e_i} = \frac{(1-\alpha)}{1+\alpha(1-\alpha)\frac{R_p}{R_i}} \Rightarrow \frac{e_o}{e_i} = -\frac{(1-\alpha)\frac{R_f}{R_i}}{1+\alpha(1-\alpha)\frac{R_p}{R_i}}$$

In your derivation, do not neglect the current to ground through the side of the variable resistor with resistance $(1-\alpha)R_p$. For applications in electronic analog computers (see the footnote to homework Problem 5.6), this arrangement of a variable resistor is called a *coefficient-setting potentiometer* or just a *pot* for short.

5.10 The circuit represented graphically below consists of two stages, each stage being built around an op-amp.



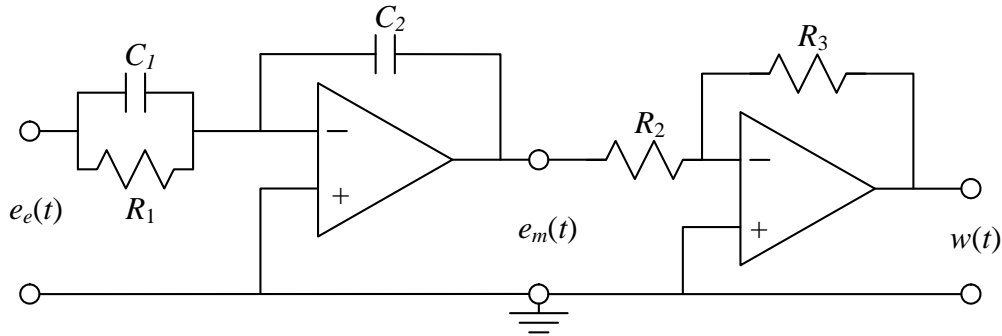
(a) Derive from the left-hand stage the following ODE for interstage voltage $e_m(t)$:

$$\dot{e}_m + \frac{1}{R_2 C} e_m = -\frac{1}{R_1 C} e_i$$

(b) Combine the result of part (a) with the effect of the right-hand stage to show that the ODE for output voltage $e_o(t)$ is $\dot{e}_o + \frac{1}{R_2 C} e_o = \frac{R_4}{R_3} \frac{1}{R_1 C} e_i$. (Note: This circuit is essentially the *electronic analog computer* (see the footnote to homework Problem 5.6) for solving the standard stable 1st order ODE (3-7), $\dot{x} + (1/\tau_1)x = bu(t)$. Input voltage $e_i(t)$ is analogous to standard input $u(t)$, output voltage $e_o(t)$ is analogous to response $x(t)$,

time constant $\tau_1 = R_2 C$, and constant $b = \frac{R_4}{R_3} \frac{1}{R_1 C}$.)

5.11 The circuit represented graphically on the next page is the basic, ideal form of electronic analog proportional-integral (PI) controller, one of the subjects of Chapter 15. (In practice, a great deal of electronic refinement and conditioning is required to produce a circuit that behaves even close to ideally.) The input voltage signal is $e_e(t)$, the intermediate voltage between the two stages is $e_m(t)$, and the output voltage from the PI controller is $w(t)$.



- (a) By applying the methods of circuit analysis described in Chapter 5, show that the ODE relating PI-controller output $w(t)$ to input $e_e(t)$, expressed in terms of the capacitor and resistor parameters of the circuit diagram, is:

$$\dot{w} = \frac{R_3 C_1}{R_2 C_2} \left(\dot{e}_e + \frac{1}{R_1 C_1} e_e \right)$$

- (b) Derive the PI-controller transfer function $TF(s) \equiv \frac{L[w(t)]|_{w_0=0}}{L[e_e(t)]|_{e_{e0}=0}}$, expressed in terms of the capacitor and resistor parameters of the circuit diagram.

Chapter 6 General time response of 1st order systems by application of the convolution integral

© 2016 by William L. Hallauer, Jr.

Up to this point in the book, we have derived time response solutions of LTI systems only for relatively simple input functions $u(t)$. The convolution integral will permit us to derive time response solutions for any physically realistic input function $u(t)$, and even to compute time response solutions if $u(t)$ is given in numerical form rather than equation form. The general convolution transform and its inverse, the convolution integral, are defined and described in this chapter, and application of the convolution integral is illustrated specifically for 1st order systems.

6-1 The convolution transform and its inverse, the convolution integral

Suppose that we have two physically realistic functions of time, $f_1(t)$ and $f_2(t)$, that are zero for all time $t < 0$ and non-zero only for $t \geq 0$. The *convolution integral* is defined (Meirovitch, 1967, pp. 16-17, 534) to be another function of time in terms of a definite integral involving $f_1(t)$ and $f_2(t)$:

$$CI(t) \equiv \int_{\tau=0}^{\tau=t} f_1(\tau) f_2(t - \tau) d\tau$$

In this definite integral, τ is the dummy variable of integration, and time t appears both in the upper limit of the integral and in argument $(t - \tau)$ of the integrand. We can express the integral differently by making the change of integration variable $\lambda = t - \tau$, so that $\tau = t - \lambda$ and $d\tau = -d\lambda$, since t is regarded as a constant within the integration:

$$\int_{\tau=0}^{\tau=t} f_1(\tau) f_2(t - \tau) d\tau = \int_{\lambda=t}^{\lambda=0} f_1(t - \lambda) f_2(\lambda) (-d\lambda) = \int_{\lambda=0}^{\lambda=t} f_1(t - \lambda) f_2(\lambda) d\lambda$$

The final right-hand-side form results because exchanging the limits of a definite integral changes its sign. In the final right-hand-side integral, λ is just the dummy variable of integration, which might as well be τ , so we can write the convolution integral in either of the following forms:

$$CI(t) = \int_{\tau=0}^{\tau=t} f_1(\tau) f_2(t - \tau) d\tau = \int_{\tau=0}^{\tau=t} f_1(t - \tau) f_2(\tau) d\tau \quad (6-1)$$

The Laplace transform $L[CI(t)]$ is called the *convolution transform*. Let's suppose that the Laplace transforms of functions $f_1(t)$ and $f_2(t)$ exist: $F_1(s) = L[f_1(t)]$ and

Chapter 6 General time response of 1st order systems by application of the convolution integral

$F_2(s) = L[f_2(t)]$. Then, as is derived in Appendix A, Section A-5, the product of these two transforms equals the convolution transform:

$$F_1(s) \times F_2(s) = L[CI(t)] = L\left[\int_{\tau=0}^{\tau=t} f_1(\tau) f_2(t-\tau) d\tau\right] = L\left[\int_{\tau=0}^{\tau=t} f_1(t-\tau) f_2(\tau) d\tau\right] \quad (6-2)$$

It follows that the inverse transform of the product is the convolution integral:

$$L^{-1}[F_1(s) \times F_2(s)] = CI(t) = \int_{\tau=0}^{\tau=t} f_1(\tau) f_2(t-\tau) d\tau = \int_{\tau=0}^{\tau=t} f_1(t-\tau) f_2(\tau) d\tau \quad (6-3)$$

For LTI systems in general, the convolution integral (6-3) will permit us to derive time response solutions for any physically realistic input function $u(t)$.

It is of interest to note that in MATLAB, the most common definition of *convolution* is a type of multiplication of two vectors. If the vectors are the coefficients of two polynomials, then MATLAB convolution amounts to the multiplication of the two polynomials. Consider, for example, the following product of two polynomials in s :

$$F_1(s) \times F_2(s) = (2s^2 + 3s + 5) \times (4s + 6) = 8s^3 + 24s^2 + 38s + 30$$

The following are MATLAB operations that execute this multiplication, using the `conv` command, and the result¹:

```
>> F1=[2 3 5]; F2=[4 6]; F3=conv(F1,F2)

F3 =
    8     24     38     30
```

Similarly, MATLAB defines *deconvolution* as a type of division of two vectors. If the vectors are the coefficients of two polynomials, then deconvolution amounts to the division of one polynomial by the other. The MATLAB command is `deconv`.

6-2 General solution of the standard stable 1st order ODE + IC by application of the convolution integral

From Eq. (3-7), we have for stable 1st order systems:

$$\text{ODE + IC: } \dot{x} + (1/\tau_1)x = bu(t), \quad x(0) = x_0, \quad \text{find } x(t) \text{ for } t > 0 \quad (6-4)$$

Solve by first taking the Laplace transform,

¹ See also the description at the end of Section 8-11 of the relationship between the *convolution sum* and multiplication of polynomials.

$$L[\text{ODE}]: sX(s) - x_0 + (1/\tau_1)X(s) = bU(s)$$

$$\Rightarrow X(s) = \frac{x_0}{s + 1/\tau_1} + b \left(\frac{1}{s + 1/\tau_1} \right) \overbrace{U(s)}^{F_2(s)}$$

Take the inverse transform, using Eq. (2-14) and convolution integral (6-3):

$$x(t) = x_0 e^{-t/\tau_1} + b \int_{\tau=0}^{\tau=t} e^{-t/\tau_1} u(t-\tau) d\tau = x_0 e^{-t/\tau_1} + b \int_{\tau=0}^{\tau=t} e^{-(t-\tau)/\tau_1} u(\tau) d\tau \quad (6-5)$$

Equations (6-5) are general solutions of problem (6-4) applicable for any input $u(t)$.² For both forms, the first term is obviously the initial-condition (IC) response and the second term is the forced response. In applications with specific $u(t)$ functions, the second form of the forced-response integral on the right-hand side of (6-5) is used more commonly than the first. The first form is also valid, but the functional nature of $u(t - \tau)$ can sometimes be difficult to interpret correctly.

The forced-response integrals in (6-5) are called convolution integrals, as in (6-1). They are also sometimes known as *superposition* integrals, because, as is shown in Section 8-10, they can be derived as the linear superposition of responses to differentially small inputs.

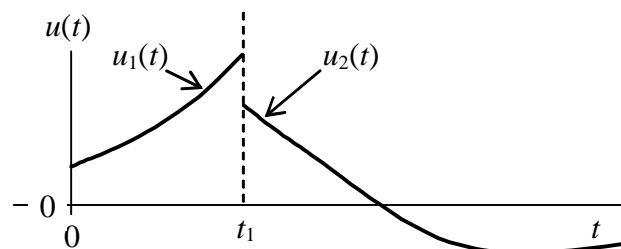
In Eqs. (6-5), constants τ_1 and b should be expressed in terms of the physical constants of the actual system analyzed, such as mass m , damping constant c , etc.

6-3 Examples of 1st order system response

Example 6-1: response of a 1st order system to piecewise continuous input functions

It is often the case that the input to a system is described by different functions, each function in effect over a different time period for $t > 0$. For example, the following equation and drawing represent an input consisting of two different general functions:

$$u(t) = \begin{cases} 0, & t < 0 \\ u_1(t), & 0 < t < t_1 \\ u_2(t), & t_1 < t \end{cases}$$



The general forced response to this type of input can be expressed nicely

² Note, however, that solutions (6-5) are not valid for a non-standard 1st order ODE, e.g., one with right-hand-side dynamics such as Eq. (5-17).

Chapter 6 General time response of 1st order systems by application of the convolution integral

in terms of convolution integrals, but we must recognize that it requires two different equations, and we must consider carefully the limits of the definite integrals. First, for the time interval $0 \leq t \leq t_1$, it is clear that the second form of Eqs. (6-5) is directly applicable, with $u(t) \equiv u_1(t)$:

$$x(t) = x_0 e^{-t/\tau_1} + b \int_{\tau=0}^{\tau=t} e^{-(t-\tau)/\tau_1} u_1(\tau) d\tau \quad , \text{ for } 0 \leq t \leq t_1 \quad (6-6a)$$

For the response during the second time interval, $t \geq t_1$, the definite integral in the second form of (6-5) still must be evaluated over the limits $\tau = 0$ to $\tau = t > t_1$, which means that both u_1 and u_2 need to be integrated, but each only over the time interval for which it is defined:

$$x(t) = x_0 e^{-t/\tau_1} + b \left[\int_{\tau=0}^{\tau=t_1} e^{-(t-\tau)/\tau_1} u_1(\tau) d\tau + \int_{\tau=t_1}^{\tau=t} e^{-(t-\tau)/\tau_1} u_2(\tau) d\tau \right] \quad , \text{ for } t \geq t_1 \quad (6-6b)$$

Note especially in (6-6b) that $\tau = t_1$ is both the upper limit of the integral that involves u_1 and the lower limit of the integral that involves u_2 . Equations (6-6) are especially useful for response to a pulse of limited duration, as is illustrated in the next example.

Example 6-2: response of a mass-damper system to a half-sine pulse

We consider again the problem for velocity of a mass moving on a viscous film, which is solved by basic ODE methods in Section 1-5:

$$\text{ODE + IC: } m \dot{v} + c v = f_x(t), \quad v(0) = v_0, \quad \text{find } v(t) \text{ for } t > 0 \quad (6-7)$$

$$f_x(t) = \begin{cases} F \sin(\pi t/t_d) \equiv F \sin \omega t & \text{where } \omega = \pi/t_d, 0 \leq t \leq t_d \\ 0, t_d < t & \end{cases}$$

Here we have $u(t) = f_x(t)$, $\tau_1 = m/c$, and $b = 1/m$. Relative to the notation of Example 6-1 above, u_1 is the half-sine pulse, and u_2 is zero.

While the pulse is active, $0 \leq t \leq t_d$, Eq. (6-6a) becomes

$$v(t) = v_0 e^{-t/\tau_1} + \frac{F}{m} e^{-t/\tau_1} \int_{\tau=0}^{\tau=t} e^{\tau/\tau_1} \sin \omega \tau d\tau \quad (6-8)$$

Chapter 6 General time response of 1st order systems by application of the convolution integral

We can evaluate the definite integral by several different methods: find it in a table of definite integrals (or indefinite integrals, but don't forget the lower limit of integration); or integrate by parts twice; or evaluate it with software that does symbolic manipulation, such as Mathematica or recent versions of MATLAB. The result is

$$\int_{\tau=0}^{\tau=t} e^{\tau/\tau_1} \sin \omega \tau d\tau = \frac{\tau_1}{1+(\omega \tau_1)^2} \left[e^{t/\tau_1} (\sin \omega t - \omega \tau_1 \cos \omega t) + \omega \tau_1 \right] \quad (6-9)$$

Combining (6-8) and (6-9) gives the velocity during the pulse duration:

$$v(t) = \left[v_0 + \frac{F}{c} \frac{\omega \tau_1}{1+(\omega \tau_1)^2} \right] e^{-t/\tau_1} + \frac{F}{c} \frac{1}{1+(\omega \tau_1)^2} (\sin \omega t - \omega \tau_1 \cos \omega t), \quad 0 \leq t \leq t_d \quad (6-10)$$

At the instant $t = t_d$ when the pulse goes to zero, $\omega t_d = \pi$, so the velocity then is

$$v(t_d) = \left[v_0 + \frac{F}{c} \frac{\omega \tau_1}{1+(\omega \tau_1)^2} \right] e^{-t_d/\tau_1} + \frac{F}{c} \frac{\omega \tau_1}{1+(\omega \tau_1)^2} \quad (6-11)$$

For the time after the pulse goes to zero, $t_d \leq t$, Eq. (6-6b) becomes

$$v(t) = v_0 e^{-t/\tau_1} + \frac{F}{m} e^{-t/\tau_1} \left(\int_{\tau=0}^{\tau=t_d} e^{\tau/\tau_1} \sin \omega \tau d\tau + \int_{\tau=t_d}^{\tau=t} e^{\tau/\tau_1} \times 0 d\tau \right) \quad (6-12)$$

With use again of Eq. (6-9), and of some algebra, (6-12) becomes

$$v(t) = v_0 e^{-t/\tau_1} + \frac{F}{c} e^{-t/\tau_1} \frac{\omega \tau_1}{1+(\omega \tau_1)^2} (1 + e^{t_d/\tau_1}) = v(t_d) e^{-(t-t_d)/\tau_1}, \quad \text{for } t \geq t_d \quad (6-13)$$

The final form on the right-hand side of (6-13) uses Eq. (6-11), and it shows that the post-pulse response is a pure exponential decay, which we would expect physically.

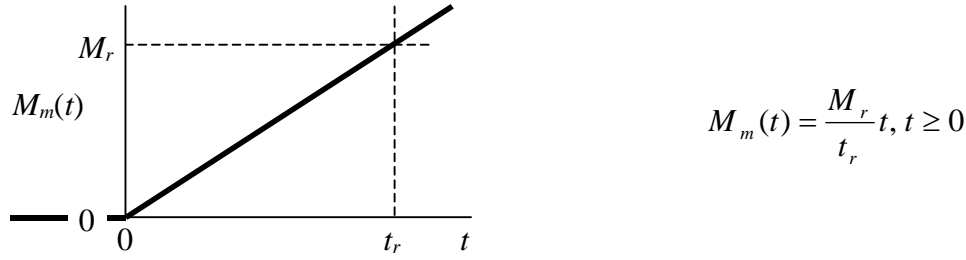
Example 6-3: response of reaction wheel spin velocity to a ramp input moment

From Section 3-3, we have the equation of motion for spin velocity $p(t)$ of a reaction wheel (Fig. 3-1) with rotational inertia J , bearing viscous damping constant c_θ , and applied motor torque $M_m(t)$:

$$\dot{p} + \frac{c_\theta}{J} p = \frac{1}{J} M_m(t) \Rightarrow \dot{p} + \frac{1}{\tau_1} p = b M_m(t) \quad \text{where } \tau_1 = \frac{J}{c_\theta} \text{ and } b = \frac{1}{J} \quad (3-2) \text{ repeated}$$

Chapter 6 General time response of 1st order systems by application of the convolution integral

Let the initial velocity be zero, $p(0) \equiv p_0 = 0$. Let the motor torque have the form of a *ramp*:



Then the second form of general solution (6-5) becomes

$$\begin{aligned} p(t) &= p_0 e^{-t/\tau_1} + b \int_{\tau=0}^{\tau=t} e^{-(t-\tau)/\tau_1} M_m(\tau) d\tau = \frac{1}{J} \int_{\tau=0}^{\tau=t} e^{-(t-\tau)/\tau_1} \frac{M_r}{t_r} \tau d\tau \\ \Rightarrow \quad p(t) &= \frac{1}{J} \frac{M_r}{t_r} e^{-t/\tau_1} \int_{\tau=0}^{\tau=t} e^{\tau/\tau_1} \tau d\tau \end{aligned}$$

We can evaluate the integral easily using integration by parts:

$$\int_{\tau=0}^{\tau=t} \tau e^{\tau/\tau_1} d\tau = \left[\tau \times \tau_1 e^{\tau/\tau_1} \right]_{\tau=0}^{\tau=t} - \int_{\tau=0}^{\tau=t} \tau_1 e^{\tau/\tau_1} d\tau = \tau_1 t e^{t/\tau_1} - \tau_1^2 (e^{t/\tau_1} - 1)$$

Therefore, the total solution is

$$p(t) = \frac{1}{J} \frac{M_r}{t_r} e^{-t/\tau_1} [\tau_1 t e^{t/\tau_1} - \tau_1^2 (e^{t/\tau_1} - 1)] = \frac{M_r}{c_\theta t_r} [t - \tau_1 (1 - e^{-t/\tau_1})] \quad (6-14)$$

By sketching a plot versus time of the dimensionless spin velocity $\frac{p(t)}{M_r/c_\theta}$, you can easily show that, as $t \rightarrow \infty$, this quantity is asymptotic to the ramp function $(t - \tau_1)/t_r$.

6-4 General solution of the standard 1st order problem: an alternate derivation

Consider again the general standard 1st order problem, Eq. (1-1), in which $u(t)$ is the known input (excitation), $x(t)$ is the output (response) that we seek, and a and b are constants, with a not necessarily negative:

$$\dot{x} - ax = bu(t), \text{ with IC } x(t_1) \text{ assumed known, find } x(t) \text{ for } t_1 \leq t \quad (6-15)$$

(We revert to the more general form now, rather than our stable standard 1st order ODE, (3-7) or (6-4), in order to make this derivation more general, applicable for any physically

Chapter 6 General time response of 1st order systems by application of the convolution integral

realistic value or polarity of the constant a .) This problem is a bit more general than we have considered previously, since we allow the initial time t_1 to be different from zero. In order to expedite indexing of array quantities in computer algorithms, we use subscript 1, instead of 0, to denote the initial time and the initial value: $x(t_1) \equiv x_1$.

To find a general solution of this 1st order problem (ODE plus IC), we use the exponential function e^{at} and closely related functions, for which we have the following basic identities:

$$e^{at} \times e^{-at_1} = e^{a(t-t_1)} \text{ and } e^{at} \times e^{-at} = e^0 = 1 \quad (6-16)$$

We begin the general solution by multiplying the ODE by the *integrating factor* e^{-at} , recognizing that this will make the left-hand side a perfect derivative:

$$e^{-at}(\dot{x} - ax = bu) \Rightarrow e^{-at}\dot{x} - e^{-at}ax = e^{-at}bu \Rightarrow \frac{d}{dt}(e^{-at}x) = e^{-at}bu$$

Now we integrate the multiplied equation from the initial time t_1 to an arbitrary time instant $t > t_1$, using τ as the variable of integration:

$$\int_{\tau=t_1}^{\tau=t} \frac{d}{d\tau}[e^{-a\tau}x(\tau)] d\tau = \int_{\tau=t_1}^{\tau=t} e^{-a\tau}bu(\tau) d\tau \Rightarrow e^{-at}x(t) - e^{-at_1}x(t_1) = \int_{\tau=t_1}^{\tau=t} e^{-a\tau}bu(\tau) d\tau$$

Finally, we multiply through by e^{at} , apply identities (6-16), move the IC term to the right-hand side, and arrive at the exact, general solution:

$$x(t) = e^{a(t-t_1)}x(t_1) + \int_{\tau=t_1}^{\tau=t} e^{a(t-\tau)}bu(\tau) d\tau, \quad t_1 \leq t \quad (6-17)$$

The term e^{at} need not be inside the integral, since it is not a function of the integration variable τ . Constant b also need not remain inside the integral. Solution (6-17) is comparable to, but more general than, the second form of convolution solution (6-5).

6-5 Numerical algorithm for the general solution of the standard 1st order problem

We seek solutions of (6-17) in time-series form, that is, at discrete, equally spaced instants in time. Accordingly, we define the following notation that employs descriptive subscripts:

$t =$	t_1	$t_2 = t_1 + \Delta t$	$t_3 = t_2 + \Delta t$	\dots	$t_n = t_{n-1} + \Delta t$	$t_{n+1} = t_n + \Delta t$	\dots
$x(t) =$	x_1	x_2	x_3	\dots	x_n	x_{n+1}	\dots
$u(t) =$	u_1	u_2	u_3	\dots	u_n	u_{n+1}	\dots

Chapter 6 General time response of 1st order systems by application of the convolution integral

Conceptually, we begin with the known values at $t = t_1$, then integrate (6-17) from t_1 to $t_2 = t_1 + \Delta t$, in which we define Δt as the constant time step; we now have known values at $t = t_2$, so we can integrate again to go from t_2 to $t_3 = t_2 + \Delta t$. We proceed in this manner from one time to the next until we have determined values of $x(t)$ at discrete instants in time over the complete time interval of interest. From (6-17), the exact, general equation for stepping from time instant t_{n-1} to the next instant t_n is

$$x_n = e^{a(t_n - t_{n-1})} x_{n-1} + \int_{\tau=t_{n-1}}^{\tau=t_n} e^{a(t_n - \tau)} b u(\tau) d\tau \quad (6-18)$$

By comparing Eq. (6-18) with Eq. (6-5), observe that the integral in (6-18) is clearly a forced-response convolution integral.

Up to this point, the solution is exact. But now we introduce what, in general, is an approximation. We assume that $u(\tau)$ varies so little over the integration time step Δt that it introduces only small error to approximate $u(\tau)$ as being constant over Δt , with its value remaining that at the beginning of the integration time:

$$u(\tau) \approx u(t_{n-1}) \equiv u_{n-1} \quad \text{for } t_{n-1} \leq \tau < t_n \quad (6-19)$$

Using approximation (6-19) and $t_n = t_{n-1} + \Delta t$, we rewrite (6-18) with the convolution integral expressed in a more easily integrable form:

$$x_n = e^{a\Delta t} x_{n-1} + \left[\int_{\tau=t_{n-1}}^{\tau=t_{n-1}+\Delta t} e^{a(t_{n-1}+\Delta t-\tau)} d\tau \right] b u_{n-1}$$

We change the variable of integration, $\xi = t_{n-1} + \Delta t - \tau$, so that the integral becomes

$$\int_{\xi=\Delta t}^{\xi=0} e^{a\xi} (-d\xi) = \int_{\xi=0}^{\xi=\Delta t} e^{a\xi} d\xi = \frac{1}{a} (e^{a\Delta t} - 1)$$

Finally, with approximation (6-19), solution (6-18) can be written as

$$x_n = e^{a\Delta t} x_{n-1} + \frac{1}{a} (e^{a\Delta t} - 1) b u_{n-1} \equiv \phi x_{n-1} + \gamma u_{n-1} \quad (6-20)$$

Equation (6-20) is a *recurrence formula* that is easy to evaluate numerically from one time instant to the next, especially since coefficients $\phi \equiv e^{a\Delta t}$ and $\gamma \equiv (e^{a\Delta t} - 1)b/a = (\phi - 1)b/a$ are invariant once Δt has been selected. Note that if the input $u(t)$ is a constant, as for a step function, then $u_n = \text{constant}$ for all $n = 1, 2, \dots$, in which case (6-20) is an exact solution because Eq. (6-19) is exact, not an approximation. Furthermore, if the actual $u(t)$ is piecewise-constant, then (6-20) can be applied to produce exact results,

Chapter 6 General time response of 1st order systems by application of the convolution integral

provided that Δt is chosen individually for each interval of constant $u(t)$ such that the interval is an integer multiple of its own Δt .

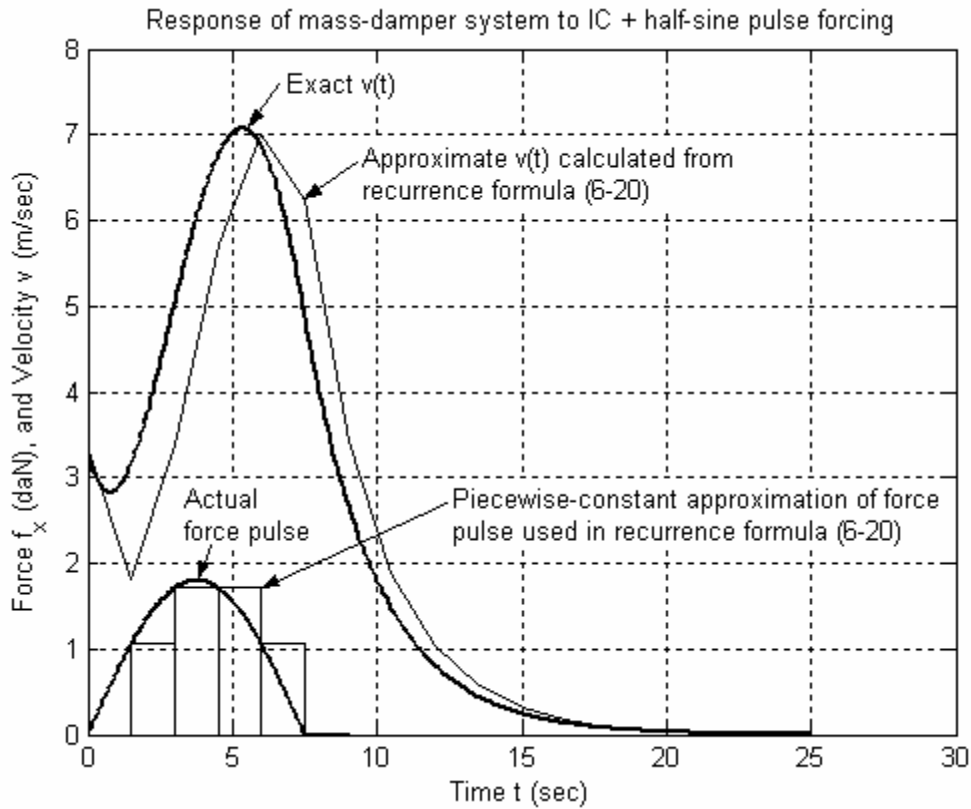
To illustrate the application of Eq. (6-20), we re-visit the numerical solution of Section 1-6, the velocity response of a mass-damper system to a half-sine force pulse. M-file `MATLABdemo11.m` of Section 1-6, which calculates the response exactly, provides the benchmark for evaluating the approximate response calculation. The MATLAB script M-file to calculate and graph the approximate response is:

```
%MATLABdemo61.m
%Mass-damper system approximate response to IC + half-sine pulse forcing
m=5;c=2; %system mass & viscous damping coefficient, SI units
a=-c/m;b=1/m;
F=18;td=7.5; %half-sine pulse, amplitude (N), pulse duration (sec)
w=pi/td; %circular frequency of half-sine pulse (rad/sec)
Dt=1.5; %time step for recurrence calculations
t=0:Dt:24;Lt=length(t); %array of time instants for recurrence calculations
phi=exp(a*Dt);gam=(phi-1)/a*b; %constants in recurrence formula
for n=1:Lt %time series array of input force pulse
    if t(n)<=7.5
        fx(n)=F*sin(pi*t(n)/td);
    else
        fx(n)=0;
    end
end
v=zeros(1,Lt);v(1)=3.3; %initialize velocity array, initial velocity (m/sec)
for n=2:Lt
    v(n)=phi*v(n-1)+gam*fx(n-1);
end
plot(t,v,'k'),bar(t+Dt/2,fx/10,1,'k')
```

Note that the implementation of recurrence formula (6-20) in `MATLABdemo61.m` is a simple three-line `for`-loop.

The figure on the next page was produced by combining the results of M-files `MATLABdemo11.m` and `MATLABdemo61.m`, and then adding explanatory labels and editing the bar graph. For this example, time step Δt was intentionally chosen to be unreasonably large, $\Delta t = 1.5$ sec (compared with system time constant $\tau_1 = 2.5$ sec), in order to produce clear distinctions between the exact and approximate dynamic variables. Nevertheless, the approximate calculation of velocity shows the correct trends qualitatively and is not highly inaccurate quantitatively. If the calculations were repeated with a more reasonable time step, $\Delta t \leq 0.1 \tau_1$, then the results would be much more accurate (homework Problem 6.4).

Observe also in the figure on the next page the bar graph of approximate force $f_x(t)$ used in Eq. (6-20), which is the graphical representation of approximation (6.19). Because of its piecewise-constant character, this is sometimes called a *stairstep* approximation. This approximation introduces a *time delay* or *lag* on the order of Δt into the approximate input. This artificial time delay is obviously transmitted to the calculated approximate response.



It is interesting and possibly useful to observe that, due to approximating $u(\tau)$ as being constant over each time step Δt , Eq. (6-20) is essentially IC + step response over each Δt . Suppose that we were to seek an even more accurate recurrence formula than (6-20) by approximating $u(\tau)$ as varying linearly with time over each time step. In that case, the solution would be essentially IC + step response + ramp response over each Δt . (Example 6-3 in Section 6-3 illustrates ramp response.) So the more refined approximate recurrence formula would be (6-20) supplemented with an additional term that represents ramp response, and we would expect that additional term to include both u_{n-1} and u_n as a consequence of the approximated linear variation of $u(\tau)$; see homework Problem 6.5.

6-6 Homework problems for Chapter 6

6.1 Consider a mass-damper system with a suddenly applied cosine forcing function beginning at $t = 0$, and let the mass have a known initial velocity. The complete problem for velocity $v(t)$ is described by the 1st order, LTI ODE $m\dot{v} + cv = F \cos \omega t$, $t > 0$, and the IC $v(0) = v_0$. Use the general solution Eq. (6-5) to write an algebraic equation for the complete solution $v(t)$ of this problem. It will be necessary to evaluate the convolution integral. You may use integration by parts and/or published tables of integrals, which are highly recommended. Symbolic software (Mathematica, MATLAB, etc.) is also a potential source of assistance with difficult integrals.

$$\text{Answer: } v(t) = \left[v_0 - \frac{F}{c} \frac{1}{1 + (\omega \tau_1)^2} \right] e^{-t/\tau_1} + \frac{F}{c} \frac{1}{1 + (\omega \tau_1)^2} (\cos \omega t + \omega \tau_1 \sin \omega t), \quad t \geq 0$$

6.2 Consider the standard 1st order LTI ODE (of a stable physical system) for dependent variable $x(t)$: $\dot{x} + (1/\tau_1)x = bu(t)$, with IC $x(0) = 0$. Let the input function be the following *flat pulse* of duration t_d :

$$u(t) = \begin{cases} 0, & t < 0 \\ U, & 0 < t < t_d \\ 0, & t_d < t \end{cases}, \text{ in which amplitude } U \text{ is constant}$$

(a) Use solutions (6-6) to write two algebraic equations for the complete response $x(t)$ of this problem. One equation should apply for the time during which the pulse is active (including initial and final times), $0 \leq t \leq t_d$, and the other equation should apply for the time after the pulse ceases, $t_d \leq t$. It will be necessary to evaluate the convolution integral.

$$\text{Answer: } x(t) = \begin{cases} bU\tau_1(1 - e^{-t/\tau_1}), & 0 \leq t \leq t_d \\ bU\tau_1(e^{-(t-t_d)/\tau_1} - e^{-t/\tau_1}), & t_d \leq t \end{cases}$$

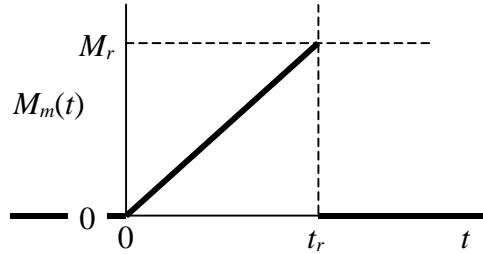
Note that the result for $t_d \leq t$ can be written also as

$$x(t) = bU\tau_1(1 - e^{-t_d/\tau_1})e^{-(t-t_d)/\tau_1}, \quad t_d \leq t$$

(b) Suppose that $t_d = \tau_1$. Sketch by hand (not by computer) a reasonably accurate time-history plot of the nondimensionalized output $\frac{x(t)}{bU\tau_1}$ versus time over the time interval $0 \leq t \leq 5\tau_1$.

6.3 Consider the equation of motion for spin velocity $p(t)$ of a reaction wheel (from Example 6-3 in Section 6-3): $\dot{p} + (c_\theta/J) p = (1/J) M_m(t)$, with IC $p(0) = 0$. Let the applied motor torque be the following *sawtooth pulse*:

$$M_m(t) = \begin{cases} 0, & t < 0 \\ \frac{M_r}{t_r} t, & 0 \leq t < t_r \\ 0, & t_r < t \end{cases}$$



Use solutions (6-6) to write two algebraic equations for the complete solution $p(t)$ of this problem. One equation should apply for the time during which the pulse is active (including initial and final times), $0 \leq t \leq t_r$, and the other equation should apply for the time after the pulse ceases, $t_r \leq t$. You may and should use without re-derivation the appropriate results from Example 6-3 in Section 6-3, in which the applied moment is a permanently increasing ramp.

6.4 Use `MATLABdemo61.m` in Section 6-5 as a template (which must be revised and supplemented with labels, grids, etc.) to calculate approximately and graph the velocity response of the same mass-damper system with the same IC, but now specifying smaller (than in Section 6-5) calculation time steps: $\Delta t = 0.5$ sec and $\Delta t = 0.25$ sec. You should find that the calculated dynamic response becomes progressively more accurate as you reduce Δt .

6.5 (a) Derive a more accurate recurrence formula than Eq. (6-20) by approximating $u(\tau)$ as varying linearly with time over each time step. In other words, use in Eq. (6-18) the linear approximation

$$u(\tau) \approx u_{n-1} + \frac{\tau - t_{n-1}}{\Delta t} (u_n - u_{n-1}) \text{ for } t_{n-1} \leq \tau \leq t_n$$

instead of the simpler approximation (6-19). By completing the integration, show (in all detail, as if the answer were not given) that the refined version of Eq. (6-20) is

$$x_n = \phi x_{n-1} + \gamma u_{n-1} + \beta (u_n - u_{n-1})$$

in which ϕ and γ are the constants defined in (6-20), and $\beta \equiv \frac{\gamma}{a \Delta t} - \frac{b}{a}$.

(b) Revise M-file `MATLABdemo61.m` of Section 6-5 to implement the refined recurrence formula of part (a). Using exactly the same numerical data as in the original program, run the revised program and plot the approximate time history $v(t)$. The approximate time history calculated by the refined recurrence formula should be substantially more accurate than that calculated by Eq. (6-20).

Chapter 6 General time response of 1st order systems by application of the convolution integral

6.6 Consider the standard 1st order LTI-ODE of a stable system, Eq. (3-7), for dependent variable $x(t)$: $\dot{x} + (1/\tau_1)x = bu(t)$. Let the initial condition be zero, $x(0) = 0$, and let the input function be a declining ramp, $u(t) = c(t_z - t)$, in which c , a dimensional constant, is the downward slope of the ramp, and t_z is the time at which the input passes through zero.

(a) Evaluate in all detail the convolution integral in Eq. (6-5) to show that the exact response solution is $x(t) = bc\tau_1[(t_z + \tau_1)(1 - e^{-t/\tau_1}) - t] = bc\tau_1[t_z + \tau_1 - t - (t_z + \tau_1)e^{-t/\tau_1}]$.

(b) Let the numerical parameters be $\tau_1 = 2.5$ sec, $t_z = 10$ sec, $b = 3.5$, and $c = 1$ (b and c in consistent units). Write a MATLAB program, or adapt the code in Section 6-5 that executes the recurrence formula, to calculate and plot an approximate numerical solution for $x(t)$ over the time interval $0 \leq t \leq 10$ sec. Adjust the time-step size Δt and the number of time steps over the 10-sec interval in your code until the graph of your approximate solution appears very similar to that of the corresponding exact solution from part (a). Submit your MATLAB code and your final graph of response.

Chapter 7 Undamped 2nd order systems: general time response; undamped vibration

© 2016 by William L. Hallauer, Jr.

The ideal 2nd order mass-damper-spring system was introduced in Section 1-9, and a theoretical response solution for an undamped system by elementary ODE methods was demonstrated in Section 1-10. In this chapter, we explore ideal undamped 2nd order systems in greater detail, deriving theoretical response solutions by means of Laplace transformation with application of the inverse convolution transform from Chapter 6. The final section of this chapter is an introduction to vibration of real structures, including actual laboratory data.

7-1 Standard form for undamped 2nd order systems; natural frequency ω_n

For the mass-damper-spring (m - c - k) system of Fig. 7-1, the ODE of motion (3-20) derived from Newton's 2nd law, with use of the FBD in Fig. 3-9, is

$$m \ddot{x} + c \dot{x} + k x = f_x(t) \quad (7-1)$$

If we neglect damping by setting $c \dot{x} = 0$ in Eq. (7-1), then we have an ideal (not real) undamped mass-spring (m - k) system. This undamped *passive* system is not fully realistic because every passive physical system is afflicted with some type and degree of energy dissipation, albeit very small in some systems.¹ Nevertheless, it is useful to study the undamped system because it reveals some important fundamental characteristics of 2nd order systems. From Eq. (7-1), the ODE for the m - k system is:

$$m \ddot{x} + k x = f_x(t) \Rightarrow \ddot{x} + \frac{k}{m} x = \frac{1}{m} f_x(t) = \frac{k}{m} \frac{f_x(t)}{k} \quad (7-2)$$

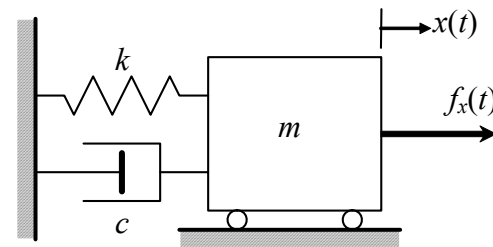


Figure 7-1 Mass-damper-spring system

Let's use Eq. (7-2) to develop the standard form that will apply for undamped 2nd order systems more generally. First, we define algebraically the *natural frequency of undamped vibration* as the positive square root of the quotient of the stiffness and mass values (both of which are positive in most passive systems):

$$\omega_n \equiv \sqrt{\frac{k}{m}} \quad (7-3)$$

¹ In an *active* system with an external source of energy and *feedback control*, it is possible that the damping might be nullified; active systems are analyzed later, beginning in Chapter 14.

The natural frequency is very important physically: it is shown in the next section that an undamped 2nd order system tends to vibrate (oscillate, pulsate, shake, quiver, ...) periodically at circular frequency ω_n radians per second. Next, we define the standard input quantity

$$u(t) \equiv \frac{1}{k} f_x(t) \quad (7-4)$$

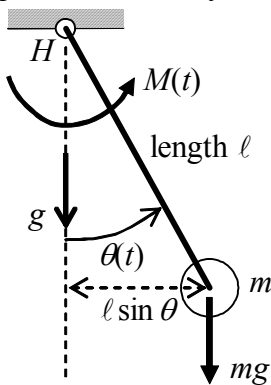
So now we define $x(t)$ as representing any appropriate output quantity (not necessarily just position as in Fig. 7-1), and we re-write (7-2) in *standard form* (standard in this book, at least, and mostly standard in engineering literature):

$$\ddot{x} + \omega_n^2 x = \omega_n^2 u(t) \quad (7-5)$$

From Eq. (7-5) we see that input $u(t)$ has exactly the same physical dimensions as output $x(t)$. In fact, we can identify $u(t)$ as being the *pseudo-static* output, $x_{ps}(t)$; that is, if $x(t)$ varies slowly enough that \ddot{x} is negligible in comparison with $\omega_n^2 x$, then ODE (7-5) reduces to a simple algebraic equation, $\omega_n^2 x \approx \omega_n^2 u(t)$, the solution of which is the pseudo-static response, $x(t) = u(t) \equiv x_{ps}(t)$. This response is called pseudo-static because it is not necessarily static (constant over time), but it varies slowly enough that the second derivative of response is negligible.

Example: the simple pendulum, a rotational 2nd order system

You have probably seen the pendulum of a grandfather clock. The ideal simple pendulum is very similar: there is a bob of mass m attached to the lower end of a rod of



length ℓ , the upper end of the rod being supported at frictionless hinge H . We assume the rod to be rigid and to have negligible inertial moment. The pendulum hangs downward and swings side-to-side with angle $\theta(t)$ in the plane of the paper, subject to the acceleration of gravity, g . For completeness, we include an agent that can impose onto the pendulum an arbitrary applied moment $M(t)$ about H . Because we neglect the inertia of the rod, the rotational inertia of the pendulum about H is $J = m\ell^2$.

Newton's 2nd law for rotation about H is

$$\Sigma(\text{all applied moments about } H) = J \times \text{rotational acceleration} = m\ell^2 \ddot{\theta}$$

$$\Rightarrow M(t) - mg \times \ell \sin \theta = m\ell^2 \ddot{\theta} \Rightarrow m\ell^2 \ddot{\theta} + mg\ell \sin \theta = M(t)$$

Chapter 7 Undamped 2nd order systems: general time response; undamped vibration

Due to the $\sin \theta$ term, the exact ODE is nonlinear. However, let's consider only small rotational angles, $|\theta| < \approx 10^\circ$, for which $\sin \theta \approx \theta$ in radians. This restriction linearizes the ODE:

$$m\ell^2\ddot{\theta} + mg\ell\theta = M(t) \Rightarrow \ddot{\theta} + \frac{g}{\ell}\theta = \frac{g}{\ell}\frac{M(t)}{mg\ell} \Rightarrow \ddot{\theta} + \omega_n^2\theta = \omega_n^2 u(t)$$

In the standardized form of the linearized ODE, the natural frequency is $\omega_n = \sqrt{g/\ell}$, and the standard input quantity (also the pseudo-static response) is $u(t) = \theta_{ps}(t) = M(t)/mg\ell$. For the pendulum at small rotational angles, the term $mg\ell\theta$ is the restoring moment that opposes motion from the unforced static equilibrium position, $\theta = 0$; essentially, gravity plays the role of a rotation spring. See homework Problem 7.4 for another interesting pendulous rotational system, a balloon carrying a basket.

7-2 General solution for output $x(t)$ of undamped 2nd order systems

Let's solve Eq. (7-5) for output $x(t)$, given any physically realistic input $u(t)$, for time $t > 0$, and given appropriate initial conditions at $t = 0$. We use Laplace transformation with application of the inverse convolution transform from Chapter 6. To simplify the notation, we denote $X(s) \equiv L[x(t)]$. Transforming (7-5) with use of Eq. (2-17) gives

$$s^2 X(s) - sx(0) - \dot{x}(0) + \omega_n^2 X(s) = \omega_n^2 L[u(t)] \quad (7-6)$$

Equation (7-6) tells us that we need two initial conditions, one on the output and one on the derivative of the output, for this 2nd order ODE. Accordingly, we simplify the writing with the definitions

ICs for 2nd order ODE: $x_0 \equiv x(0)$, initial “position”; $\dot{x}_0 \equiv \dot{x}(0)$, initial “velocity” (7-7)

Solving Eq. (7-6) for $X(s)$ with the use of notation (7-7) gives

$$X(s) = x_0 \frac{s}{s^2 + \omega_n^2} + \frac{\dot{x}_0}{\omega_n} \frac{\omega_n}{s^2 + \omega_n^2} + \omega_n \overbrace{\frac{\omega_n}{s^2 + \omega_n^2}}^{F_1(s)} \overbrace{L[u(t)]}^{F_2(s)} \quad (7-8)$$

We invert Eq. (7-8) using transforms (2-30) and (2-31), and the inverse convolution transform (6-3), to find the two equivalent general solution equations for the standard undamped 2nd order ODE, Eq. (7-5), with ICs $x(0) \equiv x_0$ and $\dot{x}(0) \equiv \dot{x}_0$:

$$x(t) = \underbrace{x_0 \cos \omega_n t + \frac{\dot{x}_0}{\omega_n} \sin \omega_n t}_{\text{IC response}} + \underbrace{\omega_n \int_{\tau=0}^{t=t} \sin \omega_n \tau \times u(t-\tau) d\tau}_{\text{forced response}} \quad (7-9a)$$

$$x(t) = \underbrace{x_0 \cos \omega_n t + \frac{\dot{x}_0}{\omega_n} \sin \omega_n t}_{IC \text{ response}} + \underbrace{\omega_n \int_{\tau=0}^t \sin \omega_n (t-\tau) \times u(\tau) d\tau}_{forced \text{ response}} \quad (7-9b)$$

7-3 Simple IC response and step response of undamped 2nd order systems

We find in this section two important special case solutions of Eqs. (7-9a,b): (1) pure initial condition response for zero input, $u(t) = 0$; and (2) pure step response with both initial conditions being zero.

For the case of pure initial condition response (also called free vibration), with $u(t) = 0$, Eqs. (7-9a,b) become

$$x(t) = x_0 \cos \omega_n t + \frac{\dot{x}_0}{\omega_n} \sin \omega_n t, \quad 0 \leq t \quad (7-10)$$

Let's use a trigonometric identity [see Eqs. (4-6)-(4-8)] to combine the two sinusoids of (7-10) into a single term. The following definition will reduce the writing required and also will turn out to be physically meaningful:

$$x_{\max} \equiv \sqrt{x_0^2 + (\dot{x}_0/\omega_n)^2} \quad (7-11)$$

$$\Rightarrow x(t) = x_{\max} \left[\cos \omega_n t \times \left(\frac{x_0}{x_{\max}} \right) - \sin \omega_n t \times \left(\frac{-\dot{x}_0 / \omega_n}{x_{\max}} \right) \right]$$

$$\Rightarrow x(t) = x_{\max} \cos(\omega_n t + \phi), \quad \phi = \tan^{-1} \left(\frac{-\dot{x}_0 / \omega_n}{x_0} \right) \quad (7-12)$$

Figure 7-2 is an annotated graph of response (7-11)-(7-12) for positive values of the ICs, $x_0 > 0$ and $\dot{x}_0 > 0$. Clearly, the output is a pure sinusoid of amplitude x_{\max} and

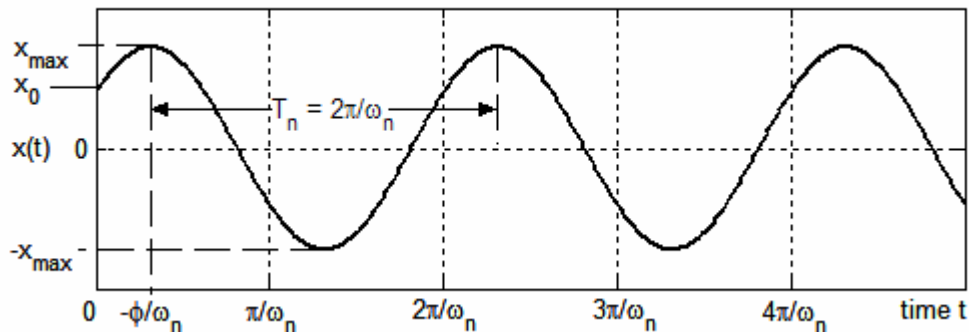


Figure 7-2 IC response of an undamped 2nd order system

Chapter 7 Undamped 2nd order systems: general time response; undamped vibration

phase angle ϕ . This form of response is called *free vibration*, because it occurs without any forcing input, $u(t) = 0$. The circular frequency of vibration is ω_n rad/sec, the natural frequency defined in Eq. (7-3). The cyclic natural frequency is $f_n = \omega_n/2\pi$ cycles/sec (Hz), and the natural period annotated on Fig. 7-2 is $T_n = 1/f_n = 2\pi/\omega_n$ sec/cycle. Free vibration at the natural frequency is one of the most important characteristics of undamped systems and, more realistically, of lightly damped systems. Damped 2nd order systems are discussed in Chapter 9.

For the case of pure step response, we set the ICs to zero, and we define the input to be a step function at time $t = 0$, with step magnitude U :

$$u(t) = U H(t) \quad (7-13)$$

The appropriate form of the general solution to use in this case is Eq. (7-9a),

$$x(t) = \omega_n \int_{\tau=0}^{\tau=t} \sin \omega_n \tau \times u(t - \tau) d\tau = \omega_n \int_{\tau=0}^{\tau=t} \sin \omega_n \tau \times U H(t - \tau) d\tau = \omega_n U \int_{\tau=0}^{\tau=t} \sin \omega_n \tau d\tau$$

Here we used the property of the unit-step function that $H(t - \tau) = 1$ for $t - \tau > 0$ (from Eq. (2-27) and Fig. 2-3); this inequality obviously is satisfied for τ over the limits of the definite integral. For most applications of the convolution integrals in Eqs. (7-9a,b), the form in (7-9b) is preferable because the integrand term $u(t - \tau)$ in (7-9a) is usually difficult to interpret and/or awkward to handle in the integration. This case, however, is an exception since $u(t - \tau)$ is easy to interpret and is extremely simple. Completing the integration gives

$$\begin{aligned} x(t) &= \omega_n U \int_{\tau=0}^{\tau=t} \sin \omega_n \tau d\tau = \omega_n U \int_{\tau=0}^{\tau=t} \left(\frac{-1}{\omega_n} \right) d(\cos \omega_n \tau) = -U [\cos \omega_n \tau]_0^t = -U (\cos \omega_n t - 1) \\ \Rightarrow \quad x(t) &= U(1 - \cos \omega_n t), \quad 0 \leq t \end{aligned} \quad (7-14)$$

Equation (7-14) is graphed for a few cycles of response in Fig. 7-3. The response is sinusoidal and periodic with the system natural period T_n , as is the free-vibration IC

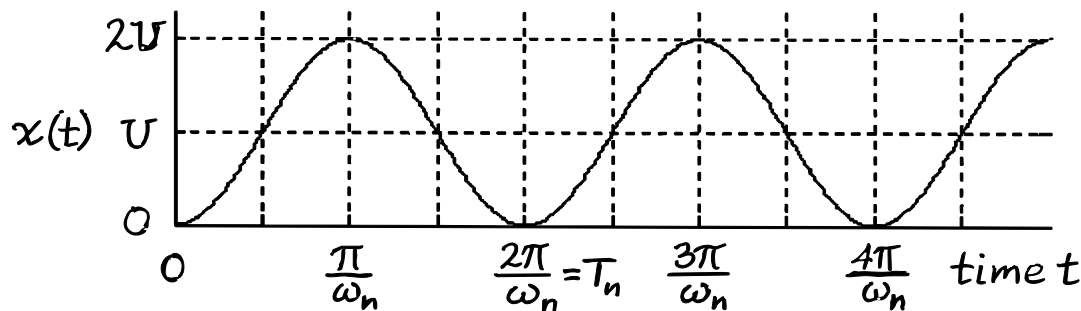
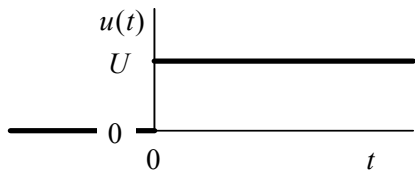


Figure 7-3 Step response of an undamped 2nd order system

response. However, (7-14) is forced response, and the input $u(t)$ is non-zero and constant for $t > 0$, so this step response vibrates around a non-zero mean value (the pseudo-static output value $x_{ps} = U$), oscillating between 0 and $2U$. In contrast, the free-vibration IC response of Eq. (7-12) and Fig. 7-2 vibrates around the zero mean value, oscillating between $-x_{max}$ and $+x_{max}$.

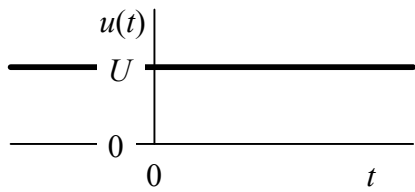
7-4 Discussion of the physical applicability of step-response solutions

The concept of step response in physical applications can be bothersome if one harbors the misconception that step response is valid only if the input is applied in an



abrupt, discontinuous manner, as on the drawing at left. This misconception is natural and honest because of the mathematical definition of the step function, Eq. (2-26) and Fig. 2-2. If we apply that strict definition to the step input analyzed in Section 7-3, without any recognition of the nature of the initial conditions, then the time history of the input would have to be a discontinuous step function.

However, it is instructive to consider also the role of initial conditions in step response. Step response solution (7-14) is derived for zero ICs, $x_0 = 0$ and $\dot{x}_0 = 0$. Imagine that some powerful external agent enforces these ICs for time $t < 0$, then at $t = 0$, the external agent abruptly releases its hold on the system. Under this circumstance, it does not matter whether the input $u(t)$ jumps discontinuously from 0 to U at $t = 0$, as in the



drawing above, or the input has value U both after and before $t = 0$, as in the drawing at left. An input value of U before $t = 0$ could not produce any effect on output $x(t)$, because it could not overpower the external agent that enforces the initial conditions before and right up to the instant $t = 0$. A practical example to which we can relate is an airplane sitting on a runway,

preparing to taxi for takeoff. With the brakes firmly engaged, the pilot increases engine thrust, but the airplane is held motionless by the brakes. In this example, the brakes play the role of “powerful external agent” that enforces the initial position and zero initial velocity, and the engine thrust plays the role of input quantity. After engine thrust has reached acceptable takeoff level, the pilot releases the brakes (at $t = 0$), and the airplane accelerates into takeoff taxi. The engine thrust exists before $t = 0$, but it produces no taxiing motion then because the brakes completely restrain the airplane.

The conclusion of this discussion is that step response is a valid physical solution even if the input is constant before and after the initiation of motion (*i.e.*, is not applied strictly like a mathematical step function), provided that initial conditions enforce the motion prior to the instant (usually $t = 0$) when the input becomes effective.

7-5 Dynamic motion of a mechanical system relative to a non-trivial static equilibrium position; dynamic free-body diagram

Consider the mass-spring system depicted in Fig. 7-4 (on the next page), which is representative in many respects of some real mechanical systems. The system is oriented vertically in a gravity field with acceleration of gravity g . Moreover, let's suppose that the spring is *close-wound*: a helical extension spring which, in its unstretched state, is wound with its coils forced into contact with each other, such that an initial tension force F_i is required to break the coil contact and allow the spring to begin stretching (Shigley and Mitchell, 1983, p. 449). Figure 7-4 illustrates three possible states of such a system. The weight of mass m is $W = mg$, and it is a constant force vector acting downward through the center of gravity of the mass. The spring has stiffness constant k and initial tension F_i , so that the spring law is $f_y = F_i + k y$ for $y \geq 0$, where y is spring stretch vertically downward. State 1 of Fig. 7-4 shows the mass supported statically by an externally applied force W acting upward, with the spring unstretched and therefore exerting no force on the mass. We define $y_t(t)$ as the total vertical motion of the mass (positive downward in this example, but not necessarily always so) relative to the unstretched-spring position. Now, if the externally applied upward force is slowly reduced, the weight of the mass is gradually transferred to the spring, and the spring stretches (provided that $W > F_i$), lowering the mass. State 2 of Fig. 7-4 is the static equilibrium state that results after the externally applied upward force shrinks to zero, with the spring stretched by the amount y_s from the State 1 position. From the FBD of State 2, the equation of vertical static force equilibrium is

$$F_i + k y_s = W \Rightarrow y_s = \frac{W - F_i}{k}, \text{ for } W \geq F_i \quad (7-15)$$

State 3 of Fig. 7-4 is a condition of dynamic response, with the dynamic force $f_y(t)$ acting on the mass. We define the dynamic position $y_d(t)$ as the motion relative to the static equilibrium position, y_s of Eq. (7-15). We see from Fig. 7-4 that the total translation (from the unstretched-spring position) and the associated acceleration are

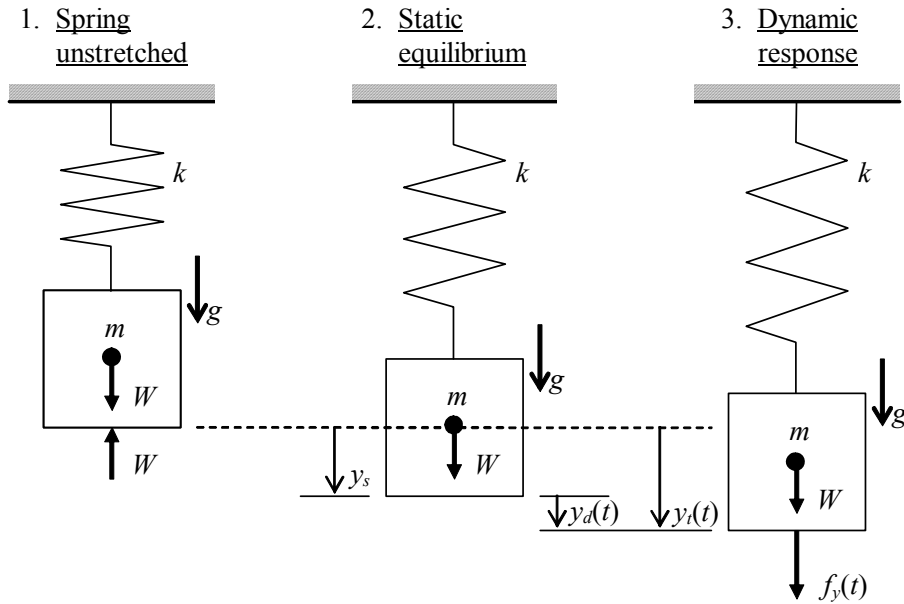
$$y_t(t) = y_s + y_d(t) \Rightarrow \ddot{y}_t(t) = \ddot{y}_d(t) \quad (7-16)$$

The acceleration equation reflects the constancy of y_s . Let's use the FBD for State 3 to write Newton's 2nd law for vertical translation:

$$\Sigma(\text{Forces})_y = m \ddot{y}_t = f_y(t) + W - (F_i + k y_t) \Rightarrow m \ddot{y}_t + k y_t = f_y(t) + W - F_i \quad (7-17)$$

Now use Eq. (7-16) to eliminate $y_t(t)$ from Eq. (7-17):

$$m \ddot{y}_d + k(y_s + y_d) = f_y(t) + W - F_i \quad (7-18)$$



FREE-BODY DIAGRAMS:

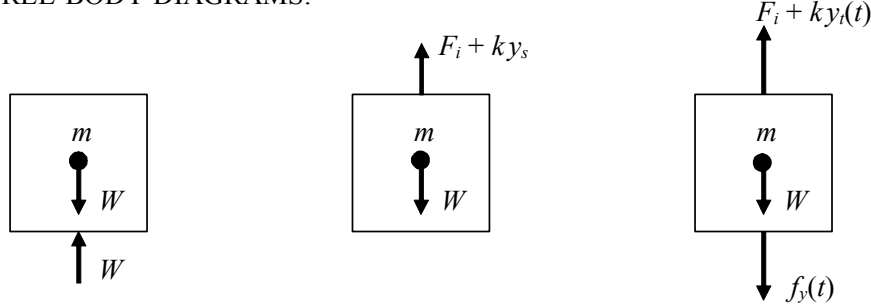


Figure 7-4 Static and dynamic positions of a hanging, spring-supported weight

Next, eliminate $k y_s = W - F_i$, Eq. (7-15), from Eq. (7-18) in order to express the ODE in terms of the motion relative to the static equilibrium position, the single dependent variable, $y_d(t)$:

$$m \ddot{y}_d + k y_d = f_y(t) \quad (7-19)$$

It is obvious physically that Eq. (7-19) is valid provided the upward dynamic motion does not exceed the static spring stretch: $y_d(t) = y_s + y_d(t) > 0$, i.e., $y_d(t) > -y_s$.

Equation (7-19) is identical in form to Eq. (7-2), which applies for a mass-spring system oriented horizontally, with no involvement of a close-wound spring or gravity. The only difference is that the unknown in (7-19) is not the total motion, but, instead, the motion relative to the static equilibrium position established by gravity and the spring initial tension. Consider the dynamic free-body diagram (DFBD) shown in Fig. 7-5 on the next page, which is similar to that of State 3 in Fig. 7-4, but without weight W and with only the spring force relative to the static equilibrium position. These changes from

the FBD of State 3 in Fig. 7-4 are equivalent to eliminating $k y_s = W - F_i$ from Eq. (7-18) in order to obtain Eq. (7-19). Clearly, applying Newton's 2nd law to the DFBD Fig. 7-5 leads again, and much more easily, to Eq. (7-19). The important conclusion here: if we want to solve only for the dynamic motion $y_d(t)$ relative to the static equilibrium position, not the total motion relative to the spring-undeformed position, then we should use a DFBD from which all static influences (weight and spring initial tension in this case) have been eliminated. The DFBD should include only dynamic forces (and/or moments) relative to the static equilibrium position.

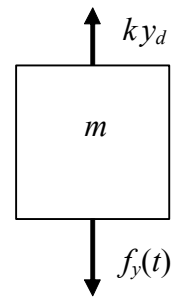


Figure 7-5
**Dynamic free-
body diagram**

This conclusion is useful more generally because, in many situations, we are, indeed, interested primarily in the dynamic response relative to the static equilibrium position. Homework Problem 7.3 is one example. Moreover, this conclusion based upon the simple mass-spring system of Fig. 7-4 has broad applicability to other mechanical systems. The subjects of Chapters 11 and 12 are more complex rotational systems and higher-order mechanical systems. It is usually convenient when analyzing those systems to deal only with the simpler DFBDs and ODEs that we use when we solve only for the dynamic motion relative to the static equilibrium position.

However, there are at least two classes of mechanical systems for which we must include (in FBDs and ODEs of motion) the weights of massive components: (1) pendulous systems for which gravity provides a spring effect, such as the simple pendulum example in Section 7-1 and the balloon-basket vehicle of homework Problem 7.4; (2) systems for which initial conditions and/or dynamic inputs (forces, moments) are defined relative to the undeformed-spring state, for example, the airplane landing contact of homework Problem 7.5.

Section 7-6 Introduction to vibrations of distributed-parameter systems

A system such as the mechanical mass-dashpot-spring system of Fig. 7-1 is often called a *lumped-parameter* system. This descriptive term is used because the essential physical features are idealized to be spatially concentrated: in Fig. 7-1, all of the mass is idealized to reside in one physical element, all of the damping in another, and all of the stiffness in yet another. Some engineering systems can be modeled accurately using idealized lumped elements; but many real systems cannot, and these latter are called *distributed-parameter* systems. A structural beam, such as that shown in Fig. 7-6 on the next page, is a prototypical distributed-parameter mechanical system. It is obvious that the mass of this beam is not concentrated at a single point in space, but instead is distributed throughout the beam's volume. Similarly, the flexibility of the beam does not reside in a discrete spring, but also is distributed over the entire spring. Finally, although there is very little damping in this particular system, it also is distributed throughout the beam in the forms of molecular "friction" within the deforming beam and fluid dynamic drag on the beam's surface if the beam is immersed in air, another gas, or liquid.

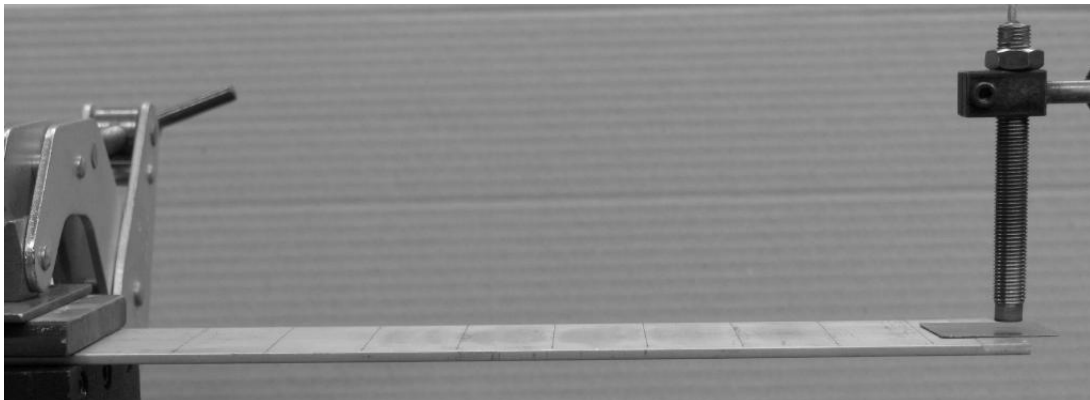


Figure 7-6 Clamped uniform aluminum beam with nominal cross section 2 inch \times 1/8 inch. Test configuration: beam clamped at left between thick steel plates, leaving 10.0 inches of overhang; non-contacting proximity (displacement) sensor over right tip; bonded onto the beam's right tip is a small, thin, steel plate, the “target” in which the proximity sensor induces eddy currents.

Figure 7-7 is an actual record of motion of the beam in Fig. 7-6 in response to a particular initial condition: the tip of the beam was bent upward statically, then released.²

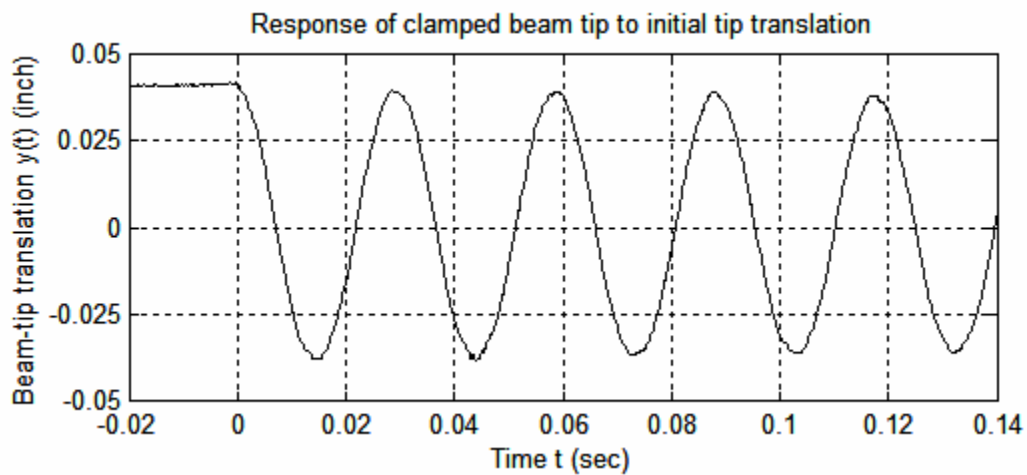


Figure 7-7 Initial-translation dynamic response of the beam in Fig. 7-6, as detected by the proximity sensor.

The subsequent time response was directly analogous to the theoretical IC response shown in Fig. 7-2, with positive initial deflection, $y_0 > 0$, but zero initial velocity, $\dot{y}_0 = 0$, $y(t)$ being vertical translation, positive upward, of the beam tip relative to the static equilibrium position under gravity loading. Note in Fig. 7-7 that the character of the measured response appears very close to that predicted theoretically in Eq. (7-10) for an undamped 2nd order system, $y(t) = y_0 \cos \omega_n t$. However, we can detect by detailed analysis of the data in Fig. 7-7 the following very small differences between actual and

² In practice, this procedure is often called *twang* testing (also *snapback*, *step-relaxation*, and *pluck* testing)—see homework Problem 9.4 for a more detailed discussion.

theoretical responses: (i) slight reductions in amplitude from one cycle to the next, due to the very light system damping and to an imperfect release of the beam from its static initial deformation; (ii) a slight eccentricity of the vibration relative to the zero-translation position, due to a small instrumentation error, which is almost unavoidable in experimental measurements; and (iii) almost imperceptibly small distortion of the waveform shape relative to a perfect cosine. (More easily observed distortion appears in Fig. 7-9, which is discussed below.) This small waveform distortion occurs because the beam is not a perfect 2nd order, lumped-parameter system; in reality, the beam is, mathematically, a much more complicated distributed-parameter system. Nevertheless, it turns out that in many circumstances, including this particular one, we can approximately model distributed-parameter structures as 2nd order systems, with acceptable accuracy for many engineering purposes.

Careful study of the experimental data in Fig. 7-7 shows that the time between any two successive peaks of the response signal, the “period” of damped vibration, is $T_d \approx 0.0294$ sec. The system of Fig. 7-6 is damped, so T_d is not a true undamped “natural” period. However, theoretical solutions for mathematical models predict that a measured period such as this for a very lightly damped system is almost equal, for all practical purposes, to the true natural period. Therefore, in the example problems below, we shall assume that the measured period is the system’s natural period, and so the undamped natural frequency is $f_n \approx 1/T_d = 34.0$ Hz.

Figure 7-8 illustrates the spatial distribution of the beam vibrating after the same type of initial condition as that of Fig. 7-7, but with a much greater magnitude of deformation. For this edge-on photo, the shutter of the digital camera was open for $\frac{1}{4}$ second, during which time the beam vibrated through 8+ complete cycles. The upper and lower limits of dynamic deformation appear as fairly distinct curved lines against the dark background in the photo, whereas the intermediate states of deformation appear as a blur. This occurs because the velocity of motion was zero at the extreme deformations; therefore the digital camera’s photosites were exposed during disproportionately longer times to the extreme deformations than to the intermediate deformations.

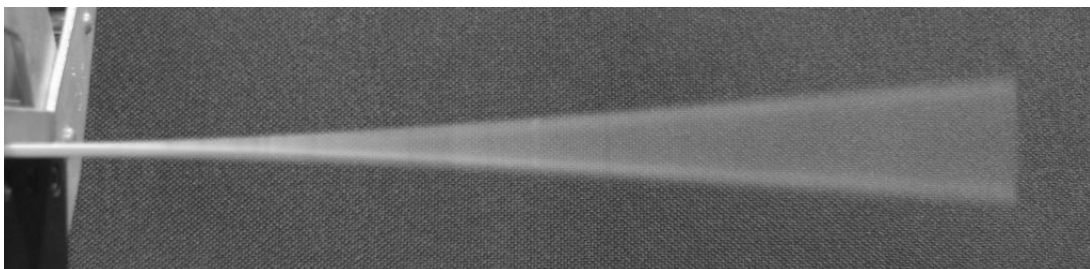


Figure 7-8 Edge-on, $\frac{1}{4}$ -second exposure photo of the beam of Fig. 7-6 vibrating after an initial static deformation and release of the beam tip.

Example Problem 7-1: a calculation of the “effective” tip mass of the vibrating beam.

Consider the system of Fig. 7-6. By loading the beam statically with small calibrated weights hanging from the beam tip, and by measuring the resulting beam-tip downward vertical deflection with the proximity sensor, students determined a beam-tip

average “effective” stiffness constant to be $k_E = 7.86 \text{ lb/inch}$. With this stiffness and the measured natural frequency $f_n = 34.0 \text{ Hz}$, we can infer a value for the “effective” tip mass from Eq. (7-3) in the form

$$m_E = \frac{k_E}{\omega_n^2} = \frac{k_E}{(2\pi f_n)^2} = \frac{7.86 \text{ lb/inch}}{(2\pi \times 34.0 \text{ sec}^{-1})^2} = 1.72e-4 \text{ lb-sec}^2/\text{inch}$$

It is appropriate to conduct a plausibility check of this result, especially since most of us find it difficult to relate intuitively to values of mass that are expressed in the traditional structural system of units (see Section 3-1). Students measured the 10.00-inch overhang of the uniform aluminum beam in Fig. 7-6 to weigh $W_b = 0.230 \text{ lb}$, and they measured the weight of the small steel target at the beam tip as 0.13 oz = 0.0081 lb. Therefore, the total mass of the beam plus the steel target is

$$m_T = W_T/g = (0.238 \text{ lb}) \div (386.1 \text{ inch/sec}^2) = 6.16e-4 \text{ lb-sec}^2/\text{inch}$$

The mass ratio is $m_E/m_T = 0.28$. In view of the photo of the vibrating beam, Fig. 7-8, it seems physically plausible that roughly 28% of the total structural mass is effectively involved in the vibration. This ends Example Problem 7-1.

Example Problem 7-2: calculations based upon ideal theory, nominal dimensions, and standard material constants

Let’s calculate an estimate of the natural frequency of the beam system of Fig. 7-6 using Eq. (7-3) in the form $f_n = \frac{1}{2\pi} \sqrt{k_E/m_E}$. In this calculation, let’s assume that we do not have measured data from actual hardware or instrumentation, *i.e.*, that we have only the type of information that would normally be available in the preliminary-design phase of an engineering project, before even a prototype is fabricated.

First, let’s calculate the theoretical effective stiffness constant k_E . From your courses and textbooks on static structural behavior, you might be familiar with the deformation under loading of structural members such as uniform (prismatic) beams and shafts that are fabricated from homogeneous, isotropic, linearly elastic materials. The theory relevant to the present situation is that for a cantilever (ideally clamped-free) beam. From any textbook with the words “mechanics of materials” or “strength of materials” in its title³, you can find that the effective stiffness at the tip of a uniform cantilever beam is $k_E = 3EI/L^3$, in which E is the material modulus of elasticity, I is the 2nd area moment (also called *area moment of inertia*) of the beam cross section, and L is the overhanging length of the beam. For the beam of Fig. 7-6, let’s use the standard (in preliminary-design calculations) elastic modulus for aluminum: $E = 10.0e+6 \text{ lb/inch}^2$. The nominal rectangular cross-sectional dimensions of the beam are width $b = 2.00$

³ Examples of such textbooks, listed in the References section: Beer and Johnston, 1992; Hibbeler, 1997; and Timoshenko and Young, 1962.

inches and depth $h = 1/8$ inch, for which the theoretical 2nd area moment is $I = bh^3/12 = 3.255e-4$ inch⁴. Using the overhang length of 10.00 inches, we calculate the effective beam-tip stiffness to be

$$k_E = \frac{3 \times (10.00 \times 10^6 \text{ lb/inch}^2) \times (3.255 \times 10^{-4} \text{ inch}^4)}{(10.00 \text{ inch})^3} = 9.766 \text{ lb/inch}$$

Next, let's calculate an effective tip mass m_E . Consider first the vibration of an ideal uniform cantilever beam alone (*i.e.*, without a concentrated tip mass such as the steel target shown on Fig. 7-6). More advanced theory⁴ shows that, for such a bare beam, the effective tip mass vibrating at the fundamental natural frequency is 0.242672 of the total beam mass, which we determine next. The weight of a uniform beam is $W_b = wAL$, in which w is the weight density (weight per unit volume), and the cross-sectional area of a rectangular beam is $A = bh$. Let's use the standard (in preliminary-design calculations) weight density of aluminum, $w = 0.1000 \text{ lb/inch}^3$, so that the weight of our ideal cantilever beam is $W_b = (0.1000 \text{ lb/inch}^3) \times (\frac{1}{4} \text{ inch}^2) \times (10.00 \text{ inches}) = 0.2500 \text{ lb}$. Hence, the effective tip mass of the bare beam alone is $m_{bE} = 0.242672 \times W_b/g = 0.242672 \times (0.2500 \text{ lb}) \div (386.1 \text{ inch/sec}^2) = 1.571e-4 \text{ lb-sec}^2/\text{inch}$. To obtain an intuitively logical estimate of the total effective tip mass, we add to m_{bE} the mass of the steel target that is bonded to the beam tip on Fig. 7-6: $m_E = m_{bE} + (0.0081 \text{ lb}) \div (386.1 \text{ inch/sec}^2) = 1.78e-4 \text{ lb-sec}^2/\text{inch}$.

Finally, the natural frequency based upon ideal theory, nominal dimensions, and standard material constants is

$$f_n = \frac{1}{2\pi} \sqrt{\frac{k_E}{m_E}} = \frac{1}{2\pi} \sqrt{\frac{9.77 \text{ lb/inch}}{1.78 \times 10^{-4} \text{ lb} \cdot \text{sec}^2/\text{inch}}} = 37.3 \text{ Hz}$$

See homework Problem 7.8 for an analysis of the discrepancy between this calculated natural frequency and the measured value of 34.0 Hz. This ends Example Problem 7-2.

The clamped-beam system of Fig. 7-6 appears to behave very much like a 2nd order system when it responds dynamically to a simple initial static deflection of the beam tip. However, when it is subjected to most other possible types of excitation, its dynamic response is more complicated. For example, when the beam tip was tapped lightly upward with a small hammer, the tip moved vertically as shown on Fig. 7-9, next page.

⁴ Theory from, among many possible sources, the following textbooks on structural dynamics that are listed in the References section: Bisplinghoff, *et al.*, 1955, Example 3-1; Craig, 1981, Example 10.3; Meirovitch, 1967, Section 5-10; and Meirovitch, 2001, Example 8.4.

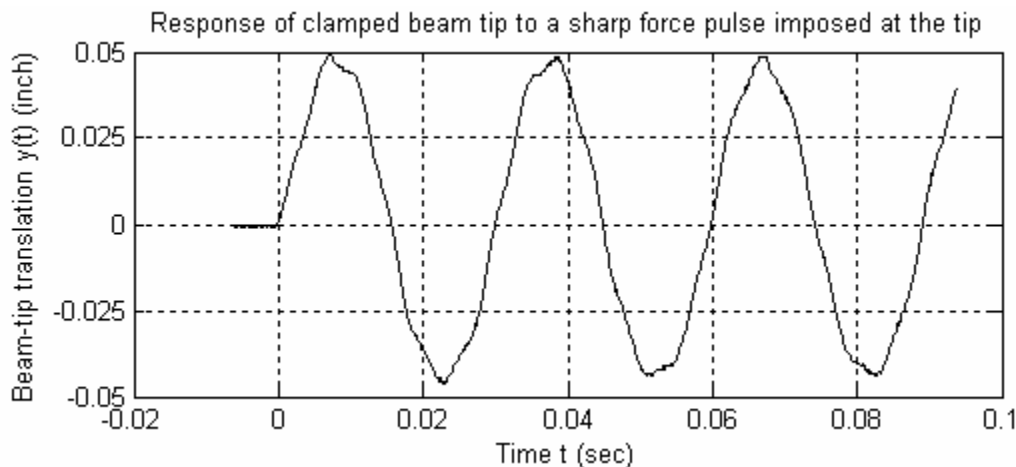


Figure 7-9 Dynamic response to a hammer tap at time $t = 0$ sec of the beam on Fig. 7-6, as detected by the proximity sensor.

The input force that stimulated the response of Fig. 7-9 was approximately a half-sine pulse (as described in Sections 1-5 and 1-6) of very short duration relative to the lightly damped period of this system, $T_d \approx 0.0294$ sec. In Chapter 8, theory is developed showing that, if the system were a true undamped 2nd order system, then the time response to such a pulse would have almost a perfect sine waveform, starting at time $t = 0$ sec. However, the waveform in Fig. 7-9 is quite different from a perfect sine waveform; in fact, it is closer to being the sum of many sinusoids, in the general spirit of a Fourier series, but without the property of Fourier series that all higher series sinusoids have frequencies that are integer multiples of the frequency of the first (fundamental) sinusoid.⁵ In the case of Fig. 7-9, the total motion consists primarily of a first sinusoid with frequency 34.0 Hz, plus a second, lower-amplitude sinusoid with frequency approximately 215 Hz. The motion at 34.0 Hz represents the *first (fundamental) mode of vibration*, and the motion at 215 Hz represents the *second mode of vibration*.

In fact, the beam system of Fig. 7-6 has many more than two modes of vibration, each with a characteristic frequency higher than that of the previous mode. The third and higher modes are not evident in Fig. 7-9 only because the particular pulse stimulus applied in this case did not noticeably excite those higher modes; however, they could be excited by any number of other stimuli, such as sharp pulses applied at particular locations, high-frequency sound-pressure waves, *etc.* In reality, every distributed-parameter system is a higher-than-2nd-order system, and, if only lightly to moderately damped, has many modes of vibration. For example, every acoustic musical instrument is a fluid or structural distributed-parameter system whose distinctive sound quality is a direct consequence of its particular modes of vibration.⁶ However, except for this short descriptive introduction, the subject of distributed-parameter systems is beyond the scope of this

⁵ The subject of Fourier series is developed in most textbooks on advanced calculus (for example, Hildebrand, 1962, pages 216-226) and in most textbooks on elementary partial differential equations.

⁶ If you are interested in the physics of musical instruments, see Cannon, 1967, Sections 13.2-13.6, for an excellent introduction written by an engineer for students of engineering.

book. The subject of vibration modes appears again in Chapter 12, which deals with undamped, 4th order, lumped-parameter systems that have two modes of vibration.

Observe from Fig. 7-9 that the translation response of the beam system of Fig. 7-6 was still dominated by the first vibration mode, even though the tip-pulse stimulus also excited the second mode, but to a much lower amplitude than that of the first mode. Hereafter in this book, the only response of any distributed-parameter system that we shall consider is the contribution of the first mode, and we shall assume that it dominates the total response. Indeed, this is often a good engineering approximation for distributed-parameter structural systems that include relatively large, spatially concentrated masses. Consider, for example, the system of Fig. 7-10, which is the same as that of Fig. 7-6 but with the addition at the beam tip of a concentrated-mass assembly that consists of two ceramic magnets and an aluminum spacer, and weighs 0.254 lb.

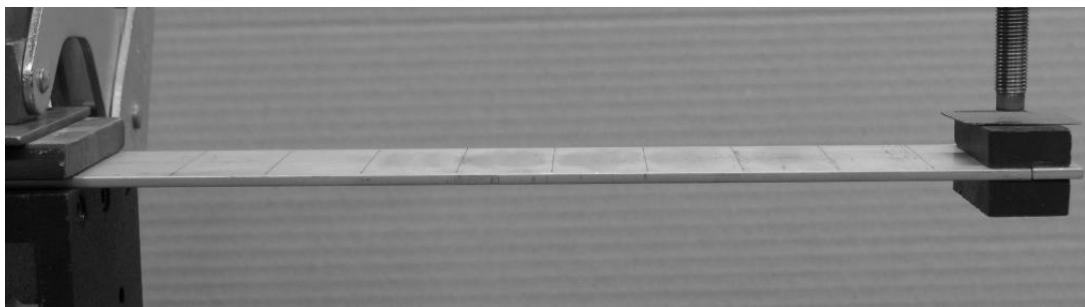


Figure 7-10 Structural system of Fig. 7-6, with the addition at the beam tip of two ceramic magnets and an aluminum spacer. Note the same steel-plate tip-target for the proximity sensor as on Fig. 7-6.

When the beam tip of Fig. 7-10 was tapped lightly upward with a small hammer, the tip moved vertically as shown on Fig. 7-11. The tip-translation response curve is a very clean sine waveform with almost no discernible distortion. The absence of significant distortion in the waveform means that, for our purposes, this beam-mass system behaves like a 2nd order system, even though it is a distributed-parameter system.

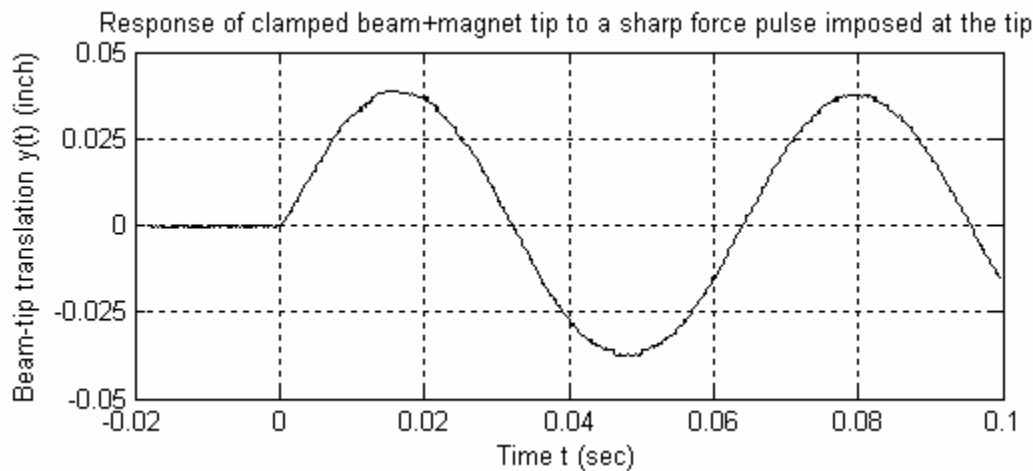


Figure 7-11 Dynamic response to a hammer tap at time $t = 0$ sec of the beam on Fig. 7-10, as detected by the proximity sensor.

The addition of a relatively large quantity of mass at the beam tip reduces considerably the frequency of the waveform on Fig. 7-11 relative to the 34.0-Hz frequency of the fundamental waveform on Figs. 7-7 and 7-9; a careful analysis of the data in Fig. 7-11 shows that the frequency of vibration is $f = 15.85$ Hz.

Example Problem 7-3: a predictive calculation of the vibration frequency of the beam-mass system of Fig. 7-10.

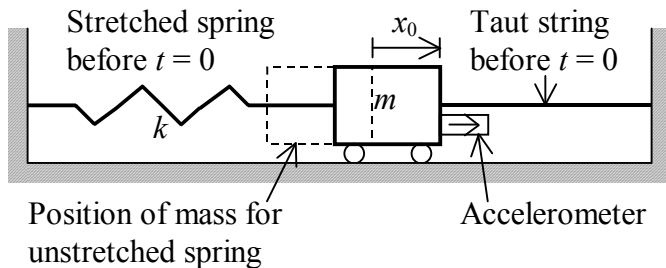
Suppose that we had wanted to predict the frequency of the beam-mass system of Fig. 7-10 before actually assembling the system and measuring the frequency. The following is an intuitively logical approach, though not necessarily theoretically rigorous. Providing that the clamped beam deforms linearly under load, the addition of mass and weight to the beam tip should not alter the beam's stiffness constant, so we use the same measured beam-tip effective stiffness as that of Example Problem 7-1, $k_E = 7.86$ lb/inch. As stated previously, the concentrated-mass assembly that was added to the beam tip weighs 0.254 lb. To obtain the total effective vibrating tip mass, it seems reasonable to add together this value and the effective tip mass of the bare beam plus the steel target, as determined in Example Problem 7-1. Thus, we find the total effective mass $m_E = 0.254$ lb/(386.1 inch/sec²) + 1.72e-4 lb·sec²/inch = 8.30e-4 lb·sec²/inch. Finally, we calculate the predicted natural frequency to be

$$f_n = \frac{1}{2\pi} \sqrt{\frac{k_E}{m_E}} = \frac{1}{2\pi} \sqrt{\frac{7.86 \text{ lb/inch}}{8.30 \times 10^{-4} \text{ lb} \cdot \text{sec}^2/\text{inch}}} = 15.5 \text{ Hz}$$

This predicted natural frequency is lower than the actual measured value of 15.85 Hz by a margin that is unexpectedly large, presuming that all assumptions underlying the theory are valid. This suggests that the actual effective stiffness during the dynamic response of Fig. 7-11 was greater than 7.86 lb/inch. This is quite possible, because the students measured the beam-tip average effective stiffness constant to be 7.86 lb/inch over a range of very small downward deformation of the beam, but they also observed that the local stiffness (slope of the curve of load versus deflection) increased progressively as the downward deformation increased. Observe on Figs. 7-6 and 7-10 at the clamped end of the beam that there appears to be a small gap between the edge of the upper steel clamping plate and the beam top surface; although not clearly visible on these photos, there is a similar gap between the lower clamping steel plate and the beam lower surface. These gaps are widest when the beam is undeformed, but as the beam is deformed downward, the lower gap gradually closes, thus slightly reducing the beam's effective length L and thereby more significantly increasing its tip stiffness, $k_E = 3EI/L^3$, from Example Problem 7-2. The static gravity load of the concentrated-mass assembly shown on Fig. 7-10 closed the lower gap, relative to its width on Fig. 7-6 without the concentrated-mass assembly. Thus, it is indeed likely that the average beam-tip stiffness during the response recorded on Fig. 7-11 was greater than that during the responses recorded on Figs. 7-7 and 7-9. The actual clamping support and restraint of the aluminum beam in this experiment is clearly not the ideal, perfectly sharp edge and completely rigid wall that the elementary theory assumes for a cantilever beam.

7-7 Homework problems for Chapter 7

- 7.1** A particular device is known to be an LTI mass-spring system having negligible damping. It is required that stiffness constant k and mass m be identified experimentally.



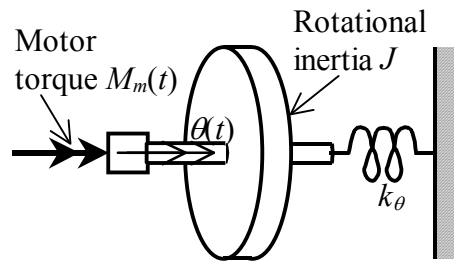
First, a static force of 100 N is applied through a string tied to the mass, producing a static translation of the mass. Next, the string is cut cleanly, allowing the system to vibrate freely from the initial static translation (with zero initial velocity). The subsequent motion is

measured by an *accelerometer*, a sensor that is attached to the system mass and measures, of course, translational acceleration of the mass. The measured acceleration is described with good accuracy by the equation

$$a(t) \equiv \ddot{x}(t) = -4.93 \cos(10\pi t) \frac{\text{m}}{\text{sec}^2}, \text{ for } 0 < t, \text{ with } t \text{ in seconds}$$

- (a) Differentiate twice Eq. (7-12) for displacement, $x(t) = x_{\max} \cos(\omega_n t + \phi)$: first, to derive the associated equation for velocity, $v(t) = \dot{x}(t)$; and second, to derive the associated equation for acceleration, $a(t) = \ddot{x}(t)$.
- (b) From the experimental data given previously and your results in part (a), infer values (with units) for stiffness constant k and mass m .

- 7.2** Consider again the reaction wheel assembly introduced in Section 3-3 (Fig. 3-1), but now suppose that there is a rotational spring with stiffness constant k_θ connecting the shaft to a rigid wall. Also, for this problem only, assume that the bearing viscous damping torque is negligible.



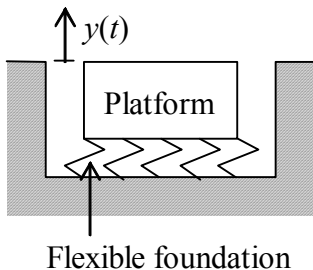
- (a) Sketch a rotational FBD (similar to that in Section 3-3, but with appropriate differences), then apply Newton's 2nd law for rotation to derive the 2nd order ODE for wheel rotation $\theta(t)$. This ODE should have the form of Eq. (7-2), but with the notation appropriate for this system.

- (b) Convert the ODE of part (a) into the standard form (7-5), $\ddot{\theta} + \omega_n^2 \theta = \omega_n^2 u(t)$. Write specific equations (in terms of this system's parameters and notation) for natural frequency ω_n and input quantity $u(t)$.

- (c) The electric torque motor that drives the rotor generates 4.00 oz-inch of torque per amp of electrical current (1 lb = 16 oz). According to the motor manufacturer, the current should be limited to 5.00 A or less in order to avoid toasting the motor, so the maximum

motor torque is 20.0 oz-inch. Suppose that this maximum torque is applied to the rotor as a step function. It is required that the subsequent rotation angle $\theta(t)$ of the rotor not exceed 45° . Calculate the minimum stiffness constant k_θ (units of lb-inch/rad) that will limit the step response $\theta(t)$ to 45° or less. Also, calculate the natural frequency in Hz of the system with this value of k_θ . The rotor has rotational inertia $J = 2.56\text{e}{-3}$ lb-sec²-inch.

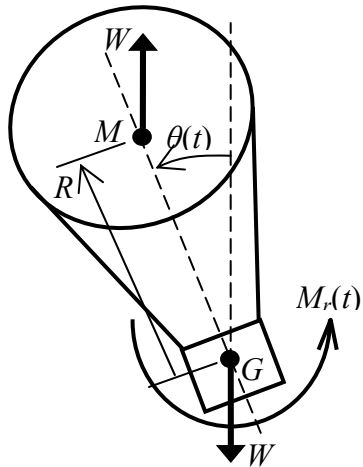
7.3 In the test laboratory of a spacecraft manufacturer, a vibration-isolation platform is supported on a flexible foundation so that the vibration induced by traffic on a busy nearby freeway will not disturb functional testing of delicate space-qualified components.



The platform weighs 907 kg_f , and the flexible foundation has nominal stiffness constant $k = 3,440 \text{ kN/m}$.

- (a) Calculate the predicted values of system natural frequency in rad/sec and Hz, and system natural period T_n . Recall from Section 3-2 that the kg_f is not a consistent unit in the SI system. (*partial answer:* $\omega_n = 61.6 \text{ rad/sec}$)
- (b) In a test to determine precisely the dynamic characteristics of this mass-spring system (having negligible damping), the platform is to be given initial downward displacement $y(0) = -0.104 \text{ mm}$ (relative to the static equilibrium position) and initial upward velocity $\dot{y}(0) = +7.20 \text{ mm/sec}$. The platform will then be allowed to vibrate freely. Write the numerical algebraic equation for the predicted response $y(t)$ in mm.

7.4 Consider the rolling motion of a balloon carrying a basket, with the vehicle neither ascending nor descending.⁷ Weight W of the vehicle acts downward through the vehicle's center of gravity G , and buoyancy force W acts upward through *center of buoyancy* M , which is the center of gravity of the volume of air displaced by the vehicle. We denote as R the separation of G and M in the vehicle's plane of symmetry. Note that with M above G , weight and buoyancy form a stabilizing couple moment, the moment arm being $R \sin \theta$. Suppose that wind, gusts, and possibly other forms of disturbance and control exert an externally applied rolling moment about G , which is denoted as $M_r(t)$. Denote the vehicle's rotational inertia about G as J_G . Assume that the vehicle rolls about point G , as if there were a frictionless hinge at G , and neglect all sources of damping.

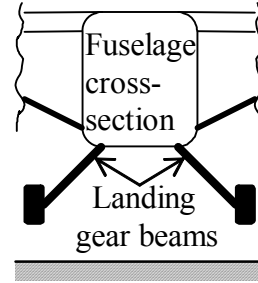


- (a) Apply Newton's 2nd law for rotation to derive the linearized 2nd order ODE for roll angle $\theta(t)$, assumed to be sufficiently small that $\sin \theta \approx \theta$ radians. This ODE should have the form of Eq. (7-2), but with the notation appropriate for this system.

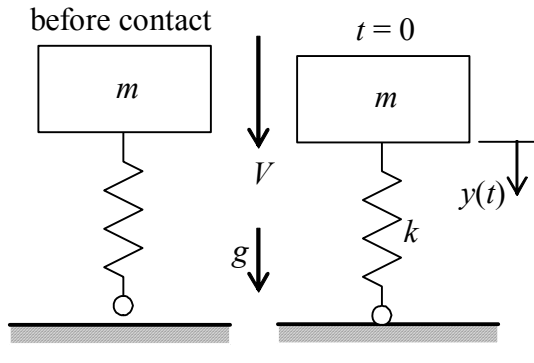
⁷ The same basic principles of dynamics and fluid statics apply if the vehicle is a submerged submarine.

- (b) Convert the ODE of part (a) into the standard form (7-5), $\ddot{\theta} + \omega_n^2 \theta = \omega_n^2 u(t)$. Write specific equations (in terms of this system's parameters and notation) for rolling natural frequency ω_n and standard input variable $u(t)$. (partial answer: $\omega_n = \sqrt{WR/J_G}$)

7.5 (adapted from Craig, 1981, Problem 5.1 on page 120) In single-engine, high-wing, general-aviation airplanes, the structures of the main landing gears are usually simple tilted cantilever beams, as illustrated in the drawing at right. When this type of airplane touches down in a landing, the beams, in combination with the flexible tires, constitute a structural spring that cushions the landing impact.



The drawings below show a simplified model used to study landing impact of a light airplane, with mass m being that of the airplane body, and stiffness k being that of the landing gear beams and tires. (The model also represents a person bouncing passively on a pogo stick.) The airplane's sinking speed just before touchdown is denoted as V , and g is the acceleration of gravity. Let's call the instant of tire contact $t = 0$ and measure the airplane's downward vertical motion $y(t)$ relative to its position at that instant, as indicated on the right-hand drawing. Hence, the initial conditions are $y(0) = 0$ and $\dot{y}(0) = V$.



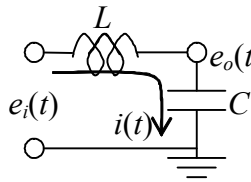
- (a) Sketch a FBD of the forces acting upon m during the time of tire contact with the ground, and use that FBD and Newton's 2nd law to write the 2nd order ODE of motion for $y(t)$. Note in this case that we measure motion relative to the spring-undeformed position, not relative to the static equilibrium position, so it is necessary to include the body weight $W = mg$ on the FBD.

- (b) Put the ODE of motion into standard form. Now combine both the IC solution (since $\dot{y}(0) = V > 0$) and the step-response solution (since W is essentially a step input) that are derived in Section 7-3 to write the algebraic equation for the response $y(t)$ during the time of tire contact. Express this equation in the form $y(t) = C_1 + C_2 \sin(\omega_n t - C_3)$, where the C_i and ω_n are positive constants that you should define in terms of the given algebraic parameters. You should find useful the trigonometric identity $\sin A \cos B \pm \cos A \sin B = \sin(A \pm B)$. If necessary, review the procedure in Section 4-3, Eqs. (4-6)-(4-8), for combining sines and cosines.

- (c) Use the correct result from part (b) above to sketch a time history of the response $y(t)$ during the time of tire contact. To make it relatively easy to sketch, suppose that the landing is hard, with $V/\omega_n = \sqrt{3} W/k$, and show that $y(t) = (W/k)[1 + 2 \sin(\omega_n t - 30^\circ)]$.

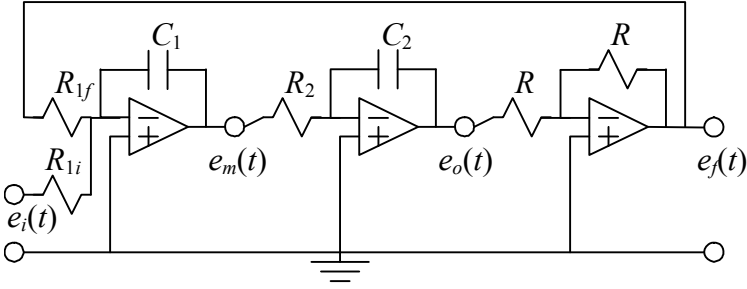
From your $y(t)$ equation and sketch, infer general algebraic equations (not applicable only for $V/\omega_n = \sqrt{3}W/k$) for the maximum value y_{\max} , the time at which $y(t) = y_{\max}$, and the time at which the tires loses contact with the ground upon rebound. For what range of landing impact velocities V does this theory predict that the tires will lose ground contact upon rebound? Is this theory completely realistic?

7.6 The ideal LC circuit⁸ drawn below is a series combination of a voltage source $e_i(t)$, an ideal inductor (having only inductance L , no resistance), and a capacitor with capacitance C . Recall that the current is the rate of change of charge $q(t)$ on the capacitor, $i = dq/dt$. Apply Kirchhoff's voltage law, as in



Electricity Example 4 of Section 5-2, and show that the ODE for $q(t)$ is $L\ddot{q} + (1/C)q = e_i(t)$. Convert this ODE into the standard 2nd order form (7-5), $\ddot{q} + \omega_n^2 q = \omega_n^2 u(t)$; write specific equations [in terms of L , C , and $e_i(t)$] for natural frequency ω_n and input quantity $u(t)$.

7.7 The circuit⁹ drawn at right consists of three stages, each built around an op-amp, and there is *feedback* of voltage $e_o(t)$ from the last (right-hand) stage to the first (left-hand) stage, where the input voltage $e_i(t)$ is applied. The circuit output voltage, $e_o(t)$, is



the output of the middle stage. For the first stage, a *summing, inverting integrator*, use the methods of Chapter 5 to derive the first ODE, $e_f/R_{1f} + e_i/R_{1i} = -C_1 \dot{e}_m$. Next, for the middle stage, an *inverting integrator*, derive the second ODE, $e_m/R_2 = -C_2 \dot{e}_o$ (homework Problem 5.6). Now differentiate the second ODE and use the result to substitute for \dot{e}_m in the first ODE. The last stage is a simple sign inverter, for which $e_f = -e_o$ from Eq. (5-13b). Substitute for e_f and show that the ODE relating output voltage $e_o(t)$ to input voltage $e_i(t)$ for the entire circuit is

$$\ddot{e}_o + \frac{1}{R_2 C_2 R_{1f} C_1} e_o = \frac{1}{R_2 C_2 R_{1f} C_1} \frac{R_{1f}}{R_{1i}} e_i.$$

Convert this ODE into the standard 2nd order form Eq. (7-5), $\ddot{e}_o + \omega_n^2 e_o = \omega_n^2 u(t)$; write specific equations (in terms of this circuit's resistances, capacitances, and input voltage) for natural frequency ω_n and input quantity $u(t)$.

⁸ The LC circuit is a simplified model for devices such as antennas and cavity resonators that transmit and receive electromagnetic energy (Halliday and Resnick, 1960, Chapters 38 and 39). Also, cascades of LC pairs are often used as passive filters in radiofrequency, 100 kHz and above, applications (Horowitz and Hill, 1980, pages 654-656).

⁹ This circuit with op-amps, capacitors, and resistors is essentially the *electronic analog computer* (see the footnote to Problem 5.6) for solving ODE (7-5).

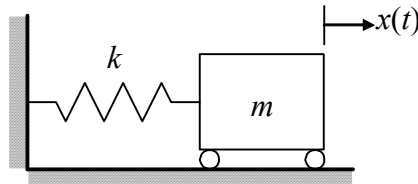
7.8 If you compare the experimental results for a beam that are presented in Example Problem 7-1 (page 7-11) with the ideal theoretical results presented in Example Problem 7-2 (page 7-12), you will observe that there are some significant differences between the two sets of results. In this problem, you will investigate some reasons for those differences.

- (a) The beam of Fig. 7-6 is an extruded aluminum “flat”. Due to manufacturing imperfections, its cross section is not completely uniform (constant) along the length; however, students made the following careful measurements of average cross-sectional dimensions: width $b = 2.00$ inches, depth $h = 0.120$ inch. The students also measured the average weight per unit length of 0.0230 lb/inch . Using this information, calculate the “actual” average weight density w in lb/inch^3 , and compare your value with the standard (in preliminary-design calculations) value for aluminum, 0.1000 lb/inch^3 , which is used in Example Problem 7-2. Also, calculate the total weight of the beam, W_b in lb, based upon the lengthwise weight density 0.0230 lb/inch , and assuming $L = 10.00$ inches.
- (b) In a series of independent tests on aluminum flats from the same manufactured lot as the beam of Fig. 7-6, students measured the average modulus of elasticity in bending $E = 9.43\text{e+6} \text{ lb/inch}^2$, which is about 6% lower than the standard (in preliminary-design calculations) value of $10.0\text{e+6} \text{ lb/inch}^2$. Use this measured value, along with the measured dimensions from part (a) to calculate the effective beam-tip stiffness constant $k_E = 3EI/L^3$, assuming that the beam overhang length is precisely $L = 10.00$ inches. Also, compare this calculated value of k_E with the measured value of 7.86 lb/inch from Example Problem 7-1 and with the ideal theoretical value of 9.766 lb/inch from Example Problem 7-2.¹⁰ [NOTE: It can be shown, by evaluation of *propagation of error*,¹¹ that a small error in the value of depth h produces three times that error in the calculated stiffness constant k_E (for example, a 2% error in h produces a 6% error in k_E); similarly, a small error in the value of length L produces three times that error in k_E .]
- (c) Use the weight W_b that you calculated in part (a) to calculate the effective tip mass of the bare beam alone from $m_{bE} = 0.242672 \times W_b/g$, in which 0.242672 is the theoretical factor introduced in Example Problem 7-2. Next, calculate the total effective tip mass, including the mass of the steel target that is bonded to the beam tip on Fig. 7-6, from $m_E = m_{bE} + (0.0081 \text{ lb}) \div (386.1 \text{ inch/sec}^2)$. Finally, use this m_E and the k_E that you calculated in part (b) to determine a corrected estimate (relative to that of Example Problem 7-2) for natural frequency f_n in Hz.

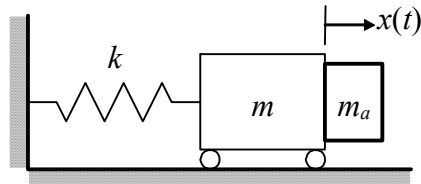
¹⁰ Example Problem 7-3 (page 7-16) describes how tiny gaps between the thick steel clamping plates and the aluminum beam surfaces might change the effective beam length L . It is worth observing also that another possible source of stiffness error, which is difficult to assess quantitatively, is some significant flexibility in the steel clamping plates. The theoretical equation for beam-tip stiffness is based on the assumption that the clamping medium is completely rigid.

¹¹ Propagation of error is discussed in textbooks on experimental instrumentation and measurements, for example, Dally, Riley, and McConnell, 1984, pages 544-545.

7.9 For the undamped (or lightly damped) mass-spring system drawn below at left, Eq. (7-3) gives the natural frequency as $\omega_n = \sqrt{k/m}$. If we attach an additional mass m_a to the original mass, as drawn below at right, then the natural frequency of the modified system is $\omega_{an} \equiv \sqrt{k/(m + m_a)}$.



Original system



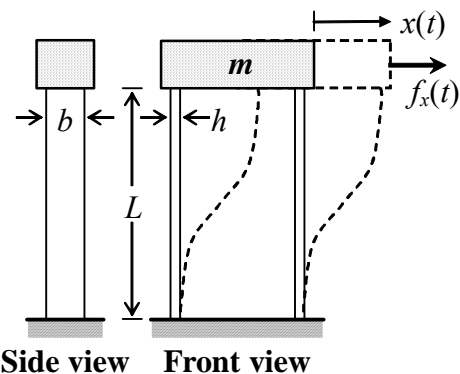
Added-mass system

(a) Suppose that the parameters m and k of the original system are unknown, but that we know the value of the added mass m_a , and that we are able to measure experimentally the natural frequencies ω_n and ω_{an} . Derive algebraically the following equation for the unknown mass m : $m = \frac{m_a}{(\omega_n/\omega_{an})^2 - 1}$.

The traditional method described here may be called the *added-mass* or *added-inertia* method.¹²

(b) Apply the added-mass method of part (a) to calculate both the 2nd order effective tip-mass quantity m_E and the 2nd order effective tip-stiffness constant k_E of the beam structural system shown on Fig. 7-6. The data that you will need is stated in Example Problems 1 and 3: the measured natural frequency of the original system is $f_n = 34.0$ Hz; the concentrated-mass assembly that was added to the beam tip (Fig. 7-10) weighs 0.254 lb; and the measured natural frequency of the added-mass system is $f_{an} = 15.85$ Hz.

7.10 A distributed-parameter structural system¹³ is shown in the drawing; the “snapshot” of a dynamic deformation state (with exaggerated magnitude) is drawn in dashed lines. This system consists of an essentially rigid block of mass m and two parallel cantilever beams. The two flexible (in bending) beams are nominally uniform and identical to each other, with rectangular cross section of width b , depth h , and cross-sectional area $A = bh$. The beams are embedded into the mass, just as they are embedded into the foundation below. In-plane rotation of mass m is suppressed by the very



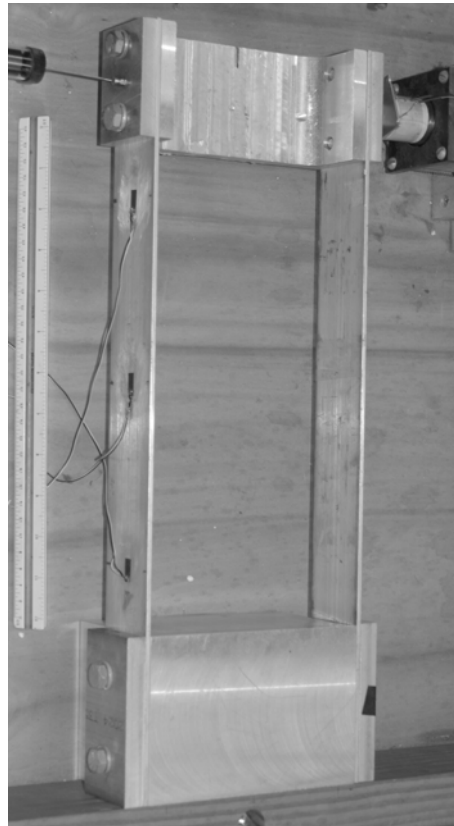
¹² The added-mass method is an elegantly simple technique for finding experimentally the unknown parameters of a 2nd order, or approximately 2nd order, linear mechanical system. The method requires only that we be able to measure accurately the free-vibration frequencies; otherwise, the motion sensors and other instrumentation can be uncalibrated. Use of the added-mass method is a simple example of *system identification*, which is discussed at greater length in Section 9-9.

¹³ This structure is a rudimentary form of one-story *shear building* that is used for studying the structural dynamics of buildings (Craig, 1981, pages 42, 265, 346, etc.; Clough and Penzien, 1974, pages 226-227). The rigid mass represents a floor slab/girder, and the flexible beams represent structural columns.

high axial stiffness of the beams and the separation of the two beams. The bending slopes of the beams where they join mass m are essentially zero due to the rigidity of mass m and of the beam-to-mass joints. Provided that forcing [such as $f_x(t)$ on the drawing] and/or initial conditions are in the plane of the paper, motion of the mass is restricted to one-dimensional translation, $x(t)$. You should be able to verify from a textbook on mechanics of materials that the total effective stiffness constant of the two beams that restrain motion of mass m is $k_E \equiv (f_x/x)_{\text{static}} = 2 \times 12EI/L^3$. We can account for the contribution of the beams' mass to the approximately 2nd order dynamics of this system by using what is known in more advanced theory as the *consistent mass* of a distributed-parameter structure. We denote the weight per unit volume of the beam material as w and the mass density as $\rho \equiv w/g$. Then the total consistent mass from the two beams, which effectively moves with mass m through translation $x(t)$, is $2m_c = 2 \times (156/420)\rho AL$ (Craig, 1981, page 387); thus, the total effective mass of the structural system is $m_E = m + 2m_c$.

(a) Write an algebraic equation for the natural frequency ω_n in rad/sec of this structural system in terms of the system parameters E, I, L, m, w, A , and g .

(b) Consider an actual fabricated version of this structural system, shown in the photograph, which is used in an instructional laboratory experiment.¹⁴ The beams are extruded aluminum "flats", from which students made the following careful measurements of average dimensions and properties: $L = 12.00$ inches, $b = 2.010$ inches, $h = 0.1259$ inch; $w = 0.0965$ lb/inch³; $E = 9.40\text{e+}6$ lb/inch². The relatively rigid mass m was machined from an aluminum block; the students measured its weight as 1.61 lb. Calculate the natural frequency f_n in Hz of this laboratory apparatus.



¹⁴ The principal plane of the actual laboratory apparatus is horizontal relative to gravity. The photograph is rotated 90° to make the plane appear vertical, in order to match the drawing on the previous page.

Chapter 8 Pulse inputs; Dirac delta function; impulse response; initial-value theorem; convolution sum

© 2016 by William L. Hallauer, Jr.

We analyzed previously the response of systems to a half-sine pulse input (e.g., in Sections 1-5 and 1-6). In this chapter, we will continue analysis of pulse excitation and subsequent dynamic response. Most importantly, we will extend the analysis to the concept of the *impulse*, which in its simplest form is $u \times t_d$, the product of excitation and the duration of excitation. In particular, the *Dirac delta* or *ideal unit-impulse* function is essential in the theory of linear systems and also useful in practical applications.

8-1 Flat pulse

This is probably the simplest form of limited-duration input. We define the *flat pulse* initially in the form of a general (standard) input quantity $u(t)$ that can be used with standard forms of system ODEs such as $\dot{x} + (1/\tau_1)x = b u(t)$ for a stable 1st order system and $\ddot{x} + 2\zeta\omega_n\dot{x} + \omega_n^2 x = \omega_n^2 u(t)$ for 2nd order systems. Figure 8-1 illustrates a flat pulse of duration t_d . It can be described mathematically with use of two unit-step functions, as defined in Section 2-4:

$$u(t) = U[H(t) - H(t - t_d)] \quad (8-1)$$

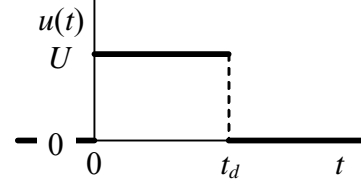


Figure 8-1 Flat pulse

The Laplace transform of Eq. (8-1), from Eqs. (2-28) and (2-29), is

$$L[u(t)] = U \left(\frac{1}{s} - \frac{e^{-st_d}}{s} \right) = \frac{U}{s} \left(1 - e^{-st_d} \right) \quad (8-2)$$

Example: response to a flat pulse of an undamped 2nd order system¹

The ODE for an undamped 2nd order system is $\ddot{x} + \omega_n^2 x = \omega_n^2 u(t)$. Let the initial conditions be zero: $x_0 = 0$, $\dot{x}_0 = 0$. The general solution then is either of the two convolution integral forms, Eqs. (7-9a) and (7-9b). Of those two, the easier one to interpret for the discontinuous flat pulse is Eq. (7-9b), which with zero ICs becomes

$$x(t) = \omega_n \int_{\tau=0}^{\tau=t} \sin \omega_n(t-\tau) \times u(\tau) d\tau \quad (8-3)$$

¹ See also homework Problem 8.3 for a simple yet elegant direct Laplace-transform solution of this problem and a physically meaningful response equation.

Rather than use Eq. (8-1) explicitly, we can observe the form of Fig. 8-1 and write Eq. (8-3) for two different time intervals:

$$x(t) = \begin{cases} \omega_n \int_{\tau=0}^{\tau=t} \sin \omega_n(t-\tau) \times U d\tau, & 0 \leq t \leq t_d \\ \omega_n \int_{\tau=0}^{\tau=t_d} \sin \omega_n(t-\tau) \times U d\tau + \omega_n \int_{\tau=t_d}^{\tau=t} \sin \omega_n(t-\tau) \times 0 d\tau, & t_d \leq t \end{cases} \quad (8-4)$$

The second integral for $t_d \leq t$ is obviously zero. This leaves us with a single integral for each time interval, each integral having the same integrand and lower limit. However, the integrals have different upper limits, so let's denote a general upper limit as T , and evaluate that common integral with use of the change of integration variable $\lambda = t - \tau \Rightarrow d\lambda = -d\tau$:

$$\int_{\tau=0}^{\tau=T} \sin \omega_n(t-\tau) d\tau = \int_{\lambda=t}^{\lambda=t-T} \sin \omega_n \lambda (-d\lambda) = \frac{1}{\omega_n} \int_{\lambda=t}^{\lambda=t-T} d(\cos \omega_n \lambda) = \frac{1}{\omega_n} [\cos \omega_n(t-T) - \cos \omega_n t]$$

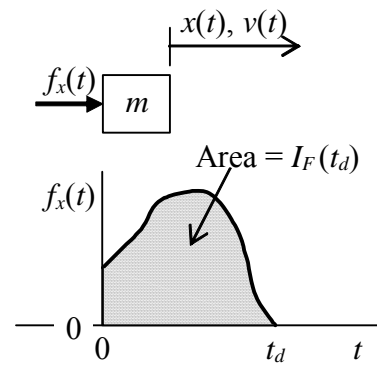
Upper limit $T \equiv t$ for $0 \leq t \leq t_d$ of Eq. (8-4), and $T \equiv t_d$ for $t_d \leq t$, so substituting the integration result into (8-4) gives the final equations,

$$x(t) = \begin{cases} U(1 - \cos \omega_n t), & 0 \leq t \leq t_d \\ U[\cos \omega_n(t-t_d) - \cos \omega_n t], & t_d \leq t \end{cases} \quad (8-5)$$

Equation (8-5) for $0 \leq t \leq t_d$ is just the simple step response of Eq. (7-14), as it logically should be. Inspection of Eq. (8-5) shows that the response $x(t)$ is continuous at $t = t_d$; by differentiating both response equations, we could show that the velocity term $\dot{x}(t)$ also is continuous at $t = t_d$. Indeed, these response quantities should be continuous, because Eq. (8-5) describes a physical response (e.g., of a mass-spring system). In fact, we could solve this problem differently from the beginning by using the requirement of continuity along with step-response (7-14) and IC response (7-12). Step response (7-14) is valid from $t = 0$ to $t = t_d$; then we could find $x(t_d)$ and $\dot{x}(t_d)$ from the step response and use those values as initial conditions for the IC solution to be valid for $t \geq t_d$.

8-2 Impulse-momentum theorem for a mass particle translating in one direction

An unrestrained mass particle subjected to force acting only in the x direction is shown in the drawing at right. The equation of motion is



$$m\ddot{x} = f_x(t) \Rightarrow m\dot{v} = f_x(t)$$

Integrating the equation of motion from time zero to any time $t > 0$ gives

$$m \int_{\tau=0}^{\tau=t} \frac{dv}{d\tau} d\tau = mv(t) - mv(0) = \int_{\tau=0}^{\tau=t} f_x(\tau) d\tau \equiv I_F(t) \quad (8-6)$$

in which $I_F(t)$ is the area under the force time history and is called the *impulse* of the force, with dimensions of force \times time. Equation (8-6), the *impulse-momentum theorem* for a mass particle, states that the change of momentum equals the impulse. For a pulse, a force of limited duration as in the drawing on the previous page, we are generally interested in the total impulse $I_F(t_d)$, which remains unchanged for $t > t_d$.

8-3 Flat impulse

The *flat impulse*, Fig. 8-2, is defined almost identically with the flat pulse, the only difference being that we specify the magnitude of the generalized impulse, I_U , which is the area under the time history of the flat pulse, then we define the magnitude of the input function in terms of the impulse and duration, $U = I_U / t_d$. Thus, for the flat impulse, from Eq. (8-1),

$$u(t) = \frac{I_U}{t_d} [H(t) - H(t - t_d)] \quad (8-7)$$

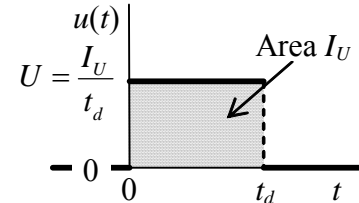


Figure 8-2 Flat impulse

8-4 Dirac delta function, ideal impulse

Consider a limit process with the flat impulse of Fig. 8-2, in which process we progressively shorten the pulse duration while maintaining constant the impulse magnitude (the shaded area), thereby progressively increasing the input magnitude, I_U / t_d . If we carry the process to the limit as $t_d \rightarrow 0$ while maintaining I_U constant, then magnitude $I_U / t_d \rightarrow \infty$. The limit process is illustrated on Fig. 8-3. The function that results is called an *ideal impulse* with magnitude I_U , and it is denoted as $u(t) = I_U \delta(t)$, in which $\delta(t)$ is called the *Dirac delta function* (after English mathematical physicist Paul Dirac, 1902-1984) or the *unit-impulse function*. The ideal impulse function $I_U \delta(t)$ is usually depicted graphically by a thick picket at $t = 0$, as on Fig. 8-3. With $I_U = 1$ in Eq. (8-7), a formal mathematical definition of the unit-impulse function is

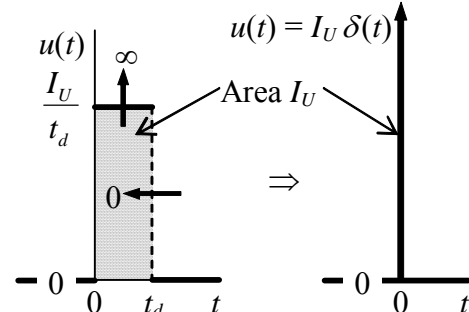
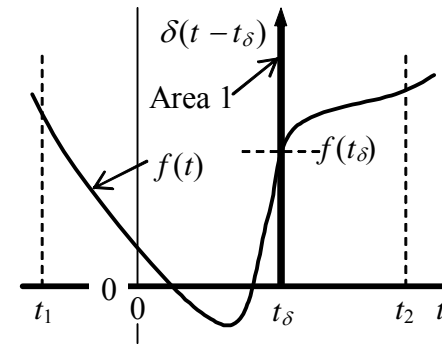


Figure 8-3 Ideal impulse

$$\delta(t) = \lim_{t_d \rightarrow 0} \frac{1}{t_d} [H(t) - H(t - t_d)] \quad (8-8)$$

Observe from Eq. (8-8) that the dimension of $\delta(t)$ is time⁻¹, since the unit-step is dimensionless, so the typical unit of $\delta(t)$ is sec⁻¹.

By definition, the area under $u(t) = I_U \delta(t)$ equals I_U , so the area under $\delta(t)$ equals 1 (hence the name unit-impulse function). This unit area under an infinitely short impulse suggests an important effect of the Dirac delta function in integrands. In order to describe this effect, we define a more general unit-impulse function, $\delta(t - t_\delta)$, which peaks infinitely at some arbitrary time t_δ that is not necessarily zero; otherwise, the nature of $\delta(t - t_\delta)$ is identical to that of $\delta(t)$ [in fact, $\delta(t) = \delta(t - t_\delta)$ for $t_\delta = 0$]. Now suppose that we have some realistic physical function $f(t)$ that is defined over the time interval $t_1 \rightarrow t_2$, and suppose that time t_δ is within this interval, as in the figure at right. Then the useful integration effect of $\delta(t - t_\delta)$ is:



$$\int_{t=t_1}^{t=t_2} f(t) \delta(t - t_\delta) dt = f(t_\delta) \quad (8-9)$$

Equation (8-9) states that, as a multiplier within the integrand, $\delta(t - t_\delta)$ essentially “selects” the value of $f(t)$ at $t = t_\delta$. Result (8-9) is intuitively clear, and it can be proved more rigorously with the theory of so-called *generalized functions* (Lighthill, 1958).

If the upper limit of integration in Eq. (8-9) is an arbitrary time $t > t_\delta$, then the result is a step function:

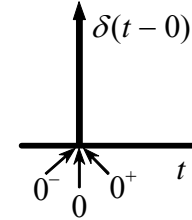
$$\int_{\tau=t_1}^{\tau=t>t_\delta} f(\tau) \delta(\tau - t_\delta) d\tau = f(t_\delta) H(t - t_\delta) \quad (8-10)$$

Setting $f(\tau) = 1$ in Eq. (8-10) leads to a fundamental integral relationship between the unit-impulse function and the unit-step function:

$$\int_{\tau=t_1}^{\tau=t>t_\delta} \delta(\tau - t_\delta) d\tau = H(t - t_\delta) \quad (8-11)$$

Next, we use Eq. (8-9) to derive the Laplace transform of delta function $\delta(t) = \delta(t - 0)$. According to the definition of Eq. (2-13), this transform would be written as $L[\delta(t)] = \int_{t=0}^{t=\infty} e^{-st} \delta(t - 0) dt$; however, there is a problem

with this particular definition: at $t = 0$, which is the lower limit of the integrand (and the initial-value instant for most ODEs that we solve using Laplace transforms), the function $\delta(t - 0)$ is nominally infinite, so the meaning of the integral is uncertain. We choose to remove the uncertainty by specifying that $\delta(t - 0)$ must lie within the limits of the integration. In order to indicate this clearly in notation, we now define three different reference instants, as depicted on the drawing at right: (1) $t = 0^-$, the instant just before activity of the ideal impulse function, at and before which $\delta(t - 0) = 0$; (2) $t = 0$, the instant when $\delta(t - 0)$ acts and is nominally infinite; and (3) $t = 0^+$, the instant just after activity of the ideal impulse function, at and after which $\delta(t - 0) = 0$. Accordingly, we re-define the Laplace transform, more generally than in Eq. (2-13), as



$$L[f(t)] = \int_{t=0^-}^{t=\infty} e^{-st} f(t) dt \quad (8-12)$$

The distinction between $t = 0$ and $t = 0^-$ in the lower limits of Eqs. (2-13) and (8-12), respectively, is meaningless for all problems considered in this book except those in which $f(t)$ involves an ideal impulse function. Application of Eqs. (8-9) and (8-12) now leads to the Laplace transform of the basic ideal impulse function:

$$L[\delta(t)] = \int_{t=0^-}^{t=\infty} e^{-st} \delta(t - 0) dt = e^{-s \times 0} = 1 \quad (8-13)$$

8-5 Ideal impulse response of a standard stable 1st order system

From Eq. (3-7), the problem statement for a standard stable 1st order system is

$$\text{ODE + IC: } \dot{x} + (1/\tau_1)x = b u(t), \quad x(0) = x_0, \quad \text{find } x(t) \text{ for } t > 0 \quad (6-4, \text{repeated})$$

Let the input function be the ideal impulse, $u(t) = I_U \delta(t)$. Although there are several methods for finding response to an ideal impulse, the conventional Laplace-transform approach is relatively simple and probably the most instructive, so we will use this method. With $L[\delta(t)] = 1$ from Eq. (8-13), the steps of the solution are:

$$L[\text{ODE}]: sX(s) - x_0 + (1/\tau_1)X(s) = bU(s) = bI_U \times 1$$

$$\Rightarrow X(s) = \frac{x_0 + bI_U}{s + 1/\tau_1} \quad (8-14)$$

$$\Rightarrow x(t) = (x_0 + bI_U)e^{-t/\tau_1} \quad (8-15)$$

As a check, we evaluate the solution at $t = 0$:

$$x(0) = (x_0 + bI_U)e^{-0/\tau_1} = x_0 + bI_U \neq x_0 \quad (8-16)$$

It appears that something is wrong with response solution Eq. (8-15), because Eq. (8-16) for $x(0)$ contradicts the original IC, $x(0) = x_0$. In order to explain this discrepancy, we must account more carefully for the nature of response to an ideal impulse, and for the distinction between the three different reference instants that are defined in the previous section: (1) $t = 0^-$, the instant just before activity of the ideal impulse function; (2) $t = 0$, the instant when $\delta(t - 0)$ acts; and (3) $t = 0^+$, the instant just after activity of the ideal impulse function. The more detailed analysis follows.

We begin by integrating the basic ODE, $\dot{x} + (1/\tau_1)x = bI_U\delta(t)$, across the ideal impulse function, just from $t = 0^-$ to $t = 0^+$:

$$\int_{\tau=0^-}^{\tau=0^+} \frac{dx}{d\tau} d\tau + \frac{1}{\tau_1} \int_{\tau=0^-}^{\tau=0^+} x d\tau = b \int_{\tau=0^-}^{\tau=0^+} I_U \delta(\tau - 0) d\tau \quad (8-17)$$

The first left-hand-side term of Eq. (8-17) is identically equal to $x(0^+) - x(0^-)$; this result introduces the new quantity $x(0^+)$, which apparently is the *post-impulse initial value* at $t = 0^+$; the *pre-impulse initial value*, $x(0^-) \equiv x_0$, is the original IC specified in Eq. (6-4), but now understood to exist at $t = 0^-$. The right-hand-side integral of Eq. (8-17) gives the finite area I_U under the infinite ideal impulse function. In contrast, the second left-hand-side term of Eq. (8-17) has a finite integrand; we can use the trapezoid rule to approximate the value of the integral and find that it is zero:

$$\int_{\tau=0^-}^{\tau=0^+} x d\tau \approx \lim_{\Delta t \rightarrow 0} \left\{ \frac{1}{2} [x(0^+) + x(0^-)] \Delta t \right\} = 0 \quad (8-18)$$

In Eq. (8-18), $\Delta t \equiv 0^+ - 0^- \rightarrow 0$, in the spirit of the idealization that the ideal impulse function acts over an infinitesimal time interval. Therefore, Eq. (8-17) gives $x(0^+) - x_0 + 1/\tau_1 \times 0 = b \times I_U$, or

$$x(0^+) = x_0 + bI_U \quad (8-19)$$

Chapter 8 Pulse inputs; Dirac delta function; impulse response; initial-value thm.; convolution sum

Comparing Eqs. (8-16) and (8-19) shows that the term $x(0)$ in the former equation really should be the post-impulse initial value, $x(0^+)$.

Equation (8-19) can also be found directly from the Laplace transform $X(s)$ by application of the *initial-value theorem*:

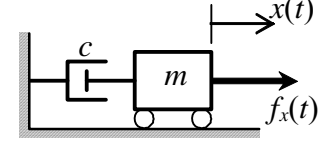
$$\lim_{t \rightarrow 0^+ \text{ from } t > 0} f(t) \equiv f(0^+) = \lim_{s \rightarrow \infty} [sF(s)] \quad (8-20)$$

We present only the relevant application of the initial-value theorem here; derivation of the theorem itself is postponed to Section 8-6. Applying Eq. (8-20) to Laplace transform solution (8-14) gives

$$x(0^+) = \lim_{s \rightarrow \infty} [sX(s)] = \lim_{s \rightarrow \infty} \left(s \times \frac{x_0 + bI_U}{s + 1/\tau_1} \right) = \lim_{s \rightarrow \infty} \left(\frac{s}{s} \times (x_0 + bI_U) \right) = x_0 + bI_U$$

This consequence of the initial-value theorem is identical to Eq. (8-19), which was derived by a different method.

Finally, we present an application of Eq. (8-19) to a mechanical system, and we show that the result conforms with a principle of mechanics. Consider a mass-damper system with mass m and viscous damping constant c , as drawn at right. The mass is initially moving with velocity $v(0^-) = v_0$ when, at $t = 0^-$, the mass is disturbed by an ideal force impulse, $f_x(t) = I_F \delta(t)$. The equation of motion is $mv + cv = f_x(t)$, or in terms of a standard stable 1st order system, $\dot{v} + (1/\tau_1)v = bu(t)$, in which $\tau_1 = m/c$, $b = 1/m$, and $u(t) = f_x(t) = I_F \delta(t)$, so that $I_U = I_F$. The initial (pre-impulse) momentum of the mass is mv_0 . According to Eq. (8-19), the post-impulse velocity of the mass is $v(0^+) = v_0 + (1/m) \times I_F = v_0 + I_F/m$, so that the post-impulse momentum of the mass is $mv(0^+) = mv_0 + I_F$. In words, the momentum of the mass is increased exactly by the magnitude of the ideal impulse, in agreement with the impulse-momentum theorem, Eq. (8-6). Force impulse $I_F \delta(t)$ is a mathematically ideal impulse, not a physically realizable excitation, so the mathematical change in momentum occurs instantly, and the viscous dashpot has no influence on this instantaneous response. From Eq. (8-15), the post-impulse response of the mass is $v(t) = (v_0 + I_F/m)e^{-t/\tau_1}$, $t > 0$.



8-6 Derivation of the initial-value theorem

Consider a physical function $f(t)$, with derivative df/dt , and with Laplace transform $L[f(t)] = F(s)$. The initial-value theorem is:

$$\lim_{\substack{t \rightarrow 0^+ \\ \text{from } t > 0}} f(t) \equiv f(0^+) = \lim_{s \rightarrow \infty} [sF(s)] \quad (8-20, \text{repeated})$$

In general, Eq. (8-20) gives the initial value $f(0^+)$ of a time function $f(t)$ based only on the Laplace transform $L[f(t)] = F(s)$, without requiring that the equation for $f(t)$ be available. If $f(t)$ is dynamic response to excitation that involves the ideal unit-impulse function $\delta(t - 0)$, then $f(0^+)$ is the post-impulse initial value, as defined in Section 8-5; otherwise, $f(0^+) \equiv f(0) \equiv f(0^-)$, which is the standard initial value known to exist before excitation occurs.

Our derivation of the initial-value theorem (from a more detailed proof in Cannon, 1967, p. 569) is based upon the form of Laplace transform that can accommodate the ideal impulse function $\delta(t - 0)$:

$$L[f(t)] = \int_{t=0^-}^{t=\infty} e^{-st} f(t) dt \quad (8-12, \text{repeated})$$

First, we need the following Laplace transform of a derivative, the transform that is associated with definition (8-12):

$$L\left[\frac{d}{dt} f(t)\right] = \int_{t=0^-}^{t=\infty} e^{-st} \frac{df}{dt} dt = sF(s) - f(0^-) \quad (8-21)$$

The derivation of Eq. (8-21) using integration by parts is almost identical to the derivation shown in Eq. (2-15a), the only difference being the lower limit of the integral at $t = 0^-$ instead of $t = 0$. We don't need the corresponding formula for higher-order derivatives right now, but it is appropriate here to state that the initial conditions at $t = 0$ in general formula (2-16) may similarly be replaced by values at $t = 0^-$:

$$L\left[\frac{d^n}{dt^n} f(t)\right] = s^n F(s) - s^{n-1} f(0^-) - s^{n-2} \dot{f}(0^-) - \cdots - {}^{(n-1)}f(0^-) \quad (8-22)$$

Next, taking the limit of all terms in Eq. (8-21) as $s \rightarrow \infty$ gives

$$\lim_{s \rightarrow \infty} L\left[\frac{df}{dt}\right] = \lim_{s \rightarrow \infty} \left(\int_{t=0^-}^{t=0^+} 1 \times \frac{df}{dt} dt + \int_{t=0^+}^{t=\infty} e^{-st} \frac{df}{dt} dt \right) = \lim_{s \rightarrow \infty} [sF(s)] - f(0^-) \quad (8-23)$$

In Eq. (8-23), we separate the definite integral into two parts: (1) a part over the interval from $t = 0^-$ to $t = 0^+$, during which we set $e^{-st} = 1$ (and during which an ideal impulse including $\delta(t - 0)$ could be acting); and (2) a part over the interval from $t = 0^+$ to $t = \infty$. The integrand of the second part includes e^{-st} , and since $s \rightarrow \infty$, we set this integral to

Chapter 8 Pulse inputs; Dirac delta function; impulse response; initial-value thm.; convolution sum

zero: $\lim_{s \rightarrow \infty} \int_{t=0^+}^{t=\infty} e^{-st} (df/dt) dt = 0$. Furthermore, the first integral, which now is independent of s , is evaluated identically as $\int_{t=0^-}^{t=0^+} (df/dt) dt = f(0^+) - f(0^-)$. Therefore, Eq. (8-23) becomes

$$\begin{aligned} \lim_{s \rightarrow \infty} L\left[\frac{df}{dt}\right] &= f(0^+) - f(0^-) = \lim_{s \rightarrow \infty} [sF(s)] - f(0^-) \\ \Rightarrow f(0^+) &= \lim_{s \rightarrow \infty} [sF(s)] \end{aligned} \quad (8-24)$$

This is the version of initial-value theorem that was applied in Section 8-5 to re-derive result (8-19).

If $f(t)$ is dynamic response to excitation that does not involves an ideal unit-impulse function $\delta(t-0)$, then there is no discontinuous jump at $t=0$, i.e., $f(0^+) - f(0^-) = 0$. For this case, therefore, Eq. (8-24) gives the more common (but less general) version of initial-value theorem:

$$f(0^-) = \lim_{s \rightarrow \infty} [sF(s)]$$

8-7 Ideal impulse response of an undamped 2nd order system

The ODE for a standard undamped 2nd order system is $\ddot{x} + \omega_n^2 x = \omega_n^2 u(t)$. Let the input function be the ideal impulse, $u(t) = I_U \delta(t)$, and let the pre-impulse initial conditions be $x(0^-) \equiv x_0$, $\dot{x}(0^-) \equiv \dot{x}_0$. Just as for the 1st order system with ideal-impulse excitation in Section 8-5, we will solve the present problem by the conventional Laplace-transform approach. Note that we will use the second-derivative form of Eq. (8-22): $L[\ddot{f}] = s^2 F(s) - s f(0^-) - \dot{f}(0^-)$. With $L[\delta(t)] = 1$ from Eq. (8-13), the steps of the solution are:

$$L[\text{ODE}]: s^2 X(s) - s x_0 - \dot{x}_0 + \omega_n^2 X(s) = b U(s) = \omega_n^2 I_U \times 1$$

$$\Rightarrow X(s) = \frac{\omega_n^2 I_U + \dot{x}_0 + s x_0}{s^2 + \omega_n^2} = \left(\omega_n I_U + \frac{\dot{x}_0}{\omega_n} \right) \frac{\omega_n}{s^2 + \omega_n^2} + x_0 \frac{s}{s^2 + \omega_n^2} \quad (8-25)$$

$$\Rightarrow x(t) = \left(\omega_n I_U + \frac{\dot{x}_0}{\omega_n} \right) \sin \omega_n t + x_0 \cos \omega_n t, \quad t \geq 0^+ \quad (8-26)$$

At the risk of being excessively repetitive, we emphasize that the discussions in Sections 8-5 and 8-6 show that response (8-26) is the post-impulse solution, certainly

valid mathematically for $t \geq 0^+$, but not necessarily correct, in particular, for the pre-impulse initial conditions at $t = 0^-$.

Solution (8-26) holds for a general undamped 2nd order system; let's adapt it specifically to a mass-spring system, with zero initial conditions, that is hit by an ideal impulse of force having magnitude I_F , with units, for example, of N-sec or lb-sec. From Eq. (7-4), we find

$$u(t) = f_x(t)/k \Rightarrow I_U \delta(t) = I_F \delta(t)/k \Rightarrow I_U = I_F/k \quad (8-27)$$

So, for translational motion $x(t)$ of the mass, Eq. (8-26) with zero initial conditions becomes (recall $k = m\omega_n^2$)

$$x(t) = \omega_n \frac{I_F}{k} \sin \omega_n t = \frac{I_F}{m\omega_n} \sin \omega_n t \quad (8-28)$$

Figure 8-4 shows a few cycles of response Eq. (8-28).

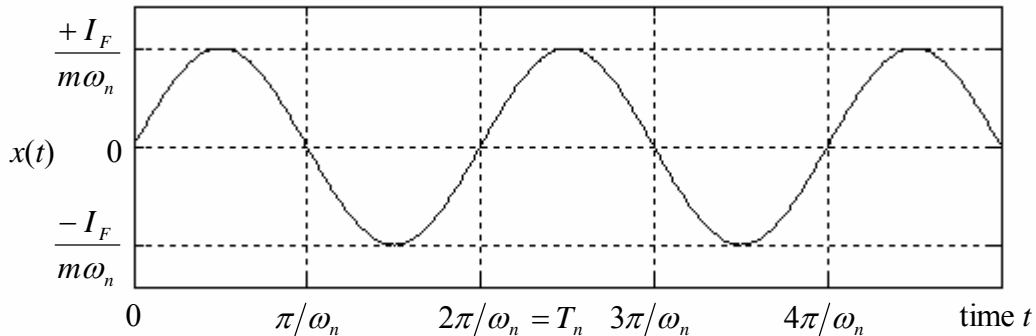


Figure 8-4 Ideal impulse response of a mass-spring system

8-8 Ideal impulse response vs. real response of systems

Section 8-5 shows that, for a 1st order system subjected to excitation by an ideal impulse function, the post-impulse initial value at $t = 0^+$ of output $x(t)$ differs from the pre-impulse initial value at $t = 0^-$. Let's now investigate the initial values in $x(t)$ and $\dot{x}(t)$ that are associated with the 2nd order system of Section 8-7. The output itself is given by Eq. (8-26): $x(t) = (\omega_n I_U + \dot{x}_0/\omega_n) \sin \omega_n t + x_0 \cos \omega_n t, t \geq 0^+$. Evaluating this equation at $t = 0^+$ shows that the post-impulse value is $x(0^+) = x_0$; this is exactly the same value as the given initial value at $t = 0^-$, so there is no discontinuous change in the initial value of $x(t)$ itself for the 2nd order system. Differentiating Eq. (8-26) gives the “velocity” function:

$$\dot{x}(t) = (\omega_n^2 I_U + \dot{x}_0) \cos \omega_n t - \omega_n x_0 \sin \omega_n t, t \geq 0^+ \quad (8-29)$$

Evaluating Eq. (8-29) at $t = 0^+$ gives

$$\dot{x}(0^+) = \omega_n^2 I_U + \dot{x}_0 \neq \dot{x}_0 = \dot{x}(0^-) \quad (8-30)$$

Thus, for the 2nd order system, there is a discontinuous change in the initial value of the “velocity” function.

The discontinuous changes that we observe in initial values for both 1st and 2nd order systems violate physical laws governing real systems, so ideal impulse response solutions appear to be defective and perhaps not applicable to real systems. The reason for this defectiveness is the ideal, not real, nature of the Dirac delta function $\delta(t)$. In physical reality, there is no such thing as a pulse of infinitely short duration and infinitely great magnitude; so $\delta(t)$ and $I_U \delta(t)$ are mathematical functions that do not represent exactly any real physical quantities.

However, the ideal impulse responses that we find can still be useful in applications to real systems, because the ideal impulse function $I_U \delta(t)$ can approximate the effect of a real, time-limited pulse that has the same impulse magnitude, I_U ; therefore, the ideal impulse response can approximate the actual physical response. Why would we use the approximate ideal impulse response rather than just determining the more precise response solution based upon the actual pulse? We would do this because it is always much easier to derive and compute the ideal impulse response than the actual pulse response; moreover, the equation for the ideal impulse response is always simpler and more amenable to practical purposes (such as *system identification*, a form of which is discussed in Section 9-9) than the equation(s) for the actual pulse response.

When is ideal impulse response a good approximation of real pulse response, and when is it not? It depends on the duration t_d of the actual input pulse relative to the shortest *characteristic time* T_c of the system that is being analyzed. The characteristic time is defined loosely as the time interval required for system response to change substantially. The system characteristic times that we know from previous chapters are *time constant* τ_1 for a 1st order system and about one quarter of a *natural period* T_n for a 2nd order system. If t_d is brief relative to the system characteristic time, $t_d \ll T_c$, then the ideal impulse response [Eq. (8-15) for a standard stable 1st order system, Eq. (8-26) for a standard undamped 2nd order system, other equations for other types of systems] will be a good approximation to the actual pulse response; on the other hand, if t_d is on the order of or greater than the system characteristic time, $O(t_d) \geq O(T_c)$, then the ideal impulse response would be a poor approximation, and we should solve for the response using the actual physical pulse. There is no hard and fast rule as to how small the ratio t_d/T_c should be to justify use of the ideal impulse response solution.

In what manner would ideal impulse response differ from the actual pulse response? Let's consider, for example, an undamped 2nd order system with zero ICs. Suppose that the duration of the actual pulse satisfies $t_d \ll \frac{1}{4}T_n$, so that, according to the discussion above, the ideal impulse response should be a good approximation to the actual response. But we already know from Eq. (8-30) that the initial velocity of the ideal impulse response will be wrong, with value $\omega_n^2 I_U$ when it ought to be zero. How will the remainder of the ideal impulse response compare with the actual response? Figure 8-5 depicts conceptually the nature of both ideal impulse response and the comparable real response for a 2nd order system during the initial portion of response. The real response shows the correct initial zero slope, $\dot{x}_0 = 0$.

For a brief period after $t = 0$, the slope of real response increases rapidly until both the response x and the slope \dot{x} essentially match the comparable values of the ideal response, but with a short time lag relative to the ideal response. In other words, the ideal response has a short, artificial time lead relative to the real response. After

the pulse ends, $t_d < t$, the real response is essentially identical to the ideal response, but the ideal response maintains the same artificial time lead for all of the remaining dynamic response. If the pulse duration is very short relative to the system quarter-period, then the artificial time lead will be very small, perhaps not even detectable on a graph of the response. In this case, ideal impulse response will clearly be an excellent approximation to the actual response, and the ideal impulse response will be much easier to derive and compute than the actual response.

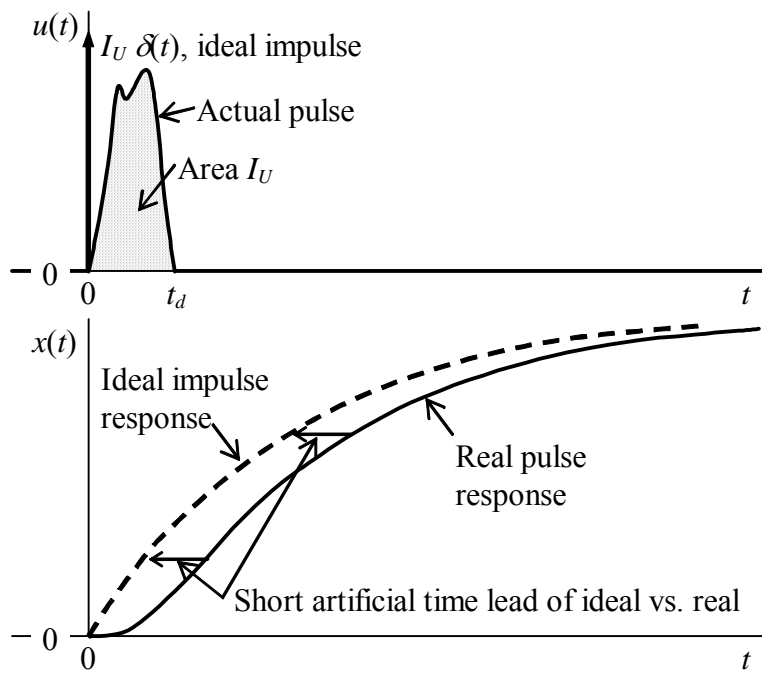


Figure 8-5 Conceptual ideal impulse response and real pulse response for an undamped 2nd order system

Note that the previous paragraph applies specifically for a 2nd order system, but not necessarily for other system types. In particular, for a 1st order system, the differences between a real pulse response and the approximating ideal impulse response have a different character (see, for example, homework Problem 8.5).

8-9 Unit-step-response function and unit-impulse-response function (IRF)

From Chapter 4, Eq. (4-24), the general equation that relates the output Laplace transform to the input transform through the system transfer function is

$$L[x(t)]|_{ICs=0} = TF(s) \times L[u(t)] \quad (8-31)$$

Equation (8-31) is valid for any LTI SISO system. Suppose that the input to such a system is the unit-step function, $u(t) = U H(t)$ with step magnitude $U = 1$:

$$u(t) = H(t) \Rightarrow \text{from Eq. (2-29), } L[u(t)] = L[H(t)] = \frac{1}{s} \quad (8-32)$$

We denote the *unit-step-response function* as $x_H(t)$; as usual for unit-step response and unit-impulse response, we specify zero ICs. Substituting Eq. (8-32) into Eq. (8-31) gives

$$L[x_H(t)] = TF(s) \times \frac{1}{s} \quad (8-33)$$

Next, suppose that the input is the ideal unit-impulse function, $u(t) = I_U \delta(t)$ with impulse magnitude $I_U = 1$:

$$u(t) = \delta(t) \Rightarrow \text{from Eq. (8-13), } L[u(t)] = L[\delta(t)] = 1 \quad (8-34)$$

We denote the *unit-impulse-response function*, with zero ICs, as $h(t)$, and we abbreviate this important function in text as IRF.² Substituting Eq. (8-34) into Eq. (8-31) gives

$$L[h(t)] = TF(s) \times 1 \equiv TF(s) \quad (8-35)$$

Equation (8-35) is an important relationship in linear-system theory: The Laplace transform of the unit-impulse-response function (IRF) equals the transfer function (TF).

Comparing Eqs. (8-32) and (8-34) shows that

$$sL[H(t)] = L[\delta(t)] \quad (8-36)$$

Next, applying Eq. (8-21), with $H(0^-) = 0$, then Eq. (8-36), gives

$$sL[H(t)] = L\left[\frac{dH}{dt}(t)\right] + H(0^-) = L\left[\frac{dH}{dt}(t)\right] = L[\delta(t)] \quad (8-37)$$

Thus, we infer from Eq. (8-37) that

² It would be consistent with notation $x_H(t)$ to denote the IRF as $x_\delta(t)$, but the symbol $h(t)$ is traditional and very common. For examples, see Cannon, 1967, pp. 210, 293 and Meirovitch, 1967, p. 14.

$$\frac{dH}{dt}(t) = \delta(t) \quad (8-38)$$

We can also derive Eq. (8-38) formally by differentiating with respect to time t the following specific form of Eq. (8-11): $H(t - 0) = \int_{\tau=0^-}^{\tau=t>0} \delta(\tau - 0) d\tau$. Expressed in words, the time derivative of the unit-step function is the unit-impulse function. These derivations of Eq. (8-38) are not mathematically rigorous, and the result might seem implausible since both $H(t)$ and $\delta(t)$ are strongly discontinuous functions. However, Eq. (8-38) can be proved with the theory of generalized functions (Lighthill, 1958), and it can also be demonstrated plausibly with the use of limiting processes on functions other than the flat impulse of Section 8-3 (e.g., homework Problem 8.6).

Comparing Eqs. (8-33) and (8-35) shows that

$$TF(s) = sL[x_H(t)] = L[h(t)] \quad (8-39)$$

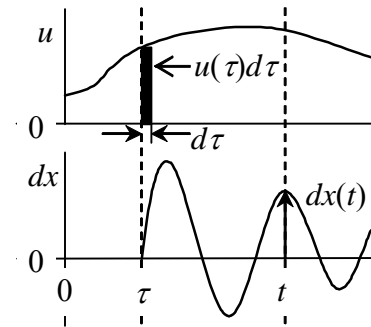
Applying Eq. (8-21) again, with $x_H(0^-) = 0$ by definition, gives

$$\frac{dx_H}{dt}(t) = h(t) \quad (8-40)$$

In words, the velocity of unit-step response equals the unit-impulse response. Equation (8-40) for responses (outputs) is directly analogous to Eq. (8-38) for excitations (inputs). The identical form of the two equations is a consequence of system linearity. Equation (8-40) is another important relationship in linear-system theory, for which we shall have a convenient application in Section 9-8.

8-10 The convolution integral as a superposition of ideal impulse responses

Suppose that an LTI system has zero ICs and that the input is an arbitrary physically realistic function, $u(t)$ for $t > 0$. Let's apply directly the principle of superposition to derive an equation for response $x(t)$ at some arbitrary instant of time $t > 0$. At any instant τ less than t , $0 < \tau < t$, the input $u(\tau)$ imposes onto the system a differentially small impulse of magnitude $dI_U = u(\tau)d\tau$, as is indicated conceptually on the figure at right. Then the differentially small response at time $t > \tau$ due to this impulse at τ is $dx(t) = dI_U \times h(t - \tau) = u(\tau)h(t - \tau)d\tau$, in which $h(t - \tau)$ is the IRF due to a unit impulse acting at instant τ . Because this system is linear, we can express the total response as the superposition of responses due to all separate inputs, as is stated in Section 1-2. In this case, there are an infinite number of separate inputs from the infinite number of instants τ between time zero and time t , so the superposition, or summation, be-



comes a definite integral:

$$x(t)|_{ICs=0} = \int_{\tau=0}^{\tau=t} dx(t) = \int_{\tau=0}^{\tau=t} u(\tau) h(t - \tau) d\tau \quad (8-41)$$

Equations such as (8-41) and its versions for specific systems [with explicit functions for $h(t - \tau)$] are often called *Duhamel integrals* (after Jean-Marie Duhamel, 1797-1872, French mathematician and physicist), especially in the literature of structural dynamics (e.g., Craig, 1981, p. 124).

Equation (8-41) is general, valid for any LTI system. To see a specific application, let's re-visit the standard undamped 2nd order system. With $I_U = 1$, Eq. (8-26) gives the IRF as $h(t) = \omega_n \sin \omega_n t$, so Eq. (8-41) becomes

$$x(t)|_{ICs=0} = \omega_n \int_{\tau=0}^{\tau=t} u(\tau) \sin \omega_n (t - \tau) d\tau \quad (8-42)$$

Equation (8-42) is the Duhamel integral response solution for the standard undamped 2nd order system, and it is identical to convolution integral response solution Eq. (7-9b) with zero ICs. Recall that Eq. (7-9b) was derived mostly from the mathematics of convolution integrals and transforms in Chapter 6. On the other hand, the derivation of Eq. (8-42) above is primarily physical, based upon the IRF and the principle of superposition for linear systems.

8-11 Approximate numerical solutions for 1st and 2nd order LTI systems based on the convolution sum

In Section 6-5, we developed a recurrence formula for the approximate numerical solution of an LTI 1st order ODE with any IC and any physically plausible input function $u(t)$. It is possible to generalize the recurrence-formula approach to 2nd and higher order LTI ODEs, but it would require development of theory and detail that are beyond the objectives of this book (see, for examples: Craig, 1982, Section 7.1; and Meirovitch, 2001, Section 4.10). There is, however, an alternative, relatively simple approach based upon the convolution integral, and this approach is readily applicable to calculating approximate numerical solutions for forced response of 1st and 2nd order LTI systems.

To describe this approach, we begin with the general convolution (Duhamel) integral for forced response, which is valid for any LTI system:

$$x(t)|_{ICs=0} = \int_{\tau=0}^{\tau=t} u(\tau) h(t - \tau) d\tau \quad (8-41, \text{repeated})$$

If initial conditions (ICs) are not zero, then appropriate IC-response solutions must be added to the convolution integral, which represents only the forced response. Examples of such IC-response solutions are given explicitly in Eqs. (6-5), (7-9), and, later, (9-20). Hereafter in this section, we will consider only the forced response, so it will be convenient to omit the “ $ICs = 0$ ” subscript from the output variable and denote it simply as $x(t)$, and later as x with subscripts, x_5 for example.

We seek approximate evaluations of Eq. (8-41) in time-series form, that is, at discrete, equally spaced instants in time. Accordingly, just as in Section 6-5, we define the following notation that employs descriptive subscripts, with the initial instant defined as time zero:

$t =$	$t_1 \equiv 0$	$t_2 = t_1 + \Delta t$ $= \Delta t$	$t_3 = t_2 + \Delta t$ $= 2\Delta t$...	$t_n = t_{n-1} + \Delta t$ $= (n-1)\Delta t$...
$x(t) =$	x_1	x_2	x_3	...	x_n	...
$u(t) =$	u_1	u_2	u_3	...	u_n	...
$h(t) =$	h_1	h_2	h_3	...	h_n	...

Let's designate as a *sequence of length N* any series of N numbers such as t_1, t_2, \dots, t_N , or x_1, x_2, \dots, x_N , and let's denote the entire sequence as $\{t\}_N$, or $\{x\}_N$. If time t is the independent variable, and quantity $f(t)$ is any time-dependent function, let's denote the values of $f(t)$ at times t_1, t_2, \dots, t_N as $\{f(t)\}_N$.

Forced-response solution Eq. (8-41) is exact. But now we introduce what, in general, is an approximation. We assume that the integrand product $u(\tau) h(t - \tau)$ varies so little over the integration time step Δt that it introduces only small error to approximate $u(\tau) h(t - \tau)$ as being constant over Δt , with its value remaining that at the beginning of the time step:

$$u(\tau) h(t - \tau) \approx u(t_{k-1}) h(t - t_{k-1}) \text{ for } t_{k-1} \leq \tau < t_k \quad (8-42)$$

In Eq. (8-42), k is an index that varies, just as τ varies over the integration limits in Eq. (8-41).

Suppose that we have matching sequences of time $\{t\}_N$, input $\{u(t)\}_N$, and IRF $\{h(t)\}_N$, and we wish to calculate the corresponding forced-response output sequence, $\{x(t)\}_N$. Then, using approximation (8-42), we express Eq. (8-41) as follows, with the convolution integral approximated as a summation:

$$\left. \begin{aligned} x(t_1) &= 0 \\ x(t_n) &= \sum_{k=1}^{n-1} u(t_k) h(t_n - t_k) \Delta t, \text{ for } 2 \leq n \leq N \end{aligned} \right\} \quad (8-43)$$

Additional explanation of Eq. (8-43) might be helpful, because the extrapolation of Eq. (8-41) from continuous time to discrete time is not completely obvious. Physically, the

forced response must be zero at the instant $t = t_1 = 0$ when forcing is begun, even if the initial input value $u(0)$ is nonzero; also, the exact convolution integral Eq. (8-41) gives the same result for the upper limit $\tau = t_1 = 0$; hence, $x(t_1) = 0$. Regarding summation over only $n - 1$ values of product $u(t_k) h(t_n - t_k) \Delta t$ in order to obtain $x(t_n)$, consider again approximation (8-42). Equation (8-42) means that the very last term in the summation of Eq. (8-43) that approximates the integral for $x(t_n)$ is the product $u(t_{n-1}) h(t_n - t_{n-1}) \Delta t$.

Equation (8-43) can be written in the following simpler form, using subscript notation and the constancy of time step Δt :

$$\left. \begin{aligned} x_1 &= 0 \\ x_n &= \Delta t \sum_{k=1}^{n-1} u_k h_{n-k}, \text{ for } 2 \leq n \leq N \end{aligned} \right\} \quad (8-44)$$

The summation in Eq. (8-44) is called a *convolution sum*.

It is instructive to write out explicitly a few terms of Eq. (8-44), and then to study a graphical interpretation of the process. Suppose that we have sequences of input values $\{u(t)\}_N$ and IRF values $\{h(t)\}_N$, with length $N \geq 4$, and we wish to find the corresponding sequence of responses $\{x(t)\}_N$. Then the first five terms in the response sequence, from Eq. (8-44), are:

$$x_1 = 0 \quad (8-45a)$$

$$x_2 = \Delta t (u_1 h_1) \quad (8-45b)$$

$$x_3 = \Delta t (u_1 h_2 + u_2 h_1) \quad (8-45c)$$

$$x_4 = \Delta t (u_1 h_3 + u_2 h_2 + u_3 h_1) \quad (8-45d)$$

$$x_5 = \Delta t (u_1 h_4 + u_2 h_3 + u_3 h_2 + u_4 h_1) \quad (8-45e)$$

Figure 8-6 on the next page is a graphical representation of many aspects of the previous discussion. The figure consists of three graphs of conceptual time-dependent functions, with the three time axes aligned. The top graph is a typical input function, $u(t)$; and one plot on the middle graph is a unit-impulse-response function (IRF), $h(t)$, which was chosen to resemble the exponential IRF of a 1st order system, with, in particular, $h(0) \neq 0$. The second (dashed) plot on the middle graph is the function $h(t_4 - t)$, and it was chosen to illustrate Eq. (8-45e) for output quantity x_5 .

Observe on the middle graph of Fig. 8-6 that $h(t_4 - t)$ is derived from $h(t)$ by “folding” $h(t)$ about a vertical line through time $t_4/2$ and then setting to zero the folded function for all times $t < 0$. One of the dictionary definitions for the word “convolution” as a noun is “a fold”, and this is apparently the reason for the use of “convolution” as the

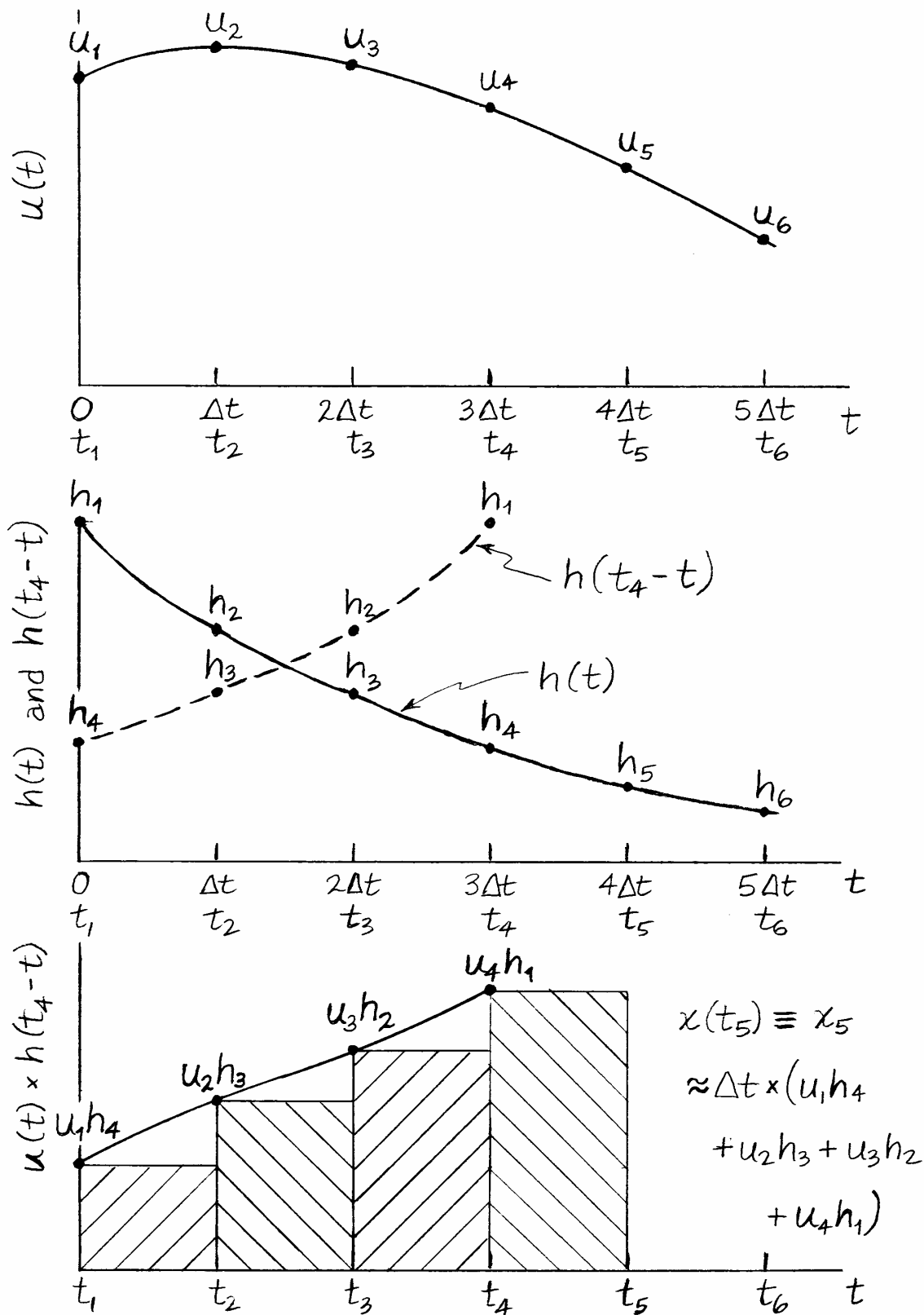


Figure 8-6 Graphical representation of the convolution sum for a conceptual problem with input function $u(t)$ and impulse-response function $h(t)$, with $h(0) \neq 0$

name of a transform, integral, or sum (Evans, 1954, pp. 199-204). It seems that “convolution sum”, for example, sounds more elegant in English than “folding sum”; however, the German noun for mathematical convolution is *Faltung*, meaning “folding” or “bending”, and *Faltung* was often used interchangeably with “convolution” in older English-language textbooks and other technical literature.

The plot on the bottom graph of Fig. 8-6 is the product $u(t) h(t_4 - t)$. At the times t_1, t_2, t_3 , and t_4 , the discrete products $u_k h_{5-k}$ are marked, and approximation (8-42) of piecewise constancy is illustrated by straight horizontal lines, each representing the time step Δt . This is a *stairstep* approximation similar to that used in Section 6-5. The bottom graph shows that Eq. (8-45e) for x_5 is the area under all the cross-hatched rectangles (the entire “staircase”); that area is an approximation of the integral from Eq. (8-41),

$$\int_{\tau=0}^{\tau=t_5} u(\tau) h(t_5 - \tau) d\tau .$$

It is obvious from this graphical interpretation of the convolution

sum that smaller values of time step Δt will produce more accurate numerical integrations, at the expense of longer calculations.

For the conceptual example of Fig. 8-6, which resembles a 1st order system that has initial IRF value $h(0) = h_1 \neq 0$, and also initial input value $u(0) = u_1 \neq 0$, Eq. (8-45b) gives $x_2 = \Delta t(u_1 h_1) \neq 0$. This is noted because it is easy to make the mistake of calculating approximate time response by applying directly the MATLAB function `conv`, as in the command line `x = conv(u, h)`, and then by taking the first N elements of the resulting sequence $\{X\}_{2N-1}$ to be the desired forced response, $\{x(t)\}_N$; this process executes the incorrect equation $x(t_n) = \sum_{k=1}^n u(t_k) h(t_{n+1} - t_k) \Delta t = x_n = \Delta t \sum_{k=1}^n u_k h_{n+1-k}$, for $1 \leq n \leq N$.

This incorrect equation calculates a sequence with $N - 1$ elements the same as those of the correct forced-response sequence, but the incorrect sequence is shifted backward in time by a single time step, Δt . In particular, the incorrect process sets $x_1 = \Delta t(u_1 h_1)$, which would be nonzero for the conceptual problem of Fig. 8-6, and might alert the analyst that something is wrong. (Recall from the discussion above that the initial forced-response value x_1 must be zero.) But for most systems other than standard 1st order systems, the initial value of the IRF is zero, $h_1 = 0$, so the error in $x_1 = \Delta t(u_1 h_1)$ would not be obvious in the calculated results. The lessons from this discussion are: (1) use of the incorrect convolution sum might produce results that are not obviously incorrect; in fact, for very small Δt , the incorrect and correct plots of approximate response versus time might be almost indistinguishable visually; and (2) if you apply directly MATLAB’s function `conv`, then, in order to obtain the correct approximate forced-response sequence, be sure to shift the sequence calculated by `conv` forward in time by a single time step, Δt , and to set $x_1 = 0$.

The following are two numerical examples of the application of Eq. (8-44), first for a 1st order ODE, next for an undamped 2nd order ODE.

Chapter 8 Pulse inputs; Dirac delta function; impulse response; initial-value thm.; convolution sum

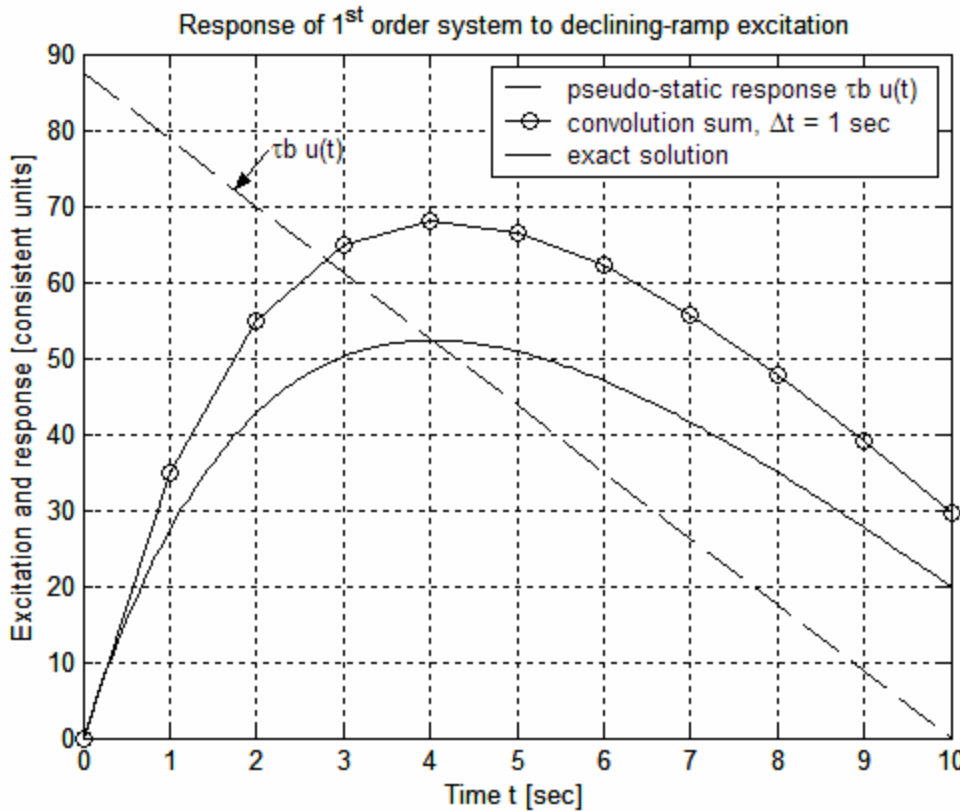
Convolution-sum Example 1: 1st order system Consider the standard 1st order LTI-ODE of a stable system, Eq. (3-7), for dependent variable $x(t)$: $\dot{x} + (1/\tau_1)x = b u(t)$, with IC $x(0) = 0$. From Section 8-5 and homework Problem 8.5(a), the unit-impulse-response function (IRF) is $h(t) = be^{-t/\tau_1}$. Let's set the input function to be a declining ramp, $u(t) = c(a - t)$, in which c , a dimensional constant, is the downward slope of the ramp, and a is the time at which the input passes through zero. For reference, the exact solution for this problem is derived from Eqs. (6-5) or (8-41):³

$$\begin{aligned} x(t) &= be^{-t/\tau_1} \int_{\tau=0}^{\tau=t} e^{\tau/\tau_1} u(\tau) d\tau = be^{-t/\tau_1} \int_{\tau=0}^{\tau=t} e^{\tau/\tau_1} c(a - \tau) d\tau \\ &= bc\tau_1 [(a + \tau_1)(1 - e^{-t/\tau_1}) - t] \end{aligned}$$

With parameters $\tau_1 = 2.5$ sec, $a = 10$ sec, $b = 3.5$, and $c = 1$ (b and c in consistent units), the MATLAB commands to calculate and plot the exact solution $x(t)$, and the approximate solution from Eq. (8-44), for the relatively large time step $\Delta t = 1$ sec, are given next, followed by the resulting graph, which was edited later to add labels, title, and legend. Observe in the MATLAB code that the declining-ramp is entered into the input sequence $\{u(t)\}_N$, as is the IRF sequence $\{h(t)\}_N$. Note that the simple code to calculate the convolution sums over the entire forced-response sequence, $\frac{x_n}{\Delta t} = \sum_{k=1}^{n-1} u_k h_{n-k}$ for $2 \leq n \leq N$, consists of a `for` loop over index k nested within a `for` loop over index n .

```
>> a=10;b=3.5;c=1;tau=2.5;
dt=1;t=0:dt:10;
N=length(t); %sequence length
u=c*(a*ones(1,N)-t); %declining-ramp excitation
plot(t,tau*b*u,'k--'),grid %pseudo-static response
h=b*exp(-t/tau); %IRF, impulse-response function
xc(1)=0; %zero initial value
for n=2:N
    sum=0;
    for k=1:(n-1)
        sum=sum+u(k)*h(n-k);
    end
    xc(n)=sum;
end
xc=dt*xc;
hold,plot(t,xc,'ko-')
te=0:0.05:10;
xe=c*b*tau*((a+tau)*(1-exp(-te/tau))-te); %exact solution
plot(te,xe,'k')
```

³ Details of the integration process are not shown. Note, however, that you can easily verify the validity of the given solution by substituting it into the ODE and IC and finding that they are satisfied.



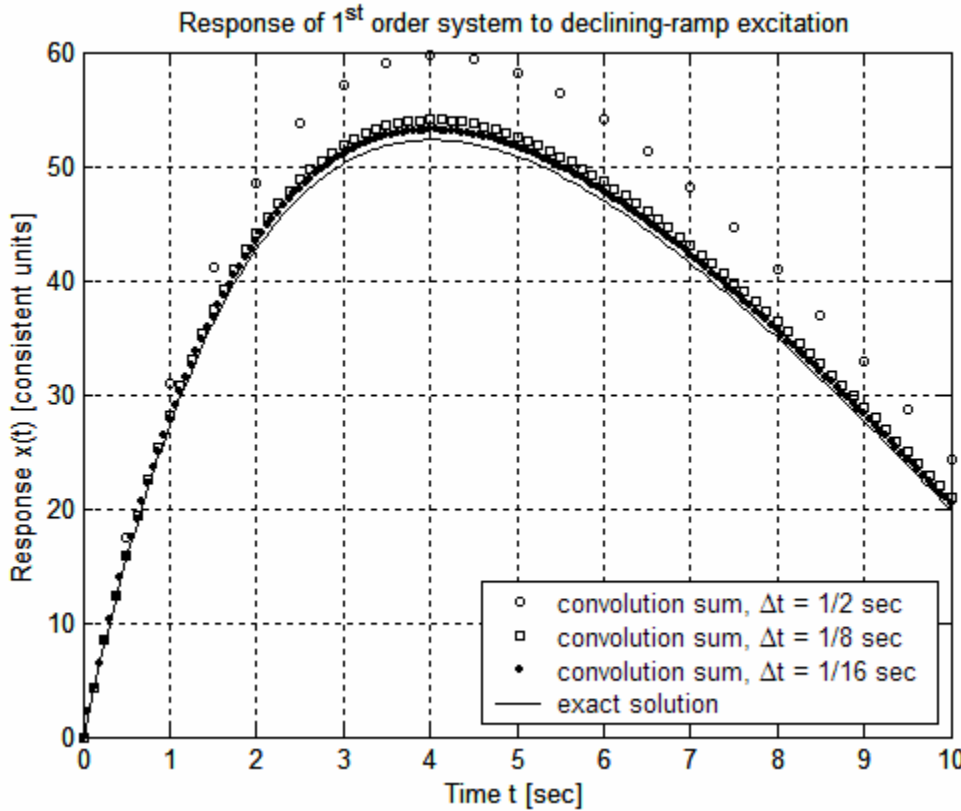
The graph above shows that Eq. (8-44) with the relatively large time step $\Delta t = 1 \text{ sec}$ produces a poor approximation to the exact solution of the 1st order ODE in this problem. The following MATLAB command lines evaluate Eq. (8-44) and plot the results for three progressively smaller values of Δt .

```

>> a=10;b=3.5;c=1;tau=2.5;
tend=10;
m=[2 8 16]; %inverses of time steps for convolution
maxln=tend*max(m)+1;
t=zeros(3,maxln);xc=zeros(3,maxln); %initialize oversized arrays
for j=1:3
    dt=1/m(j);tj=0:dt:tend;N(j)=length(tj);t(j,1:N(j))=tj;
    u=c*(a*ones(1,N(j))-tj); %excitation
    h=b*exp(-tj/tau); %IRF
    xc(j,1)=0; %zero initial value
    for n=2:N(j)
        sum=0;
        for k=1:(n-1)
            sum=sum+u(k)*h(n-k);
        end
        xc(j,n)=dt*sum;
    end
end
plot(t(1,1:N(1)),xc(1,1:N(1)), 'ko',t(2,1:N(2)),xc(2,1:N(2)), 'ks')
hold,plot(t(3,1:N(3)),xc(3,1:N(3)), 'k.')
te=0:0.05:tend;
xe=c*b*tau*((a+tau)*(1-exp(-te/tau))-te); %exact solution

```

```
plot(te,xe,'k'),grid
```



The results above demonstrate for this 1st order system that the approximate solution calculated from the convolution sum approaches the exact solution as $\Delta t \rightarrow 0$. This concludes Convolution-sum Example 1.

Convolution-sum Example 2: undamped 2nd order system Consider the LTI-ODE Eq. (7-5) for a standard undamped 2nd order system, $\ddot{x} + \omega_n^2 x = \omega_n^2 u(t)$, with ICs $x(0) = 0$ and $\dot{x}(0) = 0$. From Sections 8-7 and 8-10 [Eqs. (8-26) and (8-42)], the unit-impulse-response function (IRF) is $h(t) = \omega_n \sin \omega_n t$. Let's set the input function to be a declining-ramp pulse,

$$u(t) = \begin{cases} c(a-t), & 0 \leq t < t_d \\ 0, & t_d \leq t \end{cases}$$

in which c , a dimensional constant, is the downward slope of the ramp, ca is the input at $t = 0$, and t_d is the pulse duration. For reference, the exact solution equations for this problem are derived next from Eqs. (7-9), without details of the integration processes. For the interval during which the pulse is active, $0 \leq t \leq t_d$, we apply Eq. (7-9a), although Eq. (7-9b) would serve just as well:

$$x(t) = \omega_n \int_{\tau=0}^{\tau=t} \sin \omega_n \tau \times u(t-\tau) d\tau = \omega_n \int_{\tau=0}^{\tau=t} \sin \omega_n \tau \times c[a-(t-\tau)] d\tau$$

$$= c[a - t - a \cos \omega_n t + (1/\omega_n) \sin \omega_n t], \text{ valid for } 0 \leq t \leq t_d$$

For the time after the pulse ceases, $t_d < t$, Eq. (7-9b) is preferable since the input $u(t)$ is zero for $t_d < t$, so that the upper limit of integration is clearly t_d :

$$x(t) = \omega_n \int_{\tau=0}^{\tau=t} \sin \omega_n (t-\tau) \times u(\tau) d\tau = \omega_n \int_{\tau=0}^{\tau=t_d} \sin \omega_n (t-\tau) \times c(a-\tau) d\tau$$

$$= \omega_n c \left[\sin \omega_n t \int_{\tau=0}^{\tau=t_d} \cos \omega_n \tau \times (a-\tau) d\tau - \cos \omega_n t \int_{\tau=0}^{\tau=t_d} \sin \omega_n \tau \times (a-\tau) d\tau \right]$$

$$= c \left\{ \begin{aligned} & \sin \omega_n t [a \sin \omega_n t_d - (1/\omega_n)(\omega_n t_d \sin \omega_n t_d + \cos \omega_n t_d - 1)] \\ & - \cos \omega_n t [a(1 - \cos \omega_n t_d) - (1/\omega_n)(-\omega_n t_d \cos \omega_n t_d + \sin \omega_n t_d)] \end{aligned} \right\}, \text{ valid for } t_d < t$$

Let the parameters be: undamped natural frequency $\omega_n = \pi/4.5$ rad/sec (making the associated period 9 sec), $a = 10$ sec, $c = 1$ (in consistent units), and pulse period $t_d = 10$ sec.⁴ The MATLAB commands to calculate and plot the exact solution $x(t)$, and the approximate solution from Eq. (8-44), for the relatively large time step $\Delta t = 1$ sec, are given next, followed by the resulting graph of response, which was edited later to add labels, title, and legend. Observe in the MATLAB code that the entire declining-ramp pulse, including zeros, is entered into the input sequence $\{u(t)\}_N$, as is the IRF sequence $\{h(t)\}_N$. Also, just as in Convolution-sum Example 1, the simple code to calculate the convolution

sums over the entire forced-response sequence, $\frac{x_n}{\Delta t} = \sum_{k=1}^{n-1} u_k h_{n-k}$ for $2 \leq n \leq N$, consists of

a `for` loop over index k nested within a `for` loop over index n .

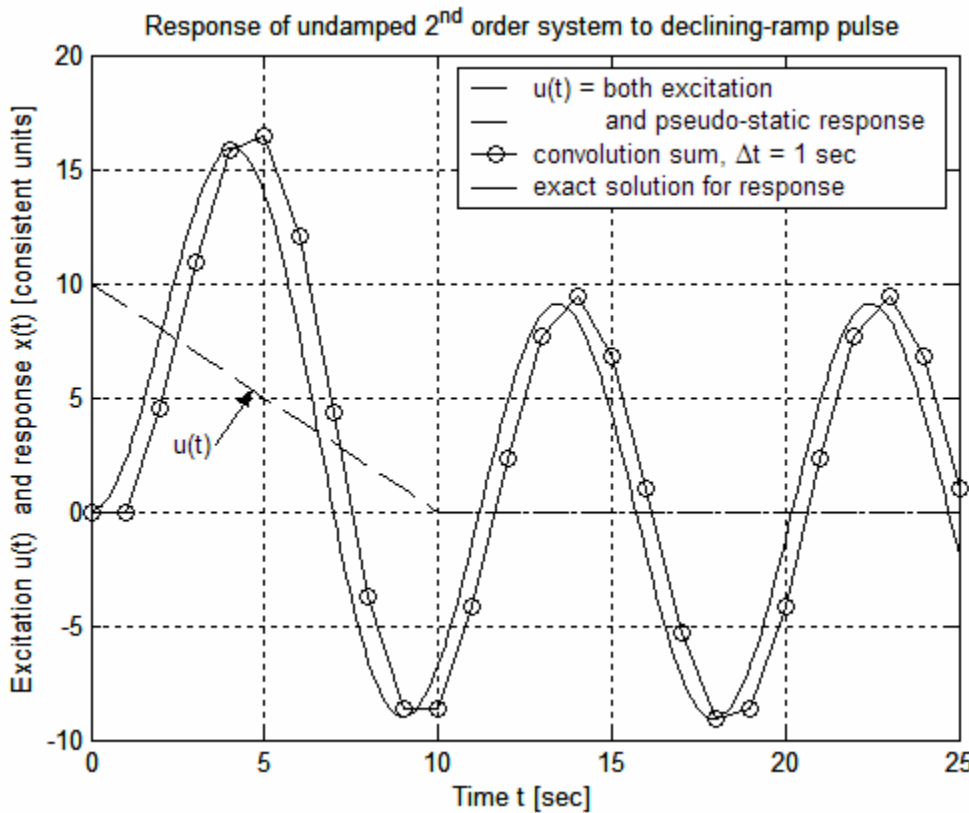
```
>> a=10;c=1;wn=pi/4.5;td=10;
tend=25; %time range (sec)
dt=1;t=0:dt:tend;
nd=td/dt+1; %warning: not necessarily an integer for arbitrary td
N=length(t); %sequence length
u=zeros(1,N);
u(1:nd)=c*(a*ones(1,nd)-t(1:nd)); %declining-ramp pulse
plot(t(1:nd),u(1:nd),'k--'),grid %pseudo-static response
hold,plot(t(nd:N),zeros(1,(N-nd+1)),'k--')
h=wn*sin(wn*t); %IRF, impulse-response function
xc(1)=0; %zero initial value
for n=2:N
    sum=0;
    for k=1:(n-1)
        sum=sum+u(k)*h(n-k);
```

⁴ With $t_d = a$, the pulse is continuous at zero when it ends.

```

    end
    xc(n)=sum;
end
xc=dt*xc;
plot(t,xc, 'ko-')
t1=0:0.1:td;t2=(td+0.1):0.1:tend;te=[t1 t2];
wt1=wn*t1;wt2=wn*t2;
x1=c*(a-t1-a*cos(wt1)+sin(wt1)/wn);
arg=wn*td;sn=sin(arg);cn=cos(arg);
S=a*sn-(arg*sn+cn-1)/wn;C=a*(1-cn)-(-arg*cn+sn)/wn;
x2=c*(S*sin(wt2)-C*cos(wt2));
xe=[x1 x2]; %exact solution
plot(te,xe,'k')

```

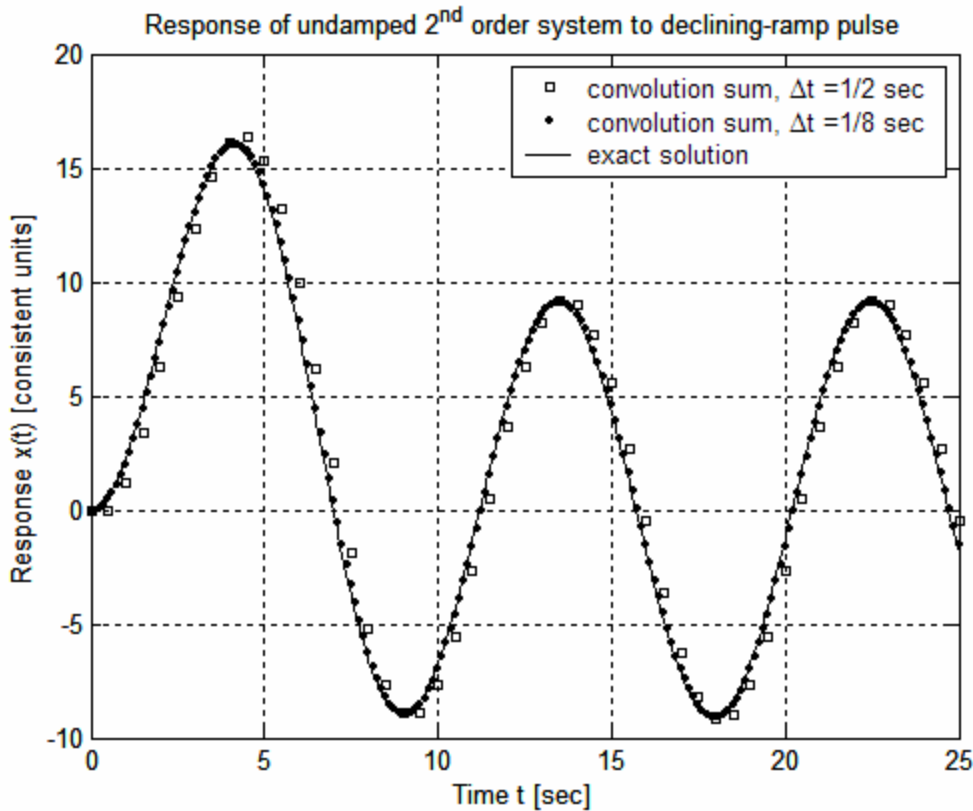


The graph above shows that Eq. (8-44) with the relatively large time step $\Delta t = 1$ sec produces only a mediocre approximation to the exact solution of the 2nd order ODE in this problem. But the plot of the convolution-sum solution also illustrates an important point: not only is $x_1 = 0$, the requirement discussed previously, but also $x_2 = u_1 h_1 = 0$ because the initial IRF value $h_1 = 0$ for the 2nd order ODE, regardless of the initial value u_1 of the input. The appropriate approximation in this case for the initial time derivative of response is $\frac{dx}{dt}(t = 0) \approx \frac{x_2 - x_1}{\Delta t} = 0$. The necessary initial conditions (ICs) for a 2nd order ODE are both $x(0)$ and $\dot{x}(0)$. As is stated at the beginning of this section, any nonzero ICs must be accounted for by separate IC-response solutions, as these ICs cannot be included in the forced-response solution, which is the convolution sum. This means that

Chapter 8 Pulse inputs; Dirac delta function; impulse response; initial-value thm.; convolution sum

we must have $x_1 = x_2 = 0$ for this, or, in fact, any correct convolution-sum approximate solution of a standard 2nd order ODE. The plot above of the convolution-sum solution also demonstrates a negative (relative to numerical accuracy) consequence of the necessary condition $x_2 = 0$: a consistent time lag, of the approximate solution relative to the exact solution, on the order of Δt . The following MATLAB command lines evaluate Eq. (8-44) and plot the results (on the next page) for two progressively smaller values of Δt .

```
>> a=10;c=1;wn=pi/4.5;td=10;
tend=25; %time range (sec)
m=[2 8]; %inverses of time steps for convolution
maxln=tend*max(m)+1;
t=zeros(2,maxln);xc=zeros(2,maxln); %initialize oversized arrays
for j=1:2
    dt=1/m(j);tj=0:dt:tend;N(j)=length(tj);t(j,1:N(j))=tj;
    nd=td/dt+1; %warning: not an integer for arbitrary td
    u=zeros(1,N(j));
    u(1:nd)=c*(a*ones(1,nd)-tj(1:nd)); %declining-ramp pulse
    h=wn*sin(wn*tj); %IRF, impulse-response function
    xc(j,1)=0; %zero initial value
    for n=2:N(j)
        sum=0;
        for k=1:(n-1)
            sum=sum+u(k)*h(n-k);
        end
        xc(j,n)=dt*sum;
    end
end
plot(t(1,1:N(1)),xc(1,1:N(1)), 'ks')
hold,plot(t(2,1:N(2)),xc(2,1:N(2)), 'k.'),grid
t1=0:0.1:td;t2=(td+0.1):0.1:tend;te=[t1 t2];
wt1=wn*t1;wt2=wn*t2;
x1=c*(a-t1-a*cos(wt1)+sin(wt1)/wn);
arg=wn*td;sn=sin(arg);cn=cos(arg);
S=a*sn-(arg*sn+cn-1)/wn;C=a*(1-cn)-(-arg*cn+sn)/wn;
x2=c*(S*sin(wt2)-C*cos(wt2));
xe=[x1 x2]; %exact solution
plot(te,xe,'k')
```



The numerical solution for time step $\Delta t = \frac{1}{2}$ sec is a fair approximate solution, but still with a noticeable time lag, relative to the exact solution, on the order of Δt . However, the numerical solution for time step $\Delta t = \frac{1}{8}$ sec is almost indistinguishable from the exact solution by eye on the graph. This concludes Convolution-sum Example 2.

Finally, we note a curious intersection of two seemingly unrelated mathematical operations, convolution sum and multiplication of polynomials. Suppose that we have two arbitrary sequences of numbers, $\{u\}_N$ and $\{h\}_M$. Consider the convolution sum in the form applied by the MATLAB command line $x = \text{conv}(u,h)$, which produces the sequence $X_n = \sum_{k=1}^n u_k h_{n+1-k}$ for $1 \leq n \leq (N + M - 1)$: $X_1 = u_1 h_1$, $X_2 = u_1 h_2 + u_2 h_1$, $X_3 = u_1 h_3 + u_2 h_2 + u_3 h_1$, $X_4 = u_1 h_4 + u_2 h_3 + u_3 h_2 + u_4 h_1$, etc. Evans (1954, pp. 201-203) observed that the convolution-sum process can be executed with use of tables in a “process similar to multiplication.” First, we define the table of sequences $\{h\}_M$ and $\{u\}_N$:

$\{h\}_M =$	h_1	h_2	h_3	h_4	\dots
$\{u\}_N =$	u_1	u_2	u_3	u_4	\dots

In order to execute the operation $X_n = \sum_{k=1}^n u_k h_{n+1-k}$ using the sequences $\{h\}_M$ and $\{u\}_N$, we construct the table of products below. The first row of the table consists of the prod-

Chapter 8 Pulse inputs; Dirac delta function; impulse response; initial-value thm.; convolution sum

ucts $u_1 \times \{h\}_M$, the second row consists of the products $u_2 \times \{h\}_M$ and this sequence is offset by one column toward the right, the third row consists of the products $u_3 \times \{h\}_M$ and this sequence is offset by two columns toward the right, etc.

	$n = 1$	$n = 2$	$n = 3$	$n = 4$...
$k = 1$	$u_1 h_1$	$u_1 h_2$	$u_1 h_3$	$u_1 h_4$...
$k = 2$		$u_2 h_1$	$u_2 h_2$	$u_2 h_3$...
$k = 3$			$u_3 h_1$	$u_3 h_2$...
$k = 4$				$u_4 h_1$...
...					...

Then each element X_n of the sequence $\{X\}_{N+M-1}$ is the sum of the products in the corresponding n^{th} column of the table of products above:

$\{X\}_{N+M-1} =$	$X_1 = u_1 h_1$	$X_2 = u_1 h_2 + u_2 h_1$	$X_3 = u_1 h_3 + u_2 h_2 + u_3 h_1$	$X_4 = u_1 h_4 + u_2 h_3 + u_3 h_2 + u_4 h_1$...
-------------------	-----------------	---------------------------	-------------------------------------	---	-----

A numerical example applying MATLAB's `conv` function to multiplication of two polynomials was given in Section 6-1. Here is another example of the process using the notation in the tables above, the product of a 1st degree polynomial, P_1 , with a 2nd degree polynomial, P_2 :

$$P_1 \times P_2 = (u_1 s + u_2) \times (h_1 s^2 + h_2 s + h_3) = u_1 h_1 s^3 + (u_1 h_2 + u_2 h_1) s^2 + (u_1 h_3 + u_2 h_2) s + u_2 h_3$$

With zero input polynomial coefficients $u_i = 0$ for $i > 2$ and $h_j = 0$ for $j > 3$, the coefficients of the product cubic polynomial (in descending order of powers of s) are the coefficients X_1 , X_2 , X_3 , and X_4 from the last table above.

If you wished to execute product $P_1 \times P_2$, you would probably use the basic algebra below for multiplication of two polynomials, which, although less general, is essentially the same as the tabular process described above.

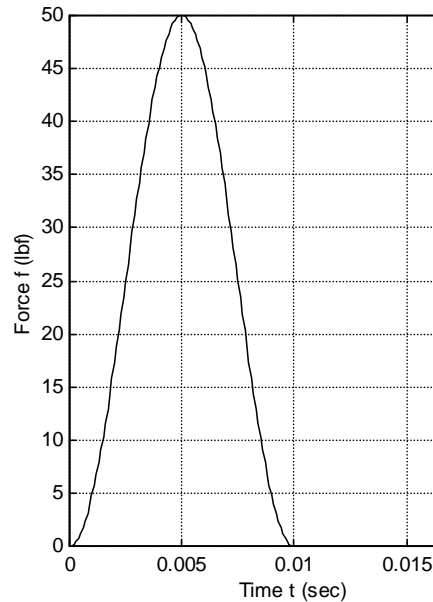
$$\begin{array}{r}
 \text{Polynomial } P_2 = \quad h_1 s^2 + \quad h_2 s + \quad h_3 \\
 \text{Polynomial } P_1 = \quad u_1 s + \quad u_2 \\
 \hline
 u_1 s \times P_2 = \quad u_1 h_1 s^3 + \quad u_1 h_2 s^2 + \quad u_1 h_3 s \\
 u_2 \times P_2 \text{ (offset)} = \quad \quad \quad u_2 h_1 s^2 + \quad u_2 h_2 s + \quad u_2 h_3 \\
 \hline
 P_1 \times P_2 = \text{column sums} = \quad u_1 h_1 s^3 + \quad (u_1 h_2 + u_2 h_1) s^2 + \quad (u_1 h_3 + u_2 h_2) s + \quad u_2 h_3
 \end{array}$$

8-12 Homework problems for Chapter 8

8.1 A “shaped”, 10-millisecond force pulse in pounds is described by the equation

$$f_x(t) = [50 \sin^2(100\pi t)] \text{ lb} \\ \times [H(t) - H(t - 0.01 \text{ sec})]$$

which is graphed at right. In a calculation of system response to this input force, we wish to approximate the force as an ideal impulse function, $f_x(t) \approx I_F \delta(t)$. What is the value (with units) of I_F ? (Hint: before embarking on a long integration, examine the graph carefully for symmetries that will make the calculation almost trivial.)



8.2 Consider an undamped mass-spring system. The mass weighs 20.0 lb including an air-jet thruster that is attached to it, and the spring is calibrated to stretch 0.279 inch when subjected to 100 lb of tension. The air-jet thruster has been designed and calibrated to provide 0.767 lb of thrust in a nearly perfect flat pulse. Let's study the dynamic position response $x(t)$ of the mass, starting from zero ICs, to this force input from the thruster.

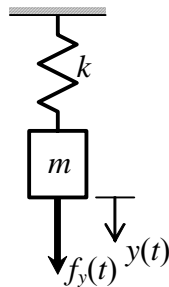
(a) Calculate the natural frequency of the mass-spring system in rad/sec and Hz, and the natural period of the system in seconds and milliseconds. Calculate the impulse magnitude I_F delivered by the air-jet thruster in a blast of duration $t_d = 4.00$ milliseconds.
(Partial answers: $T_n = 75.53$ msec, $I_F = 3.068 \times 10^{-3}$ lb-sec)

(b) Model the 4.00-msec air-jet blast as a perfect flat pulse of force. For this input, write equations that describe the real pulse response $x(t)$ (in inches); for help, see Eq. (8-5) and Eq. (7-4); don't re-derive anything that is already available. Use MATLAB to make an accurate time history plot of this real pulse response $x(t)$ (in inches) over the time interval $0 \leq t \leq 40$ msec.

(c) Approximate the air-jet force input as an ideal impulse with the same impulse magnitude I_F as calculated in part (a). Use Eq. (8-28) to write the numerical equation for the ideal impulse response $x(t)$ in inches.

(d) Use MATLAB to make two accurate time history plots, on the same graph, of $x(t)$ (in inches) over the time span $0 \leq t \leq 40$ msec: the real pulse response of part (b) and the ideal impulse response of part (c).

8.3 Consider the mass-spring system drawn below with $m = 8.03 \text{ kg}$ and $k = 317 \text{ N/m}$. This system is initially at rest in the static equilibrium position when it is hit by a flat force pulse $f_y(t) = F[H(t) - H(t - t_d)]$ of magnitude $F = 4.50 \text{ N}$ and short duration $t_d = 0.05 \text{ sec}$. In this problem, we analyze the dynamic displacement of the mass relative to the initial static equilibrium position.



- (a) The following succinct response equation can be derived easily with use of transform Eq. (8-2) and the general Laplace transform of a function that is translated in time: $L[f(t - t_d)H(t - t_d)] = e^{-st_d} F(s)$.

$$y(t) = \frac{F}{k} [(1 - \cos \omega_n t)H(t) - (1 - \cos \omega_n (t - t_d))H(t - t_d)]$$

Show that this equation is fully equivalent to the response equations in the two-part solution Eq. (8-5). Note from Eq. (7-4) that $U = F/k$.

Next, use MATLAB to plot the response curve of $y(t)$ versus t from $t = 0$ to $t = 1 \text{ sec}$, the period of the mass-spring system.

(b) In order to compare with the real response, plot [on the same graph as part (a)] the ideal impulse response of the system, $y(t) = (I_F / m\omega_n) \sin \omega_n t$, Eq. (8-28), using for I_F the value of the actual impulse from given data. Label clearly which curve is the real response and which is the ideal impulse response; title and label your graph appropriately.

8.4 In this exercise, let's apply the initial-value theorem to the problem of Section 8-7: the standard undamped 2nd order system that has non-zero initial conditions and is disturbed by an ideal impulse, $u(t) = I_u \delta(t)$.

(a) Determine the post-impulse initial value, $x(0^+)$, by using Eq. (8-25) for $X(s)$ in the initial-value theorem. Is your result the same as that found directly from Eq. (8-26)?

(b) Use Eq. (8-25) for $L[x(t)]$ to find the Laplace transform $L[\dot{x}(t)]$ of the “velocity” function; be sure to include both terms of Eq. (8-21) for the transform of a derivative.

(c) Determine the post-impulse initial “velocity”, $\dot{x}(0^+)$, by using your $L[\dot{x}(t)]$ from part (b) in the initial-value theorem. Is your result the same as that of Eq. (8-30)?

8.5 Consider the standard 1st order LTI-ODE (of a stable physical system) for dependent variable $x(t)$: $\dot{x} + (1/\tau_1)x = bu(t)$, with IC $x(0) = 0$, and with excitation by an ideal impulse, $u(t) = I_u \delta(t)$.

(a) Infer from the results of Section 8-5 the unit-impulse-response function (IRF), $h(t)$.

(b) Use the result from part (a) to write the Duhamel integral response solution for the standard stable 1st order system, which is comparable to Eq. (8-42) for the standard undamped 2nd order system.

(c) The object of this part is to compare numerically the ideal impulse response derived in Section 8-5 with the response to a real, flat pulse that has the same impulse magnitude as the ideal impulse and a pulse duration that is short relative to the system time constant. Use MATLAB to make two accurate time history plots, on the same graph, of the dimensionless output $x(t)/bI_U$ versus dimensionless time t/τ_1 over the time interval $0 \leq t/\tau_1 \leq 1$. One plot will be the response to the ideal impulse. The other plot will be the response to a flat pulse having dimensionless duration $t_d/\tau_1 = 0.2$; for this plot, use the response equations derived in homework Problem 6.2. You should find that the ideal impulse response is much easier to calculate than the real-pulse response. However, is the ideal impulse response a sufficiently accurate approximation to the real response, and, if so, is it accurate over all time, or over just some portion of the response time?

8.6 If you compare Fig. 2-2 for the Heaviside unit-step function $H(t)$ with Fig. 3-3 for step response of a stable 1st order system, you can see that as time constant τ_1 becomes progressively smaller, the 1st order step response looks progressively more like the unit-step function. Using Eq. (2-26) for $H(t)$ as a model, let's define the "exponential-unit-step" function $H_e(t)$:

$$H(t) = \begin{cases} 0 & \text{for } t < 0 \\ 1 & \text{for } t > 0 \end{cases} \Rightarrow H_e(t) \equiv \begin{cases} 0 & \text{for } t < 0 \\ 1 - e^{-t/\tau_1} & \text{for } t > 0 \end{cases}$$

It is clear that $H(t)$ can be defined as a limit of $H_e(t)$: $H(t) = \lim_{\tau_1 \rightarrow 0} H_e(t)$. Now, let's define the "exponential-unit-impulse" function $\delta_e(t)$:

$$\delta_e(t) \equiv \begin{cases} 0 & \text{for } t < 0 \\ \frac{d}{dt} (1 - e^{-t/\tau_1}) = \frac{1}{\tau_1} e^{-t/\tau_1} & \text{for } t > 0 \end{cases}$$

Sketch by hand an over-and-under pair of graphs, the upper graph being $H_e(t)$ vs. t and the lower graph being $\delta_e(t)$ vs. t . Sketch conceptually the two exponential functions for a few values of time constant τ_1 ; show in particular how $H_e(t)$ and $\delta_e(t)$ evolve as τ_1 becomes progressively smaller. Describe the character of $\delta_e(t)$ as $\tau_1 \rightarrow 0$. Is it plausible physically to define the Dirac delta function as $\delta(t) = \lim_{\tau_1 \rightarrow 0} \delta_e(t)$, which, with the definition $H(t) = \lim_{\tau_1 \rightarrow 0} H_e(t)$, is equivalent to $\delta(t) = dH/dt$? [This is one of many possible limit-process definitions of $\delta(t)$; Eq. (8-8) is a more commonly used definition.]

8.7 Consider the mass-spring system (with damping neglected) of Fig. 1-4, for which the ODE of motion is $m\ddot{x} + kx = f_x(t)$, and the system parameters are $m = 2.20$ kg and $k = 770$ N/m. Initial conditions are zero: $x(0) = 0$ and $\dot{x}(0) = 0$. The excitation is a ramped exponential force pulse, $f_x(t) = F_m (t/t_m) \exp(1 - t/t_m)$, with $F_m = 6.0$ N and $t_m = 1/12$ sec. Write a MATLAB program, or adapt the code of Convolution-sum Example 2 in Section 8-11, to calculate and plot an approximate numerical solution for $x(t)$ over the time interval $0 \leq t \leq 1$ sec. Adjust the time-step size Δt and number of time steps over the 1-sec interval in your code until the graph of your approximate solution appears very similar to that on Fig. 1-5 of the corresponding exact solution. Submit your MATLAB code and your final graph of response.

Chapter 9 Damped 2nd order systems: general time response

© 2016 by William L. Hallauer, Jr.

9-1 Homogeneous solutions for damped 2nd order systems; viscous damping ratio ζ

For the mass-dashpot-spring (m - c - k) system of Fig. 9-1, the equation of motion (3-20) derived from Newton's 2nd law, with use of the FBD in Fig. 3-9, is

$$m \ddot{x} + c \dot{x} + k x = f_x(t) \quad (9-1)$$

Although 2nd order systems appear in many different mechanical and electrical forms, the m - c - k system of Fig. 9-1 is generally considered to be the prototype.

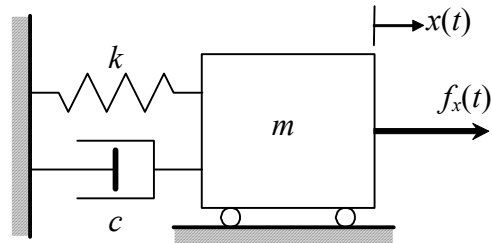


Figure 9-1 Mass-dashpot-spring system

To provide direction for developing a standard form of damped 2nd order ODE, let's consider the homogeneous form of Eq. (9-1) and seek a homogeneous solution $x_h(t)$ using the conventional method that is described in Section 1-5 [Eq. (1-6) and the subsequent discussion]:

$$m \ddot{x}_h + c \dot{x}_h + k x_h = 0 \quad (9-2)$$

We seek $x_h(t) = C e^{\lambda t}$, in which C and λ are unknown:

$$\Rightarrow (m\lambda^2 + c\lambda + k)C e^{\lambda t} = 0$$

Now $x_h(t) = C e^{\lambda t} \neq 0$ for a non-trivial solution, leading to the characteristic equation:

$$m\lambda^2 + c\lambda + k = 0 \quad (9-3)$$

We solve Eq. (9-3) for characteristic values λ using the quadratic formula, recognizing $k/m = \omega_n^2$ from Eq. (7-3):

$$\lambda = \frac{-c \pm \sqrt{c^2 - 4mk}}{2m} = -\frac{c}{2m} \pm \sqrt{\left(\frac{c}{2m}\right)^2 - \frac{k}{m}} = -\frac{c}{2m} \pm \sqrt{\left(\frac{c}{2m}\right)^2 - \omega_n^2}$$

The dimensionless *viscous damping ratio* ζ and the *critical* viscous damping constant c_c are defined as follows:

Chapter 9 Damped 2nd order systems: general time response

$$\zeta \equiv \frac{c}{2m\omega_n} = \frac{c}{2\sqrt{mk}} \equiv \frac{c}{c_c} \quad \text{where} \quad c_c \equiv 2m\omega_n = 2\sqrt{mk} \quad (9-4)$$

Recall that constants m , c , and k are normally positive for a passive, stable system, so that ζ and c_c also are normally positive. With definitions (9-4), the characteristic values take the form

$$\lambda = -\left(\frac{c}{2m\omega_n}\right)\omega_n \pm \sqrt{\left(\frac{c}{2m\omega_n}\right)^2 \omega_n^2 - \omega_n^2} = -\zeta\omega_n \pm \omega_n\sqrt{\zeta^2 - 1} \quad (9-5)$$

Depending upon the value of ζ relative to 1, there are three possible distinct solution types for characteristic value λ and the associated homogeneous solution $x_h(t)$:

Type 1: $\zeta > 1$, overdamped or supercritically damped system

Both roots are real and negative:

$$\lambda_{I,II} = -\zeta\omega_n \pm \omega_n\sqrt{\zeta^2 - 1} \quad (9-6)$$

The corresponding homogeneous solution is an exponentially decaying response with two distinct time constants:

$$x_h(t) = C_I e^{\lambda_I t} + C_{II} e^{\lambda_{II} t} = C_I e^{-t/\tau_I} + C_{II} e^{-t/\tau_{II}} \quad \text{where} \quad \tau_{I,II} \equiv -1/\lambda_{I,II} \quad (9-7)$$

If we were given initial conditions $x_h(0)$ and $\dot{x}_h(0)$, we could now solve for constants C_I and C_{II} in terms of the ICs, and thus obtain an IC solution for the overdamped $m-c-k$ system. We will obtain such a solution in Section 9-10, using different methods.

Type 2: $\zeta = 1$, critically damped system

The two roots (9-5) are equal and negative:

$$\lambda_{I,II} = -\omega_n \quad (9-8)$$

Due to the existence of repeated roots, the homogeneous solution involves both a pure exponential decay term and a term multiplied by time t that also decays, but more slowly than exponential:

$$x_h(t) = C_I e^{-\omega_n t} + C_{II} t e^{-\omega_n t} \quad (9-9)$$

Chapter 9 Damped 2nd order systems: general time response

The case of critical damping is more of academic than practical interest, since it is rare in practice that physical parameters lead to the exact value $\zeta = 1$. (see homework Problem 9.11)

Type 3: $0 \leq \zeta < 1$, underdamped or subcritically damped system

In this case, the terms in Eq. (9-5) within the square root are negative, so we have two complex characteristic values, each with a negative real part:

$$\lambda_{I,II} = -\zeta\omega_n \pm j\omega_n\sqrt{1-\zeta^2} \equiv -\zeta\omega_n \pm j\omega_d \quad \text{where } \omega_d \equiv \omega_n\sqrt{1-\zeta^2} \quad (9-10)$$

Frequency ω_d is called the *damped natural frequency*. The corresponding homogeneous solution is

$$x_h(t) = C_I e^{\lambda_I t} + C_{II} e^{\lambda_{II} t} = C_I e^{(-\zeta\omega_n + j\omega_d)t} + C_{II} e^{(-\zeta\omega_n - j\omega_d)t} = e^{-\zeta\omega_n t} (C_I e^{j\omega_d t} + C_{II} e^{-j\omega_d t})$$

By applying Euler's equation (2-8) and combining constants C_I and C_{II} appropriately to form two new constants D_I and D_{II} , we can re-write this homogeneous solution in the form of an exponentially decaying sinusoid:

$$x_h(t) = e^{-\zeta\omega_n t} (D_I \cos \omega_d t + D_{II} \sin \omega_d t) \quad (9-11)$$

If we were given initial conditions $x_h(0)$ and $\dot{x}_h(0)$, we could now solve for real constants D_I and D_{II} in terms of the ICs, and thus obtain an IC solution for the underdamped *m-c-k* system. We will obtain this solution in Section 9-4, using the general solution for $x(t)$ obtained from Laplace transformation. Underdamped systems are the most important and common in practical applications and the most interesting, so we will devote more attention to them than to the other two types of damped 2nd order systems.

9-2 Standard form of ODE for damped 2nd order systems

Using the concepts and notation developed in the previous section, we now derive the “standard” form of ODE governing response of damped 2nd order systems, beginning with ODE (9-1) for an *m-c-k* system:

$$m\ddot{x} + c\dot{x} + kx = f_x(t) \Rightarrow \ddot{x} + 2\frac{c}{2\sqrt{mk}}\sqrt{\frac{k}{m}}\dot{x} + \frac{k}{m}x = \frac{1}{m}f_x(t) = \frac{k}{m}\frac{f_x(t)}{k} \quad (9-12)$$

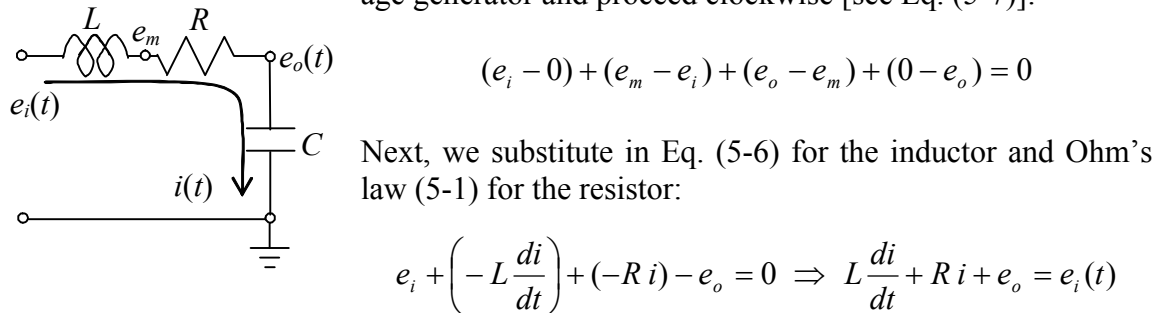
Using the definitions from the previous section and the standard input quantity (7-4), $u(t) \equiv f_x(t)/k$, we re-write Eq. (9-12) in the standard form:

$$\ddot{x} + 2\zeta\omega_n\dot{x} + \omega_n^2x = \omega_n^2u(t) \quad (9-13)$$

In Eq. (9-13), $x(t)$ represents any appropriate output quantity (not necessarily just position as in Fig. 9-1) for a damped 2nd order system. Recall from Chapter 7 that we can identify $u(t)$ as being the pseudo-static output, $x_{ps}(t)$; if $x(t)$ varies slowly enough that the terms \ddot{x} and $2\zeta\omega_n\dot{x}$ are negligible in comparison with ω_n^2x , then ODE (9-13) reduces to a simple algebraic equation, $\omega_n^2x \approx \omega_n^2u(t)$, the solution of which is the pseudo-static response, $x(t) = u(t) \equiv x_{ps}(t)$.

Example 9-1: the LRC circuit, a 2nd order electrical system

Let's derive an ODE governing the dynamic behavior of the *LRC* circuit in the figure below. To write Kirchhoff's voltage law for this circuit, we start at the input voltage generator and proceed clockwise [see Eq. (5-7)]:



For the capacitor, we use (5-3), then differentiate the result and substitute into the ODE:

$$i = C \frac{d(e_o - 0)}{dt} = C \dot{e}_o \Rightarrow \frac{di}{dt} = C \ddot{e}_o \Rightarrow LC \ddot{e}_o + RC \dot{e}_o + e_o = e_i(t)$$

Therefore, we can write the ODE in the standard 2nd order form (9-13) as¹

$$\ddot{e}_o + \frac{R}{L} \dot{e}_o + \frac{1}{LC} e_o = \frac{1}{LC} e_i(t)$$

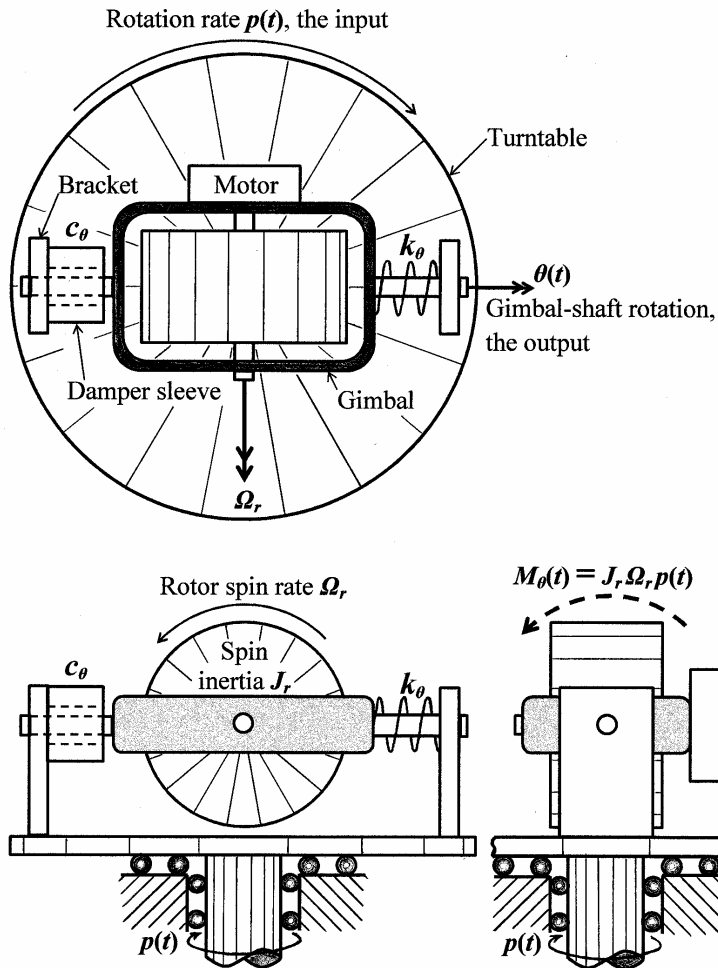
From this standard form, we see that the undamped natural frequency is $\omega_n = 1/\sqrt{LC}$, and the viscous damping ratio is $\zeta = (1/2\omega_n)(R/L) = \frac{1}{2}R\sqrt{C/L}$.

Example 9-2: the rate gyroscope, a 2nd order mechanical system

The schematic three-view engineering sketch on the next page represents the basic functional form of a single-axis *rate gyroscope* (gyro), a sensor of rotational velocity.² The supporting turntable in the sketch could be a fixture in a laboratory setup for cali-

¹ In Appendix B, Section B-3, this ODE is derived by an alternative method using energy and power. The rate of change of system energy is equated with the power supplied to the system.

² Gyroscopes have been used in sensors and actuators for both aerospace vehicles and water-borne vehicles. Some examples are described by Cannon, 1967, pages 159-163, 617-626, 696-697, and by Den Hartog, 1956, pages 108-112.



rotational spring with constant k_θ , and by a rotational viscous damper with constant c_θ . (Drag is imposed by viscous liquid within a gap between the outer surface of the shaft segment and the inner surface of the sleeve, which is attached to the bracket.) The polar rotational inertia of the gimbal-shaft assembly about the gimbal axis is J_θ . Due to the inertia J_r and high speed Ω_r of the spinning rotor, turntable rotation $p(t)$ induces an inertial moment about the gimbal axis, $M_\theta(t) = J_r \Omega_r p(t) \cos \theta(t)$ [as derived from Newton's laws of rigid-body dynamics by, e.g., Cannon, 1967, pages 152-163]; we assume that $\theta(t)$ is small enough that $\cos \theta(t) \approx 1$, so that $M_\theta(t) \approx J_r \Omega_r p(t)$, as labeled on the sketch.. From Eq. (3-1), Newton's 2nd law for rotation of the gimbal-shaft assembly about the gimbal axis is

$$\Sigma(\text{Moments})_{\text{about gimbal axis}} = (\text{rotational inertia}) \times (\text{rotational acceleration})_{\text{about gimbal axis}}$$

$$M_\theta(t) - c_\theta \dot{\theta} - k_\theta \theta = J_\theta \ddot{\theta} \Rightarrow J_\theta \ddot{\theta} + c_\theta \dot{\theta} + k_\theta \theta = J_r \Omega_r p(t)$$

Therefore, we can write the ODE in the standard 2nd order form (9-13) as

$$\ddot{\theta} + \frac{c_\theta}{J_\theta} \dot{\theta} + \frac{k_\theta}{J_\theta} \theta = \frac{J_r \Omega_r}{J_\theta} p(t) = \frac{k_\theta}{J_\theta} \frac{J_r \Omega_r}{k_\theta} p(t)$$

brating the sensor; the turntable rotates clockwise (as viewed from above) with rotational velocity (rate) $p(t)$. At the heart of the rate gyro is a spinning rotor with polar rotational inertia J_r about its spin axis; it is driven by a motor to spin counterclockwise (as viewed from the front) at the high constant spin rate (rotational speed) Ω_r , which is usually orders of magnitude greater than $|p(t)|$. The motor and spinning rotor are attached to a gimbal (rotating frame) and shaft segments that fit into bearings within brackets projecting from the turntable. The gimbal-shaft assembly (including the motor and spinning rotor) can rotate through small angle $\theta(t)$ about the so-called “gimbal axis”. This $\theta(t)$ rotation is resisted by a ro-

Chapter 9 Damped 2nd order systems: general time response

From this standard form, we see that the undamped natural frequency is $\omega_n = \sqrt{k_\theta/J_\theta}$, and the viscous damping ratio is $\zeta = (c_\theta/J_\theta)/(2\omega_n)$, and the standard input quantity, with the same dimensions as rotation-angle output $\theta(t)$, is $u(t) = (J_r \Omega_r/k_\theta) p(t) \equiv \theta_{ps}(t)$, the pseudo-static output.

In practical application of a rate gyro, a transducer detects the rotation of the gimbal-shaft assembly and generates an electrical signal proportional to $\theta(t)$, which might be displayed and/or recorded by a data-acquisition-and-processing system, and might also serve as an input to a control system. Spinning-rotor rate gyros come in various sizes and shapes; typical units are around the size of a one- or two-pound can of vegetables, and their cases can be cylindrical or box-shaped.³

9-3 General solution for output $x(t)$ of underdamped 2nd order systems

We want to solve Eq. (9-13) for output $x(t)$ during positive time $t > 0$, given any input $u(t)$, and given appropriate initial conditions at $t = 0$. We will use Laplace transformation with application of the inverse convolution transform. To simplify the notation, let's denote $X(s) \equiv L[x(t)]$. Transforming Eq. (9-13) with use of Eq. (2-17) gives

$$s^2 X(s) - sx(0) - \dot{x}(0) + 2\zeta\omega_n [sX(s) - x(0)] + \omega_n^2 X(s) = \omega_n^2 L[u(t)]$$

We denote the two initial conditions, $x_0 \equiv x(0)$ initial “position” and $\dot{x}_0 \equiv \dot{x}(0)$ initial “velocity”. Collecting terms algebraically and rearranging the equation gives

$$(s^2 + 2\zeta\omega_n s + \omega_n^2) X(s) = (s + 2\zeta\omega_n) x_0 + \dot{x}_0 + \omega_n^2 L[u(t)] \quad (9-14)$$

Note that up to this point in the derivation, no restriction has been placed on the value of damping ratio ζ .

To cast Eq. (9-14) into an easily solvable form, we use two algebraic tricks that are not obvious *a priori*. The first trick is to re-write the left-hand-side quadratic term [which, essentially, is the same as the quadratic term in characteristic equation (9-3)]:

$$s^2 + 2\zeta\omega_n s + \omega_n^2 = (s + \zeta\omega_n)^2 + \omega_n^2 - (\zeta\omega_n)^2 = (s + \zeta\omega_n)^2 + \omega_d^2 \quad (9-15)$$

We shall regard ω_d^2 as a positive parameter in the following, so Eq. (9-15) is nominally valid only for an underdamped system ($0 \leq \zeta < 1$). The second trick is to split into a particular form the IC terms on the right-hand side of Eq. (9-14):

$$(s + 2\zeta\omega_n) x_0 + \dot{x}_0 = (s + \zeta\omega_n) x_0 + (\dot{x}_0 + \zeta\omega_n x_0) \quad (9-16)$$

³ This type of spinning-rotor gyro can be considered a “legacy” design, not necessarily the most modern or the best for current applications. Rotation sensors using laser optics and microelectromechanics (MEMS) have been developed more recently.

Chapter 9 Damped 2nd order systems: general time response

Applying Eqs. (9-15) and (9-16) to Eq. (9-14), then solving for $X(s)$ gives:

$$X(s) = \frac{s + \zeta\omega_n}{(s + \zeta\omega_n)^2 + \omega_d^2} x_0 + \frac{\omega_d}{(s + \zeta\omega_n)^2 + \omega_d^2} \left(\frac{\dot{x}_0 + \zeta\omega_n x_0}{\omega_d} \right) \\ + \frac{\omega_n^2}{\omega_d} \underbrace{\frac{F_1(s)}{(s + \zeta\omega_n)^2 + \omega_d^2}}_{\omega_d} \underbrace{L[u(t)]}_{F_2(s)} \quad (9-17)$$

The motivation for casting the solution into form (9-17) is a relevant general Laplace transform pair that has not appeared previously in this book: given a function $f(t)$, its Laplace transform $F(s)$, and the exponential function $e^{\sigma t}$, where σ is a constant, then the Laplace transform of the product $e^{\sigma t}f(t)$ is

$$L[e^{\sigma t} f(t)] = \int_{t=0}^{t=\infty} e^{-st} e^{\sigma t} f(t) dt = \int_{t=0}^{t=\infty} e^{-(s-\sigma)t} f(t) dt \equiv F(s - \sigma) \quad (9-18)$$

The associated inverse transform is

$$L^{-1}[F(s - \sigma)] = e^{\sigma t} f(t) \quad (9-19)$$

Returning to Eq. (9-17), we identify $\sigma = -\zeta\omega_n$ and invert the two IC-response terms using Eq. (9-19) in conjunction with sine and cosine transforms (2-30) and (2-31). To invert the forced-response term, we apply both Eq. (9-19) and inverse convolution transform (6-3). This leads to the two equivalent general equations for output $x(t)$ of an underdamped 2nd order system:

$$x(t) = e^{-\zeta\omega_n t} \overbrace{\left[x_0 \cos \omega_d t + \left(\frac{\dot{x}_0 + \zeta\omega_n x_0}{\omega_d} \right) \sin \omega_d t \right]}^{IC \text{ response}} + \overbrace{\frac{\omega_n^2}{\omega_d} \int_{\tau=0}^{\tau=t} e^{-\zeta\omega_n \tau} \sin \omega_d \tau \times u(t - \tau) d\tau}^{forced \text{ response}} \quad (9-20a)$$

$$x(t) = e^{-\zeta\omega_n t} \left[x_0 \cos \omega_d t + \left(\frac{\dot{x}_0 + \zeta\omega_n x_0}{\omega_d} \right) \sin \omega_d t \right] + \frac{\omega_n^2}{\omega_d} \int_{\tau=0}^{\tau=t} e^{-\zeta\omega_n (t-\tau)} \sin \omega_d (t-\tau) \times u(\tau) d\tau \quad (9-20b)$$

Note the emphasis that Eqs. (9-20) are valid for underdamped systems. This solution is nominally not valid for overdamped systems, although we will see in Section 9-10 that it can be converted easily. The nominal restriction to underdamped systems stems from the use of sinusoidal transforms (2-30) and (2-31), which are valid in this case only for positive ω_d^2 , which holds only if $0 \leq \zeta < 1$, from Eq. (9-10). For example, we used the in-

Chapter 9 Damped 2nd order systems: general time response

verse transform $L^{-1}\left[\frac{\omega}{s^2 + \omega^2}\right] = \sin \omega t$, valid for $\omega^2 > 0$, in order to find (9-20), but the following transform holds for a negative term in the denominator: $L^{-1}\left[\frac{\omega}{s^2 - \omega^2}\right] = \sinh \omega t$, a hyperbolic sine.

9-4 Initial-condition transient response of underdamped 2nd order systems

One form of transient, free vibration is response from non-zero initial conditions, with input $u(t) = 0$ for all time. With $u(t) = 0$, response (9-20) becomes

$$x(t) = e^{-\zeta \omega_n t} \left[x_0 \cos \omega_d t + \left(\frac{\dot{x}_0 + \zeta \omega_n x_0}{\omega_d} \right) \sin \omega_d t \right], \text{ for } 0 \leq t \text{ and } 0 \leq \zeta < 1 \quad (9-21a)$$

By following the procedure of Eqs. (7-11)-(7-12) for combining the two sinusoids of Eq. (9-21a), we can also express the IC, free-vibration response as

$$x(t) = x_{\max} e^{-\zeta \omega_n t} \cos(\omega_d t + \phi), \text{ for } 0 \leq t \text{ and } 0 \leq \zeta < 1 \quad (9-21b)$$

$$\text{where } x_{\max} = \sqrt{x_0^2 + \left(\frac{\dot{x}_0 + \zeta \omega_n x_0}{\omega_d} \right)^2} \quad \text{and} \quad \phi = \tan^{-1} \left[- \left(\frac{\dot{x}_0 + \zeta \omega_n x_0}{\omega_d} \right) / x_0 \right]$$

Note that for $\zeta = 0$, response equations (9-21) reduce to the results (7-10) and (7-12) derived for an undamped system in Chapter 7. In this regard, it is useful to keep in mind the definition of the damped natural frequency, $\omega_d \equiv \omega_n \sqrt{1 - \zeta^2}$.

The equation $\omega_d \equiv \omega_n \sqrt{1 - \zeta^2}$ also shows that damping reduces the frequency of free vibration, and increases the period, $T_d \equiv 2\pi/\omega_d$. However, the words “frequency” and “period” are used loosely in this case, because the damped response is not truly periodic. More correctly, T_d is defined as the time between successive local crests or troughs of the response, and between successive positive-going or negative-going zeros.

Figure 9-2 on the next page is an annotated sketch of response (9-21) for positive values of the ICs, $x_0 > 0$ and $\dot{x}_0 > 0$, and for the small damping ratio $\zeta = 0.11$. The output is a sinusoid, $\cos(\omega_d t + \phi)$, modulated by a decaying *exponential envelope*, $\pm x_{\max} e^{-\zeta \omega_n t} \equiv \pm x_{\max} e^{-t/\tau_2}$. In this equation for the exponential envelope, we define the *time constant* τ_2 appropriate for underdamped 2nd order systems as

$$\tau_2 \equiv \frac{1}{\zeta \omega_n} \quad (9-22)$$

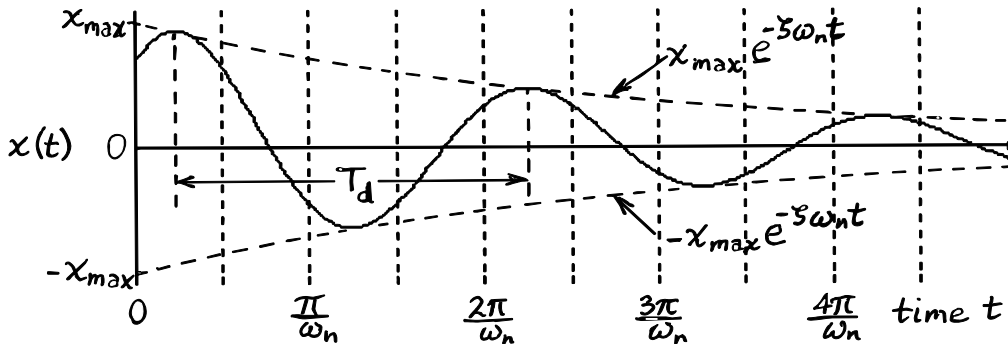


Figure 9-2 IC response of a damped 2nd order system, $\zeta = 0.11$

It is often necessary to measure experimentally the dynamic response of mechanical systems, which requires sensors (transducers) that sense a response quantity and convert it into an electrical voltage. The sensors most abundant and relatively inexpensive for mechanical systems are translational accelerometers (see homework Problem 10.12). Velocity sensors and translation (displacement) sensors are also used, but less commonly. It is appropriate, therefore, that we find from “displacement” Eqs. (9-21) the corresponding equations for free-vibration “velocity” and “acceleration.” One differentiation of (9-21b) gives

$$\dot{x}(t) = x_{\max} e^{-\zeta \omega_n t} [-\zeta \omega_n \cos(\omega_d t + \phi) - \omega_d \sin(\omega_d t + \phi)]$$

Next, we combine the two sinusoidal terms with use of the trigonometric identity $\sin A \cos B + \cos A \sin B = \sin(A + B)$ and the equation $\omega_d \equiv \omega_n \sqrt{1 - \zeta^2}$, leading to

$$\dot{x}(t) = -\omega_n x_{\max} e^{-\zeta \omega_n t} \sin(\omega_d t + \phi + \sin^{-1} \zeta), \text{ for } 0 \leq t \text{ and } 0 \leq \zeta < 1 \quad (9-23)$$

One more differentiation of (9-23) followed by a similar combination procedure gives

$$\ddot{x}(t) = -\omega_n^2 x_{\max} e^{-\zeta \omega_n t} \cos(\omega_d t + \phi + 2 \sin^{-1} \zeta), \text{ for } 0 \leq t \text{ and } 0 \leq \zeta < 1 \quad (9-24)$$

We see that displacement, velocity, and acceleration all have the same damped sinusoidal form. Therefore, experimental measurements of any of the three can be used for identification of system parameters such as ζ and ω_d , a subject addressed in subsequent sections.

9-5 Calculation of viscous damping ratio ζ from free-vibration response

Consider an underdamped 2nd order system in a state of free vibration, *i.e.*, with zero input, $u(t) = 0$. This free vibration can be an initial-condition response or the resid-

ual response after input excitation has ceased, e.g., for $t > t_d$ if the input is a pulse. Then the free-decay response will have the form of Fig. 9-3. On the figure, a reference local extreme value $x(t_0) \equiv x_0$ is annotated (at a crest on Fig. 9-3, but it could just as well be at a trough), and subsequent local extreme values (both crests and troughs) also are annotated. We wish to calculate viscous damping ratio ζ from the graph of response. Note also that the exponential envelope is indicated on Fig. 9-3 with dashed lines.

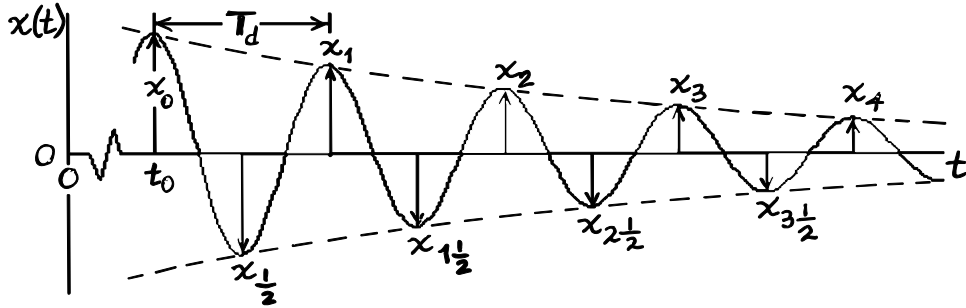


Figure 9-3 Free-vibration response of a damped 2nd order system

We use Eq. (9-21b) for free-vibration response:

$$x(t) = x_{\max} e^{-\zeta \omega_n t} \cos(\omega_d t + \phi) \quad (9-21b) \text{ repeated}$$

From this equation, we form the ratio x_0/x_r of the reference extreme absolute value $|x(t_0)|$ divided by the r^{th} crest or trough absolute value, where r as shown on Fig. 9-3 can have either integer or half-integer values. Note that $|\cos(\omega_d t + \phi)| = 1$ at each of the local extreme values, and that the time of the r^{th} extreme value is $t_r = t_0 + rT_d$, where $T_d = 2\pi/\omega_d$ is the damped natural period. So the required ratio is

$$\frac{x_0}{x_r} = \frac{e^{-\zeta \omega_n t_0}}{e^{-\zeta \omega_n (t_0 + rT_d)}} = e^{\zeta \omega_n rT_d} = \exp\left(\zeta \omega_n r \frac{2\pi}{\omega_n \sqrt{1-\zeta^2}}\right) = \exp\left(2\pi r \frac{\zeta}{\sqrt{1-\zeta^2}}\right) \quad (9-25)$$

Taking the natural logarithm of Eq. (9-25) gives the so-called *logarithmic decrement*:

$$\ln\left(\frac{x_0}{x_r}\right) = 2\pi r \frac{\zeta}{\sqrt{1-\zeta^2}} \Rightarrow \frac{\zeta}{\sqrt{1-\zeta^2}} = \frac{\ln(x_0/x_r)}{2\pi r} \equiv \zeta_s \quad (9-26)$$

In the last term of Eq. (9-26), we define ζ_s as being the accurate approximation for “small” damping ratio ζ . It is very common for a system to have positive, but *small damping*. We define damping to be small if $\sqrt{1-\zeta^2} \approx 1$, which simplifies considerably equations such as (9-26). For $\zeta = 0.2$, $\sqrt{1-\zeta^2} = 0.980$, so this is a reasonable upper

Chapter 9 Damped 2nd order systems: general time response

limit for “smallness.” We can find the exact equation for ζ by squaring (9-26) and then proceeding algebraically to derive

$$\zeta = \frac{\zeta_s}{\sqrt{1 + \zeta_s^2}}, \text{ for } 0 \leq \zeta < 1 \quad (9-27)$$

It might appear that the preceding derivation requires the values of x_0 and x_r to be at crests and troughs of the response plot, and that these should be zero-to-peak values; but neither of these restrictions is necessary. The values of x_0 and x_r can be at any convenient instants along the time history (zeros of the response, as well as extremes), provided that we interpret x_0 and x_r as being the magnitudes of the exponential envelope at the chosen instants. Normally, only the free-vibration response plot is available (from a storage oscilloscope, strip-chart recorder, etc.), so we should sketch in the exponential envelope to aid in measuring x_0 , x_r and r . Moreover, rather than measuring zero-to-peak values, it is more accurate and easier to measure x_0 and x_r as peak-to-peak values, from the lower exponential boundary to the upper exponential boundary.

Let's summarize the procedure for measuring/calculating ζ from a plot of free-vibration response. First, sketch in the exponential envelope. Next, choose time instants along the graph at which you can measure with reasonable accuracy the number of periods r (usually an integer, half-integer, or quarter-integer) and the magnitudes x_0 and x_r between the exponential boundaries. Next, substitute the measured values of r , x_0 , and x_r into Eq. (9-26) and calculate ζ_s . If this ζ_s is ≤ 0.2 , then $\zeta \approx \zeta_s$ with sufficient engineering accuracy. However, if $0.2 < \zeta_s < 1$, then calculate ζ more accurately from Eq. (9-27).

There is a simplified version of Eq. (9-26) that is often used for quick calculation of small ζ . If possible, we find the reference magnitude and the r^{th} magnitude such that $x_0/x_r = 2$, and we label the number of periods as $r_{1/2}$. Hence, $\ln(x_0/x_r)/2\pi \equiv 0.110$, which leads us from Eq. (9-26) to the *half-amplitude formula* for small ζ :

$$\zeta_s = \frac{0.110}{r_{1/2}} \approx \zeta \quad (9-28)$$

Finally, the preceding derivation was based upon Eq. (9-21b) for “displacement” response $x(t)$. However, the formulas derived for ζ are equally valid if the measurements are made from graphs of “velocity” $\dot{x}(t)$ or “acceleration” $\ddot{x}(t)$. This is so because, from Eqs. (9-23) and (9-24), the derivatives of $x(t)$ have the same exponentially-bounded sinusoidal form as $x(t)$ itself.

9-6 Step response of underdamped 2nd order systems

For step response, we set the ICs to zero, and we define the input to be a step function at time $t = 0$, with step magnitude U : $u(t) = U H(t)$. The appropriate form of the general solution to use is Eq. (9-20a), which becomes [with $H(t - \tau) = 1$ for $\tau < t$]

$$\begin{aligned} x(t) &= \frac{\omega_n^2}{\omega_d} \int_{\tau=0}^{t=t} e^{-\zeta\omega_n\tau} \sin \omega_d \tau \times u(t - \tau) d\tau = \frac{\omega_n^2}{\omega_d} \int_{\tau=0}^{t=t} e^{-\zeta\omega_n\tau} \sin \omega_d \tau \times U H(t - \tau) d\tau \\ &= U \frac{\omega_n^2}{\omega_d} \int_{\tau=0}^{t=t} e^{-\zeta\omega_n\tau} \sin \omega_d \tau d\tau \end{aligned}$$

This integral can be evaluated by hand (*e.g.*, using integration by parts), but the process is tedious. The following evaluation was completed with use of a table of integrals:

$$\begin{aligned} x(t) &= U \frac{\omega_n^2}{\omega_d} \frac{1}{(-\zeta\omega_n)^2 + \omega_d^2} \left[e^{-\zeta\omega_n t} (-\zeta\omega_n \sin \omega_d t - \omega_d \cos \omega_d t) \right]_{\tau=0}^{t=t} \\ &= U \frac{1}{\omega_d} \left[e^{-\zeta\omega_n t} (-\zeta\omega_n \sin \omega_d t - \omega_d \cos \omega_d t) - 1(-\omega_d) \right] \\ x(t) &= U \left[1 - e^{-\zeta\omega_n t} \left(\cos \omega_d t + \frac{\zeta\omega_n}{\omega_d} \sin \omega_d t \right) \right], \text{ for } 0 \leq t \text{ and } 0 \leq \zeta < 1 \quad (9-29) \end{aligned}$$

Note that the coefficient of $\sin \omega_d t$ in Eq. (9-29) is dependent only on the damping ratio:

$$\frac{\zeta\omega_n}{\omega_d} = \frac{\zeta\omega_n}{\omega_n \sqrt{1 - \zeta^2}} = \frac{\zeta}{\sqrt{1 - \zeta^2}} = \zeta_s \quad [\text{see Eq. (9-26)}]$$

Step response (9-29) for small damping ratio $\zeta = 0.11$ is plotted over a few cycles of response on Fig. 9-4. Relative to the pseudo-static response, $x_{ps} = U$, the actual

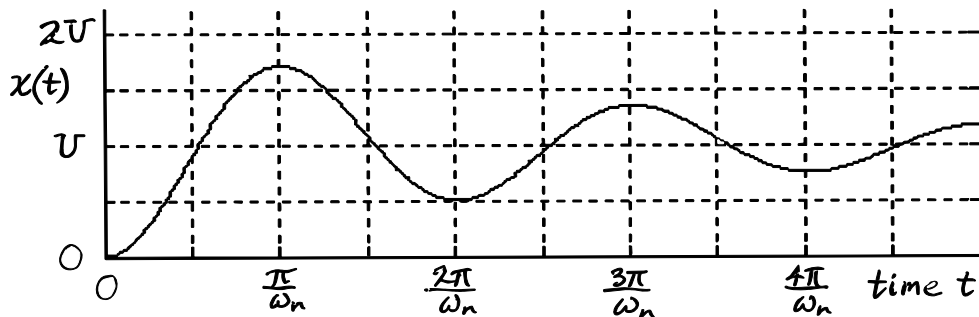


Figure 9-4 Step response of a damped 2nd order system, $\zeta = 0.11$

step response of a damped system initially overshoots, then undershoots, then overshoots again, then undershoots again, *etc.*, *etc.* But damping dissipates the energy of vibration, causing the response eventually (not shown on Fig. 9-4) to settle statically at $\lim_{t \rightarrow \infty} x(t) = x_{ps} = U$. Several step-response characteristics (called *specifications*, or *specs* in engineering jargon) of a system can be quantified and often are of great interest in practice. For example, the *rise time* is the time required for the response first to reach U , which on Fig. 9-4 is just a bit longer than $\frac{1}{2}\pi/\omega_n$. However, before studying those characteristics in more detail, it is appropriate that we first consider impulse response.

9-7 Ideal impulse response of underdamped 2nd order systems

For impulse response, we set the ICs to zero, and we define the input to be an ideal impulse at time $t = 0$, with impulse magnitude I_U : $u(t) = I_U \delta(t)$. The more appropriate form of the general solution to use is Eq. (9-20b), which becomes

$$x(t) = \frac{\omega_n^2}{\omega_d} \int_{\tau=0}^{\tau=t} e^{-\zeta\omega_n(t-\tau)} \sin \omega_d(t-\tau) \times u(\tau) d\tau = \frac{\omega_n^2}{\omega_d} \int_{\tau=0}^{\tau=t} e^{-\zeta\omega_n(t-\tau)} \sin \omega_d(t-\tau) \times I_U \delta(\tau) d\tau$$

Using the integration property of $\delta(\tau)$, Eq. (8-11), we find the relatively simple result:

$$x(t) = I_U \frac{\omega_n^2}{\omega_d} e^{-\zeta\omega_n t} \sin \omega_d t, \text{ for } 0 < t \text{ and } 0 \leq \zeta < 1 \quad (9-30)$$

Ideal impulse response (9-30) for small damping ratio $\zeta = 0.11$ is plotted over a few cycles of response on Fig. 9-5. Observe that this ideal response violates the specified

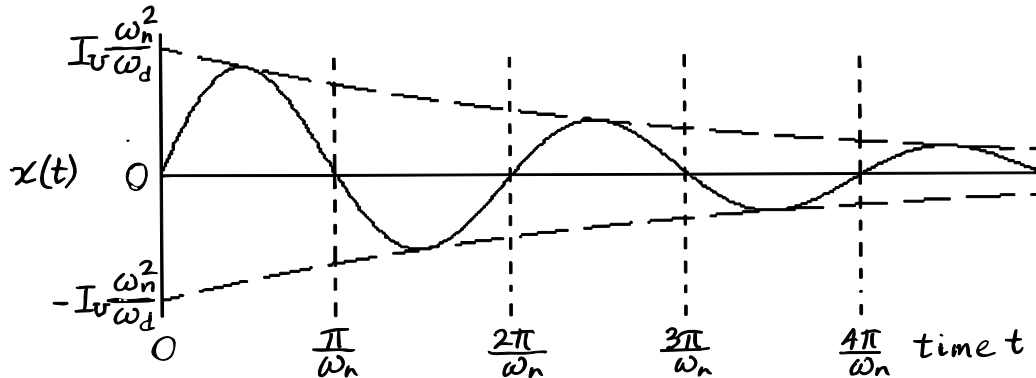


Figure 9-5 Ideal impulse response of a damped 2nd order system, $\zeta = 0.11$

initial condition $\dot{x}(0) = 0$; thus, the solution is defective in this respect, as is discussed in Section 8-7. Figure 9-5 shows the exponential envelope; note, in particular, the values at $t = 0$ of the exponential envelope, $\pm I_U \omega_n^2 / \omega_d$. This magnitude is easily measurable from a graph, after we have sketched in the exponential envelope, if necessary, and it is

Chapter 9 Damped 2nd order systems: general time response

essential in the process of estimating mechanical system parameters from an experimental response to a short force pulse (Section 9-9).

From Eq. (9-30), we find the unit-impulse-response function (IRF, as defined in Section 8-7) for underdamped 2nd order systems:

$$h(t) \equiv x(t)|_{I_U=1} = \frac{\omega_n^2}{\omega_d} e^{-\zeta\omega_n t} \sin \omega_d t, \text{ for } 0 < t \text{ and } 0 \leq \zeta < 1 \quad (9-31)$$

Further, from Eq. (8-25), we find the Duhamel integral giving general response to input $u(t)$, with zero ICs, for underdamped 2nd order systems:

$$x(t)|_{ICs=0} = \int_{\tau=0}^{t=t} u(\tau) h(t-\tau) d\tau = \frac{\omega_n^2}{\omega_d} \int_{\tau=0}^{t=t} u(\tau) e^{-\zeta\omega_n(t-\tau)} \sin \omega_d(t-\tau) d\tau \quad (9-32)$$

Duhamel integral (9-32) is identical to convolution-integral response solution (9-20b) with zero ICs.

Finally, it is worthy of mention that convolution sum Eq. (8-44) for approximate numerical forced response applies just as well to damped 2nd order systems as to 1st order and undamped 2nd order systems. Therefore, to calculate approximate forced response of an underdamped 2nd order system, we would apply exactly the same procedure described in Convolution-sum Example 2 of Section 8-11, but instead of calculating in Eq. (8-44) the IRF $h(t) = \omega_n \sin \omega_n t$ for an undamped system, we would calculate Eq. (9-31).

9-8 Step-response specifications for underdamped systems

Engineering systems are often designed so that the time history of an output quantity will mimic as closely as possible the time history of the input quantity. An example, with reference to Section 3-5, is the aileron-induced rolling of an airplane, for which the original input is the control wheel angle set manually (“commanded”) by the pilot, and the ultimate output is the airplane roll rate. Another example is the modern automobile; we usually describe a car as being “responsive” if the steering (or the acceleration, or the braking) mimics quickly and precisely the driver’s commands set by hand or foot.

Step response of a system is often used for measuring and quantifying dynamic “responsiveness.” Ideally, step response would mimic exactly the step input, but system characteristics such as inertia and damping prevent such instantaneous response. The degree to which step response fails to mimic step input is quantified in the following four *step-response specifications*: rise time, t_r ; peak time, t_p , maximum overshoot ratio, \bar{x}_p , and settling time, t_s . These step-response quantities are illustrated on Fig. 9-6 on the next page. They are called “specifications” or “specs” because it is common in the beginning of a project to specify them as design targets; later, these step-response quantities are measured experimentally on prototype and/or production test articles.

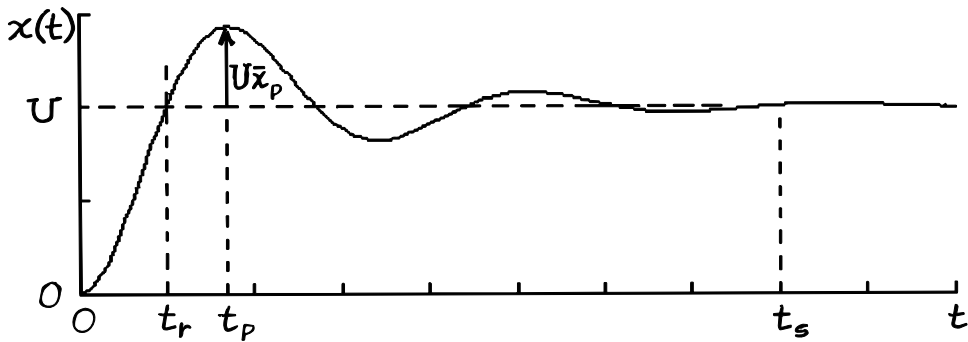


Figure 9-6 Step-response specifications of an underdamped system

For underdamped 2nd order systems, we can apply step-response solution (9-29) and impulse-response solution (9-30) to derive specific equations for the step-response specifications:

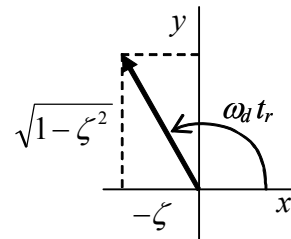
Rise time, t_r

From Fig. 9-6, we evaluate Eq. (9-29) at $t = t_r$, the first time when $x(t) = U$:

$$\begin{aligned} x(t_r) = U &= U \left[1 - e^{-\zeta \omega_n t_r} \left(\cos \omega_d t_r + \frac{\zeta \omega_n}{\omega_d} \sin \omega_d t_r \right) \right] \Rightarrow \cos \omega_d t_r + \frac{\zeta \omega_n}{\omega_d} \sin \omega_d t_r = 0 \\ \Rightarrow \tan \omega_d t_r &= -\frac{\omega_d}{\zeta \omega_n} = -\frac{\sqrt{1-\zeta^2}}{\zeta} = -\frac{1}{\zeta_s} \end{aligned}$$

This last equation shows that as $\zeta \rightarrow 0$ from positive values, then $\tan \omega_d t_r \rightarrow -\infty$ from negative values; therefore, $\omega_d t_r \rightarrow \frac{1}{2}\pi \times n$ from higher values, where $n = 1, 5, 9, \dots$; and the first time when $x(t) = U$ corresponds to $n = 1$: $\omega_d t_r \rightarrow \frac{1}{2}\pi$ from higher values. We can see this in Fig. 9-4, where t_r is just a bit after $\frac{1}{2}\pi/\omega_n$ (keep in mind that $\omega_d \leq \omega_n$). This leads to the conclusion that the rise time is given by

$$t_r = \frac{1}{\omega_d} \tan^{-1} \left(\frac{\sqrt{1-\zeta^2}}{-\zeta} \right) \quad (9-33)$$



In Eq. (9-33), we take the value of the four-quadrant inverse tangent that is between $\frac{1}{2}\pi$ and π , as shown on the drawing at right.

Chapter 9 Damped 2nd order systems: general time response

Peak time, t_p

From Fig. 9-6, t_p is the time at which $x(t)$ is maximum and the first time after $t = 0$ that $\dot{x}(t) = 0$. So we need to differentiate Eq. (9-29), set it to zero, and solve for t_p from the resulting equation. From the appearance of Eq. (9-29), though, that differentiation will be long and tedious. But that drudgery will not be necessary, because a fundamental relationship derived in Section 8-7 will come to our rescue. We identify the unit-step response as Eq. (9-29) with step magnitude $U = 1$:

$$x_H(t) = 1 \times \left[1 - e^{-\zeta\omega_n t} \left(\cos \omega_d t + \frac{\zeta\omega_n}{\omega_d} \sin \omega_d t \right) \right] = 1 - e^{-\zeta\omega_n t} \left(\cos \omega_d t + \frac{\zeta\omega_n}{\omega_d} \sin \omega_d t \right) \quad (9-34)$$

Clearly, t_p is independent of step magnitude U . Now, Eq. (8-24) gives the derivative of Eq. (9-34) as $dx_H/dt = h(t)$, where the IRF $h(t)$ in this case is Eq. (9-31). Therefore, the equation leading to t_p that we seek is

$$\frac{dx_H}{dt} = h(t) = \frac{\omega_n^2}{\omega_d} e^{-\zeta\omega_n t} \sin \omega_d t = 0 \text{ at } t = t_p \quad (9-35)$$

The required solution of Eq. (9-35) is the lowest positive value of t that satisfies $\sin \omega_d t = 0$, which is

$$t_p = \frac{\pi}{\omega_d} \quad (9-36)$$

The graphical equivalent of this mathematical derivation of Eq. (9-36) is evident in an examination of Figs. 9-4 and 9-5, where we can see that both the peak of the step response and the first zero of the ideal impulse response occur at an instant t just a bit after π/ω_n (recall that $\omega_d \leq \omega_n$).

Maximum overshoot ratio, \bar{x}_p

From Fig. 9-6, Eq. (9-29), and Eq. (9-36), the maximum overshoot ratio is

$$\begin{aligned} \bar{x}_p &= \frac{x(t_p) - U}{U} = -e^{-\zeta\omega_n t_p} \left(\cos \omega_d t_p + \frac{\zeta\omega_n}{\omega_d} \sin \omega_d t_p \right) = -\exp\left(-\zeta\omega_n \frac{\pi}{\omega_d}\right) \left(\cos \pi + \frac{\zeta\omega_n}{\omega_d} \sin \pi \right) \\ &\Rightarrow \bar{x}_p = \exp\left(-\frac{\zeta}{\sqrt{1-\zeta^2}} \pi\right) \leq 1, \text{ valid for } 0 \leq \zeta < 1 \end{aligned} \quad (9-37)$$

Chapter 9 Damped 2nd order systems: general time response

So the maximum overshoot ratio is a function only of viscous damping ratio ζ . Conversely, ζ can be determined from a measurement of \bar{x}_p by taking the natural logarithm of Eq. (9-37):

$$\ln \bar{x}_p = -\frac{\zeta}{\sqrt{1-\zeta^2}} \pi \Rightarrow -\frac{\ln \bar{x}_p}{\pi} = \frac{\zeta}{\sqrt{1-\zeta^2}} \equiv \zeta_s, \text{ valid for } 0 < \bar{x}_p \leq 1 \quad (9-38)$$

Note the similarity of Eq. (9-38) to Eq. (9-26) for the logarithmic decrement. Therefore, we arrive again at Eq. (9-27), the exact equation giving ζ for any overshoot in the range $0 < \bar{x}_p \leq 1$: $\zeta = \zeta_s / \sqrt{1 + \zeta_s^2}$, for $0 \leq \zeta < 1$, now with $\zeta_s = -\ln \bar{x}_p / \pi$.

If damping is small such that $\sqrt{1 - \zeta^2} \approx 1$, i.e., $0 \leq \zeta \leq 0.2$, then Eqs. (9-37) and (9-38) are approximated as:

$$\bar{x}_p \approx e^{-\zeta \pi} \quad \text{and} \quad \zeta \approx -\frac{\ln \bar{x}_p}{\pi} \quad \text{valid for } 0 \leq \zeta \leq 0.2 \text{ and } 0.534 \leq \bar{x}_p \leq 1 \quad (9-39)$$

Settling time, t_s

This specification is defined as the time required for response $x(t)$ to settle to within $\pm 2\%$ of the final steady-state (pseudo-static) value, U . For this underdamped 2nd order system, the time constant of the exponential envelope is Eq. (9-22), $\tau_2 \equiv 1/\zeta\omega_n$. From Chapter 3, we have $1 - e^{-4} = 0.982$ (see Fig. 3-3), so the settling time is defined as

$$t_s = 4\tau_2 \equiv \frac{4}{\zeta\omega_n} \quad (9-40)$$

It is appropriate here to evaluate the variation in step response of a standard 2nd order system as damping varies. Figure 9-7 on the next page displays 2nd order step responses for a range of viscous damping ratios ζ . [The response curves of Fig. 9-7 are calculated as follows: for underdamping, $0 \leq \zeta < 1$, from Eq. (9-29); for critical damping, $\zeta = 1$, from the result of homework Problem 9.11; for overdamping, $\zeta = 1.2$, from the result of homework Problem 9.16. The time reference is undamped natural period $T_n = 2\pi/\omega_n$.] As engineers designing a system, we might wish to design into the system a quantity of damping ζ that makes the time history of an output quantity mimic as closely as possible the time history of the input quantity. This means, in the context of step response, we would want both to make rise time as fast as possible and to minimize overshoot. However, Fig. 9-7 shows that we cannot simultaneously do both for a standard 2nd order system: rise time is fastest for small ζ , but overshoot is minimized or eliminated with larger ζ . Therefore, we would have to compromise and select a value of ζ that produces practically acceptable values of both rise time and overshoot, even

though neither response parameter would be the best possible. Observe from Fig. 9-7 that overshoot exists only for underdamping.

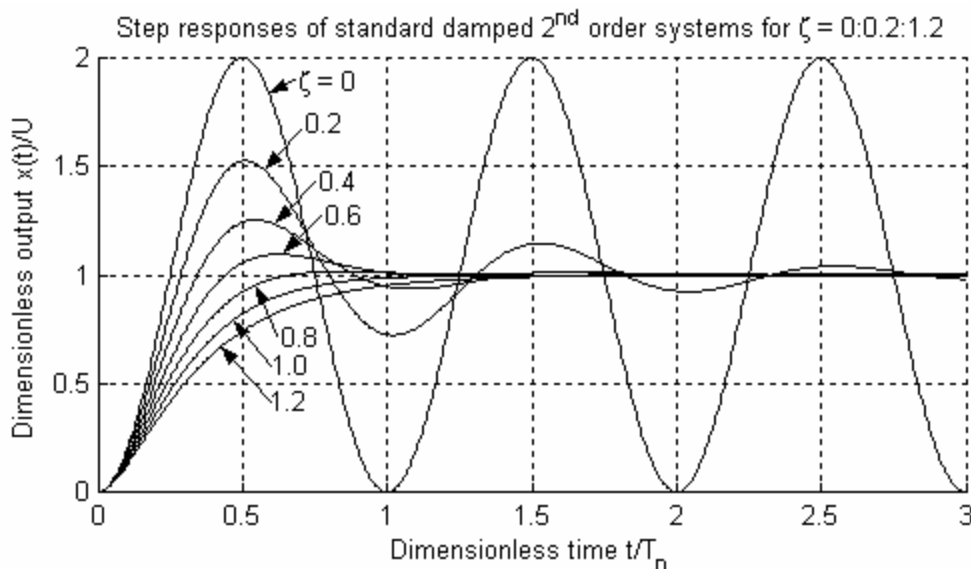


Figure 9-7 Step responses of standard 2nd order systems as viscous damping varies

The transient response of engineered control systems is very important in practice, so there is more analysis and discussion of subjects such as rise time and overshoot later in the book, beginning in Chapter 14.

9-9 Identification of a mass-damper-spring system from measured response to a short force pulse

Suppose we have a mechanical system that is known to be an $m-c-k$ system (or a close enough approximation thereto, for engineering purposes), such as that of Fig. 9-1, and suppose we need to estimate from experimental measurements the system parameters: mass m , effective viscous damping constant c , and stiffness constant k . This is a form of the process known generally as *system identification* (ID). There are many methods of system ID using both transient response and frequency response. In this section, we illustrate one common method based upon pulse response.

The theoretical basis for system ID by pulse testing of a mechanical $m-c-k$ system is the ideal impulse response given by Eq. (9-30), with use of Eq. (8-13), $I_U = I_F/k$, and the equation for natural frequency, $\omega_n^2 = k/m$:

$$x(t) = \frac{I_F}{k} \frac{k/m}{\omega_d} e^{-\zeta\omega_n t} \sin \omega_d t = \frac{I_F}{m\omega_d} e^{-\zeta\omega_n t} \sin \omega_d t \quad (9-41)$$

Similarly, the values at $t = 0$ of the upper and lower boundaries of the exponential envelope (for guidance, see Fig. 9-5) are

$$\pm I_U \frac{\omega_n^2}{\omega_d} = \pm \frac{I_F}{m\omega_d} \quad (9-42)$$

The practical implementation of these equations is based upon using them to approximate the real response from a short force pulse, as is discussed extensively in Section 8-6.

The experimental procedure is as follows. An engineer or technician strikes the mass lightly but sharply with a specially designed hammer. A force sensor mounted in the head of the hammer measures the pulse. A displacement sensor measures motion of the mass due to the force pulse. For accuracy of the system ID, it is essential that the pulse duration t_d of the hammer strike be very short relative to a quarter of the system natural period: $t_d \ll \frac{1}{4} T_n$; achieving this might require some experimental iteration, testing hammer contact tips of different degrees of hardness. The time history $f_x(t)$ of force input to the mass is recorded; this force pulse might be somewhat irregular, such as Fig. 8-5, or it might appear to have a more regular form, such as a half-sine. The time history of displacement response, $x(t)$, also is recorded; with a properly short pulse duration, response $x(t)$ should look very much like the damped sinusoid of Fig. 9-5, ideal impulse response. The steps of the subsequent calculation algorithm are:

1. Calculate from measurements on the $x(t)$ graph the damped natural frequency f_d (Hz) and the viscous damping ratio ζ . In order to obtain reasonably accurate values of f_d and ζ , be sure to average over as many cycles as possible of the damped sinusoid. To aid in the calculation of ζ , first sketch in the exponential envelope. Next, use the values of f_d and ζ to calculate the two circular natural frequencies in rad/sec: $\omega_d = 2\pi f_d$ and $\omega_n = \omega_d / \sqrt{1 - \zeta^2}$. For small ζ , these two frequencies will be essentially identical.
2. From the $f_x(t)$ graph, use graphical or approximate theoretical integration to calculate the actual force impulse I_F . From the $x(t)$ graph, find the value at $t = 0$ of the upper and lower boundaries of the exponential envelope, which are approximately $\pm I_F / m\omega_d$ from Eq. (9-42). It is important in this step to be very careful with the units of these quantities measured from experimental data. Now, you have the data required to calculate the mass from the identity

$$m = \left[\omega_d \times \frac{1}{I_F} \times \frac{I_F}{m\omega_d} \right]^{-1} \quad (9-43)$$

3. Finally, calculate the stiffness constant using $k = m\omega_n^2$, and calculate the effective viscous damping constant from Eq. (9-4), $c = 2\zeta m\omega_n = 2\zeta \sqrt{mk}$.

It is always essential in engineering practice to check your calculations as much as is practical. After you have calculated m , c , and k from the procedure described above, you can check the validity of your values by using MATLAB (or some similar calcula-

tion software) to graph the ideal impulse response of your calculated system, Eq. (9-41); then compare the calculated graph with the recorded experimental response. If the two graphs are very similar, then your system ID is probably correct, provided that you calculated I_F correctly. However, suppose that you use an incorrect value of I_F , then calculate wrong values of m , c , and k based upon this wrong I_F ; if you then graph the ideal impulse response, using these wrong values in Eq. (9-41), the result will look very much like the recorded experimental response, giving you a false indication that your system ID is correct. Therefore, be sure to calculate correctly the force impulse I_F .

9-10 Deriving response equations for overdamped 2nd order systems

For $\zeta > 1$, we can consider the damped natural frequency to be an imaginary number:

$$\omega_d = \omega_n \sqrt{1 - \zeta^2} = j\omega_n \sqrt{\zeta^2 - 1} \equiv j\mu_d \quad \text{where } \mu_d \equiv \omega_n \sqrt{\zeta^2 - 1} \text{ is real} \quad (9-44)$$

The general method of deriving transient response equations for the overdamped case is to substitute (9-44) into the Laplace transform (9-17), and then proceed to invert the resulting equation, leading to general expressions that include IC response terms and convolution integrals, analogous to Eqs. (9-20).

There is an easier method for finding overdamped-system response equations if the comparable underdamped-system equations have already been derived. The method is to use Eq. (9-44) in order to convert trigonometric terms of the $\zeta < 1$ equations into hyperbolic terms for the $\zeta > 1$ equations. From homework Problem 2.13, we have the following conversions valid for $\zeta > 1$:

$$\cos \omega_d t = \cosh \mu_d t \quad \text{and} \quad \frac{\sin \omega_d t}{\omega_d} = \frac{\sinh \mu_d t}{\mu_d} \quad (9-45)$$

An example of applying Eqs. (9-44) and (9-45) is conversion of IC response Eq. (9-21a) from the underdamped ($\zeta < 1$) form into the overdamped ($\zeta > 1$) form:

$$x(t) = e^{-\zeta \omega_n t} \left[x_0 \cos \omega_d t + \left(\frac{\dot{x}_0 + \zeta \omega_n x_0}{\omega_d} \right) \sin \omega_d t \right] \text{ for } 0 \leq \zeta < 1$$

$$\Rightarrow x(t) = e^{-\zeta \omega_n t} \left[x_0 \cosh \mu_d t + \left(\frac{\dot{x}_0 + \zeta \omega_n x_0}{\mu_d} \right) \sinh \mu_d t \right] \text{ for } \zeta > 1 \quad (9-46a)$$

in which $\mu_d = \omega_n \sqrt{\zeta^2 - 1}$. This IC-response equation is valid for $0 \leq t$ and $\zeta > 1$. The hyperbolic functions are defined in terms of exponential functions as

Chapter 9 Damped 2nd order systems: general time response

$$\cosh \mu_d t = \frac{e^{\mu_d t} + e^{-\mu_d t}}{2} \quad \text{and} \quad \sinh \mu_d t = \frac{e^{\mu_d t} - e^{-\mu_d t}}{2}$$

Therefore, IC-response equation (9-46a) can be written a bit more clearly as

$$x(t) = \frac{1}{2} e^{-\zeta \omega_n t} \left[e^{\mu_d t} \left(x_0 + \frac{\dot{x}_0 + \zeta \omega_n x_0}{\mu_d} \right) + e^{-\mu_d t} \left(x_0 - \frac{\dot{x}_0 + \zeta \omega_n x_0}{\mu_d} \right) \right] \quad (9-46b)$$

All terms in Eq. (9-46b) are exponentially damped. Even the first term within the square brackets decays away exponentially because $-\zeta \omega_n + \mu_d = -\zeta \omega_n + \omega_n \sqrt{\zeta^2 - 1} = -(\zeta - \sqrt{\zeta^2 - 1})\omega_n < 0$ for $\zeta > 1$.

Example 9-3: RC band-pass filter, an overdamped 2nd order system

We re-visit Section 5-4, where the input voltage to the *RC* band-pass filter is defined as $e_i(t)$, the mid-circuit voltage between low-pass and high-pass stages is $e_m(t)$, and the output voltage is $e_o(t)$; also, the 1st order time constants of the low-pass and high-pass stages are τ_L and τ_H , respectively, defined in terms of resistance and capacitance values in the circuit. The two coupled 1st order ODEs derived in Section 5-4 are

$$\text{for the low-pass filter stage, } \tau_L \dot{e}_m + e_m = e_i \quad (5-16) \text{ repeated}$$

$$\text{for the high-pass filter stage, } \tau_H \dot{e}_o + e_o = \tau_H \dot{e}_m \quad (5-17) \text{ repeated}$$

We combine these coupled 1st order ODEs into a single 2nd order ODE with the following operations: differentiate Eqs. (5-16) and (5-17); in the differentiated (5-16), replace \dot{e}_m using the original (5-17), and replace \ddot{e}_m using the differentiated (5-17); rearrange and collect terms to find the ODE relating output $e_o(t)$ to input $e_i(t)$:

$$\tau_L \tau_H \ddot{e}_o + (\tau_L + \tau_H) \dot{e}_o + e_o = \tau_H \dot{e}_i \quad (9-47)$$

Due to the right-hand-side dynamics (the presence of \dot{e}_i rather than just e_i), we cannot cast this entire equation into the standard form (9-13); see homework Problem 9.15 for a modified standard form of ODE and for convolution-integral response solutions. However, the order of the circuit is determined only by the left-hand-side terms, and it is clearly 2nd order, with natural frequency and damping ratio defined as

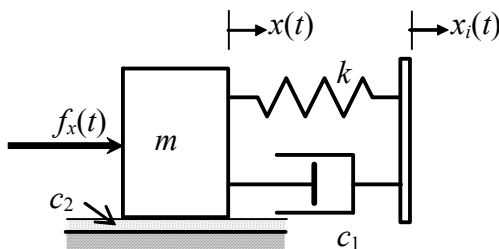
$$\omega_n = \frac{1}{\sqrt{\tau_L \tau_H}} \quad \text{and} \quad \zeta = \frac{1}{2\omega_n} \frac{\tau_L + \tau_H}{\tau_L \tau_H} = \frac{1}{2} \frac{\tau_L + \tau_H}{\sqrt{\tau_L \tau_H}}$$

Chapter 9 Damped 2nd order systems: general time response

Suppose, for example, that a particular circuit has the high-pass and low-pass break frequencies $f_H = 10$ Hz and $f_L = 500$ Hz, respectively. Then the time constants are $\tau_H = 1/\omega_H = 1/(2\pi f_H) = 1.592\text{e-}2$ sec, and $\tau_L = 1/\omega_L = 1/(2\pi f_L) = 3.183\text{e-}4$ sec, and the undamped natural frequency is $\omega_n = 4.443\text{e}2$ rad/sec ($f_n = \omega_n/2\pi = 70.71$ Hz). Finally, the damping ratio is $\zeta = 3.606$, which means that this is a strongly overdamped system.

9-11 Homework problems for Chapter 9

- 9.1** In the system drawn below, mass m is attached to a movable support by viscous dashpot c_1 and spring k , and the mass also slides on a lubricated surface, which causes viscous damping with constant c_2 . There are two independent input quantities: (1) support displacement $x_i(t)$ shown (displacement control, e.g., by a cam), which is often called *base excitation*,⁴ and (2) force $f_x(t)$ shown. The output quantity is displacement $x(t)$ of the mass.



Sketch and label clearly appropriate free-body diagrams, then use your FBD to derive the differential equation of motion for $x(t)$ in terms of constants m , c_1 , c_2 and k , and variable inputs $x_i(t)$ and $f_x(t)$. Your ODE of motion should include some non-standard right-hand-side dynamics.

- 9.2** Given, a standard $m-c-k$ system, Fig. 9-1, with the following parameters: weight of the mass $W = 0.386$ lb, so that $m = \frac{W}{g} = \frac{0.386 \text{ lb}}{386 \text{ inch/sec}^2} = 0.001 \frac{\text{lb} - \text{sec}^2}{\text{inch}}$; damper viscous constant $c = 1.1 \times 10^{-3}$ lb/inch/sec; spring stiffness constant $k = 3.025$ lb/inch.

- (a) Calculate the following quantities, all to at least 3 significant figures: ω_n in rad/sec, f_n in Hz, ζ , ω_d in rad/sec, f_d in Hz, and $T_d \equiv 1/f_d$. You may calculate these quantities in MATLAB, if you wish, using the command `format short e`.
- (b) Given initial conditions $x(0) = 0.5$ inch and $\dot{x}(0) = 35$ inch/sec, calculate and graph with MATLAB the free-vibration response due to the ICs over about 20 complete decaying cycles. Since you are multiplying sinusoidal time functions by an exponential time function, it is necessary that you use array multiplication (`*`) in MATLAB. Draw grids on your graph and add an appropriate title and appropriate axis labels.
- (c) Sketch by hand the exponential envelope on your graph, then use the grids and/or a graduated straight edge to measure amplitudes of local peaks of the decaying sinusoid. In particular, find (approximately) the quantity $r_{1/2} \equiv$ the number of decaying cycles to decay to half amplitude (not necessarily an integer). Now calculate the dimensionless ratio $0.110/r_{1/2}$; the value that you calculate should match closely with your previously calculated value of ζ .

⁴ Base excitation is displacement input imposed at the “ground” or “base” side of the spring instead of directly upon the mass. It is very common to consider base excitation in analyses of earthquake-induced response of buildings, automobile tires rolling over bumpy roads, and vibration isolation of sensitive devices such as delicate payloads in rocket boosters.

Chapter 9 Damped 2nd order systems: general time response

9.3 The free-vibration response to initial conditions of a standard damped 2nd order system is given by $x(t) = 2.24 e^{-0.300t} \cos(12.00t - 1.11)$ mm, where t is in seconds. Calculate (i) the damped natural frequency f_d in Hz, (ii) the damping time constant τ_2 in seconds, and (iii) the viscous damping ratio ζ (use the small- ζ approximation). Show your calculations.

9.4 A simple type of vibration testing often used for underdamped mechanical systems, such as the $m-c-k$ system of Fig. 9-1, is called *twang testing* (named after the sharp, ringing sound made by plucking a string of a musical instrument; Section 7-6 demonstrates twang testing of a flexible beam): the mass is displaced from its static equilibrium position by amount x_0 (with zero initial velocity, $\dot{x}_0 = 0$), then it is released. From the record of subsequent transient response, we can calculate directly the damped natural frequency f_d and the viscous damping ratio ζ . If we know initially either the mass m or the stiffness constant k , then we can use the measured f_d and ζ to calculate the other constant and the effective viscous damping constant c . Use Eq. (9-21b) to show that twang test response is

$$x(t) = x_{\max} e^{-\zeta \omega_n t} \cos(\omega_d t + \phi), \text{ for } 0 \leq t \text{ and } 0 \leq \zeta < 1$$

$$\text{where } x_{\max} = x_0 / \sqrt{1 - \zeta^2} \quad \text{and} \quad \phi = \tan^{-1}(-\zeta / \sqrt{1 - \zeta^2})$$

For a very lightly damped system, the preferred simple approximation of this twang response is

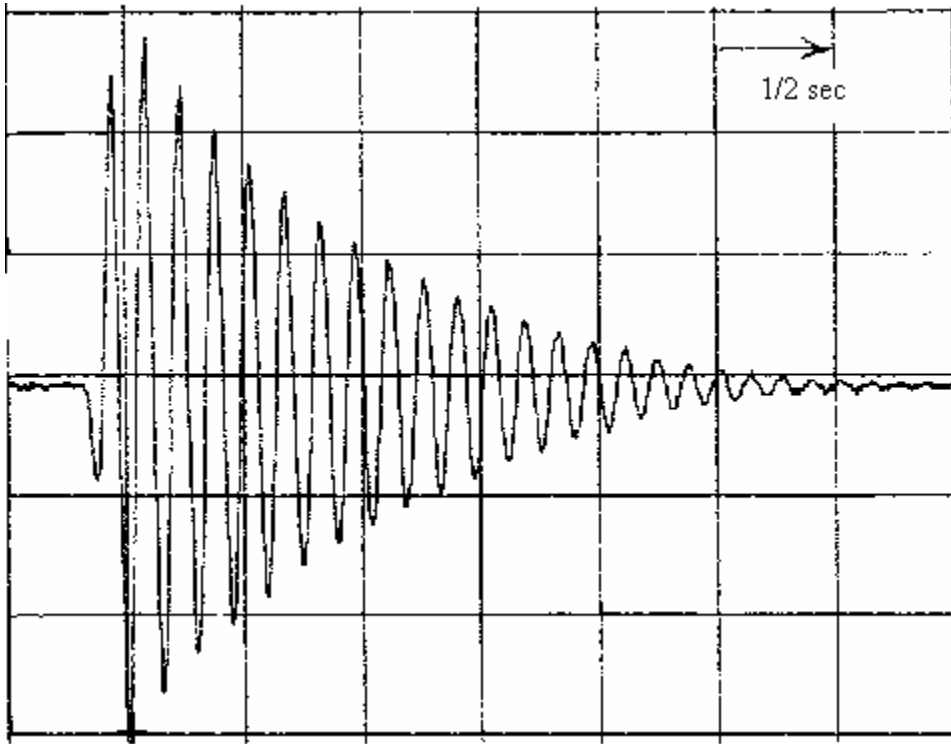
$$x(t) \approx x_0 e^{-\zeta \omega_n t} \cos(\omega_n t), \text{ with } \phi \approx 0$$

How small must ζ be so that phase lag ϕ is so small (say, $|\phi| \leq 5^\circ$) that it can't be distinguished from zero phase lag, $\phi \approx 0$? [NOTE: the measurement resolution on a typical analog graphical record of transient-decay vibration response (for example, from a small oscilloscope screen) is so limited that the resolution of calculated phase is probably only around $\pm 5^\circ$.]

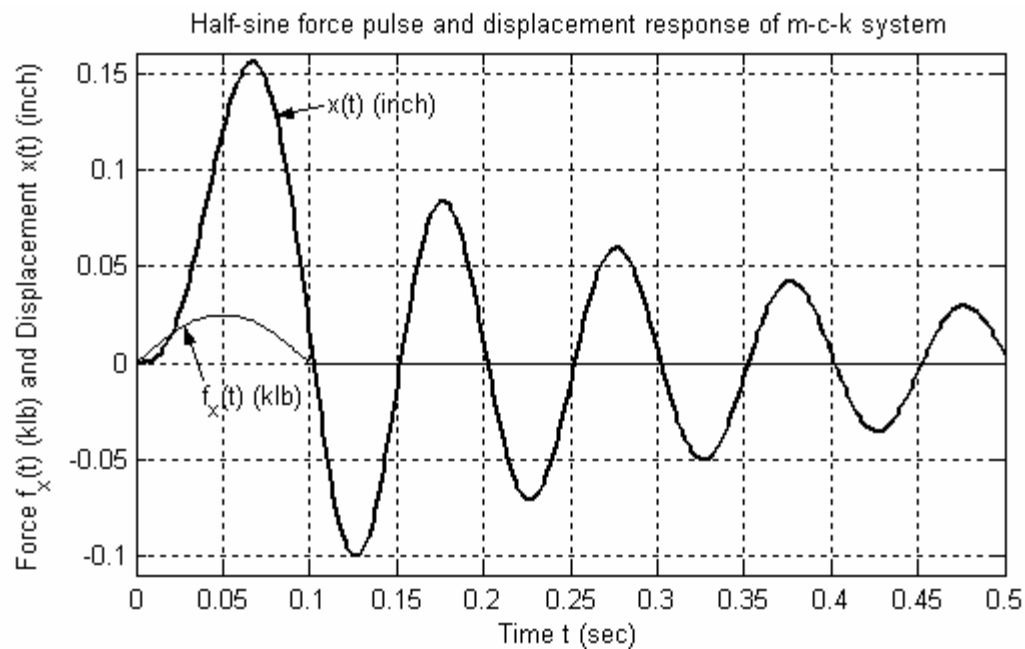
9.5 A laboratory mass-damper-spring system was set into motion and then allowed to vibrate freely. The time-history acceleration on the next page was sensed by a light-weight accelerometer attached to the mass. The graph was copied from the screen of a digital oscilloscope. Calculate from measurements on a photocopy of the graph the damped natural frequency f_d (Hz) = $\omega_d / 2\pi$ and the viscous damping ratio ζ . In order to obtain reasonably accurate values for f_d and ζ , be sure to average over many cycles of the damped sinusoid. To calculate ζ , first sketch in the exponential envelope. Also, note that the zero level of the acceleration signal is offset from the center horizontal grid line; therefore, peak-to-peak amplitude measurements are more appropriate than zero-to-peak measurements, as well as more accurate. Annotate your measurements on the graph (submit the annotated graph), and show your calculations clearly. From your values for f_d and ζ , calculate the undamped natural frequency f_n (Hz). For a lightly damped system

Chapter 9 Damped 2nd order systems: general time response

such as this one, is the difference between f_d and f_n numerically significant, given the limited precision of the measured quantities?



9.6 A standard $m-c-k$ system is initially at rest. Then an engineer strikes the mass with a soft-tipped hammer that produces a relatively slow half-sine force pulse of amplitude 25 lb and duration 0.1 sec [$f_x(t) = 25 \text{ lb} \times \sin(10\pi t)$ for $0 \leq t \leq 0.1 \text{ sec}$]. Both the force pulse $f_x(t)$ and the displacement response $x(t)$ of the mass are recorded on the graph below. To support the calculations assigned (next page), annotate your measurements on a



Chapter 9 Damped 2nd order systems: general time response

photocopy of the graph (hand in the annotated graph), and show your calculations clearly.

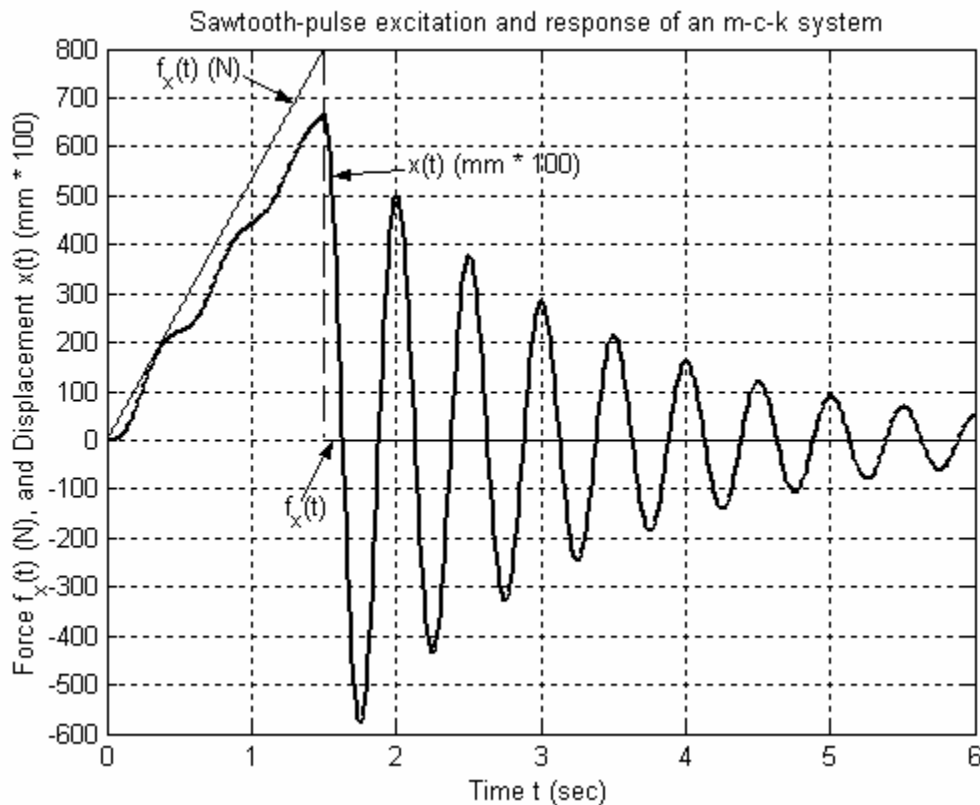
(a) Calculate from the $f_x(t)$ equation the impulse I_F produced by the force. However, you should not use this I_F in Eq. (9-43) to determine m . Explain why not.

(b) Calculate from the graph, with as much accuracy as the data permits, the damped natural frequency f_d (Hz), and the viscous damping ratio ζ of the system.

(c) The system's mass m is known to be 0.0652 lb-sec²/inch. Calculate stiffness constant k and damping constant c .

9.7 A large mass-damper-spring ($m-c-k$) system is initially at rest. Then a machine imposes upon the mass a slowly varying force in the form of a sawtooth pulse of amplitude 800 N and pulse duration 1.5 sec, $f_x(t) = \frac{800 \text{ N}}{1.5 \text{ sec}} \times t$ for $0 \leq t \leq 1.5 \text{ sec}$. Both the force

pulse $f_x(t)$ and the displacement response $x(t)$ of the mass are recorded on the graph below. The unusual displacement scale “ $x(t)$ (mm * 100)” is employed in order to accommodate the ranges of both $f_x(t)$ and $x(t)$ on the same graph; this scale simply means that the range of displacements on the graph is $-6.00 \text{ mm} \leq x(t) \leq +8.00 \text{ mm}$. To support the calculations assigned (next page), annotate your measurements on a photocopy of the graph (hand in the annotated graph), and show your calculations clearly.



Chapter 9 Damped 2nd order systems: general time response

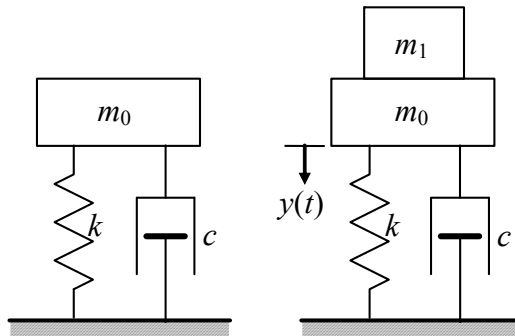
- (a)** Calculate the total impulse I_F produced by the force. However, you should not use this I_F in Eq. (9-43) to determine m . Explain why not.
- (b)** Calculate from the graph, with as much accuracy as the data permits, the damped natural frequency f_d (Hz), and the viscous damping ratio ζ of the system.
- (c)** The system's stiffness constant k is known from static testing to be 120.0 kN/m. Calculate mass m and damping constant c .
- (d)** Find the algebraic/numerical equation for the pseudo-static response $x_{ps}(t)$ while the pulse is active ($0 \leq t \leq 1.5$ sec), and compare your $x_{ps}(t)$ with the actual response $x(t)$ on the graph.

9.8 Consider the mass-damper-spring system shown in the figure below, with:

(a) $m_0 = 10.0$ kg, $c = 40.0$ N-sec/m, $k = 400$ N/m, and $m_1 = 2.00$ kg;

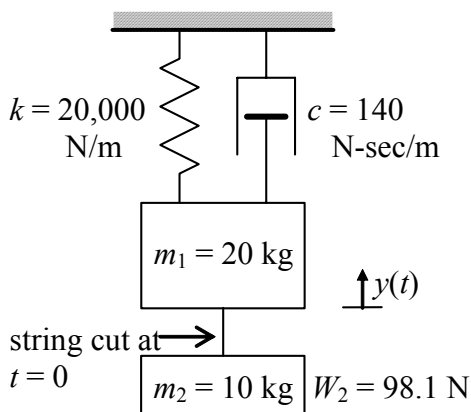
(b) $m_0g = 225$ lb, $c = 2.10$ lb-sec/inch, $k = 30.5$ lb/inch, and $m_1g = 105$ lb.

The system is initially at rest (the left-hand figure) in the static equilibrium position for weight m_0g . At $t = 0$, mass m_1 is gently placed upon m_0 and then released. This imposes an m_1g step force (the weight, due to gravity) onto the system. Note also that mass m_1 changes the system, since the total vibrating mass now will be $m_0 + m_1$, not just m_0 . Use Eq. (9-29) for underdamped 2nd order system step response to write the numerical equation for response $y(t)$ in inches of combined mass $m_0 + m_1$ (relative to the static equilibrium position for the weight of m_0 alone, as indicated on the figure). Then use MATLAB to plot the response curve of $y(t)$ versus t from $t = 0$ until the mass has settled to within at least 2% of its final steady-state position. This means plot to at least four time constants, $t = 4\tau_2$, where $\tau_2 = (\zeta\omega_n)^{-1}$. Since you are multiplying sinusoidal time functions by an exponential time function, it is necessary that you use array multiplication (\cdot^*) in MATLAB. Provide appropriate grids, titles, and labels on your graph. It is not required, but you can check from your graph that the response has the values of frequency, steady-state (final static, pseudo-static) displacement, and viscous damping ratio that you can calculate from the original data for mass, damping, stiffness, and applied force.



9.9 For the $m\text{-}c\text{-}k$ system and step input/response of homework Problem 9.8 [part (a) or (b), whichever is assigned], use the equations of Section 9-8 to calculate rise time t_r , peak time t_p , maximum overshoot ratio \bar{y}_p , and settling time t_s . These calculations should agree with the comparable results that you can measure from your MATLAB step-response graph for homework Problem 9.8, assuming that your graph is correct.

9.10 Weight $W_2 = 98.1$ N (mass $m_2 = 10.0$ kg) is suspended by a string from weight $W_1 = 196.2$ N (mass $m_1 = 20.0$ kg), which is attached to the ceiling by spring k and viscous dashpot c , as shown below. The system is in static equilibrium when, at time $t = 0$, the string is cut cleanly, dropping W_2 . (This simulates the release of a bomb from a flexible airplane wing.) Consider the subsequent motion $x(t)$, $t \geq 0$, of m_1 . With the $y(t)$ datum shown on the drawing, you can think of this as step-response, with the release of W_2 being equivalent to imposing upon m_1 an upward step force equal to W_2 .



(a) Calculate the undamped natural frequency f_n (Hz), the damping ratio ζ , the damped natural frequency f_d (Hz), and the damped period of oscillation T_d (sec).

(b) Calculate the final (as $t \rightarrow \infty$) static value of y and the settling time t_s required for the motion to settle within 2% of that final static value.

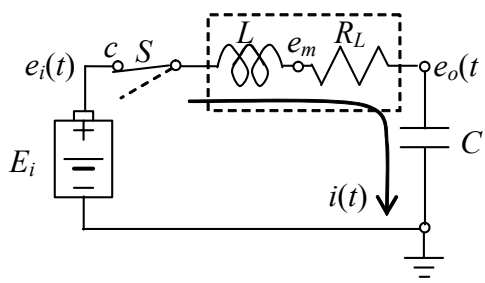
(c) Sketch a plot of the response $y(t)$ versus t from $t = 0$ until about $t = t_s$. Don't carry out extensive calculations; just use the results of parts

(a) and (b) to sketch an engineer's back-of-the-envelope type of quick graph that clearly shows the principal features of the response, but is not precise like a computer-generated graph.

9.11 Derive the algebraic equation for step response $x(t)$ with zero ICs of critically damped 2nd order systems: $\ddot{x} + 2\omega_n \dot{x} + \omega_n^2 x = \omega_n^2 U$, for $t \geq 0$, with $x(0) = 0$ and $\dot{x}(0) = 0$. One easy method of solution, the conventional approach of Section 1-5, is to use homogeneous solution (9-9), add to it an appropriate particular solution, then enforce the ICs to determine the unknown constants. (Answer: $x(t) = U[1 - (1 + \omega_n t)e^{-\omega_n t}]$, $t \geq 0$)

9.12 Having solved by inverse convolution transform for step and impulse responses of underdamped 2nd order systems, we can now use those results to obtain rather easily two messy Laplace transform pairs. Use Eq. (9-17) first with Eq. (9-29) and next with Eq. (9-31) to obtain $f_H(t) = L^{-1}\left[\frac{\omega_n^2}{s[(s + \zeta\omega_n)^2 + \omega_d^2]}\right]$ and $f_\delta(t) = L^{-1}\left[\frac{\omega_n^2}{(s + \zeta\omega_n)^2 + \omega_d^2}\right]$, both for $0 \leq t$, $|\zeta| < 1$, and $\omega_d^2 > 0$. Write the algebraic equations for $f_H(t)$ and $f_\delta(t)$.

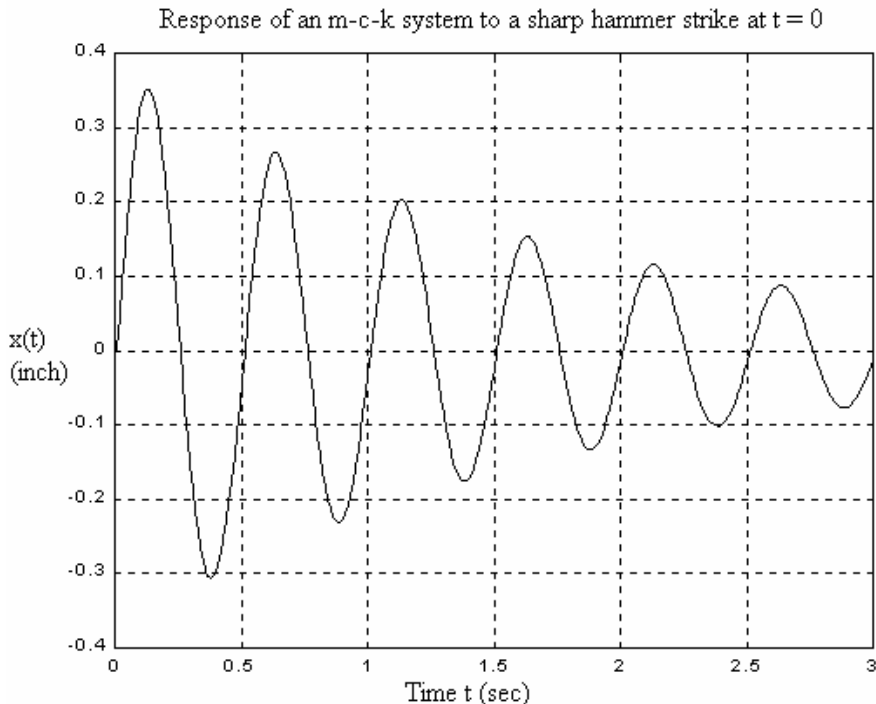
- 9.13** Consider the *LRC* circuit drawn below. The ODE describing output voltage $e_o(t)$



in terms of input voltage $e_i(t)$ is derived in Example 9-1 of Section 9-2. Because an inductor consists primarily of coiled wire, and because coiled wire accumulates resistance, a real inductor has resistance as well as inductance. A common, simple, approximate circuit model for such a real inductor is a series combination of an ideal inductor and a resistor, L and R_L , as shown in the drawing. Suppose that one small circuit

component has the values $L = 1.4 \text{ H}$ and $R_L = 210 \Omega$, and that it is in series with a capacitance of $C = 0.25 \mu\text{F}$ (micro-farad), as shown in the drawing. Calculate the natural frequency f_n (Hz) and damping ratio ζ of this circuit. Suppose further that the input voltage is $e_i(t) = 1.50 H(t)$ volts (a 1.5-volt battery is connected suddenly by switch S), and that all ICs are zero (in particular, there is no initial charge on the capacitor). Use MATLAB to plot output voltage $e_o(t)$ over a time interval from zero until $e_o(t)$ settles to within at least 2% of its final steady-state value.

- 9.14** A particular device is known to be a mass-damper-spring system. It is required that the mass m , the viscous damping constant c , and the stiffness constant k be identified experimentally from a transient-response test. In this test, an engineer strikes the mass sharply with a specially designed hammer that is instrumented with a force sensor. The force input to the mass is recorded, and examination of the actual force time history shows that it is closely approximated by a particular half-sine force pulse that lasts only 20 milliseconds, $f_x(t) = 58.9 \sin 50\pi t [H(t) - H(t - 0.02 \text{ sec})]$ lb. The measured displacement response of the mass is shown on the graph below. Use this information to



calculate m , c , and k in consistent units and with as much accuracy as the data permits. To support these calculations, annotate your measurements on the graph (hand in a photocopy of the annotated graph), and show your calculations clearly. The input force pulse is very short relative to the oscillatory period of the system. Therefore, for the purpose of approximate parameter identification, you should assume that the response is very close to ideal impulse response of the system to an ideal impulse, $f_x(t) = I_F \delta(t)$, with I_F having the value of the impulse of the actual half-sine force pulse. [NOTE: after you calculate m , c , and k , you can easily check the validity of your values by graphing (with MATLAB) the ideal impulse response of your system and then comparing that graph with the actual time history of response. However, this check is valid only if you use the correct value of impulse I_F , so first be 100% certain that your I_F is correct.]

9.15 For systems with the particular type of right-hand-side dynamics of Eq. (9-47), we can define a physical constant T having dimensions of time, then write a modified form of standard ODE (9-13) as $\ddot{x} + 2\zeta\omega_n \dot{x} + \omega_n^2 x = \omega_n^2 T u(t)$. [You can easily verify, for example, that $T = \tau_H$ for the band-pass filter, Eq. (9-47).] The pure IC-response of this equation is the same as Eq. (9-21), so let's focus on the forced response and set all ICs = 0. Also, let's assume initially that $|\zeta| < 1$, so that $\omega_d^2 = \omega_n^2(1 - \zeta^2) > 0$.

- (a) For this modified ODE, follow the steps from Eqs. (9-14) to (9-17), and assume also that $u(0) = 0$. to find $L[x(t)] = \frac{\omega_n^2 T}{\omega_d} \frac{s \omega_d}{(s + \zeta \omega_n)^2 + \omega_d^2} L[u(t)]$. Next, use a Laplace transform pair developed, in effect, between Eqs. (9-17) and (9-20) to solve for $x(t)$ if the input is step function $u(t) = U H(t)$. Which of the zero ICs is or is not preserved in this solution?
- (b) Use the inverse transform for step response of part (a), and the general transform $L[\dot{f}(t)] = s F(s) - f(0)$ to derive the following inverse transform:

$$L^{-1}\left[\frac{s \omega_d}{(s + \zeta \omega_n)^2 + \omega_d^2} \right] = e^{-\zeta \omega_n t} (\omega_d \cos \omega_d t - \zeta \omega_n \sin \omega_d t)$$

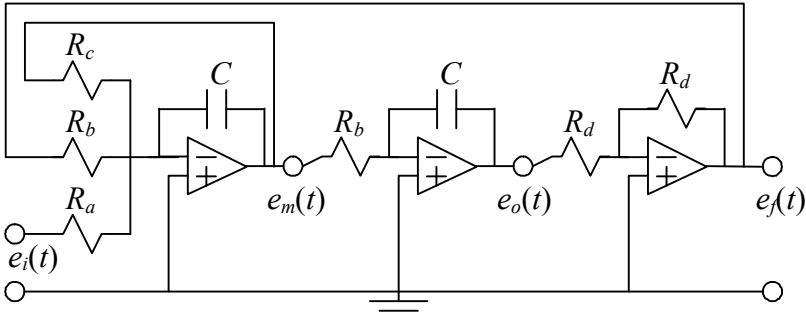
- (c) Use the result of part (b) and the inverse convolution transform to write $x(t)|_{ICs=0}$ equations, which involve convolution integrals, that apply for arbitrary input function $u(t)$.
- (d) Use the result of part (b) and Eq. (8-24) to show that the algebraic equation for the unit-impulse-response function (IRF) valid for the modified 2nd order ODE with right-hand side dynamics is $h(t) = \omega_n^2 T e^{-\zeta \omega_n t} [\cos \omega_d t - (\zeta \omega_n / \omega_d) \sin \omega_d t]$. Now use this IRF to write a Duhamel integral equation, Eq. (8-25), for $x(t)|_{ICs=0}$ that applies for arbitrary input function $u(t)$.

(e) The results of parts (a)-(d) apply for an underdamped 2nd order system, $|\zeta| < 1$. But Example 9-3 in Section 9-10 shows that an *RC* band-pass filter, for one, is an over-damped 2nd order system, so we need to convert the previous results to obtain results valid for $|\zeta| > 1$. Use the methods of Section 9-10 to write an algebraic equation for IRF $h(t)$ and an integral equation for $x(t)|_{ICs=0}$, both valid for the modified over-damped 2nd order ODE with right-hand side dynamics and the latter valid for arbitrary input function $u(t)$.

9.16 Figure 9-7 includes a curve that is step response of a standard overdamped 2nd order system. Use the methods of Section 9-10 to derive the algebraic equation from which that particular curve was calculated. *Answer:*

$$x(t) = U \left[1 - e^{-\zeta \omega_n t} \left(\cosh \mu_d t + \frac{\zeta \omega_n}{\mu_d} \sinh \mu_d t \right) \right], \text{ for } 0 \leq t \text{ and } \zeta > 1, \mu_d \equiv \omega_n \sqrt{\zeta^2 - 1}$$

9.17 The circuit drawn at right⁵ consists of three stages, each built around an op-amp, and there is *feedback* of voltage $e_f(t)$ from the last (right-hand) stage to the first (left-hand) stage, where the input voltage $e_i(t)$ is applied. The circuit output voltage, $e_o(t)$, is the output of the middle stage. The first stage is a *summing, inverting integrator*; use the methods of Chapter 5 to derive the first ODE, $e_m/R_c + e_f/R_b + e_i/R_a = -C \dot{e}_m$. Next, for the middle stage, an *inverting integrator*, derive the second ODE, $e_m/R_b = -C \dot{e}_o$ (homework Problem 5.6); now use the second ODE to substitute for e_m in the first ODE, and differentiate the second ODE and use the result to substitute for \dot{e}_m in the first ODE. The last stage of the circuit is a simple sign inverter, for which $e_f = -e_o$ from Eq. (5-13b); substitute for e_f and show that the ODE relating output voltage $e_o(t)$ to input voltage $e_i(t)$ for the entire circuit is $\ddot{e}_o + \frac{1}{R_c C} \dot{e}_o + \left(\frac{1}{R_b C} \right)^2 e_o = \left(\frac{1}{R_b C} \right)^2 \frac{R_b}{R_a} e_i$. Convert this ODE into the standard damped 2nd order form (9-13), $\ddot{e}_o + 2\zeta\omega_n \dot{e}_o + \omega_n^2 e_o = \omega_n^2 u(t)$; write specific equations (in terms of this circuit's resistances, capacitances, and input voltage) for undamped natural frequency ω_n , viscous damping ratio ζ , and input quantity $u(t)$.



⁵ This circuit is essentially the *electronic analog computer* (see the footnote to homework Problem 5.6) for solving ODE (9-13).

9.18 One rate gyroscope (Example 9-2 in Section 9-2) has the following rotor parameters: polar rotational inertia $J_r = 2.9 \times 10^{-4}$ kg-m², and spin rate $\Omega_r = 2,100$ revolutions per minute (rpm); also, it has the following gimbal-shaft parameters: polar rotational inertia $J_\theta = 2.2 \times 10^{-4}$ kg-m², and damping constant $c_\theta = 0.0046$ N-m/(rad/sec), and stiffness constant $k_\theta = 0.096$ N-m/rad. Consider output gimbal-shaft rotation $\theta(t)$ in response to an input turntable rotational rate that approximates step function $p(t) \approx P \times H(t)$. (Only a physically impossible ideal impulse moment acting on the turntable could produce an exact step change in rotational rate; therefore, imagine for this problem that a very short but very large moment pulse produces the approximate step function, but use the equations that apply for an exact step function.) For the step magnitude $P = 15$ degrees/sec, calculate the following response quantities: pseudo-static gimbal-shaft rotation, θ_{ps} (in degrees); and rise time, t_r ; and peak time, t_p ; and maximum overshoot ratio, \bar{x}_p . (*Partial answer:* $t_p = 0.174$ sec) The theory developed in Example 9-2 is accurate only if gimbal-shaft rotation $\theta(t)$ is sufficiently small that $\cos\theta(t) \approx 1$, say, $\cos\theta(t) > 0.95$. For the parameters in this problem, is this criterion for accuracy satisfied?

9.19 Another type of single-axis gyroscopic sensor is similar to the rate gyro described in Example 9-2 of Section 9-2 except that there is no spring to restrain the rotation of the gimbal-shaft assembly, so $k_\theta = 0$ in the equations derived in Example 9-2. Therefore, the equation of motion becomes effectively a 1st order ODE in dependent variable $\dot{\theta}(t)$, the rate of gimbal-shaft rotation:

$$J_\theta \ddot{\theta} + c_\theta \dot{\theta} = J_r \Omega_r p(t)$$

Observe from the ODE that the pseudo-static response is $(\dot{\theta})_{ps} = (J_r \Omega_r / c_\theta) p(t)$. But the electrical transducer of this device detects $\theta(t)$, not $\dot{\theta}(t)$, which means that the sensed quantity has the form $\theta(t) = \int_t \dot{\theta}(\tau) d\tau = (J_r \Omega_r / c_\theta) \int_t p(\tau) d\tau$. Therefore, this type of sensor is called a *rate-integrating gyroscope*; its output is proportional, not to the rotational rate, but to the actual rotational angle of the turntable, $\psi(t) = \int_t p(\tau) d\tau$, where $p \equiv \dot{\psi}$.

Consider output gimbal-shaft rotational rate $\dot{\theta}(t)$ and rotation $\theta(t)$ in response to an input turntable rotational rate that approximates the following *flat pulse* of duration t_d :

$$p(t) = \begin{cases} 0, & t < 0 \\ P, & 0 < t < t_d \\ 0, & t_d < t \end{cases}, \text{ in which magnitude } P \text{ is constant}$$

(Only physically impossible ideal impulse moments acting on the turntable could produce exact step changes in rotational rate; therefore, imagine for this problem that very short but very large moment pulses produce the approximate step changes, but use the equations that apply for the exact flat pulse.)

Chapter 9 Damped 2nd order systems: general time response

(a) The mathematical solution for response of a standard stable 1st order system to a flat-pulse input is given in homework Problem 6.2(a). Adapt this solution to write response equations for the rate-integrating gyro's gimbal-shaft rotational rate, $\dot{\theta}(t)$, given the IC $\dot{\theta}(0) = 0$. Next, integrate appropriately (show all details!) the $\dot{\theta}(t)$ equations, given the IC $\theta(0) = 0$, to derive the following equations for gimbal-shaft rotation:

$$\theta(t) = \begin{cases} bP\tau_1[t - \tau_1(1 - e^{-t/\tau_1})], & 0 \leq t \leq t_d \\ \theta(t_d) + bP\tau_1^2(1 - e^{-t_d/\tau_1})(1 - e^{-(t-t_d)/\tau_1}), & t_d \leq t \end{cases}$$

where $b \equiv J_r \Omega_r / J_\theta$ and $\tau_1 \equiv J_\theta / c_\theta$.

(b) One rate-integrating gyro has the following rotor parameters: polar rotational inertia $J_r = 2.9 \times 10^{-4}$ kg-m², and spin rate $\Omega_r = 420$ revolutions per minute (rpm); also, it has the following gimbal-shaft parameters: polar rotational inertia $J_\theta = 8.5 \times 10^{-4}$ kg-m², and damping constant $c_\theta = 9.2 \times 10^{-3}$ N-m/(rad/sec). For the flat-pulse rotational-rate magnitude $P = 5$ degrees/sec and pulse duration $t_d = 2.5$ sec, calculate and plot from the equations of part (a) the gimbal-shaft rotation $\theta(t)$ (in degrees) over the time interval $0 \leq t \leq 5$ sec. The theory developed in Example 9-2 is accurate only if gimbal-shaft rotation $\theta(t)$ is sufficiently small that $\cos \theta(t) \approx 1$, say, $\cos \theta(t) > 0.95$. For the parameters in this problem, is this criterion for accuracy satisfied?

(c) Since $(\dot{\theta})_{ps} = (J_r \Omega_r / c_\theta)p(t) = (J_r \Omega_r / c_\theta)\dot{\psi}(t)$, it is clear the rate-integrating gyro's output is designed to be proportional, as closely as its dynamics permit, to the actual rotational angle of the turntable, *i.e.*, $\theta(t) \approx (J_r \Omega_r / c_\theta)\psi(t)$; therefore, the equation that estimates $\psi(t)$ from the measured gimbal-shaft rotation is $\psi(t) \approx [c_\theta / (J_r \Omega_r)]\theta(t)$. Use your calculated $\theta(t)$ from part (b) to calculate and plot the quantity $[c_\theta / (J_r \Omega_r)]\theta(t)$ over the same time interval, $0 \leq t \leq 5$ sec. Next, calculate the actual turntable rotational angle from $\psi(t) = \int_0^t p(\tau) d\tau$, given the IC $\psi(0) = 0$, and plot it on the same graph for comparison with $[c_\theta / (J_r \Omega_r)]\theta(t)$. In this case, how well does the rate-integrating gyro follow the actual turntable rotation?

Chapter 10 2nd order systems: frequency response; beating response to suddenly applied sinusoidal (SAS) excitation

© 2016 by William L. Hallauer, Jr.

10-1 Frequency response of undamped 2nd order systems; resonance

As discussed in Section 7-1, a truly undamped 2nd order passive system is physically unrealistic. Nevertheless, it is useful to derive the frequency response for this ideal type of system because the results reveal important characteristics of the resonating behavior of general underdamped 2nd order systems. Moreover, the frequency response of an undamped 2nd order system is, for many practical purposes, a simple yet satisfactory engineering approximation to the frequency response of the corresponding lightly damped 2nd order system.

Consider the standard ODE for idealized undamped 2nd order systems:

$$\ddot{x} + \omega_n^2 x = \omega_n^2 u(t) \quad (10-1), \text{ Eq. (7-5) repeated}$$

To derive frequency response, we let $u(t) = U \cos \omega t$ and seek the steady-state sinusoidal response in the form $x(t) = X_S(\omega) \cos \omega t$, in which $X_S(\omega)$ is the unknown quantity. We find an equation for $X_S(\omega)$ by substituting into Eq. (10-1):

$$\begin{aligned} & (-\omega^2 + \omega_n^2) X_S(\omega) \cos \omega t = \omega_n^2 U \cos \omega t \\ \Rightarrow \quad \frac{X_S(\omega)}{U} &= \frac{\omega_n^2}{\omega_n^2 - \omega^2} = \frac{1}{1 - (\omega/\omega_n)^2} \end{aligned} \quad (10-2)$$

Note from Eq. (10-2) that $X_S(\omega)$ is a signed quantity; it can be positive or negative depending upon the value of frequency ratio ω/ω_n relative to 1. But our conventional notation for a frequency response function is $FRF(\omega) = \frac{X(\omega)}{U} e^{j\phi(\omega)}$, Eq. (4-41), in which magnitude $X(\omega) \geq 0$. Therefore, we infer from Eq. (10-2) the following magnitude-ratio and phase functions in the conventional notation:

$$\frac{X(\omega)}{U} = \left| \frac{1}{1 - (\omega/\omega_n)^2} \right|, \quad \phi(\omega) = \begin{cases} 0^\circ & \text{for } 0 \leq \omega/\omega_n < 1 \\ -180^\circ & \text{for } 1 < \omega/\omega_n \end{cases} \quad (10-3a, b)$$

Chapter 10 2nd order systems: frequency response; beating response to SAS excitation

Equations (10-3) give the frequency response function (FRF) of an undamped 2nd order system. The magnitude ratio $X(\omega)/U$ and phase $\phi(\omega)$ are plotted on Fig. 10-1 as functions of excitation frequency ratio ω/ω_n .

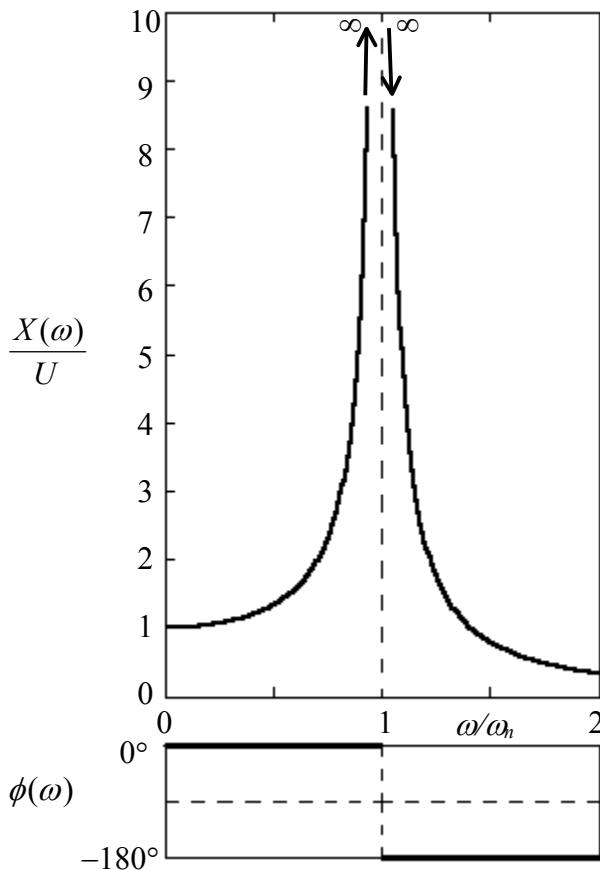


Figure 10-1 Frequency response function of an undamped 2nd order system

very important characteristic of lightly damped 2nd order systems. There is additional discussion of resonance in the next section.

FRF (10-3) contains not only the magnitude but also the phase ϕ : for $\omega < \omega_n$, the phase is 0° , so the response is exactly in phase with the excitation; however, for $\omega > \omega_n$, the phase is -180° , so the response is exactly out of phase with the excitation.

10-2 Frequency response of damped 2nd order systems

From Section 9-2, the standard form of the 2nd order ODE is:

$$\ddot{x} + 2\zeta\omega_n\dot{x} + \omega_n^2x = \omega_n^2u(t) \quad (10-4), \text{ Eq. (9-13) repeated}$$

To derive frequency response, we take the Laplace transform of (10-4), with zero ICs:

$$\left(s^2 + 2\zeta\omega_n s + \omega_n^2 \right) L[x(t)] \Big|_{ICs=0} = \omega_n^2 L[u(t)] \quad (10-5)$$

Definition (4-23) for the transfer function gives

$$TF(s) = \frac{L[x(t)]}{L[u(t)]} \Big|_{ICs=0} = \frac{\omega_n^2}{s^2 + 2\zeta\omega_n s + \omega_n^2} \quad (10-6)$$

Then the fundamental relationship (4-41) between the transfer function and the complex frequency response function gives

$$FRF(\omega) = TF(j\omega) = \frac{\omega_n^2}{-\omega^2 + j2\zeta\omega_n\omega + \omega_n^2} = \frac{1}{\left(1 - \omega^2/\omega_n^2\right) + j2\zeta\omega/\omega_n} \quad (10-7)$$

To simplify notation, we define the dimensionless excitation frequency ratio, the excitation frequency relative to the system undamped natural frequency:

$$\beta \equiv \frac{\omega}{\omega_n} \quad (10-8)$$

With notation (10-8), the relationship (4-41) between $FRF(\omega)$ and the magnitude ratio $X(\omega)/U$ and phase angle $\phi(\omega)$ of the frequency response gives

$$FRF(\omega) = \frac{1}{(1 - \beta^2) + j2\zeta\beta} = \frac{X(\omega)}{U} e^{j\phi(\omega)} \quad (10-9)$$

After the standard manipulation of the complex fraction in Eq. (10-9), we find the following equations for magnitude ratio and phase angle [homework Problem 2.6(a)]:

$$\frac{X(\omega)}{U} = \frac{1}{\sqrt{(1 - \beta^2)^2 + (2\zeta\beta)^2}}, \quad \phi(\omega) = \tan^{-1}\left(\frac{-2\zeta\beta}{1 - \beta^2}\right), \quad \beta \equiv \frac{\omega}{\omega_n} \quad (10-10)$$

Note that results (10-10) are valid for any non-negative value of viscous damping ratio, $\zeta \geq 0$; unlike most of the time-response equations derived in Chapter 9, Eqs. (10-10) alone apply for underdamped, critically damped, and overdamped 2nd order systems.

Results (10-10) are plotted on Fig. 10-2 (page 10-5) for viscous damping ratios varying from 0 to 1. The graphs of Fig. 10-2 were produced with use of MATLAB (Version 6 or later). First, an M-file was programmed to calculate and graph FRFs using the method described in the statement of homework Problem 4.3 [starting with complex FRF (10-9), not the real equations (10-10)]:

Chapter 10 2nd order systems: frequency response; beating response to SAS excitation

```
%frf2orddamped.m
%Fig. 10-2 Frequency response, damped 2nd order
%Magnitude ratio for zero damping, zeta=0
bt0a=logspace(-1,log10(0.998),100);
frf0a=(1)./(1-bt0a.^2);
loglog(bt0a,frf0a,'k'),hold on
bt0b=logspace(log10(1.002),1,100);
frf0b=(1)./(bt0b.^2-1);
loglog(bt0b,frf0b,'k')
%Magnitude ratio for several cases of zeta > 0
bt1=logspace(-1,1,400);
zt=[ 0.05 0.1 0.2 0.5 1/sqrt(2) 1];nzts=length(zt);
for i=1:nzts
    frf=(1)./(1-bt1.^2+j*2*zt(i).*bt1);
    magrat=abs(frf);
    loglog(bt1,magrat,'k')
end
hold off
%Phase angle in degrees for zero damping, zeta=0
bt0a=[0.1 1];faz0a=zeros(1,2);
figure,semilogx(bt0a,faz0a,'k'),hold on
bt0b=[1 10];faz0b=-180*ones(1,2);
semilogx(bt0b,faz0b,'k')
%Phase angle in degrees for several cases of zeta > 0
for i=1:nzts
    frf=(1)./(1-bt1.^2+j*2*zt(i).*bt1);
    faz=angle(frf)*180/pi;
    semilogx(bt1,faz,'k')
end
```

After the M-file was executed, the extensive figure editing features of MATLAB were used to set axis limits and to generate titles, labels, and curve annotations.

Even though Fig. 10-2 was produced by computer-aided graphics, it is still important that you understand how to evaluate Eqs. (10-10) with a hand calculator. These equations appear simple, but they can be tricky, particularly for the special case $\zeta = 0$. See homework Problem 2.6(b) for help with understanding how to evaluate Eqs. (10-10) numerically.

There are several noteworthy characteristics of the frequency response of damped 2nd order systems, from Eqs. (10-10) and Fig. 10-2:

* Resonance: maximum (peak) magnitude ratio The frequency at which the peak magnitude ratio occurs is called the *resonance frequency*, denoted ω_r , and this frequency is lower than natural frequency ω_n if damping is positive, $\zeta > 0$. To find the maximum, we differentiate the magnitude ratio of Eqs. (10-10), set the result to zero, and solve for the associated frequency (you can verify the result yourself, or see Meirovitch, 2001, pp. 115-116 for the details of calculus and algebra; also, there are instructive alternative approaches in Ogata, 1998, pp. 480-481 and in Clark, 1962, pp. 316-322):

$$\frac{d}{d\beta} \left(\frac{X(\beta)}{U} \right) = 0 \Rightarrow \beta_r = \sqrt{1 - 2\zeta^2} \Rightarrow \omega_r = \omega_n \sqrt{1 - 2\zeta^2} \quad (10-11)$$

Chapter 10 2nd order systems: frequency response; beating response to SAS excitation

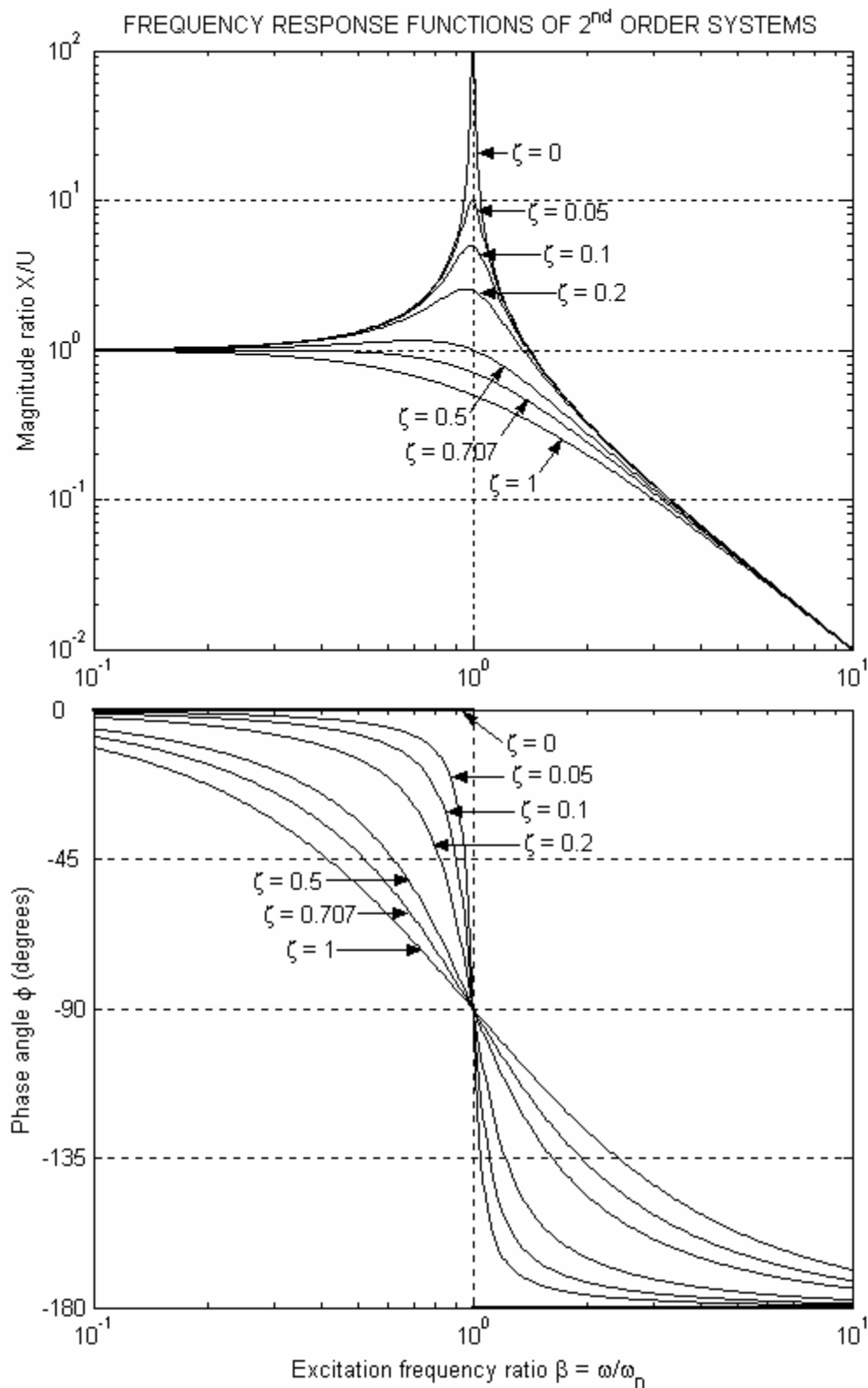


Figure 10-2 Frequency response functions for standard 2nd order systems with viscous damping ratios ζ varying from 0 to 1

Subscript r in Eq. (10-11) denotes a resonance quantity corresponding to the peak magnitude ratio X_r/U . The excitation frequency must be real and greater than or equal to zero, so $\omega_r = \omega_n \sqrt{1 - 2\zeta^2}$ is valid only for $0 \leq \zeta \leq 1/\sqrt{2} = 0.707$. If ζ is positive but very small, then X_r/U occurs almost at the natural frequency, $\omega_r \approx \omega_n$. As ζ increases from very small positive values, ω_r decreases until, for $\zeta = 1/\sqrt{2}$, $\omega_r = 0$. However, dynamic amplification is insignificant for values of ζ greater than about 0.5. Substituting Eq. (10-11) back into $X(\omega)/U$ of Eqs. (10-10) gives (after more algebra) the resonance value:

$$\frac{X(\beta_r)}{U} = \frac{X_r}{U} = \frac{1}{2\zeta \sqrt{1 - \zeta^2}} \quad (10-12)$$

Note from Eq. (10-12) that for $\zeta = 1/\sqrt{2}$ [the maximum permissible value for validity of Eq. (10-11)], we have $X_r/U = 1$ at $\omega_r = 0$. As indicated by the trend on Fig. 10-2, for higher damping ratios, $\zeta \geq 1/\sqrt{2}$, the magnitude $X(\omega)/U$ is maximum at $\omega = 0$, and decreases monotonically as ω increases.

* Response at the natural frequency The frequency response at $\omega = \omega_n$, $\beta = 1$, consists of phase angle $\phi(\omega_n) = -90^\circ$ regardless of the value of viscous damping ratio ζ , and magnitude ratio $X(\omega_n)/U = 1/(2\zeta)$. Also, the peak magnitude response occurs essentially at $\omega = \omega_n$ if damping is small, as discussed next.

* Small viscous damping, small- ζ approximation If damping is so small that $\sqrt{1 - 2\zeta^2} \approx 1$, then we can use the following accurate approximations of the values associated with response at resonance, from Eqs. (10-11) and (10-12):

$$\omega_r = \omega_n \sqrt{1 - 2\zeta^2} \approx \omega_n \quad (10-13)$$

$$\frac{X_r}{U} = \frac{1}{2\zeta \sqrt{1 - \zeta^2}} \approx \frac{X(\omega_n)}{U} = \frac{1}{2\zeta} \quad (10-14)$$

The upper limit of viscous damping ratio for which the small- ζ approximation is practically useful is about $\zeta = 0.2$, which we can see on Fig. 10-2. At this upper limit, the approximation is in error on the order of 4%, since $\sqrt{1 - 2(0.2)^2} = 0.959$. The small- ζ resonance amplification factor (10-14) is sometimes called the *quality factor*, and it is denoted $Q = 1/(2\zeta)$. The “quality” reference is to tuning, especially of a receiving device such as a radio (Hammond, 1961, pp. 106-114). When you turn the analog tuning dial of an old radio, you are varying the value of capacitance in an *LRC* electrical tuning circuit in order to produce resonance with the electromagnetic carrier signal, which gives

the strongest possible reception. Clearly, a high Q is desirable in the tuning circuit of a radio. On the other hand, high Q is often undesirable in mechanical systems, because it can lead to structural failure or other negative consequences. For example, if the system consisting of a car's tire, suspension spring, and damping strut happens to resonate with the waves in a washboard dirt road, then the resulting vibration will produce poor ride quality and might even break car parts.

Note on the Fig. 10-2 graph of magnitude ratio that the $\zeta = 0$ curve bounds the curves for all $\zeta > 0$, and that it provides a good approximation for small ζ at all frequencies except those close to ω_n ; for small damping, therefore, the simple equation (10-3a) for magnitude ratio will, for some calculations, be sufficiently accurate.

* Phase angles of frequency response Figure 10-2 shows that the more lightly damped a system is, the closer its response is to being in phase with excitation below the natural frequency, and out of phase with excitation above the natural frequency. Furthermore, for excitation at the natural frequency, $\omega = \omega_n$, response lags excitation by exactly 90°, regardless of the level of viscous damping; this so-called *quadrature phase* is an important characteristic often used to help determine natural frequencies in vibration testing of machines and structures.

* 2nd order low-pass filter A moderately damped ($0.5 \leq \zeta \leq 1$) 2nd order system can function as a low-pass filter, with natural frequency ω_n being the break (corner) frequency. Compare the magnitude ratio curve for $\zeta = 1/\sqrt{2} = 0.707$ on Fig. 10-2 with the magnitude ratio curve for a 1st order low-pass filter, Fig. 4-2. The most significant difference between the two curves is in their high-frequency asymptotes: the 2nd order magnitude ratio rolls off at the rate of two decades for each decade increase of frequency (40 dB/decade rolloff), twice as steeply as the 1st order magnitude ratio. Thus, the 2nd order filter functions much more effectively than the 1st order filter. However, an important practical deficiency (in some potential applications) of both types of low-pass filters is that they impose on the low-passed output large phase lags relative to the input.

10-3 Frequency response of mass-damper-spring systems, and system identification by sinusoidal vibration testing

Reviewing the basic 2nd order mechanical system from Fig. 9-1 and Section 9-2, we have the $m-c-k$ and standard 2nd order ODEs:

$$m\ddot{x} + c\dot{x} + kx = f_x(t) \Rightarrow \ddot{x} + 2\zeta\omega_n\dot{x} + \omega_n^2 x = \omega_n^2 u(t) \quad (10-15)$$

with the definitions

$$\omega_n = \sqrt{\frac{k}{m}}, \quad \zeta \equiv \frac{c}{2m\omega_n} = \frac{c}{2\sqrt{mk}} \equiv \frac{c}{c_c}, \quad u(t) \equiv \frac{1}{k} f_x(t) \quad (10-16)$$

So we can use the correspondence $U = F/k$ to adapt FRF (10-10) directly for $m\text{-}c\text{-}k$ systems:

$$\frac{X(\omega)}{F/k} = \frac{1}{\sqrt{(1-\beta^2)^2 + (2\zeta\beta)^2}}, \quad \phi(\omega) = \tan^{-1}\left(\frac{-2\zeta\beta}{1-\beta^2}\right), \quad \beta \equiv \frac{\omega}{\sqrt{k/m}} \quad (10-17)$$

In the conceptually simplest form of forced-vibration testing of a 2nd order, linear mechanical system, a force-generating *shaker* (an electromagnetic or hydraulic translational motor) imposes upon the system's mass a sinusoidally varying force at cyclic frequency f , $f_x(t) = F \cos(2\pi f t)$. The resulting steady-state sinusoidal translation of the mass is $x(t) = X \cos(2\pi f t + \phi)$. Calibrated sensors detect $f_x(t)$ and $x(t)$, and then F , X , f and ϕ are measured from the electrical signals of the sensors. In principle, the testing involves a *stepped-sine sweep*: measurements are made first at a lower-bound frequency in a steady-state *dwell*, then the frequency is stepped upward by some small increment and steady-state measurements are made again; this frequency stepping is repeated again and again until the desired frequency band has been covered and smooth plots of X/F and ϕ versus frequency f can be drawn.

For system identification (ID) of 2nd order, linear mechanical systems, it is common to write the frequency-response magnitude ratio of Eq. (10-17) in the form of a dimensional magnitude of *dynamic flexibility*:¹

$$\frac{X(\omega)}{F} = \frac{1}{k} \frac{1}{\sqrt{(1-\beta^2)^2 + (2\zeta\beta)^2}} = \frac{1}{\sqrt{(k-m\omega^2)^2 + c^2\omega^2}} \quad (10-18)$$

Also, in terms of the basic $m\text{-}c\text{-}k$ parameters, the phase angle of Eq. (10-17) is

$$\phi(\omega) = \tan^{-1}\left(\frac{-c\omega}{k-m\omega^2}\right) \quad (10-19)$$

Note that if $\omega \rightarrow 0$, dynamic flexibility (10-18) reduces just to the *static flexibility* (the inverse of the stiffness constant), $X(0)/F = 1/k$, which makes sense physically. In fact, the first step in the system ID process is to determine the stiffness constant. Electromagnetic shakers are not very effective as static loading machines, so a static test independent of the vibration testing might be required. In principle, static force F imposed on the mass by a loading machine causes the mass to translate an amount $X(0)$, and the stiffness constant is computed from

$$k = \frac{F}{X(0)} \quad (10-20)$$

¹ However, see homework Problem 10.16 for the practical reasons why it might often be better to measure *dynamic stiffness*, Eq. (10-31), rather than dynamic flexibility.

However, suppose that it is more convenient to shake the mass at a relatively low frequency (that is compatible with the shaker's capabilities) than to conduct an independent static test. Note from Fig. 10-2 that if the excitation frequency is less than about 25% of natural frequency ω_n , then the magnitude of dynamic flexibility is essentially the same as the static flexibility, so a good approximation to the stiffness constant is

$$k \approx \left(\frac{X(\omega \leq 0.25\omega_n)}{F} \right)^{-1} \quad (10-21)$$

Even if it is possible to generate frequency response data at frequencies only as low as 60-70% of ω_n , one can still knowledgeably extrapolate the dynamic flexibility curve down to very low frequency and apply Eq. (10-21) to obtain an estimate of k that is probably sufficiently accurate for most engineering purposes.

Assuming that all necessary experimental data have been collected, and assuming that the system can be modeled reasonably as an LTI, SISO, $m-c-k$ system with viscous damping, then the steps of the subsequent system ID calculation algorithm are:

1. Calculate k from Eq. (10-20) and/or Eq. (10-21), preferably both, in order to check that both static and dynamic testing lead to the same result.
2. Determine natural frequency ω_n from the frequency response curves. The frequency at which the phase angle is -90° is the natural frequency, regardless of the level of damping. Also, if viscous damping ratio ζ is small, less than about 0.2, then the frequency at which the dynamic flexibility peaks is essentially the natural frequency. With ω_n and k known, calculate the mass: $m = k/\omega_n^2$.
3. Measure the resonance (peak) dynamic flexibility, X_r/F . Then the maximum dynamic amplification equation (10-12) gives the following equation from which any viscous damping ratio $\zeta \leq 1/\sqrt{2}$ can be calculated:

$$\frac{X_r}{F/k} = k \left(\frac{X_r}{F} \right) = \frac{1}{2\zeta\sqrt{1-\zeta^2}} \quad (10-22)$$

The calculation is simplified considerably if ζ is small, less than about 0.2:

$$\frac{1}{2\zeta} \approx k \left(\frac{X_r}{F} \right) \Rightarrow \zeta \approx \frac{1}{2} \left[k \left(\frac{X_r}{F} \right) \right]^{-1} \quad (10-23)$$

Finally, the viscous damping constant is calculated from Eq. (10-16):

$$c = c_c \times \zeta = 2\zeta\sqrt{mk} = 2\zeta m\omega_n \quad (10-24)$$

10-4 Frequency-response function of an *RC* band-pass filter

We re-visit once again Section 5-4 and the example of Section 9-10, where it is demonstrated that a typical *RC* band-pass filter, as depicted below, is an overdamped 2nd order system with right-hand-side dynamics. Our goal now is to derive the FRF of this filter circuit.

Rather than analyze 2nd order ODE (9-47) directly, it is instructive to start with the coupled 1st order ODEs of the two stages: Eq. (5-16), $\tau_L \dot{e}_m + e_m = e_i$, with $\tau_L = R_L C_L$, for the upstream, low-pass filter; and Eq. (5-17), $\tau_H \dot{e}_o + e_o = \tau_H \dot{e}_m$, with $\tau_H = R_H C_H$, for the downstream, high-pass filter. In this approach, we represent a system (the band-pass filter, in this case) as an assemblage of stages or lower-order sub-systems (the low-pass and high-pass filters, in this case). This section is a preview of the more general discussion beginning in Chapter 13.

Taking the Laplace transform of the ODE for the low-pass stage, with the assumption that all ICs are zero, gives

$$(\tau_L s + 1)L[e_m] \Big|_{ICs=0} = L[e_i] \Rightarrow L[e_m] \Big|_{ICs=0} = \frac{1}{\tau_L s + 1} L[e_i] \quad (10-25)$$

Next, we take the Laplace transform of the ODE for the high-pass stage, still with the assumption that all ICs are zero, and then substitute Eq. (10-25) into the result:

$$\begin{aligned} (\tau_H s + 1)L[e_o] \Big|_{ICs=0} &= \tau_H s L[e_m] \Big|_{ICs=0} \\ \Rightarrow L[e_o] \Big|_{ICs=0} &= \frac{\tau_H s}{\tau_H s + 1} L[e_m] \Big|_{ICs=0} = \frac{\tau_H s}{\tau_H s + 1} \times \frac{1}{\tau_L s + 1} L[e_i] \end{aligned} \quad (10-26)$$

So the transfer function of the entire *RC* band-pass filter circuit, clearly displaying right-hand-side dynamics, is

$$TF(s) \equiv \frac{L[e_o] \Big|_{ICs=0}}{L[e_i]} = \frac{\tau_H s}{(\tau_H s + 1)(\tau_L s + 1)} \quad (10-27)$$

Finally, the system complex frequency-response function is

$$FRF(\omega) = TF(j\omega) = \frac{j\omega\tau_H}{(j\omega\tau_H + 1)(j\omega\tau_L + 1)} \quad (10-28)$$

See homework Problem 10.11 for a numerical evaluation of this frequency response that demonstrates the practical function for which a band-pass filter is designed.

10-5 Common frequency-response functions for electrical and mechanical-structural systems

The term *frequency-response function* (FRF) is general, meaning physically the magnitude and phase in steady-state sinusoidal variation with time of some subject variable, relative to the magnitude and phase of some other reference variable. Often, but not always, the subject variable is clearly a physical response (output), and the reference variable is clearly a physical excitation (input). During over a century of development, engineers have found uses for many different types of FRF subject and reference variables, and names for these types are widely recognized. Many of the most common of these FRF definitions, their names, and examples are presented in this section.

Diagrams such as Fig. 4-1 and Figs. 10-1 and 10-2 display FRFs graphically, and there are many different forms of these diagrams. One of the most well-known and useful forms is the *Bode diagram*, on which relative magnitude and phase are plotted separately against the sinusoidal frequency, which is on a logarithmic scale (as on Fig. 10-2). Relative magnitude is usually plotted on the *decibel scale* [$\text{dB} = 20 \times \log_{10}(\text{relative magnitude})$], and relative phase is usually expressed in degrees. Another useful graphical format for FRFs is the *Nyquist diagram or plot* (after Harry Nyquist, Swedish-born American electrical engineer and physicist, 1889-1976), which is described at length in Section 17-2. Application of Bode diagrams and Nyquist diagrams to analysis of control systems is discussed in Chapter 17.

The use of FRFs apparently began during the 1880s with the definitions of *admittance* and *impedance* in the context of electrical engineering. Electrical *admittance* is traditionally assigned the symbol $Y(\omega)$. With $\Delta e(t)$ being a specified voltage difference and $i(t)$ being a specified current, admittance is defined by the equation

$$Y(\omega) = \left\{ \frac{L[i(t)]}{L[\Delta e(t)]} \right\}_{s=j\omega} \quad (10-29)$$

Keep in mind that the Laplace transforms in Eq. (10-29) and all other definitions of FRFs are for zero initial conditions. Electrical *impedance* is traditionally assigned the symbol $Z(\omega)$, and it is defined to be the inverse of admittance: $Z(\omega) = 1/Y(\omega)$. In general, admittance is the degree to which an electrical system admits (or permits, if you prefer) the flow of current, and impedance is the degree to which the system impedes the flow of current. The simplest examples of electrical admittance and impedance are for an ideal linear resistor of resistance R , with voltage difference $\Delta e(t)$ across the resistor and current

$i(t)$ flowing through it. Ohm's law, Eq. (5-1), is $\Delta e(t) = R \times i(t)$, so $Y(\omega) = 1/R$ and $Z(\omega) = R$, the same for all frequencies.²

The electrical FRFs for an ideal linear capacitor with capacitance C are more complicated. The relationship between voltage difference $\Delta e(t)$ across a capacitor and current $i(t)$ flowing through it is Eq. (5-3): $i(t) = C \times d[\Delta e(t)]/dt$. Taking the Laplace transform of this equation gives $L[i(t)] = C \times sL[\Delta e(t)]$, so, from Eq. (10-29), a capacitor's admittance is $Y(\omega) = j\omega C$, and its impedance is $Z(\omega) = 1/(j\omega C) = -j \times 1/(\omega C)$. The magnitude of this impedance is called *capacitive reactance* (Hammond, 1961, pp. 97-100), and is usually written as $X_C = 1/(\omega C) = 1/(2\pi f C)$. Physically, for a given magnitude of voltage difference and a given capacitance C , the magnitude of current permitted by a capacitor is directly proportional to frequency ω or f , and the current leads the voltage difference by 90°.

The relationship between voltage difference $\Delta e(t)$ across an ideal linear inductor and current $i(t)$ flowing through it is Eq. (5-6): $\Delta e(t) = \mathcal{L} \times d i(t)/dt$ (denoting inductance $\equiv \mathcal{L}$ in this paragraph only, to distinguish it from Laplace transform operator L). You can show easily that the associated admittance and impedance are, respectively, $Y(\omega) = 1/(j\omega \mathcal{L}) = -j \times 1/(\omega \mathcal{L})$ and $Z(\omega) = j\omega \mathcal{L}$. The magnitude of this impedance is called *inductive reactance*, and is usually written as $X_{\mathcal{L}} = \omega \mathcal{L} = 2\pi f \mathcal{L}$. Physically, for a given magnitude of voltage difference and a given inductance \mathcal{L} , the magnitude of current permitted by an inductor is inversely proportional to frequency ω or f , and the current lags the voltage difference by 90°.

The subject and reference variables of FRFs commonly used for mechanical and structural systems are, of course, different than those used for electrical systems. During much of the 20th century, conflicting and ambiguous names for these FRFs appeared in the engineering literature, but the names in English have been more uniformly standardized in recent years, as described by Ewins, 1984, pp. 26-27, and by Maia and Silva, 1997, pp. 38-39. In the following, we will derive theoretical FRF equations for an *m-c-k* system; however, in engineering practice, these FRF definitions are also applied both theoretically and experimentally for much more general and more complicated mechanical and structural systems.

For *mechanical admittance*, the subject variable is a physical displacement (translation or rotation) at some point and in some direction on the mechanical or structural system, and the reference variable is a physical action (force or moment) imposed at some point and in some direction onto the system (Bisplinghoff *et al.*, 1955, pp. 663-665). Thus, for an *m-c-k* system, from Laplace transformation of the ODE $m\ddot{x} + c\dot{x} + kx = f_x(t)$, and with use of notation defined in Eqs. (10-8) and (10-16), the equation for complex mechanical admittance is

² Clearly, the SI unit for impedance is the ohm (Ω), that of resistance; apparently since admittance is the inverse of impedance, the SI unit for admittance was given the whimsical name *mho* (Ω^{-1}).

$$\left\{ \frac{L[x(t)]}{L[f_x(t)]} \right\}_{s=j\omega} = \frac{1}{(k - \omega^2 m) + j\omega c} = \frac{1}{k} \left[\frac{1}{(1 - \beta^2) + j2\zeta\beta} \right] \quad (10-30)$$

The magnitude ratio and phase angle associated with Eq. (10-30) were written earlier in Eqs. (10-18) and (10-19). Some synonyms in English for mechanical admittance are *dynamic flexibility*, *dynamic compliance*, and *receptance*.

The inverse of mechanical admittance is known as *dynamic stiffness* (occasionally also *mechanical impedance*, but this name usually denotes a different FRF, as described below); thus, the dynamic stiffness of an *m-c-k* system is

$$\left\{ \frac{L[f_x(t)]}{L[x(t)]} \right\}_{s=j\omega} = (k - \omega^2 m) + j\omega c = k[(1 - \beta^2) + j2\zeta\beta] \quad (10-31)$$

The definition of Eq. (10-31), with the Laplace transform of action in the numerator and that of displacement in the denominator, might seem unorthodox, since an action (force or moment) is usually the physical input and a displacement is usually the physical output. However, this type of FRF is useful in practice for experimental measurements, as is described in homework Problem 10.16. Dynamic stiffness is also the basis of an advanced method for analyzing theoretically the dynamics of distributed-parameter structures (Clough and Penzien, 1975, Chapter 20; Fergusson and Pilkey, 1991).

For mechanical and structural systems, the first and second time derivatives of displacement are also of interest, primarily because velocity sensors and, especially, accelerometers are often used to measure motion. Accordingly, appropriate FRFs have been defined. For *mobility*, the subject variable is a velocity, and the reference variable is an action. Since $L[\dot{x}(t)] = s \times L[x(t)]$, the mobility of an *m-c-k* system, from Eq. (10-30), is

$$\left\{ \frac{L[\dot{x}(t)]}{L[f_x(t)]} \right\}_{s=j\omega} = \frac{j\omega}{(k - \omega^2 m) + j\omega c} = \frac{1}{c} \left[\frac{j2\zeta\beta}{(1 - \beta^2) + j2\zeta\beta} \right] \quad (10-32)$$

The inverse of mobility is usually given the name *mechanical impedance*. Accordingly, the mechanical impedance of an *m-c-k* system is

$$\left\{ \frac{L[f_x(t)]}{L[\dot{x}(t)]} \right\}_{s=j\omega} = \frac{(k - \omega^2 m) + j\omega c}{j\omega} = c \left[1 - j \left(\frac{1 - \beta^2}{2\zeta\beta} \right) \right] \quad (10-33)$$

For *accelerance* (also known as *inertance*), the subject variable is an acceleration, and the reference variable is an action. Since $L[\ddot{x}(t)] = s^2 \times L[x(t)]$, the accelerance of an *m-c-k* system, from Eq. (10-30), is

$$\left\{ \frac{L[\ddot{x}(t)]}{L[f_x(t)]} \right\}_{s=j\omega} = \frac{(j\omega)^2}{(k - \omega^2 m) + j\omega c} = \frac{1}{m} \left[\frac{-\beta^2}{(1 - \beta^2) + j2\zeta\beta} \right] \quad (10-34)$$

It is worth noting that for static loading ($\omega = 0$), mechanical admittance equals a nonzero static flexibility, but both mobility and accelerance are zero. The inverse of accelerance is called *apparent mass*, as motivated by the following expression for an $m-c-k$ system:

$$\left\{ \frac{L[f_x(t)]}{L[\ddot{x}(t)]} \right\}_{s=j\omega} = \frac{(k - \omega^2 m) + j\omega c}{(j\omega)^2} = m \left[\left(1 - \frac{1}{\beta^2} \right) - j \frac{2\zeta}{\beta} \right] \quad (10-35)$$

All of the mechanical and structural FRFs described in this section have dimensional units. For example, common units of accelerance used in the dynamic testing of structures are G 's or meters/sec² (of acceleration) per pound or newton (of force).

10-6 Beating response of 2nd order systems to suddenly applied sinusoidal excitation

Thus far in Chapter 10, we have considered only the pure frequency response of 2nd order systems, *i.e.*, the steady-state sinusoidal response to sinusoidal excitation. In frequency-response analysis based upon Eq. (4-41), initial conditions are ignored, as is any non-steady-sinusoidal start-up portion of the excitation; in other words, both pure sinusoidal excitation and response are idealized to start at some indefinite time in the past. But any real excitation must start at some definite time, at which time any real dynamic system has some initial conditions. After the initiation of sinusoidal excitation, there will be a transitional interval of response between the initial conditions and, provided the system is stable, the achievement of steady-state sinusoidal response. Section 4-2 illustrates such a transitional interval for a stable 1st order system, which does not exhibit natural oscillatory behavior. In this section, we consider a form of transitional response, *beating*, that is often observed in lightly damped vibrating systems, the simplest forms of which are underdamped 2nd order systems.

The basic character of beating response to sinusoidal excitation is best illustrated theoretically by the idealized undamped 2nd order system. Consider again the standard ODE for undamped 2nd order systems, Eq. (10-1). Suppose now that $u(t) = 0$ for $t < 0$, and let's define the suddenly applied sinusoidal (SAS) excitation as $u(t) = U \sin \omega t$ for $t \geq 0$. (We use $\sin \omega t$ here rather than the customary $\cos \omega t$ because it is more natural, especially for mechanical systems, that the excitation begins continuously from zero at $t = 0$, rather than with a discontinuity.) Thus, the ODE Eq. (10-1) becomes

$$\ddot{x} + \omega_n^2 x = \omega_n^2 u(t) = \omega_n^2 U \sin \omega t, \text{ for } t \geq 0 \quad (10-36)$$

For simplicity, we let the initial conditions be zero: $\dot{x}(0) = 0$ and $x(0) = 0$. The complete algebraic solution of ODE (10-36) with these rest ICs is found in homework Problem 1.12 by the method of undetermined coefficients:

$$x(t) = \frac{U}{1 - (\omega/\omega_n)^2} [\sin \omega t - (\omega/\omega_n) \sin \omega_n t], \text{ valid for } \omega \neq \omega_n, t \geq 0 \quad (10-37)$$

Equation (10-37) is valid only if the excitation frequency is different than the natural frequency, $\omega \neq \omega_n$; however, this is not a serious practical restriction, because it is almost impossible in reality to excite a system exactly at its natural frequency. [But see homework Problem 1.12(d) for the theoretical solution valid if $\omega = \omega_n$.]

It is appropriate to write the response solution Eq. (10-37) in a slightly different algebraic form:

$$x(t) = \frac{U}{1 - (\omega/\omega_n)^2} [\sin \omega t - \sin \omega_n t + (1 - \omega/\omega_n) \sin \omega_n t] \quad (10-38)$$

This form of $x(t)$ allows us to invoke a useful trigonometric identity:

$$\sin \omega t - \sin \omega_n t = 2 \cos \frac{1}{2}(\omega t + \omega_n t) \times \sin \frac{1}{2}(\omega t - \omega_n t) \quad (10-39)$$

Now we can express the solution (10-38) in an equation that more clearly displays the characteristics of beating:

$$x(t) = \frac{U}{1 - (\omega/\omega_n)^2} [2 \cos \frac{1}{2}(\omega + \omega_n)t \times \sin \frac{1}{2}(\omega - \omega_n)t + (1 - \omega/\omega_n) \sin \omega_n t] \quad (10-40)$$

For computation, with definitions of driving frequency ratio $\beta \equiv \omega/\omega_n$ and natural period $T_n \equiv 2\pi/\omega_n$, we express Eq. (10-40) in the dimensionless form:

$$\frac{x(t)}{U} = \frac{1}{1 - \beta^2} \left[2 \cos \left((\beta + 1)\pi \frac{t}{T_n} \right) \times \sin \left((\beta - 1)\pi \frac{t}{T_n} \right) + (1 - \beta) \sin \left(2\pi \frac{t}{T_n} \right) \right] \quad (10-41)$$

Let's use numerical evaluation and graphical display to help us examine the parts of Eqs. (10-40) and (10-41); Figure 10-3 on the next page includes plots of both suddenly applied sinusoidal excitation and the associated response calculated from Eq. (10-41), with the excitation frequency set at 90% of the natural frequency, $\omega = 0.9 \omega_n$ or $\beta = 0.9$.

With use of Fig. 10-3, we can identify the roles of the terms within square brackets of Eqs. (10-40) and (10-41) for any case in which the excitation frequency ω is somewhat close to the system natural frequency ω_n . The dominant (in magnitude) term that closely resembles the excitation is $2 \cos \frac{1}{2}(\omega + \omega_n)t$, a sinusoid whose frequency is the average of the excitation and natural frequencies. But this dominant term is multiplied by $\sin \frac{1}{2}(\omega - \omega_n)t$, which is a slowly varying amplitude modulator whose frequency is half the difference between the excitation and natural frequencies. For the case of Fig.

10-3 with $\omega/\omega_n = 0.9$, we have $\left|\frac{1}{2}(\omega - \omega_n)\right| = 0.05\omega_n$. Therefore, the full period of the amplitude-modulating term is $2\pi/0.05\omega_n = 20T_n$; from Fig. 10-3, this period is the total interval between time $t = 0$ sec and the second subsequent minimum of the amplitude-modulating envelope. Furthermore, the beating terms are minimal in amplitude at every half-period of the amplitude-modulating term, in this case 0, $10T_n$, $20T_n$, ..., and the beating terms are maximal in amplitude at instants between the half-period instants, in this case $5T_n$, $15T_n$, $25T_n$,

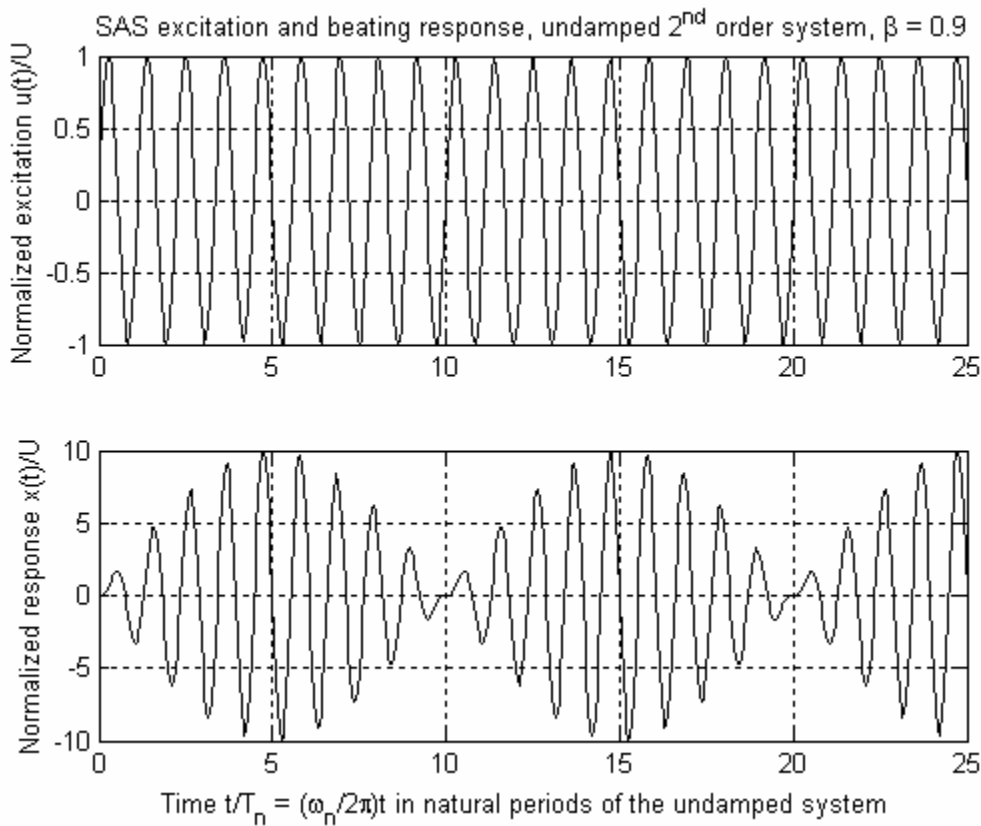


Figure 10-3 Upper graph: suddenly applied (at $t = 0$) sinusoidal (SAS) excitation with frequency $\omega = 0.9\omega_n$; lower graph: response from zero initial conditions of a standard undamped 2nd order system having natural frequency ω_n .

The apparent period of beating is the interval between successive minima or successive maxima of response, $10T_n$ in the case of Fig. 10.3, which is half the period of the amplitude-modulating term. Therefore, the apparent frequency of beating is $|\omega - \omega_n|$, which is twice the frequency of the amplitude-modulating term. Similarly, when we hear two musical tones of close but not identical pitches (frequencies), the frequency of beating that we perceive is the difference between the two tonal frequencies.

Let's consider now the remaining term, $(1 - \omega/\omega_n)\sin \omega_n t$, within the brackets of Eqs. (10-40) and (10-41). Pure undamped beating, in general, is the combination of two

sinusoids that have different but closely spaced frequencies, as the two sinusoids pass into and out of phase with each other. The beating of the undamped 2nd order system shown on Fig. 10-3 is the combination of two sinusoids in the term $\sin \omega t - \sin \omega_n t$ of Eq. (10-38). These two sinusoids represent (1) the driven response of the system at the excitation frequency ω , and (2) most of the free-vibration response of the system at its natural frequency ω_n . When these two sinusoids are in phase, they combine and, together with the smaller contribution of the term $(1 - \omega/\omega_n)\sin \omega_n t$, form the maximal response; when they are out of phase, they nullify each other completely, leaving only the small remaining part of the free-vibration response due to the term $(1 - \omega/\omega_n)\sin \omega_n t$.

Thus far, we have examined response to suddenly applied sinusoidal excitation of a physically unrealistic undamped 2nd order system. Let's consider next the influence of more realistic subcritical damping by solving for complete time response of an under-damped 2nd order system the ODE $\ddot{x} + 2\zeta\omega_n\dot{x} + \omega_n^2 x = \omega_n^2 u(t)$ with $u(t) = 0$ for $t < 0$ and $u(t) = U \sin \omega t$ for $t \geq 0$, and with rest ICs $x(0) = 0$ and $\dot{x}(0) = 0$. An appropriate convolution-integral solution is Eq. (9-20a):

$$x(t) = \frac{\omega_n^2}{\omega_d} \int_{\tau=0}^{t=t} e^{-\zeta\omega_n\tau} \sin \omega_d \tau \times u(t-\tau) d\tau = \frac{\omega_n^2}{\omega_d} \int_{\tau=0}^{t=t} e^{-\zeta\omega_n\tau} \sin \omega_d \tau \times U \sin \omega(t-\tau) d\tau$$

The damped frequency is $\omega_d \equiv \omega_n \sqrt{1 - \zeta^2}$, so we can express the response integral in dimensionless form as

$$\frac{x(t)}{U} = \frac{\omega_n}{\sqrt{1 - \zeta^2}} \int_{\tau=0}^{t=t} e^{-\zeta\omega_n\tau} \sin \omega_n \sqrt{1 - \zeta^2} \tau \times \sin \omega(t-\tau) d\tau \quad (10-42)$$

After evaluation of the formidable integral in Eq. (10-42), the solution is³

$$\frac{x(t)}{U} = \frac{e^{-\zeta\omega_n t} \beta \left[2\zeta \cos \omega_d t - \frac{(1 - \beta^2 - 2\zeta^2)}{\sqrt{1 - \zeta^2}} \sin \omega_d t \right] + (1 - \beta^2) \sin \omega t - 2\zeta\beta \cos \omega t}{(1 - \beta^2)^2 + (2\zeta\beta)^2} \quad (10-43)$$

The equation for response of an undamped 2nd order system that is most similar in algebraic form to Eq. (10-43) is Eq. (10-37), and you can easily show that for $\zeta = 0$ Eq. (10-43) reduces to Eq. (10-37). However, unlike Eq. (10-37), Eq. (10-43) apparently cannot be reconfigured into a form comparable to Eq. (10-40) that is amenable to physical interpretation relative to beating behavior. To learn the physical character of Eq. (10-43), it seems that the best we can do is to evaluate it computationally with relevant numerical parameters and then interpret the results. For computation of Eq. (10-43), with

³ The author derived Eq. (10-43) first with MATLAB by applying the `syms`, `int`, `simple`, and `pretty` symbolic operations, and then by implementing the human touch with pencil and paper to simplify further the MATLAB result. See homework Problems 1.6 and 1.9.

definitions of driving frequency ratio $\beta \equiv \omega/\omega_n$ and natural period $T_n \equiv 2\pi/\omega_n$, we can express the time-dependent function arguments of Eq. (10-43) in the following forms in terms of dimensionless time t/T_n : $-\zeta\omega_n t = -2\pi\zeta(t/T_n)$, $\omega_d t = 2\pi\sqrt{1-\zeta^2}(t/T_n)$, and $\omega t = 2\pi\beta(t/T_n)$. Figure 10-4 includes plots of SAS response calculated from Eq. (10-43) for zero damping and for light viscous damping ratios $\zeta = 0.01$ and 0.02 , with the excitation frequency set at 90% of the natural frequency, $\omega = 0.9\omega_n$ or $\beta = 0.9$, the same as for Fig. 10-3.

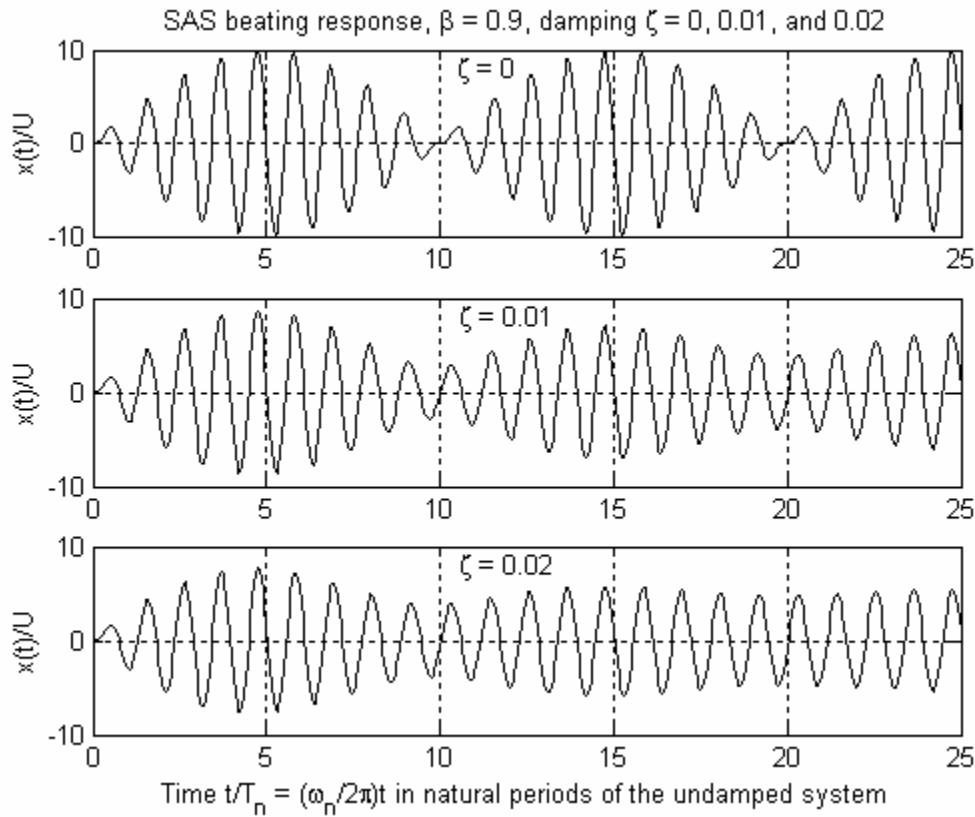


Figure 10-4 Calculations of Eq. (10-43) for a standard 2nd order system having undamped natural frequency ω_n , with zero damping (top) and two positive values of viscous damping ratio, $\zeta = 0.01$ and 0.02 ; response from rest initial conditions to a suddenly applied (at $t = 0$) sinusoidal (SAS) excitation with frequency $\omega = 0.9\omega_n$.

The response in Fig. 10-4 for $\zeta = 0$ is, of course, the same as that in Fig. 10-3, with very significant beating. However, the responses for $\zeta = 0.01$ and 0.02 show that even these relatively small quantities of damping suppress the beating, at least for this case of $\omega = 0.9\omega_n$. Although less obvious than for zero damping, the apparent period of beating for $\zeta = 0.01$, $\sim 10T_n$, is still quite evident. However, for $\zeta = 0.02$, the response in Fig. 10-4 after 25 natural periods has almost settled into its steady-state condition, for which you can calculate from Eq. (10-10) that the steady-state frequency-response magnitude ratio is $X/U = 5.171$. To investigate the nature of beating for any other case of damping ratio $\zeta > 0$ and excitation frequency ratio $\beta \equiv \omega/\omega_n$, we would need again to evaluate Eq. (10-43) numerically; see, for example, homework Problem 10.17.

10-7 Homework problems for Chapter 10

Problems 10.1–10.4 are frequency response problems (inspired by Myklestad, 1944) about standard 2nd order mass-damper-spring systems. In each case, the mass is excited by sinusoidal force $f_x(t) = F \cos \omega t$, and it responds with steady-state sinusoidal displacement $x(t) = X \cos(\omega t + \phi)$, where excitation frequency in Hz is $f = \omega/2\pi$. Some partial answers are given to help you see if you are on the right track; you still must calculate these values as if the answers were not given. To derive maximum benefit from these problems, use the appropriate equations for calculations, but also figure out how the results are represented in the FRF magnitude and phase graphs, Figs. 10-1 and 10-2. Be sure to use the appropriate value for g , either 386.1 inch/sec² or 9.807 m/sec².

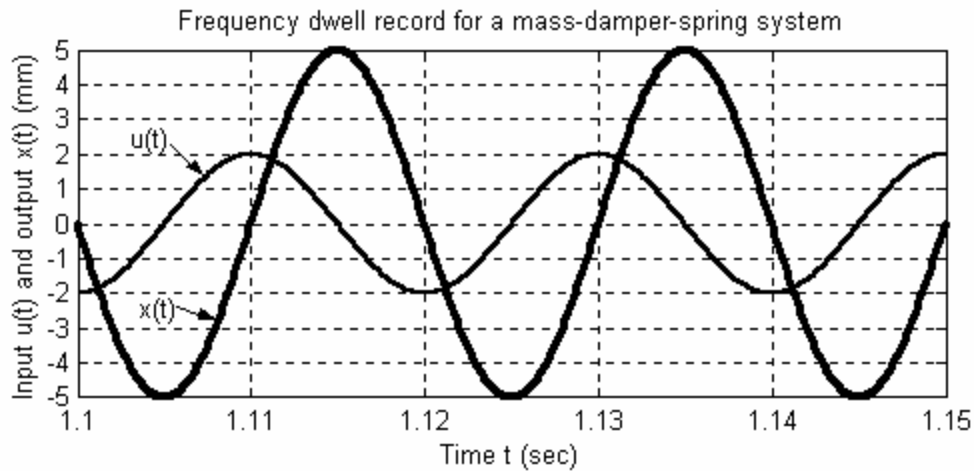
10.1 (Myklestad, 1944, p. 61) Suppose that damping is negligibly small. The measured weight of the mass is $W = 19.0$ lb, and the spring stiffness is $k = 13.0$ lb/inch. With $F = 5.00$ lb at a certain frequency of excitation, the response amplitude is $X = 0.750$ inch. Calculate the dimensionless dynamic amplification $X/(F/k)$. There are two different excitation frequencies, $f_1 < f_2$, that can produce this particular dynamic amplification; calculate both frequencies (in Hz), and the response phase ϕ (in degrees) at both frequencies. (*partial answers:* $\phi_1 = 0^\circ, f_2 = 3.18$ Hz)

10.2 Suppose that damping is negligibly small. The measured weight of the mass is $W = 8.50$ kg_f, and the spring stiffness is $k = 2.50$ kN/m. With $F = 5.00$ N at a certain frequency of excitation, the response amplitude is $X = 20.0$ mm. Calculate the dimensionless dynamic amplification $X/(F/k)$. There are two different excitation frequencies, $f_1 < f_2$, that can produce this particular dynamic amplification; calculate both frequencies (in Hz), and the response phase ϕ (in degrees) at both frequencies. (*partial answer:* $f_2 = 2.86$ Hz)

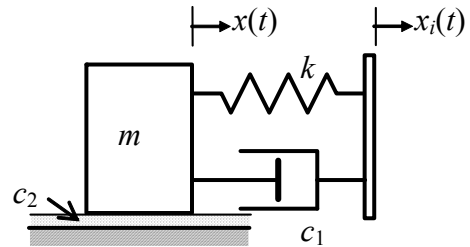
10.3 The mass weighs $W = 1.26$ kN, and the viscous damping and spring constants are, respectively, $c = 2,400$ N-sec/m and $k = 1.12$ MN/m. Calculate the undamped natural frequency f_n in Hz and the viscous damping ratio ζ . Suppose that the response amplitude is $X = 2.50$ mm when the phase $\phi = -90.0^\circ$; calculate the corresponding amplitude F of the excitation force. (*partial answer:* $F = 560$ N)

10.4 (Myklestad, 1944, p. 113) The mass weighs $W = 2.36$ lb, and the spring and viscous damping constants are, respectively, $k = 37.8$ lb/inch, and $c = 0.0169$ lb-sec/inch. The force amplitude is $F = 0.785$ lb. Calculate the critical damping constant c_c , the damping ratio ζ , the maximum possible amplitude of response X_r , and the amplitude X and phase ϕ (in degrees) for excitation at 13.0 Hz. (Note: to calculate ϕ correctly, you must account carefully for the quadrant of the fraction in the arctangent argument; if you just calculate the fraction and use the arctan function on your calculator, you will get the wrong answer; if you need some help, see the atan2 command in MATLAB). Is the small- ζ approximation appropriate for this system? (*partial answers:* $X_r = 0.591$ inch, $\phi = -155^\circ$)

10.5 A frequency response measurement is conducted on a standard 2nd order $m\text{-}c\text{-}k$ system with known stiffness constant k , so that the input pseudo-static displacement is calculated from the measured input force, $u(t) = f_x(t)/k$. A measured graph of the input and output displacements at one particular excitation frequency is shown below. Calculate from the graph, with as much accuracy as the data permits, the following quantities: the frequency (in Hz); the FRF magnitude ratio X/U ; the FRF phase ϕ (in degrees). What are the natural frequency f_n (in Hz) and the damping ratio ζ of this system?



10.6 The mechanical system of homework Problem 9.1 [with $f_x(t) = 0$] has *base excitation* input $x_i(t)$ and output $x(t)$. The ODE of motion is $m\ddot{x} + (c_1 + c_2)\dot{x} + kx = c_1\dot{x}_i + kx_i$, which includes right-hand-side (RHS) dynamics, where m is the mass, c_1 and c_2 are viscous damping constants, and k is the stiffness constant.



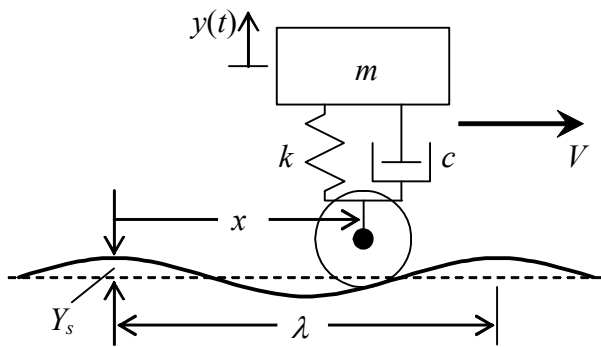
(a) Derive for this system the transfer function $TF(s) = L[x(t)]|_{ICs=0}/L[x_i(t)]$.

(b) Use the fundamental result $TF(j\omega) = FRF(\omega) = [X(\omega)/X_i]e^{j\phi(\omega)}$ and the result from part (a) to derive the relatively simple algebraic equation for real magnitude ratio $X(\omega)/X_i$. This equation should be in terms of physical parameters m , c_1 , c_2 , and k , and excitation frequency ω . [NOTE: You should implement complex division by the polar method described on pages 2-3 and 2-4; do not use the rectangular method, because it will produce an awful algebraic mess!] If you wish, you may derive the associated relatively simple algebraic/trigonometric equation for the real phase angle $\phi(\omega)$ (in radians), but that is not required.

(c) Let the system constants be $m = 128.5$ kg, $c_1 = 1,600$ N-sec/m, $c_2 = 800$ N-sec/m, and $k = 1.12$ MN/m. Calculate and plot the frequency response (magnitude ratio X/X_i , and phase ϕ in degrees) over the range of excitation frequencies 0-30 Hz. Use the over-under graphical format of Fig. 10-2, except plot both graphs on linear (not log) scales. As in the

script that produced Fig. 10-2, let MATLAB do most of the work for you by starting with the complex frequency response function $FRF(\omega)$ from part (b), then using MATLAB's capability for performing complex arithmetic with the `abs` and `angle` functions. If you need some help with the array multiplications required for this FRF, see the "`frf=...`" command lines in the script that produced Fig. 10-2. Submit your MATLAB script along with your FRF graphs.

10.7 The drawing represents a very simplified model of a land vehicle driving over a wavy (washboard) road with constant forward velocity V . The vehicle mass is m , and it is connected to the rolling wheel through the shock strut that has viscous damping constant c and stiffness constant k . The deviation of the road surface from flatness is denoted as $y_s(x) = Y_s \cos(2\pi x/\lambda)$, in which x is horizontal distance traveled from a reference position, Y_s is the amplitude (wave height at the crests), and λ is the wave length. We make the following assumptions for this model: the wheel itself is rigid, it rolls without slipping, and it maintains contact with the road at all times due to the weight of mass m ; also, wave height Y_s is small relative to wheel radius, so that, in effect, the contact point is always directly beneath the wheel axle, which means that y_s plays the role of *base excitation*, and essentially is a function of time: $y_s(x) = Y_s \cos \omega t$.



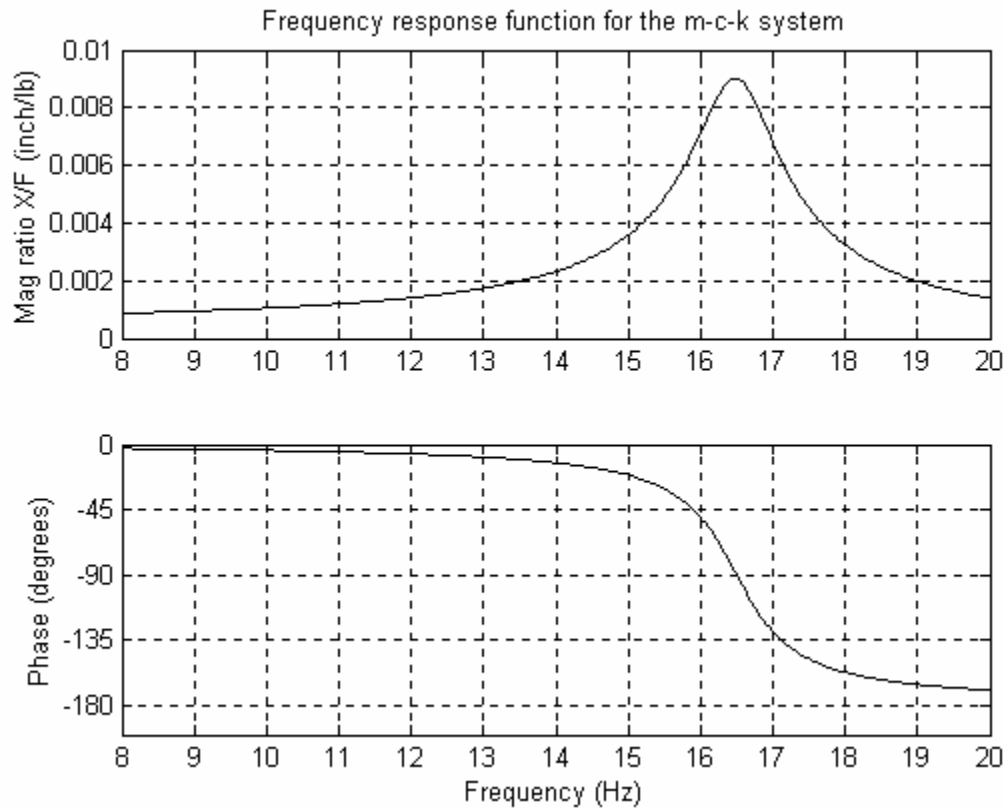
(a) Assume for the moment that $y_s(t)$ is arbitrary base excitation. Draw a dynamic free-body diagram of mass m , and derive from your DFBD the ODE of vertical dynamic motion $y(t)$, measured relative to the static equilibrium position for a flat road surface. First, write the ODE in terms of constants m , c , and k ; second, use the standard definitions from Eqs. (7-3) and (9-4) to write the ODE in terms of natural frequency ω_n and viscous damping ratio ζ .

(b) Use the second ODE of part (a) to derive the complex frequency response function for arbitrary input $y_s(t)$ and output $y(t)$ as $FRF(\omega) = \frac{1 + j2\zeta\beta}{(1 - \beta^2) + j2\zeta\beta} \equiv \frac{Y(\omega)}{Y_s} e^{j\phi(\omega)}$, in

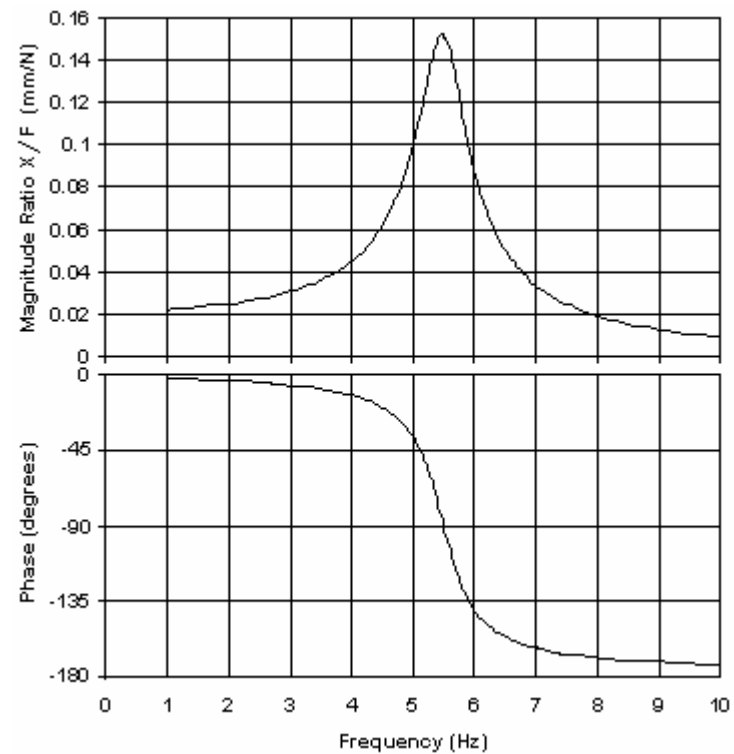
which $\beta \equiv \omega/\omega_n$. Even though this system has right-hand-side dynamics that influence response, let's consider the condition $\omega = \omega_n$. Derive equations for FRF magnitude ratio $Y(\omega_n)/Y_s$ and phase $\phi(\omega_n)$, in terms of ζ . (NOTE: To obtain the most manageable algebra, implement complex division by the polar method described on pages 2-3 and 2-4, not by the rectangular method.) If ζ is small, e.g., $\zeta = 0.05$, how close are your values of $Y(\omega_n)/Y_s$ and $\phi(\omega_n)$ to the values at $\omega = \omega_n$ that would prevail if there were no right-hand-side dynamics?

- (c) For the washboard road surface, we use the kinematic relation $x = Vt$ to express the base excitation as a sinusoidal function: $y_s(t) = Y_s \cos(2\pi Vt/\lambda) \equiv Y_s \cos \omega t$, in which $\omega \equiv 2\pi V/\lambda$. Write the algebraic equation, in terms of m , k , and λ , for the velocity V_n at which base excitation frequency equals the undamped natural frequency, $\omega = \omega_n$.

10.8 A particular device is known to be an LTI mass-damper-spring system. You (the engineer) are required to identify experimentally the mass m , the viscous damping constant c , and the stiffness constant k . First, you apply a static force of 162 lb, and you observe that the mass deflects statically by 0.108 inch. Next, you run a stepped-sine frequency-response test, applying sinusoidal force onto the mass, with the frequency increasing in small increments from 8 to 20 Hz. You measure at each frequency the steady-state input force magnitude F (in lbs), the output translation magnitude X (in inches) and the phase of translation relative to force. The frequency response is plotted below. Use this information to calculate m , c , and k in consistent units and with as much accuracy as the data permits. Show all calculations.



10.9 A particular device is known to be an LTI mass-damper-spring system, but the mass m , viscous damping constant c , and stiffness constant k are unknown. It is required that



the system parameters be identified experimentally with a combination of static and vibration testing. First, a static force of 52.0 N is applied, and the mass is measured to deflect statically by 1.13 mm. Next, sinusoidal force is applied to the mass by an electromagnetic shaker, with the frequency increased in small increments from 1 to 10 Hz. The steady-state input force magnitude F and output translation magnitude X are measured at each frequency, as is the phase ϕ of translation relative to force. The frequency-response translation-to-force magnitude ratio and phase are plotted at left. Use this information to calculate

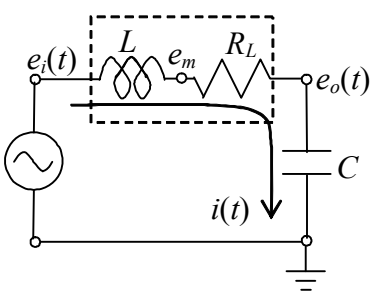
m , c , and k in consistent SI units and with as much accuracy as the data permits. Show all calculations.

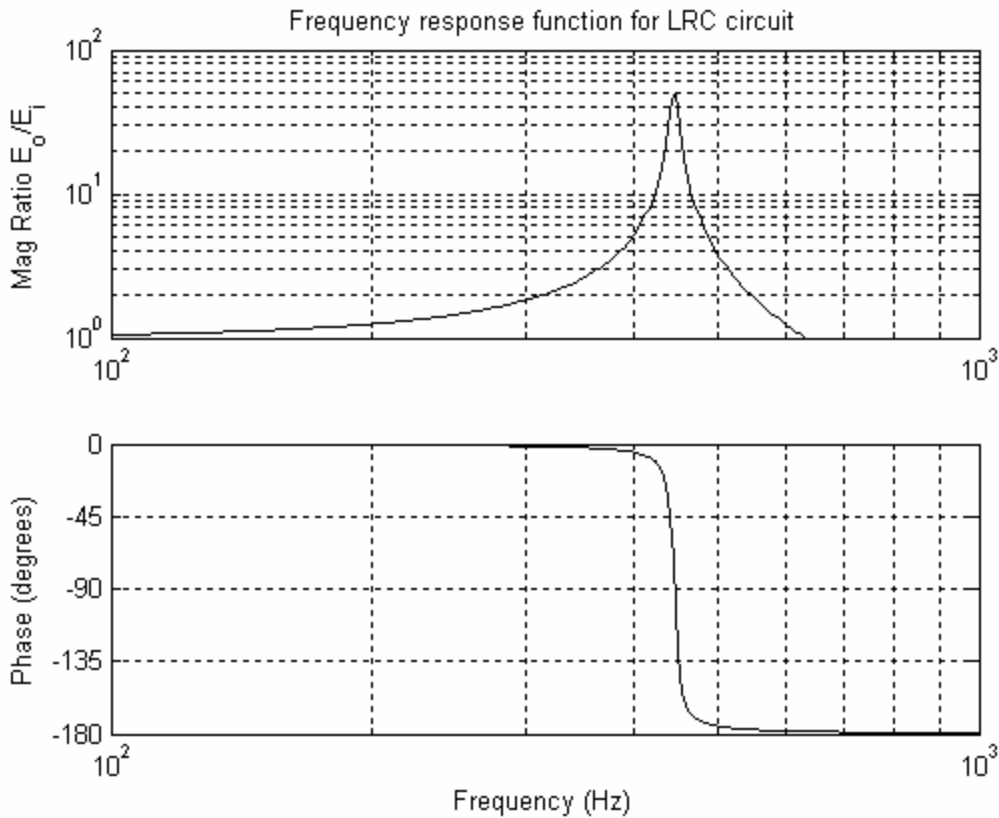
10.10 You, the engineer, are asked to determine experimentally the electrical constants (inductance L and resistance R_L) of a small coil, based upon the simple model of inductor and resistor in series, to see if these constants match the design specifications. You elect to infer these constants from a frequency response test on an LRC circuit driven by a sine-

wave voltage generator, with the coil connected in series to a calibrated capacitor with capacitance $C = 0.500 \mu\text{F}$. The circuit is shown in the drawing (from the example in Section 9-2), and its ODE in standard 2nd order form is

$$\ddot{e}_o + \frac{R}{L} \dot{e}_o + \frac{1}{LC} e_o = \frac{1}{LC} e_i(t).$$

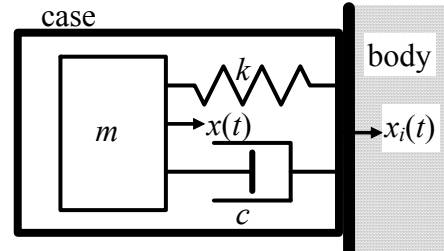
You run a stepped-sine frequency-response test, applying sinusoidal input voltage of constant magnitude $E_i = 1.00 \text{ V}$, with the frequency increasing in small increments from 100 to 1,000 Hz. You measure at each frequency the steady-state output voltage magnitude E_o , and the phase ϕ of output voltage relative to input voltage. The frequency response is plotted on the next page. Use this information to calculate L and R_L in consistent units and with as much accuracy as the data permits. Show all calculations.





10.11 Consider the *RC* band-pass filter described in Section 10-4, for which the frequency response function is $FRF(\omega) = TF(j\omega) = \frac{j\omega\tau_H}{(j\omega\tau_H + 1)(j\omega\tau_L + 1)}$. The purpose of this problem is to demonstrate the practical function for which that filter is designed, by means of FRF graphs. Let $\tau_H = \frac{1}{2\pi \times 10}$ sec and $\tau_L = \frac{1}{2\pi \times 500}$ sec to make the high-pass and low-pass break frequencies be, respectively, 10 Hz and 500 Hz. Now, use MATLAB to calculate and plot the FRF magnitude ratio and phase (in degrees) over the frequency range 0.1 to 10,000 Hz. Use the graphical format described in homework Problem 4.3 (log-log for magnitude ratio, semilog for phase in degrees, magnitude ratio graph directly over phase graph). As in Problem 4.3, let MATLAB do most of the work for you by starting with the complex FRF representation, and then using MATLAB's capability for performing complex arithmetic. Recall, in particular, that the MATLAB function `abs` calculates the absolute value (magnitude) of a complex number, and the MATLAB function `angle` calculates the angle in radians of a complex number.

10.12 An idealized mechanical model for motion sensors of the *seismic* type is shown in the figure. Such a sensor is entirely mounted on a moving body (is said to be “structure-borne”), unlike, for example, the proximity displacement sensor shown in Figs. 7-6 and 7-10. The mechanical part of the



sensor is a mass-damper-spring system sealed within a sturdy case, which is attached firmly to the body whose motion is sensed. The stimulus to the sensor is *base excitation*: translation $x_i(t)$ of the body and the case. The absolute translation of seismic mass m is $x(t)$. A transducer within the case detects the relative translation $z(t) \equiv x(t) - x_i(t)$ and generates an electrical signal⁴ proportional to $z(t)$, which typically is displayed and/or recorded by a data-acquisition-and-processing system, and may also serve as an input to a control system.

- (a) Sketch and label appropriate free-body diagrams, then use your FBDs to derive an ODE of motion for $z(t)$ [not $x(t)$] in terms of constants m , c , and k , and variable input quantity $x_i(t)$ or its derivatives. Convert your ODE into the standard form Eq. (10-4), except with $z(t)$ [not $x(t)$] as the dependent variable: $\ddot{z} + 2\zeta\omega_n\dot{z} + \omega_n^2 z = \omega_n^2 u(t)$. Write an explicit equation for standard input quantity $u(t)$ in terms of the appropriate constants and $x_i(t)$ or its derivatives.
- (b) Evaluate the use of this seismic sensor as a translational *accelerometer*, a sensor of the body's acceleration in the direction defined by $x(t)$ and $x_i(t)$. First, use the results of part (a) to show that the pseudo-static response is $z_{ps}(t) = -(m/k)\ddot{x}_i(t)$. This means that if the quantity $\ddot{z} + 2\zeta\omega_n\dot{z}$ is small (or zero) in comparison with $\omega_n^2 z$, then the seismic sensor acts as an accelerometer, since then $z(t)$ and its corresponding electrical signal are directly proportional to $\ddot{x}_i(t)$.⁵ This pseudo-static response is reflected clearly in the FRF graphs of Fig. 10-2: If the frequencies of motion within base excitation $x_i(t)$ are substantially below the natural frequency of the sensor ($\beta \equiv \omega/\omega_n = 1$), then both the magnitude and phase of response follow closely those of excitation. *An accelerometer is a seismic sensor intended to measure frequencies that are considerably lower than the sensor's own natural frequency.* Suppose you are designing an accelerometer that will measure with reasonable engineering accuracy body accelerations whose frequencies are no higher than 25% of the sensor's natural frequency. What is the highest value of damping ratio ζ (to three significant digits) that your sensor can have in order that phase error will be less than 5°, and what is the maximum magnitude error for that ζ ? Use Fig. 10-2 to find an estimate, then make trial-and-error iterative calculations (preferably with MATLAB) to determine more precisely the required ζ and magnitude ratio.
- (c) Evaluate the use of this seismic sensor as a translational *seismometer*, a sensor of the body's translation $x_i(t)$. Now, due to the right-hand-side second derivative \ddot{x}_i , your first ODE from part (a) is not in the standard form Eq. (10-4), so it is necessary to derive new response equations. The appropriate transfer function is defined as $TF(s) = L[z(t)]|_{ICs=0} \div L[x_i(t)]|_{ICs=0}$. Derive this $TF(s)$, then use it to derive the corresponding FRF:

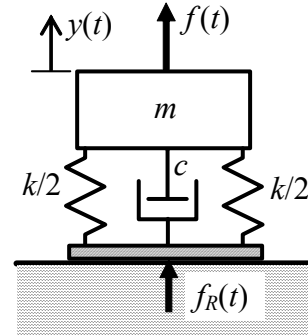
⁴ For most commercially available sensors, the electrical signal passes through wires connected to the sensor, but some modern sensors send the signal wirelessly. The size of such a sensor ranges typically from that of an aspirin tablet to that of a large soda bottle.

⁵ Although the theoretical constant of proportionality is $-m/k$, the true constant, including polarity, of any real sensor is always measured by laboratory calibration.

$$FRF(\omega) \equiv \frac{Z(\omega)}{X_i} e^{j\phi(\omega)} = \frac{\beta^2}{(1-\beta^2) + j2\zeta\beta}, \text{ with } \beta = \frac{\omega}{\omega_n} = \frac{\omega}{\sqrt{k/m}}, \text{ and } \zeta = \frac{c}{2m\omega_n}$$

Suppose that a seismometer has damping ratio $\zeta = 0.22$, high enough to dampen resonant response quickly. Plot over the range $0.1 \leq \beta \leq 10$ the frequency response magnitude ratio $Z(\omega)/X_i$ and, separately, phase angle $\phi(\omega)$ in degrees. (If necessary, see for guidance the description of producing Fig. 10-2 with MATLAB.) From these graphs, and if you wish from low- and high-frequency asymptotes of $Z(\omega)/X_i$, you should recognize that: *A translational seismometer is a seismic sensor intended to measure frequencies that are considerably higher than the sensor's own natural frequency.* Suppose this seismometer is intended to measure with reasonable engineering accuracy body translations whose frequencies are no lower than five (5) times that of the sensor's natural frequency. Calculate the greatest values of sensor error, percent of magnitude ratio and degrees of phase angle?⁶ Describe physically the motion of the seismic mass in response to base-motion frequencies that are considerably higher than the seismometer's natural frequency.

10.13 The drawing at right is the prototypical idealized model for the subject of *vibration isolation*. Suppose that mass m in the drawing houses a reciprocating internal combustion engine with a single vertically oriented piston-cylinder pair, and that the damper-spring-base assembly attaches the mass to the floor. The engine exerts an oscillatory vertical force $f(t)$ on mass m , and the mass-damper-spring system transmits force through the rigid base to the stiff floor, which reacts the transmitted force with oscillatory vertical force $f_R(t)$.⁷ For the benefit of the floor and its superstructure (building, vehicle, *etc.*) and for the comfort of the occupants, it is usually desirable to design the damper-spring support so that $f_R(t)$ is as small as practical, in other words, to isolate the engine from the floor. In practice, the damper-spring support often is an elastomeric (rubber-like) padding.



(a) Use a dynamic free-body diagram (DFBD), if necessary, to write the ODE of dynamic motion $y(t)$ relative to the static equilibrium position, in terms of excitation force $f(t)$ and constants m , c , and k . Take the Laplace transform of the ODE (assuming zero ICs) to obtain an equation for transform $L[y(t)] \equiv Y(s)$, which equation will include as the input quantity transform $L[f(t)] \equiv F(s)$. Next, write an equation for dynamic reaction force $f_R(t)$ in terms of $y(t)$ and its derivative and the appropriate constants, then take its Laplace transform to find an equation for transform $L[f_R(t)] \equiv F_R(s)$. Next, combine the two transform equations appropriately to find the transfer function $TF(s) = F_R(s)/F(s)$ relating the floor-reaction dynamic force to the excitation force. Finally, use the standard definitions

⁶ For the phase-angle error, regard a 180° phase difference as being equivalent to 0° , because it is simply a sign difference that is corrected in calibration and/or data processing.

⁷ The floor's true reaction is distributed force, *i.e.* stress, acting against the base over the area of contact. Discrete force $f_R(t)$ in the drawing is the equivalent *resultant* of the distributed force, that is, $f_R(t)$ has the magnitude of the total force distribution and its point of application is the center of the distribution.

of ω_n , ζ , and β to show that the corresponding complex frequency-response function, known as *transmissibility*, is $TF(j\omega) \equiv FRF(\omega) \equiv \frac{F_R(\omega)}{F} e^{j\phi(\omega)} = -\frac{1 + j2\zeta\beta}{(1 - \beta^2) + j2\zeta\beta}$.⁸

(b) Plot on a single graph the transmissibility magnitude ratio $F_R(\omega)/F$ for the cases of zero damping, $\zeta = 0$, and the relatively high damping ratio $\zeta = 0.25$; plot these curves on linear (not logarithmic) scales over the frequency ratios $0 \leq \beta \leq 4$, and display the magnitude ratio only over the range $0 \leq F_R(\omega)/F \leq 2.5$. (If necessary, see for guidance the description of producing Fig. 10-2 with MATLAB.) Explain how your graph shows (don't bother with any theory) that there is effective vibration isolation only if $\beta > \sqrt{2}$. Suppose that you know mass m and excitation frequency ω ; what is the range of spring constant k for which there is effective vibration isolation? Physically, should the springs be stiff or soft, and how stiff or soft? Does positive damping either increase or decrease the effectiveness of vibration isolation at all excitation frequencies, or is damping a mixed blessing, helpful in some range of frequencies, but not so much in others?

10.14 The translational velocity $v(t)$ of a point on an object is sometimes measured with use of a structure-borne accelerometer (see homework Problem 10.12). An accelerometer is a transducer that senses translational acceleration in one direction, e.g. $a(t) = \ddot{x}(t)$, and converts the motion into an electrical voltage signal, $e_a(t)$, which can be displayed, or recorded, or processed, or used in a control system. The transducer's output signal is nominally $e_a(t) = C_{ea} a(t) + n(t) + \varepsilon$: C_{ea} is the sensor's calibration factor, with units such as volts per meter/sec; $n(t)$ is small, randomly varying electrical "noise"; and ε is a small, constant offset voltage. Error voltage $n(t) + \varepsilon$ is unrelated to the sensed motion; it is an unwanted but practically unavoidable by-product of a transducer's circuitry. Acceleration is the rate of change of velocity, $\dot{v}(t) = a(t)$, so the accelerometer's output signal must be integrated to produce an electrical signal $e_v(t)$ that is proportional to velocity. Thus, the basic ODE that an exact integrator (in analog circuitry or a digital algorithm) would solve is $\dot{e}_v(t) = (1/T) e_a(t)$, where T is a physical constant having dimensions of time (e.g., $T = -RC$ for the op-amp-circuit integrator of homework Problem 5.6). However, in practice exact integration of an accelerometer's signal is not desirable due to constant error ε , because $\int e_a(t) dt = \int [C_{ea} a(t) + n(t) + \varepsilon] dt = \int C_{ea} a(t) dt + \int n(t) dt + \varepsilon t$. The term $\int n(t) dt$ typically is negligible because random $n(t)$ has average value of zero. On the other hand, the error term εt is artificial drift that grows with time and distorts the exact integrator's output signal, regardless of how small ε is. Therefore, it is necessary to use approximate integration that is not vulnerable to artificial drift but is still sufficiently accurate for practical purposes. Perhaps the simplest approximate integrator, which we name the low-pass approximate integrator, is defined by the 1st order ODE $\dot{e}_v + \Omega e_v = (1/T) e_a(t)$; the static response to non-zero constant e_a is clearly non-zero, $e_v = e_a / (\Omega T)$. This non-zero static response makes the low-pass approximate integrator unsuitable for

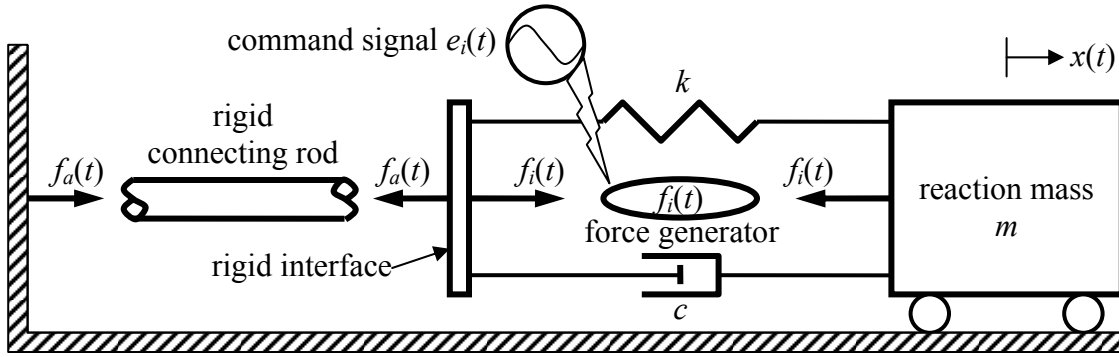
⁸ This FRF applies for a vibration isolator with viscous damping. However, the *internal-friction* mathematical model of structural damping is more realistic than viscous damping. In Appendix B, Section B-5, the internal-friction model is described and applied for vibration isolation.

applications that require the device's output to have zero offset voltage. To avoid such an artificial constant static response, we have the band-pass approximate integrator defined by the 2nd order ODE $\ddot{e}_v + \Omega \dot{e}_v + \Omega^2 e_v = (1/T) \dot{e}_a(t)$, which has right-hand-side dynamics.

(a) Using the definition of dimensionless excitation frequency $\beta \equiv \omega/\Omega$, derive and show that the complex frequency-response functions of the exact integrator, the low-pass approximate integrator, and the band-pass approximate integrator can be written in the forms, respectively, $[\Omega T \times FRF(\omega)]_{\text{exact}} = 1/(j\beta)$, and $[\Omega T \times FRF(\omega)]_{\text{low-pass}} = 1/(1 + j\beta)$, and $[\Omega T \times FRF(\omega)]_{\text{band-pass}} = j\beta/(1 - \beta^2 + j\beta)$.

(b) Plot on one graph the magnitudes versus β (at least over the range $0.1 \leq \beta \leq 10$) of $[\Omega T \times FRF(\omega)]_{\text{exact}}$, and $[\Omega T \times FRF(\omega)]_{\text{low-pass}}$, and $[\Omega T \times FRF(\omega)]_{\text{band-pass}}$. Plot on another graph the phases versus β (over the same range) of these three frequency-response functions. Your graphs should clearly display features noted earlier such as the static responses of the low-pass and band-pass approximate integrators, and they should show that for $\beta \equiv \omega/\Omega > 6$ both approximate integrators have negligible magnitude error, relative to the exact integrator, and phase error less than 10° .

10.15 Consider the *reaction-mass actuator* (RMA) drawn schematically below, which includes an $m-c-k$ system that is augmented with an internal force generator, $f_i(t)$. An external dynamic voltage signal $e_i(t)$ commands the force generator to impose equal and opposite dynamic forces $f_i(t)$ upon reaction mass m and the rigid interface, forces $f_i(t)$ that are proportional to input $e_i(t)$. The intended function of the RMA is to “react” against m in order to impose a dynamic force $f_a(t)$ through the connecting rod onto the rigid wall drawn at left. However, due to the dynamics of the $m-c-k$ system, the actuation force $f_a(t)$ actually transmitted through the connecting rod is different than internal force $f_i(t)$.



Reaction-Mass Actuator (RMA) in a calibration setup

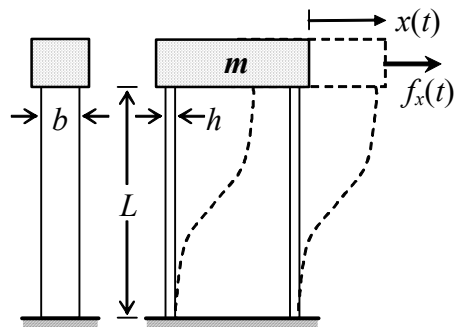
Your tasks in this problem are to derive the mathematical relationship between the output actuation force $f_a(t)$ and the input voltage signal $e_i(t)$, and then to calculate and plot frequency response that illustrates the character of RMA functioning.

(a) Derive the very simple ODE relating translation $x(t)$ of reaction mass m to the actuation force $f_a(t)$ shown acting onto the rigid interface. (The masses of the internal components—spring, damper, and force generator—are negligible relative to m .) Then derive from that ODE the transfer function $F_a(s)/X(s)$, where $F_a(s)$ and $X(s)$ are the Laplace transforms, respectively, of $f_a(t)$ and $x(t)$.

- (b) The linear relationship between generated internal force $f_i(t)$ and input voltage signal $e_i(t)$ is $f_i(t) = G e_i(t)$, where gain (calibration) constant G has units such as newtons/volt. Derive the ODE relating the translation $x(t)$ of reaction mass m to the internal force $f_i(t)$ shown acting onto m , and then to input signal $e_i(t)$. Then derive from that ODE the transfer function $X(s)/E_i(s)$, where $E_i(s)$ is the Laplace transform of $e_i(t)$.
- (c) Multiply the transfer functions of parts (a) and (b) in order to show that the required transfer function relating the output actuation force $f_a(t)$ to the input voltage signal $e_i(t)$ is $F_a(s)/E_i(s) = G s^2 / (s^2 + 2\zeta\omega_n s + \omega_n^2)$, where, as usual, $\omega_n^2 = k/m$ and $\zeta = c/(2m\omega_n)$.
- (d) During the 1990s, a team of aerospace companies designed a specialized RMA and fabricated several units of the device for use as vibration-control actuators in experiments on a test bed that simulated a space-satellite laser-beam-director structure [Dettmer, 1995, which uses another common name, *proof-mass actuator* (PMA) for the device].⁹ Imagine that these RMAs are restored for a new project and that you, as an instrumentation engineer, are assigned to perform system identification and calibration tests on one of them. First, you run free-vibration tests with the force generator turned off, $f_i(t) = 0$. You excite vibration by displacing reaction mass m from $x = 0$, then releasing it (twang testing, see homework Problem 9.4). You measure the frequency of the resulting free vibration of m to be 5.00 Hz, with very light inherent damping that reduces the amplitude of vibration in half in exactly 9 full cycles [in Eq. (9-28), $r_{1/2} = 9.00$]. The RMA has a flange allowing you to bolt a calibrated mass of 3.00 kg firmly to reaction mass m ; so you run a second twang test, from which you measure the frequency of free vibration of reaction mass plus added mass, $m + 3.00$ kg, to be 4.23 Hz (see homework Problem 7.9). Next, you remove the 3.00-kg added mass and turn on the force actuator. In static testing, you measure a linear relationship between applied voltage e_i and translation x , with maximum voltage $e_i = +10.0$ V moving m the distance $x = -6.00$ mm (and, conversely, -10.0 V producing $+6.00$ mm). Use your measured data to infer values for the components m , c , k , and G of the RMA system (*Partial answer:* $G = 4.47$ N/V). Finally, calculate the frequency-response function corresponding to transfer function $F_a(s)/E_i(s)$ of part (c), and plot it in the format of Fig. 10-2 [log(magnitude ratio) vs. log(frequency in Hz), linear(phase in degrees) vs. log(frequency in Hz)] over the excitation-frequency range 1-100 Hz. These graphs should indicate that the RMA produces output actuation force $f_a(t)$ nicely representative of input voltage signal $e_i(t)$ for frequencies above about twice the RMA's natural frequency, but that $f_a(t)$ is not at all representative of $e_i(t)$ for frequencies near and below the RMA's natural frequency.

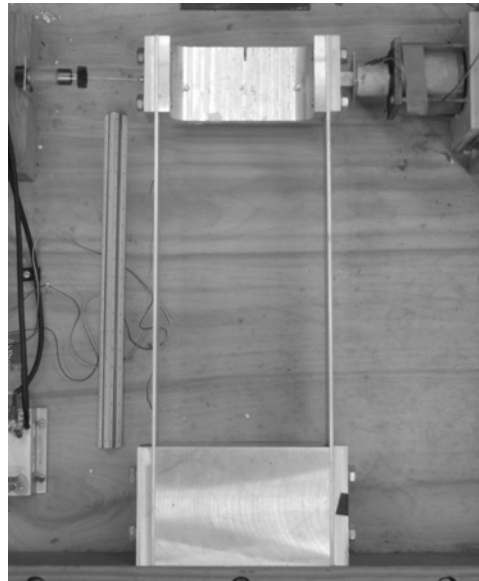
⁹ The schematic drawing for this problem shows the connecting rod attached to a rigid wall, which is a configuration suitable for calibrating an RMA; however, in any end-user practical application, the connecting rod would be attached to a flexible structure. RMAs are applied in practice to impose dynamic forces upon structures, both to provide excitation for vibration testing, and to suppress unwanted vibration as actuators in control systems. An RMA can be structure-borne, meaning it can be completely supported by the structure onto which it imposes dynamic force. For example, large RMAs have been installed in the top floors of tall buildings in order to reduce bending vibration excited by wind and ground tremors; an RMA in this civil engineering application is often called an *active tuned-mass damper* (ATMD). The internal force generators of ATMDs are hydraulic motors, whereas those of small RMAs (having total weight on or under the order of 100 lb) are electromagnetic linear motors.

10.16 A distributed-parameter *shear-building* structural model used in an instructional laboratory is shown in the drawing and the photograph, and is described in detail in



Side view Front view

homework Problem 7.10. Measurements by students give the effective vibrating mass as $m_E = 0.00473 \text{ lb}\cdot\text{sec}^2/\text{inch}$, and the lateral stiffness due to the two $L = 12$ -inch aluminum beams as $k_E = 43.6 \text{ lb/inch}$. The inherent structural and aero-acoustic damping of the vibrating beams and mass is very, very small, but a supplementary dashpot (near top left in the photo) attached between the mass and ground increases the total measured effective viscous damping constant to $c_E = 0.0309 \text{ lb}\cdot\text{sec/inch}$.



(a) Calculate the undamped natural frequency f_n in Hz and the damping ratio ζ . (Answers: $f_n = 15.3 \text{ Hz}$, $\zeta = 0.0340$)

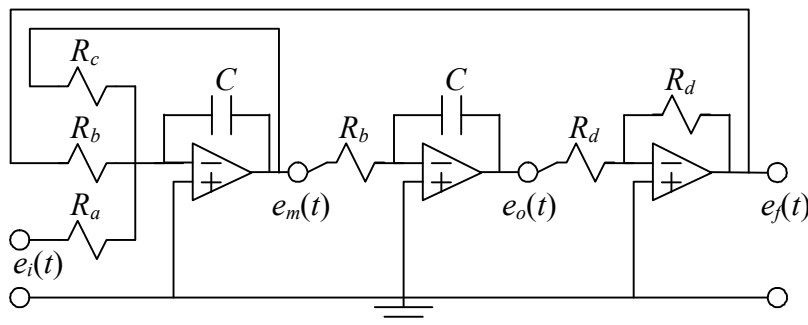
(b) A small electromagnetic shaker¹⁰ is attached to the right-hand side of the mass, and it produces the time-varying force $f_x(t)$ labeled on the drawing. Any real force actuator has a maximum *stroke*, the range of motion of the device's moving parts, over which: (i) the output force $f_x(t)$ is proportional to the input electrical command signal, and/or (ii) the moving parts of the device can deflect without damaging themselves or other parts within the device. It is important to recognize that the moving parts of the shaker are attached directly to the structure, so they experience the same deflection as the attachment point on the structure. Hence, the structural vibration can actually cause the maximum shaker stroke to be exceeded, especially at or near resonance. Suppose you want to run an experiment to measure an FRF of the shear-building model, in a stepped-sine sweep of excitation frequency f in Hz from $0.5 f_n$ to $1.5 f_n$. The shaker will drive the mass with sinusoidal force $f_x(t) = F \cos(2\pi f t)$, and the mass will respond with steady-state sinusoidal translation $x(t) = X \cos(2\pi f t + \phi)$. Suppose the shaker in this case has the maximum

¹⁰ This device is similar to the driver of a speaker in a sound system. The primary components are a wire voice coil and a magnetic field structure, within which is a small but strong permanent magnet. The wire coil is wrapped around and bonded to a spool, which is attached directly to the mass. The coil is embedded within a magnetic field that acts across an annular gap in the front of the field structure. Electrical current driven through the coil by a power amplifier interacts with the magnetic field to produce a force onto the coil and spool that is proportional to the current. The force is transmitted to the mass through the spool.

stroke of ± 0.05 inch and maximum force magnitude $F_{\max} = 2$ lb (typical values for a small commercial off-the-shelf shaker). If you were to run the stepped-sine sweep so as to measure directly the *mechanical admittance* (also known as *dynamic flexibility*) by holding the force magnitude constant at 80% of its capability, $F = 0.8F_{\max}$, what are the theoretically predicted magnitudes X of structural (and shaker moving parts) translation at the frequencies $0.5f_n$, f_n , and $1.5f_n$? (*Partial answer:* $X(f_n) = 0.539$ inch) Why would this dynamic-flexibility approach not work in real life?

- (c) Suppose you run a stepped-sine sweep, with the same shaker properties as defined in part (b), in such a way as to measure directly the *dynamic stiffness*, instead of the dynamic flexibility. For example, imagine that at each discrete excitation frequency in the sweep you adjust the shaker force magnitude so that the response magnitude equals 80%, $X = 0.04$ inch, of the maximum shaker stroke. Calculate the theoretically predicted magnitudes F of required shaker force at the excitation frequencies $f = 0$ (the static condition), $0.5f_n$, $1.0f_n$, and $1.5f_n$. (*Partial answer:* $F(f_n) = 0.119$ lb) For what (if any) range of excitation frequencies would this dynamic-stiffness approach work in real life?
- (d) Calculate and plot the theoretically predicted dynamic stiffness (magnitude and phase) of this structural system for excitation frequency over the range $0 \leq f \leq 1.5f_n$.

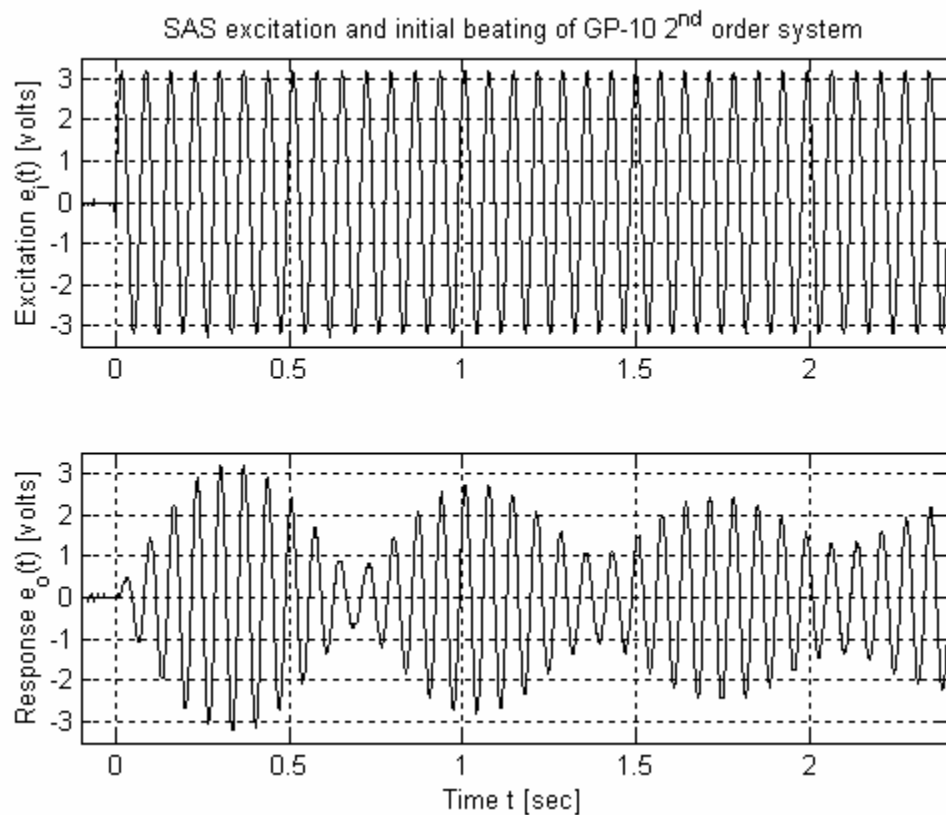
10.17 Evaluate Eq. (10-43) numerically (using MATLAB or your choice of software) to calculate and plot the time response from rest ICs to a suddenly applied sinusoidal (SAS) input into the electronic analog computer circuit at right. The ODE relating output voltage $e_o(t)$ to input voltage $e_i(t)$ derived in homework Problem 9.17, is,



in standard 2nd order form, $\ddot{e}_o + \frac{1}{R_c C} \dot{e}_o + \left(\frac{1}{R_b C} \right)^2 e_o = \left(\frac{1}{R_b C} \right)^2 \frac{R_b}{R_a} e_i(t)$. The input voltage is zero for time $t < 0$ and $e_i(t) = E_i \sin(2\pi f t)$ for $t \geq 0$, in which $E_i = 3.20$ V and $f = 14.2$ Hz.

The circuit component values are: $R_a = R_d = 50.0$ k Ω , $R_b = 5.00$ k Ω , $R_c = 500$ k Ω , and $C = 2.04$ μ F. Calculate and plot both excitation and response over the time interval $-0.1 \leq t \leq 2.4$ sec, at increments of 0.001 sec (to produce suitable graphical resolution). This circuit was “patched” (programmed with plug-in wires) on a Comdyna GP-10 analog computer, and the given input voltage was produced by a sine-wave generator; graphs of the actual measured time-varying input excitation and output response are on the next page. Do the numerically simulated excitation and response that you calculate look very similar to the measured excitation and response? (If not, they should!) Although the circuit is lightly damped, there is still clear beating behavior. Show that the period and frequency of beating evident in the time-response graph are what you would expect, based upon Eq. (10-40) for beating of an undamped 2nd order system.

Chapter 10 2nd order systems: frequency response; beating response to SAS excitation



Chapter 11 Mechanical systems with rigid-body plane translation and rotation

© 2016 by William L. Hallauer, Jr.

Up to this point, we have considered mechanical systems with motion consisting of either translation in only one direction or rotation about one axis, but not both together. Simple rotational systems have appeared in previous chapters (for example, in Sections 3-3, 3-5, and 7-1), but now we will treat rigid-body plane motion more generally, as consisting of both translation and rotation, and with the two forms of motion possibly coupled together by system components and system geometry. The focus in this chapter is on deriving correctly the equations of motion, which generally are higher-order, coupled sets of ODEs. Chapter 12 introduces some methods for solving such equations, leading to fundamental characteristics of an important class of higher-order systems.

11-1 Equations of motion for a rigid body in general plane motion

Consider a rigid body that is restricted to motion in the xy plane. Figure 11-1 shows the body in its reference static equilibrium position (solid lines) and in a position of motion (dashed lines) relative to the reference position. The xy axis system shown is an inertial reference with its origin at point O , which is either motionless or translating at a constant velocity. We will use vectors and vector operations, so we need to recognize that the inertial reference system is really the three-dimensional Cartesian xyz axis system, with the z axis being perpendicular to the xy plane and pointed toward us, in the sense of the right-hand rule. We denote the fixed unit vectors in the reference Cartesian directions as $\mathbf{1}_x$, $\mathbf{1}_y$, and $\mathbf{1}_z$. From the background of your previous dynamics and physics courses, you should be familiar with vectors, vector algebra and calculus, and vector

kinematics and dynamics; if necessary, you should review these concepts in your engineering dynamics textbook.

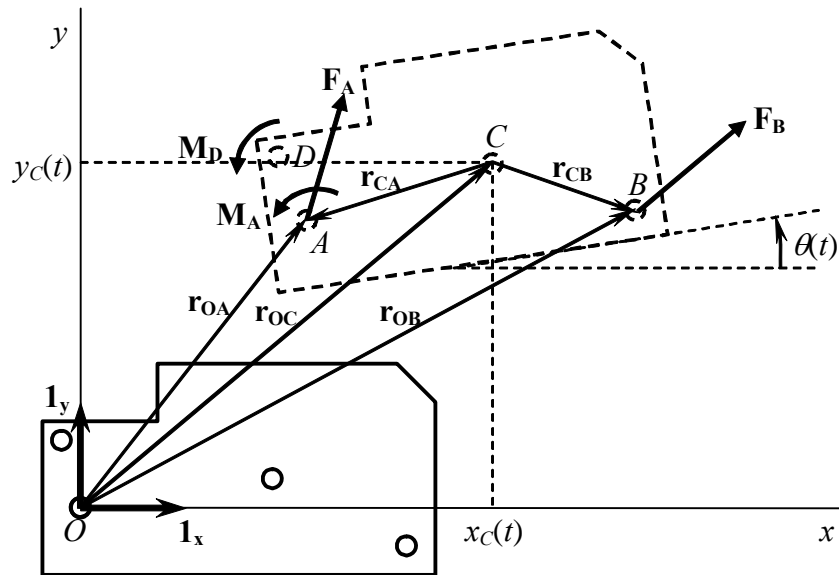


Figure 11-1 Rigid body in general plane motion

Of particular interest is the position and orientation of the rigid body's center of mass C . At any instant of time t , C has relative position coordinates $[x_C(t), y_C(t)]$. Thus, the vector position of C relative to some absolutely fixed

point P is $\mathbf{r}_C(t) = \mathbf{r}_O(t) + \mathbf{r}_{OC}(t) = \mathbf{r}_O(t) + x_C(t)\mathbf{1}_x + y_C(t)\mathbf{1}_y$, where $\mathbf{r}_O(t)$ is the known instantaneous position of O relative to P . Similarly, the vector velocity of C relative to absolutely fixed point P is $\mathbf{v}_C(t) = \mathbf{v}_O(t) + \mathbf{v}_{OC}(t) = \mathbf{v}_O(t) + \dot{x}_C(t)\mathbf{1}_x + \dot{y}_C(t)\mathbf{1}_y$, where $\mathbf{v}_O(t)$ is the constant velocity of O relative to P . Because $\mathbf{v}_O(t)$ is constant, the absolute vector acceleration of C is $\mathbf{a}_C(t) = \mathbf{a}_{OC}(t) = \ddot{x}_C(t)\mathbf{1}_x + \ddot{y}_C(t)\mathbf{1}_y$. We denote as $\theta(t)$ the positive-counterclockwise rotational orientation of mass center C (indeed, of the entire body, since it is rigid). Position $\mathbf{r}_O(t)$ of O is known, so if we can determine at any instant the three motion quantities $x_C(t)$, $y_C(t)$, and $\theta(t)$, then we can calculate from simple geometry the position of any point on the rigid body. These three quantities are independent in general plane motion, and only these three [plus known $\mathbf{r}_O(t)$] are required to describe completely the position in space of the rigid body. Therefore, $x_C(t)$, $y_C(t)$, and $\theta(t)$ are called *degrees of freedom*, and general plane rigid-body motion is called a *three-degrees-of-freedom (3-DOF) problem*.

For generality, we identify three other points fixed to the rigid body, at which point actions (forces or moments) are applied by sources external to the body. (In general, there can be more or fewer points of externally applied actions; analyzing such situations will require only minor modifications to the present derivation.) Point A is a connection to the external environment, possibly through springs, dampers, *etc.*; actions applied at Point A are vector reaction force $\mathbf{F}_A = F_{Ax}\mathbf{1}_x + F_{Ay}\mathbf{1}_y$ and vector reaction moment $\mathbf{M}_A = M_A\mathbf{1}_z$. It is useful to express the vector position of point A in terms of that of mass center C : $\mathbf{r}_{OA} = \mathbf{r}_{OC} + \mathbf{r}_{CA}$ (see Fig. 11-1). An arbitrary vector force $\mathbf{F}_B = F_{Bx}\mathbf{1}_x + F_{By}\mathbf{1}_y$ is applied at point B , and that point's vector position is expressed as $\mathbf{r}_{OB} = \mathbf{r}_{OC} + \mathbf{r}_{CB}$. Finally, an arbitrary vector moment $\mathbf{M}_D = M_D\mathbf{1}_z$ acts at point D .

We denote as m the mass of the rigid body. Newton's 2nd law for forces, written in vector form, is

$$m\mathbf{a}_C = \mathbf{F}_A + \mathbf{F}_B \quad (11-1)$$

Expressing Eq. (11-1) in terms of scalar components gives the two scalar ODEs:

$$m\ddot{x}_C = F_{Ax} + F_{Bx} \quad (11-2a)$$

$$m\ddot{y}_C = F_{Ay} + F_{By} \quad (11-2b)$$

We denote as J_C the rotational inertia of the rigid body about an axis normal to the plane of motion and passing through mass center C . Newton's 2nd law for moments relevant to this plane-motion case states that the inertial moment about mass center C equals the sum of all applied moments about mass center C ; it is expressed as follows in vector notation, including vector cross products:

$$J_C \ddot{\theta} \mathbf{1}_z = \mathbf{r}_{CA} \times \mathbf{F}_A + \mathbf{r}_{CB} \times \mathbf{F}_B + (M_A + M_D) \mathbf{1}_z \quad (11-3)$$

Despite the vector notation, Eq. (11-3) is actually a scalar equation, because the vector cross products obviously produce vectors in the z direction; the use of these cross products just provides economy of notation.¹

We shall see an application of general-plane-motion Eqs. (11-2) and (11-3) to a specific aeroelastic system in Section 11-3 (Example 11-3); but, first, it is appropriate to develop in Section 11-2 and to illustrate in Section 11-3 (Examples 11-1 and 11-2) the special case of pure plane rotational motion about a fixed point.

11-2 Equation of motion for a rigid body in pure plane rotation

An important special case of general plane motion is pure rotation about a fixed pivot or hinge, as depicted in Fig. 11-2. To analyze this case, let's suppose that reaction point A of Fig. 11-1 is the hinge point, and let's position the xyz origin O at point A . To emphasize the character of this hinge point, we re-label it as H ; in other words, both points A and O on Fig. 11-1 now become hinge point H on Fig. 11-2. We can use the

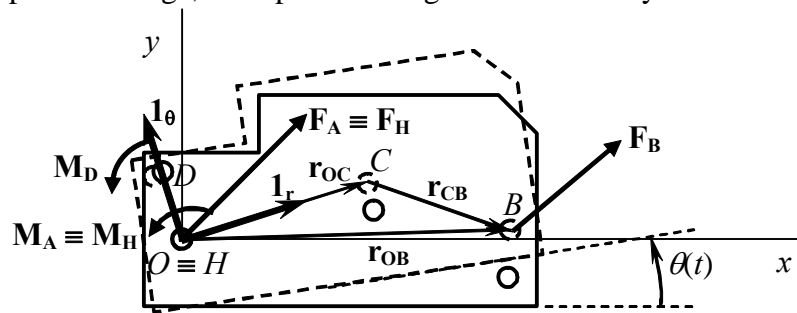


Figure 11-2 Rigid body in pure rotation about point O

previous equations simply by setting position vector \mathbf{r}_{OA} on Fig. 11-1 equal to zero: $\mathbf{r}_{OA} = \mathbf{0} = \mathbf{r}_{OC} + \mathbf{r}_{CA} \Rightarrow \mathbf{r}_{CA} = -\mathbf{r}_{OC} \equiv -\mathbf{r}_{HC}$. It is helpful also to express \mathbf{r}_{CB} on Fig. 11-1 in terms of \mathbf{r}_{OC} : $\mathbf{r}_{CB} = \mathbf{r}_{OB} - \mathbf{r}_{OC}$. Using these substitutions in Eq. (11-3) gives

$$J_C \ddot{\theta} \mathbf{1}_z = -\mathbf{r}_{OC} \times \mathbf{F}_A + (\mathbf{r}_{OB} - \mathbf{r}_{OC}) \times \mathbf{F}_B + (M_A + M_D) \mathbf{1}_z \quad (11-4a)$$

After we replace subscripts O and A with H and re-arrange terms, Eq. (11-4a) becomes

$$J_C \ddot{\theta} \mathbf{1}_z + \mathbf{r}_{HC} \times (\mathbf{F}_H + \mathbf{F}_B) = \mathbf{r}_{HB} \times \mathbf{F}_B + (M_H + M_D) \mathbf{1}_z \quad (11-4b)$$

Next, substituting Eq. (11-1) into Eq. (11-4b) gives

$$J_C \ddot{\theta} \mathbf{1}_z + \mathbf{r}_{HC} \times m \mathbf{a}_C = \mathbf{r}_{HB} \times \mathbf{F}_B + (M_H + M_D) \mathbf{1}_z \quad (11-5a)$$

¹ For Eqs. (11-2) and (11-3), the reference xyz axis system is inertial, either stationary in space or moving at a constant translational velocity, and motion of the rigid body is measured relative to this inertial system. However, for many problems in dynamics, it is preferable to derive equations of motion using a reference axis system that is fixed in the body and moves with it. A plane-motion problem of this type is the leading-lagging rotation of a hinged helicopter rotor blade, as analyzed by Bramwell, 1976, pp. 51-52.

Since hinge point H is fixed, let's simplify notation by writing $\mathbf{r}_{HC} \equiv \mathbf{r}_C$ and $\mathbf{r}_{HB} \equiv \mathbf{r}_B$. Also, we can express the acceleration as $\mathbf{a}_C \equiv \ddot{\mathbf{r}}_C$, so Eq. (11-5a) becomes

$$J_C \ddot{\theta} \mathbf{1}_z + \mathbf{r}_C \times m \ddot{\mathbf{r}}_C = \mathbf{r}_B \times \mathbf{F}_B + (M_H + M_D) \mathbf{1}_z \quad (11-5b)$$

We can simplify the $\ddot{\mathbf{r}}_C$ term on the left-hand side of Eq. (11-5b) by using the kinematics of rigid-body, plane, pure rotation about point H . For this task, it is convenient to work in polar rather than Cartesian coordinates, so we define on Fig. 11-2 the orthogonal rotating unit vectors $\mathbf{1}_r$ and $\mathbf{1}_\theta$; thus, we can express the position vector to mass center C as $\mathbf{r}_C = r_C \mathbf{1}_r$, where r_C is the constant radius from hinge point H to mass center C . We express the rotational velocity vector as $\boldsymbol{\omega} = \dot{\theta} \mathbf{1}_z$. (In this context, the vector symbol $\boldsymbol{\omega}$ denotes rotational velocity, which is standard in dynamics textbooks, whereas everywhere else in this book the scalar symbol ω denotes frequency of vibration.) Therefore, the first derivative of the mass-center position vector is

$$\dot{\mathbf{r}}_C = \boldsymbol{\omega} \times \mathbf{r}_C = \dot{\theta} \mathbf{1}_z \times r_C \mathbf{1}_r = r_C \dot{\theta} \mathbf{1}_\theta \quad (11-6)$$

To obtain the second derivative, we differentiate product (11-6), recognizing that r_C is constant, but that $\mathbf{1}_\theta$ is rotating:

$$\ddot{\mathbf{r}}_C = r_C [\ddot{\theta} \mathbf{1}_\theta + \dot{\theta} \dot{\mathbf{1}}_\theta] = r_C [\ddot{\theta} \mathbf{1}_\theta + \dot{\theta} (\dot{\theta} \mathbf{1}_z \times \mathbf{1}_\theta)] = r_C [\ddot{\theta} \mathbf{1}_\theta - \dot{\theta}^2 \mathbf{1}_r] \quad (11-7)$$

With Eq. (11-7), the vector cross product on the left-hand side of Eq. (11-5b) becomes

$$\mathbf{r}_C \times \ddot{\mathbf{r}}_C = r_C \mathbf{1}_r \times r_C [\ddot{\theta} \mathbf{1}_\theta - \dot{\theta}^2 \mathbf{1}_r] = r_C^2 \ddot{\theta} \mathbf{1}_z \quad (11-8)$$

With Eq. (11-8), the left-hand side of Eq. (11-5b) becomes

$$J_C \ddot{\theta} \mathbf{1}_z + \mathbf{r}_C \times m \ddot{\mathbf{r}}_C = (J_C + m r_C^2) \ddot{\theta} \mathbf{1}_z \equiv J_H \ddot{\theta} \mathbf{1}_z \quad (11-9)$$

In Eq. (11-9), we use the parallel-axis theorem to define the rotational inertia of the rigid body about center of rotation H , $J_H = J_C + m r_C^2$. Thus, Eq. (11-5b) becomes

$$J_H \ddot{\theta} \mathbf{1}_z = \mathbf{r}_B \times \mathbf{F}_B + (M_H + M_D) \mathbf{1}_z \equiv \Sigma(\text{all active and reactive moments about } H) \mathbf{1}_z \quad (11-10)$$

To summarize, for a rigid-body in pure plane rotation about point H , the only degree of freedom is rotation $\theta(t)$, and the single, relatively simple ODE of motion is

$$J_H \ddot{\theta} = \Sigma(\text{all active and reactive moments about } H) \quad (11-11)$$

in which J_H is the rotational inertia of the rigid body about center of rotation H .

Note that the reaction force at hinge H does not appear in ODE (11-11). In fact, to find this reaction force, you would have to solve (11-11) for $\theta(t)$, then find the acceleration of C , then substitute the results back into Eqs. (11-1) or (11-2).

11-3 Examples of equations of motion for rigid bodies in plane motion

Example 11-1: damped, spring-supported rigid bar, hinged at point H

Let's derive the specific ODE of motion for the system of Fig. 11-3, assuming small angles of rotation. The bar has rotational inertia J_H about hinge H , which we assume to have negligible friction. The bar is shown in the reference static equilibrium position, subject to static gravity but before applied dynamic force $F(t)$ becomes active. Dynamic degree of freedom $\theta(t)$ shown with dashed lines is the small rotation relative to the static equilibrium position. (It is this book's graphical convention for this and all subsequent systems of this type that the rigid body is drawn in its static equilibrium position, and dynamic motion relative to this reference position is indicated with dashed lines and annotation.) Note the rotation spring with spring constant k_θ at hinge H ; this spring resists rotation by generating an opposing moment of magnitude $k_\theta \times \dot{\theta}$. Typical units for k_θ are lb-inch/radian and N-m/radian.

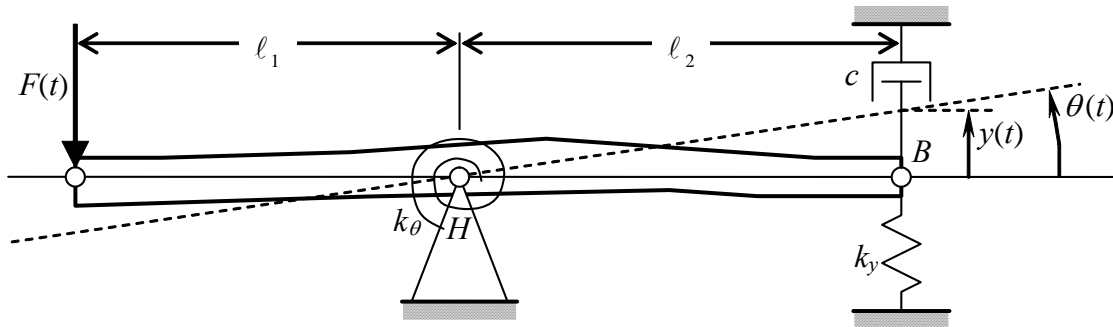


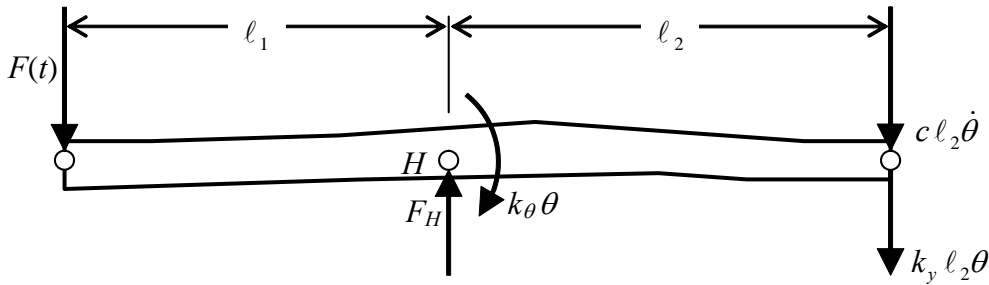
Figure 11-3 Example 11-1: damped, spring-supported, hinged rigid bar

Before drawing a dynamic free-body diagram (DFBD, as defined in Section 7-5), we need to express appropriately the reaction forces on the bar at point B from the translational spring ($k_y \times y$) and the translational viscous damper ($c \times \dot{y}$). Observe that point B moves in a circular arc of radius ℓ_2 , so that $y = \ell_2 \sin \theta$. For arbitrarily large θ , the term $\sin \theta$ and its time derivative would make equation of motion (11-11) nonlinear. However, the assumption of small rotation, $|\theta(t)| < \approx 10^\circ$, linearizes that ODE; the geometry of small rotation gives approximate linear equations in terms of θ for stretch y of the translational spring due to motion of point B , and for damper-piston velocity \dot{y} :

$$y = \ell_2 \sin \theta \approx \ell_2 \theta \quad (\theta \text{ in radians}), \quad \text{and} \quad \dot{y} = \ell_2 \cos \theta \times \dot{\theta} \approx \ell_2 \dot{\theta}$$

The geometry of small rotation was used previously in the example of Section 7-1 to linearize the pendulum equation of motion. For the system of Fig. 11-3, the assumption of small rotation is physically plausible as well as mathematically expedient, because the translational and rotational springs most likely would restrict rotation of the bar to small angles relative to the static equilibrium position.

The appropriate DFBD is drawn below. Note that we do not include bar weight among the applied forces. We omit bar weight because we are interested only in dynamic



motion relative to the static equilibrium position, and because this bar is approximately horizontal so that gravity has no pendulous effect on it; if you are not sure why we neglect weight in this case, then review Section 7-5.

From the DFBD and Eq. (11-11), the ordinary differential equation of motion is

$$J_H \ddot{\theta} = \ell_1 F(t) - k_\theta \theta - \ell_2 (c \ell_2 \dot{\theta} + k_y \ell_2 \theta)$$

$$\Rightarrow J_H \ddot{\theta} + c \ell_2^2 \dot{\theta} + (k_\theta + k_y \ell_2^2) \theta = \ell_1 F(t) \quad (11-12)$$

Equation (11-12) can be put into the standard form for a 2nd order damped system, and all of the relevant results of Chapters 9 and 10 can be expressed in terms of the physical parameters of this particular mechanical system. For example, we can immediately find equations for the system undamped natural frequency and viscous damping ratio:

$$\omega_n = \sqrt{\frac{k_\theta + k_y \ell_2^2}{J_H}}, \quad 2\zeta\omega_n = \frac{c \ell_2^2}{J_H} \Rightarrow \zeta = \frac{1}{2} \frac{c \ell_2^2}{\sqrt{J_H (k_\theta + k_y \ell_2^2)}} \quad (11-13)$$

NOTE: It is easy to make mistakes in algebra when we derive results such as (11-13). One good, easy type of partial check that you can use is to evaluate the physical dimensions of algebraic results. (It is only a partial check because dimensional consistency is a necessary condition, but it does not guarantee the correctness of an algebraic equation.) Do Eqs. (11-13) have the correct physical dimensions? You should be able to show that the equation for ω_n has the dimension (time)⁻¹ and that the equation for ζ is dimensionless. Don't forget that rotation θ is dimensionless and that the radian, the natural metric of rotation, is unitless. If you are more comfortable working with units than dimensions, it's satisfactory to check units instead. Table 3-1 should be helpful relative to mechanical units.

Example 11-2: 1-DOF typical-section model for study of aeroelastic wing twist

Since the beginning of modern aeronautical engineering in the late 1800s and early 1900s, the interaction of aerodynamic pressure with airplane structural flexibility has often produced unexpected and sometimes disastrous consequences. The subject of these phenomena became known as *aeroelasticity*. During and after World War I, high-aspect-ratio, cantilevered monoplane wings tended to be susceptible both to aeroelastic *flutter*, undamped vibration that can escalate to destruction of wing and airplane, and to aeroelastic *divergence*, the gradual twisting-off of a wing in, for example, pull-up from a dive.² In their attempts to analyze these aeroelastic phenomena, early aeronautical engineers used simplified, low-degrees-of-freedom dynamic models of wing structures. The basis of these models is called a *typical section*: one “typical” cross-section of a high-aspect-ratio, straight, unswept wing is treated aerodynamically as an airfoil in two-dimensional flow (without spanwise flow), and structurally as a spring-supported rigid body (without spanwise beam bending and twisting).

The simplest typical-section model is the one-degree-of-freedom (1-DOF) system drawn in Fig. 11-4. It is helpful to visualize this as a physical model mounted for testing in a wind tunnel. *Elastic axis EA* (the hinge) is assumed to be frictionless, and rotation spring k_θ represents wing torsional stiffness. (The term *elastic axis* refers to the line along the span of a high-aspect-ratio, straight, unswept wing about which the wing chordwise sections rotate if a pure twisting moment is imposed upon the wing.) This model is intended primarily for the study of aeroelastic divergence. Figure 11-4 shows the typical

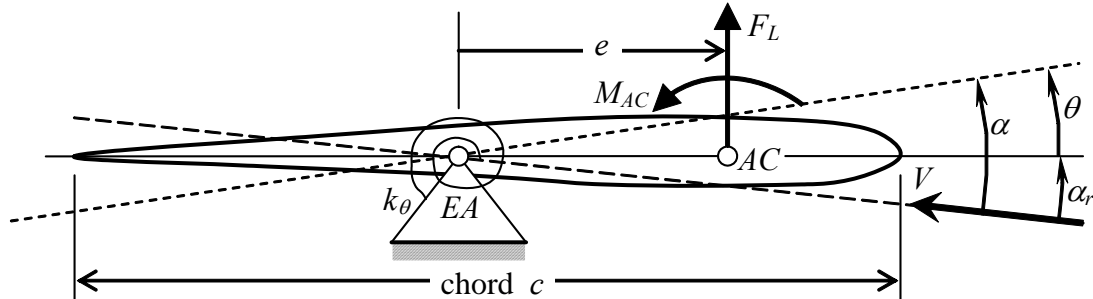
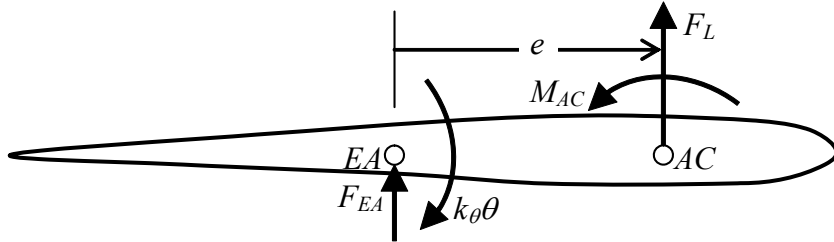


Figure 11-4 Example 11-2: 1-DOF typical section in an airstream

section in the reference static equilibrium position before the wind tunnel fan is turned on. Turning on the wind tunnel fan then produces an airstream of steady free-stream velocity V flowing over the typical section at small angle of incidence α_r relative to the reference chordline of the typical section. The airstream creates a resultant lifting force F_L that acts through *aerodynamic center AC*, and a resultant pitching moment M_{AC} that acts about AC . For most cases of practical interest, AC is forward of EA by some positive distance e , as shown on Fig. 11-4; the polarity $e > 0$ is very important relative to divergence. Aerodynamic actions F_L and M_{AC} impose moments upon rotation spring k_θ , and the spring flexibility permits structural rotation θ relative to the reference position.

² For the early history of aeroelastic divergence, see Bisplinghoff *et al.*, 1955, pp. 3-7, and Gordon, 1978, pp. 259-270.

The DFBD associated with Fig. 11-4 is drawn below. The equation of motion comes directly from the DFBD and Eq. (11-11), with the assumption of small angles of



incidence and rotation, $|\alpha_r| < \approx 10^\circ$ and $|\theta(t)| < \approx 10^\circ$, and with J_{EA} being the rotational inertia of the typical section about EA:

$$J_{EA} \ddot{\theta} = F_L e + M_{AC} - k_\theta \theta \Rightarrow J_{EA} \ddot{\theta} + k_\theta \theta = F_L e + M_{AC} \quad (11-14)$$

We can cast Eq. (11-14) into a more interesting and useful form by relating the aerodynamic actions to the structural rotation. We assume that the airstream direction coincides with the zero-lift attitude of the airfoil, *i.e.*, that F_L would be zero for any value of airspeed V if the airfoil incidence were fixed at $\alpha_r = 0$. Consequently, the total *angle of attack* of the airfoil relative to the zero-lift attitude is $\alpha = \alpha_r + \theta$. Then aerodynamic lift and moment can be expressed as

$$F_L = \bar{q} S C_{L\alpha} \alpha = \bar{q} S C_{L\alpha} (\alpha_r + \theta), \quad \text{and} \quad M_{AC} = \bar{q} S c C_{MAC} \quad (11-15)$$

Note especially in Eqs. (11-15) that an aerodynamic action (in this case, lift F_L) is dependent upon structural deformation (in this case, rotation θ); this type of interaction between aerodynamics and structural flexibility is an important characteristic of all aeroelastic phenomena. The symbols used in (11-15) beyond those previously defined are:

$\bar{q} = \frac{1}{2} \rho V^2$ is the free-stream dynamic pressure (lb/ft^2 or N/m^2).

ρ is air density (slug/ft^3 or kg/m^3).

$S = b c$ is the planform area of the typical section (ft^2 or m^2).

b is the span of the typical section into the plane of the paper (ft or m).

$C_{L\alpha} > 0$ is the slope of the curve of section lift coefficient ($F_L / \bar{q} S$) versus angle of attack (rad^{-1}), which we assume here to be constant for small angles of attack.

C_{MAC} is the dimensionless coefficient of pitching moment about AC, normally positive for a positively cambered airfoil, but zero for an uncambered thin airfoil.

Wind tunnel experiments and aerodynamic theory show that aerodynamic action Eqs. (11-15) are valid only for steady flow, for which angle of attack α does not vary with time. However, we will approximate a bit here and assume that Eqs. (11-15) are at least qualitatively valid for slowly-time-varying angle of attack, $\alpha(t) = \alpha_r + \theta(t)$. This approximation is sometimes called *quasi-static* or *quasi-steady* aerodynamics. Substituting Eqs. (11-15) into Eq. (11-14) gives

$$\begin{aligned} J_{EA} \ddot{\theta} + k_\theta \theta &= \bar{q} S C_{L\alpha} (\alpha_r + \theta) e + \bar{q} S c C_{MAC} \\ \Rightarrow J_{EA} \ddot{\theta} + (k_\theta - \bar{q} S C_{L\alpha} e) \theta &= \bar{q} S C_{L\alpha} \alpha_r e + \bar{q} S c C_{MAC} \end{aligned} \quad (11-16)$$

Note in Eq. (11-16) that the total stiffness constant, $k_\theta - \bar{q} S C_{L\alpha} e$ (structural stiffness plus aerodynamic “stiffness”) can, for $e > 0$, become zero or even negative if dynamic pressure \bar{q} is sufficiently large. This is critically important relative to the stability of the system. Consider steady flow, for example, for which $\ddot{\theta} = 0$; in this case we can solve Eq. (11-16) algebraically for the static structural rotation:

$$\theta = \frac{\bar{q} S (C_{L\alpha} \alpha_r e + c C_{MAC})}{k_\theta - \bar{q} S C_{L\alpha} e} \equiv \frac{\bar{q} (C_{L\alpha} \alpha_r e + c C_{MAC})}{C_{L\alpha} e (\bar{q}_D - \bar{q})} \quad (11-17)$$

In Eq. (11-17), we define the *divergence dynamic pressure* in terms of other fixed system parameters as

$$\bar{q}_D \equiv \frac{k_\theta}{S C_{L\alpha} e} \quad (11-18)$$

If it is possible for a given set of physical parameters to increase the wind-tunnel airspeed V up to the point that $\bar{q} \rightarrow \bar{q}_D = k_\theta / S C_{L\alpha} e$, then, from Eq. (11-17), clearly something very interesting will happen. From your knowledge of aerodynamics and structures, what types of physical behavior do you think are possible? Keep in mind that Eq. (11-17) is predicated on the assumptions of small angles and complete linearity of both aerodynamics and structures (in this system, the rotation spring).

A conventional airplane control surface is mounted on the trailing edge of a major lifting surface, with the leading edge of the control surface hinged to the lifting surface (e.g., an aileron on a wing). In this case, the aerodynamic center of the control surface is aft of the elastic axis, making the moment arm e negative (see Fig. 11-4). From Eq. (11-16), this produces the negative moment $\bar{q} S C_{L\alpha} \alpha_r e$, which is called a *blowdown* moment, and it also augments the structural stiffness in the total stiffness constant $k_\theta - \bar{q} S C_{L\alpha} e$. Therefore, a conventional trailing-edge control surface cannot diverge aeroelastically.

Example 11-3: 2-DOF *typical-section* model for coupled wing bending and torsion

We now return to general-plane-motion Eqs. (11-2a), (11-2b), and (11-3), which are three ODEs in three unknown DOFs: $x_C(t)$, $y_C(t)$, and $\theta(t)$. In practice, these ODEs are often coupled by system geometry and the nature of the active and reactive actions. Moreover, if motion is allowed to have arbitrarily large magnitude, then the equations are usually nonlinear. In general, these arbitrary-plane-motion equations can be solved only in numerical form, not in the form of algebraic equations. However, the mechanical systems considered in this book are limited, in most cases, to those for which center-of-mass translation is small relative to rigid-body dimensions, and for which rotation is small, $|\theta(t)| < \approx 10^\circ$ (e.g., Examples 11-1 and 11-2 in this section); these limitations allow us to linearize the ODEs into more easily solvable forms.

One of the first forms of aeroelastic wing flutter that was observed and carefully analyzed during the early 1900s involves coupled bending and torsional vibration (Bisplinghoff *et al.*, 1955, Section 9-2). The two-degrees-of-freedom (2-DOF) typical section depicted in Fig. 11-5 is a very simplified structural model used to study wing bending-torsion flutter.³ The airfoil section is hinged without friction at elastic axis EA to a vertical bar (assumed rigid and of negligible inertial force), which is restricted to vertical translation by frictionless linear bearings. Rotational spring k_θ simulates wing torsional stiffness, and translational spring k_y simulates wing bending stiffness. The theory of unsteady aerodynamics, even for two-dimensional flow, is very complicated, so we shall simply represent the aerodynamic resultant actions generally as lift $F_L(t)$ and pitching moment about the aerodynamic center $M_{AC}(t)$, and we shall focus on the structural dynamics.

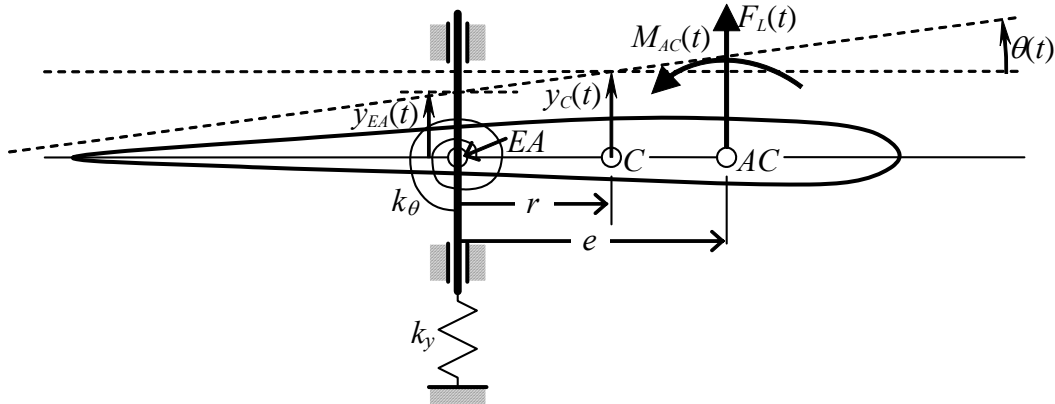


Figure 11-5 Example 11-3: 2-DOF typical section

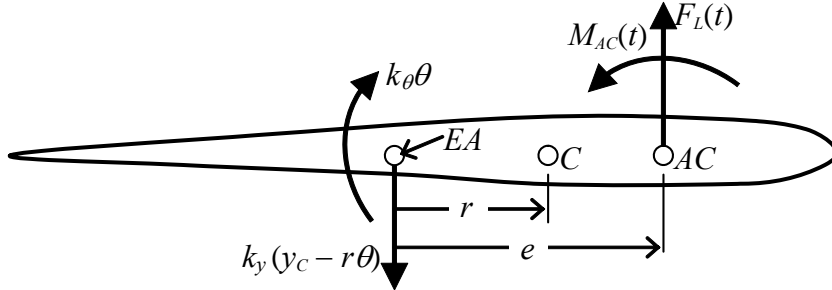
³ Physical typical-section airfoils were designed, fabricated, and tested in recent wind-tunnel experimental research studies of unsteady aerodynamics (as summarized by Bennett, 2000), and of feedback control to suppress flutter (DeMarqui, *et al.*, 2005 and 2006). Homework Problem 16.11 applies an approximate theory of unsteady aerodynamics in a simulation of one such experimental project.

Chapter 11 Mechanical systems with rigid-body plane translation and rotation

In order to write the equations of motion for this typical section, we select as degrees of freedom the vertical translation $y_C(t)$ of mass center C , and pitching rotation $\theta(t)$, both relative to the reference static equilibrium position. The geometry of small rotation is represented by the relationship between $y_C(t)$ and $y_{EA}(t)$:

$$y_C(t) = y_{EA}(t) + r \sin \theta(t) \approx y_{EA}(t) + r\theta(t) \Rightarrow y_{EA}(t) \approx y_C(t) - r\theta(t) \quad (11-19)$$

The DFBD associated with Fig. 11-5 is drawn below, with approximation (11-19) used to annotate the force due to translation spring k_y .



Using this DFBD, we write the two relevant equations of motion, (11-2b) and (11-3) in scalar form, as

$$m \ddot{y}_C = F_L(t) - k_y(y_C - r\theta) \quad (11-20a)$$

$$J_C \ddot{\theta} = (e - r)F_L(t) + M_{AC}(t) - k_\theta\theta + r k_y(y_C - r\theta) \quad (11-20b)$$

It is appropriate to express Eqs. (11-20) with all terms involving degrees of freedom $y_C(t)$ and $\theta(t)$ transposed to the left-hand sides:

$$m \ddot{y}_C + k_y y_C - r k_y \theta = F_L(t) \quad (11-21a)$$

$$J_C \ddot{\theta} - r k_y y_C + (k_\theta + r^2 k_y) \theta = (e - r)F_L(t) + M_{AC}(t) \quad (11-21b)$$

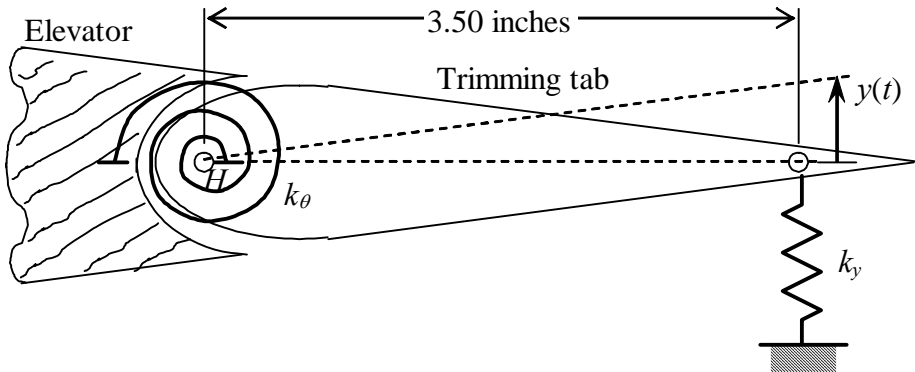
Equations (11-21) are a pair of 2nd order, *coupled* ODEs in unknowns $y_C(t)$ and $\theta(t)$. Just as Eqs. (1-15a) and (1-15b), Eqs. (11-21a) and (11-21b) are described as being coupled because each equation contains both dependent variables and neither equation can be solved independently of the other. It is possible, though we won't bother doing it, to combine these two equations into a single 4th order ODE in a single unknown function of time; therefore, this 2-DOF typical section is actually a 4th order system. It is appropriate and common also to express the set of ODEs (11-21) in matrix form:

$$\underbrace{\begin{bmatrix} m & 0 \\ 0 & J_C \end{bmatrix}}_{\text{inertia matrix}} \begin{bmatrix} \ddot{y}_C \\ \ddot{\theta} \end{bmatrix} + \underbrace{\begin{bmatrix} k_y & -r k_y \\ -r k_y & k_\theta + r^2 k_y \end{bmatrix}}_{\text{structural stiffness matrix}} \begin{bmatrix} y_C \\ \theta \end{bmatrix} = \begin{bmatrix} F_L(t) \\ (e - r)F_L(t) + M_{AC}(t) \end{bmatrix} \quad (11-22)$$

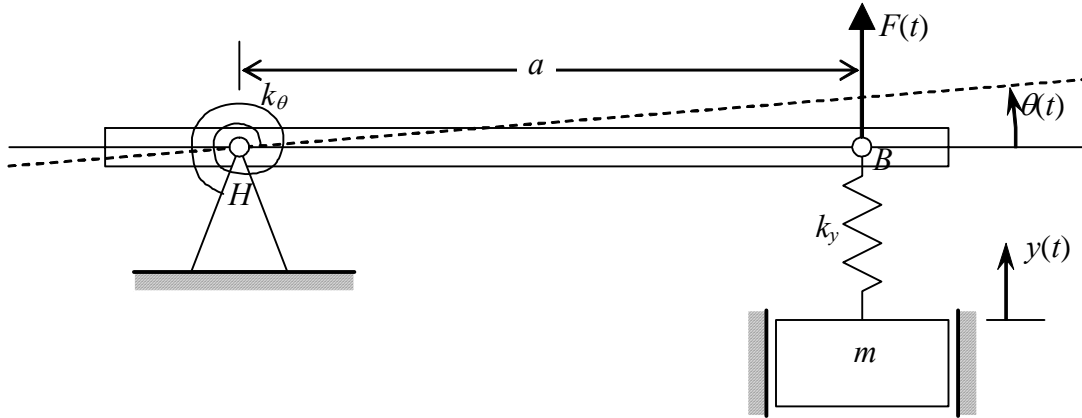
The labeled left-hand-side coefficient matrices of Eq. (11-22) are typical for structural dynamic systems, and they exhibit some important general properties. The *inertia matrix* in this case is diagonal; more generally, it will be non-diagonal but symmetric. The inertia matrix will always be *positive definite* because all matter has positive mass; therefore, the determinant of the inertia matrix will always be positive. In (11-22), that determinant is simply the product $m J_C > 0$. The *structural stiffness matrix* in (11-22) is symmetric, and this is a general property resulting from linearity between applied actions and structural deformations. Moreover, if a structure is restrained by grounded supports, such as the rotational spring k_θ and translational spring k_y of the typical section, then each of the diagonal elements of the stiffness matrix will be positive, and the stiffness matrix itself will be positive definite. You can check easily that the determinant of the stiffness matrix in (11-22) is the product $k_y k_\theta > 0$. The coupling between vertical translation $y_c(t)$ and pitching rotation $\theta(t)$ of the typical section is both produced by and displayed by the non-zero off-diagonal terms of the stiffness matrix, each being $-rk_y$.

11-4 Homework problems for Chapter 11

11.1 The trimming tab of a small airplane is attached to the elevator by a hinge at axis H and a rotational spring (the actuator linkage) with constant k_θ , as shown in the drawing below. You are required to determine experimentally both rotational inertia J_H of the elevator about the hinge, and rotational stiffness k_θ . The field experiment consists of two separate *twang* tests. (See homework Problem 9.4 for a detailed description of twang testing and relevant equations.) First, the rotational spring is disconnected from the tab, and a vertical translational support spring of known stiffness $k_y = 15.6 \text{ lb/inch}$ (and low mass, producing negligible inertial force) is attached near the trailing edge, as shown. Then the tab is twanged (displaced statically from the static equilibrium position, then released). A non-contacting displacement sensor picks up the dynamic motion at a point near the support spring: $y(t) = 0.107 e^{-0.144t} \cos(59.9t)$ inch (t in seconds). (There is slight damping due to friction at the hinge, internal structural damping in the spring, and drag of the surrounding air.) From this first twang test, calculate J_H (in $\text{lb}\cdot\text{sec}^2\cdot\text{inch}$). Next, translational spring k_y is removed, rotational spring k_θ is re-connected, and the tab is again twanged. The same displacement sensor as in the first twang test now measures dynamic motion $y(t) = 0.132 e^{-0.112t} \cos(66.0t)$ inch. From the previous results and this second twang test, calculate k_θ (in $\text{lb}\cdot\text{inch}/\text{radian}$).



11.2 The system depicted on the next page consists of a rigid bar, a mass, and springs. The rigid bar is supported at frictionless hinge H , where it is elastically restrained by rotational spring k_θ , and the rotational inertia of the bar about point H is J_H . Mass m is connected to the bar by translational spring k_y at point B , and the mass is restrained to move only vertically by frictionless walls. An externally applied vertical force $F(t)$ acts on the bar at point B . Degrees of freedom $y(t)$ and $\theta(t)$ are the small motions relative to the static equilibrium position. Sketch and label a DFBD for the bar and a DFBD for mass m , then use these diagrams to derive the two coupled differential equations of motion for this system. (Hints: Show that for small bar rotation, the stretch of spring k_y is $a\theta - y$. Do not include mg or bar weight among the applied forces, because we are interested only in dynamic motions relative to the static equilibrium position; if you are not sure why we neglect weights in these equations of motion, then review Section 7-5.)



11.3 The two-degrees-of-freedom system drawn below consists of a pendulum supported at frictionless hinge H , and a mass-spring connected by a viscous damper to the pendulum rod. The inertial moment of the lightweight pendulum rod is negligible, so pendulum rotational inertia about H is $J_H = m_p \ell^2$. Degrees of freedom $x(t)$ and $\theta(t)$ are small motions relative to the static equilibrium position. Show that the velocity of the damper cylinder relative to the damper piston is $\dot{x} - a\dot{\theta}$.

Both gravity and the externally applied horizontal force $F(t)$ act on mass m_p of the pendulum bob. Sketch and label an FBD for the pendulum and an FBD for mass m , then use these diagrams to derive the two coupled differential equations of motion for this system. In addition to the motion and force variables

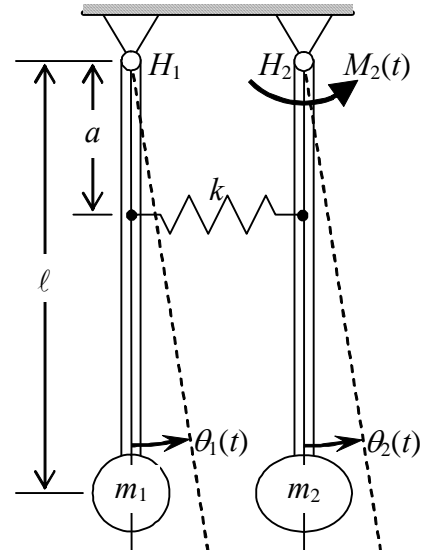
and the constant parameters shown on the drawing, the acceleration of gravity acting vertically downward is denoted g . For this problem, unlike for Problems 11.1 and 11.2 and the examples in Section 11-3, you should sketch your pendulum FBD with the pendulum rotated through a small angle, so that you can indicate the restraining effect of weight $m_p g$ on pendulum rotation; see the pendulum example in Section 7-1.

11.4 The form of the typical-section ODEs of motion represented by Eqs. (11-21) and (11-22) is not unique. Suppose, for example, you want to define $y_{EA}(t)$ as the vertical translation degree of freedom, instead of $y_C(t)$. With use of geometry, inertia, and algebraic manipulation, you can cast the ODEs into a cosmetically different, but mathematically equivalent form. First, substitute Eq. (11-19) into Eqs. (11-21) in order to replace $y_C(t)$ with appropriate terms that include $y_{EA}(t)$ and small-rotation $\theta(t)$; next, use the parallel-axis theorem to replace J_C with the rotational inertia about the elastic axis, J_{EA} , and a term including mass m ; finally, perform any additional algebraic substitution required to write the ODEs of motion in the following relatively simple matrix form:

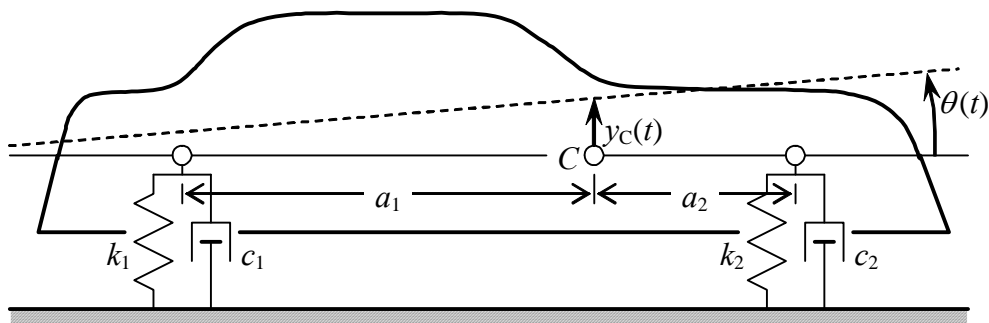
$$\underbrace{\begin{bmatrix} m & mr \\ mr & J_{EA} \end{bmatrix}}_{\text{inertia matrix}} \begin{bmatrix} \ddot{y}_{EA} \\ \ddot{\theta} \end{bmatrix} + \underbrace{\begin{bmatrix} k_y & 0 \\ 0 & k_\theta \end{bmatrix}}_{\text{structural stiffness matrix}} \begin{bmatrix} y_{EA} \\ \theta \end{bmatrix} = \begin{bmatrix} F_L(t) \\ eF_L(t) + M_{AC}(t) \end{bmatrix}$$

Which terms in this matrix equation produce and display the coupling between vertical translation $y_{EA}(t)$ and pitching rotation $\theta(t)$? Will this coupling still exist if the applied aerodynamic actions $F_L(t)$ and $M_{AC}(t)$ are either constant or vary slowly enough that the response is pseudo-static? Prove the positive definiteness of these inertia and structural stiffness matrices by finding the values and polarities of their determinants.

11.5 Consider the pendulum-spring system depicted below. The inertial moments of the lightweight pendulum rods are negligible, so pendulum rotational inertias about their hinges are $J_i = m_i \ell^2$, $i = 1, 2$. Degrees of freedom $\theta_1(t)$ and $\theta_2(t)$ are small rotations relative to the vertical hanging static equilibrium positions. A horizontal translational spring with stiffness constant k connects the two pendulums, and it is undeformed when the pendulums are in the vertical hanging static equilibrium positions. Show that the stretch of the spring is given by $a(\theta_2 - \theta_1)$. Externally applied moment $M_2(t)$ acts on pendulum 2 at its hinge (applied, for example, by a motor). Sketch and label an FBD for each pendulum, then use these diagrams to derive the two coupled differential equations of motion for this system. In addition to the motion and applied action variables and the constant parameters shown on the drawing, the acceleration of gravity acting vertically downward is denoted g . In this problem, you should sketch your FBDs with the pendulums rotated through small angles, so that you can indicate the restraining effect of the weights $m_i g$, $i = 1, 2$, on the rotations; see the pendulum example in Section 7-1.



11.6 The drawing below depicts a very simplified model for the pitch-translation dynamics of an automotive vehicle. The body and frame are considered to be rigid, with center of mass C located as shown, and having mass m and rotational inertia J_C about C .



Chapter 11 Mechanical systems with rigid-body plane translation and rotation

The wheel-axle assemblies are considered to have negligible inertial forces. The flexibilities of tires and suspension systems are lumped together into a single rear-axle translational spring k_1 and a single front-axle translational spring k_2 . Damping is provided by shock struts and rubber tires, and it is lumped into viscous dashpots c_1 and c_2 arranged in parallel with the respective springs. Sketch and label a DFBD for this vehicle model, then use it to derive the two coupled differential equations of motion for this system, in terms of the given parameters. Use as degrees of freedom the small vertical translation $y_C(t)$ and the small pitching rotation $\theta(t)$, both relative to the static equilibrium position.

Chapter 12 Vibration modes of undamped mechanical systems with two degrees of freedom

© 2016 by William L. Hallauer, Jr.

12-1 Introduction: undamped mass-spring system

The subject of this chapter is free vibration of undamped mechanical systems, beginning with the one-degree-of-freedom (1-DOF) mass-spring system of Fig. 12-1. We evaluated the $m-k$ system more generally in Chapter 7, but we will re-visit it here using a different approach. Free vibration can arise from initial translation of the mass (relative to the static equilibrium position) and/or initial velocity, and also from excitation that has ceased, which might provide the mass with both initial translation and initial velocity at the instant when excitation ceases. However, it is easiest conceptually to visualize this motion as response to only non-zero initial translation relative to the static equilibrium position. Doing so sacrifices a little generality because we cannot also account for a non-zero initial velocity, but the essential characteristics of the free vibration are revealed by this approach. Consider an undamped mass-spring system with non-zero initial translation, $y(0) = y_0$, and zero initial velocity, $\dot{y}(0) = 0$, but without forcing excitation, so that $f_y(t) = 0$. From Eq. (7-2), the ODE of free vibration is

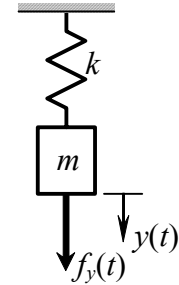


Figure 12-1

$$m \ddot{y} + k y = f_y(t) = 0 \quad (12-1)$$

We now ask the questions: Can motion exist in the form $y(t) = Y \cos \omega t$, and, if so, what are the constants Y and ω ? To find the answers, we substitute the presumed form of motion into ODE (12-1), perform the differentiations and algebra, and see where the process leads:

$$m(-\omega^2 Y \cos \omega t) + k Y \cos \omega t = (-\omega^2 m + k) Y \cos \omega t = 0$$

This equation can be satisfied in general, for a non-trivial solution, only if

$$\omega^2 = k/m \equiv \omega_n^2 \Rightarrow \omega = \omega_n = \sqrt{k/m}$$

Moreover, we can use the initial condition to find Y :

$$\begin{aligned} y(0) &= y_0 = Y \cos(\omega \times 0) = Y \\ \Rightarrow y(t) &= y_0 \cos \omega_n t \end{aligned} \quad (12-2)$$

This simple result was already derived in Eq. (7-10); we re-derive it differently here just to establish the approach that will be useful next for higher-order systems.

12-2 Undamped two-mass-two-spring system

Next, we analyze the two-degrees-of freedom (2-DOF) undamped mass-spring system of Fig. 12-2. Dynamic translations $y_1(t)$ and $y_2(t)$ shown are relative to the static equilibrium positions. As usual for the purpose of drawing forces on dynamic free-body diagrams (DFBDs, as defined in Section 7-5), we let the translational springs be stretched at the instant depicted, so that, in particular, the dynamic tension in the lower spring is $k_2(y_2 - y_1)$. From the DFBDs, Newton's 2nd law gives the ODEs of motion:

$$\begin{aligned} m_1 \ddot{y}_1 &= f_1(t) + k_2(y_2 - y_1) - k_1 y_1 \\ m_2 \ddot{y}_2 &= f_2(t) - k_2(y_2 - y_1) \end{aligned} \quad (12-3)$$

Transposing dependent-variable terms to the left-hand sides, and collecting terms gives

$$\begin{aligned} m_1 \ddot{y}_1 + (k_1 + k_2)y_1 - k_2 y_2 &= f_1(t) \\ m_2 \ddot{y}_2 - k_2 y_1 + k_2 y_2 &= f_2(t) \end{aligned} \quad (12-4)$$

Now, expressing Eqs. (12-4) in the same matrix form as Eq. (11-22) gives

$$\underbrace{\begin{bmatrix} m_1 & 0 \\ 0 & m_2 \end{bmatrix}}_{\text{inertia matrix}} \begin{bmatrix} \ddot{y}_1 \\ \ddot{y}_2 \end{bmatrix} + \underbrace{\begin{bmatrix} k_1 + k_2 & -k_2 \\ -k_2 & k_2 \end{bmatrix}}_{\text{structural stiffness matrix}} \begin{bmatrix} y_1 \\ y_2 \end{bmatrix} = \begin{bmatrix} f_1(t) \\ f_2(t) \end{bmatrix} \quad (12-5)$$

You can verify easily that, just as in Eq. (11-22), the inertia and structural stiffness matrices of Eq. (12-5) are positive definite, and all diagonal elements of both matrices also are positive definite.

Next, we want to solve matrix Eq. (12-5) for free vibrations, so we set to zero the applied forces, $f_1(t) = f_2(t) = 0$. Following the procedure in Section 12-1 for the 1-DOF system, let's seek response to non-zero initial translations, with zero initial velocities. Accordingly, we assume motion solutions of the unforced 2-DOF system in the form $y_1(t) = Y_1 \cos \omega t$ and $y_2(t) = Y_2 \cos \omega t$, in which ω , Y_1 , and Y_2 are the unknown quantities. It is efficient and appropriate to express the assumed solution in matrix form:

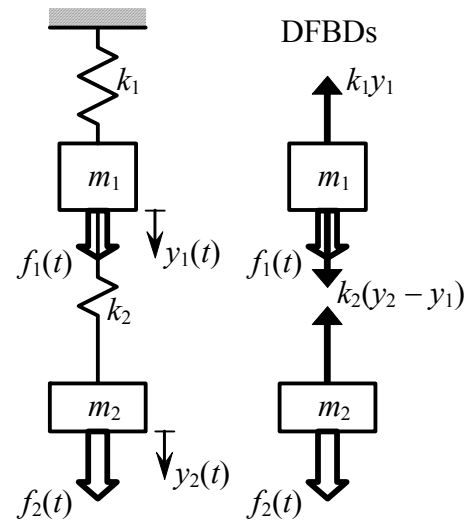


Figure 12-2 Two-mass-two-spring mechanical system

$$\begin{bmatrix} y_1(t) \\ y_2(t) \end{bmatrix} = \begin{bmatrix} Y_1 \\ Y_2 \end{bmatrix} \cos \omega t \quad (12-6)$$

Substituting Eq. (12-6) into Eq. (12-5) with zero forcing gives

$$\begin{bmatrix} m_1 & 0 \\ 0 & m_2 \end{bmatrix} \begin{bmatrix} Y_1 \\ Y_2 \end{bmatrix} (-\omega^2) \cos \omega t + \begin{bmatrix} k_1 + k_2 & -k_2 \\ -k_2 & k_2 \end{bmatrix} \begin{bmatrix} Y_1 \\ Y_2 \end{bmatrix} \cos \omega t = \begin{bmatrix} 0 \\ 0 \end{bmatrix} \quad (12-7)$$

The common multiple $\cos \omega t$ in Eq. (12-7) cannot be zero in general, so we cancel it out of the equation. Further, we consolidate all of the coefficients of Y_1 and Y_2 into a single matrix, giving

$$\begin{bmatrix} k_1 + k_2 - \omega^2 m_1 & -k_2 \\ -k_2 & k_2 - \omega^2 m_2 \end{bmatrix} \begin{bmatrix} Y_1 \\ Y_2 \end{bmatrix} = \begin{bmatrix} 0 \\ 0 \end{bmatrix} \quad (12-8)$$

Before dealing with Eq. (12-8), let's review a little from your mathematics background about solving two linear algebraic equations in two unknowns. In general, the equations are expressed in matrix notation as

$$\begin{bmatrix} a_{11} & a_{12} \\ a_{21} & a_{22} \end{bmatrix} \begin{bmatrix} x_1 \\ x_2 \end{bmatrix} = \begin{bmatrix} b_1 \\ b_2 \end{bmatrix}, \text{ with } \begin{bmatrix} a_{11} & a_{12} \\ a_{21} & a_{22} \end{bmatrix} \equiv [\mathbf{a}], \text{ and } \begin{bmatrix} x_1 \\ x_2 \end{bmatrix} \equiv \{\mathbf{x}\}, \text{ and } \begin{bmatrix} b_1 \\ b_2 \end{bmatrix} \equiv \{\mathbf{b}\} \quad (12-9)$$

in which the a_{ij} 's are known constant coefficients, the x_i 's are the unknowns, and the b_i 's are known right-hand-side constants. It is useful to express the matrix equation symbolically by using bold fonts, brackets, and parentheses: $[\mathbf{a}]\{\mathbf{x}\} = \{\mathbf{b}\}$. Then the *determinant* and the *adjoint matrix* of the coefficient matrix are, respectively,

$$\det[\mathbf{a}] = a_{11}a_{22} - a_{21}a_{12} \quad (12-10)$$

$$\text{adj}[\mathbf{a}] = \begin{bmatrix} a_{22} & -a_{12} \\ -a_{21} & a_{11} \end{bmatrix} \quad (12-11)$$

The solution of Eq. (12-9) for the unknowns involves the inverse $[\mathbf{a}]^{-1}$ of the coefficient matrix, which is defined in terms of the determinant and the adjoint matrix:

$$\{\mathbf{x}\} = [\mathbf{a}]^{-1}\{\mathbf{b}\} = \frac{\text{adj}[\mathbf{a}]}{\det[\mathbf{a}]} \{\mathbf{b}\} \quad (12-12)$$

If $\{\mathbf{b}\} = \mathbf{0}$, which is the case for Eq. (12-8), then there are two possible types of solutions: (i) if $\{\mathbf{b}\} = \mathbf{0}$ and $\det[\mathbf{a}] \neq 0$, then the solution must be the trivial result $\{\mathbf{x}\} = \mathbf{0}$; (ii) however, if $\{\mathbf{b}\} = \mathbf{0}$ and $\det[\mathbf{a}] = 0$, then the right-hand side of Eq. (12-12) has the indetermi-

Chapter 12 Vibration modes of undamped mechanical systems with two degrees of freedom

nate form $0/0$, so that there exists, and we can solve for a non-trivial $\{\mathbf{x}\} \neq \mathbf{0}$, but any constant multiple of $\{\mathbf{x}\}$ is also a solution since $\{\mathbf{b}\} = \mathbf{0}$ in Eq. (12-9). Therefore, for our current application, Eq. (12-8), we must seek a type (ii) solution.

To find the same type (ii) result as in the last paragraph, but without using matrices or theory from linear algebra, let's write Eq. (12-8) as two separate scalar equations, and then attempt to solve them algebraically for Y_1 and Y_2 :

$$(k_1 + k_2 - \omega^2 m_1) Y_1 - k_2 Y_2 = 0 \Rightarrow Y_2 = \frac{1}{k_2} (k_1 + k_2 - \omega^2 m_1) Y_1 \quad (12-13a)$$

$$-k_2 Y_1 + (k_2 - \omega^2 m_2) Y_2 = 0 = -k_2 Y_1 + (k_2 - \omega^2 m_2) \frac{1}{k_2} (k_1 + k_2 - \omega^2 m_1) Y_1 \quad (12-13b)$$

Re-arranging the last part of Eq. (12-13b) a bit differently gives

$$\left[(k_1 + k_2 - \omega^2 m_1)(k_2 - \omega^2 m_2) - k_2^2 \right] \frac{Y_1}{k_2} = 0 \quad (12-14)$$

We want to solve Eq. (12-14) for a non-zero Y_1 , which leads us to conclude that: (1) the bracketed term multiplying Y_1/k_2 must be zero [Note that the bracketed term is the determinant of the coefficient matrix in Eq. (12-8).]; and (2) we cannot yet assign any specific value to Y_1 (but we will be able to do so later if we chose to regard this problem as being time response to specific initial translations).

The bracketed term in Eq. (12-14) must be zero; upon carrying out the multiplications, we see that it leads to a quadratic equation in the unknown ω^2 :

$$m_1 m_2 (\omega^2)^2 + [-m_1 k_2 - m_2 (k_1 + k_2)] \omega^2 + k_1 k_2 = 0 \quad (12-15)$$

This type of polynomial equation is generally called the *characteristic equation* of the free-vibration problem. For any realistic values of the mass and stiffness constants, Eq. (12-15) has two real, positive roots, which we denote as ω_1^2 and ω_2^2 .

Let's consider a numerically simplified case for which the masses are equal, $m_1 = m_2 \equiv m$, and the stiffness constants also are equal, $k_1 = k_2 \equiv k$. In this case, the quadratic equation (12-15) becomes

$$m^2 (\omega^2)^2 - 3mk\omega^2 + k^2 = 0 \quad (12-16)$$

Using the standard solution of quadratic equations, Eq. (2-2), we find the roots of Eq. (12-16) to be

$$\omega^2 = \frac{3 \pm \sqrt{5}}{2} \frac{k}{m} = (0.382, 2.618) \frac{k}{m} \quad (12-17)$$

For future reference, note that the lower of the \pm signs gives the smaller (the “first”) of the two ω^2 roots, and that the upper sign gives the larger (the “second”) of the two ω^2 roots. Only positive circular frequencies are physically meaningful, and they are:

$$\omega = (0.618, 1.618) \sqrt{k/m} \Rightarrow \omega_1 = 0.618 \sqrt{k/m} \quad \text{and} \quad \omega_2 = 1.618 \sqrt{k/m} \quad (12-18)$$

Of the two circular frequencies in Eqs. (12-18), the smaller value ω_1 is called the *first* or *fundamental natural frequency*, and the larger value ω_2 is called the *second natural frequency*. By convention, natural frequencies are always numbered in ascending order for all higher-order systems that have two or more natural frequencies. It is mathematically systematic to define an integer subscript n that is either 1 or 2, and to identify the natural frequencies more generally as ω_n , $n = 1, 2$. (In this case, the symbol n performs double-duty, because it both implies *natural* frequency of vibration and takes the values 1 or 2 to distinguish the two natural frequencies from each other.)

Next, let’s seek values of Y_1 and Y_2 associated with each of the natural frequencies. It is appropriate and efficient to extend use of the subscript n to these motion magnitude values by labeling as Y_{1n} and Y_{2n} the values associated with frequency ω_n , $n = 1, 2$. Let’s re-write Eqs. (12-13) using this notation and the numerically simplified case of equal masses and equal stiffness constants:

$$(2k - \omega_n^2 m) Y_{1n} - k Y_{2n} = 0 \Rightarrow Y_{2n} = \frac{1}{k} (2k - \omega_n^2 m) Y_{1n} \quad (12-19a)$$

$$-k Y_{1n} + (k - \omega_n^2 m) Y_{2n} = 0 \Rightarrow Y_{2n} = \frac{k}{k - \omega_n^2 m} Y_{1n} \quad (12-19b)$$

As is stated in the discussion of Eq. (12-14), we cannot yet assign any specific value to Y_{1n} . If we leave Y_{1n} arbitrary (but not zero) for now, then Eqs. (12-19) appear to give two different ways of solving for Y_{2n} in terms of Y_{1n} . Let’s use natural frequency Eq. (12-17) to evaluate both equations:

$$Y_{2n} = \frac{1}{k} (2k - \omega_n^2 m) Y_{1n} = \left(2 - \omega_n^2 \frac{m}{k} \right) Y_{1n} = \left(2 - \frac{3 \pm \sqrt{5}}{2} \right) Y_{1n} = \frac{1 \mp \sqrt{5}}{2} Y_{1n} \quad (12-20a)$$

$$\begin{aligned}
 Y_{2n} &= \frac{k}{k - \omega_n^2 m} Y_{1n} = \frac{1}{1 - \omega_n^2 \frac{m}{k}} Y_{1n} = \frac{1}{1 - \frac{3 \pm \sqrt{5}}{2}} Y_{1n} = \frac{2}{-1 \mp \sqrt{5}} Y_{1n} \\
 &= \frac{2}{-1 \mp \sqrt{5}} \times \frac{1 \mp \sqrt{5}}{1 \mp \sqrt{5}} Y_{1n} = \frac{1 \mp \sqrt{5}}{2} Y_{1n}
 \end{aligned} \tag{12-20b}$$

Both equations (12-20) give the same answer! Mathematically, this result is related to the zero of the determinant of the coefficient matrix in Eq. (12-8), but the detailed theory is best left to a more advanced book (for example, Craig, 1981, Section 13.1). For our purposes, it is enough to recognize from this example that, in this type of problem, both equations have the same solution, so it is necessary to solve only one of them.

Next, let's collect together from Eqs. (12-18) and (12-20) all the numerical results for each value of the index n into *modes of vibration*, the physical significance of which will become clear later. We have observed already that Y_{1n} is some arbitrary non-zero value, so nothing is lost if we set $Y_{1n} = 1$ (with dimension of translation, *i.e.*, length) for both modes of vibration.

$n = 1$, first (fundamental) mode of vibration: [the lower sign in Eqs. (12-20)]

$$\omega_1 = 0.618 \sqrt{\frac{k}{m}}, \quad Y_{21} = \frac{1 + \sqrt{5}}{2} Y_{11} = 1.618 \Rightarrow \begin{bmatrix} Y_{11} \\ Y_{21} \end{bmatrix} = \begin{bmatrix} 1 \\ 1.618 \end{bmatrix} \tag{12-21a}$$

$n = 2$, second mode of vibration: [the upper sign in Eqs. (12-20)]

$$\omega_2 = 1.618 \sqrt{\frac{k}{m}}, \quad Y_{22} = \frac{1 - \sqrt{5}}{2} Y_{12} = -0.618 \Rightarrow \begin{bmatrix} Y_{12} \\ Y_{22} \end{bmatrix} = \begin{bmatrix} 1 \\ -0.618 \end{bmatrix} \tag{12-21b}$$

For reasons that will become clear later, the column matrices $\begin{bmatrix} Y_{11} \\ Y_{21} \end{bmatrix}$ and $\begin{bmatrix} Y_{12} \\ Y_{22} \end{bmatrix}$ are called the *mode shapes* of, respectively, the first and second modes of vibration. NOTE: In Eqs. (12-21) we set $Y_{11} = Y_{12} = 1$ with dimension of length, but that does not necessarily imply that the magnitudes of physical responses $y_1(t)$ and $y_2(t)$ are one meter or one foot or one inch (depending upon the unit system in use). The actual physical response magnitudes are determined by initial conditions, as is discussed in the next paragraph.

Recall that we are seeking response to non-zero initial deformation, with zero initial velocity, and so we chose the solution in the form $\begin{bmatrix} y_1(t) \\ y_2(t) \end{bmatrix} = \begin{bmatrix} Y_1 \\ Y_2 \end{bmatrix} \cos \omega t$, Eq. (12-6).

In view of the free-vibration results (12-21), it is quite plausible physically (and it can be

Chapter 12 Vibration modes of undamped mechanical systems with two degrees of freedom

proved rigorously) that the general initial-translation response can be written as the linear sum of two terms like Eq. (12-6), one for each of the vibration modes:

$$\begin{bmatrix} y_1(t) \\ y_2(t) \end{bmatrix} = C_1 \begin{bmatrix} Y_{11} \\ Y_{21} \end{bmatrix} \cos \omega_1 t + C_2 \begin{bmatrix} Y_{12} \\ Y_{22} \end{bmatrix} \cos \omega_2 t \quad (12-22)$$

In Eq. (12-22), the dimensionless multiplying constants C_1 and C_2 show the contribution to the total response due to each mode of vibration; they are found from given initial translations $y_1(0)$ and $y_2(0)$ by writing (12-22) for $t = 0$:

$$\begin{bmatrix} y_1(0) \\ y_2(0) \end{bmatrix} = C_1 \begin{bmatrix} Y_{11} \\ Y_{21} \end{bmatrix} + C_2 \begin{bmatrix} Y_{12} \\ Y_{22} \end{bmatrix} = \begin{bmatrix} Y_{11} & Y_{12} \\ Y_{21} & Y_{22} \end{bmatrix} \begin{bmatrix} C_1 \\ C_2 \end{bmatrix} \quad (12-23)$$

The determinant of the 2×2 *mode-shape matrix* $[\mathbf{Y}]$ in Eq. (12-23) is non-zero, so that matrix can be inverted and the equation can be solved by application of Eq. (12-12), for arbitrary known $y_1(0)$ and $y_2(0)$, to give mode contribution constants C_1 and C_2 :

$$\begin{bmatrix} C_1 \\ C_2 \end{bmatrix} = \frac{1}{\det[\mathbf{Y}]} \begin{bmatrix} Y_{22} & -Y_{12} \\ -Y_{21} & Y_{11} \end{bmatrix} \begin{bmatrix} y_1(0) \\ y_2(0) \end{bmatrix} \quad (12-24)$$

Now, suppose that the initial translation is chosen to have the shape of the first mode, in other words, to be proportional to $\begin{bmatrix} Y_{11} \\ Y_{21} \end{bmatrix}$ with dimensionless constant of proportionality D_1 : $\begin{bmatrix} y_1(0) \\ y_2(0) \end{bmatrix} = D_1 \begin{bmatrix} Y_{11} \\ Y_{21} \end{bmatrix}$. Substituting this initial translation into Eq. (12-24) gives

$$\begin{bmatrix} C_1 \\ C_2 \end{bmatrix} = \frac{1}{\det[\mathbf{Y}]} \begin{bmatrix} Y_{22} & -Y_{12} \\ -Y_{21} & Y_{11} \end{bmatrix} D_1 \begin{bmatrix} Y_{11} \\ Y_{21} \end{bmatrix} = \frac{D_1}{\det[\mathbf{Y}]} \begin{bmatrix} Y_{22}Y_{11} - Y_{12}Y_{21} \\ -Y_{21}Y_{11} + Y_{11}Y_{21} \end{bmatrix} = \begin{bmatrix} D_1 \\ 0 \end{bmatrix}$$

Therefore, the total response (12-22) is $\begin{bmatrix} y_1(t) \\ y_2(t) \end{bmatrix} = D_1 \begin{bmatrix} Y_{11} \\ Y_{21} \end{bmatrix} \cos \omega_1 t$ for $t \geq 0$. Let's express this mathematical result in words: if we impose the initial translation in the shape of the first mode of vibration, then the subsequent free vibration of the system will be pure sinusoidal motion at the first natural frequency, and the relative positions of the two masses at each instant of time will remain in the first mode shape. In other words, both masses will vibrate with frequency ω_1 , and at each instant $t \geq 0$ the ratio $y_2(t)/y_1(t)$ will have the same value, Y_{21}/Y_{11} , which is 1.618 for the numerical example of Eqs. (12-16)-(12-18) and (12-20)-(12-21). In this case, the two masses move in the same direction at each instant, so they are said to move *in phase* with each other.

Suppose next that the initial translation is chosen to have the shape of the second mode, to be proportional to $\begin{bmatrix} Y_{12} \\ Y_{22} \end{bmatrix}$ with dimensionless constant of proportionality D_2 .

By following the procedure of the last paragraph, we can find that the total response Eq. (12-22) is $\begin{bmatrix} y_1(t) \\ y_2(t) \end{bmatrix} = D_2 \begin{bmatrix} Y_{12} \\ Y_{22} \end{bmatrix} \cos \omega_2 t$ for $t \geq 0$. In words, the subsequent free vibration of the system will be pure sinusoidal motion at the second natural frequency, and the relative positions of the two masses at each instant of time will remain in the second mode shape: both masses will vibrate with frequency ω_2 , and at each instant $t \geq 0$ the ratio $y_2(t)/y_1(t)$ will have the same value, Y_{22}/Y_{12} , which is -0.618 for the numerical example of Eqs. (12-16)-(12-18) and (12-20)-(12-21). In this case, the two masses move in opposite directions at each instant, so they are said to move *out of phase*.

The modes of vibration of this 2-DOF mass-spring system, the numerical example of Eqs. (12-16)-(12-18) and (12-20)-(12-21), are depicted graphically in Fig. 12-3. The

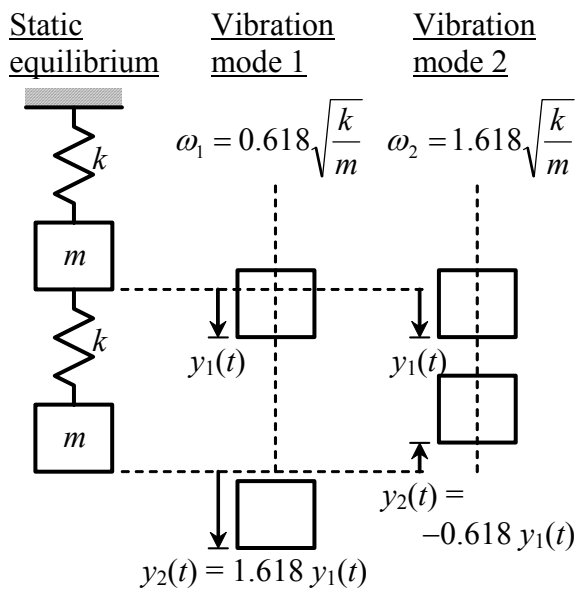


Figure 12-3 Vibration modes of the 2-DOF mass-spring system that has equal masses and equal springs

system is shown in its static equilibrium position for reference, and in deformed positions corresponding to each of the modes of vibration. We can't animate on the printed page the dynamic motion of a vibration mode, so we imagine that we are viewing a snapshot of the masses taken at one instant of time when the deformations are non-zero during any cycle of vibration.

The object in this chapter is to derive and illustrate the physical character of modes of vibration of undamped 2-DOF systems. The clearest and most direct way to do this is to restrict attention to response resulting from simple initial deformation, with zero initial velocity and zero input action. We will not go further in this book, but you should be informed that the theory started here can be ex-

tended to account for arbitrary non-zero initial conditions (both deformation and velocity) and arbitrary non-zero input actions imposed on damped 2-DOF systems. Indeed, the theory can be extended to damped higher-order systems having any number of degrees of freedom, which are often called *N-DOF systems*, with $N \geq 2$. The general method of analysis is called *modal analysis*, and it is used extensively in engineering practice and research for both mathematical and experimental studies. This book just scratches the surface of modal analysis; the theory is extended to general response of LTI mechanical

systems by more advanced books on linear-systems analysis and structural dynamics, two examples being Meirovitch, 2001, Chapter 7 and Craig, 1981, Chapters 13-15.

12-3 Vibration modes of an undamped 2-DOF typical-section model of a wing

From Example 3 of Section 11-3, the system is depicted again in Fig. 12-4:

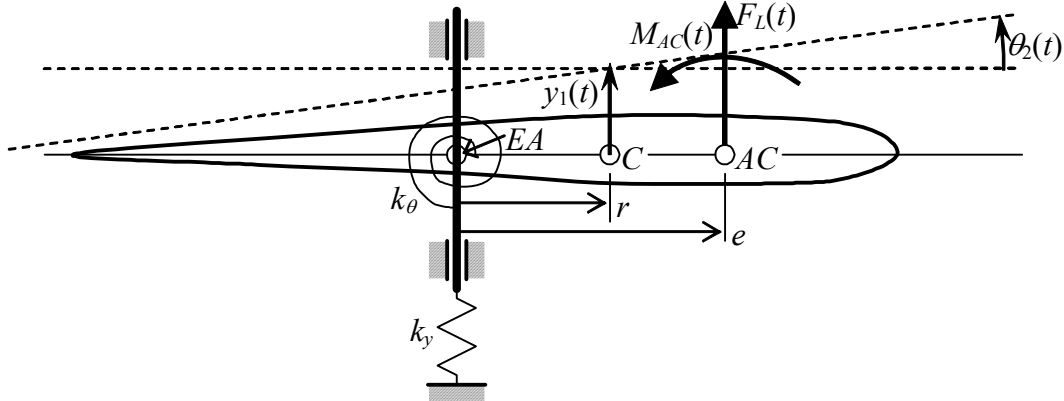


Figure 12-4 2-DOF typical section

The degree-of-freedom symbols $y_C(t)$ and $\theta(t)$ used in Chapter 11 are changed here, respectively, to $y_1(t)$ and $\theta_2(t)$, in order to denote clearly that these motion quantities are, respectively, degrees of freedom (DOFs) #1 and #2.

The matrix equation of motion in DOFs $y_1(t)$ and $\theta_2(t)$, from Eq. (11-22) is

$$\begin{bmatrix} m & 0 \\ 0 & J_C \end{bmatrix} \begin{bmatrix} \ddot{y}_1 \\ \ddot{\theta}_2 \end{bmatrix} + \begin{bmatrix} k_y & -rk_y \\ -rk_y & k_\theta + r^2 k_y \end{bmatrix} \begin{bmatrix} y_1 \\ \theta_2 \end{bmatrix} = \begin{bmatrix} F_L(t) \\ (e-r)F_L(t) + M_{AC}(t) \end{bmatrix} \quad (12-25)$$

To analyze Eq. (12-25) for modes of free vibration following the procedure described in the previous section, we set to zero the applied aerodynamic actions, and we seek motion solutions of the unforced system in the form:

$$\begin{bmatrix} y_1(t) \\ \theta_2(t) \end{bmatrix} = \begin{bmatrix} Y_1 \\ \Theta_2 \end{bmatrix} \cos \omega t \quad (12-26)$$

Substituting Eq. (12-26) into Eq. (12-25), canceling the common $\cos \omega t$ term, and collecting all coefficients in a single square matrix leads to

$$\begin{bmatrix} k_y - \omega^2 m & -rk_y \\ -rk_y & k_\theta + r^2 k_y - \omega^2 J_C \end{bmatrix} \begin{bmatrix} Y_1 \\ \Theta_2 \end{bmatrix} = \begin{bmatrix} 0 \\ 0 \end{bmatrix} \quad (12-27)$$

Setting to zero the determinant of the coefficient matrix gives the quadratic equation for the natural frequencies (the characteristic equation of the free-vibration problem),

$$mJ_C(\omega^2)^2 + \left[-m(k_\theta + r^2 k_y) - J_C k_y \right] \omega^2 + k_y k_\theta = 0 \quad (12-28)$$

For physically realistic values of the parameters in Eq. (12-28), there are two positive real roots, $\omega_1^2 < \omega_2^2$, one for each of the vibration modes, $n = 1, 2$. After these roots have been found, they can be substituted back into either scalar equation of matrix Eq. (12-27) to give equations for the mode shapes. We choose to use the first scalar equation (because it has fewer terms than the second), and we solve for pitch mode shape component Θ_2 in terms of vertical translation component Y_1 :

$$(k_y - \omega_n^2 m) Y_{1n} - r k_y \Theta_{2n} = 0 \Rightarrow \Theta_{2n} = \frac{k_y - \omega_n^2 m}{r k_y} Y_{1n}, \quad n = 1, 2 \quad (12-29)$$

There is an interesting physical feature of motion in a pure vibration mode that is sometimes exhibited by bodies such as the typical-section model of Fig. 12-4, bodies that both translate and rotate: whereas most of the body is vibrating at a natural frequency ω_n , there might be a particular point on the body that is completely motionless. Such a point is called a *node* or *nodal point* of the vibration mode. We can determine the location of a nodal point on the typical section by referring to Fig. 12-5, which shows both the airfoil in the static equilibrium position and the displaced chord line at some arbitrary instant during a cycle of pure modal vibration. We define on the diagram a stationary x axis with its origin at mass center C of the airfoil in the static equilibrium position. The

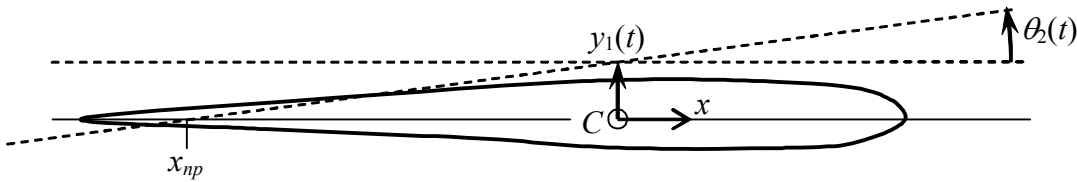


Figure 12-5 Nodal point of the 2-DOF typical section in a mode of vibration

coordinate x_{np} shown at the intersection of the static equilibrium chord line and the displaced chord line is the nodal point. Using the geometry of small rotation and the notation on Fig. 12-5, we have $y_1(t) \approx -x_{np} \theta_2(t)$; the minus sign is necessary because x_{np} as shown is negative (aft of point C), but the values of $y_1(t)$ and $\theta_2(t)$ shown are positive. Therefore, the location of the nodal point for vibration mode n is given by

$$(x_{np})_n = -\frac{y_1(t)}{\theta_2(t)} = -\frac{Y_{1n}}{\Theta_{2n}} \quad (12-30)$$

Chapter 12 Vibration modes of undamped mechanical systems with two degrees of freedom

If mode n is mostly translation, with little rotation, then the coordinate $(x_{np})_n$ might have such a large magnitude that there is no motionless point along the chord of the airfoil. However, if there is a nodal point on a typical section in a vibration test, one can easily observe it by sprinkling a little sand on the airfoil in the vicinity of the nodal point. As the body vibrates, the sand will migrate away from oscillating surfaces and accumulate on the motionless nodal point.

Rather than deal with an excessive number of algebraic symbols in equations such as (12-28), it is convenient now to consider a numerical example. A certain wind-tunnel typical section has a chord of 12 inches, weighs $mg = 5.00$ lb, has rotational “weight” about its mass center $J_C g = 90.0$ lb-inch², and has its mass center located $r = 3.00$ inches forward of the axis at which it is supported by lightweight flexible beams that function as springs. The spring constants provided by the beams are $k_y = 51.0$ lb/inch and $k_\theta = 920$ lb-inch/radian. The MATLAB session printed below evaluates Eqs. (12-28) through (12-30) for this numerical case.

```
>> mg=5.00;Jcg=90.0;r=3.00;g=386.1; %mass and inertia constants
>> ky=51.0;kt=920;format short e %stiffness constants
>> p=[mg*Jcg/g^2 -(mg*(kt+ky*r^2)+Jcg*ky)/g ky*kt] %coeffs of Eq.(12-28)

p =
3.0187e-003 -2.9746e+001 4.6920e+004

>> w_sqrd=roots(p) %roots w^2 of quadratic Eq.(12-28)

w_sqrd =
7.8822e+003
1.9720e+003

>> wn=[sqrt(w_sqrd(2)) sqrt(w_sqrd(1))] %circular natural frequencies
(in rad/sec) arranged in ascending order

wn =
4.4407e+001 8.8782e+001

>> fn=wn/2/pi %cyclic natural frequencies (in Hz)

fn =
7.0676e+000 1.4130e+001

>> Th2n=(ky-mg/g*wn.^2)/(r*ky) %Eq.(12-29) for mode shape components Θ2n,
with Y1n = 1 inch

Th2n =
1.6642e-001 -3.3382e-001

>> XNPn=(-1)./Th2n %Eq.(12-30) for locations of the nodal points
```

Chapter 12 Vibration modes of undamped mechanical systems with two degrees of freedom

XNPn =

-6.0087e+000 2.9956e+000

The numerical results of the MATLAB calculations are summarized in the following table:

Mode of vibration n	1	2
Natural frequency ω_n and $f_n = \omega_n / 2\pi$	$\omega_1 = 44.41 \text{ rad/sec}$ $f_1 = 7.068 \text{ Hz}$	$\omega_2 = 88.78 \text{ rad/sec}$ $f_2 = 14.13 \text{ Hz}$
Mode shape	$\begin{bmatrix} Y_{11} \\ \Theta_{21} \end{bmatrix} = \begin{bmatrix} 1 \text{ inch} \\ 0.1664 \text{ rad} \end{bmatrix}$	$\begin{bmatrix} Y_{12} \\ \Theta_{22} \end{bmatrix} = \begin{bmatrix} 1 \text{ inch} \\ -0.3338 \text{ rad} \end{bmatrix}$
Nodal point location $(x_{np})_n$	-6.01 inch	+3.00 inch

The vibration modes of this typical section are also displayed effectively in a graphical format, Fig. 12-6, which is comparable to Fig. 12-3 for the mass-spring system. Figure 12-6 indicates the airfoil in its reference position with a solid chord line, and in a modal displaced position with a dashed chord line. Let's suppose that mass center C is located 5 inches aft of leading edge LE along the 12-inch chord. In this case, the nodal points of both modes (listed in the table above) are located on the airfoil as shown on Fig. 12-6, not forward of LE or aft of trailing edge TE . For graphical clarity, the magnitudes of motions $y_1(t)$ and $\theta_2(t)$ are shown greatly exaggerated relative to the 12-inch chord. Actual motions of a realistic typical section would be tens or hundreds of times smaller.

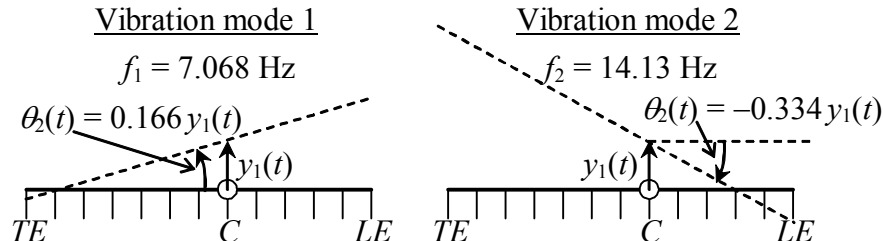
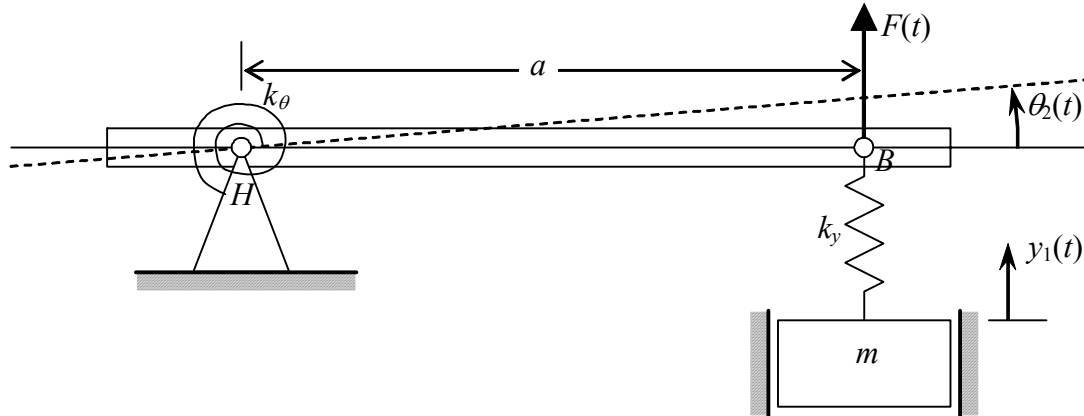


Figure 12-6 Vibration modes of the example typical section

12-4 Homework problems for Chapter 12

12.1 Consider again the 2-DOF system of homework Problem 11.2, depicted below.



The two coupled differential equations of motion for this system, as derived for homework Problem 11.2 and now expressed in matrix form, are

$$\begin{bmatrix} m & 0 \\ 0 & J_H \end{bmatrix} \begin{bmatrix} \ddot{y}_1 \\ \ddot{\theta}_2 \end{bmatrix} + \begin{bmatrix} k_y & -ak_y \\ -ak_y & k_\theta + a^2 k_y \end{bmatrix} \begin{bmatrix} y_1 \\ \theta_2 \end{bmatrix} = \begin{bmatrix} 0 \\ a F(t) \end{bmatrix}$$

All the parameters in these equations are defined on the figure except J_H , which is the rotational inertia of the bar about frictionless hinge H . Consider the free-vibration problem, with $F(t) = 0$. First, show that the characteristic equation in general is

$$m J_H (\omega^2)^2 + [-m(k_\theta + a^2 k_y) - J_H k_y] \omega^2 + k_y k_\theta = 0$$

Now, consider the following situation. Suppose that you are a design engineer working on a new satellite project for an aerospace company. You have designed a sensor package that includes a small mechanical device in the form of the subject 2-DOF system. The satellite has been fabricated, and is now being subjected to functional ground testing. The primary attitude-control actuator for the satellite is a *control-moment gyroscope* (CMG), the rotor of which spins at 11,400 rpm in normal operation. The spin-up time for this CMG is about four hours. During the first functional test, at the very end of the CMG spin-up, test engineers observe a short period of loud buzzing coming from the vicinity of your sensor package. The buzzing suddenly stops, and nobody thinks anything more about it until functional tests begin on your sensor. Unfortunately, the readings from your sensor are gibberish. The sensor package is removed and opened up, and examination shows that the 2-DOF device is completely destroyed: both springs are fractured, the bar is badly bent, the mass is detached, and the bar and mass have banged against near-by circuit boards within the package. It is now your responsibility to determine what went wrong. One experienced test engineer speculates that the 2-DOF device might have resonated due to base excitation caused by the CMG. Although the rotors of space-qualified CMGs are always carefully balanced, it is impossible to remove all im-

balance. Consequently, rotor-spin imbalance imposes small periodic forces at the spin rate onto the CMG supports, and these forces produce vibration that is transmitted in waves throughout the spacecraft structure. With the assistance of calibration technicians, you determine that the numerical parameters of the 2-DOF device are: $m = 19.2 \text{ g} = 0.0192 \text{ kg}$, $J_H = 37.3\text{e-}6 \text{ kg-m}^2$, $k_y = 16.9 \text{ N/mm} = 16.9 \text{ kN/m}$, $k_\theta = 12.8 \text{ N-m/rad}$, and $a = 30.0 \text{ mm} = 0.0300 \text{ m}$. Calculate the vibration modes of this system (natural frequencies, mode shapes, and sketches of the mode shapes), and discuss in a few sentences the probable cause of the structural failure within your satellite sensor package.

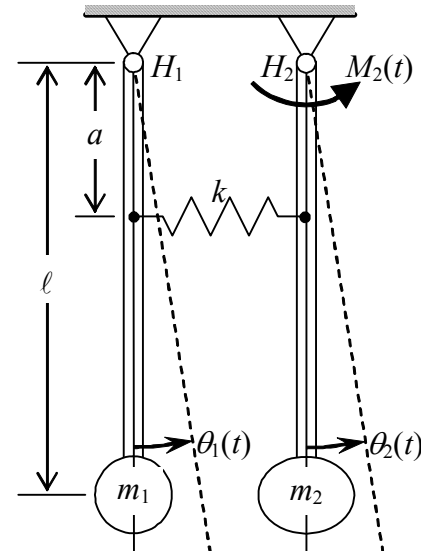
12.2 Consider again the 2-DOF pendulum-spring system of homework Problem 11.5, depicted below. The two coupled differential equations of motion for this system, as derived for homework Problem 11.5 and now expressed in matrix form, are

$$\begin{bmatrix} m_1\ell^2 & 0 \\ 0 & m_2\ell^2 \end{bmatrix} \begin{bmatrix} \ddot{\theta}_1 \\ \ddot{\theta}_2 \end{bmatrix} + \begin{bmatrix} m_1g\ell + ka^2 & -ka^2 \\ -ka^2 & m_2g\ell + ka^2 \end{bmatrix} \begin{bmatrix} \theta_1 \\ \theta_2 \end{bmatrix} = \begin{bmatrix} 0 \\ M_2(t) \end{bmatrix}$$

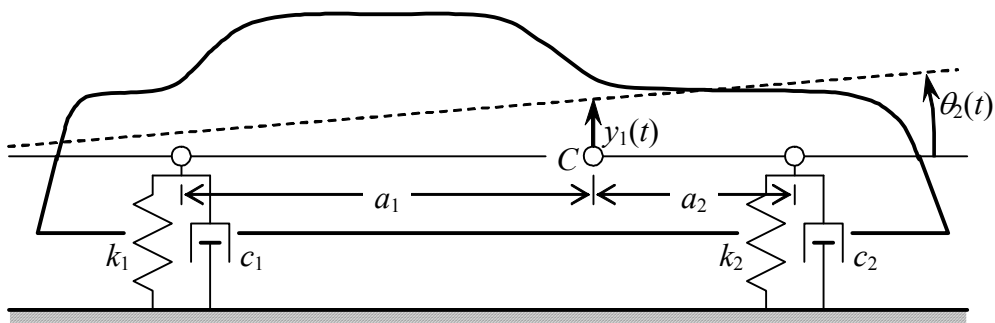
Consider the free-vibration problem, with $M_2(t) = 0$. It will simplify the writing if, initially, you will use the following notational abbreviations: $J_1 = m_1\ell^2$, $J_2 = m_2\ell^2$, $k_1 = m_1g\ell + ka^2$, $k_2 = m_2g\ell + ka^2$, and $k_c = ka^2$ (the “coupling” coefficient). First, show that the characteristic equation in general is

$$J_1 J_2 (\omega^2)^2 + (-J_2 k_1 - J_1 k_2) \omega^2 + k_1 k_2 - k_c^2 = 0$$

Now consider the special case with $m_1 = \frac{1}{2}m_2$ and $k_c = ka^2 = m_2g\ell$. Express all the coefficients of the characteristic equation in terms of m_2 , g , and ℓ , and then show that this quadratic equation can be put into the form $(\omega^2)^2 - 5(g/\ell)\omega^2 + 4(g/\ell)^2 = 0$. For this special case, solve for the natural frequencies and mode shapes, and sketch the mode shapes.



12.3 Consider again from homework Problem 11.6 the simplified model for pitching-translation dynamics of an automotive vehicle, depicted below. The rigid body frame has mass m and rotational inertia J_C about center of mass C .



The two coupled differential equations of motion for this system, as derived for homework Problem 11.6 and now expressed in matrix form, are

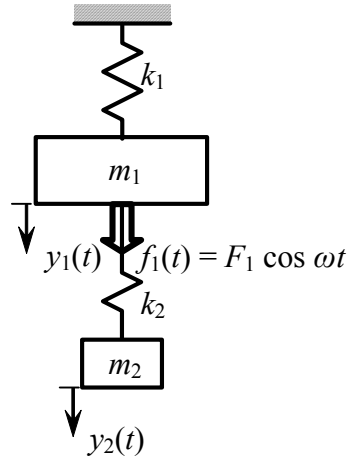
$$\begin{bmatrix} m & 0 \\ 0 & J_C \end{bmatrix} \begin{bmatrix} \ddot{y}_1 \\ \ddot{\theta}_2 \end{bmatrix} + \begin{bmatrix} c_1 + c_2 & c_2 a_2 - c_1 a_1 \\ c_2 a_2 - c_1 a_1 & c_1 a_1^2 + c_2 a_2^2 \end{bmatrix} \begin{bmatrix} \dot{y}_1 \\ \dot{\theta}_2 \end{bmatrix} + \begin{bmatrix} k_1 + k_2 & k_2 a_2 - k_1 a_1 \\ k_2 a_2 - k_1 a_1 & k_1 a_1^2 + k_2 a_2^2 \end{bmatrix} \begin{bmatrix} y_1 \\ \theta_2 \end{bmatrix} = \begin{bmatrix} 0 \\ 0 \end{bmatrix}$$

To obtain the vibration modes of the undamped system, we set $c_1 = c_2 = 0$, which deletes the entire second term of the matrix equation. The following data are representative for a compact four-door sedan: $mg = 2,150$ lb, $J_C g = 5.47e6$ lb-inch 2 , $k_1 = k_2 = 155$ lb/inch, $a_1 = 82.7$ inches, and $a_2 = 35.4$ inches. Calculate the natural frequencies, mode shapes, and nodal point locations, and sketch the mode shapes.

12.4 Consider again Fig. 12-2, but now suppose that the entire undamped mass-spring system consists of a primary sub-system, with mass m_1 and spring k_1 , plus a smaller auxiliary sub-system, with mass m_2 and spring k_2 ; also, that a steady sinusoidal force $f_1(t) = F_1 \cos \omega t$ acts upon m_1 , but no externally applied force acts upon m_2 , $f_2(t) = 0$. Your assignment is to solve for and evaluate the steady-state forced sinusoidal responses $y_1(t) = Y_1(\omega) \cos \omega t$ and $y_2(t) = Y_2(\omega) \cos \omega t$. To solve, use the theory developed in Section 12-2, not the more general procedure described in Section 4-7 for finding frequency-response functions.

- (a) Determine algebraic equations for $Y_1(\omega)$ and $Y_2(\omega)$ in terms of m_1 , k_1 , m_2 , k_2 , F_1 , and ω . Also, write the characteristic equation of the free-vibration problem, and explain what happens if its roots are substituted into the equations for $Y_1(\omega)$ and $Y_2(\omega)$.

Partial answer:
$$Y_2(\omega) = \frac{k_2 F_1}{(k_1 + k_2 - \omega^2 m_1)(k_2 - \omega^2 m_2) - k_2^2}$$

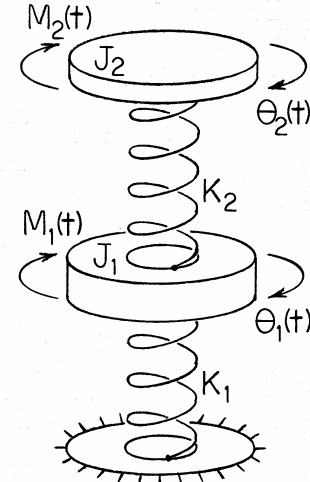


- (b) Suppose that this is a system for which *vibration isolation* is required: primary mass m_1 includes an unbalanced reciprocating motor or machine that oscillates with specific frequency $\omega = \Omega$, which tends to cause m_1 to vibrate vertically at frequency Ω ; but it is desirable to protect from that vibration the supporting structure to which primary spring k_1 is attached. (See homework Problem 10.13 for additional discussion of vibration isolation.) According to your solution in part (a), what happens to motion amplitudes $Y_1(\Omega)$ of m_1 and $Y_2(\Omega)$ of m_2 if you tune the single-DOF frequency of the auxiliary mass and spring, m_2 and k_2 , to the excitation frequency, *i.e.*, if you design the auxiliary sub-system so that $k_2/m_2 \equiv \Omega^2$? With $k_2/m_2 \equiv \Omega^2$, what is the sinusoidal force $k_2[y_2(t) - y_1(t)]$ that spring k_2 imposes on primary mass m_1 ? With the correct answers to these questions, you will have explained the functioning of an ideal *undamped dynamic vibration absorber*.

(c) An ideal undamped dynamic vibration absorber is unattainable in reality because systems always have some damping. Moreover, even if we could magically eliminate all damping, the ideal absorber would still have a serious deficiency: if the excitation frequency were to differ from the nominal value, which usually happens in practice during motor start-up or off-nominal operation, then the system could experience a 2-DOF resonance failure. Suppose, for example, we have the following numerical parameters: $m_1 = 25.3 \text{ kg}$, $k_1 = 2.62 \text{ MN/m}$, $\Omega/2\pi = 50 \text{ Hz}$, and the auxiliary sub-system is tuned to 50 Hz with $m_2 = 5.066 \text{ kg}$ and $k_2 = 0.5 \text{ MN/m}$. First, solve the characteristic equation to calculate the two system natural frequencies in Hz, $f_1 = \omega_1/2\pi < f_2 = \omega_2/2\pi$; if you wish, you may use the `roots` MATLAB function for this task. Next, calculate and plot versus excitation frequency (in Hz) the frequency-response dynamic flexibility, $Y_1(\omega)/F_1$, of the primary sub-system. The range of excitation frequencies over which you plot this response must include at least all three frequencies, f_1 , $\Omega/2\pi$, and f_2 ; it probably should even extend somewhat below the lowest of these three and somewhat above the highest. Be sure to include appropriate axis labels on your graph. Your graph should display clearly both the strengths and the weaknesses of the ideal undamped dynamic vibration absorber for these particular numerical parameters.¹

12.5 The drawing at right represents a rotational mechanical system that is directly analogous to the translational mechanical system of Fig. 12-2. Rotational inertias J_1 and J_2 are analogous, respectively, to masses m_1 and m_2 on Fig. 12-2; rotational springs K_1 and K_2 are analogous to translational springs k_1 and k_2 ; applied moments $M_1(t)$ and $M_2(t)$ are analogous to applied forces $f_1(t)$ and $f_2(t)$; and rotations $\theta_1(t)$ and $\theta_2(t)$ are analogous to translations $y_1(t)$ and $y_2(t)$. Therefore, the matrix equation of motion for this rotational system is directly analogous to Eq. (12-5) for the translational system:

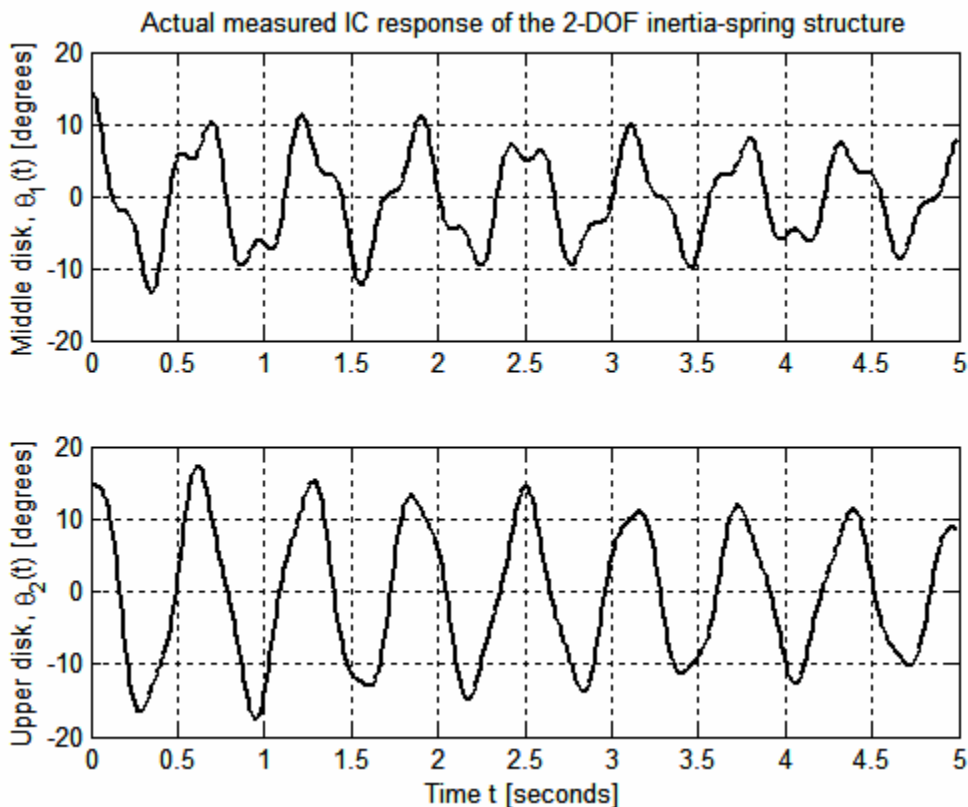
$$\underbrace{\begin{bmatrix} J_1 & 0 \\ 0 & J_2 \end{bmatrix}}_{\text{inertia matrix}} \underbrace{\begin{bmatrix} \ddot{\theta}_1 \\ \ddot{\theta}_2 \end{bmatrix}}_{\text{structural stiffness matrix}} + \begin{bmatrix} K_1 + K_2 & -K_2 \\ -K_2 & K_2 \end{bmatrix} \begin{bmatrix} \theta_1 \\ \theta_2 \end{bmatrix} = \begin{bmatrix} M_1(t) \\ M_2(t) \end{bmatrix}$$



Consider a 2-DOF inertia-spring system with rotational inertias $J_1 = J_2 = 0.01042 \text{ kg-m}^2$ and rotational stiffness constants $K_1 = K_2 = 2.77 \text{ N-m/rad}$. Your assignment is to calculate and plot, over the time interval $0 \leq t \leq 5$ seconds, the unforced initial-condition (IC) responses, rotations $\theta_1(t)$ and $\theta_2(t)$, of this system if the initial rotations are $\theta_1(0) = \theta_2(0) = 14.58$ degrees, and the initial rotational velocities are zero. Use the theory (and even the appropriate calculations, if you wish) of Section 12-2. The given inertias and stiffness constants are those of a real structural system, which is described on the next two pages, and the given initial conditions were imposed on that system, producing the measured responses shown on the graph following this paragraph. Your theoretical responses should

¹ Homework Problem 12.4 is only an introduction to the subject of dynamic vibration absorbers. See Den Hartog, 1956, Sections 3.2 and 3.3, for a more advanced and extensive treatment of this subject.

appear somewhat similar to the measured responses, but the theoretical and measured responses should differ in one significant respect. Read the description below of the actual structural system, then identify the property of all real mechanical dynamic systems that is not modeled by the theory of Chapter 12, and explain how this modeling deficiency is illustrated in the differences between the theoretical and measured responses shown on the graphs.



The photograph on the next page shows the relevant structural portion of the actual laboratory system² that is represented by the drawing on the previous page, and from which the IC-response graph above was measured. Three steel disks are attached to a continuous steel shaft of diameter about 3.2 mm. Each disk is 20 cm in diameter and 0.5 cm thick, with four radial slots to accommodate added masses. The total length of shaft between lower and upper disks is about 68 cm. The shaft is supported near the middle and upper disks by bearings, which impose some damping on the structure. The lower disk is clamped to the frame, so the shaft is fixed at the bottom but is free to twist everywhere else along its length. Two metal cylinders, each of nominal mass 0.5 kg, are bolted symmetrically at 9-cm radii to each of the middle and upper disks. The rotational inertias of the two bulked-up disks are orders of magnitude greater than that of the shaft, so this system is effectively a 2-DOF rotational structure, those DOFs being rotations $\theta_1(t)$ and $\theta_2(t)$ of the middle and upper disks, respectively. $\theta_1(t)$ and $\theta_2(t)$ are sensed by the optical encoders shown on the photograph; each encoder shaft is connected to the

² This is a Model 205a Torsional Plant designed and fabricated by Educational Control Products of Bell Canyon, California, USA.

structural shaft by a lightweight belt and pulleys, which add to the system some damping but negligible inertia.

A clever student determined experimentally the inertias and stiffness constants of this system, rather than relying on purely theoretical calculations, mostly by using the added-inertia method (from homework Problem 7.9). To determine J_2 and K_2 , the student clamped the middle disk to the frame, and then measured free-vibration frequencies of the upper disk [$\theta_2(t)$ with $\theta_1(t) = 0$], both bare and with symmetrically added combinations of the metal cylinders. The student determined J_1 and $K_1 + K_2$ by clamping the upper disk, and then measuring free-vibration frequencies of the middle disk [$\theta_1(t)$ with $\theta_2(t) = 0$]. The values of the parameters determined by this process are $J_1 = J_2 = 0.01042$ (± 0.00003) kg-m² and $K_1 = K_2 = 2.77$ (± 0.04) N-m /rad.

The initial rotations, $\theta_1(0) = \theta_2(0) = 14.58^\circ$, were imposed on the middle and upper disks by twang, also known as snapback, excitation: a fine thread was tied around the front cylinder of the middle disk, the thread was pulled laterally and the opposite end was anchored, thus imposing onto the middle disk the static initial rotation, then the thread was cut with scissors, abruptly releasing the middle and upper disks to free vibration. The structural shaft was fixed only at the bottom, so the initial rotation of the upper disk was the same as that of the middle disk.



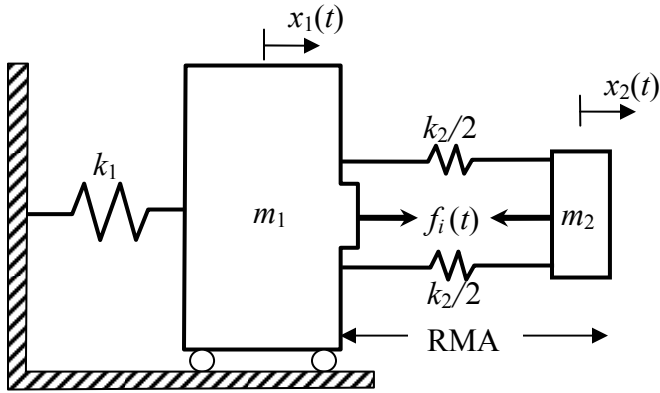
12.6 A structure's fundamental mode of vibration is represented in the drawing below by mass m_1 and spring k_1 , with the translation of m_1 denoted as $x_1(t)$. Suppose we wish to exercise active control over that vibration by use of an attachment to the structure: a reaction-mass actuator (RMA), represented in the diagram by reaction mass m_2 , spring k_2 , and internally generated force $f_i(t)$ acting equally and oppositely on m_2 and m_1 , with the translation of m_2 denoted as $x_2(t)$. (To simplify the equations here, we neglect the normally small natural passive damping inherent in both structures and RMAs.) Use Eq. (12-5) to write the matrix equation of motion for this combination of structure and RMA. Next, revise this equation to include the particular type of feedback vibration control described in the following. Suppose that reaction mass m_2 carries a transducer that senses the translational velocity of m_2 relative to that of m_1 and generates an electrical voltage signal proportional to that relative velocity, $e_v(t) = V(\dot{x}_2 - \dot{x}_1)$, where V is a calibration constant with units such as volt per meter/sec. Homework Problem 10.15 explains that an external voltage signal $e_i(t)$ [not shown on this drawing] commands internal force $f_i(t)$ according to the linear relationship $f_i(t) = G e_i(t)$, G being a constant with units such as newton per volt. Suppose that we multiply the relative velocity signal $e_v(t)$ by a variable gain factor F (using, e.g., a non-inverting amplifier, homework Problem 5.8) and then feed the multiplied signal back to serve as the force-command signal, $e_i(t) = F e_v(t) = F V(\dot{x}_2 - \dot{x}_1)$. Therefore, the generated internal force is $f_i(t) = G e_i(t) = GFV(\dot{x}_2 - \dot{x}_1) \equiv C(\dot{x}_2 - \dot{x}_1)$, where we define the overall feedback constant $C \equiv GFV$ with units such as newton per meter/sec. Revise your matrix equation of motion to reflect the feedback vibration control described here; in particular, show that the feedback produces an *artificial viscous damping matrix*,

$$C \begin{bmatrix} 1 & -1 \\ -1 & 1 \end{bmatrix}$$

With sufficiently large feedback gain factor F and sufficient authority of the RMA's internal force generator, this form of control can impose significant positive damping upon a structure's vibration.

NOTE: It is not required in this problem, but it might be of interest to you that replacing dependent variable $x_2(t)$ with the relative translation of reaction mass m_2 , $z(t) = x_2(t) - x_1(t)$ can transform the matrix equation of motion into the following form, in which the inertia matrix becomes full and symmetric, but the artificial damping and stiffness matrices become simpler and diagonal:

$$\begin{bmatrix} m_1 + m_2 & m_2 \\ m_2 & m_2 \end{bmatrix} \begin{bmatrix} \ddot{x}_1 \\ \ddot{z} \end{bmatrix} + \begin{bmatrix} 0 & 0 \\ 0 & C \end{bmatrix} \begin{bmatrix} \dot{x}_1 \\ \dot{z} \end{bmatrix} + \begin{bmatrix} k_1 & 0 \\ 0 & k_2 \end{bmatrix} \begin{bmatrix} x_1 \\ z \end{bmatrix} = \begin{bmatrix} 0 \\ 0 \end{bmatrix}$$



Chapter 13 Laplace block diagrams, and additional background material for the study of feedback-control systems

© 2016 by William L. Hallauer, Jr.

We will consider in Chapter 13 a graphical format, the Laplace block diagram, which is useful in the analysis of complicated systems that consist of more than one subsystem. While developing closed-loop block diagrams, we will also analyze the equation of motion and the time response of a base-excited mass-damper-spring system, which turns out to be an instructive prototype for output feedback control. All of this is preparation for the more general study of feedback-control systems beginning in Chapter 14.

13-1 Laplace block diagrams for an *RC* band-pass filter

To introduce the Laplace block diagram for a simple case, we re-visit again the *RC* band-pass filter considered previously in Sections 5-4, 9-10, and 10-4. As shown in Fig. 5-10, this circuit consists of a low-pass-filter stage to the left of the voltage follower, and a high-pass-filter stage to the right. The Laplace transforms derived for these stages in Section 10-4, assuming zero ICs, are: for the low-pass stage, with $\tau_L = R_L C_L$,

$$L[e_m] = \frac{1}{\tau_L s + 1} L[e_i] \quad (13-1)$$

and for the high-pass stage, with $\tau_H = R_H C_H$,

$$L[e_o] = \frac{\tau_H s}{\tau_H s + 1} L[e_m] \quad (13-2)$$

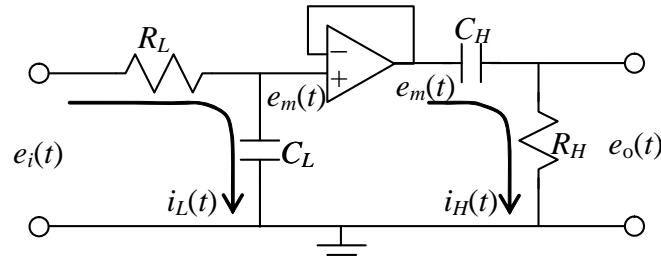


Figure 5-10 (repeated) *RC* band-pass filter

Figure 13-1 shows a convenient graphical format, the *block diagram*, for representing these Laplace-transform output-to-input relationships. From Eqs. (13-1) and (13-2), we have the individual transfer functions of the low-pass and high-pass stages:

$$TF_L(s) = \frac{L[e_m]}{L[e_i]} = \frac{1}{\tau_L s + 1} \quad (13-3)$$

$$TF_H(s) = \frac{L[e_o]}{L[e_m]} = \frac{\tau_H s}{\tau_H s + 1} \quad (13-4)$$

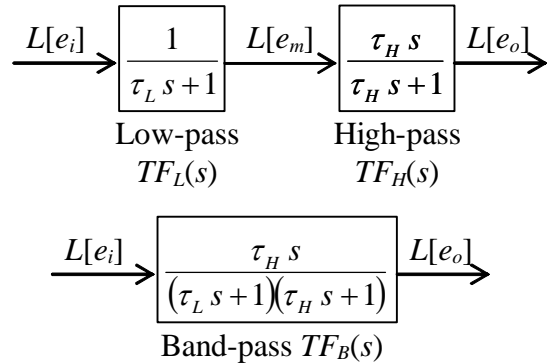


Figure 13-1 Laplace block diagrams of the *RC* band-pass filter

In the upper row of Fig. 13-1, transfer functions (13-3) and (13-4) are shown as individual blocks, and the Laplace transforms are shown as input and output “signals” relative to the blocks. The most basic rule of “block-diagram algebra” is that the input signal (transform) multiplied by the block transfer function equals the output signal (transform), which gives Eqs. (13-1) and (13-2).

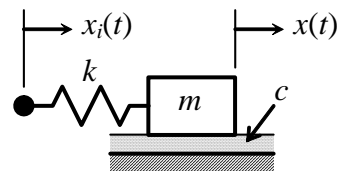
One common objective in construction of Laplace block diagrams is to simplify the process of deriving the transfer function of the overall system from the transfer functions of individual sub-systems. To help achieve this objective, we have the second basic rule of block-diagram algebra: multiply the transfer functions of two adjacent blocks in order to obtain the more general transfer function relating the output signal from the downstream block to the input signal into the upstream block. The result of this operation in the present case is shown in the lower row of Fig. 13-1, where transfer function (10-27) of the entire *RC* band-pass filter circuit is derived once again:

$$TF_B(s) = \frac{L[e_o]}{L[e_i]} = \frac{\tau_H s}{(\tau_H s + 1)(\tau_L s + 1)} \quad (13-5)$$

Each of the block diagrams in Fig. 13-1 has a single *forward* (left-to-right) *path* or *branch*. A more general type of block diagram has a forward branch and also one or more *backward paths* denoting signal flow in the opposite direction; such a right-to-left path is called a *feedback branch*. A forward branch combined with a feedback branch forms a *closed loop*, and a block diagram that includes closed loops is called a closed-loop block diagram. Accordingly, a block diagram with only a forward branch is called an *open-loop* block diagram. The next section develops the concept of closed-loop block diagrams in the context of a familiar mechanical system.

13-2 Laplace block diagram with feedback branches for an *m-c-k* system with base excitation

Let's proceed beyond the most basic aspects of Laplace block diagrams by analyzing the *m-c-k* system with base excitation shown on Fig. 13-2. The input is base translation $x_i(t)$, and the output is mass translation $x(t)$. The ODE of motion for this system (from homework Problem 9.1) is



$$m \ddot{x} + c \dot{x} + k x = k x_i(t) \quad (13-6)$$

Figure 13-2 *m-c-k* system with base excitation

It is convenient to denote the input transform as $L[x_i(t)] = X_i(s)$ and the output transform as $L[x(t)] = X(s)$. Taking the Laplace transform of Eq. (13-6) with zero ICs, for the purpose of deriving the transfer function, gives

$$m s^2 X(s) + c s X(s) + k X(s) = k X_i(s) \quad (13-7)$$

Equation (13-7) clearly leads to the transfer function,

$$TF(s) \equiv \frac{X(s)}{X_i(s)} = \frac{k}{m s^2 + c s + k} \quad (13-8) \quad \xrightarrow{X_i(s)} \boxed{\frac{k}{m s^2 + c s + k}} \xrightarrow{X(s)}$$

Equation (13-8) is represented in the simple open-loop Laplace block diagram just above.

It will be instructive for our later study of feedback control to develop now an alternative but equivalent block diagram from Eq. (13-7). First, we transpose to the right-hand side all terms other than the $X(s)$ term of highest order:

$$m s^2 X(s) = k X_i(s) - c s X(s) - k X(s) \quad (13-9)$$

Now we “solve” algebraically for $X(s)$ on the left-hand side of Eq. (13-9) simply by dividing through by the coefficient of the left-hand-side $X(s)$:

$$X(s) = \frac{1}{s} \left\{ \frac{1}{m s} [k X_i(s) - k X(s) - c s X(s)] \right\} \quad (13-10)$$

Observe in Eq. (13-10) that output transform $X(s)$ appears in the right-hand-side terms as well as on the left-hand side; these right-hand-side terms imply *feedback*. Using (13-10) leads to the following block diagram with several different transfer-function blocks and with two feedback branches:

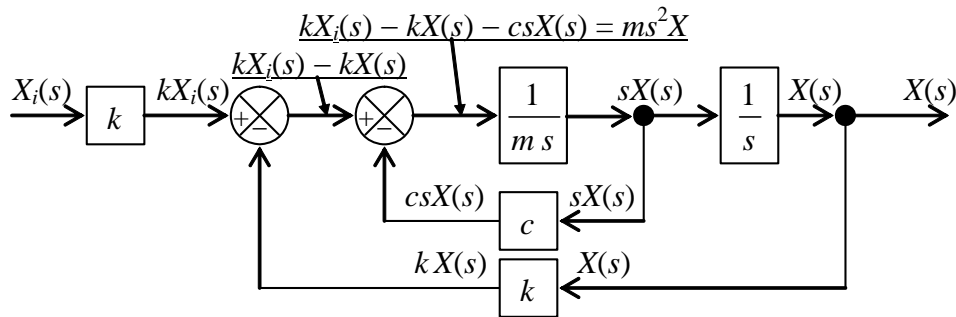
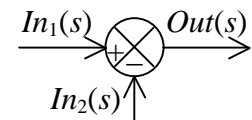


Figure 13-3 Laplace block diagram with feedback branches for a base-excited $m-c-k$ system

The input and output signals for every block are labeled on Fig. 13-3 in order to help you relate the block diagram to Eq. (13-10), and you should carefully compare the equation and the diagram until you are certain that you understand.

Also, block diagram Fig. 13-3 introduces two kinds of *junctions*. The first kind is a simple *branch point* (black circle), from which the same block-output “signal” travels onward on two different branches, as is indicated by the signal labels on Fig. 13-3. The second kind is a *summing junction*, shown at right with input and output signals la-



beled. This summing junction is configured for negative feedback, so it differences the two input signals, $Out(s) = In_1(s) - In_2(s)$.

In this section, we started with ODE (13-6) and developed from it Laplace block diagram Fig. 13-3. This approach is primarily for the purpose of presenting some important features of block diagrams. This approach is actually the reverse of the standard procedure for analysis of feedback-control systems, which we will consider in later chapters. There, we will start with the block diagram of a system, something like Fig. 13-3, and derive from it the *closed-loop transfer function*, $CLTF(s)$), which in this case is just Eq. (13-8). The process of deriving $CLTF(s)$ from the system block diagram will require some new operations in block-diagram algebra; it is expedient to postpone the descriptions of these operations until we need them in later chapters.

13-3 Forced response of an $m-c-k$ system with base excitation

It will be helpful for our introduction to feedback control in Chapter 14 if we now examine the relationship between input motion $x_i(t)$ and output motion $x(t)$ for the mechanical system of Fig. 13-2 and Eq. (13-6). Let's adopt the perspective here that we want to use $x_i(t)$ in order to control $x(t)$; in particular for this system, let's suppose that we want to make motion $x(t)$ of mass m be as close as possible to input motion $x_i(t)$. You can visualize intuitively from Fig. 13-2 that if $x_i(t)$ is imposed very slowly, then $x(t)$ will be essentially the same as $x_i(t)$; in this case, the inertial force of mass m will be negligible, and spring k will deform only slightly, therefore acting essentially as a rigid link. (You can, of course, prove theoretically this qualitative analysis, for example, by finding frequency response at a very low input frequency.)

But can output motion $x(t)$ be made close to input $x_i(t)$ if $x_i(t)$ is not imposed slowly? Your intuition probably fails to answer this question because, in this case, spring k might deform significantly, and the inertial force of mass m might not be negligible. We will have to analyze this situation theoretically. Let's do so specifying that input motion $x_i(t)$ is a step function of magnitude X_H imposed at time $t = 0$. An ideal step input is not merely fast; it is in fact the fastest imaginable (though not physically realizable) base excitation, because base position changes with infinite velocity at $t = 0$ from $x_i = 0$ to $x_i = X_H$. So this ideal input poses a formidable challenge to the control objective: can output translation $x(t)$ approximate in some reasonable manner the input translation $x_i(t)$, even though initially the input translation is infinitely fast?

In order to analyze this case, let's first adapt ODE (13-6) to the standard ODE for damped 2nd order systems as it is defined in Chapter 9. Dividing Eq. (13-6) through by m , and then applying the standard definitions (7-3) for undamped natural frequency, $\omega_n = \sqrt{k/m}$, and (9-4) for viscous damping ratio, $\zeta = c/(2\sqrt{mk})$, casts the ODE into the form $\ddot{x} + 2\zeta\omega_n\dot{x} + \omega_n^2x = \omega_n^2x_i(t)$. Comparing this ODE with Eq. (9-13) shows that in-

put $x_i(t)$ for this particular base-excited $m\text{-}c\text{-}k$ system is exactly equal to the standard input quantity: $x_i(t) \equiv u(t)$. We define step input $x_i(t) = X_H H(t)$. Therefore, $X_H \equiv U$, which is the general step-input magnitude of Section 9-6, and we can write the step-response solution for $|\zeta| < 1$ directly from Eq. (9-29):

$$x(t) = X_H \left[1 - e^{-\zeta\omega_n t} \left(\cos \omega_d t + \frac{\zeta\omega_n}{\omega_d} \sin \omega_d t \right) \right], \text{ for } 0 \leq t \quad (13-11)$$

In Eq. (13-11), the damped natural frequency is $\omega_d \equiv \omega_n \sqrt{1 - \zeta^2}$. Also, for use in Fig. 13-4, the period of the undamped system is $T_n = 2\pi/\omega_n$. Recall that our control objective is to make the output motion at least approximately equal to the input motion. At $t = 0$, input motion $x_i(t)$ jumps discontinuously from 0 to X_H , then x_i remains constant thereafter, so we would like the output motion $x(t)$ to approximate that step input as closely as possible. In particular, we want the final, steady-state value of $x(t)$ to be X_H .

It is instructive to calculate and graph Eq. (13-11) for a few different values of ζ , assuming that the system is underdamped, $0 \leq \zeta < 1$. The step-response graphs are shown on Fig. 13-4. If the system is undamped, $c = 0$, then the mass oscillates forever (in theory) about the desired final position, $x = X_H$; in this ideal (with zero damping) case, the control objective cannot be achieved.

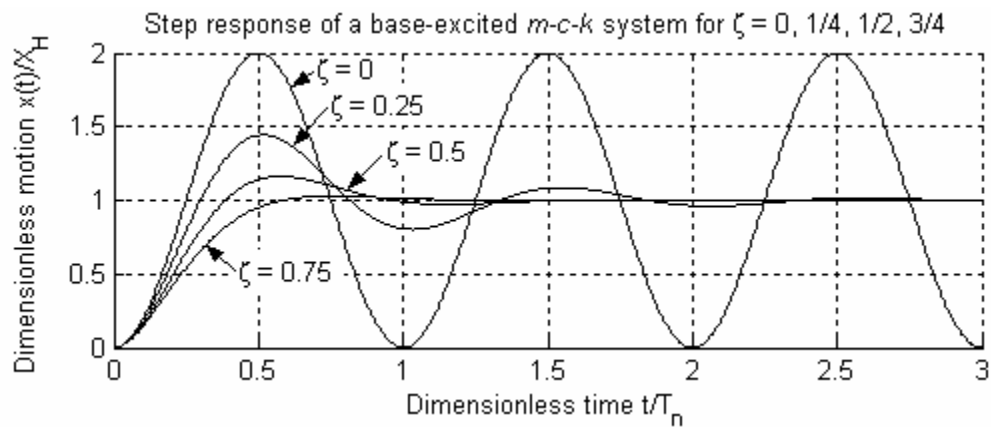


Figure 13-4 Base-excitation control of mass position for an $m\text{-}c\text{-}k$ system

However, Fig. 13-4 also demonstrates that, if there is positive damping, $\zeta > 0$, then the motion output $x(t)$ does, indeed, approximate the step input, $x_i(t) = X_H H(t)$: $x(t)$ rises from 0, though with finite velocity, and it eventually settles at the desired final value, $x = X_H$.

Chapter 13 Laplace block diagrams; background material for the study of feedback-control systems

Note that the equations for step-response specifications (rise time, peak time, maximum overshoot ratio, and settling time) derived in Section 9-8 are applicable to this case of excitation of an $m-c-k$ system by base motion.

The base-excited mass-damper-spring system of Fig. 13-2 is an instructive prototype for output feedback control of mechanical position, which is the subject of Chapter 14. Therefore, we shall refer back to this system and to the results of Sections 13-2 and 13-3 in order to clarify and justify some of the control-system developments presented in Chapter 14.

13-4 Homework problems for Chapter 13

13.1 Consider the standard ODE (3-7) for a stable 1st order system, $\dot{x} + (1/\tau_1)x = bu(t)$, in which $u(t)$ is the input quantity, $x(t)$ is the output quantity, τ_1 is the positive time constant, and b is a constant. Denote the Laplace transforms as $L[u(t)] = U(s)$ and $L[x(t)] = X(s)$. Derive and draw for this system a Laplace block diagram with feedback, a block diagram of the same type as Fig. 13-3. The input signal on the left side of your block diagram is $U(s)$, and the output signal on the right side is $X(s)$.

13.2 With input and output voltages $e_i(t)$ and $e_o(t)$, respectively, the governing ODE for the electrical LRC series circuit is $L\ddot{e}_o + R\dot{e}_o + (1/C)e_o = (1/C)e_i(t)$, as derived in Section 9-2. Denote the Laplace transforms as $L[e_i(t)] = E_i(s)$ and $L[e_o(t)] = E_o(s)$, then derive and draw for this system a Laplace block diagram with feedback, a block diagram of the same type as Fig. 13-3. The input signal on the left side of your block diagram is $E_i(s)$, and the output signal on the right side is $E_o(s)$.

13.3 A certain 3rd order system has excitation $u(t)$ and response $x(t)$, and its governing ODE is $a_1\ddot{x} + a_2\dot{x} + a_3x = bu(t)$, in which all a_i and b are constants. Denote the Laplace transforms as $L[u(t)] = U(s)$ and $L[x(t)] = X(s)$. Derive and draw for this system a Laplace block diagram with feedback, a block diagram of the same type as Fig. 13-3, but somewhat more complicated. The input signal on the left side of your block diagram is $U(s)$, and the output signal on the right side is $X(s)$. Your block diagram should have three feedback branches.

13.4 Consider the higher-order (4th order in this case), 2-DOF mechanical system of homework Problems 11.2 and 12.1, for which the coupled matrix equation of motion is

$$\begin{bmatrix} m & 0 \\ 0 & J_H \end{bmatrix} \begin{bmatrix} \ddot{y}_1 \\ \ddot{\theta}_2 \end{bmatrix} + \begin{bmatrix} k_y & -ak_y \\ -ak_y & k_\theta + a^2k_y \end{bmatrix} \begin{bmatrix} y_1 \\ \theta_2 \end{bmatrix} = \begin{bmatrix} 0 \\ aF(t) \end{bmatrix}$$

(a) From the matrix equation, write the two separate scalar ODEs that are coupled by the term $-ak_y\theta_2$ in the “ $y_1(t)$ ODE” (i.e., the ODE that includes acceleration \ddot{y}_1), and the term $-ak_y y_1$ in the “ $\theta_2(t)$ ODE.” This system has the single input, force $F(t)$, but two output quantities, translation $y_1(t)$ of the mass, and rotation $\theta_2(t)$ of the rigid bar.

(b) Denote the Laplace transforms as $L[F(t)]$, $L[y_1(t)] = Y(s)$, and $L[\theta_2(t)] = \Theta(s)$. Take the Laplace transforms of both ODEs, with zero ICs. Now, derive and draw for this system a Laplace block diagram (in the form of Fig. 13-3, but with differences) that has feedback and also “feed-across” between the forward-flowing branch that develops from the $y_1(t)$ ODE and the forward-flowing branch that develops from the $\theta_2(t)$ ODE. The input signal on the left side of your block diagram is $L[F(t)]$, and the two output signals on the right side are $Y(s)$ and $\Theta(s)$, one from each of the forward-flowing branches.

Chapter 14 Introduction to feedback control: output operations for control of rotational position

© 2016 by William L. Hallauer, Jr.

14-1 Initial definitions and terminology

As an introduction to feedback control and related matters, this chapter considers a common task for many engineering systems: *remote (indirect) control* of the rotational position of some solid body; let's refer to this solid body generically as the *rotor*. The input to a rotation-control system is typically a *command* issued by a human operator using a device such as a steering wheel, control column, dial, computer keyboard, *etc.*; the input can also be a computer-generated signal that carries previously programmed instructions. The output is the rotational position of the rotor. The modifiers “remote” and “indirect” of “control” mean that there is no direct, rigid, mechanical linkage between the input device and the rotor; instead, for a remote control system, there might exist between the input device and the rotor such engineering equipment as sensors, electrical circuits, signal processors (analog and/or digital), flexible links or cables, electromagnetic or acoustic transmitters and receivers, and actuators of many types (motors, thrusters, *etc.*).

The following are a few of the many “rotors” in modern engineering practice with which you are probably familiar: aerodynamic and hydrodynamic control surfaces, such as rudders, elevators, and ailerons; the steering mechanisms that guide land vehicles and taxiing airplanes; nozzles of rocket engines or vectored-thrust jet engines; any entire vehicle itself, the three-dimensional rotational orientation (roll, pitch, yaw) of which is generally called the vehicle’s *attitude*. You can probably add other rotors to this list from your own experience.

In general, the mass center of a solid body can have three degrees of rotational freedom. However, in order to keep the rotational dynamics simple here and to focus on feedback control, we will restrict our attention to rigid rotors that rotate in a plane about a fixed point, so that there is only one degree of rotational freedom.

Consider the simple generic rotor shown in Fig. 14-1. Let's specify that it is restricted to rotating about the shaft axis, that its rotation angle relative to some reference

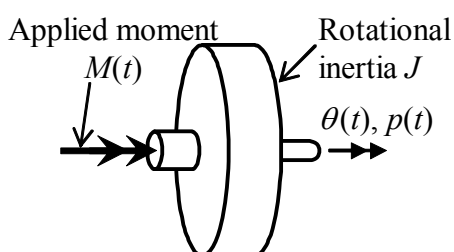


Figure 14-1 Generic rotor, the *plant*

position is $\theta(t)$, and that its angular velocity is $p(t) \equiv \dot{\theta}$. The rotational inertia of the rotor about the axis of rotation is denoted as J , and the total moment applied onto the rotor by all sources is denoted as $M(t)$. This is the physical object that we wish to control; in the terminology of control, the object or process to be controlled is often called the *plant*.

Provided that there is no damping moment proportional to $p(t)$ imposed upon the rotor, the equation of motion for the plant of Fig. 14-1 is a simplified version of Eq. (3-1):

$$J \dot{\theta} = J \ddot{\theta} = M(t) \quad (14-1)$$

Let's derive the transfer function of the plant, $PTF(s)$, by taking the Laplace transform of Eq. (14-1) with zero initial conditions:

$$J s^2 L[\theta(t)] = L[M(t)] \Rightarrow PTF(s) \equiv \frac{L[\theta(t)]}{L[M(t)]} = \frac{1}{J s^2} \quad (14-2)$$

In our previous work, we usually assumed that $M(t)$ is known, and we then solved for the resulting $p(t)$ and/or $\theta(t)$. Now, our objective is different: for control, we want to command a desired rotor-position time history. The command usually is something like a steering-wheel position or dial setting, or a signal carrying computer-generated instructions. In order to distinguish the input command from the output rotor angle, we introduce a different symbol for the command:

$$r(t) \equiv \text{operator setting intended to produce the desired } \theta(t) \quad (14-3)$$

Operator setting $r(t)$ is the *reference* input quantity, which is transmitted to the system by electrical circuitry, mechanical linkages or cables, electromagnetic or acoustic waves, *etc.*

14-2 More definitions, and examples of open-loop control systems

As an initial attempt to produce the desired motion history $\theta(t)$, it is probably most natural simply to seek the input setting $r(t)$ that will do the job completely, without the need for any further design refinement. This type of control is called *open-loop* control, for reasons that will be given later. Figure 14-2 depicts an open-loop control system.

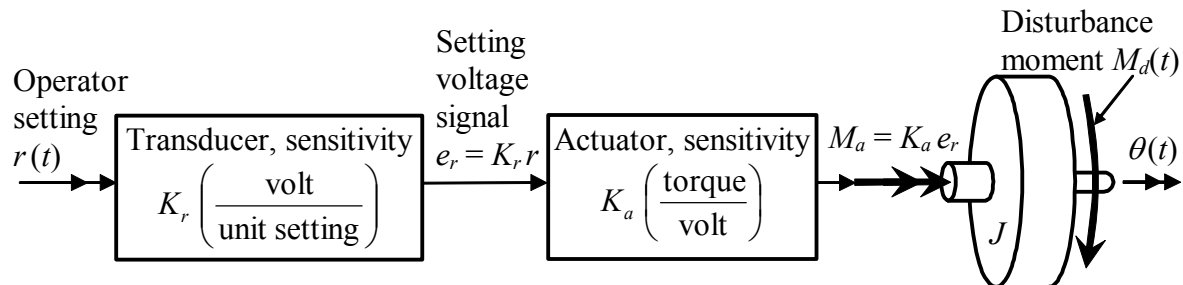


Figure 14-2 Functional diagram of open-loop rotor-position control system

Operator setting $r(t)$ is shown in Fig. 14-2 as a general quantity, and the input transducer is assumed to be a general linear device that produces voltage signal $e_r(t) = K_r r(t)$; if the input device were a rotary dial, for example, the operator setting might be a rotational position in degrees, and the transducer might be a variable resistor in a voltage divider circuit (see homework Problems 5.1 and 5.9), with accurately calibrated sensitivity of K_r volts per degree. The actuator also is assumed to be a general linear device

that produces control moment $M_a(t) = K_a e_r(t) = K_a K_r r(t)$; if it were an electromagnetic actuator, for example, it would probably consist of a power amplifier and a motor, both of which are designed to function linearly. In practice, device sensitivity constants do not have to be positive and often are negative, but let's assume here that all are positive ($K_a > 0, K_r > 0$, etc.) just to avoid unnecessary complications.

Also shown on Fig. 14-2 is *disturbance* moment $M_d(t)$ acting upon the rotor. In the terminology of control, a disturbance is some extraneous action upon the plant, not the intended control action. In the system of Fig. 14-2, for example, an actuator moment produced by unwanted electrical noise in the circuitry would be an *internal* disturbance, and a moment produced by wind or impact from solid objects onto the rotor would be an *external* disturbance. Disturbances are often random, or at least unpredictable, so that we usually cannot write equations to describe their variation with time. In most cases, disturbances tend to influence adversely the performance of a control system.

Let's analyze the control system of Fig. 14-2. The total moment acting upon the rotor is $M_a(t) + M_d(t)$, so that Eq. (14-1) becomes

$$J\ddot{\theta} = M_a(t) + M_d(t) = K_a K_r r(t) + M_d(t) \quad (14-4)$$

Disturbance $M_d(t)$ in Eq. (14-4) is the nemesis of open-loop control, so let's consider initially the case with zero disturbance, $M_d(t) = 0$. If we have an equation for the desired motion history $\theta(t)$, then we can solve (14-4) directly for the required operator setting:

$$r(t) = \frac{J}{K_a K_r} \ddot{\theta} \quad (14-5)$$

This method for finding $r(t)$ is easy, and open-loop control appears to be a feasible engineering tool. However, open-loop control has some serious deficiencies. A more detailed example will help to reveal these deficiencies, so we consider next an application of open-loop attitude control for a spacecraft.

Suppose that a capsule carrying astronauts is re-entering Earth's atmosphere, Fig. 14-3, and that pitch angle $\theta(t)$ must be controlled in order to position the heat shield for optimal functioning and to prevent unstable tumbling. Two collinear pairs of gas thrusters (usually fueled by liquid chemicals) are separated by moment arm e so that they actuate rotation by a couple (pure moment), without causing mass center C to translate. Firing of the two thrusters shown active on Fig. 14-3 produces a positive couple, and firing of the two opposite collinear thrusters would produce a negative couple. To simplify the analysis, let's assume that the thrusters are continuously throttleable, so that thrust force is related linearly to the operator setting by

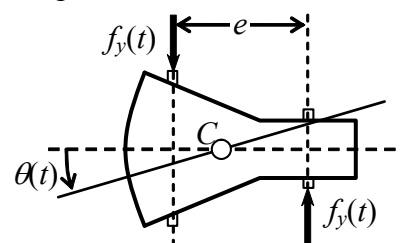


Figure 14-3 Pitch control of a re-entry capsule

$$f_y(t) = K r(t) \quad (14-6)$$

In Eq. (14-6), K is a positive sensitivity constant, with appropriate dimensions depending upon the specific character of $r(t)$. Then the control moment is $M_a(t) = e f_y(t) = e K r(t)$, so that the equation of motion equivalent to Eq. (14-4) is

$$J \ddot{\theta} = M_a(t) + M_d(t) = e K r(t) + M_d(t) \quad (14-7)$$

in which J is the capsule's rotational inertia about mass center C . If we neglect all possible disturbances, $M_d(t) = 0$, then we can solve Eq. (14-7) for the required operator setting in terms of the desired pitching maneuver:

$$r(t) = \frac{J}{eK} \ddot{\theta} \quad (14-8)$$

For example, let's require that the spacecraft rotate smoothly from $\theta = 0$ to final pitch angle $\theta = \theta_f$ during t_f seconds, according to the lower time history graphed on Fig. 14-4, which is expressed by the equation¹

$$\theta(t) = \frac{\theta_f}{\pi} \left[\frac{\pi}{t_f} t - \frac{1}{2} \sin\left(\frac{2\pi}{t_f} t\right) \right] \quad (14-9)$$

for $0 \leq t \leq t_f$. Differentiating Eq. (14-9) twice and then substituting the result into Eq. (14-8) leads to

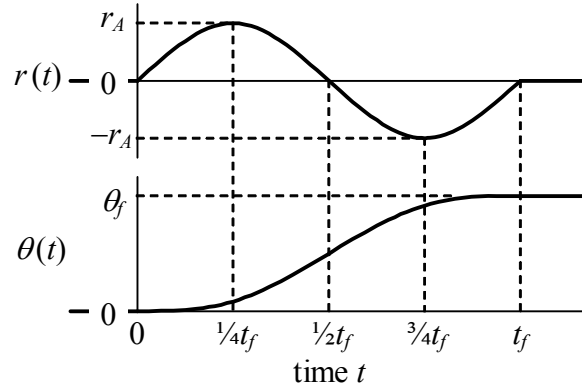


Figure 14-4 Example operator setting and resulting pitch maneuver for re-entry capsule

$$r(t) = r_A \sin\left(\frac{2\pi}{t_f} t\right), \quad r_A \equiv \frac{2\pi J \theta_f}{e K t_f^2}, \quad \text{for } 0 \leq t \leq t_f \quad (14-10)$$

This reference input setting $r(t)$ is shown on the upper graph of Fig. 14-4.

Note that Eqs. (14-9) and (14-10) and Fig. 14-4 illustrate the impulse-momentum theorem for 1-DOF rotation, which is directly analogous to the impulse-momentum theorem for 1-DOF translation (Section 8-2). The control moment is proportional to $r(t)$, $M_a(t) = e K r(t)$, so the $r(t)$ time history shows that the total moment impulse (area under the moment curve) in this maneuver is zero; since the total impulse is zero, the final ($t \geq$

¹ Maneuver time history Eq. (14-9) comes from Sarafin, 1995, pages 644-645, a book that includes additional interesting discussions of spacecraft attitude control.

t_f) angular momentum also is zero, $J\dot{\theta} = 0$, so the spacecraft is rotated to the final position $\theta = \theta_f$ with zero final rotational velocity, $\dot{\theta} = 0$.

Let's pause for a reality check. One feature of the control equipment described for this spacecraft maneuver is not practically realistic: space qualified gas thrusters in common use are nonlinear on-off (approximately) force generators; they are not continuously throttleable as assumed in this example, Eq. (14-6). Gas thrusters are, in fact, used to actuate spacecraft attitude and position control, but their on-off character produces rougher motion (abrupt changes in acceleration) than that of Eq. (14-9); see Sarafin, 1995, pp. 636-637. A smooth maneuver such as Eq. (14-9) would be actuated in practice by a space-qualified reaction wheel or control-moment gyroscope. We have assumed the hypothetical throttleable gas thrusters for this example just because it is easy to visualize this situation and to describe it in equations.

Now, with reference to the example above of spacecraft attitude control, let's evaluate open-loop control as represented generally by Fig. 14-2, with particular interest in identifying the following deficiencies:

1. Note from Fig. 14-4 that output $\theta(t)$ is not a single-valued, monotonic function of operator setting $r(t)$. For example, to $r = 0$ there correspond three different output values: $\theta = 0$ before the maneuver, $\theta = \frac{1}{2}\theta_f$ during the maneuver, and $\theta = \theta_f$ after the maneuver. This type of complicated functional relationship is not necessarily an operational deficiency, but it certainly is counter-intuitive to the natural engineering expectation of a unique, monotonic, often linear relationship between cause and effect.
2. Equations (14-5), (14-8), and (14-10) show that the validity of derived operator setting $r(t)$ is directly dependent upon the accuracy of the plant parameters and control system sensitivities, and upon the fidelity of the theoretical model of the system. If, for example, we use an inaccurate value of rotational inertia J (a distinct possibility for most vehicles, since burning of fuel changes inertias), or if the thrusters fail to function exactly as we model them, then the derived $r(t)$ clearly will not lead to the exact desired rotation time history, $\theta(t)$.
3. The $r(t)$ equations (14-5) and (14-8) are predicated on the absence of disturbances; but if $M_d(t) \neq 0$, then the derived $r(t)$ will fail to produce the exact desired $\theta(t)$. In practice, unpredictable disturbances are common, and they should not be ignored. For example, moments that can act upon a re-entering spacecraft might be produced by atmospheric drag, impact from space debris, astronauts shifting position within the vehicle, etc.

Deficiencies 2 and 3 above can be described in a more general manner: the performance of an open-loop control system is strongly dependent upon the quality of the theoretical model of the system and its environment; in other words, the control performance is

highly sensitive to imperfections in the theoretical model, which are inevitable for most real engineering situations.²

It is a fundamental characteristic and weakness of open-loop control that the actual output is not measured and compared with the desired output, for the purposes of assessing the output error and attempting to reduce the error. A simple and natural remedy for this weakness is to “close the loop” with feedback, which is described in the next section. Note that the absence of a feedback branch from Fig. 14-2 leads to the designation “open-loop.” But even this designation is at least a little misleading because there is no “loop” at all; there is simply a single branch that carries forward-flowing signals!

14-3 Closed-loop control of rotor position using position feedback

Let’s modify the open-loop control system of Fig. 14-2 in the following manner: measure the output with a rotational-position sensor, and send the voltage output from this sensor back to a summing junction that forms the *error signal*, which is the difference between the signal representing the operator setting and the signal representing the actual output. The feedback branch and summing junction convert the open-loop system into the *closed-loop* system depicted on Fig. 14-5.

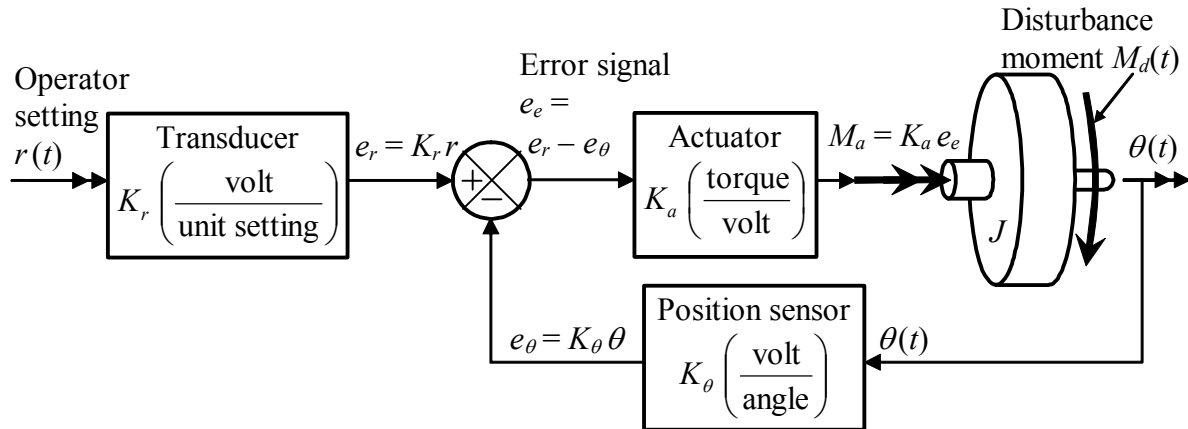


Figure 14-5 Functional diagram of position-feedback control system

The elements of the closed-loop system are the same as those of the open-loop system, Fig. 14-2, but with the addition of the output sensor and the summing junction (defined in Section 13-2). We assume that the sensor is a device such as an optical encoder, with accurately calibrated positive sensitivity K_θ (volt per degree or radian). The summing junction could be a simple circuit consisting of an inverting amplifier (Fig. 5-8) and a summing inverting amplifier (homework Problem 5.7).

This closed-loop system tends to be *self-correcting*. We can understand this tendency by writing in detail the equation for the control moment, from the signals labeled on Fig. 14-5:

² In the language of control engineering, a control system is described as *robust* if its performance and stability are insensitive to potentially detrimental influences such as disturbances, deficiencies in the theoretical model of the plant, and inaccurate response measurements due to sensor dynamics.

$$M_a(t) = K_a e_e(t) = K_a [e_r(t) - e_\theta(t)] = K_a [K_r r(t) - K_\theta \theta(t)] \quad (14-11)$$

From Eq. (14-11), the control moment is zero when $K_r r(t) - K_\theta \theta(t) = 0$, so that

$$\theta(t) = \frac{K_r}{K_\theta} r(t) \quad (14-12)$$

Equation (14-12) clearly is the desired instantaneous linear relation of output $\theta(t)$ to input $r(t)$. At instants when (14-12) is not satisfied, the control actuator imposes a corrective moment. Suppose, for example, that at a certain instant both $\theta(t)$ and $r(t)$ are positive, but that the output is less than the desired value, $\theta(t) < [K_r / K_\theta] r(t)$; at this instant, then, the error signal is $K_r r(t) - K_\theta \theta(t) = e_e(t) > 0$, and $M_a(t) = K_a e_e(t) > 0$; thus, when the output is less than it ought to be, the closed-loop control system imposes a positive moment to increase the output. Moreover, by reversing the inequality signs above, you can show that the control system imposes a negative moment to decrease the output when the output is greater than it ought to be.

Because the corrective moment is proportional to the output error and is independent of the theoretical model, the self-correcting tendency of this closed-loop control system is in effect regardless of how well the theoretical model represents the system and its environment.

To infer more information about the closed-loop system of Fig. 14-5, let's derive the ODE of motion by substituting Eq. (14-11) into Eq. (14-4):

$$\begin{aligned} J\ddot{\theta} &= M_a(t) + M_d(t) = K_a [K_r r(t) - K_\theta \theta(t)] + M_d(t) \\ \Rightarrow J\ddot{\theta} + K_a K_\theta \theta &= K_a K_r r(t) + M_d(t) \end{aligned} \quad (14-13)$$

From Eq. (14-13), we make the following observations: (1) the feedback control in Fig. 14-5 has the effect of attaching between the operator setting and the rotor inertia an artificial restoring spring with stiffness constant $K_a K_\theta$; (2) if only operator input $r(t)$ acts, i.e., if $M_d(t) = 0$, then the desired output (14-12) is actually the pseudo-static response of the system (as defined in Section 7-1),

$$K_a K_\theta \theta_{ps} = K_a K_r r(t) \Rightarrow \theta_{ps}(t) = \frac{K_r}{K_\theta} r(t) \quad (14-14)$$

(3) if only operator input $r(t)$ acts, and if the input-transducer sensitivity equals the output-sensor sensitivity, $K_r = K_\theta$, then the closed-loop system is directly analogous to an undamped, base-excited mass-spring system [as described by Eq. (13-6) with $c = 0$]; (4) the self-correcting tendency even counteracts the adverse influence of many types of

disturbance, which we can conclude from our previous experience with forced-response solutions for 2nd order systems. If, for example, the disturbance is time-limited, such as a pulse, then post-pulse response due to the pulse will oscillate about zero but will not contain any constant steady-state component. If, for another example, the disturbance is sinusoidal, then the resulting response will oscillate about zero but will not contain any constant steady-state component; however, we can also see that if the frequency of the sinusoidal disturbance is in the neighborhood of the closed-loop system natural frequency, $\omega_n = \sqrt{K_a K_\theta / J}$, then the disturbance could produce resonance, which this particular control system could not prevent.

To establish the method for analysis later of more complicated control systems, let's draw and analyze the Laplace block diagram corresponding to functional diagram Fig. 14-5. For this task, we define the following Laplace transforms: $L[r(t)] \equiv R(s)$, $L[\theta(t)] \equiv \Theta(s)$, $L[e_r(t)] \equiv E_r(s)$, $L[e_\theta(t)] \equiv E_\theta(s)$, $L[e_e(t)] \equiv E_e(s)$, $L[M_a(t)] \equiv M_a(s)$, $L[M_d(t)] \equiv M_d(s)$, and $L[M(t)] \equiv M(s)$. The Laplace block diagram, Fig. 14-6, is similar to the functional diagram, except that we replace the rotor in Fig. 14-5 with its transfer function, $PTF(s)$ of Eq. (14-2), and we use a summing junction to denote the actions upon the rotor of both control moment $M_a(t)$ and disturbance moment $M_d(t)$.

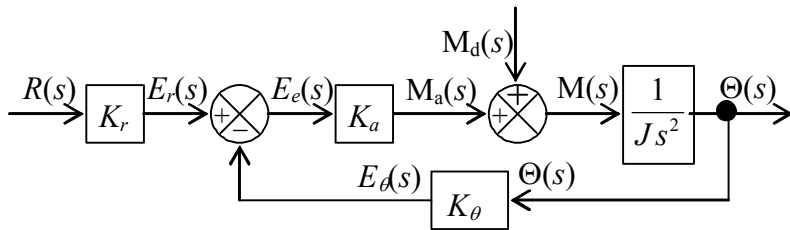


Figure 14-6 Laplace block diagram, including disturbance input, of position-feedback control system

This system actually has two independent inputs, $r(t)$ and $M_d(t)$, so it is not strictly a single-input-single-output (SISO) system. However, the most important fundamental relationship for this control system is that between the reference input and output $\theta(t)$, so we now will focus on that relationship by setting $M_d(t) = 0$. Therefore, $M_d(s) = 0$, and we re-draw Fig. 14-6 as the SISO block diagram at right, with the objective of deriving from it the closed-loop transfer function, $CLTF(s) \equiv \Theta(s)/R(s)$.

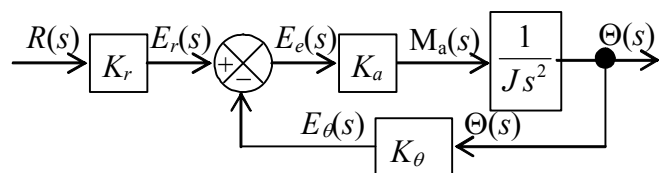


Figure 14-7 Laplace block diagram of SISO position-feedback control system

Three distinct steps of block-diagram algebra are required to reduce Fig. 14-7 to a single block, the $CLTF(s)$, that separates input and output signals:

1. Combine (multiply) the two block transfer functions within the forward branch of the loop, as shown at right.

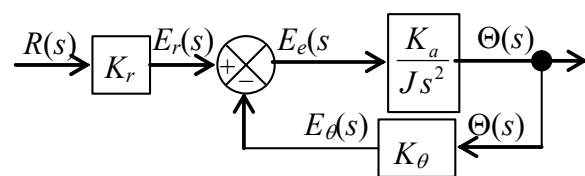
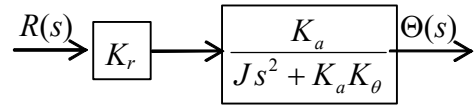


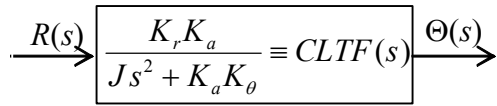
Figure 14-7a

This multiplication operation is derived in Section 13-1.

2. Resolve the forward-branch and feedback-branch transfer functions of the closed loop into the single equivalent transfer function shown at right. The block-diagram algebra used in this step is derived in the next section; it is an important basic tool for the analysis of control systems.



3. Finally, and obviously, just multiply the remaining two blocks to produce the required result shown at right.

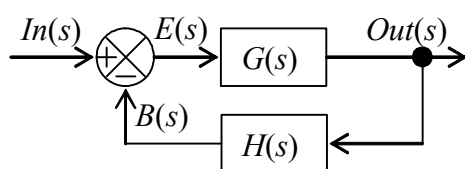


For this relatively simple system, the SISO version of ODE of motion (14-13) is $J\ddot{\theta} + K_a K_\theta \theta = K_a K_r r(t)$. It is very easy to derive the same $CLTF(s)$ directly from this ODE, but we have derived $CLTF(s)$ here using block-diagram algebra in order to establish the approach that is appropriate for more complicated systems.

We shall re-visit this position-feedback control system in Section 14-5, with the objectives of evaluating its control performance and then developing an addition to the system that will improve the performance.

14-4 Transfer function of a single closed loop

Consider Figure 14-8, which is a more general version, in standard notation, of the closed loop in Fig. 14-7a. General functions $G(s)$ and $H(s)$ are, respectively, the forward-branch and feedback-branch transfer functions.



$E(s)$ is the actuating error signal, and $B(s)$ is the feedback signal. We seek the closed-loop transfer function, the ratio $Out(s)/In(s)$. All of the quantities labeled on Fig. 14-8 are denoted as functions of Laplace variable s , but it is important to recognize that there are two fundamentally different types of functions: (1) the

Figure 14-8 Laplace block diagram of general closed loop

“signals” $In(s)$, $E(s)$, $B(s)$, and $Out(s)$, which actually are Laplace transforms of time-dependent variables such as motion and voltage; and (2) the transfer functions $G(s)$ and $H(s)$, which represent in the Laplace domain the characteristics of systems and objects such as inertias, actuators, and circuits. To emphasize the difference in the following derivation of $Out(s)/In(s)$, let’s omit the functional notation “ (s) ” from the signals, at least in the intermediate steps. The steps follow naturally from Fig. 14-8:

$$E = In - B \quad \text{and} \quad B = Out \times H(s),$$

$$\begin{aligned} \Rightarrow \quad Out &= E \times G(s) = [In - B] \times G(s) = [In - Out \times H(s)] \times G(s) \\ &= In \times G(s) - Out \times H(s) \times G(s) \end{aligned}$$

$$\Rightarrow \text{Out} \times [1 + G(s)H(s)] = \text{In} \times G(s)$$

$$\Rightarrow \frac{\text{Out}(s)}{\text{In}(s)} = \frac{G(s)}{1 + G(s)H(s)} \quad (14-15)$$

Equation (14-15) is an important, general, labor-saving tool for analysis of loops in any control system, not just the systems discussed in this chapter. To illustrate its application, let's use it to derive in detail the loop transfer function written in Step 2 of the block-diagram algebra of Section 14-3. From Step 1 of that process (or from Fig. 14-7a), we identify: $G(s) = K_a/Js^2$ and $H(s) = K_\theta$. Substituting these into Eq. (14-15) gives

$\frac{\text{Out}(s)}{\text{In}(s)} = \frac{K_a/Js^2}{1 + (K_a/Js^2)K_\theta} = \frac{K_a}{Js^2 + K_a K_\theta}$, which is the loop transfer function shown in the block diagram as the result of Step 2.

A transfer function in Eq. (14-15) often has the form of a ratio of polynomials in s , such as $G(s)$ in the previous paragraph, so it is useful to derive a version of (14-15) in terms of the polynomials. First, we define numerator and denominator polynomials that make up $G(s)$ and $H(s)$:

$$G(s) \equiv \frac{N_G(s)}{D_G(s)} \quad \text{and} \quad H(s) \equiv \frac{N_H(s)}{D_H(s)} \quad (14-16)$$

Next, we carry out the algebra of Eq. (14-15), dropping the functional notation “(s)” from the transfer functions and polynomials in the interest of notational conciseness:

$$\frac{\text{Out}(s)}{\text{In}(s)} = \frac{G}{1 + GH} = \frac{N_G/D_G}{1 + (N_G/D_G) \times (N_H/D_H)} = \frac{N_G D_H}{D_G D_H + N_G N_H} \quad (14-17)$$

For the example of the previous paragraph, the simple polynomials are $N_G = K_a$, $D_G = Js^2$, $N_H = K_\theta$, and $D_H = 1$; substituting these terms into Eq. (14-17) obviously leads to the $\text{Out}(s)/\text{In}(s)$ result derived in the previous paragraph, but with a bit less algebra because the algebra has been completed in (14-17). Equation (14-17) expresses the closed-loop transfer function as a ratio of polynomials, and it applies in general, not just to the problems of this chapter.

Finally, we will use later an even more specialized form of Eqs. (14-15) and (14-17) for the case of *unity feedback*, $H(s) = 1 = 1/1$:

$$\frac{\text{Out}(s)}{\text{In}(s)} = \frac{G}{1 + G} = \frac{N_G}{D_G + N_G} \quad (14-18)$$

Equations (14-15), (14-17), and (14-18) are very useful for the analysis of feedback control. In the future, whenever you encounter a simple loop with the form of Fig. 14-8 in the Laplace block diagram of a system, you may (and usually should) apply whichever of these equations is most appropriate to derive the loop transfer function, without repeating the algebra that goes into the derivation of these equations.

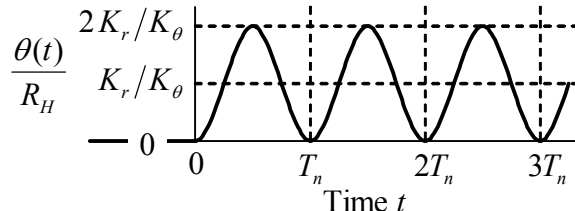
14-5 Closed-loop control of rotor position using position feedback plus rate feedback

Let's re-visit the position-feedback control system of Section 14-3 in order, first, to evaluate its control performance and, next, to develop an addition to the system that will improve the performance.

It is easy to evaluate the control performance just by considering the SISO version of ODE of motion (14-13), which is

$$J\ddot{\theta} + K_a K_\theta \theta = K_a K_r r(t) \quad (14-19)$$

As was noted earlier, the pseudo-static response of Eq. (14-19) is $\theta_{ps}(t) = [K_r / K_\theta]r(t)$; this would be good controlled response, but it is not necessarily the total response. Therefore, let's consider in more detail the total transient response. Equation (14-19) is an undamped 2nd order ODE of the type analyzed extensively in Chapter 7. By dividing (14-19) through by J and then defining appropriate parameters, we can adapt this ODE to the standard form (7-5), $\ddot{\theta} + \omega_n^2 \theta = \omega_n^2 u(t)$, in which the natural frequency is $\omega_n = \sqrt{K_a K_\theta / J}$, and the standard input quantity is $u(t) = [K_r / K_\theta]r(t)$. We can also adapt any appropriate response solutions already derived in Chapters 7 and 8 to this position-feedback control system. For example, if the operator setting is the step function $r(t) = R_H H(t)$, then $u(t) = [K_r / K_\theta]R_H H(t) \equiv U H(t)$, so the standard solution (7-14) leads to step response $\theta(t) = (K_r / K_\theta)R_H(1 - \cos \omega_n t)$. This step response is plotted on the figure at right, with the period defined as $T_n = 2\pi / \omega_n$. Due to the absence of damping, the response oscillates forever about the desired constant pseudo-static response, $\theta_{ps} = (K_r / K_\theta)R_H$. The response never settles at θ_{ps} , so the control system fails to deliver the desired performance.



We must conclude from this example that the absence of damping renders the position-feedback control system of Section 14-3 (Fig. 14-5) unsuitable for most, if not all engineering applications of control. However, there is a relatively simple design feature that can be added to the control system, a feature that will provide damping to the system and will greatly improve the control performance.

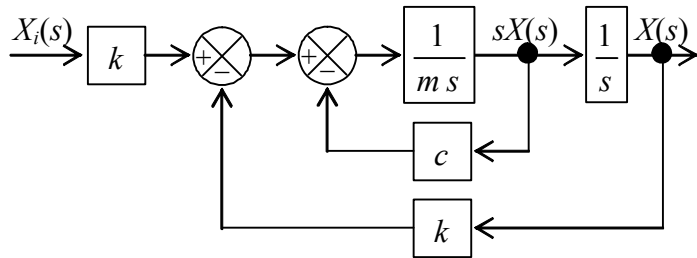


Figure 14-9 Laplace block diagram with feedback branches for a base-excited $m\text{-}c\text{-}k$ system

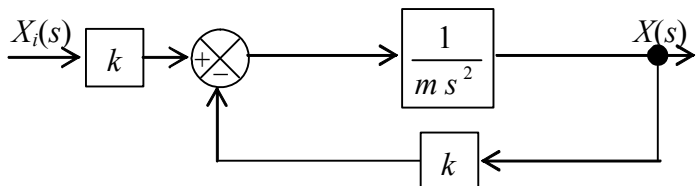


Figure 14-10 Laplace block diagram with feedback branch for a base-excited $m\text{-}k$ system

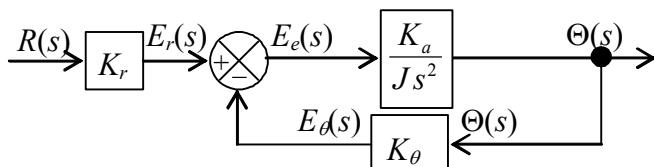


Figure 14-7a (repeated) Laplace block diagram of SISO position-feedback control system

repeated here. The Laplace block diagrams of the two systems have nearly identical forms, with, for example, constants K_r and K_a/J in Fig. 14-7a being directly analogous, respectively, to constants k and $1/m$ in Fig. 14-10. Only the possibility on Fig. 14-7a that input block constant K_r and feedback block constant K_θ can be different keeps Fig. 14-7a from being completely analogous to Fig. 14-10. This is a minor difference that has no substantive effect in the following discussion.

Let's exploit the similarities between the base-excited $m\text{-}c\text{-}k$ system and the rotor-position control system in order to guide us toward a method for improving the latter. First, we refer back to the solution in Section 13-3 for response of the base-excited $m\text{-}c\text{-}k$ system to step input $x_i(t) = X_H H(t)$. The step response is presented graphically on Fig. 13-4, which is repeated on the next page for your convenience.

Recall the following definitions for the $m\text{-}c\text{-}k$ system: $\omega_n = \sqrt{k/m}$, $T_n = 2\pi/\omega_n$, and $\zeta = c/(2\sqrt{mk})$. Note on Fig. 13-4 that the addition of positive damping ($c > 0 \Rightarrow \zeta > 0$) to the undamped system produces output $x(t)$ that approximates the input; therefore, the positively damped $m\text{-}c\text{-}k$ system is, indeed, a suitable control system, whereas the undamped $m\text{-}k$ system is not.

In order to describe the motivation for this new feature of the control design, let's revisit the base-excited $m\text{-}c\text{-}k$ system of Sections 13-2 and 13-3. The principal elements of Fig. 13-3, that system's Laplace block diagram, are reproduced on Fig. 14-9. The inner feedback loop makes Fig. 14-9 more complicated than any control system block diagram that we have encountered previously in this chapter. Consider, however, the case of zero damping, $c = 0$, for which the system is an undamped, base-excited mass-spring ($m\text{-}k$) system, and Fig. 14-9 loses the inner feedback loop, taking on the simpler appearance of Fig. 14-10. Now, let's compare the Laplace block diagram of the base-excited $m\text{-}k$ system with that of the rotor position-feedback control system, Fig. 14-7a, which is re-

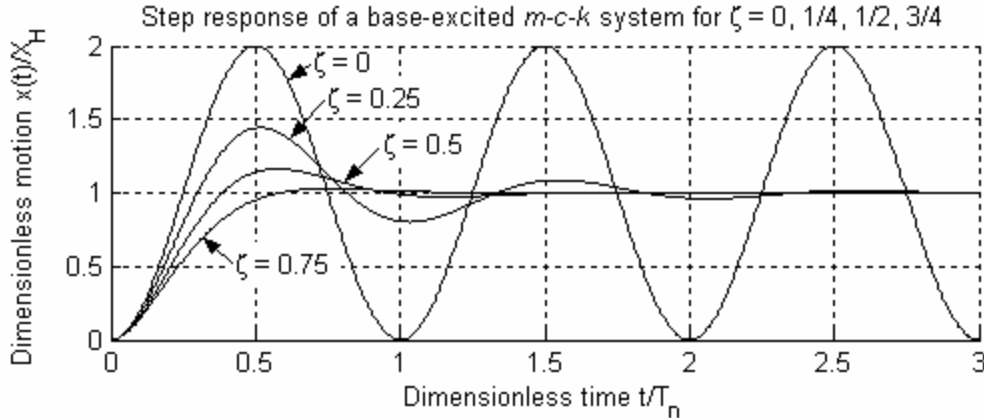


Figure 13-4 (repeated) Base-excitation control of mass position for an *m-c-k* system

Can we modify the undamped rotor-position control system in such a way that it has the same type of positive damping, and therefore suitable control performance, as the *m-c-k* system? Block diagram Fig. 14-9 for the positively damped *m-c-k* system suggests that we might improve the rotor-position control system by adding an inner feedback loop to its block diagram, Fig. 14-7a, a loop that is similar to the inner loop of Fig. 14-9. But are there practical physical operations and devices corresponding to the purely mathematical addition of this type of loop to Laplace block diagram Fig. 14-7a? To answer this question, let's observe that the Laplace feedback signal of the inner loop on Fig. 14-9 is $sX(s)$, which is the Laplace transform of velocity $\dot{x}(t)$. Therefore, the inner loop on Fig. 14-9 represents mathematically the physical operations of detecting the output velocity and multiplying that velocity by negative constant $-c$ to create a damping force that opposes motion of mass *m*. We can perform the analogous physical operation for the rotor-position control system by measuring output rotational velocity $p(t) \equiv \dot{\theta}(t)$ with an appropriate sensor (such as a rate gyroscope) and feeding that signal negatively back to the input of the actuator. Figure 14-11 depicts the modified rotor-position control system, with both this rate feedback (to provide positive damping) and the original position feedback (to provide positive stiffness).

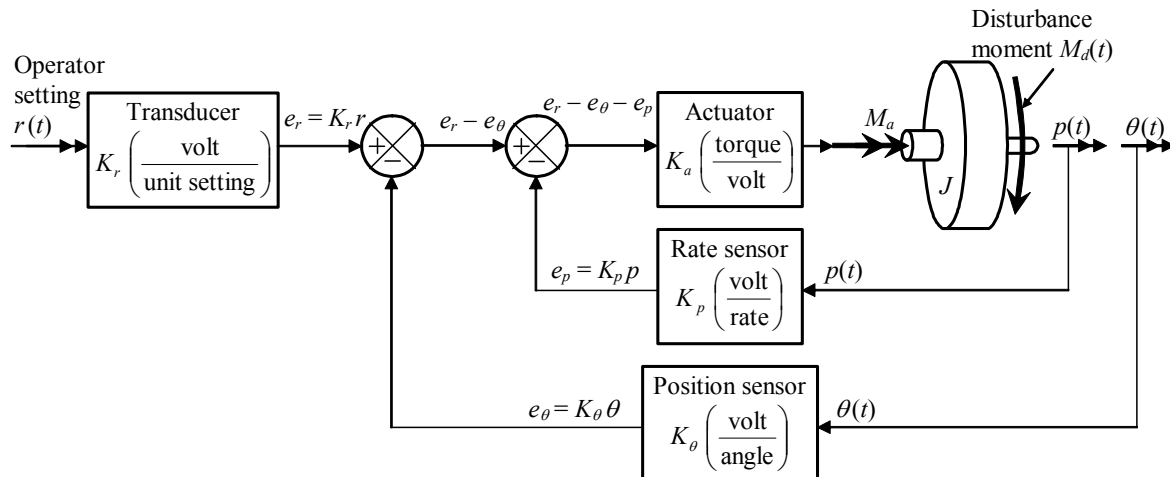


Figure 14-11 Functional diagram of rotor-position control system with both position feed-back and rate feedback

Figure 14-12 is the Laplace block diagram corresponding to functional diagram Fig. 14-11. For measuring and feeding back the rotational velocity, the appropriate form of plant ODE of motion (14-1) is $J\ddot{\theta} = M(t)$, so the appropriate plant transfer function in the new inner loop is $L[p(t)] / L[M(t)] \equiv P(s) / M(s) = 1 / (Js)$. Also, the definition of rotational velocity $\dot{\theta}(t) \equiv p(t)$ leads to the forward-branch integration transfer function, $\Theta(s) / P(s) = 1/s$. Comparing Fig. 14-12 with Fig. 14-9 for the base-excited $m-c-k$ system, we see that the two Laplace block diagrams have nearly identical forms, except for the presence of the disturbance moment on Fig. 14-12. Thus, and to summarize, we have modified the rotor-position control system to add positive damping, using the base-excited $m-c-k$ system as a model.

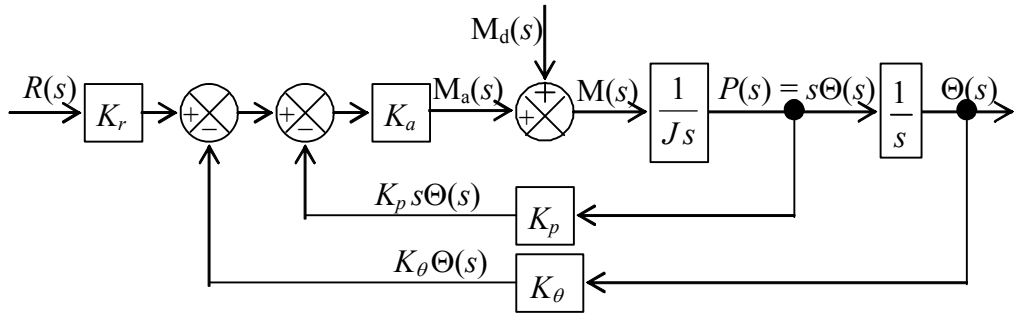


Figure 14-12 Laplace block diagram of rotor-position control system with both position feedback and rate feedback

The position-feedback and rate-feedback types of control illustrated by Figs. 14-11 and 14-12 are relatively simple *output operations*: this control involves no more than basic arithmetic operations on the sensed output signals, without any modification of the error signal in the forward branch. Chapter 15 introduces control by *input error operations*, which involves more general mathematical operations upon a single error signal.

Next, let's analyze in detail the SISO version of the modified rotor-position control system. Thus, we set $M_d(t) = 0$ and $M_d(s) = 0$, and we re-draw Fig. 14-12 as SISO block diagram Fig. 14-13. Our objectives are: first, to derive from Fig. 14-13 the closed-loop transfer function, $CLTF(s) \equiv \Theta(s)/R(s)$; second, to infer from $CLTF(s)$ the characteristics of the SISO system.

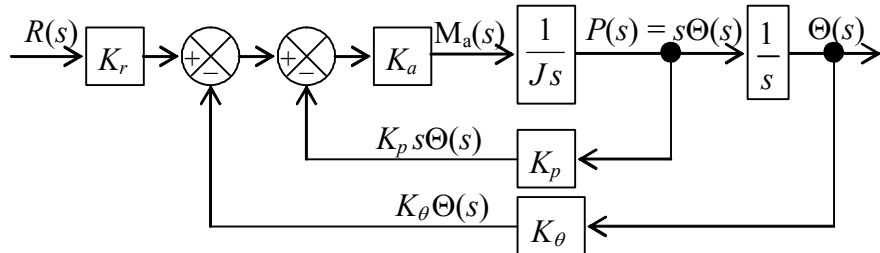
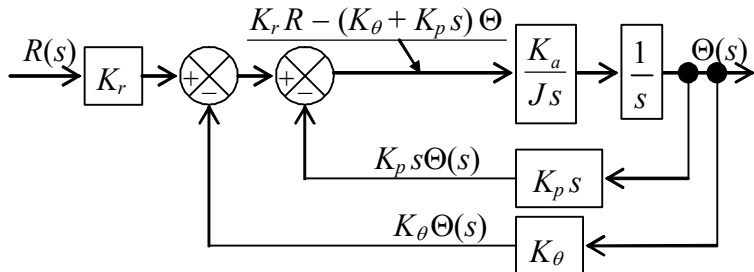
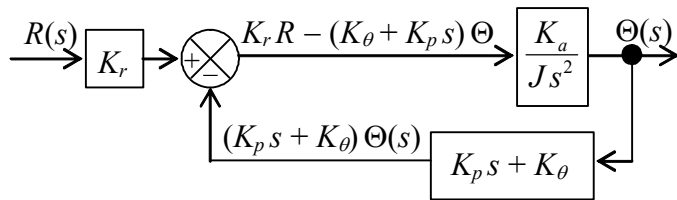


Figure 14-13 Laplace block diagram of SISO rotor-position control system with both position feedback and rate feedback

We could resolve block diagram Fig. 14-13 by the “brute-force” method of applying Eq. (14-17) first to the inner loop, then to the outer loop. However, we can achieve the same result more simply by using some sensible block-diagram algebra. The approach in each step is to modify a block and/or branch so as to simplify the diagram without changing the most important output signals. The obvious first step, is to combine the two blocks in the forward branch of the inner loop on Fig. 14-13 into transfer function $K_a/(Js)$. Next, we move the branch point of the inner loop to the right of the integration block, and modify accordingly the feedback transfer function of the inner loop, as shown at right.



Next, we multiply the two blocks of the forward branch inside the loops into transfer function $K_a / (Js^2)$. Now, both feedback branches essentially originate at the same branch point and terminate at the same summing junction, so we combine them into a single feedback branch with an appropriate transfer function, as shown at right. This block diagram has only a single loop, so we can apply Eq. (14-17)



with the following transfer-function polynomials: $N_G = K_a$, $D_G = Js^2$, $N_H = K_p s + K_\theta$, and $D_H = 1$. The result is:

$$\frac{N_G D_H}{D_G D_H + N_G N_H} = \frac{K_a \times 1}{Js^2 \times 1 + K_a \times (K_p s + K_\theta)} = \frac{K_a}{Js^2 + K_a K_p s + K_a K_\theta}$$

Finally, multiplying this loop transfer function by the input transducer sensitivity gives

$$CLTF(s) \equiv \frac{\Theta(s)}{R(s)} = \frac{K_r K_a}{Js^2 + K_a K_p s + K_a K_\theta} \quad (14-20)$$

Let’s cast system transfer function (14-20) into a form that displays more clearly the fundamental characteristics of the closed-loop system. We again use as a guide the base-excited $m-c-k$ system of Section 13-2. The undamped natural frequency of that system is $\omega_n = \sqrt{k/m}$, and the viscous damping ratio is $\zeta = c/(2\sqrt{mk})$. Using these definitions, we can express transfer function (13-8) in terms of these fundamental system characteristics rather than the physical parameters m , c , and k :

$$TF(s) \equiv \frac{X(s)}{X_i(s)} = \frac{k}{m s^2 + c s + k} = \frac{k/m}{s^2 + (c/m)s + k/m} = \frac{\omega_n^2}{s^2 + 2\zeta \omega_n s + \omega_n^2} \quad (14-21)$$

Manipulating (14-20) in a similar manner, with an additional step to account for the possibility that $K_r \neq K_\theta$, gives:

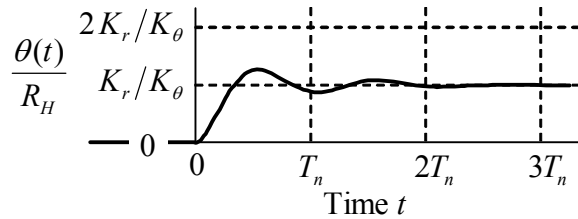
$$CLTF(s) = \frac{\Theta(s)}{R(s)} = \frac{K_r}{K_\theta} \times \frac{K_a K_\theta / J}{s^2 + (K_a K_p / J)s + K_a K_\theta / J} = \frac{K_r}{K_\theta} \times \frac{\omega_n^2}{s^2 + 2\zeta\omega_n s + \omega_n^2} \quad (14-22)$$

In Eq. (14-22) the undamped natural frequency and viscous damping ratio of the rotor-position control system are

$$\omega_n = \sqrt{\frac{K_a K_\theta}{J}} \quad \text{and} \quad \zeta = \frac{K_a K_p}{2J\omega_n} \quad (14-23)$$

Equation (14-22) differs in form from Eq. (14-21) only in the presence of pseudo-static multiplier K_r/K_θ , which is defined in Eq. (14-14).

The system with transfer function (14-21) behaves as a control system should: in this case, as a positively damped, 2nd order system. For example, if the parameters in Eq. (14-22) are selected such that ζ is in the range 0.3 to 0.5, and if the operator setting is step function $r(t) = R_H H(t)$, then the inverse Laplace transform developed in homework Problem 9.12 gives the type of step response shown on the figure at right. The output cannot exactly follow this infinitely fast input, but it rises quickly and settles quickly to the desired pseudo-static response. This example illustrates a general characteristic of control systems: it is generally impossible to achieve absolute accuracy instantly (in this case, the pseudo-static response), but a good control system can achieve practically acceptable accuracy, with a practically acceptable time lag between the input and the desired output.



It was observed earlier that position feedback through the sensor with gain K_θ has the effect of attaching between the operator setting and the rotor inertia an artificial restoring spring with stiffness constant $K_a K_\theta$. We see now, additionally, that rate feedback through the sensor with gain K_p has the effect of imposing upon the absolute motion of the rotor an artificial viscous damper with damping constant $K_a K_p$.

Finally, let's note that the favorable and stable performance of this rotor-position control system is strongly dependent upon the positivity of constants $K_a K_\theta$ and $K_a K_p$. In practice, it is possible (in fact, too easy) to make these constants negative, usually by accident or negligence, which could cause the system to be unstable. Chapters 16 and 17 examine in more detail the important issue of system stability.

14-6 Comments regarding classical control theory and modern control theory

In the words of Brogan, 1974, page 1, “Control theory can be divided into two major categories, classical and modern.” Chapters 14-17 of this book constitute an introduction to the former, namely, classical control theory for linear, time-invariant (LTI) systems. Whereas classical control theory focuses on relatively simple single-input-single-output (SISO) systems, modern control theory, which is based upon the *state-space* mathematical representation of systems, is very well suited for design and analysis of control for both simple systems and much more complicated multiple-input-multiple-output (MIMO) systems.³

The state-space representation of systems is a generalization of the standard 1st order ODE Eq. (1-1), $\dot{x} - ax = bu(t)$, which has only the single input $u(t)$ and the single dependent variable $x(t)$. In the generalization to an LTI-MIMO system of, say, r inputs and n dependent variables, scalar $x(t)$ becomes the $n \times 1$ *state vector* (column matrix) $\mathbf{x}(t)$ of dependent variables, scalar $u(t)$ becomes the $r \times 1$ vector of inputs $\mathbf{u}(t)$, single constant a becomes the $n \times n$ matrix \mathbf{A} of system constants, single constant b becomes the $n \times r$ matrix \mathbf{B} of input constants, and single ODE $\dot{x} - ax = bu(t)$ becomes the system of n coupled 1st order ODEs written in matrix form, $\dot{\mathbf{x}} - \mathbf{Ax} = \mathbf{Bu}(t)$. All of the 2nd order systems analyzed in this book can be expressed in state-space form with $\mathbf{x}(t)$ being 2 \times 1 state vectors; for example, the two scalar Eqs. (1-15) can clearly be written as the following single matrix ODE:

$$\begin{bmatrix} \dot{x} \\ \dot{v} \end{bmatrix} - \begin{bmatrix} 0 & 1 \\ -k/m & -c/m \end{bmatrix} \begin{bmatrix} x \\ v \end{bmatrix} = \begin{bmatrix} 0 \\ 1/m \end{bmatrix} f_x(t)$$

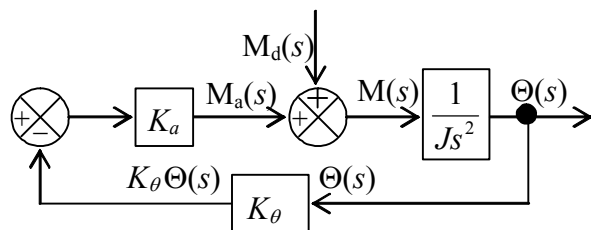
Further, the 2-DOF systems of Chapters 11 and 12 can be expressed in state-space form with $\mathbf{x}(t)$ being 4 \times 1 state vectors.

Chapters 14-17 of this book should provide adequate preparation for study of the fundamental aspects of modern control theory. Three appropriate textbooks, among the many available, are Brogan, 1974, Franklin, *et al.*, 1991, and Ogata, 2001.

³ Franklin, *et al.*, 1991, page 361, wrote that the adjective “modern” is misleading “... since the state-space method of description for differential equations is over 100 years old and was introduced to control design in the late 1950s, ...”. Those authors prefer the designations “transform methods” rather than “classical control” and “state-space methods” rather than “modern control”.

14-7 Homework problems for Chapter 14

14.1 In Section 14-3 for the rotor-position control system with position feedback, the transfer function relating output rotor position to input operator setting, with zero disturbance, is derived by a series of block-diagram algebraic operations to resolve (simplify) Fig. 14-7. In practice, for assessment of control system quality, it is often required also to determine the transfer function that relates output rotor position to the disturbance, with zero operator setting. The appropriate block diagram for that task in

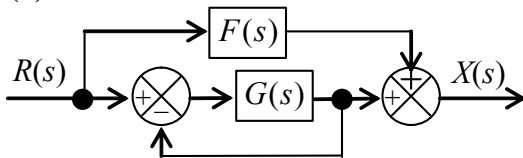


this case comes from Fig. 14-6, with $R(s) = 0$, as shown at left. Derive from this block diagram the transfer function $\frac{\Theta(s)}{M_d(s)} = \frac{1}{Js^2 + K_a K_\theta}$. This task is not difficult: just write $M_a(s)$ in terms of $\Theta(s)$, then $M(s) = M_a(s) + M_d(s)$, and

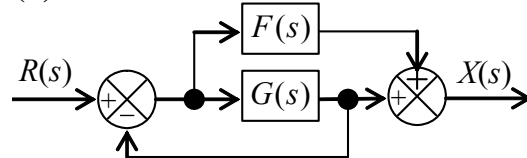
$M(s) \times 1/Js^2 = \Theta(s)$, which steps should lead you to the required result. This result can also be derived directly from the ODE of motion (14-13), but the assignment here is to derive it from the block diagram, to give you practice with block-diagram algebra.

14.2 In some systems, information is fed forward as well as backward. Each of the Laplace block diagrams (a) and (b) shown below includes both a *feedforward* branch and a *unity-feedback* branch. Transfer functions $F(s)$ and $G(s)$ represent arbitrary plant, filter, sensor, etc. system elements. (We could also include a transfer-function block in the unity-feedback branch, but its value would be simply 1, so it is standard practice to omit that obvious block.) For the part(s) assigned, derive the algebraic equation for the system transfer function, $X(s)/R(s)$, in terms of $F(s)$ and $G(s)$.

(a)

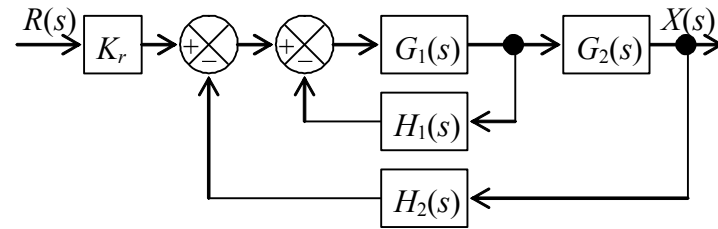


(b)



(c) The idealized series damper-spring high-pass mechanical filter shown in Fig. 3-12 has the governing ODE with right-hand-side (RHS) dynamics, $\dot{x}_o + (1/\tau_1)x_o = \dot{x}_i(t)$, Eq. (3-24). The transfer function from this ODE is clearly $X_o(s)/X_i(s) = s/(s + 1/\tau_1)$, where $L[x_i(t)] \equiv X_i(s)$ and $L[x_o(t)] \equiv X_o(s)$. With the definition of a new independent variable $x_d(t)$ and the auxiliary equation $x_o(t) = x_d(t) + x_i(t)$, the ODE is converted into an alternate form without RHS dynamics, $\dot{x}_d + (1/\tau_1)x_d = -(1/\tau_1)x_i(t)$, Eq. (3-26). Construct a Laplace block diagram using the alternate ODE and the auxiliary equation; this diagram should have input $X_i(s)$ on the left and output $X_o(s)$ on the right, and it should include a feedforward branch. Use block-diagram algebra on this diagram to derive again the system transfer function $X_o(s)/X_i(s) = s/(s + 1/\tau_1)$.

- 14.3** Consider a system represented by the somewhat general Laplace block diagram at the right. Constant K_r is an input sensor gain, and transfer functions $G_1(s)$, $G_2(s)$, $H_1(s)$, and $H_2(s)$ represent arbitrary plant, filter, sensor, etc. system elements. Use block-diagram algebra to show in detail that the closed-loop transfer function is

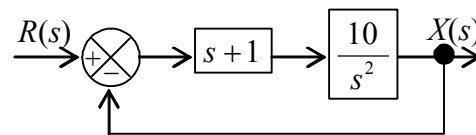


$$CLTF(s) \equiv \frac{X(s)}{R(s)} = \frac{K_r G_1 G_2}{1 + G_1 H_1 + G_1 G_2 H_2}$$

- 14.4** Consider a system represented by the block diagram below. The feedback branch is a *unity-feedback* path; we could include a transfer-function block in that branch, but its value would be simply 1, so it is standard practice to omit that obvious block.

- (a) Show that the closed-loop transfer function is

$$CLTF(s) = \frac{X(s)}{R(s)} = \frac{10(s+1)}{s^2 + 10s + 10}$$

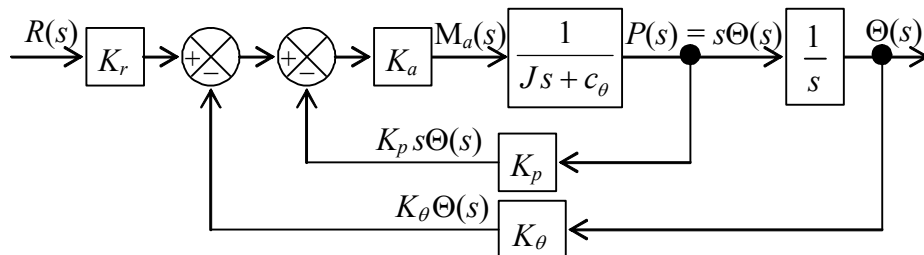


- (b) Evaluate the denominator quadratic equation to calculate the viscous damping ratio ζ , which should indicate that the closed-loop system is overdamped.

- (c) Factor the denominator quadratic into the form $(s - p_1)(s - p_2)$, find the values of poles p_1 and p_2 . (*partial answer:* $p_1 = -1.127 \text{ sec}^{-1}$)

- (d) Suppose that the ICs are zero and that the input is a step function, $r(t) = 5 H(t)$. Determine the complete algebraic equation for output $x(t)$. First express $X(s)$ in a partial-fraction expansion, then find the inverse Laplace transform. Use your $x(t)$ equation to find the final value, $\lim_{t \rightarrow \infty} x(t)$, after all dynamic motion has damped out. (*partial answer:* one of the terms in the equation for $x(t)$ should be $-5.728 e^{-8.873 t}$.)

- 14.5** Consider position control of a reaction wheel (from Section 3-3) by position feedback plus rate feedback, for which the system Laplace block diagram is:



This block diagram is identical to Fig. 14-13, except that the plant transfer function from Eq. (3-1) is $1/(Js + c_\theta)$, not just $1/Js$, due to the presence of bearing friction with assumed viscous damping constant c_θ . The following data were measured for a small laboratory reaction-wheel assembly:

$$J = 2.56 \times 10^{-3} \text{ lb-inch-sec}^2, c_\theta = 0.020 \frac{\text{ounce inch}}{\text{rad/sec}}, K_a = 0.950 \frac{\text{ounce inch}}{\text{V}}$$

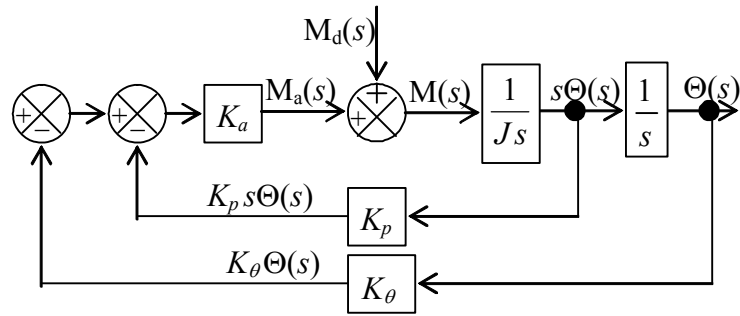
For the case(s) assigned, the control system transducer and sensor sensitivities are as shown in columns 2, 3, and 4 of the following table:

Case	K_r (V/rad)	K_θ (V/rad)	K_p (V-sec/rad)	t_r (sec)	\bar{x}_p
1	15	10	0.36	0.1280	0.3858
2	1.5	1.5	0.27	0.4507	0.1117
3	14	21	0.35	0.08163	0.5355
4	3.5	3.5	0.24	0.2255	0.3260

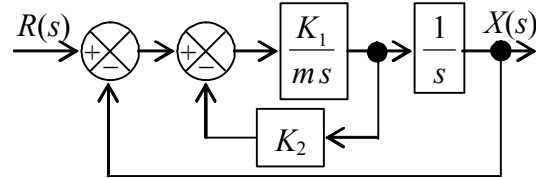
- (a) Calculate from the values in table columns 2, 3, and 4 the following quantities for this closed-loop system: pseudo-static multiplier K_r/K_θ , undamped natural frequency ω_n (rad/sec), viscous damping ratio ζ , and damped natural frequency ω_d (rad/sec).
- (b) Suppose that the input is a step function, $r(t) = R_H H(t)$, with magnitude $R_H = 30$ degrees. For the subsequent step response, calculate the rise time t_r , the peak time t_p , the maximum overshoot ratio \bar{x}_p , and the settling time t_s (see Section 9-8). Also, calculate the final static value of wheel position, $\lim_{t \rightarrow \infty} \theta(t)$ in degrees, after all dynamic motion has damped out. *Partial answers are given in columns 5 and 6 of the table above to help you know if you are, or are not on the right track, but you still must show all derivations and calculations leading to these answers.*
- (c) For the same step input as in part (b), use MATLAB to calculate and plot the step response $\theta(t)$ in degrees from $t = 0$ until at least the settling time $t = t_s$.

14.6 In Section 14-5 for the rotor-position control system with position feedback and rate feedback, the transfer function relating output rotor position $\Theta(s)$ to input operator setting $R(s)$, with zero disturbance, is derived by a series of block-diagram algebraic operations to resolve (simplify) Fig. 14-13. In practice, for assessment of control system quality, it is often required also to determine the transfer function that relates output rotor position to the disturbance, with zero operator setting. The appropriate Laplace block diagram for

that task in this case comes from Fig. 14-12, with $R(s) = 0$, as shown on the figure at right. Derive from this block diagram the algebraic equation for transfer function $\frac{\Theta(s)}{M_d(s)}$.



14.7 Consider a system represented by the Laplace block diagram at right. The outer feedback branch is a *unity feedback* path; we could include a transfer-function block in that branch, but its value would be simply 1, so it is standard practice to omit that obvious block.



- (a) Use the result of Problem 14.3 or any other method of your choice to show that the closed-loop transfer function is

$$\frac{X(s)}{R(s)} = \frac{K_1}{ms^2 + K_1 K_2 s + K_1}$$

- (b) Suppose that the ICs are zero and that the input to this system is a step function, $r(t) = R_H H(t)$. For the case(s) assigned, the value of the mass-like parameter m (in consistent units) is given in column 2 of the table below. Calculate the values of constants K_1 and K_2 (in consistent units) that will produce the values of maximum overshoot ratio \bar{x}_p and peak time t_p given in columns 3 and 4 of the table (see Section 9-8). Note that this is a design exercise: you are calculating values of system parameters that are intended to produce specified control objectives. Complete the problem by calculating also the rise time t_r and the settling time t_s . *Partial answers are given in columns 5 and 6 of the table below to help you know if you are, or are not on the right track, but you still must show all derivations and calculations leading to these answers.*

Case	m	\bar{x}_p	t_p (sec)	K_2	t_s (sec)
1	150	0.25	0.35	0.08230	1.010
2	0.085	0.75	0.015	8.672e-4	0.2086
3	35	0.055	1.1	0.3490	1.517
4	2.5	0.125	0.75	0.2198	1.443

- (c) Let the step magnitude of part (b) be $R_H = 0.753$ (in consistent units). Calculate the final value, $\lim_{t \rightarrow \infty} x(t)$, after all dynamic motion has damped out.

Chapter 15 Input-error operations: proportional, integral, and derivative types of control

© 2016 by William L. Hallauer, Jr.

15-1 Initial definitions; proportional-integral-derivative (PID) control

Figure 15-1 is a general functional block diagram that represents many engineering control systems. The term *input-error operation* can be defined in the context of this diagram: a single output quantity is fed back and differenced from the operator-setting input quantity, and the error signal is manipulated mathematically by a *controller*, also called *control processor* or *filter*, in such a way as to produce effective control. The controller usually consists of analog electronic circuitry and/or a digital processor.

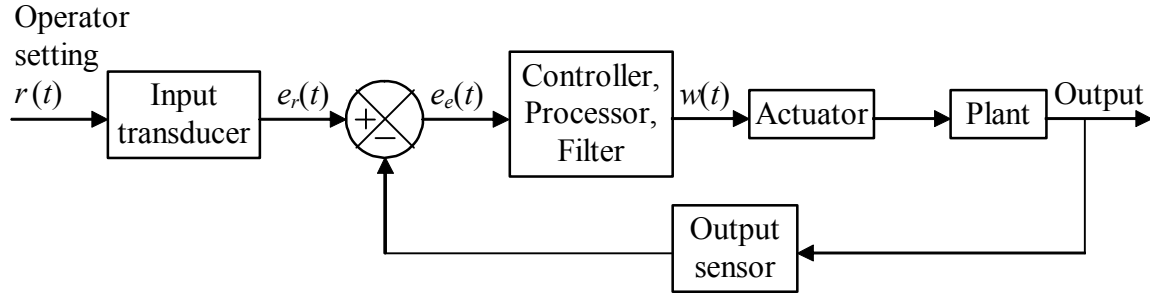


Figure 15-1 Functional block diagram of general control system using input-error operations

Proportional-integral-derivative (PID) control is a class of input-error operations used widely in industry. Let $e_e(t)$ be the error voltage signal that is input to the controller and $w(t)$ be the output voltage from the controller, as shown on Fig. 15-1. The mathematical operations performed by an ideal PID controller are described by the equation

$$w(t) = P \left[e_e(t) + b_i \frac{1}{\tau_i} \int_{\tau=0}^{\tau=t} e_e(\tau) d\tau + b_d \tau_d \frac{de_e}{dt}(t) \right] \quad (15-1)$$

The physical constants in Eq. (15-1) are *proportional gain* P , *integral time constant* τ_i , and *derivative time constant* τ_d . Each of the binary constants b_i and b_d has dimensionless value 1 or 0, depending upon whether or not integral and/or derivative actions are included in the control. Determining what these constants should be for a particular application is a major part of the control design process. To find the transfer function of the ideal PID controller, we define the Laplace transforms $L[e_e(t)] \equiv E_e(s)$ and $L[w(t)] \equiv W(s)$. Taking the Laplace transform of Eq. (15-1) gives the ideal-PID-controller transfer function:

$$\frac{W(s)}{E_e(s)} = P \left[1 + b_i \frac{1}{\tau_i s} + b_d \tau_d s \right] \quad (15-2)$$

We shall consider in examples three subsets of PID control that are in common usage: for proportional (P) control, only the first term inside the brackets of Eqs. (15-1) and (15-2) is used, so $b_i = b_d = 0$; for proportional-integral (PI) control, only the first and second terms are used, so $b_i = 1$ and $b_d = 0$; and for proportional-derivative (PD) control, only the first and third terms are used, so $b_i = 0$ and $b_d = 1$.

To make the concept of PI control, for example, more concrete, Fig. 15-2 depicts a specific analog electrical circuit that, in principle, acts as an ideal PI controller. (In practice, a great deal of electronic refinement and conditioning is required to produce a

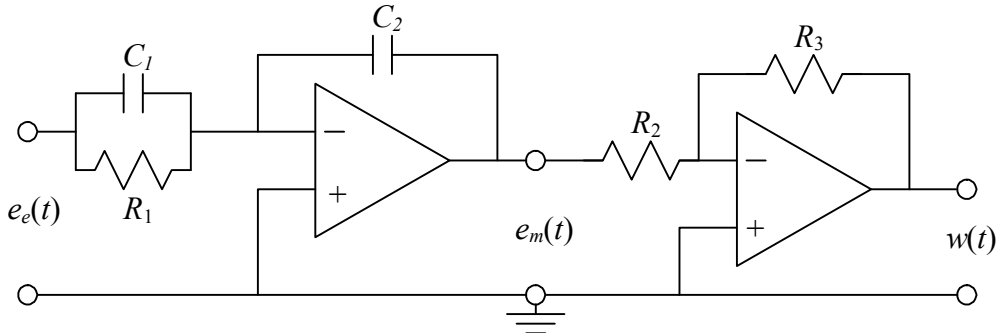


Figure 15-2 Electronic analog PI controller

circuit that behaves even close to ideally.) By applying the methods of circuit analysis described in Chapter 5 (homework Problem 5.11), we can show that the PI ($b_i = 1$ and $b_d = 0$) constants in Eqs. (15-1) and (15-2), expressed in terms of the circuit parameters of Fig. 15-2, are:

$$P = \frac{R_3 C_1}{R_2 C_2}, \quad \tau_i = R_1 C_1 \quad (15-3)$$

The detailed design of PID controllers involves a great deal of engineering art as well as engineering science, and it has been developed extensively; see, e.g., Ogata, 2001, Chapter 10. The present chapter is just an introduction to PID control, so we will not delve deeply into design details; instead, we shall explore some of the more general characteristics of P, PI, and PD types of control in the context of relatively simple examples.

15-2 Examples of proportional (P) and proportional-integral (PI) control

Figure 15-3 on the next page depicts a mechanical plant that is appropriate for the purpose of illustrating P control and PI control. A lightweight rotor is immersed in a viscous liquid, so that the damping moment imposed upon the rotor is $-c_\theta \dot{\theta}$. The rotor is attached to the mechanical operator-setting device (a control wheel, for example) through a highly flexible torsion spring that has rotational stiffness constant k_θ . The rotor has

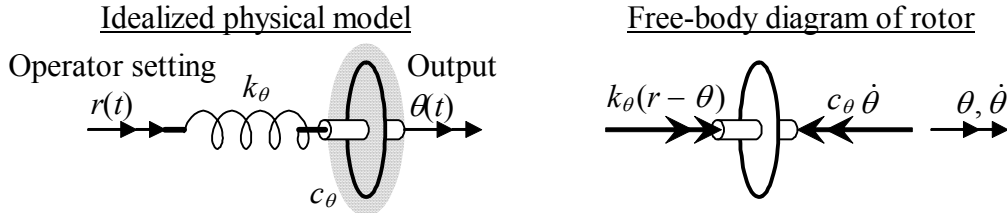


Figure 15-3 Lightweight rotor immersed in a viscous liquid, with connection to the input through a soft torsion spring

sufficiently low rotational inertia J , and viscous damping constant c_θ is sufficiently large, that we assume inertial moment $-J\ddot{\theta}$ to be negligible in comparison with the damping and structural moments.

The equation of motion comes from the FBD on Fig. 15-3:

$$k_\theta(r - \theta) - c_\theta \dot{\theta} = J\ddot{\theta} \approx 0 \Rightarrow \frac{c_\theta}{k_\theta} \dot{\theta} + \theta = r \Rightarrow \tau_1 \dot{\theta} + \theta = r(t), \text{ where } \tau_1 = \frac{c_\theta}{k_\theta} \quad (15-4)$$

Taking the Laplace transform of Eq. (15-4) gives the basic plant transfer function:

$$PTF(s) = \frac{L[\theta(t)]}{L[r(t)]} \equiv \frac{\Theta(s)}{R(s)} = \frac{1}{\tau_1 s + 1} \quad (15-5)$$

Clearly, this idealized open-loop mechanical plant by itself is a simple 1st order system with time constant $\tau_1 = c_\theta/k_\theta$; furthermore, this system is the rotational equivalent of the translational series damper-spring low-pass filter described by Fig. 3-12 and Eq. (3-23).

The input to the plant is operator-setting angle $r(t)$, and the output is rotor position $\theta(t)$. From ODE (15-4), we see that the pseudo-static output is exactly equal to the input, $\theta_{ps}(t) = r(t)$. So let's specify that our control objective for this system is to make the actual output $\theta(t)$ be as close as possible to input $r(t)$. To develop a physical feel for the behavior of the open-loop plant in Fig. 15-3, let's suppose that the operator quickly moves the control wheel to one side so that input $r(t)$ is close to a step function. The torsion spring will immediately be wound up more tightly, and will impose a moment upon the rotor. However, as we can visualize intuitively, the viscous restraint upon the rotor will prevent it from moving as quickly as the input, and the rotor angle will lag the input. As time goes on and the torsion spring gradually unwinds, the rotor angle will eventually settle to the input angle.

Let's suppose that the open-loop response is too slow for our purposes, and that we want to speed-up the response by using sensors, an actuator, feedback, and P or PI control in the system depicted on the next page, in functional form on Fig. 15-4, and as a corresponding Laplace block diagram on Fig. 15-5. The transfer function on Fig. 15-5 for the P or PI controller comes from Eq. (15-2), and the transfer function for the rotor-spring-liquid plant comes from Eq. (15-5). The input transducer and the output position

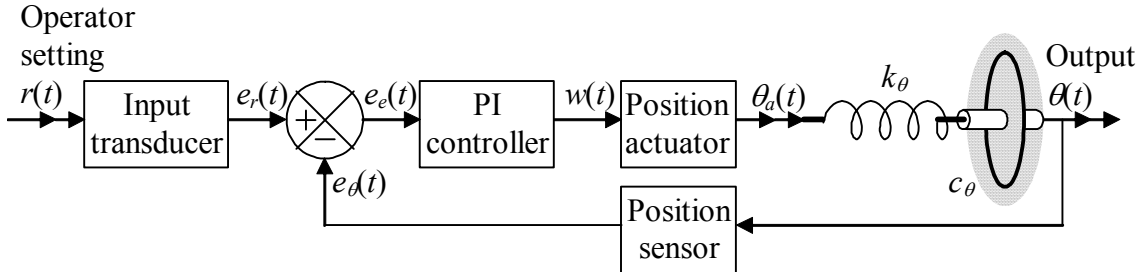


Figure 15-4 Functional diagram of a system for controlling the position of a spring-connected rotor in a viscous liquid, based on proportional-integral control

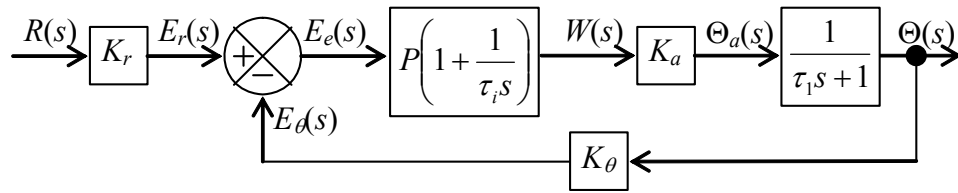


Figure 15-5 Laplace block diagram of a system for controlling the position of a spring-connected rotor in a viscous liquid, based on proportional-integral

sensor shown on Figs. 15-4 and 15-5 are familiar from Chapter 14 (on Fig. 14-5, for example). But the “position actuator” is something new. Whereas the output of most motors is torque, the output of this position actuator is specified to be rotational position. To make an actuator behave in this manner requires a feedback control system within the actuator itself; this is a characteristic of control systems that we now **pause** to examine.

In fact, most actuators and sensors of all types are themselves complicated dynamic systems, often with internal feedback circuits. But this begs the following question: if there are control systems within actuators and/or sensors, then why aren't the details of these systems included in the device or sub-system transfer functions shown on block diagrams such as Fig. 15-5?

A general response to this question is based upon the relative “speeds” of different systems. To illustrate this concept of system speed, we imagine that two standard 2nd order systems, A and B, have equivalent values of subcritical viscous damping ratio ζ , but that System A’s undamped natural frequency is 100 times that of System B, $\omega_{nA}/\omega_{nB} = 100$. Consequently, System A’s settling time for step inputs, $t_{sA} = 4/(\zeta\omega_{nA})$ [Eq. (9-40)], is only 0.01 that of System B; in this case, we regard “the dynamics of System A” as being “100 times faster” than “the dynamics of System B.” Engineers usually select for a control system sensors¹ and, when possible, actuators that are much faster than the dynamics of the plant under control; in such cases, we usually approximate the behavior of a sensor or actuator with a simple linear sensitivity constant, in equations such as $e_r(t) = K_r r(t)$, $e_\theta(t) = K_\theta \theta(t)$, and $\theta_a(t) = K_a w(t)$, all of which are represented on Fig.

¹ Examples that appear in this book of such sensors are the accelerometer [homework Problem 10.12(b)], the rate gyroscope (Example 9-2 in Section 9-2, and homework Problem 9.18), and the rate-integrating gyroscope (homework Problem 9.19).

15-5. In these cases, we are making the approximation that the dynamics of the sensors and actuators are essentially infinitely fast and are independent of, or “uncoupled from” the dynamics of the plant.

Be aware, though, that the full dynamics of devices used for control, especially actuators, cannot always be considered uncoupled from the dynamics of the plant. For one example, the dynamics of a reaction-mass actuator (homework Problem 10.15) in a vibration-control system are usually inextricably coupled with those of the structural plant, as in homework Problem 12.6. For another example, homework Problem 15.7 is an exercise of incorporating the dynamics of a position actuator into a control-system model; in this case, the process involves even more than just inserting the actuator’s transfer function in series within the block diagram of the overall system. In yet another example, Dettmer, 1995, Section 1.3.4 describes a control system for which it was necessary to account for the dynamic characteristics of both sensors and actuators.

Returning now to the rotor-position control system of Figs. 15-4 and 15-5, our objective is to make the output follow the input, $\theta(t) \approx r(t)$, so it is appropriate to define a revised (relative to Fig. 15-3) open-loop configuration. If the feedback loop in Fig. 15-5 were broken, and if the PI controller were not present ($P = 1, b_i = 0$), then the transfer function for this open-loop system clearly would be $K_r \times K_a \times 1/(\tau_1 s + 1)$. We want this to be the same as that of the bare (devoid of control devices) plant, Eq. (15-5), so let’s suppose that we have the ability to set the sensitivities of the input transducer and the position actuator so that $K_r \times K_a = 1$. Also, it will greatly simplify the algebra in the following developments if we suppose further that we can use identical sensors on the input angle and the output angle in the feedback path, so that $K_r = K_\theta$. To summarize, we shall apply the following restrictions on the device sensitivities:

$$K_r \times K_a = 1 \quad \text{and} \quad \frac{K_\theta}{K_r} = 1 \quad (15-6)$$

To compare open-loop and closed-loop system performances, let’s consider response (from zero initial conditions) to step input $r(t) = R_H H(t) \Rightarrow R(s) = R_H/s$. Then, for the open-loop system, using transfer function (15-5) and partial-fraction expansion gives

$$\Theta(s) = R_H \frac{1}{s} \frac{1}{\tau_1 s + 1} = R_H \left(\frac{1}{s} - \frac{1}{s + 1/\tau_1} \right) \quad (15-7)$$

Taking the inverse Laplace transform gives the step response of the open-loop system:

$$\theta(t) = R_H (1 - e^{-t/\tau_1}), \text{ for } t \geq 0 \quad (15-8)$$

Equation (15-8) is simple 1st order step response of the type shown on Fig. 3-3. At the end of this section, there is a comparative numerical evaluation of this open-loop response and step responses for P and PI types of closed-loop control. For now, though,

Chapter 15 Input-error operations: proportional, integral, and derivative types of control

let's just observe from (15-8) that the asymptotic or "final" value of response for times much greater than time constant τ_1 equals the magnitude of the step input, as required:

$$\lim_{t \rightarrow \infty} \theta(t) = R_H \quad (15-9)$$

Next, let's analyze closed-loop proportional (P) control, for which $b_i = 0$ on Fig. 15-5. Thus, for the closed loop on Fig. 15-5, we have for Eq. (14-16) the polynomials $N_G = P \times K_a$, $D_G = \tau_1 s + 1$, $N_H = K_\theta$, and $D_H = 1$, which we use to find the following $CLTF(s)$:

$$\frac{\Theta(s)}{R(s)} = K_r \times \frac{N_G D_H}{D_G D_H + N_G N_H} = \frac{K_r P K_a}{\tau_1 s + 1 + P K_a K_\theta} = K_r K_a \frac{P}{\tau_1 s + 1 + K_r K_a \frac{K_\theta}{K_r} P}$$

With simplifying assumptions (15-6), this becomes

$$CLTF(s) = \frac{\Theta(s)}{R(s)} = \frac{P}{\tau_1 s + 1 + P} = \frac{P}{1 + P} \frac{1}{\left(\frac{\tau_1}{1 + P}\right)s + 1} \equiv \frac{P}{1 + P} \frac{1}{\tau_{1P}s + 1} \quad (15-10)$$

in which the new time constant for the proportionally controlled system is

$$\tau_{1P} \equiv \frac{\tau_1}{1 + P} \quad (15-11)$$

For step input $r(t) = R_H H(t) \Rightarrow R(s) = R_H / s$, Eq. (15-10) gives the transform

$$\Theta(s) = \frac{R_H}{s} \times CLTF(s) = R_H \frac{P}{1 + P} \times \frac{1}{s} \frac{1}{\tau_{1P}s + 1} \quad (15-12)$$

Hence, we find the step response of the proportionally controlled system just by comparing Eq. (15-12) with Eq. (15-7) and then modifying Eq. (15-8) appropriately:

$$\theta(t) = R_H \frac{P}{1 + P} (1 - e^{-t/\tau_{1P}}), \text{ for } t \geq 0 \quad (15-13)$$

The asymptotic or "final" value of proportionally controlled step response for times much greater than time constant τ_{1P} is:

$$\lim_{t \rightarrow \infty} \theta(t) = R_H \frac{P}{1 + P} \quad (15-14)$$

This situation provides the opportunity to introduce the *final-value theorem* and to illustrate its application; this is a useful mathematical tool that is derived in the next section. This theorem allows us to find the finite asymptotic value of a time function $f(t)$,

Chapter 15 Input-error operations: proportional, integral, and derivative types of control

assuming that such a value exists, based only on the Laplace transform $L[f(t)] = F(s)$, without requiring that the equation for $f(t)$ be available:

$$\lim_{t \rightarrow \infty} f(t) = \lim_{s \rightarrow 0} [sF(s)] \quad (15-15)$$

For step response of the proportionally controlled system, the final-value theorem and Eq. (15-12) give

$$\begin{aligned} \lim_{t \rightarrow \infty} \theta(t) &= \lim_{s \rightarrow 0} s \times \Theta(s) \\ &= \lim_{s \rightarrow 0} \left(s \times R_H \frac{P}{1+P} \frac{1}{s} \frac{1}{\tau_{1P}s + 1} \right) = \lim_{s \rightarrow 0} \left(R_H \frac{P}{1+P} \frac{1}{\tau_{1P}s + 1} \right) = R_H \frac{P}{1+P} \end{aligned}$$

This is another, easier method for finding result (15-14). The final-value theorem was not needed to derive the correct asymptotic solution for this simple case, but it will be a useful, labor-saving tool for more complicated cases in the future.

Comparing Eq. (15-14) with the required asymptotic value $\lim_{t \rightarrow \infty} \theta(t) = R_H$, Eq. (15-9), we see that, because $P/(1+P) \neq 1$, the proportionally controlled system fails to satisfy the requirement exactly. Let's examine possible values of proportional gain P . Equation (15-11) requires that $P > -1$ so that the system is stable, $\tau_{1P} > 0$. Equation (15-13) requires that $P > 0$ so that the response has the same sign as the input. Moreover, P should be a positive number as large as possible, within practical hardware limitations, because (1) the greater the value of P , the smaller is time constant τ_{1P} , making the system faster than the open-loop system, and (2) the greater the value of P , the closer is the asymptotic value of the output to the value of the input, from Eq. (15-14). The value $P = 4$ is a commonly used proportional gain. But even for a large, positive value of P , the steady-state response will be at least a little smaller than the input. The *steady-state output error*, also known as *offset*, is defined as

$$\Delta\theta_{\text{offset}} \equiv R_H - R_H \frac{P}{1+P} = \frac{R_H}{1+P} \quad (15-16)$$

A large value, $P > 9$, is required to reduce the offset to less than 10% of the desired steady-state output.

There is a simple explanation for the offset produced by proportional (P) control, which also will suggest a remedy. Block diagrams Fig. 15-4 and Fig. 15-5 show that the final value of θ_a must be non-zero, equal to the final value of output θ . In other words, the torsion spring must be completely relaxed (unloaded) at the end of the control process, which is obvious physically. Furthermore, by tracing backwards on the forward branches of the loops on Figs. 15-4 and 15-5, we find the other relevant final values: $w = \theta_a/K_a = \theta/K_a$, and, with $b_i = 0$, $e_e = w/P = \theta_a/(K_a P) = \theta/(K_a P) \neq 0$. Ideally, the final error signal $e_e = e_r - e_\theta$ should be zero, corresponding to the output being exactly the

desired final value; however, the preceding argument shows that the final error for P control alone is inevitably non-zero. This argument also suggests that we seek some way to make the final error equal zero, $e_e = 0$, but still to preserve non-zero input into the position actuator, $w \neq 0$, so that $\theta_a \neq 0$, and so that the final output equals the desired value, $\theta = r$. Integral (I) action can produce this effect: if we add a term to w that is proportional to the integral of the error signal, $\int_{\tau=0}^{\tau=t} e_e(\tau) d\tau$, then we can have a final non-zero control signal, $w \neq 0$, even though the final error itself is zero, $e_e = 0$.

Therefore, let's next find the closed-loop transfer function for closed-loop proportional-integral (PI) control ($b_i = 1$). For the closed loop on Fig. 15-5, the forward-branch transfer function is $G = P \left(1 + \frac{1}{\tau_i s} \right) \times K_a \times \frac{1}{\tau_1 s + 1} = \frac{PK_a(\tau_i s + 1)}{\tau_i s (\tau_1 s + 1)}$, so $N_G = PK_a(\tau_i s + 1)$ and $D_G = \tau_i s (\tau_1 s + 1)$. For the feedback branch, $N_H = K_\theta$ and $D_H = 1$. Therefore, Eq. (14-16) gives the following $CLTF(s)$:

$$\begin{aligned} \frac{\Theta(s)}{R(s)} &= K_r \times \frac{N_G D_H}{D_G D_H + N_G N_H} = \frac{K_r P K_a (\tau_i s + 1)}{\tau_i s (\tau_1 s + 1) + P K_a (\tau_i s + 1) K_\theta} \\ &= K_r K_a \frac{P(\tau_i s + 1)}{\tau_i s (\tau_1 s + 1) + K_r K_a \frac{K_\theta}{K_r} P(\tau_i s + 1)} \end{aligned}$$

With simplifying assumptions (15-6), this becomes

$$\frac{\Theta(s)}{R(s)} = \frac{P(\tau_i s + 1)}{\tau_i s (\tau_1 s + 1) + P(\tau_i s + 1)} = \frac{P(\tau_i s + 1)}{\tau_i \tau_1 s^2 + (1 + P) \tau_i s + P} \quad (15-17)$$

Before analyzing Eq. (15-17) in more detail, let's first determine if, as predicted above, PI control eliminates the P-control offset of Eq. (15-16). For step input $r(t) = R_H H(t) \Rightarrow R(s) = R_H / s$, Eq. (15-17) gives the transform

$$\Theta(s) = \frac{R_H}{s} \frac{P(\tau_i s + 1)}{\tau_i s (\tau_1 s + 1) + P(\tau_i s + 1)} \quad (15-18)$$

Applying final-value theorem (15-15) to Eq. (15-18) gives

$$\lim_{t \rightarrow \infty} \theta(t) = \lim_{s \rightarrow 0} s \times \Theta(s) = \lim_{s \rightarrow 0} \left(\frac{R_H P(\tau_i s + 1)}{\tau_i s (\tau_1 s + 1) + P(\tau_i s + 1)} \right) = \lim_{s \rightarrow 0} \left(R_H \frac{P}{s} \right) = R_H \quad (15-19)$$

Therefore, integral action does indeed eliminate the error that is inevitable from purely proportional control.

Chapter 15 Input-error operations: proportional, integral, and derivative types of control

Returning to transfer function (15-17), we see that integral action has increased the order of the system to 2nd order from the 1st order of the plant. Accordingly, we can re-write the transfer function in terms of parameters appropriate for a 2nd order system:

$$\frac{\Theta(s)}{R(s)} = \frac{\frac{P}{\tau_i \tau_1} (\tau_i s + 1)}{s^2 + \frac{1+P}{\tau_1} s + \frac{P}{\tau_i \tau_1}} \equiv \frac{\omega_n^2 (\tau_i s + 1)}{s^2 + 2\zeta \omega_n s + \omega_n^2} \quad (15-20)$$

in which the undamped natural frequency and the viscous damping ratio are, respectively,

$$\omega_n = \sqrt{\frac{P}{\tau_i \tau_1}} \quad \text{and} \quad \zeta = \frac{1}{2\omega_n} \frac{1+P}{\tau_1} = \frac{1}{2} \sqrt{\frac{\tau_i}{\tau_1}} \frac{1+P}{\sqrt{P}} \quad (15-21)$$

Note that this system is not a standard 2nd order system, as defined in Eq. (9-13). The term $\omega_n^2 \tau_i s$ in the numerator of Eq. (15-20) makes this system non-standard; that term corresponds to right-hand-side dynamics in the ODE describing the system, which is $\ddot{\theta} + 2\zeta \omega_n \dot{\theta} + \omega_n^2 \theta = \omega_n^2 (\tau_i \dot{r} + r)$. The non-standard character means, among other things, that the step-response specifications derived in Section 9-8 do not apply exactly for this system.

For comparison with the previous cases of open-loop and P control, let's solve for response of the PI-controlled system to step input $r(t) = R_H H(t) \Rightarrow R(s) = R_H / s$. Eq. (15-20) gives the transform

$$\Theta(s) = \frac{R_H}{s} \frac{\omega_n^2 (\tau_i s + 1)}{s^2 + 2\zeta \omega_n s + \omega_n^2} = R_H \left[\frac{\omega_n^2 \tau_i}{\omega_d} \frac{\omega_d}{(s + \zeta \omega_n)^2 + \omega_d^2} + \frac{1}{s} \frac{\omega_n^2}{(s + \zeta \omega_n)^2 + \omega_d^2} \right] \quad (15-22)$$

The second form of Eq. (15-22) is written subject to the condition $|\zeta| < 1$, so that $\omega_d^2 \equiv \omega_n^2 (1 - \zeta^2) > 0$; since $\zeta > 0$ from Eq. (15-21), this means that we assume the system to be underdamped, at least initially. With Eq. (15-22) in the second form, we can apply the following inverse Laplace transforms. First, Eqs. (9-17) and (9-20) give:

$$L^{-1} \left[\frac{\omega_d}{(s + \zeta \omega_n)^2 + \omega_d^2} \right] = e^{-\zeta \omega_n t} \sin \omega_d t \quad (15-23)$$

Next, Eqs. (9-17) and (9-29) give (see homework Problem 9.12):

$$L^{-1} \left[\frac{1}{s (s + \zeta \omega_n)^2 + \omega_d^2} \right] = 1 - e^{-\zeta \omega_n t} \left(\cos \omega_d t + \frac{\zeta \omega_n}{\omega_d} \sin \omega_d t \right) \quad (15-24)$$

Chapter 15 Input-error operations: proportional, integral, and derivative types of control

Substituting (15-23) and (15-24) into the inverse transform of (15-22), then combining terms appropriately, gives the step response of the PI-controlled underdamped system:

$$\theta(t) = R_H \left[1 - e^{-\zeta \omega_n t} \left(\cos \omega_d t + \frac{\zeta \omega_n - \omega_n^2 \tau_i}{\omega_d} \sin \omega_d t \right) \right], \text{ for } 0 \leq \zeta < 1 \text{ and } 0 \leq t \quad (15-25)$$

In the numerical example to follow, we shall encounter cases of both underdamping and overdamping; therefore, it is appropriate to apply conversion Eq. (9-45) to underdamped response equation (15-25) in order to write the following equation for step response of the PI-controlled overdamped system:

$$\theta(t) = R_H \left[1 - e^{-\zeta \omega_n t} \left(\cosh \mu_d t + \frac{\zeta \omega_n - \omega_n^2 \tau_i}{\mu_d} \sinh \mu_d t \right) \right], \text{ for } 1 < \zeta \text{ and } 0 \leq t \quad (15-26)$$

in which $\mu_d = \omega_d \sqrt{\zeta^2 - 1}$.

Now that we have derived the equations for step response, let's evaluate a numerical case with physically plausible parameters; in particular, let's calculate and compare the step responses: Eq. (15-8) for the open-loop system; Eq. (15-13) for the P-controlled system; and Eq. (15-25) or Eq. (15-26) for the PI-controlled system. We let the time constant of the open-loop system have the value $c_\theta/k_\theta \equiv \tau_1 = 1$ sec, and we use the typical value $P = 4$ for the proportional gain. For the PI-controlled system, we consider three different integral time constants, $\tau_i = 1/3, 2/3$, and 1 sec. The following is a MATLAB M-file that calculates the step responses and plots them on a single graph:

```
%MATLABdemo151.m
%1st order system: spring-connected rotor in a viscous fluid
%Step responses: open-loop, P-controlled, and PI-controlled
t=0:.01:4;
taul=1;%time constant of open-loop system = 1 sec
thOL=1-exp(-t/taul);%open-loop step response ratio
P=4;taulP=taul/(1+P);
thP=P/(1+P)*(1-exp(-t/taulP));%step response ratio, P control
plot(t,thOL,t,thP),hold
taui=[1/3 2/3 1];%step response ratios, three cases of PI control
for ni=1:3,
    wn=sqrt(P/(taui(ni)*taul));zeta=(1+P)/(2*wn*taul);
    sig=zeta*wn;case_taui_zeta=[ni taui(ni) zeta]
    if zeta < 1
        wd=wn*sqrt(1-zeta^2);
        thPI(ni,:)=1-exp(-sig*t).*(cos(wd*t)+(sig-wn^2*taui(ni))/wd*sin(wd*t));
    else
        md=wn*sqrt(zeta^2-1);
        thPI(ni,:)=1-exp(-sig*t).*(cosh(md*t)+(sig-wn^2*taui(ni))/md*sinh(md*t));
    end
    plot(t,thPI(ni,:),'k')
end
grid,xlabel('Time t (sec)'),ylabel('Step response ratio \theta(t)/R_H')
title('Position control of a spring-connected rotor in a viscous fluid')
```

Chapter 15 Input-error operations: proportional, integral, and derivative types of control

The MATLAB command and resulting output are printed below. The three cases shown are for PI control with integral time constant (“ τ_i ”) $\tau_i = 1/3$, $2/3$, and 1 sec; note the values of viscous damping ratio (“ ζ ”): the system is underdamped for $\tau_i = 1/3$ sec, but overdamped for $\tau_i = 2/3$ and 1 sec.

```
>> MATLABdemo151
Current plot held

case_taui_zeta =
    1.0000    0.3333    0.7217

case_taui_zeta =
    2.0000    0.6667    1.0206

case_taui_zeta =
    3.0000    1.0000    1.2500
```

Figure 15-6 is the graphical output from the MATLAB M-file.

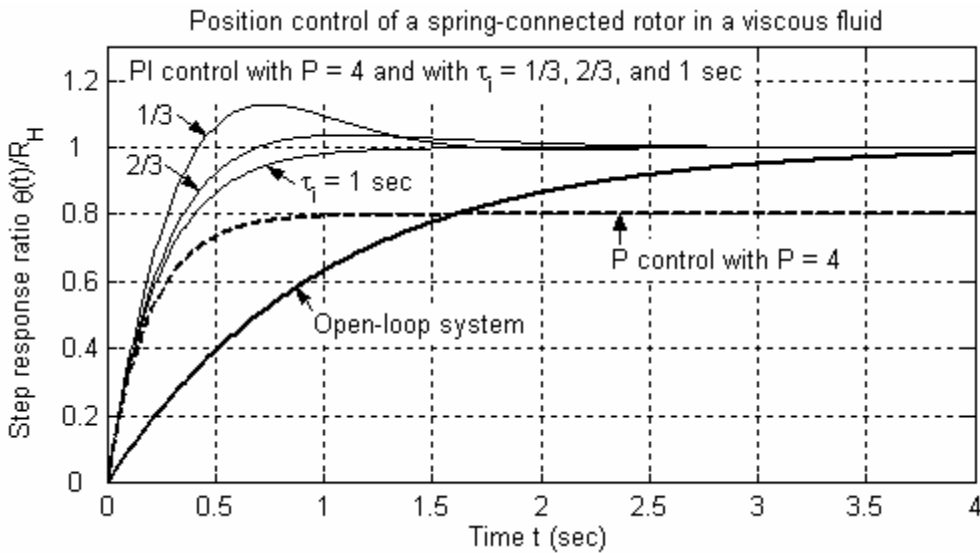


Figure 15-6 Step responses for no control (open-loop), proportional (P) control, and proportional-integral (PI) control

Figure 15-6 illustrates clearly the results derived previously regarding the time constants for open-loop and P control, and the final values of step response for open-loop, P control and PI control. The new and interesting results on Fig. 15-6 relate to step response of the system under PI control. For all three values of τ_i , the speed of response is much faster than that of the open-loop system, and comparable to that for P control. Moreover, there is a design trade-off for this 2nd order system between rise time and overshoot. Recall from Section 9-8 that rise time is the time required for the response first to reach the desired value, and overshoot is the maximum amount by which the response exceeds the desired value. For most cases, the control designer would like to make rise time as fast as possible, and to minimize overshoot. However, Fig. 15-6 shows that we

cannot simultaneously do both in this case: rise time is fastest for small τ_i , but overshoot is minimized or eliminated with larger τ_i . Therefore, the control designer must compromise and select a value of τ_i that produces practically acceptable values of both rise time and overshoot, even though neither response parameter would be the best possible.

It is interesting to observe also from Fig. 15-6 that, for this non-standard 2nd order system, there is overshoot for $\tau_i = 2/3$ sec $\Rightarrow \zeta = 1.02$; in other words, there is overshoot even though the system is overdamped. This is different from the step response of a positively damped standard 2nd order system (Section 9-8), for which overshoot can occur only if $0 \leq \zeta < 1$.

15-3 Derivation of the final-value theorem

Consider a continuous physical function $f(t)$, with continuous derivative df/dt , and with Laplace transform $L[f(t)] = F(s)$. The final-value theorem expresses the final, steady-state value of $f(t)$ in terms of $F(s)$ as:

$$\lim_{t \rightarrow \infty} f(t) = \lim_{s \rightarrow 0} [sF(s)] \quad (15-15) \text{ repeated}$$

This theorem is useful for finding the final value because it is almost always easier to derive the Laplace transform and evaluate the limit on the right-hand side, than to derive the equation for $f(t)$ and evaluate the limit on the left-hand side. Final-value theorem (15-15) is valid provided that $\lim_{t \rightarrow \infty} f(t)$ exists (*i.e.*, is a finite, constant value). But we must apply Eq. (15-15) with care, because the theorem itself fails to distinguish between functions for which the limit exists and functions which have no limit. Indeed, the theorem can predict falsely that an unstable system has a limit when, in fact, there is none, *i.e.*, that $\lim_{t \rightarrow \infty} f(t) \rightarrow \pm\infty$.

Derivation of the final-value theorem is based upon definition (2-13) of a Laplace transform and the Laplace transform (2-15b) of a derivative:

$$L\left[\frac{d}{dt} f(t)\right] = \int_{t=0}^{t=\infty} e^{-st} \left[\frac{d}{dt} f(t)\right] dt = sF(s) - f(0)$$

Taking the limit of all terms as $s \rightarrow 0$ gives

$$\lim_{s \rightarrow 0} L\left[\frac{d}{dt} f(t)\right] = \int_{t=0}^{t=\infty} 1 \times \left[\frac{d}{dt} f(t)\right] dt = \lim_{s \rightarrow 0} [sF(s)] - f(0)$$

Now the integral is evaluated easily:

$$\int_{t=0}^{t=\infty} \left[\frac{d}{dt} f(t) \right] dt \equiv f(\infty) - f(0) = \lim_{s \rightarrow 0} [sF(s)] - f(0)$$

$$\Rightarrow f(\infty) \equiv \lim_{t \rightarrow \infty} f(t) = \lim_{s \rightarrow 0} [sF(s)]$$

This completes the derivation of final-value theorem (15-15), which was applied earlier to re-derive result (15-14) and in Eq. (15-19).

15-4 Example of proportional-derivative (PD) control

Next, we consider the effect of derivative control, the third type of operation on the error signal indicated in Eqs. (15-1) and (15-2). The derivative term (with $b_d = 1$) in the actuator signal $w(t)$ is $P\tau_d \times de_e/dt$. This term is proportional to the rate of change of the error signal, so it anticipates, in a sense, any increase in the error, and it acts to oppose that increase. Derivative action is used in combination with proportional action or proportional-integral action, but not by itself. Whereas proportional action has the effect of a restoring linear spring, derivative action has the effect of a viscous damper. Therefore, derivative control by itself would fail to provide action that forces system output toward the desired value.

A reality check is appropriate at this point. The derivative output $x_d(t) \equiv \dot{e}_e$ of an ideal PID controller in Eq. (15-1) is physically unrealistic, because it is not possible to measure exactly, in real time, the derivative \dot{e}_e of the error signal. Exact real-time measurement of a derivative at an instant would require information about future values of the signal, but future values are unknown. Another manifestation of the unrealism of the derivative term is the associated transfer function, $X_d/E_e = s/1$, which is written here as a fraction on the right-hand side so as to emphasize that the polynomial order (in s) of the numerator is higher than that of the denominator. Thus, this transfer function is *acausal*, meaning that the current output of the ideal differentiator must be dependent upon future, as well as past and present, values of the error signal (see Bélanger, 1995, p. 440).

Since the exact differentiator of Eq. (15-1) cannot be realized physically, an actual PD controller often includes an approximate differentiator in the form of a 1st order *high-pass filter* described by the ODE $\varepsilon\tau_d \dot{x}_d + x_d = \dot{e}_e$; in this ODE, τ_d is the derivative time constant, and ε is a small positive number typically selected to be in the range 0.1 to 0.3 (Ogata, 2001, pages 700 and 727). The transfer function of this approximate differentiator is $X_d(s)/E_e(s) = s/(\varepsilon\tau_d s + 1)$, which is *causal*, therefore physically realizable. For error signals that are slowly varying in time relative to the high-pass-filter break frequency $1/(\varepsilon\tau_d)$ rad/sec, this approximate differentiator is very accurate, but for faster error signals the device's output fails to approximate the derivative of the error signal (see homework Problem 15.4). In practice, therefore, the selection of parameters τ_d and ε is based at least partly on the speed of signals that the PD controller is expected to process. The operation of an actual PD controller using the approximate differentiator is

Chapter 15 Input-error operations: proportional, integral, and derivative types of control

$w(t) = P[e_e(t) + \tau_d x_d(t)]$; you can easily show that the transfer function of the actual PD controller is $\frac{W(s)}{E_e(s)} = P\left(1 + \tau_d \frac{X_d(s)}{E_e(s)}\right) = P\left(1 + \frac{\tau_d s}{\varepsilon \tau_d s + 1}\right) = P\left(\frac{(1 + \varepsilon)\tau_d s + 1}{\varepsilon \tau_d s + 1}\right)$.

It is standard in introductory discussions to describe PD control in the context of the ideal (though physically unrealizable) differentiator $x_d \equiv \dot{e}_e$, rather than the more realistic approximate differentiator $\varepsilon \tau_d \dot{x}_d + x_d = \dot{e}_e$. The approximate differentiator leads to a higher-order system and much more complicated algebra, from which it is difficult to infer basic physical characteristics of PD control. Therefore, in the rest of this section, and in the continued examination of this same example in homework Problem 15.1 and in Section 16-2, we shall follow the standard introductory procedure and use the ideal PD-controller transfer function $P(1 + \tau_d s)$ from Eq. (15-2). Most of the theoretical results produced by this approach are good approximations to what would be realized from a properly designed real PD controller, at least for sufficiently slowly varying inputs and outputs.

To illustrate proportional-derivative (PD) control, we consider again the problem of controlling position $\theta(t)$ of a rotor with significant inertia J , as discussed in Chapter 14 [Figs. 14-1, 14-2, and 14-5, and Eqs. (14-1) and (14-2)]. Recall that the input to the system is operator setting $r(t)$. Let's neglect disturbance moments, $M_d(t) = 0$. Figure 15-7 is the Laplace block diagram for the P-controlled system, from which the loop transfer functions are $G(s) = PK_a/(Js^2)$ and $H(s) = K_\theta$. Hence, we use Eq. (14-16) to find

$$CLTF(s) = \frac{\Theta(s)}{R(s)} = K_r \times \frac{N_G D_H}{D_G D_H + N_G N_H} = K_r \times \frac{PK_a}{Js^2 + PK_a K_\theta} \equiv \frac{K_r}{K_\theta} \frac{\omega_n^2}{s^2 + \omega_n^2}$$

Undamped natural frequency in this $CLTF(s)$ is defined by $\omega_n^2 = PK_a K_\theta / J$. Suppose that the input is a step function with magnitude R_H : $r(t) = R_H H(t)$. For this input, the Laplace

transform of response is $\Theta(s) = \frac{R_H}{s} \frac{K_r}{K_\theta} \frac{\omega_n^2}{s^2 + \omega_n^2}$. Application of inverse transform (15-

24), with $\zeta = 0$, gives the step response $\theta(t) = (R_H K_r / K_\theta)(1 - \cos \omega_n t)$. This is undamped motion that oscillates forever about the desired final value, $\theta = R_H K_r / K_\theta$ [see Eq. (7-14) and Fig. 7-3], so it is unacceptable for a position control system. In this case, P control alone has the effect of a restoring linear spring, but it provides no damping.

In order to improve the control performance, we add derivative action, upgrading from P control to ideal PD control. From Eq. (15-2) with $b_i = 0$ and $b_d = 1$, the ideal PD-controller

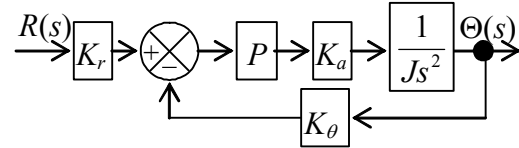


Figure 15-7 Proportional control of rotor position

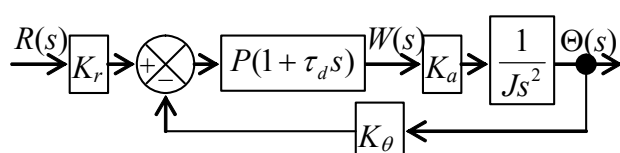


Figure 15-8 Ideal proportional-derivative (PD) control of rotor position

transfer function is $P(1 + \tau_d s)$, so the Laplace block diagram for the closed-loop system becomes that shown in Fig. 15-8. In this case, the loop forward-branch transfer function is $G(s) = P(1 + \tau_d s)K_a/(Js^2)$, so the closed-loop transfer function of the system is

$$\frac{\Theta(s)}{R(s)} = K_r \times \frac{N_G D_H}{D_G D_H + N_G N_H} = K_r \times \frac{P(1 + \tau_d s)K_a}{Js^2 + P(1 + \tau_d s)K_a K_\theta} = \frac{K_r P K_a (1 + \tau_d s)}{Js^2 + P K_a K_\theta \tau_d s + P K_a K_\theta}$$

As we did in Eqs. (15-20) and (15-21), which apply to PI control (but of a different plant), we can now re-write this PD closed-loop transfer function in terms of parameters appropriate for a damped 2nd order system:

$$\frac{\Theta(s)}{R(s)} = \frac{K_r}{K_\theta} \frac{(PK_a K_\theta / J)(\tau_d s + 1)}{s^2 + (PK_a K_\theta / J)\tau_d s + (PK_a K_\theta / J)} \equiv \frac{K_r}{K_\theta} \frac{\omega_n^2 (\tau_d s + 1)}{s^2 + 2\zeta\omega_n s + \omega_n^2} \quad (15-27)$$

In Eq. (15-27) the undamped natural frequency and the viscous damping ratio are, respectively:

$$\omega_n = \sqrt{\frac{PK_a K_\theta}{J}} \quad \text{and} \quad \zeta = \frac{1}{2\omega_n} \frac{PK_a K_\theta}{J} \tau_d = \frac{1}{2} \omega_n \tau_d \quad (15-28)$$

The obvious effect of the derivative action is to add damping to the 2nd order system, and this damping improves the control performance (see homework Problem 15.1). Note also that the term $\omega_n^2 \tau_d s$ in the numerator of Eq. (15-27) makes this system non-standard relative to definition (9-13) of the standard 2nd order ODE. The non-standard character means, among other things, that the step-response specifications derived in Section 9-8 do not apply exactly for this system.

15-5 Homework problems for Chapter 15

15.1 Consider closed-loop transfer function (15-27), with definitions (15-28), for position control of a rotor by an ideal PD controller.

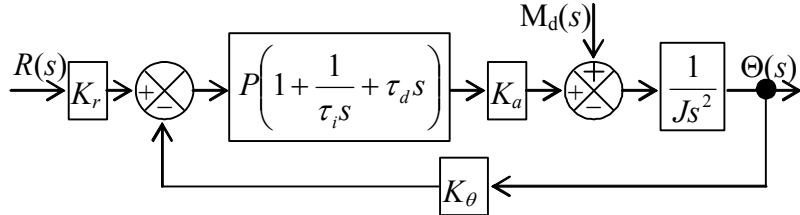
- (a) Suppose that we know rotational inertia J , actuator sensitivity K_a , and equal input and feedback transducer sensitivities, $K_r = K_\theta$, and that we want to specify (*i.e.*, “design”) the undamped natural frequency ω_n and the viscous damping ratio ζ for this controlled system. Hence, we need to determine appropriate values for proportional gain P and derivative time constant τ_d , which we would set in the PD controller. For a particular system, we have $J = 2.56\text{e-}3 \text{ lb-sec}^2\text{-inch}$ (the value for a small aluminum wheel about four inches in diameter, Fig. 3-1), and the product $K_r K_a = 0.0350 \text{ lb-inch/rad}$; let’s specify $f_n = \omega_n / 2\pi = 1.00 \text{ Hz}$ (so that step-response rise time will be around $\frac{1}{4} \text{ sec}$) and $\zeta = +0.1$ (too low for most practical control systems, but it suits the overall purposes of this problem). Calculate the required values of P and τ_d (sec).
- (b) Use the MATLAB `residue` operation (see homework Problem 2.15) to expand the transfer function [with the numerical values of part (a)] into a partial-fraction expansion. The poles are critical to the stability of any system, which is the subject of Chapter 16. For this system, you should find a pair of poles that are complex conjugates, and their real part should be negative—this means that the system is stable.
- (c) Let the input be a step, $r(t) = R_H H(t)$. First, apply the final-value theorem to find $\lim_{t \rightarrow \infty} \theta(t)$. Next, use inverse transforms (15-23) and (15-24) [or just appropriately adapt step response (15-25) to this case] to show that the step response is

$$\theta(t) = R_H \left[1 - e^{-\zeta\omega_n t} \left(\cos \omega_d t - \frac{\zeta\omega_n}{\omega_d} \sin \omega_d t \right) \right], \text{ for } |\zeta| < 1 \text{ and } \omega_d = \omega_n \sqrt{1 - \zeta^2}$$

Finally, let the input step magnitude be $R_H = 0.1$ radian, with the numerical values of part (a), and use MATLAB to plot the output $\theta(t)$ over the time interval 0-2.5 sec, about $2\frac{1}{2}$ cycles.

- (d) To simulate what would happen if you made a mistake and got the wrong sign for τ_d (and therefore for ζ), let $\zeta = -0.1$, and repeat the operations of parts (b) and (c). If you can plot $\theta(t)$ for both $\zeta = +0.1$ and $\zeta = -0.1$ on the same graph, it will enhance comparison of the two cases. For $\zeta = -0.1$, you should find the real part of the complex conjugate poles to be positive; the associated time history $\theta(t)$ should indicate system instability. Observe for this unstable system that the final-value theorem incorrectly predicts a finite steady-state value for this step response.

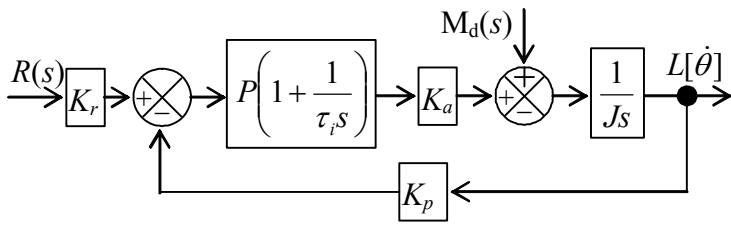
15.2 Consider ideal PID control of the position of a rotor that has significant inertia J . Let's also account for a disturbance moment $M_d(t)$ acting upon the rotor. The Laplace block diagram for this 3rd order system is drawn above. In the following exercises, assume that this system is stable.



(a) For zero disturbance, $M_d(s) = 0$, derive the algebraic equation for closed-loop transfer function $\Theta(s)/R(s)$. For step input, $r(t) = R_H H(t)$, apply the final-value theorem to find $\lim_{t \rightarrow \infty} \theta(t)$.

(b) For zero input, $R(s) = 0$, derive the algebraic equation for closed-loop transfer function $\Theta(s)/M_d(s)$. For step disturbance, $M_d(t) = M_H H(t)$, apply the final-value theorem to find $\lim_{t \rightarrow \infty} \theta(t)$. A control system should suppress permanent output due to a step disturbance.

15.3 Consider PI control of the speed (not position) of a rotor that has significant inertia J . The sensor on the output is a tachometer with gain constant K_p , so the electrical signal that is fed back is $K_p \dot{\theta}$. (This configuration illustrates a general rule-of-thumb in control-system design: sense and feed back the quantity that you want to control.) This is a sim-



plified model, for example, of an automobile's cruise-control system. Let's also allow for a disturbance moment $M_d(t)$ acting upon the rotor. The Laplace block diagram for this system is at left.

(a) For zero disturbance, $M_d(s) = 0$, derive the algebraic equation in terms of all parameters on the Laplace block diagram for the closed-loop transfer function $L[\dot{\theta}]/R(s)$ that relates output rotational velocity $\dot{\theta}(t)$ to input command $r(t)$. For step input, $r(t) = R_H \times H(t)$, apply the final-value theorem to find the algebraic equation for $\lim_{t \rightarrow \infty} \dot{\theta}(t)$, assuming that this asymptotic value exists. Explain (perhaps using an example from your own experience, such as a cruise-control system) the physical significance of the ratio K_r/K_p of the input-transducer sensitivity to the tachometer sensitivity.

(b) Derive algebraic equations for undamped natural frequency ω_n and viscous damping ratio ζ of this controlled system, in terms of inertia J , actuator sensitivity K_a , tachometer sensitivity K_p , proportional gain P , and integral time constant τ_i .

15.4 In this problem, you will produce graphically and compare the frequency-response functions of the exact, but physically unrealizable differentiator $x_d \equiv \dot{e}_e$ (which is used in this book for ideal PD control) and an approximate, but physically realizable differentiator that has the character of a high-pass filter.

(a) Section 15-4 gives the ODE of the approximate differentiator as $\varepsilon\tau_d\dot{x}_d + x_d = \dot{e}_e$, with τ_d being the positive derivative time constant and ε being a small positive number in the range 0.1-0.3; show that the complex frequency-response function (FRF) of output signal $x_d(t)$ relative to input signal $e_e(t)$ is $FRF(\omega) = j\omega/(1 + j\omega\varepsilon\tau_d)$.

(b) For frequency response, the input signal has the steady-state sinusoidal form $e_e(t) = E_e \cos \omega t$ and the output signal has the corresponding form $x_d(t) = X_d(\omega) \cos(\omega t + \phi)$. Use the FRF of part (a) to show that the equations for FRF magnitude ratio and phase of the approximate differentiator are $\frac{X_d(\omega)}{\omega_b E_e} = \frac{\bar{\omega}}{\sqrt{1 + \bar{\omega}^2}}$ and $\phi(\omega) = \frac{\pi}{2} - \tan^{-1} \bar{\omega}$, in which

the break frequency is $\omega_b \equiv 1/(\varepsilon\tau_d) = 2\pi f_b$ and the dimensionless frequency ratio is $\bar{\omega} \equiv \omega/\omega_b = f/f_b$. Use the magnitude-ratio equation to derive equations for the low-frequency and high-frequency asymptotes, and sketch those asymptotes on a log-log graph such as Fig. 4-2. The approximate differentiator should exhibit the character of a *high-pass filter*, analogous to the system of homework Problem 4.4. Use the asymptotes as an envelope to guide you in sketching the actual curve of $X_d(\omega)/(\omega_b E_e)$, as is done on Fig. 4-2. Finally, on a semi-log graph below the log-log graph (analogous to Fig. 4-1), sketch the variation with frequency of phase $\phi(\omega)$.

(c) Now consider the exact differentiator, with equation $x_d \equiv \dot{e}_e$. Repeat all the steps of parts (a) and (b) for the exact differentiator, sketching the magnitude-ratio and phase curves on the part (b) graphs, but in some different color or line style, so that the curves for exact and approximate differentiators are clearly distinguishable. You should be able to infer from these final graphs the ranges of frequency over which the approximate differentiator is reasonably accurate, or inaccurate.

15.5 Consider the transfer function of the PD-controlled rotor position of Section 15-4, Eq. (15-27) with equal input and feedback transducer sensitivities, $K_r = K_\theta$, in the form $\Theta(s) = \frac{K_r P K_a (1 + \tau_d s)}{R(s) = J s^2 + K_r P K_a \tau_d s + K_r P K_a}$. Use this transfer function and the block diagram of

Fig. 15-8 to write the algebraic equation for the transfer function of the PD controller, $W(s)/R(s)$. Now, examine the nature of $W(s)/R(s)$ in the following steps:

(a) Find the order m of the numerator polynomial and the order n of denominator polynomial of $W(s)/R(s)$. Is this transfer function causal or acausal, and what does that mean in theory regarding the physical realism of $W(s)/R(s)$?

(b) Suppose that the input is the infinitely fast step function $r(t) = R_H H(t)$ of homework Problem 15.1(c). Show that the controller-output transform $W(s)$ must have a constant *direct term*, as defined in homework Problem 2.15. What is the component of time response $w(t)$ that corresponds to the direct term of $W(s)$, and is this a physically realizable signal from a real device? Your conclusions from parts (a) and (b) should be compatible.

(c) If you conclude in parts (a) and (b) that something is physically unrealistic about these theoretical results, then what is there in the theoretical analysis that makes the results defective? Propose a remedy that should produce physically realizable results, and show succinctly, with appropriate algebraic equations and written explanation (but no calculations), why your proposed remedy should work.

15.6 Consider control of a spacecraft's pitch attitude, $\theta(t)$, for which the ODE of motion, from Eq. (14-7), is $J\ddot{\theta} = M_a(t) + M_d(t)$, where $M_d(t)$ is a disturbance moment. In this problem, you will apply a physically realizable form of PD control, with the control actuator moment defined as $M_a(t) = K_a \times w(t)$, where K_a is the actuator sensitivity. The output signal from the realizable PD controller is $w(t) = P[e_e(t) + \tau_d x_d(t)]$, where $x_d(t)$ is the dependent variable in the ODE $\varepsilon\tau_d \dot{x}_d + x_d = e_e$ (see the relevant discussion in Section 15-4). The input error is $e_e(t) = K_r r(t) - K_\theta \theta(t)$, where $r(t)$ is the input operator setting, and K_r and K_θ are the transducer sensitivities at, respectively, the input and output feedback.

(a) Draw and label completely the Laplace block diagram of this system, from input $R(s) \equiv L[r(t)]$ to output $\Theta(s) \equiv L[\theta(t)]$, including disturbance moment signal $M_d(s) = L[M_d(t)]$.

(b) For $M_d(s) = 0$, derive from the block diagram of part (a) the closed-loop transfer function $CLTF(s) = \Theta(s)/R(s) = Num(s)/Den(s)$, where $Num(s)$ and $Den(s)$ are polynomials in powers of s . *Partial answer:* $Den(s) = Js^2(\varepsilon\tau_d s + 1) + PK_a K_\theta [\tau_d(1 + \varepsilon)s + 1]$

(c) For step input, $r(t) = R_H H(t)$, apply the final-value theorem to find $\lim_{t \rightarrow \infty} \theta(t)$, provided that the system is stable.

(d) How does $CLTF(s)$ in part (b), for a physically realizable form of PD control, differ from the corresponding closed-loop transfer function that applies for an ideal but unrealizable PD controller, for which $w(t) = P[e_e(t) + \tau_d \dot{e}_d(t)]$? [Do not re-derive this $CLTF(s)$ from scratch; instead, just make a simple substitution in the $CLTF(s)$ of part (b).] Discuss in one or two sentences.

15.7 Consider the “position actuator” depicted on functional diagram Fig. 15-4, which represents a system for control of a rotor immersed in a viscous liquid. Suppose that the position actuator is the rotor-position control system of Fig. 14-11, and that Fig. 14-12 is the actuator’s Laplace block diagram. Your assignment in this problem is to revise the immersed-rotor control system’s Laplace block diagram, Fig. 15-5, to incorporate the po-

sition-actuator dynamics, replacing the simplified block of actuator gain K_a with an appropriate version of Fig. 14-12, and making any other necessary modifications. There are at least three significant changes required, the first two being notational. (1) You should re-label the input of the modified Fig. 14-12 to $W(s) \equiv L[w(t)]$, replacing $R(s)$, and also re-label the output to $\Theta_a(s) \equiv L[\theta_a(t)]$, replacing $\Theta(s)$. (2) In order to avoid notational ambiguity, you should re-label all system components on Fig. 14-12 having subscripted symbol K , with subscripted symbol Q , e.g., on the revised Fig. 14-12, $K_r \rightarrow Q_r$, and $K_a \rightarrow Q_a$, etc. (3) It is necessary to recognize that the rotational spring with stiffness k_θ shown on Fig. 15-4 imposes upon the position actuator a moment $k_\theta(\theta - \theta_a)$. The quantities labeled on Figs. 14-11 and 14-12 that can represent moment $k_\theta(\theta - \theta_a)$ are, respectively, $M_d(t)$ and $M_d(s)$, for example, $M_d(s) = k_\theta[\Theta(s) - \Theta_a(s)]$. (However, the moment $k_\theta(\theta - \theta_a)$ is clearly defined and not at all random or unpredictable mathematically, so it is not truly a *disturbance* in the sense defined in Section 14-2, with reference to Fig. 14-2.) Accounting for items (1)-(3) and any other necessities, draw a Laplace block diagram of the immersed-rotor control system, a diagram that incorporates the position-actuator dynamics from Fig. 14-12. This block diagram will be somewhat longer than others appearing in this book. It is not required that you simplify this block diagram to derive an algebraic expression for the closed-loop transfer function; it is possible to do so using the operations of block-diagram algebra described in Chapters 13 and 14, but the process would be complicated algebraically, and it would produce a very long and messy equation for $CLTF(s)$. Modern processes using specialized computer software are more appropriate than algebra-by-hand for a task such as this. For example, if you had numerical values for all the system parameters (J , k_θ , Q_r , ..., τ_1 , P , etc.), then you could easily generate a single equation for $CLTF(s)$ with MATLAB by using the functions `tf`, and `feedback`, and `series` (or, rather than `series`, simply the operation of transfer function multiplication).

Chapter 16 Introduction to system stability: time-response criteria

© 2016 by William L. Hallauer, Jr.

Section 16-1 is a lengthy and detailed, perhaps almost tedious, development of the theory underlying time-response stability criteria. Section 16-2, on the other hand, is a specific example, based upon a control system from Chapter 15, which illustrates explicitly many of the theoretical results of Section 16-1. Rather than reading the two sections sequentially, in series, you, the student, might find the material more interesting and instructive if you read Sections 16-1 and 16-2 together, in parallel.

16-1 General time-response stability criterion for linear, time-invariant systems

For any linear, time-invariant (LTI), single-input-single-output (SISO) physical system, we denote the input as $u(t)$ [or $r(t)$, the reference operator setting for controlled systems] and the output as $x(t)$. For an n^{th} order system, in general, the input and output are related by an ODE of the form

$$a_1 \frac{d^n x}{dt^n} + a_2 \frac{d^{n-1} x}{dt^{n-1}} + \dots + a_n \frac{dx}{dt} + a_{n+1} x = b_1 \frac{d^m u}{dt^m} + b_2 \frac{d^{m-1} u}{dt^{m-1}} + \dots + b_m \frac{du}{dt} + b_{m+1} u \quad (16-1)$$

Symbols a_1, \dots, a_{n+1} and b_1, \dots, b_{m+1} are constants (with the numbering system keyed to MATLAB notation), and $m \leq n$. With use of Eq. (2-16), especially for initial-condition terms, the Laplace transform of Eq. (16-1) is

$$\begin{aligned} & (a_1 s^n + a_2 s^{n-1} + \dots + a_n s + a_{n+1}) L[x(t)] - a_1 \left[s^{n-1} x(0) + s^{n-2} \frac{dx}{dt}(0) + \dots + \frac{d^{n-1} x}{dt^{n-1}}(0) \right] \\ & - a_2 \left[s^{n-2} x(0) + s^{n-3} \frac{dx}{dt}(0) + \dots + \frac{d^{n-2} x}{dt^{n-2}}(0) \right] - \dots - a_n x(0) \quad (16-2) \\ & = (b_1 s^m + b_2 s^{m-1} + \dots + b_m s + b_{m+1}) L[u(t)] \end{aligned}$$

The initial-condition terms on the left-hand side are algebraically messy; it will suit our purposes to combine together known a_k constants and known initial conditions into constant coefficients denoted as IC_k , and to express the initial-condition terms in the following simpler algebraic form, arranged in order of descending powers of s :

$$\begin{aligned} & -\overbrace{a_1 x(0)}^{\equiv IC_1} s^{n-1} - \overbrace{\left[a_1 \frac{dx}{dt}(0) + a_2 x(0) \right]}^{\equiv IC_2} s^{n-2} - \dots - \overbrace{\left[a_1 \frac{d^{n-1} x}{dt^{n-1}}(0) + a_2 \frac{d^{n-2} x}{dt^{n-2}}(0) + \dots + a_n x(0) \right]}^{\equiv IC_n} \\ & \equiv -IC_1 s^{n-1} - IC_2 s^{n-2} - \dots - IC_{n-1} s - IC_n \end{aligned}$$

Therefore, we can express Eq. (16-2) in the algebraically simpler form,

Chapter 16 Introduction to system stability: time-response criteria

$$\begin{aligned}
 & (a_1 s^n + a_2 s^{n-1} + \dots + a_n s + a_{n+1}) L[x(t)] - IC_1 s^{n-1} - IC_2 s^{n-2} - \dots - IC_{n-1} s - IC_n \\
 & = (b_1 s^m + b_2 s^{m-1} + \dots + b_m s + b_{m+1}) L[u(t)]
 \end{aligned} \tag{16-3}$$

The algebraic solution of Eq. (16-3) for the Laplace transform of the output is:

$$L[x(t)] = \frac{IC_1 s^{n-1} + IC_2 s^{n-2} + \dots + IC_{n-1} s + IC_n}{a_1 s^n + a_2 s^{n-1} + \dots + a_n s + a_{n+1}} + \frac{b_1 s^m + b_2 s^{m-1} + \dots + b_m s + b_{m+1}}{a_1 s^n + a_2 s^{n-1} + \dots + a_n s + a_{n+1}} L[u(t)] \tag{16-4}$$

It is appropriate now to examine the nature of transform solution (16-4). Let's refer to the first term on the right-hand side as the "IC-response transform," and to the second term as the "forced-response transform." Observe first that the coefficient of input transform $L[u(t)]$ in the forced-response transform is the system transfer function, from Eq. (4-23),

$$TF(s) \equiv \frac{L[x(t)]}{L[u(t)]} = \frac{b_1 s^m + b_2 s^{m-1} + \dots + b_m s + b_{m+1}}{a_1 s^n + a_2 s^{n-1} + \dots + a_n s + a_{n+1}} \tag{16-5}$$

If the system is controlled with use of feedback, then Eq. (16-5) represents the closed-loop transfer function, which we usually denote as $CLTF(s)$. It is conventional to express $TF(s)$ in the following form, with both numerator and denominator polynomials factored:

$$TF(s) = \frac{b_1 s^m + b_2 s^{m-1} + \dots + b_m s + b_{m+1}}{a_1 s^n + a_2 s^{n-1} + \dots + a_n s + a_{n+1}} \equiv \frac{Num(s)}{Den(s)} = \frac{b_1(s - z_1)(s - z_2)\dots(s - z_m)}{a_1(s - p_1)(s - p_2)\dots(s - p_n)} \tag{16-6}$$

The m roots z_k of polynomial equation $Num(z) = 0$ are called the *zeros* of the transfer function, since $TF(s) = 0$ if s equals any z_k . The n roots p_k of polynomial equation $Den(p) = 0$ are called the *poles* of the transfer function, because $TF(s) \rightarrow \infty$ if s equals any p_k . [Imagine the complex space surface $TF(s)$ graphed as a function of coordinates $\text{Re}(s)$ and $\text{Im}(s)$: for s in the vicinity of any p_k , the surface will look something like that of a circus tent near where it is held up by a structural pole; however, whereas the circus-tent pole has finite length, the mathematical pole is infinitely long.]

Observe next that both right-hand-side terms of Eq. (16-4) have in their denominators the term $Den(s)$ defined in Eq. (16-6). This term is the key to system stability. The n^{th} degree polynomial equation $Den(p) = 0$ is the general¹ *characteristic equation* of the system, and its n roots are the poles p_k , $k = 1, 2, \dots, n$. System stability is determined by the signs of the real parts of the poles. The general result is:

If $\text{Re}(p_k) < 0$ for all $k = 1, 2, \dots, n$, then the system is stable. If, on the other hand, there is at least one pole for which $\text{Re}(p_k) > 0$, then the system is unstable.

¹ The characteristic equation of the free-vibration problem described in Chapter 12 is a specific form, applicable only to undamped free vibration, of this general characteristic equation.

In order to justify this general stability criterion, we shall continue the analysis of Eq. (16-4) by deriving the inverse transform conceptually; however, it is appropriate first to state the criterion above, without proof, so that you can see the simple yet very important result of the analysis without being burdened by all the details of the derivation.

First, let's review without proof some basic results from the theory of polynomial equations with real coefficients, a subject covered in most algebra textbooks. The roots of such equations are either real or complex. Moreover, complex roots always appear in conjugate pairs. For example, if one of the roots of $\text{Den}(p) = 0$ is complex, $p_k = \sigma_k + j\omega_k$, where σ_k and ω_k are real, then one of the other roots is the complex conjugate, $p_{k+1} = \bar{p}_k = \sigma_k - j\omega_k$.

Returning to Eq. (16-4), let's evaluate first the IC-response transform. The numerator polynomial is of degree less than n , that of the denominator polynomial, so we can usually expand the entire term into simple partial-fraction form [see the discussion surrounding Eq. (2-25)]:

$$\frac{IC_1 s^{n-1} + IC_2 s^{n-2} + \dots + IC_{n-1} s + IC_n}{a_1 s^n + a_2 s^{n-1} + \dots + a_n s + a_{n+1}} = \frac{IC_1 s^{n-1} + IC_2 s^{n-2} + \dots + IC_{n-1} s + IC_n}{a_1(s-p_1)(s-p_2)\dots(s-p_n)} = \sum_{k=1}^n \frac{C_k}{s-p_k} \quad (16-7)$$

Right-hand-side constants C_k in Eq. (16-7) are called *residues*. Some relevant results from the theory of fractions of polynomials with real coefficients are: if pole p_k is real, then the associated residue C_k also is real; if pole p_k is complex, then the associated residue C_k also is complex, and the residue associated with the complex conjugate pole p_{k+1} is the conjugate of C_k , $C_{k+1} = \bar{C}_k$. It will be useful in derivations that follow to express a complex residue in polar form, $C_k \equiv |C_k| e^{j\angle C_k}$, in which $|C_k|$ is the absolute value (as in the MATLAB function `abs`), and $\angle C_k$ is the angle (as in the MATLAB function `angle`). See Section 2-1 for a review of complex numbers and complex arithmetic.

Taking the inverse transform of Eq. (16-7) to find initial-condition response, we deal, in general, with two “Types” of terms: (1) terms that have real poles and real residues; and (2) pairs of terms that have complex conjugate poles and complex conjugate residues. The inverse of any Type 1 term is a simple real exponential, from Eq. (2-14):

$$L^{-1}\left[\frac{C_k}{s-p_k}\right] = C_k e^{p_k t}, \quad C_k \text{ real, and } p_k \text{ real} \quad (16-8)$$

In Eq. (16-8), if $p_k < 0$, then the term decays exponentially as time increases, which is stable response. Such a term decays eventually to a static equilibrium state of zero; let's call this *exponential stability*. However, if $p_k > 0$, then the term is a permanently growing exponential as time increases, which is unstable response. Finally, if $p_k = 0$, then the term

Chapter 16 Introduction to system stability: time-response criteria

is constant in time; such response is bounded and therefore not unstable, which is good for practical purposes; but it is also not so stable that it eventually decays to zero.

Next, let's consider Type 2 terms, as defined above Eq. (16-8), and derive the inverse transform of a pair of terms that have complex conjugate poles and complex conjugate residues. In the following sequence of operations, we apply: first, Eq. (2-14); next, identities derived in homework Problems 2.3(a) and 2.4; and, finally, Euler's equation, Eq. (2-8):

$$\begin{aligned}
 L^{-1}\left[\frac{C_k}{s-p_k} + \frac{\bar{C}_k}{s-\bar{p}_k}\right] &= C_k e^{p_k t} + \bar{C}_k e^{\bar{p}_k t} = C_k e^{p_k t} + \overline{C_k e^{p_k t}} = 2 \times \operatorname{Re}[C_k e^{p_k t}] \\
 &= 2 \times \operatorname{Re}\left[\left(|C_k| e^{j\angle C_k}\right) e^{(\sigma_k + j\omega_k)t}\right] = 2|C_k| e^{\sigma_k t} \times \operatorname{Re}\left[e^{j(\omega_k t + \angle C_k)}\right] \\
 &= 2|C_k| e^{\sigma_k t} \cos(\omega_k t + \angle C_k)
 \end{aligned} \tag{16-9}$$

Equation (16-9)² varies with time as a sinusoid modulated by an exponential envelope. With respect to stability, the critical term is the exponential envelope, $e^{\sigma_k t}$, and its character is determined by the sign of $\sigma_k \equiv \operatorname{Re}(p_k)$. If $\operatorname{Re}(p_k) < 0$, then $e^{\operatorname{Re}(p_k)t}$ is a decaying exponential, and the total response is a stable positively damped oscillation. However, if $\operatorname{Re}(p_k) > 0$, then $e^{\operatorname{Re}(p_k)t}$ is a permanently growing exponential, and the total response is an unstable ever-expanding oscillation. Finally, if $\operatorname{Re}(p_k) = 0$, then $e^{\operatorname{Re}(p_k)t}$ is constant in time, and the total response is a sinusoid of constant magnitude; such response is bounded and therefore not unstable; but it is also not so stable that it eventually decays to a static equilibrium state, *i.e.*, it is not exponentially stable.

Now that we have derived the stability criterion for the IC-response terms of Eq. (16-4), let's turn our attention to the forced-response transform,

$$L[x_f(t)] \equiv \frac{b_1 s^m + b_2 s^{m-1} + \dots + b_m s + b_{m+1}}{a_1 s^n + a_2 s^{n-1} + \dots + a_n s + a_{n+1}} L[u(t)] = \frac{b_1(s-z_1)(s-z_2)\dots(s-z_m)}{a_1(s-p_1)(s-p_2)\dots(s-p_n)} L[u(t)]$$

We shall consider explicitly in this derivation only transfer functions for which the following practically common conditions apply: $m < n$; no pole is repeated; no zero equals any pole. With these restrictions and with another restriction described in the next paragraph, this particular derivation does not apply to all conceivable LTI systems. However, the general derivation is more involved than necessary for our purposes. The stability criterion that we shall derive applies to any LTI system, even though we will not prove it in general. In Section 16-2, a specific, non-trivial system is analyzed in detail, in order to illustrate all of the theory that is developed in this section.

² When applying Eq. (16-9), you should assign the title of p_k to the one root (of the complex conjugate pair of roots) for which $\operatorname{Im}(p_k) \equiv \omega_k > 0$, in order to define the oscillatory frequency as being positive. Then you should assign the title of C_k to the residue that is associated with the root for which $\operatorname{Im}(p_k) > 0$.

Chapter 16 Introduction to system stability: time-response criteria

In order to find the conceptual inverse of Eq. (16-10), let's consider the nature of transform $L[u(t)]$ for physically common input functions $u(t)$. In this derivation, we shall consider explicitly only the type of input function whose Laplace transform is a fraction of polynomials in the Laplace variable s , with the numerator polynomial being of lower degree than the denominator polynomial. (However, the same stability criterion that we derive for this special type of input function can be derived for any physically realizable input function.) The following are simple examples of this type of input function, which are defined to be non-zero only for $t \geq 0$: ideal step $H(t)$, for which $L[H(t)] = 1/s$; exponential-unit-impulse $e^{-t/\tau}/\tau$, for which $L[e^{-t/\tau}/\tau] = 1/(\tau s + 1)$; exponential-unit-step $1 - e^{-t/\tau}$, for which $L[1 - e^{-t/\tau}] = 1/[s(\tau s + 1)]$ (see homework Problem 8.6 for a discussion of the exponential-unit-step and exponential-unit-impulse functions); ramped exponential pulse $t e^{-t/\tau}$, for which $L[t e^{-t/\tau}] = 1/(s + 1/\tau)^2$; and sinusoid $\cos \omega t$, for which $L[\cos \omega t] = s/(s^2 + \omega^2)$. Let's denote the Laplace transform of such input functions in a general form:

$$L[u(t)] \equiv \frac{N_u(s)}{D_u(s)} = \frac{d_1 s^{mu} + d_2 s^{mu-1} + \dots + d_{mu} s + d_{mu+1}}{c_1 s^{nu} + c_2 s^{nu-1} + \dots + c_{nu} s + c_{nu+1}} = \frac{d_1(s - w_1)(s - w_2)\dots(s - w_{mu})}{c_1(s - q_1)(s - q_2)\dots(s - q_{nu})} \quad (16-11)$$

Constants c_i and d_i are known coefficients of powers of s , and constants q_i and w_i are, respectively, poles and zeros of the input transform. Keep in mind that we assume $N_u(s)$ in Eq. (16-11) to have lower degree than $D_u(s)$, $mu < nu$.

Proceeding with the conceptual forced-response solution, we substitute Eq. (16-11) into Eq. (16-10):

$$L[x_f(t)] = \frac{b_1(s - z_1)(s - z_2)\dots(s - z_m)}{a_1(s - p_1)(s - p_2)\dots(s - p_n)} \times \frac{d_1(s - w_1)(s - w_2)\dots(s - w_{mu})}{c_1(s - q_1)(s - q_2)\dots(s - q_{nu})} \quad (16-12)$$

Forced-response transform (16-12) is a fraction of polynomials in s , with numerator polynomial degree $m + mu$ being less than denominator polynomial degree $n + nu$. Therefore, we can, in principle, usually expand (16-12) into the following form, in which terms that are associated explicitly with the transfer-function poles have simple partial-fraction form, including residues CU_k :

$$L[x_f(t)] = \sum_{k=1}^n \frac{CU_k}{s - p_k} + F(s; q_i) \quad (16-13)$$

The symbol $F(s; q_i)$ denotes terms associated explicitly with poles q_i of the input transform. Depending upon the specific nature of $L[u(t)]$, these terms might or might not have simple partial-fraction form. In any case, the terms in $F(s; q_i)$ have the same poles q_i as the input transform, which are always stable poles, so these terms cannot produce

instability. Therefore, instability of the forced-response can exist only in the terms $\sum_{k=1}^n CU_k/(s - p_k)$, i.e., the terms containing the poles of the system transfer function.

The forced-response terms $\sum_{k=1}^n CU_k/(s - p_k)$ are identical in form to the IC-response terms $\sum_{k=1}^n C_k/(s - p_k)$ of Eq. (16-7). Recall that the analysis of stability for IC-response [Eqs. (16-8) and (16-9) and the associated discussion] was based upon that form. Therefore, the analysis of stability for forced-response is identical to that for IC-response, so we need not repeat it. However, it is worth repeating, for emphasis, the general stability criterion for LTI systems that has been derived (albeit, not generally) here:

For an n^{th} order LTI system, the poles of the transfer function are denoted as p_k , $k = 1, 2, \dots, n$. If $\text{Re}(p_k) < 0$ for all $k = 1, 2, \dots, n$, then the system is stable. If, on the other hand, there is at least one pole for which $\text{Re}(p_k) > 0$, then the system is unstable.

Observe from the derivation that the stability or instability of an LTI system does not depend upon ICs or forcing—it is an intrinsic property of the system. However, by referring to general transform solution (16-4), one might make the mathematical argument that if all initial conditions were zero, and if forcing input $u(t)$ also were zero, then the solution would be $x(t) = 0$, and therefore even a system that has an unstable pole, $\text{Re}(p_k) > 0$, would be stable if there were no stimulus. In physical reality, though, there is always some perturbation or excitation, no matter how small, acting upon a system; and even the tiniest IC or forcing input, which would be negligible for a stable system, will always be enough to provoke the instability of an unstable LTI system.

16-2 Stable and unstable PD-controlled-rotor systems

In this section, we analyze in detail a specific example of the theory developed in Section 16-1. The situation considered is ideal proportional-derivative (PD) control of position $\theta(t)$ of a rotor with significant inertia J , as described in Section 15-4 and homework Problem 15.1. The sensitivity of identical input and output-feedback transducers is denoted $K_r = K_\theta$, moment actuator sensitivity is K_a , and, for the ideal PD controller, proportional gain is P and derivative time constant is τ_d . The transfer function of this system, from Eqs. (15-27) and (15-28), is

$$\frac{\Theta(s)}{R(s)} = \frac{\omega_n^2(\tau_d s + 1)}{s^2 + 2\zeta\omega_n s + \omega_n^2} \quad (16-14)$$

with 2nd order-system standard parameters defined as

$$\omega_n = \sqrt{\frac{K_r K_a P}{J}} \quad \text{and} \quad \zeta = \frac{1}{2} \omega_n \tau_d \quad (15-28) \text{ repeated}$$

Chapter 16 Introduction to system stability: time-response criteria

The first useful thing that we can do with transfer function (16-14) is infer the system ordinary differential equation (ODE) by inverse Laplace transformation:

$$[s^2 + 2\zeta\omega_n s + \omega_n^2]\Theta(s) = [\omega_n^2(\tau_d s + 1)]R(s) \Rightarrow \ddot{\theta} + 2\zeta\omega_n \dot{\theta} + \omega_n^2 \theta = \omega_n^2(\tau_d \dot{r} + r) \quad (16-15)$$

Recall that the transfer function is based upon zero ICs for the output. But we want to account for ICs now, so let's take the complete Laplace transform of the ODE, including the possibly non-zero ICs, initial rotation rate $\dot{\theta}(0) \equiv \dot{\theta}_0$ and initial position $\theta(0) \equiv \theta_0$:

$$[s^2 + 2\zeta\omega_n s + \omega_n^2]\Theta(s) - s\theta_0 - \dot{\theta}_0 - 2\zeta\omega_n \theta_0 = [\omega_n^2(\tau_d s + 1)]R(s) \quad (16-16)$$

The solution of Eq. (16-16) for the output transform is

$$\Theta(s) = \frac{\theta_0 s + (\dot{\theta}_0 + 2\zeta\omega_n \theta_0)}{s^2 + 2\zeta\omega_n s + \omega_n^2} + \frac{\omega_n^2(\tau_d s + 1)}{s^2 + 2\zeta\omega_n s + \omega_n^2} R(s) \quad (16-17)$$

Compare specific transform solution (16-17) with the general form (16-4). Next, let's factor the denominator polynomial of the transfer function. It is convenient for this purpose to assume that $|\zeta| < 1$, and to define the positive, real, damped natural frequency as $\omega_d = \omega_n \sqrt{1 - \zeta^2}$. You can easily derive from the quadratic formula (or just substitute in the right-hand side to verify) the factoring:

$$s^2 + 2\zeta\omega_n s + \omega_n^2 = (s - p)(s - \bar{p}), \text{ where the complex pole is } p = -\zeta\omega_n + j\omega_d \quad (16-18)$$

Hence, we re-write transform (16-17), and express it in terms of IC-response and forced-response components:

$$\Theta(s) = \frac{\theta_0 s + (\dot{\theta}_0 + 2\zeta\omega_n \theta_0)}{(s - p)(s - \bar{p})} + \frac{\omega_n^2(\tau_d s + 1)}{(s - p)(s - \bar{p})} R(s) \equiv \Theta_{ic}(s) + \Theta_f(s) \quad (16-19)$$

The IC-response term of Eq. (16-19) is expanded into partial-fraction form:

$$\Theta_{ic}(s) \equiv \frac{\theta_0 s + (\dot{\theta}_0 + 2\zeta\omega_n \theta_0)}{(s - p)(s - \bar{p})} = \frac{C}{(s - p)} + \frac{\bar{C}}{(s - \bar{p})} \quad (16-20)$$

Using the conventional labor-saving partial-fraction-expansion method of Sections 2-2 and 2-3, and $p = -\zeta\omega_n + j\omega_d$ from Eq. (16-18), and a little algebra, we find the following complex residue of Eq. (16-20):

$$C = [(s - p)\Theta_{ic}(s)]_{s=p} = \left[\frac{\theta_0 p + (\dot{\theta}_0 + 2\zeta\omega_n \theta_0)}{(s - \bar{p})} \right]_{s=p} = \frac{1}{2} \left(\theta_0 - j \frac{\dot{\theta}_0 + \zeta\omega_n \theta_0}{\omega_d} \right) \quad (16-21)$$

Chapter 16 Introduction to system stability: time-response criteria

Hence, substituting Eqs. (16-18) and (16-20) into inverse transform (16-9) gives the IC-response [with C given by Eq. (16-21)]:

$$\theta_{ic}(t) = L^{-1}[\Theta_{ic}(s)] = 2|C|e^{-\zeta\omega_n t} \cos(\omega_d t + \angle C) \quad (16-22)$$

Next, let's derive the forced response of this controlled system to a specific, non-trivial input, the ramped exponential pulse $r(t) = R_p(t/\tau)e^{-t/\tau}$, the maximum value of which is $r_{\max} = r(t = \tau) = R_p e^{-1}$. The Laplace transform of this pulse is $R(s) = (R_p/\tau)/(s + 1/\tau)^2$. The transform of the forced response, from Eq. (16-19), is

$$L[\theta_f(t)] = \frac{\omega_n^2(\tau_d s + 1)}{(s - p)(s - \bar{p})} R(s) = \frac{\omega_n^2(\tau_d s + 1)}{(s - p)(s - \bar{p})} \frac{R_p/\tau}{(s + 1/\tau)^2} = R_p \frac{\omega_n^2}{\tau} \frac{\tau_d s + 1}{(s - p)(s - \bar{p})(s + 1/\tau)^2} \quad (16-23)$$

The fraction of polynomials in Eq. (16-23) can be expanded in the following form:

$$L[\theta_f(t)] \Big/ R_p \frac{\omega_n^2}{\tau} \equiv F_f(s) = \frac{\tau_d s + 1}{(s - p)(s - \bar{p})(s + 1/\tau)^2} = \frac{CR}{s - p} + \frac{\overline{CR}}{s - \bar{p}} + \frac{A}{(s + 1/\tau)^2} + \frac{B}{s + 1/\tau} \quad (16-24)$$

CR , A , and B are constants that we need to find. We have not previously encountered a case of repeated poles such as this. The last two right-hand-side terms in Eq. (16-24) show the form that a partial-fraction expansion must have for repeated poles (Ogata, 1998, p. 33). We find complex residue CR using the conventional method:

$$CR = [(s - p)F_f(s)]_{s=p} = \frac{\tau_d p + 1}{(p - \bar{p})(p + 1/\tau)^2} = \frac{\tau_d p + 1}{j 2\omega_d(p + 1/\tau)^2} \quad (16-25)$$

in which $p = -\zeta\omega_n + j\omega_d$. To find constants A and B , it is useful to multiply through Eq. (16-24) by the denominator factor with repeated poles (Ogata, 1998, p. 33):

$$(s + 1/\tau)^2 F_f(s) = \frac{\tau_d s + 1}{(s - p)(s - \bar{p})} = (s + 1/\tau)^2 \left(\frac{CR}{s - p} + \frac{\overline{CR}}{s - \bar{p}} \right) + A + (s + 1/\tau)B \quad (16-26)$$

From Eq. (16-26), we easily find constant A using the conventional method:

$$A = [(s + 1/\tau)^2 F_f(s)]_{s=-1/\tau} = \frac{-\tau_d/\tau + 1}{(-1/\tau - p)(-1/\tau - \bar{p})} = \frac{1 - \tau_d/\tau}{(1/\tau + p)(1/\tau + \bar{p})} \quad (16-27)$$

Finding constant B is expedited by first differentiating Eq. (16-26) with respect to s , so that constant B stands alone in the last right-hand-side term:

Chapter 16 Introduction to system stability: time-response criteria

$$\begin{aligned}
 \frac{d}{ds} \left[(s+1/\tau)^2 F_f(s) \right] &= \frac{(s-p)(s-\bar{p})\tau_d - (\tau_d s + 1)(2s - p - \bar{p})}{[(s-p)(s-\bar{p})]^2} \\
 &= \frac{d}{ds} \left[(s+1/\tau)^2 \left(\frac{CR}{s-p} + \frac{\overline{CR}}{s-\bar{p}} \right) \right] + B \\
 &= 2(s+1/\tau) \left(\frac{CR}{s-p} + \frac{\overline{CR}}{s-\bar{p}} \right) + (s+1/\tau)^2 \frac{d}{ds} \left(\frac{CR}{s-p} + \frac{\overline{CR}}{s-\bar{p}} \right) + B
 \end{aligned} \tag{16-28}$$

Hence, we find constant B by evaluating Eq. (16-28) at $s = -1/\tau$:

$$\begin{aligned}
 B &= \left. \left\{ \frac{(s-p)(s-\bar{p})\tau_d - (\tau_d s + 1)(2s - p - \bar{p})}{[(s-p)(s-\bar{p})]^2} \right\} \right|_{s=-1/\tau} \\
 &= \frac{(1/\tau + p)(1/\tau + \bar{p})\tau_d + (1 - \tau_d/\tau)(2/\tau + p + \bar{p})}{[(1/\tau + p)(1/\tau + \bar{p})]^2}
 \end{aligned} \tag{16-29}$$

Even though p is complex, $p = -\zeta\omega_n + j\omega_d$, the constants A in Eq. (16-27) and B in Eq. (16-29) turn out to be real. The factors that appear to be complex are: $(1/\tau + p)(1/\tau + \bar{p}) = (1/\tau - \zeta\omega_n + j\omega_d)(1/\tau - \zeta\omega_n - j\omega_d) = (1/\tau - \zeta\omega_n)^2 + \omega_d^2$, which is real; and $2/\tau + p + \bar{p} = 2(1/\tau - \zeta\omega_n)$, which also is real. Thus, the final, more clearly real formulas for constants A in Eq. (16-27) and B in Eq. (16-29) are

$$A = \frac{1 - \tau_d/\tau}{(1/\tau - \zeta\omega_n)^2 + \omega_d^2}, \quad B = \frac{[(1/\tau - \zeta\omega_n)^2 + \omega_d^2]\tau_d + 2(1 - \tau_d/\tau)(1/\tau - \zeta\omega_n)}{[(1/\tau - \zeta\omega_n)^2 + \omega_d^2]^2} \tag{16-30}$$

With complex residue CR from Eq. (16-25), and real constants A and B from Eq. (16-30), the forced-response equation is found from the inverse transform of Eq. (16-24):

$$\theta_f(t) = R_p \frac{\omega_n^2}{\tau} L^{-1}[F_f(s)] = R_p \frac{\omega_n^2}{\tau} [2|CR|e^{-\zeta\omega_n t} \cos(\omega_d t + \angle CR) + (At + B)e^{-t/\tau}] \tag{16-31}$$

The terms $(At + B)e^{-t/\tau}$ in Eq. (16-31) are associated with the poles of the forcing function $r(t) = R_p(t/\tau)e^{-t/\tau}$. Observe that these terms vary in time similarly to $r(t)$, but that they have no influence over the positive or negative stability of the system. Only the exponential function $e^{-\zeta\omega_n t}$, which is in the term associated with the system (transfer-function) poles, determines the state of system stability.

The complete output equation is the combination of IC-response (16-22) and forced-response (16-31):

$$\theta(t) = \theta_{ic}(t) + \theta_f(t) \tag{16-32}$$

Chapter 16 Introduction to system stability: time-response criteria

Let's calculate and plot responses for a particular system. The basic parameters are: rotor inertia $J = 0.00256 \text{ lb-sec}^2\text{-inch}$ (the inertia of a small aluminum wheel about four inches in diameter); and product of sensitivities $K_r K_a = 0.0350 \text{ lb-inch/radian}$. Let's specify for the closed-loop system: undamped natural frequency $f_n = \omega_n/(2\pi) = 1.0 \text{ Hz}$ (so that step-response rise time would be around $\frac{1}{4} \text{ sec}$); and damping ratios $\zeta = +0.12$ for a case of positive stability, and $\zeta = -0.03$ for a case of instability. The MATLAB M-file below uses Eq. (15-28) to calculate the proportional gain $P = \omega_n^2 J / (K_r K_a) = 2.888$ and the derivative time constants $\tau_d = 2\zeta/\omega_n = 0.0382 \text{ sec}$ and -0.00955 sec listed in the alphanumeric output for the two different cases.

In order to have non-trivial initial conditions, let's specify initial rotation rate $\dot{\theta}(0) \equiv \dot{\theta}_0 = -0.29 \text{ rad/sec}$ and initial position $\theta(0) \equiv \theta_0 = -0.025 \text{ radian}$. For the ramped-exponential input function $r(t) = R_p(t/\tau)e^{-t/\tau}$, let's specify magnitude $R_p = 0.1 \times e$ radian = 0.2718 radian and time constant $\tau = 1.5 \text{ sec}$, so that $r_{\max} = R_p e^{-1} = 0.1 \text{ radian}$ at time $t = 1.5 \text{ sec}$. (Most of the input values specified above were chosen by trial and error to produce clear and instructive graphical output.)

A MATLAB script M-file for computing and graphing the response follows:

```
%MATLABdemo161.m
%Stability of a PD-controlled rotor
%Excitation with initial conditions and a ramped exponential pulse
J=2.56e-3;KrKa=0.035;fn=1;wn=2*pi*fn;P=wn^2*J/KrKa;
disp('P ='),disp(P)
zeta=[0.12 -0.03];
for nc=1:2;
zt=zeta(nc);wd=wn*sqrt(1-zt^2);p=-zt*wn+j*wd;Td=2*zt/wn;
disp('Case #, zeta, Td, p ='),disp([nc zt Td p])
%Initial-condition response
th0=-0.025;dth0=-0.29;
C=(th0-j*(dth0+zt*wn*th0)/wd)/2;abC=abs(C);anC=angle(C);
t=0:.05:10;
thic=2*abC*exp(-zt*wn*t).*cos(wd*t+anC);
%Forced response
Rp=0.1*exp(1);tau=1.5;r=Rp/tau*t.*exp(-t/tau);
CR=(Td*p+1)/(j*2*wd*(p+1/tau)^2);abCR=abs(CR);anCR=angle(CR);
c1=1-Td/tau;c2=1/tau-zt*wn;c3=c2^2+wd^2;A=c1/c3;
B=(c3*Td+2*(1-Td/tau)*c2)/c3^2;
thf=Rp*wn^2/tau*(2*abCR*exp(-zt*wn*t).*cos(wd*t+anCR)+(A*t+B).*exp(-t/tau));
subplot(2,1,nc),plot(t,thic+thf,t,r),grid
end
```

The command to execute the M-file, and the resulting alphanumeric output and graphical output (after use of MATLAB's editing features for annotation and graphical enhancement) are:

```
>> MATLABdemo161

P =
2.8876

Case #, zeta, Td, p =
1.0000          0.1200          0.0382          -0.7540 + 6.2378i
```

Chapter 16 Introduction to system stability: time-response criteria

Case #, zeta, T_d , p =
 2.0000 -0.0300 -0.0095 0.1885 + 6.2804i

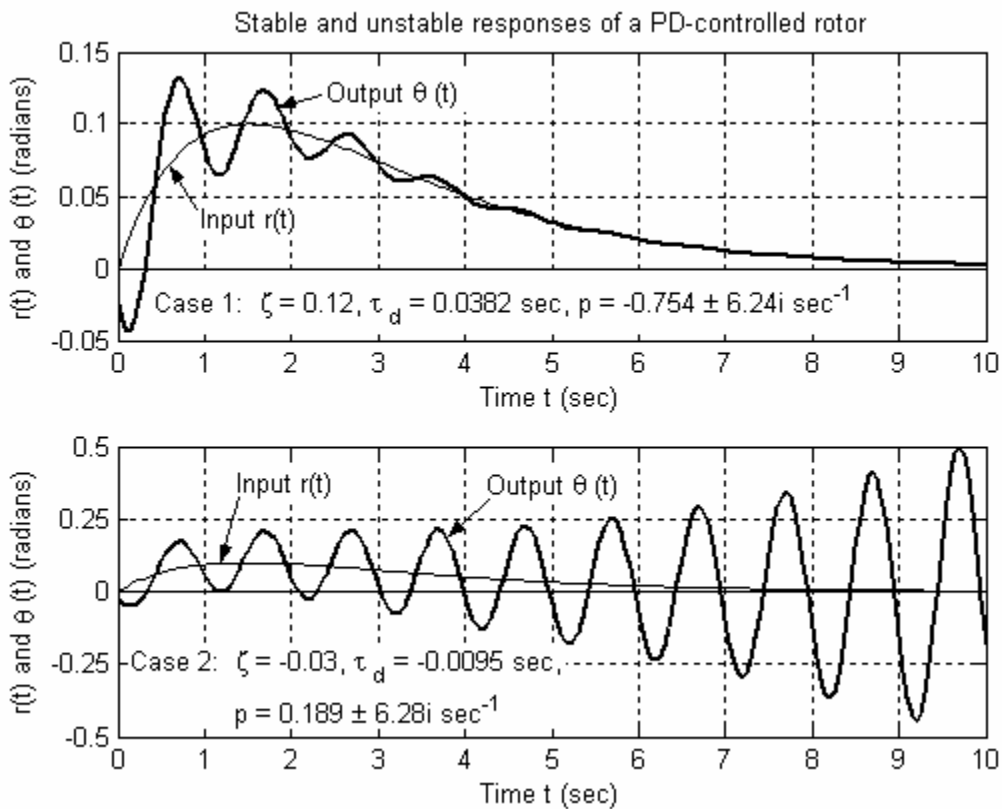


Figure 16-1 Ramped-exponential input operator setting $r(t)$ and output rotor positions $\theta(t)$ for an ideal proportional-derivative (PD) controlled rotor, with two different derivative time constants

Case 1 of Fig. 16-1 displays good performance of the PD control system: despite rather adverse initial conditions, the output follows the input nicely, especially after the initial transient response has decayed. In normal engineering practice, derivative time constant τ_d would probably be set considerably higher than in this academic case, which would suppress the transient oscillation even more quickly and produce even better controlled response.

Case 2, on the other hand, exhibits a serious dynamic instability, which would be unacceptable in normal engineering practice. Note the different y -axis scales for Cases 1 and 2. In real life, the oscillations would continue to grow exponentially until some mechanical or electrical part would fail (possibly a protective fuse that is designed to fail under excessive load), or some mechanical governor would limit motion, or some electrical component (e.g., an op-amp) would saturate, or until the control system would somehow be disabled intentionally. This example demonstrates that feedback control systems can be dangerous; engineers should design and test any feedback control system with great care in order to make certain that it is positively stable and safe.

16-3 Routh's stability criteria

We denote the transfer function of an n^{th} order LTI system as $TF(s) = \frac{Num(s)}{Den(s)}$, in which $Den(s)$ is an n^{th} degree polynomial in s . As derived in Section 16-1, the system is stable or unstable depending upon the signs of the roots of the characteristic equation,

$$Den(p) = a_1 p^n + a_2 p^{n-1} + \cdots + a_n p + a_{n+1} = 0 \quad (16-33)$$

For positive stability, we must have $\text{Re}(p_k) < 0$ for all roots, $k = 1, 2, \dots, n$. The roots are dependent upon the polynomial coefficients $a_1, a_2, \dots, a_n, a_{n+1}$, so it would seem that the state of stability could be determined directly from these coefficients, without the necessity of calculating the roots. This is indeed the case, and the conditions that these coefficients must satisfy for positive stability are known as Routh's stability criteria (after Edward John Routh, 1831-1907, English mathematician, physicist, and educator, who developed the systematic framework). These quantitative criteria can be written for a system of any order n , but they become progressively more complicated as n increases. For that reason, we examine in this section only the criteria for 1st, 2nd, and 3rd order systems; Routh's criteria for 4th order systems are presented in homework Problem 16.9(c).

The first requirement for a system of any order, for the system to be positively stable, is that all coefficients of characteristic equation (16-33) be non-zero and have the same sign. This is a necessary condition but, for $n > 2$, not a sufficient condition for stability. Consider the simplest case, any 1st order system:

$$Den(p) = a_1 p + a_2 = 0 \Rightarrow p = -\frac{a_2}{a_1} \quad (16-34)$$

It is clear that $p < 0$ if a_1 and a_2 are both non-zero and of the same polarity, so no other condition is required for stability. Consider next any 2nd order system:

$$Den(p) = a_1 p^2 + a_2 p + a_3 = 0 \quad (16-35)$$

The quadratic formula gives the following roots of Eq. (16-35):

$$p_{1,2} = -\frac{a_2}{2a_1} \pm \sqrt{\left(\frac{a_2}{2a_1}\right)^2 - \frac{a_3}{a_1}} \quad (16-36)$$

Careful study of Eq. (16-36) shows that these roots have negative real parts only if a_1, a_2 and a_3 all are non-zero and have the same sign. Therefore, for the 2nd order system, the requirement that all three polynomial coefficients be non-zero and have the same sign is a sufficient as well as necessary condition for stability. Note that $a_2 = 0$ means the system has zero damping; if, in addition, a_1 and a_3 have the same sign, then the free-vibration

response of the system is pure sinusoidal oscillation (at the natural frequency) with constant amplitude. In this case, the system is not unstable, since the response is bounded, but it is also not exponentially stable; the response does not decay away to a static equilibrium state.

Finally, let's consider the more challenging 3rd order system:

$$Den(p) = a_1 p^3 + a_2 p^2 + a_3 p + a_4 = 0 \quad (16-37)$$

For the system to be stable, a_1, a_2, a_3 and a_4 all must be non-zero and have the same sign. The other requirement for positive stability of a 3rd order system establishes upper and lower bounds on the product $a_1 \times a_4$:

$$a_2 \times a_3 > a_1 \times a_4 > 0 \quad (16-38)$$

The derivation of these two Routh criteria for stability of a 3rd order system is relatively simple, but more lengthy than necessary for our study; it is presented clearly by Cannon, 1967, pages 406-409.

Let's evaluate Routh's stability criteria applied to the 3rd order system depicted on Fig. 16-2. It is similar to the system of Section 14-3 for output-position-feedback control of rotor position, but there are two additions to that system. First, there is bearing friction that produces a passive rotational moment, $-c_\theta \dot{\theta}$, with c_θ being the viscous damping constant. Second, there is, in the feedback branch downstream of the position sensor, an electrical 1st order low-pass filter with time constant τ_L . The filtering of sensor voltage signals in this fashion is very common in practice. The usual purpose for low-pass filtering is to cut out high-frequency electrical components from the sensor signal. Such unwanted components might arise from the electronics in a "noisy" sensor, from stray electromagnetic fields and/or improperly shielded electrical cables, and even from extraneous mechanical vibrations. So the amplitude-reduction function of a low-pass filter is almost always beneficial to control-system functioning. However, a low-pass filter also changes the phase of sensor signals, as well as reducing the amplitude of high-frequency

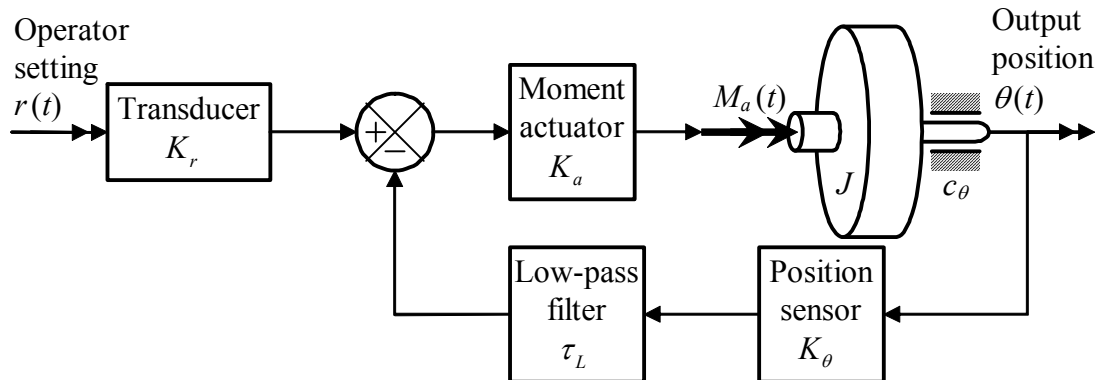


Figure 16-2 Functional diagram of a rotor position-feedback control system with a 1st order low-pass filter in the feedback branch

noise, as shown on Fig. 4-1. Phase shifts can produce adverse effects on control systems, including reduction of control effectiveness and degradation of system stability, even to instability. From Fig. 4-1, we see that the extreme phase shift introduced by a 1st order low-pass filter is -90° , and we can think of this as “almost changing the sign” of the signal that goes through the filter. According to Routh’s criteria, the change of a sign can produce instability. (The effect on stability would be even more dramatic if there were a 2nd order, rather than 1st order, low-pass filter in the feedback branch, Fig. 10-2 with $\zeta > \sim 0.5$; the extreme phase shift produced by a 2nd order filter is -180° , which is a complete sign change in the signal that goes through the filter. See homework Problem 16.5.)

The ODE of motion for the damped rotor comes from Eq. (3-1): $J\ddot{\theta} + c_\theta\dot{\theta} = M_a(t)$. With the notation $L[\theta(t)] \equiv \Theta(s)$, the Laplace transform for zero ICs of the ODE of motion is $(Js^2 + c_\theta s)\Theta(s) = L[M_a(t)]$, so that the transfer function of the basic damped-rotor plant is

$$\frac{\Theta(s)}{L[M_a(t)]} = \frac{1}{Js^2 + c_\theta s} \quad (16-39)$$

With plant transfer function Eq. (16-39) and low-pass-filter transfer function Eq. (13-3), Fig. 16-3 is the Laplace block diagram for the system of Fig. 16-2. The branch transfer functions for the loop in Fig.

16-3 are $G(s) = \frac{K_a}{Js^2 + c_\theta s}$ and $H(s) = \frac{K_\theta}{\tau_L s + 1}$. Hence, with

use of Eq. (14-16), we find the following closed-loop transfer function:

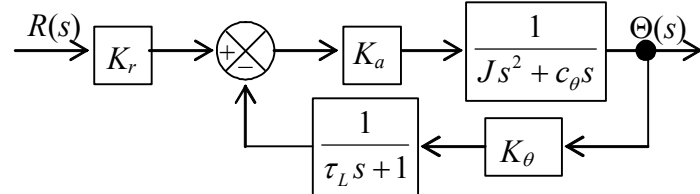


Figure 16-3 Laplace block diagram of position-feedback control system with low-pass filtering

$$\frac{\Theta(s)}{R(s)} = K_r \times \frac{N_G D_H}{D_G D_H + N_G N_H} = K_r \times \frac{K_a (\tau_L s + 1)}{(Js^2 + c_\theta s)(\tau_L s + 1) + K_a K_\theta}$$

Algebraic manipulation of this transfer function casts it into the following more useful forms:

$$\frac{\Theta(s)}{R(s)} = \frac{K_r K_a}{J} \frac{s + 1/\tau_L}{s \left(s + \frac{c_\theta}{J} \right) \left(s + \frac{1}{\tau_L} \right) + \frac{K_a K_\theta}{J \tau_L}} = \frac{K_r K_a}{J} \frac{s + 1/\tau_L}{s^3 + \left(\frac{1}{\tau_L} + \frac{c_\theta}{J} \right) s^2 + \frac{c_\theta}{J} \frac{1}{\tau_L} s + \frac{K_a K_\theta}{J \tau_L}} \quad (16-40)$$

The two final algebraic forms of Eq. (16-40) are intended to expedite both evaluation by Routh’s criteria next and by a more general analysis of stability in Section 16-4.

Chapter 16 Introduction to system stability: time-response criteria

From transfer function (16-40), we find the characteristic equation:

$$Den(p) \equiv a_1 p^3 + a_2 p^2 + a_3 p + a_4 = p^3 + \left(\frac{1}{\tau_L} + \frac{c_\theta}{J} \right) p^2 + \frac{c_\theta}{J} \frac{1}{\tau_L} p + \frac{K_a K_\theta}{J \tau_L} = 0 \quad (16-41)$$

Routh's first set of criteria for positive stability requires that all polynomial coefficients be non-zero and of the same sign. Since $a_1 = 1$, the following inequalities are necessary but not sufficient conditions for positive stability:

$$a_2 = \frac{1}{\tau_L} + \frac{c_\theta}{J} > 0, \quad a_3 = \frac{c_\theta}{J} \frac{1}{\tau_L} > 0, \text{ and} \quad a_4 = \frac{K_a K_\theta}{J \tau_L} > 0 \quad (16-42)$$

Rotational inertia J and filter time constant τ_L should always be positive physical constants, so Eqs. (16-42) require for positive stability that damping constant c_θ must be positive, and that the product of sensitivities $K_a K_\theta$ must be positive. Routh's final requirement for positive stability of a 3rd order system is Eq. (16-38):

$$a_2 \times a_3 > a_1 \times a_4 > 0 \Rightarrow \left(\frac{1}{\tau_L} + \frac{c_\theta}{J} \right) \frac{c_\theta}{J} \frac{1}{\tau_L} > \frac{K_a K_\theta}{J \tau_L} > 0 \Rightarrow \left(\frac{1}{\tau_L} + \frac{c_\theta}{J} \right) \frac{c_\theta}{J} > \frac{K_a K_\theta}{J} > 0 \quad (16-43a)$$

The common factor $1/\tau_L$ was removed to produce the final form of Eq. (16-43a).

Let's suppose that parameters J , c_θ , and τ_L are positive and fixed, but that the positive product of sensitivities $K_a K_\theta$ is a control gain which we have the ability to vary in order to modify the performance and/or stability of the control system. It will be convenient for continued analysis to define a special symbol that denotes the varying fraction in Eq. (16-43a) and to express the stability requirement in terms of that symbol:

$$\frac{K_a K_\theta}{J} \equiv \Lambda \Rightarrow \left(\frac{1}{\tau_L} + \frac{c_\theta}{J} \right) \frac{c_\theta}{J} > \Lambda > 0 \quad (16-43b)$$

Equation (16-43b) establishes upper and lower stability boundaries for $K_a K_\theta / J \equiv \Lambda$. To illustrate, let's express the stability criterion numerically for some plausible system values. Suppose that the circular break frequency of the low-pass filter is $\omega_b \equiv 1/\tau_L = 300$ rad/sec, corresponding to cyclic break frequency $f_b = \omega_b/2\pi = 47.75$ Hz, a realistic value for a low-pass filter used in the control of a mechanical system. Suppose also that the plant parameters have values such that $c_\theta/J = 100 \text{ sec}^{-1}$. Substituting these constants into Eq. (16-43b) gives the criterion: $40,000 \text{ sec}^{-2} > \Lambda > 0$ for positive stability.

To test the correctness of Routh's criteria, let's calculate with MATLAB some responses of this system to the initial condition $\theta(0) \equiv \theta_0 = 0.1$ radian, with all other ICs zero and with zero input, $r(t) = 0$. Let's find the IC response for these three cases:

Case I $\Lambda_I = 0.75 \times \left(\frac{1}{\tau_L} + \frac{c_\theta}{J} \right) \frac{c_\theta}{J} = 30,000 \text{ sec}^{-2}$; this should give stable response.

Case II $\Lambda_{II} \equiv 1.00 \times \left(\frac{1}{\tau_L} + \frac{c_\theta}{J} \right) \frac{c_\theta}{J} = 40,000 \text{ sec}^{-2}$, the upper boundary of stability;

but Λ is supposed to be less than $40,000 \text{ sec}^{-2}$ for stability (not equal to it), so what will be the nature of this response?

Case III $\Lambda_{III} = 1.25 \times \left(\frac{1}{\tau_L} + \frac{c_\theta}{J} \right) \frac{c_\theta}{J} = 50,000 \text{ sec}^{-2}$; this should give unstable response.

To solve for IC responses of this system, we adapt Eq. (16-2) to this problem. A little algebra leads us from Eq. (16-2) to the following transform of the IC response:

$$\Theta(s) = \frac{\theta_0(a_1 s^2 + a_2 s + a_3)}{a_1 s^3 + a_2 s^2 + a_3 s + a_4} \quad (16-44)$$

The a_k constants in Eq. (16-44) are defined in Eq. (16-42), and the numerical parameters are given in the paragraph following Eq. (16-43b). For the numerical values of Cases I, II, and III described above, the partial-fraction expansion of Eq. (16-44) has the form

$$\Theta(s) = \sum_{k=1}^3 \frac{C_k}{s - p_k} = \frac{C_1}{s - p_1} + \frac{C_2}{s - p_2} + \frac{\overline{C}_2}{s - \overline{p}_2} \quad (16-45)$$

in which residue C_1 and pole p_1 are real constants, with p_1 negative for all three cases, and residue C_2 and pole $p_2 \equiv \sigma_2 + j\omega_2$ are complex constants. Therefore, from Eqs. (16-8) and (16-9), the time response has the form

$$\theta(t) = C_1 e^{p_1 t} + 2|C_2| e^{\sigma_2 t} \cos(\omega_2 t + \angle C_2) \quad (16-46)$$

The MATLAB script M-file below computes the constants of transform (16-45), using MATLAB's `residue` operation (see homework Problem 2.15), and it computes and plots time response (16-46).

```
%MATLABdemo162.m
%Stability of a damped rotor with low-pass-filtered position feedback
%Excitation with initial position
wb=300;covrJ=100;a2=wb+covrJ;a3=wb*covrJ;Lmub=a2*covrJ;
th0=0.1;t=0:0.0004:0.16;format short e,figure,hold
Lm=[0.75 1 1.25]*Lmub;
for nc=1:3;
    a4=Lm(nc)*wb;
    Num=th0*[1 a2 a3];Den=[1 a2 a3 a4];[C,p,k]=residue(Num,Den);
    disp('Case #, Lambda ='),disp([nc Lm(nc)])
    disp('Poles p ='),disp(p.'),disp('Residues C ='),disp(C.')
    sig=real(p(2));wd=imag(p(2));abC=abs(C(2));anC=angle(C(2));
    th=C(1)*exp(p(1)*t)+2*abC*exp(sig*t).*cos(wd*t+anC);
    plot(t,th,'k')
```

Chapter 16 Introduction to system stability: time-response criteria

```

end
grid,xlabel('Time t (sec)'),ylabel('Position \theta (t) (radian)')
title('Response of a 3^rd order system with different control gains')

```

The command to execute the M-file, and the resulting alphanumeric output and graphical output (after use of MATLAB's editing features for annotation and graphical enhancement) follow:

```

>> MATLABdemo162
Current plot held

Case #, Lambda =
1      30000

Poles p =
-3.8302e+002      -8.4887e+000 +1.5305e+002i -8.4887e+000 -1.5305e+002i

Residues C =
1.4354e-002      4.2823e-002 -2.0336e-002i  4.2823e-002 +2.0336e-002i

Case #, Lambda =
2      40000

Poles p =
-4.0000e+002      -4.3965e-014 +1.7321e+002i -4.3965e-014 -1.7321e+002i

Residues C =
1.5789e-002      4.2105e-002 -1.8232e-002i  4.2105e-002 +1.8232e-002i

Case #, Lambda =
3      50000

Poles p =
-4.1484e+002      7.4222e+000 +1.9001e+002i  7.4222e+000 -1.9001e+002i

Residues C =
1.6864e-002      4.1568e-002 -1.6786e-002i  4.1568e-002 +1.6786e-002i

```

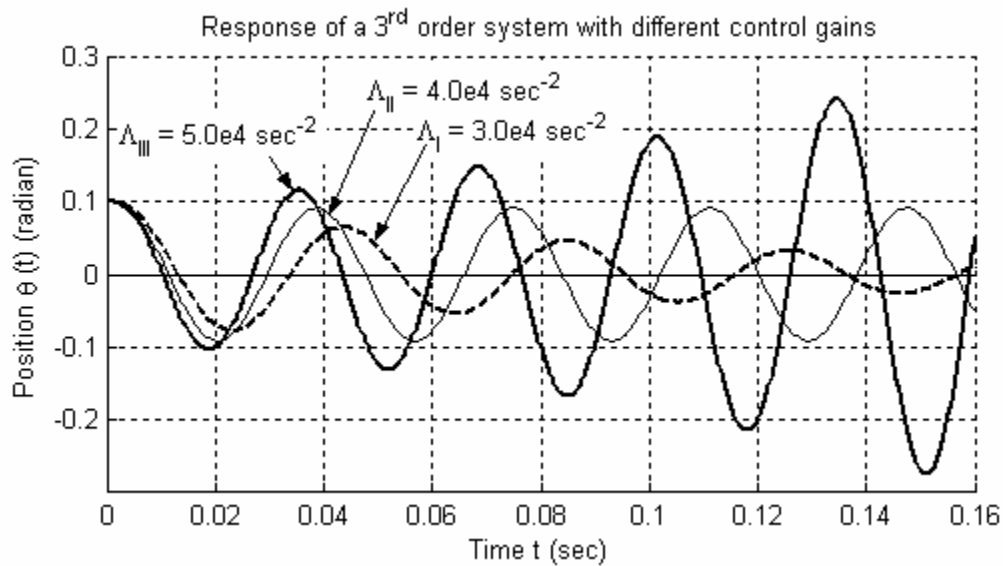


Figure 16-4 Initial-condition response of a rotor output-position-feedback control system with a 1st order low-pass filter in the feedback branch

For this system with three poles, at least one pole must be real. For Cases I, II, and III evaluated above, this real pole, p_1 , turns out to be strongly negative, so it does not contribute to any instability. The second pole, p_2 , is complex, and the third pole is the conjugate of the second. (The other possibility for a 3rd order system is that all three poles can be real, but the gains Λ used in this example preclude that.) For gain Λ_I , $\text{Re}(p_2)$ is negative; consequently, the Case I system is positively stable, as predicted by Routh, Eq. (16-43b). For gain Λ_{III} , $\text{Re}(p_2)$ is positive; consequently, the Case III system is unstable, also as predicted by Routh. Gain Λ_{II} is on the upper boundary between positive and negative stability, according to Routh, and the alphanumeric output above shows that $\text{Re}(p_2) = 0$. (The tiny number calculated, $-4.4\text{e-}14$, is non-zero due to round-off error; comparison of this number with the values of the other poles shows that it is effectively zero.) We see from Fig. 16-4 that the time response associated with Case II is a pure, undamped sinusoid; the response is bounded, therefore not unstable, but it is not exponentially stable, *i.e.*, it does not decay to zero.

The control system of Figs. 16-2 and 16-3 has two major dynamic sub-systems: the damped rotor with transfer function $1/[s(Js + c_\theta)]$; and the low-pass filter with transfer function $1/(\tau_L s + 1)$. Each of these *passive* sub-systems by itself dissipates energy, *i.e.*, acts as an *energy sink*, and is positively stable. But the complete system is clearly capable of being unstable. The complete system includes an *energy source*, the moment actuator, and therefore is said to be *active*. Any system that includes feedback and an energy source is potentially capable of being unstable.

Observe that Routh's criteria essentially tell us only that a system is stable or unstable, the nature of stability in an *absolute* sense. They do not tell us the type of response (monotonic-exponential or oscillatory) or the degree of stability (essentially, the magnitudes of the real parts of transfer-function poles), which is also known as *relative stability*. The method introduced in the next section finds the relative stability.

16-4 Loci of roots for 2nd order systems

Let's seek both the type of response and the degree of stability, by directly solving for the roots of the characteristic equation $\text{Den}(p) = 0$ [*i.e.*, the poles of $TF(s)$ or $CLTF(s)$, whichever is appropriate]. Further, we will observe how these roots vary as some particular system parameter is changed. The graphical representation of this variation in the complex p -plane is known commonly as *locus of roots*; however, systems of 2nd and higher orders always have multiple roots, so it is more correct to use the Latin plural: *loci* of roots. Stability analysis using loci of roots is more general than the basic Routh's criteria, and more informative about the character of a system and the nature of its stability.

We begin by studying the roots of any 2nd order system. This will be instructive and will also establish the basis for interpretation of loci-of-roots graphs for LTI systems of higher order. The characteristic equation of any 2nd order system can be expressed as:

$$Den(p) = p^2 + 2\zeta\omega_n p + \omega_n^2 = 0 \quad (16-47)$$

Some examples of 2nd order system transfer functions that lead to Eq. (16-47) are Eqs. (10-6), (10-27), (13-8), (14-21), (15-20), and (15-27). We are accustomed to studying stable systems for which ζ and ω_n^2 are positive values. However, these parameters are not necessarily always positive in systems; they can be negative, especially for feedback control systems and for *self-excited* systems. An example of a self-excited system is a flexible wing in an airstream, as discussed in Examples 11-2 and 11-3 of Section 11-3.

First, let's study the roots of Eq. (16-47) when ζ varies, in both magnitude and sign, while ω_n is fixed and positive, $\omega_n > 0$. Solving first for $|\zeta| \geq 1$, using the quadratic formula, gives the two real-valued poles:

$$p_{1,2} = -\zeta\omega_n \pm \omega_n\sqrt{\zeta^2 - 1} \quad (16-48a)$$

For $|\zeta| \leq 1$, the poles are the complex conjugate pair:

$$p_{1,2} = -\zeta\omega_n \pm j\omega_n\sqrt{1 - \zeta^2} \equiv -\zeta\omega_n \pm j\omega_d \quad (16-48b)$$

Figure 16-5 shows the loci of roots Eqs. (16-48) as ζ varies from more negative than -1 to more positive than $+1$. Note that the x -axis is the real part of the roots, $Re(p)$, and the

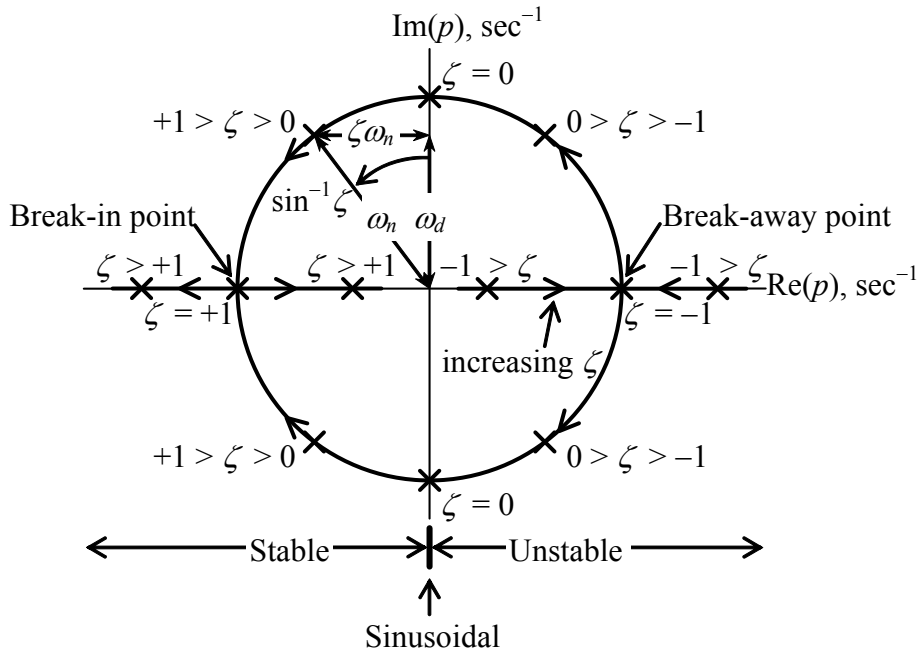


Figure 16-5 Loci of roots of $p^2 + 2\zeta\omega_n p + \omega_n^2 = 0$ as ζ varies from less than -1 to greater than $+1$, with $\omega_n > 0$ held constant

y -axis is the imaginary part, $Im(p)$; these two axes encompass the complex p -plane. For selected values of ζ , the roots are indicated by 'x's and the ζ values are labeled. The directions of the loci as ζ increases are indicated by arrowheads.

For $-1 > \zeta$, the two real roots, (16-48a), are in the right (“east”) half of the p -plane, on the $\text{Re}(p)$ axis; the type of time response associated with these roots is monotonically growing exponential, an instability. At $\zeta = -1$, these two real roots come together with value $+\omega_n$; this is called a “break-away” point because, for the slightest increase in ζ above -1 , the roots separate into complex conjugates, (16-48b), one root headed directly “northward” and the other directly “southward.” The type of response associated with complex conjugate roots that are in the right half-plane off the $\text{Re}(p)$ axis is oscillation modulated by a growing exponential envelope, an instability. For $+1 > \zeta > -1$, the loci of roots form a perfect circle of radius ω_n and centered on the origin: $x^2 + y^2 = (-\zeta\omega_n)^2 + (\pm\omega_d)^2 = \omega_n^2$. The roots for $\zeta = 0$ are imaginary, $p_{1,2} = \pm j\omega_n$, for which the time response has pure, undamped sinusoidal form. For $+1 > \zeta > 0$, the complex conjugate roots are in the left (“west”) half-plane off the $\text{Re}(p)$ axis; the type of time response associated with these complex conjugate roots is oscillation modulated by a decaying exponential envelope, which is stable response. As increasing ζ approaches the value $+1$, the two complex roots come together and become real, with value $-\omega_n$, at the “break-in” point. Finally, as ζ increases above $+1$, one real root heads farther westward on the $\text{Re}(p)$ axis, and the other creeps eastward toward the origin; the type of time response associated with these real roots in the left half-plane is monotonically decaying exponential, which is stable response.

Keep in mind that both monotonic-exponential response and oscillatory response are bounded by the exponential envelope $e^{\text{Re}(p)t}$. If $\text{Re}(p) < 0$, in the left half-plane, then we define, as in Eq. (9-22), the 2nd order *time constant*, $\tau_2 \equiv -1/\text{Re}(p) > 0$, so that the decaying exponential envelope is e^{-t/τ_2} ; τ_2 is the time for the stable exponential envelope to decrease by the factor e^{-1} . The degree of positive stability associated with a particular stable root increases as $\text{Re}(p)$ becomes progressively more negative and τ_2 becomes progressively smaller. In other words, the farther westward from the origin that a pole is located, the greater is the degree of positive stability associated with that pole. On the other hand, if $\text{Re}(p) > 0$, in the right half-plane, then $+1/\text{Re}(p)$ is the time for the unstable exponential envelope to increase by the factor e^{+1} . The degree of instability associated with a particular unstable root increases progressively as $\text{Re}(p)$ becomes progressively more positive; in other words, the instability worsens as the unstable pole moves farther eastward from the origin. Although these observations are made in the context of Fig. 16-5, they are equally applicable to the loci of roots of any LTI system having any order.

Note on Fig. 16-5 the construction of a right triangle consisting of horizontal leg $\zeta\omega_n$, vertical leg ω_d , and hypotenuse ω_n , which extends from the origin to a complex pole p . This right triangle is based on the definition $\omega_d^2 = \omega_n^2(1 - \zeta^2) = \omega_n^2 - (\zeta\omega_n)^2$, which is valid for $|\zeta| < 1$. Thus, the frequency of vibration (in rad/sec) associated with this particular complex pole is the vertical leg ω_d along the $\text{Im}(p)$ axis. Further, the horizontal leg $\zeta\omega_n$ (if in the left half-plane) determines the time constant, $\tau_2 = 1/\zeta\omega_n$ (in sec). Finally, the value of damping ratio ζ is the sine of the angle labeled on Fig. 16-5 between

the $\text{Im}(p)$ axis and hypotenuse ω_n ; for a stable pole p in the left half-plane, as drawn on Fig. 16-5, ζ is positive; for an unstable pole p in the right half-plane, ζ would be negative. Although this derivation is based on Fig. 16-5, these methods derived for determining the frequency ω_d , time constant τ_2 , and damping ratio ζ associated with a particular complex pole are applicable to the loci of roots of any LTI system.

Figure 16-5 shows the loci of roots of a 2nd order system as generalized damping, represented by ζ , varies. Next, let's consider the loci of roots for a 2nd order system as generalized stiffness varies. Rather than using the symbols ζ and ω_n , it is better for this task to revert back to the notation of Section 9-1 representing a generalized mass-damper-spring system. Accordingly, we have Eq. (7-3), $\omega_n^2 = k/m$, and from Eq. (9-4), $\zeta\omega_n = c/(2m)$. In these definitions, we specify that k represents a generalized stiffness, which will vary, and that c and m represent, respectively, generalized damping and generalized inertia, which are considered positive constants and will remain fixed while k varies. For convenience, let's use the following simplified notation:

$$\omega_n^2 = k/m \equiv K \quad \text{and} \quad \zeta\omega_n = c/(2m) \equiv C \quad (16-49)$$

Therefore, for the case $c/2m \geq k/m$, we re-write the real roots (16-48a) as

$$p_{1,2} = -\zeta\omega_n \pm \sqrt{(\zeta\omega_n)^2 - \omega_n^2} = -C \pm \sqrt{C^2 - K} \quad (16-50a)$$

For $k/m \geq c/2m$, the complex conjugate roots (16-48b) are

$$p_{1,2} = -\zeta\omega_n \pm j\sqrt{\omega_n^2 - (\zeta\omega_n)^2} = -C \pm j\sqrt{K - C^2} \quad (16-50b)$$

Figure 16-6 is an incomplete graph of loci of roots Eqs. (16-50) as K varies with $C > 0$ fixed. (Homework Problem 16.3 is an exercise for completing the task.) Partial annotation shows the locations of the two real poles for $K = 0$. Note, in particular, that for $K < 0$ one real locus is entirely in the right half-plane. The type of time response associated with this locus is monotonically growing exponential, an instability. (Of course, Routh also shows that the system is unstable for $K < 0$ and $C > 0$, since then coefficients of the characteristic equa-

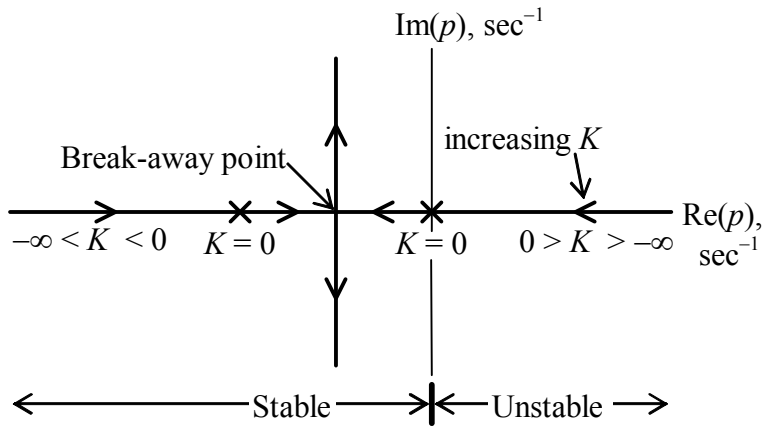


Figure 16-6 Loci of roots of $p^2 + 2Cp + K = 0$ as K varies from $-\infty$ to greater than C^2 , with $C > 0$ held constant

tion have different signs.) The passive mechanical springs with which we are familiar always have positive stiffness, so it might appear that this type of instability is purely academic, without any practical significance. Such is not the case. Recall that, in the present discussion, k (and therefore K also) represents generalized or total stiffness, not just mechanical stiffness. An elastically restrained airfoil within an air stream is one practical engineering system for which the total stiffness is not necessarily positive. As shown in the discussion accompanying Eq. (11-16), the total mechanical plus aerodynamic stiffness of this system can become zero or even negative at high airspeeds; the resulting unbounded pitching of the airfoil, called *aeroelastic divergence*, is an important example of the type of instability represented in Fig. 16-6 for $K < 0$.

Developing loci-of-roots graphs Figs. 16-5 and 16-6 for 2nd order systems is relatively simple, but useful as an instructive introduction to this type of stability analysis. In the next section, we will consider the more demanding task of determining loci of roots for systems of higher order.

16-5 Loci of roots for a 3rd order system

In Section 16-4, we used the quadratic formula to evaluate easily the loci of roots for 2nd order systems. It is more typical in practice, however, that engineering systems have higher orders than 2nd order, so that determining loci of roots requires repeatedly solving polynomial equations of 3rd and higher degrees, which can be a challenging task. This section introduces by example the methods of solution for higher-order systems that are commonly used in practice.

For this example, we consider again the system described in Section 16-3 (Figs. 16-2, 16-3, and 16-4), a rotor position-feedback control system with a 1st order low-pass filter in the feedback branch. Closed-loop transfer function (16-40) gives the 3rd degree characteristic equation in two different algebraic forms, one of which is

$$Den(p) = a_1 p^3 + a_2 p^2 + a_3 p + a_4 = p^3 + \left(\frac{1}{\tau_L} + \frac{c_\theta}{J} \right) p^2 + \frac{c_\theta}{J} \frac{1}{\tau_L} p + \frac{K_a K_\theta}{J \tau_L} = 0 \quad (16-51a)$$

In Section 16-3, we held constant rotor inertia J , viscous damping constant c_θ of the bearings, and time constant τ_L of the 1st order low-pass filter, all positive values; in particular, we chose for numerical evaluation the values $c_\theta/J = 100 \text{ sec}^{-1}$, and, for the filter break frequency, $\omega_b \equiv 1/\tau_L = 300 \text{ rad/sec}$. We allowed the value of product $K_a K_\theta$ of control system sensitivities to vary. Using Routh's criteria, we determined the lower and upper stability boundaries for the parameter $K_a K_\theta/J \equiv \Lambda$: the system is positively stable provided that $0 < \Lambda < 40,000 \text{ sec}^{-2}$.

Now, let's conduct a more detailed evaluation of stability by calculating and plotting the loci of roots as Λ varies, using the same numerical values of the other constants as in Section 16-3. We solve numerically for the roots of polynomial (16-51a) using MATLAB's `root` operation: for each value of Λ , the input is the array of coefficients

Chapter 16 Introduction to system stability: time-response criteria

$[a_1 \ a_2 \ a_3 \ a_4]$, and the output is the 3×1 matrix of roots. We will calculate and plot the loci of roots twice: first, for a set of Λ values that we choose (guess) somewhat arbitrarily to encompass the entire possible range of practical interest; second, for another set of Λ values that are refined, based upon the results of the first pass, to focus on the specific roots of greatest practical significance.

For the first pass, we vary Λ from $-30,000 \text{ sec}^{-2}$ to $+70,000 \text{ sec}^{-2}$ in increments of $10,000 \text{ sec}^{-2}$. The following is a MATLAB script M-file that computes the roots of polynomial (16-51a) repeatedly over these values of Λ , then prints the input and output values in a table, then plots the loci of roots:

```
%MATLABdemo163.m
%Stability of a damped rotor with low-pass-filtered position feedback
%Loci of roots
wb=300;covrJ=100;a2=wb+covrJ;a3=wb*covrJ;
Lm=[-3 -2 -1 0 1 2 3 4 5 6 7]*1.0e4;Np=length(Lm);
for i=1:Np;
    a4=Lm(i)*wb;
    p(i,1:3)=roots([1 a2 a3 a4]).';
end
nc=1:Np;anout=[nc' Lm' p'];
disp('Roots #, Lambda, p'),disp(anout)
plot(p,'kx'),grid,xlabel('Real part of pole (sec^-^1)')
ylabel('Imag part of pole (sec^-^1)')
title('Loci of roots of a 3^r^d order system as \Lambda varies')
```

The command to execute the M-file, and the resulting tabular output follows:

```
>> MATLABdemo163

Roots #, Lambda, p
1.0e+004 *

0.0001      -3.0000      -0.0253 + 0.0141i   -0.0253 - 0.0141i   0.0107
0.0002      -2.0000      -0.0242 + 0.0111i   -0.0242 - 0.0111i   0.0085
0.0003      -1.0000      -0.0227 + 0.0056i   -0.0227 - 0.0056i   0.0055
0.0004          0          0                  -0.0300                   -0.0100
0.0005      1.0000      -0.0337      -0.0031 + 0.0089i   -0.0031 - 0.0089i
0.0006      2.0000      -0.0363      -0.0019 + 0.0127i   -0.0019 - 0.0127i
0.0007      3.0000      -0.0383      -0.0008 + 0.0153i   -0.0008 - 0.0153i
0.0008      4.0000      -0.0400      -0.0000 + 0.0173i   -0.0000 - 0.0173i
0.0009      5.0000      -0.0415      0.0007 + 0.0190i   0.0007 - 0.0190i
0.0010      6.0000      -0.0428      0.0014 + 0.0205i   0.0014 - 0.0205i
0.0011      7.0000      -0.0440      0.0020 + 0.0217i   0.0020 - 0.0217i
```

The associated loci-of-roots plot (after use of MATLAB's editing features for annotation and graphical enhancement) is Fig. 16-7, on the next page.

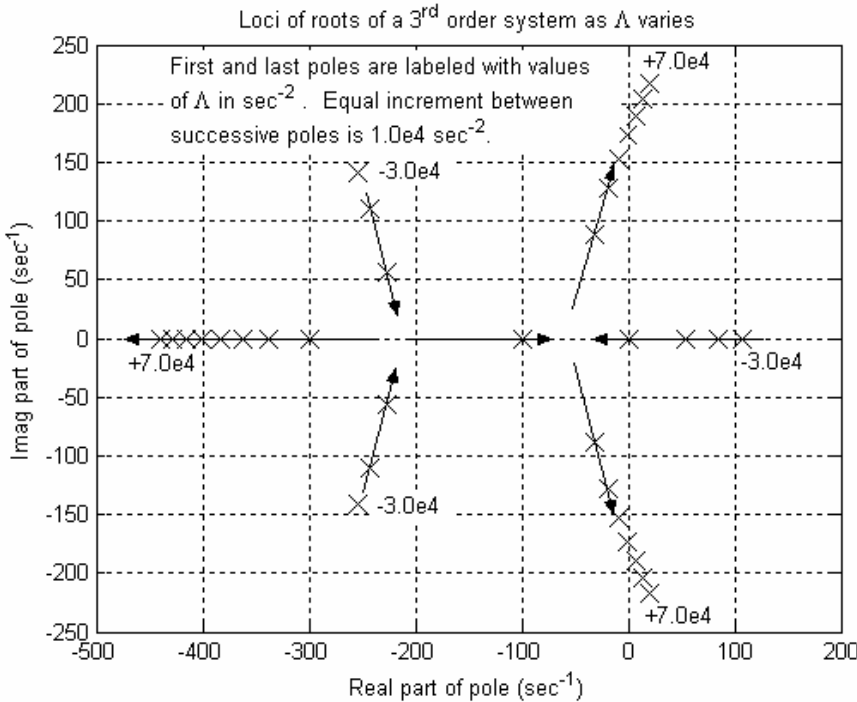


Figure 16-7 First-pass loci of roots of Eq. (16-51a) for varying control parameter $\Lambda = K_a K_\theta / J$

We infer from Fig. 16-7 the following relevant information. For $\Lambda < 0$, the system has an unstable pole associated with monotonic exponentially growing time response; we already knew from Routh that the system is unstable for $\Lambda < 0$, but Routh did not reveal the type of response. For $\Lambda = 0$, the poles are all real and have the values 0, -100 , and -300 sec^{-1} . This is also obvious in the alternate algebraic form of the 3rd degree characteristic equation that comes from closed-loop transfer function (16-40):

$$Den(p) = p(p + c_\theta/J)(p + \omega_b) + \omega_b \Lambda = 0 \quad (16-51b)$$

From (16-51b) with $\Lambda = 0$, the poles are clearly $p_1 = 0$, $p_2 = -c_\theta/J = -100 \text{ sec}^{-1}$, and $p_3 = -\omega_b \equiv -1/\tau_L = -300 \text{ sec}^{-1}$. The arrows on Fig. 16-7 indicate the directions of loci as Λ increases. The arrows show that there is a break-in point (as defined on Fig. 16-5) for Λ somewhere in the range $-10,000 \text{ sec}^{-2} < \Lambda < 0$, and a break-away point for Λ somewhere in the range $0 < \Lambda < +10,000 \text{ sec}^{-2}$. For future reference, let's denote the break-away value of Λ as Λ_{ba} , which is not yet determined. We also observe from Fig. 16-7 and the tabulated roots that the upper boundary of stability (with purely complex roots, $p_{2,3} = \pm j173 \text{ rad/sec}$) is $\Lambda = 40,000 \text{ sec}^{-2}$, and that the time response is oscillatory for values of Λ in the vicinity of the upper boundary; we knew from Routh the value of the upper boundary, but not the type of response. Moreover, since the real pole for $\Lambda > \Lambda_{ba}$ is associated with heavily damped exponential decay, the complex loci for $\Lambda > \Lambda_{ba}$ of Fig. 16-7 suggest that the time response is primarily oscillatory for $\Lambda > \Lambda_{ba}$. See Fig. 16-4 for examples of this primarily oscillatory response. For $\Lambda > \Lambda_{ba}$, this system has a heavily

damped exponential *mode of response* and a lightly damped oscillatory mode, and the latter, with poles closest to the imaginary axis, is the *dominant* mode.

Now let's refine the loci-of-roots calculation, using a new set of Λ values that would be of greatest practical interest. This set probably would consist of values for which the system is stable, namely $0 < \Lambda < 40,000 \text{ sec}^{-2}$. The value Λ_{ba} is significant: it is the boundary between a system (with $0 < \Lambda < \Lambda_{ba}$) for which all transient response is decaying exponential and a system (with $\Lambda_{ba} < \Lambda$) for which the dominant transient response is oscillatory. We certainly could choose the refined set of Λ values by numerical trial and error, letting MATLAB do most of the work. However, this situation provides the opportunity for introduction of a theoretical and more systematic approach, which we shall consider next. This approach is general, but our limited objective in this introduction will be to determine theoretically only the upper boundary of stability, $\Lambda \equiv \Lambda_{ub}$, and the break-away value Λ_{ba} .

This approach is based upon form (16-51b) of the characteristic equation, which we re-write as

$$p(p + c_\theta/J)(p + \omega_b) = -\omega_b \Lambda \quad (16-52)$$

It is important that the sub-system poles are separated into factors on the left-hand side of Eq. (16-52). Each factor is a complex number, in general, and it can be expressed in complex polar form, as described in Section 2-1. It is helpful to regard each factor as a two-dimensional complex vector with its tail at the sub-system pole, so that we write

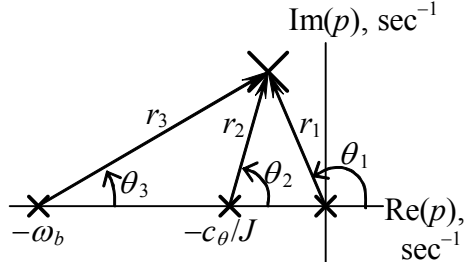
$$p = p - 0 \equiv r_1 e^{j\theta_1}, \quad p + c_\theta/J = p - (-c_\theta/J) \equiv r_2 e^{j\theta_2}, \quad p + \omega_b = p - (-\omega_b) \equiv r_3 e^{j\theta_3} \quad (16-53)$$

The real right-hand side of Eq. (16-52) also is written in polar form: $-\omega_b \Lambda = \omega_b \Lambda \exp[j(\pm\pi, \pm 3\pi, \dots)]$. Therefore, the entire characteristic equation is expressed in the following polar form, which any root must satisfy:

$$r_1 e^{j\theta_1} \times r_2 e^{j\theta_2} \times r_3 e^{j\theta_3} = r_1 r_2 r_3 e^{j(\theta_1 + \theta_2 + \theta_3)} = \omega_b \Lambda \exp[j(\pm\pi, \pm 3\pi, \dots)] \quad (16-54)$$

The drawing at right is a graphical representation of both the polar vectors of Eq. (16-53) and characteristic equation (16-54). The small \times 's are the sub-system poles, at which the tails of the complex vectors are located. The large \mathbf{X} is a pole of the complete system, i.e., a root of Eq. (16-51b), and a value that satisfies Eq. (16-54). Complex equation (16-54) includes two real equations, both of which must be satisfied by any system pole. The first equation is the equality of angles on the two sides of (16-54):

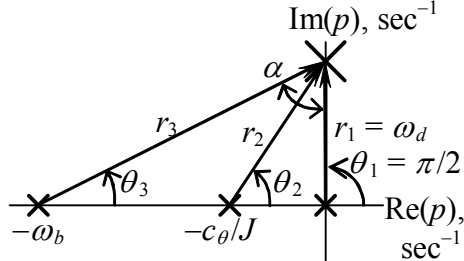
$$\theta_1 + \theta_2 + \theta_3 = \pm\pi, \pm 3\pi, \dots \quad (16-55)$$



The second equation is the equality of magnitudes:

$$r_1 r_2 r_3 = \omega_b \Lambda \Rightarrow \Lambda = \frac{r_1 r_2 r_3}{\omega_b} \quad (16-56)$$

For our first application of this approach, let's use Eq. (16-55) to find the pole $j\omega_d$ at the upper stability boundary Λ_{ub} , and then Eq. (16-56) to find the value of Λ_{ub} itself. The pole is shown on the drawing at right. We have by definition for this stability boundary: $r_1 = \omega_d$ and $\theta_1 = \pi/2$. Therefore, Eq. (16-55) gives $\theta_2 + \theta_3 = \pi/2$. [We



rule out the other possibilities $-\pi, \pm 3\pi, \dots$ in Eq. (16.55) just by inspecting the figure.] Some trigonometry is required now. Angle α between the arrowheads of r_1 and r_3 is labeled on the drawing. Angles α and θ_3 are the complementary acute angles of a right triangle, so we have also $\alpha + \theta_3 = \pi/2$. Therefore, $\alpha = \theta_2$. Hence, we find ω_d by equating the tangents of the two similar right triangles:

$$\tan \theta_2 = \frac{\omega_d}{c_\theta/J} = \tan \alpha = \frac{\omega_b}{\omega_d} \Rightarrow \omega_d = \sqrt{\omega_b \frac{c_\theta}{J}} = \sqrt{300 \text{ sec}^{-1} \times 100 \text{ sec}^{-1}} = 173.2 \frac{\text{rad}}{\text{sec}}$$

Having $\omega_d = r_1$, we can use the theorem of Pythagoras to find $r_2 = \sqrt{\omega_d^2 + (c_\theta/J)^2} = \sqrt{\omega_b (c_\theta/J) + (c_\theta/J)^2}$ and $r_3 = \sqrt{\omega_d^2 + \omega_b^2} = \sqrt{\omega_b (c_\theta/J) + \omega_b^2}$. Finally, we find Λ_{ub} by applying Eq. (16-56), which, after a little algebra, gives

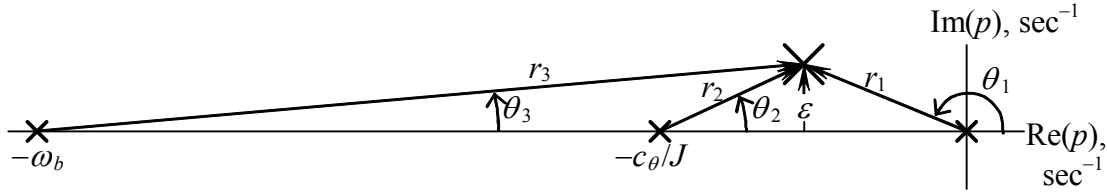
$$\Lambda_{ub} = \frac{r_1 r_2 r_3}{\omega_b} = \omega_b \frac{c_\theta}{J} + \left(\frac{c_\theta}{J} \right)^2 = 300 \text{ sec}^{-1} \times 100 \text{ sec}^{-1} + (100 \text{ sec}^{-1})^2 = 40,000 \text{ sec}^{-2}$$

This result for Λ_{ub} is, of course, identical to the upper boundary found by Routh's criteria in Eq. (16-43b).

For a more subtle application of this theoretical approach, let's: first, use Eq. (16-55) to find the value of the two identical poles at the break-away point, which is evident on Fig. 16-7 (on the real axis, somewhere between the origin and $-c_\theta/J = -100 \text{ sec}^{-1}$); and then, use Eq. (16-56) to find the associated value of Λ_{ba} . It is obvious that Eq. (6-55) is satisfied identically right at the break-away point, where $\theta_1 = \pi$ and $\theta_2 = \theta_3 = 0$, so this does not provide any useful information. But Eq. (6-55) must apply also for all other points on the loci of roots, in particular now, for points that are close to the break-away point; this fact will lead to a useful result. Suppose that Λ is just slightly greater than Λ_{ba} so that one of the complex poles is a small distance ε above the break-away point on the

Chapter 16 Introduction to system stability: time-response criteria

real axis, as shown on the drawing below. As ε shrinks but remains > 0 , the acute angles



between the sub-system radii and the real axis become very small, so we can use in Eq. (16-55) the approximation $\theta \approx \sin \theta$. Hence, Eq. (16-55) gives

$$\theta_1 + \theta_2 + \theta_3 = \left(\pi - \frac{\varepsilon}{r_1} \right) + \frac{\varepsilon}{r_2} + \frac{\varepsilon}{r_3} = \pi \Rightarrow \varepsilon \left(-\frac{1}{r_1} + \frac{1}{r_2} + \frac{1}{r_3} \right) = 0$$

This equation must be valid even if ε is very small but non-zero, so we conclude that

$$-\frac{1}{r_1} + \frac{1}{r_2} + \frac{1}{r_3} = 0 = \frac{-r_2 r_3 + r_1 r_3 + r_1 r_2}{r_1 r_2 r_3} \Rightarrow -r_2 r_3 + r_1 r_3 + r_1 r_2 = 0$$

In the limit as the pole goes to the break-away point on the real axis, $\varepsilon = 0$, the radii are related as $r_1 + r_2 = c_\theta/J$ and $r_1 + r_3 = \omega_b$. Substituting into the equation above to eliminate r_2 and r_3 gives $-r_2 r_3 + r_1(r_3 + r_2) = -(c_\theta/J - r_1)(\omega_b - r_1) + r_1(\omega_b - r_1 + c_\theta/J - r_1) = 0$, and this leads, after some algebra, to a quadratic equation in unknown r_1 :

$$3r_1^2 - 2\left(\omega_b + \frac{c_\theta}{J}\right)r_1 + \omega_b \frac{c_\theta}{J} = 0$$

Solving for r_1 with the quadratic formula gives

$$r_1 = \frac{1}{3} \left[\left(\omega_b + \frac{c_\theta}{J} \right) \pm \sqrt{\left(\omega_b + \frac{c_\theta}{J} \right)^2 - 3\omega_b \frac{c_\theta}{J}} \right]$$

Substituting into this equation $\omega_b = 300 \text{ sec}^{-1}$ and $c_\theta/J = 100 \text{ sec}^{-1}$ gives the roots 221.53 and 45.14 sec^{-1} , with the latter root corresponding to the break-away pole that we seek between the origin and -100 sec^{-1} on the real axis, i.e., $r_1 = 45.14 \text{ sec}^{-1}$. Then Eq. (16-56) gives the associated value of the varying control parameter:

$$\Lambda_{ba} = \frac{r_1 r_2 r_3}{\omega_b} = \frac{r_1 (c_\theta/J - r_1)(\omega_b - r_1)}{\omega_b} = 2,103.77 \text{ sec}^{-2}$$

The approach used above to determine theoretically the stability-upper-bound and break-away values of the varying control parameter Λ , based upon Eqs. (16-52)-(16-56),

Chapter 16 Introduction to system stability: time-response criteria

is a small portion of an extensive set of procedures for completely determining loci of roots, which is known as the *root-locus method*. Walter R. Evans (1920-1999, American electrical engineer) developed and published this elegant method around 1950. Using the root-locus method, an experienced engineer can develop quickly, without the need for a digital computer, complete loci of roots, even for systems of somewhat higher order. For about a quarter-century after this method became widely known, the slide rule was still an engineer's primary computational tool, and the root-locus method profoundly influenced the design and analysis of control systems during that era. Now that digital computers and highly specialized software are readily available, Evans' root-locus method is no longer so essential if you need only to analyze a given system. However, if you want to design control systems logically and efficiently, then the concepts underlying Evans' method, represented in this example by Eqs. (16-52)-(16-56), will be extremely valuable. Details of Evans' method are available in many references, one of the clearest and most complete being Cannon, 1967, Sections 11.8 and 11.9 and Chapter 21.

Let's return now to the task of choosing a refined set of Λ values and using MATLAB to calculate and graph loci of roots for this refined set. We specify that this set consists of values for which the system is stable, $0 < \Lambda < 40,000 \text{ sec}^{-2}$, with particular emphasis on the range of values associated with the dominant oscillatory mode of response, $\Lambda_{ba} < \Lambda < 40,000 \text{ sec}^{-2}$. Therefore, the value $\Lambda_{ba} = 2,103.77 \text{ sec}^{-2}$ calculated above is useful, and is included in the refined set of Λ values. The other values are chosen by trial and error to produce moderately uniform spacing between the complex poles in the p -plane; the complete set, in ascending order is $\Lambda = 0, 1,000, 1,800, \Lambda_{ba}, 2,300, 3,500, 6,250, 10,000, 20,000, \text{ and } 40,000 \text{ sec}^{-2}$. Except for this different set of Λ values, the MATLAB script M-file is the same as that which produced Fig. 16-7. The command to execute the M-file, and the resulting tabular output follows:

```
>> MATLABdemo164

Roots #, Lambda, p
1.0e+004 *

0.0001      0          0      -0.0300      -0.0100
0.0002      0.1000    -0.0305    -0.0083      -0.0012
0.0003      0.1800    -0.0308    -0.0064      -0.0027
0.0004      0.2104    -0.0310    -0.0045 + 0.0000i  -0.0045 - 0.0000i
0.0005      0.2300    -0.0311    -0.0045 + 0.0015i  -0.0045 - 0.0015i
0.0006      0.3500    -0.0315    -0.0042 + 0.0039i  -0.0042 - 0.0039i
0.0007      0.6250    -0.0326    -0.0037 + 0.0066i  -0.0037 - 0.0066i
0.0008      1.0000    -0.0337    -0.0031 + 0.0089i  -0.0031 - 0.0089i
0.0009      2.0000    -0.0363    -0.0019 + 0.0127i  -0.0019 - 0.0127i
0.0010      3.0000    -0.0383    -0.0008 + 0.0153i  -0.0008 - 0.0153i
0.0011      4.0000    -0.0400    -0.0000 + 0.0173i  -0.0000 - 0.0173i
```

The associated loci-of-roots plot, Fig. 16-8, is on the next page. MATLAB's editing features for annotation and graphical enhancement were used on Fig. 16-8. In particular, the axes were set to be "equal," which means in this case that the x axis [*i.e.*, $\text{Re}(p)$] and the y axis [*i.e.*, $\text{Im}(p)$] have exactly the same linear scale.

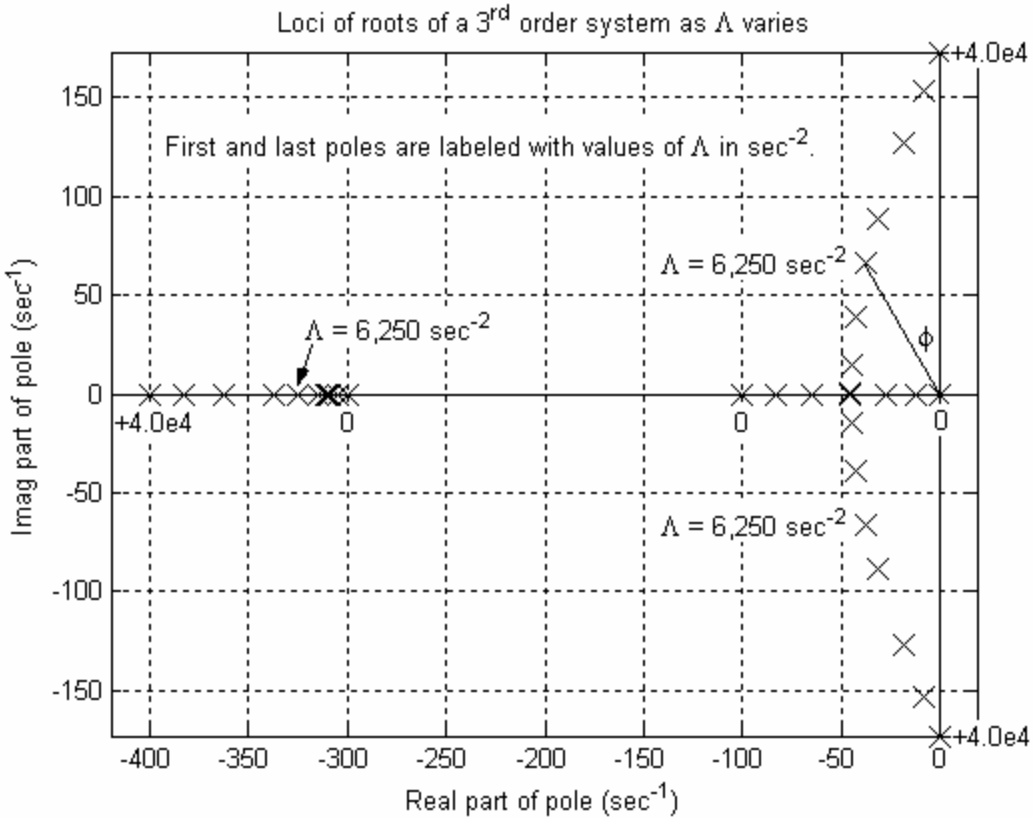


Figure 16-8 Refined loci of roots of Eq. (16-51a) for varying control parameter $\Lambda = K_a K_\theta / J$

The roots on Fig. 16-8 for one example value, $\Lambda = 6,250 \text{ sec}^{-2}$, are labeled in order to illustrate calculation of basic 1st order and 2nd order parameters for a higher-order system. The real root is $p_1 = -326 \text{ sec}^{-1}$ (taken approximately from Fig. 16-8, but more precisely from the table of roots on the previous page). The associated 1st order time constant is $\tau_1 = -1/p_1 = 3.07e-3 \text{ sec} = 3.07 \text{ msec}$. The imaginary roots for $\Lambda = 6,250 \text{ sec}^{-2}$ are $p_{2,3} = -37 \pm j66 \text{ sec}^{-1}$, and the angle labeled on Fig. 16-8 is $\phi \approx 30^\circ$ (for its relevance, see Fig. 16-5). The associated 2nd order response parameters are: time constant $\tau_2 = -1/\text{Re}(p_{2,3}) = 27 \text{ msec}$ (much longer than τ_1); frequency $\omega_d = \text{Im}(p_2) = 66 \text{ rad/sec}$; and damping ratio $\zeta = \sin \phi \approx 0.5$. We can use MATLAB's poles to calculate more precisely the damping ratio associated with a stable complex pole, $p_k = \sigma_k + j\omega_k$ (the notation of Section 16-1), by recognizing that $\sigma_k = \text{Re}(p_k) \equiv -(\zeta\omega_n)_k$ and $\omega_k = \text{Im}(p_k) \equiv (\omega_d)_k$, and that (dropping the k subscripts temporarily) $\omega_d^2 = \omega_n^2 - (\zeta\omega_n)^2$:

$$\zeta^2 = \frac{(\zeta\omega_n)^2}{\omega_n^2} = \frac{(\zeta\omega_n)^2}{(\zeta\omega_n)^2 + \omega_d^2} \equiv \frac{\sigma^2}{\sigma^2 + \omega^2} = \frac{1}{1 + (\omega/\sigma)^2}$$

Therefore (restoring the k subscripts), the damping ratio is

$$\zeta_k = \frac{1}{\sqrt{1 + (\omega_k/\sigma_k)^2}} \quad (16-57)$$

Applying Eq. (16-57) for $\Lambda = 6,250 \text{ sec}^{-2}$ gives $\zeta_2 = 1/\sqrt{1 + (66/37)^2} = 0.49$.

The calculations in the previous paragraph suggest the following question: why does this 3rd order system have one real pole that corresponds to monotonic exponential 1st order response, and a pair of complex conjugate poles that correspond to damped oscillatory 2nd order response? In fact, this is a simple example of an important general property of linear time-invariant systems. Every LTI system has *modes of response* that are associated with its poles, the roots of the system's characteristic equation. We show this by re-writing characteristic equation (16-33) in the general factored form:

$$Den(p) = a_1 p^n + a_2 p^{n-1} + \cdots + a_n p + a_{n+1} = a_1 \prod_{k=1}^n (p - p_k) = 0 \quad (16-58)$$

where the symbol $\prod_{k=1}^n$ denotes multiplication of n terms. Since all coefficients a_k are real, this equation can always be factored into 1st order terms with real poles and 2nd order terms with complex conjugate poles for which $|\zeta_j| < 1$:

$$\frac{1}{a_1} Den(p) = \prod_{k=1}^n (p - p_k) = \dots (p - p_i) \dots (p^2 + 2\zeta_j \omega_j p + \omega_j^2) \dots \quad (16-59)$$

It might be conceptually clearest to think of the modes in terms of response to initial conditions, without the complication of forcing inputs. The mode of IC response associated with any real pole [p_i in Eq. (16-59)] is monotonic exponential, exactly that of a basic 1st order system. The mode of IC response associated with any pair of complex conjugate poles $[-\zeta_j \omega_j \pm j\omega_j \sqrt{1 - \zeta_j^2}$ in Eq. (16-59)] is oscillation modulated by an exponential envelope, exactly that of a basic 2nd order system for which $|\zeta| < 1$. The total time response of an LTI system to initial conditions and forcing inputs is the superposition of the responses of all of its individual 1st order and 2nd order modes. If the response is stable, then the greatest contributors to this total response typically are a few, at most, dominant modes, those whose poles are closest to the imaginary axis.

The *modes of vibration* introduced in Section 7-6 and Chapter 12 represent a special case of the more general modes of response discussed in the previous paragraph. An undamped structural system of the type considered in Chapter 12 always has even order (*i.e.*, $n = 2, 4, 6, \dots$), so that its characteristic equation has an even number of roots. These roots appear in purely imaginary conjugate pairs, each pair for a particular mode of vibration; the absolute value of any root is the natural frequency of that particular mode.

Before proceeding, we should observe a general feature of loci-of-roots diagrams. The poles are either real or, if complex, appear in conjugate pairs, as is expressed by Eq.

(16-59). Therefore, loci-of-roots diagrams are always symmetric about the $\text{Re}(p)$ axis. This symmetry is evident in Figs. 16-5, 16-7, and 16-8.

16-6 Open-loop transfer functions and loci of roots

Let's review and consider again Fig. 14-8, the general Laplace block diagram for an SISO closed-loop system with feedback. In Section 14-4, we used Fig. 14-8 to derive the closed-loop transfer function, $\text{Out}(s)/\text{In}(s)$:

$$\text{CLTF}(s) = \frac{G}{1 + GH} = \frac{N_G D_H}{D_G D_H + N_G N_H} \quad (16-60)$$

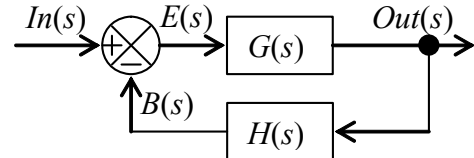


Fig. 14-8 (repeated) Laplace block diagram of general closed loop

It is common practice also to refer to the ratio $B(s)/E(s)$ as the *open-loop transfer function*, which is expressed more completely as

$$\frac{B(s)}{E(s)} \equiv \text{OLTF}(s) = G(s)H(s) = \frac{N_G(s)N_H(s)}{D_G(s)D_H(s)} \equiv C \times \frac{\prod_{k=1}^m (s - Z_k)}{\prod_{k=1}^n (s - P_k)} \quad (16-61)$$

In Eq. (16-61), C is some physical constant, the finite zeros Z_k of $\text{OLTF}(s)$ are the roots of $N_G(s)N_H(s) = 0$, and the poles P_k of $\text{OLTF}(s)$ are the roots of $D_G(s)D_H(s) = 0$. [For $n > m$, there are also $n - m$ zeros of $\text{OLTF}(s)$ as $s \rightarrow \infty$.]

The n^{th} degree characteristic polynomial of the closed-loop system is Eq. (16-58), $a_1 \prod_{k=1}^n (p - p_k) = 0$. Note that the denominator of $\text{CLTF}(s)$, Eq. (16-60), equals the denominator plus the numerator of $\text{OLTF}(s)$, Eq. (16-61). Therefore, after we divide out coefficient a_1 , the characteristic equation for closed-loop system poles p can generally be put into one of the following forms:

$$D_G(p)D_H(p) + N_G(p)N_H(p) = 0 \Rightarrow \begin{cases} \prod_{k=1}^n (p - P_k) + c \Lambda = 0 & \text{(a)} \\ \prod_{k=1}^n (p - P_k) + c \Lambda \prod_{k=1}^m (p - Z_k) = 0 & \text{(b)} \end{cases} \quad (16-62)$$

In Eqs. (16-62), c is some known physical constant, and Λ is the varying control parameter. The system evaluated by root-locus methods in Section 16-5 includes open-loop poles P_k (called there the “sub-system poles”), but not any finite open-loop zeros Z_k , so that system’s characteristic equation, Eq. (16-51b), is of form (16-62a). On the other hand, the systems of homework Problems 16.8, 16.9, and 16.10 have both open-loop poles and open-loop zeros, so their characteristic equations have form (16-62b).

Some simple but general features of loci of closed-loop roots can be inferred from Eqs. (16-62). Both equations show clearly that when $\Lambda = 0$, the closed-loop poles are exactly the same as the open-loop poles. At the other extreme, as Λ becomes very large, $\Lambda \rightarrow \infty$, m of the loci \rightarrow the finite open-loop zeros Z_k . This is obvious from Eq. (16-62b), because the term including the open-loop poles becomes progressively less significant in relative size as the magnitude of Λ increases.

As $\Lambda \rightarrow \infty$ in Eq. (16-62a), in order for an equation of magnitude equality such as Eq. (16-56), $r_1 r_2 r_3 = \omega_b \Lambda$, to remain satisfied, all n of the loci of that equation must go to some ∞ locations in the p -plane. Similarly, as $\Lambda \rightarrow \infty$ in Eq. (16-62b), although m of the loci terminate at the finite open-loop zeros Z_k , the remaining $n - m$ loci must go to some ∞ locations in the p -plane. For both Eqs. (16-62) as $\Lambda \rightarrow \infty$, the values of the finite open-loop zeros Z_k and of the open-loop poles P_k have a secondary influence, so the directions θ_A in the p -plane of the $n - m$ straight-line asymptotes of the $\Lambda \rightarrow \infty$ loci are the solutions for angles of $p^{n-m} + c\Lambda = 0$, which leads to:

$$(re^{j\theta_A})^{n-m} = c\Lambda \exp[j(\pm\pi, \pm 3\pi, \dots)] \Rightarrow (n-m)\theta_A = \pm\pi, \pm 3\pi, \dots$$

$$\theta_A = \frac{1}{n-m}(\pm\pi, \pm 3\pi, \dots) \quad (16-63)$$

However, Eq. (16-63) neglects the values of Z_k and P_k , so it implies incorrectly that the asymptotes “radiate” (or “emanate”) from the origin of the p -plane; in fact, it can be proved (Cannon, 1967, pages 658-659) that all $n - m$ asymptotes emanate from a point on the real axis defined by the equation:

$$p_A = \frac{1}{n-m} \left(\sum_{k=1}^n \operatorname{Re}[P_k] - \sum_{k=1}^m \operatorname{Re}[Z_k] \right) \quad (16-64)$$

It is useful also to know the directions in which loci “depart” from the open-loop poles as Λ increases from zero. Suppose that we seek the direction (angle) of departure $(\theta_j)_{dep}$ of the locus of closed-loop roots from open-loop pole P_j . Let’s use the following notation: $(\theta P)_{kj}$ is the angle from open-loop pole P_k to open-loop pole P_j ; and $(\theta Z)_{kj}$ is the angle from open-loop zero Z_k to open-loop pole P_j . Provided that all of the open-loop poles and zeros are single (not repeated or multiple) roots, then the required angle is calculated from the equation (Cannon, 1967, pages 660-661):

$$(\theta_j)_{dep} = \pi - \sum_{\substack{k=1 \\ k \neq j}}^n (\theta P)_{kj} + \sum_{k=1}^m (\theta Z)_{kj} \quad (16-65)$$

We use Section 16-5’s numerical example to illustrate the information about loci of roots that is provided by open-loop poles; that example is a 3rd order system for which $n = 3$ and $m = 0$. From Eq. (16-51b) with $\Lambda = 0$, the open-loop poles are $p_1 = 0 \text{ sec}^{-1}$, $p_2 = -100 \text{ sec}^{-1}$, and $p_3 = -300 \text{ sec}^{-1}$. These open-loop poles are marked by \times ’s on Fig. 16-9. There are no open-loop zeros, so as $\Lambda \rightarrow \infty$, the three loci must go to some ∞ locations in

the p -plane; the directions of the lines asymptotic to these loci are given by Eq. (16-63) as $\theta_A = \pm\pi/3$ and $\theta = \pi$. The point on the real axis from which all three asymptotes emanate is given by Eq. (16-64) as $p_A = (0 - 100 - 300)/3 = -133\frac{1}{3} \text{ sec}^{-1}$. The asymptotes are the straight dashed lines on Fig. 16-9. Equation (16-65) gives the angles of departure from open-loop poles as $(\theta_1)_{dep} = \pi - (0 + 0) = \pi$, $(\theta_2)_{dep} = \pi - (\pi + 0) = 0$, and $(\theta_3)_{dep} = \pi - (\pi + \pi) = -\pi$. These angles of departure are represented on Fig. 16-9 by short, bold arrows. Although the directions of departure for this particular system are either due east or due west, this is not always the case; for systems in general, a direction of departure can be any angle.

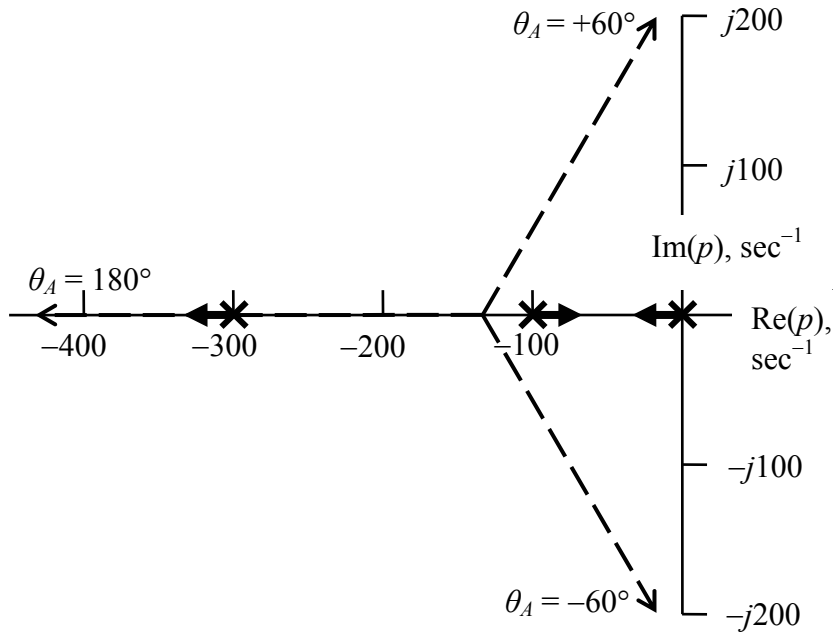


Figure 16-9 Example of information about loci of roots that is provided by the open-loop poles

We can make educated guesses as to the appearance of the completed diagram of root loci, even from the incomplete diagram Fig. 16-9. First, it seems likely that the locus originating (*i.e.*, for $\Lambda = 0$) at open-loop pole $p_3 = -300 \text{ sec}^{-1}$ just proceeds westerly along the asymptote $\theta_A = \pi$, without straying away from the $\text{Re}(p)$ axis. That being the case, then the loci originating from the open-loop poles $p_1 = 0 \text{ sec}^{-1}$ and $p_2 = -100 \text{ sec}^{-1}$ must initially approach each other, then come together somewhere between p_1 and p_2 , and then break away from the $\text{Re}(p)$ axis and become the complex conjugate pair of curves to which the asymptotes $\theta_A = \pm\pi/3$ are tangent as $\Lambda \rightarrow \infty$. Certainly, the incomplete diagram Fig. 16-9 is qualitatively similar to the exact diagram Fig. 16-8, and Fig. 16-9 even includes some of the same significant quantitative information.

When you use software to determine loci of roots, you should also make the easy calculations presented in this section based upon open-loop poles and zeros. If the software calculations match yours, then this check will validate (partially, at least) that the software is correct and that you are using it correctly.

16-7 Homework problems for Chapter 16

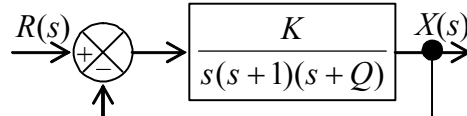
16.1 Examine whichever of the following characteristic equations are assigned, using Routh's criteria to determine if all of their roots have negative real parts so that the associated systems are positively stable.

(a) $p - 3 = 0$ (b) $2p + 11 = 0$ (c) $p^2 + 2p + 8 = 0$ (d) $2p^2 - 9p + 29 = 0$

(e) $2p^3 + 4p^2 + 4p + 12 = 0$ (f) $p^3 + 6p^2 + 12p + 8 = 0$ (g) $p^4 - p^3 + 7p^2 + p - 8 = 0$

16.2 Consider the conceptual Laplace closed-loop-system block diagram below, with two possibly variable system parameters, K and Q .

Write the equation for the closed-loop transfer function. Next, expand the denominator (characteristic) polynomial and apply Routh's stability criteria to write all of the algebraic inequality relationships involving K and Q (in general) that must be satisfied in order for the system to be positively stable. (Don't worry about the units of K and Q , just assume that they are consistent.) Calculate the range of K for which the system is positively stable for whichever of the following cases is assigned: (a) $Q = -0.5$ and $+0.5$; (b) $Q = -1.0$ and $+1.0$; (c) $Q = -1.5$ and $+1.5$.



16.3 Consider the characteristic equation $p^2 + 2Cp + K = 0$. With mass m being positive-definite, this is the characteristic equation of the standard mass-damper-spring system described by equation of motion $m\ddot{x} + c\dot{x} + kx = f_x(t)$, but with the notation $C \equiv c/(2m)$ and $K \equiv k/m$. The roots of this 2nd degree polynomial equation are the poles of the system transfer function. Suppose that damping constant $C = 6 \text{ sec}^{-1}$, and that you want to evaluate the system stability characteristics for different values of stiffness constant $K \text{ sec}^{-2}$. Consider first non-negative values of K . For what positive value of $K \equiv K_c$ is the damping critical, and what values do the polynomial roots have for $K \equiv K_c$? (Definition: if damping is positive but less than critical, then the roots are complex, corresponding to initial-condition response that is oscillation modulated by a decaying exponential envelope; if, on the other hand, damping is equal to or greater than critical, then the roots are negative real, corresponding to monotonic exponentially decaying initial-condition response.) What values are the roots for $K = 0$ and for $K = 2K_c$? Show each of these roots by marking large X's at the correct positions on a complex p -plane graph [x-axis is $\text{Re}(p)$, y-axis is $\text{Im}(p)$, both in sec^{-1}]; label the axes and the linear scale of the axes, the same scale on both axes, as on the MATLAB graph Fig. 16-8. Explain concisely what quality of the roots indicates that the system is stable for all values of $K > 0$. Now calculate the values of the roots for a negative stiffness, say $K = -3K_c$, and mark those roots on your p -plane graph. From the roots for a negative stiffness, what can you state conclusively about the system stability for all negative values of K ? Indicate clearly on your p -plane graph the loci of roots as K increases from $-3K_c$ to 0, then from 0 to $+K_c$, then from K_c to $2K_c$, and finally for $K_c > 2K_c$. Is there a break-away point on your loci of roots; if so, for what value of K ?

16.4 The following characteristic equations are expressed in completely or partially factored forms. For whichever equations are assigned, find the order n of the associated system, solve for the roots and mark their locations with large X's on a sketch of the complex p -plane, and state whether the system is stable or unstable; give the reason(s) for your conclusion.

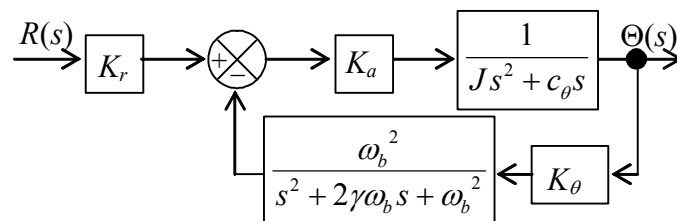
(a) $(p - 4)(p + 3)(p + 4)(p + 5) = 0$

(b) $p(p + 2)(p^2 - 6p + 34) = 0$

(c) $(p + 1)(p + 3 - j5)(p + 3 + j5) = 0$

(d) $(p + 3)(p^2 + 2p + 2)(p^2 + 4p + 20) = 0$

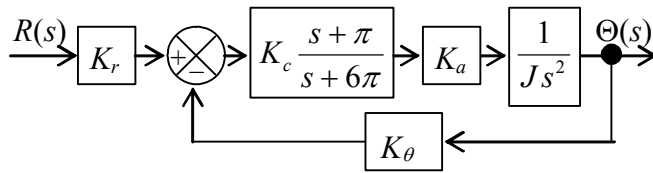
16.5 The Laplace block diagram at right represents a system similar to that of Figs. 16-2 and 16-3: it is a damped rotor with position feedback that is low-pass-filtered. But the low-pass filter in this case is 2nd order, whereas the filter of Fig. 16-3 is 1st order. The filter transfer function on the block diagram is from Eq. (10-6): low-pass break frequency ω_b is the undamped natural frequency, and γ is the filter viscous damping ratio. We specify the value $\gamma = 1/\sqrt{2}$; as shown on the frequency-response magnitude-ratio graph of Fig. 10-2, for this γ , the magnitude attenuation at $\omega = \omega_b$ is $1/\sqrt{2}$ (same as for a 1st order filter), and the high frequency roll-off is two decades for each decade increase of frequency (twice as steep as the roll-off of a 1st order filter). (See also the discussion of 2nd order low-pass filters at the end of Section 10-2.)



(a) Derive from the block diagram the algebraic equation for the closed-loop transfer function, $CLTF(s) \equiv \Theta(s)/R(s)$ (in terms of the symbols shown, without numbers at this stage). From your $CLTF(s)$, write the characteristic equation, $Den(p) = 0$.

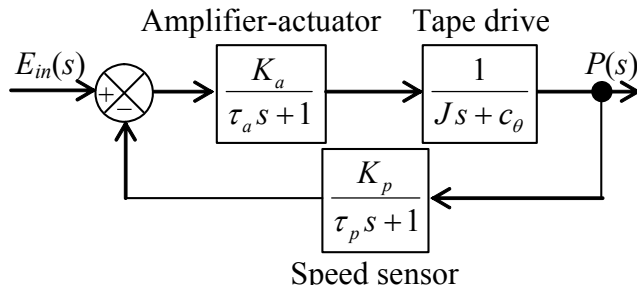
(b) Use the same values as for the calculations of Chapter 16: $\omega_b = 300$ rad/sec and $c_\theta/J = 100$ sec⁻¹, as well as $\gamma = 1/\sqrt{2}$. Also as in Chapter 16, denote the varying control-system parameter as $\Lambda \equiv K_a K_\theta / J$. Use MATLAB's `root` operation to calculate, print out, and plot the loci of roots of this system over the entire range of Λ values for which the system is positively stable. Your graph and numerical output should show with at least 2-3 significant-figure precision any break-away points and the upper and lower boundaries of stability. Find by trial and error the approximate value of Λ for which the dominant oscillatory mode of response has the system damping ratio $\zeta \approx 1/\sqrt{2}$, and also calculate the time constant τ_2 and the frequency ω_d for this value of Λ .

16.6 The Laplace block diagram here represents a system to control the angular position of a satellite in one plane. The unfamiliar input-error block in the forward branch of the loop is the transfer function of a *compensator*, which in this case is designed to place a pair of the system's closed-loop poles at $2\pi(-1 \pm j1)$ sec $^{-1}$ in the *p*-plane, for one value of control parameter $\Lambda \equiv K_c K_a K_\theta / J$. For these poles, the frequency is $f_d = \omega_d / 2\pi = 1$ Hz, and the viscous damping ratio is $\zeta = 1/\sqrt{2}$.



- (a) Derive from the block diagram the algebraic equation for the closed-loop transfer function, $\Theta(s)/R(s)$, then write the characteristic equation, $Den(p) = 0$.
- (b) Use MATLAB's `root` operation to calculate, print out, and plot the loci of roots of this system over the parameter range $0 \leq \Lambda \leq 200$ sec $^{-2}$.
- (c) Use Evans' root-locus method to determine the numerical value of Λ that produces poles $2\pi(-1 \pm j1)$ sec $^{-1}$.

16.7 (Adapted from Franklin, *et al.*, 1991, Problem 5.25 on page 347) The Laplace block diagram of the speed-control system of a magnetic-tape drive is shown in the figure below. The operator setting is input voltage signal $e_{in}(t)$, the Laplace transform of which is $E_{in}(s)$. Each major sub-system of the control system functions as a 1st order system. The sub-system consisting of a power amplifier and a torque actuator has variable sensitivity K_a (N-m/V) and time constant $\tau_a = 1.0$ sec. The tape drive has rotational inertia $J = 4.0$ N-m per rad/sec 2 and lubricated-shaft viscous damping constant $c_\theta = 1.0$ N-m per rad/sec; the output of the tape drive in this application is rotational speed $p(t)$ in rad/sec [with Laplace transform $P(s)$], not rotational position $\theta(t)$. The rotational-speed sensor in the feedback branch has sensitivity $K_p = 1.250$ V per rad/sec; this sensor is sufficiently slow relative to the other sub-systems that we must account for its time constant, $\tau_p = 0.5$ sec.



- (a) Derive the closed-loop transfer function $P(s)/E_{in}(s)$, and then show that the characteristic equation of this system can be expressed as

$$(p + c_\theta/J)(p + \tau_a^{-1})(p + \tau_p^{-1}) + \Lambda = 0, \text{ or } r_1 e^{j\theta_1} \times r_2 e^{j\theta_2} \times r_3 e^{j\theta_3} = \Lambda \exp[j(\pm\pi, \pm 3\pi, \dots)]$$

where the variable control parameter is defined as $\Lambda = K_a K_p / (J \tau_a \tau_p)$, with units of sec $^{-3}$.

- (b)** Determine (by hand, not MATLAB) all of the open-loop poles, all of the asymptotes (as $\Lambda \rightarrow \infty$) of the closed-loop poles, and the directions of departure of the root loci from the open-loop poles as Λ increases from zero. Sketch on graph paper a p -plane, and indicate on it the information that you determined for this system. See Fig. 16-9 for an example of the type of diagram that yours should be. Make educated guesses and sketch on your diagram the forms you think the root loci should have.
- (c)** From part (a), any point on a locus of roots must satisfy the angle equality: $\theta_1 + \theta_2 + \theta_3 = \pm\pi, \pm 3\pi, \dots$. Use this equality to write a transcendental equation that can be solved for the closed-loop pole $j\omega_d$ at the upper stability boundary Λ_{ub} of the complex oscillatory loci; your equation will include trigonometric functions for the θ_i angles that involve ω_d and the numerical values of the open-loop poles. It is not necessary for you to solve the transcendental equation, but you may show just by substitution that $\omega_d = 1.6583124 \text{ sec}^{-1} = \sqrt{11}/2 \text{ sec}^{-1}$ is the solution. Finally, again using the result of part (a), solve for the value $\Lambda_{ub} = r_1 \times r_2 \times r_3$; your equation will include terms for the r_i magnitudes that involve ω_d and the numerical values of the open-loop poles. [Note: you could also solve this part by applying Routh's criteria, Eqs. (16-37) and (16-38), to calculate Λ_{ub} , then substituting Λ_{ub} back into the characteristic equation to solve for $p = j\omega_d$.]

16.8 The open-loop transfer function of a certain control system is

$$G(s)H(s) \equiv OLT(s) = \Lambda \frac{s^2 + 4s + 104}{(s+1)(s^2 + 2s + 26)}$$

where Λ (with units sec^{-1}) is a variable parameter with possible range $0 \leq \Lambda < +\infty$.

- (a)** Determine (by hand, not MATLAB) all of the open-loop poles and open-loop zeros of this system, any asymptotes (as $\Lambda \rightarrow \infty$) of the closed-loop poles, and the directions of departure of the root loci from the open-loop poles as Λ increases from zero. Sketch on graph paper a p -plane, and indicate on it the information that you determine for this system. See Fig. 16-9 for an example of the type of diagram that yours should be. However, whereas Fig. 16-9 does not display any open-loop zeros, your diagram should; it is traditional to mark an open-loop zero by an **o**, just as an open-loop pole is marked by an **x**. Make educated guesses and sketch on your diagram the forms you think the root loci should have.

- (b)** Show that the characteristic equation of the closed-loop system is

$$p^3 + (3 + \Lambda)p^2 + 4(7 + \Lambda)p + 26(1 + 4\Lambda) = 0$$

Apply Routh's criteria, Eqs. (16-37) and (16-38), to calculate bounds and ranges of Λ for stability; in particular, solve a quadratic equation in unknown Λ to show that two of the bounds are $\Lambda_{1,2} = 8 \pm \sqrt{49.5} \text{ sec}^{-1} = 0.964376 \text{ sec}^{-1}$ and 15.0356 sec^{-1} . In order to inter-

pret the significance of these bounds relative to stability, calculate the quadratic equation for values of Λ slightly above and below these two bounds. Next, substitute the values Λ_1 and Λ_2 back into the characteristic equation as $p = j\omega_{d1}$ and $p = j\omega_{d2}$ to solve for the oscillatory frequencies ω_{d1} and ω_{d2} at Λ_1 and Λ_2 , respectively—there will be both a real and an imaginary part of the equation that you can solve; calculate the $\omega_{d1,2}$ from the easier part, then just substitute that value of $\omega_{d1,2}$ into the harder part to show that it also is satisfied. What is the significance of $\omega_{d1,2}$ and $\Lambda_{1,2}$ on your diagram in part (a)?

16.9 The characteristic equation of a certain LTI-SISO system can be expressed as

$$1 + G(p)H(p) = 1 + \Lambda \frac{p+1}{(p-1)(p+3)(p^2+2p+2)} = 0$$

where Λ is a variable gain parameter with possible range $0 \leq \Lambda < +\infty$.

(a) Determine (by hand, not MATLAB) all of the open-loop poles and the open-loop zero of this system, all of the asymptotes (as $\Lambda \rightarrow \infty$) of the closed-loop poles, and the directions of departure of the root loci from the open-loop poles as Λ increases from zero.

Sketch on graph paper a p -plane, and indicate on it the information that you determine for this system. See Fig. 16-9 for an example of the type of diagram that yours should be. However, whereas Fig. 16-9 does not display any open-loop zeros, your diagram should; it is traditional to mark an open-loop zero by an **o**, just as an open-loop pole is marked by an **x**. Make educated guesses and sketch on your diagram the forms you think the root loci should have.

(b) Your information in part (a) should suggest that one locus of roots is on the $\text{Re}(p)$ axis, starting from an open-loop pole at $p = +1$ (for $\Lambda = 0$), and terminating on an open-loop zero at $p = -1$ (for $\Lambda \rightarrow \infty$). If that is true, then this particular locus must, for some value of Λ between 0 and ∞ , cross the origin of the p -plane from $p > 0$ (unstable) to $p < 0$ (stable). Your assignment is to express the characteristic equation in polar form [in the manner of Eqs. (16-53)- (16-56)], use that form to prove the segment $-1 \leq p \leq +1$ of the $\text{Re}(p)$ axis is or is not a locus, and, if it is, find the value of Λ at $p = 0$, the boundary between instability and stability.

(c) Your solution from part (b) should indicate: there is a locus on the segment $-1 \leq p \leq +1$ of the $\text{Re}(p)$ axis; and that locus has stable roots for Λ greater than its value at $p = 0$. On the other hand, your information from part (a) should show there is a pair of complex conjugate open-loop poles in the stable western half-plane; it also should suggest that the loci departing from those complex open-loop poles (for $\Lambda = 0$) then proceed in an easterly direction as Λ increases from zero, then, for some positive value of Λ , cross over the $\text{Im}(p)$ axis into the unstable eastern half-plane. So, as Λ increases from zero, one real locus of closed-loop roots goes from being unstable to stable, but a pair of complex conjugate loci go from being stable to unstable. Therefore, we must ask if there is any range of Λ for which all of the loci are in the western half-plane and the closed-loop system is stable? Perhaps the best way to answer this question is to use Routh's stability criteria.

Chapter 16 Introduction to system stability: time-response criteria

Consider a general 4th order characteristic equation: $a_1 p^4 + a_2 p^3 + a_3 p^2 + a_4 p + a_5 = 0$. The associated system is stable if and only if all of the following conditions are satisfied (Ogata, 2001, pages 275-277):

* all $a_i > 0$, $i = 1, 2, 3, 4, 5$;

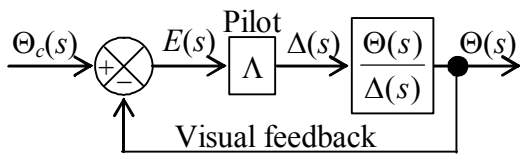
* $R_2 \equiv a_2 \times a_3 - a_1 \times a_4 > 0$;

* $R_3 \equiv R_2 \times a_4 - a_2^2 \times a_5 > 0$.

Use Routh's stability criteria to determine the range of Λ for which the closed-loop system is stable, if there is such a range.

16.10 (adapted from Nelson, 1989, Problem 7.7 on pages 222-223) The 1903 Wright Flyer by itself was inherently unstable in longitudinal motion (coupled pitch and vertical translation). However, Wilbur and Orville Wright stabilized, just barely, the system of airplane + pilot by providing sufficient control authority with a canard and by developing flying skill through extensive experimentation and practice with piloted gliders. A mathematical model³ of the system was formulated, the Laplace block diagram for which is shown below. The input to the system is commanded pitch attitude $\Theta_c(s)$, and the output

is actual pitch attitude $\Theta(s)$. Incremental canard position is $\Delta(s)$, for which the Laplace transform is $\Delta(s)$. The canard-position-to-pitch-attitude transfer function incorporates both rigid-body dynamics and aerodynamics; the estimated model of this transfer function is



$$\frac{\Theta(s)}{\Delta(s)} = \frac{11.0(s + 0.5)(s + 3.0)}{(s^2 + 5.9s - 11.9)(s^2 + 0.72s + 1.44)} = \frac{11.0(s + 0.5)(s + 3.0)}{(s - 1.589)(s + 7.489)(s^2 + 0.72s + 1.44)}$$

(a) Determine (by hand, not MATLAB) all of the open-loop poles and open-loop zeros of this system, all of the asymptotes (as pilot gain $\Lambda \rightarrow \infty$) of the closed-loop poles, and the directions of departure of the root loci from the open-loop poles as Λ increases from zero. Sketch on graph paper a p -plane, and indicate on it the information that you determined for this system. See Fig. 16-9 for an example of the type of diagram that yours should be. However, whereas Fig. 16-9 does not display any open-loop zeros, your diagram should; it is traditional to mark an open-loop zero by an **o**, just as an open-loop pole is marked by an **x**.

(b) Show in detail that the characteristic polynomial equation in the form $a_1 p^4 + a_2 p^3 + a_3 p^2 + a_4 p + a_5 = 0$, with all a_i coefficients either numerical or combinations of numbers and pilot gain Λ , is given by:

³ Culick, F.E.C.: "Building a 1903 Wright 'Flyer'—by Committee," AIAA Paper 88-0094, 1988

Chapter 16 Introduction to system stability: time-response criteria

$$p^4 + 6.62p^3 + (11\Lambda - 6.212)p^2 + (38.5\Lambda - 0.072)p + (16.5\Lambda - 17.136) = 0$$

- (c) If we wish at this point to program into software the calculation of loci of roots, we know only to consider $0 < \Lambda < \infty$; but, without more information, it is difficult to know what specific range or even order of magnitude of Λ to enter initially in the calculations. However, Routh's stability criteria can provide that necessary additional information. Use Routh's criteria [homework Problem 16.9(c)] and the characteristic-equation coefficients to evaluate the absolute stability of the Wright Flyer system, thereby determining quantitatively a candidate range of Λ for use in calculation of loci of roots.⁴ (*Answer:* for stability, $\Lambda > 1.3096$)
- (d) Use MATLAB's `root` operation to calculate, print out, and plot the loci of roots of this system over a range of Λ values for which the system is stable. From Eq. (9-28), viscous damping ratio $\zeta = 0.11$ of the oscillatory mode produces 50% amplitude decay during each cycle; show from your calculations that $\Lambda = 3.24$ is the lower pilot gain for which $\zeta = 0.11$, to reasonable engineering accuracy. From your results for $\Lambda = 3.24$, do you expect an oscillatory mode to be dominant in time response, or an exponential mode, or perhaps a combination of the two?

- (e) It is of interest to examine in more detail the case of pilot gain $\Lambda = 3.24$, beginning with the closed-loop transfer function $CLTF(s)$. Note that we essentially already have the denominator of $CLTF(s)$: in the characteristic equation of part (b), just replace $p \rightarrow s$ and set $\Lambda = 3.24$. Show that the closed-loop transfer function, in the form of Eq. (16-5), is:

$$CLTF(s) = \frac{\Theta(s)}{\Theta_c(s)} = \frac{35.64(s^2 + 3.5s + 1.5)}{s^4 + 6.62s^3 + 29.428s^2 + 124.668s + 36.324}$$

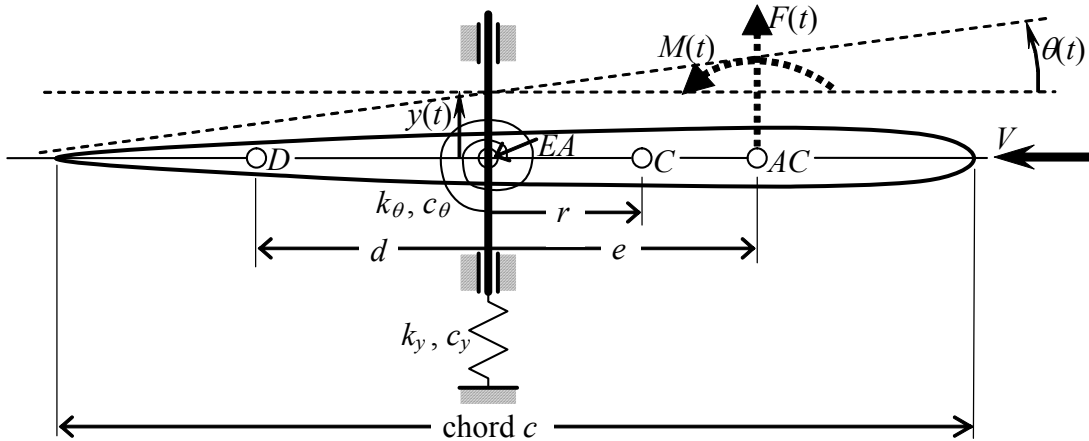
Now apply MATLAB's `residue` operation (see homework Problem 2.15) to calculate the residues and poles of $CLTF(s)$, and write out the partial-fraction expansion form of $CLTF(s)$. Note that the poles found in this step should match those of part (d) for $\Lambda = 3.24$.

- (f) Finally, consider a forced-response solution in time, with zero initial conditions. Suppose the pilot commands a short pulse to the pitch-control lever; represent this pulse approximately with a Dirac delta function (Section 8-4): $\theta_c(t) = I_\theta \delta(t)$, for which the Laplace transform is $\Theta_c(s) = I_\theta$. Let the impulse magnitude be $I_\theta = 2$ degree-sec. Use the partial-fraction expansion form of $CLTF(s)$ from part (e) to derive the equation for the

⁴ This exercise requires several calculations. Rather than calculating manually, you might prefer to use symbolic software. If you use MATLAB's Symbolic Math Toolbox (see homework Problem 1.6), be aware that this symbolic software performs calculations exactly, expressing numbers as fractions of integers if at all possible. But the integers in these fractions can become quite large and unwieldy. You can convert these fractions into decimal numbers by using “variable precision arithmetic.” For example, if a symbolic term is expressed as $v = 4115/2263*w$, you can convert the fractional coefficient into a five-digit decimal with the operations `>> digits(5); v5=vpa(v)`, the result of which is $v5 = 1.8184*w$.

pitch response $\theta(t)$ to this control excitation, and then calculate and plot this transient response over a 15-sec interval.

16.11 We know from Chapter 16 that the process of calculating and plotting loci of roots is useful in analysis of control-system stability; the objective of this problem is to illustrate another important application of root-loci: analysis of the stability of a system for which the potentially destabilizing feedback is natural and intrinsic, not human-designed. Systems with this characteristic are often described as *self-excited* (see, e.g., Den Hartog, 1956, Chapter 7). The particular phenomenon we consider here, aeroelastic dynamic response of a typical-section airfoil, including unstable flutter, originated in aeronautical engineering but is relevant also to many other applications of force-generating objects that are immersed within moving fluids (e.g., hydrofoils, wind-turbine blades, and propellers). The typical-section airfoil is described in Section 11-3, Examples 11-2 and 11-3, and we consider here the form depicted below, an uncambered, symmetric thin airfoil supported by springs in a wind tunnel, and immersed within an incompressible airstream of density ρ and freestream velocity V .



Structural dynamic equations of motion with vertical translation of mass center C , $y_{AC}(t)$, and pitch $\theta(t)$ as degrees of freedom (DOFs) are derived and expressed in matrix form in Eq. (11-22). However, a more appropriate vertical translation DOF for this problem is $y_{EA}(t) \equiv y(t)$ of the elastic axis EA , as labeled on the figure above; the equations of motion for DOFs $y(t)$ and $\theta(t)$ are derived in homework Problem 11.4 and are expressed below, with the addition of a damping matrix that represents approximately the energy dissipation within the springs (using the viscous-damping mathematical model described in Appendix B, Section B-5).

$$\begin{bmatrix} m & mr \\ mr & J_{EA} \end{bmatrix} \begin{bmatrix} \ddot{y} \\ \ddot{\theta} \end{bmatrix} + \begin{bmatrix} c_y & 0 \\ 0 & c_\theta \end{bmatrix} \begin{bmatrix} \dot{y} \\ \dot{\theta} \end{bmatrix} + \begin{bmatrix} k_y & 0 \\ 0 & k_\theta \end{bmatrix} \begin{bmatrix} y \\ \theta \end{bmatrix} = \begin{bmatrix} F(t) \\ M(t) + F(t)e \end{bmatrix} \quad (\text{P16.11-1})$$

We assume that aerodynamic resultant lift force and moment (positive nose-up) are due both to the motions of the typical section itself (self-excitation), and to sources such as gusts that are independent of the motion, which we denote as lift $F_G(t)$ and moment

$M_G(t)$. There is no exact and readily applicable theory of unsteady, motion-dependent aerodynamics; therefore, we use here one of the many approximate theories, the *quasi-steady* aerodynamics of Fung, 1955, pages 191-193. In these equations of unsteady lift and moment, we replace Fung's lift-curve slope for an airfoil of infinite span, $C_{L\alpha} = 2\pi$ per radian, with a reduced value of $C_{L\alpha}$ that applies for an airfoil of finite span. This is appropriate for the specific numerical parameters considered below in part (b), which are chosen to represent an actual experimental research investigation of typical-section aeroelasticity. Since dynamic pressure is $\bar{q} = \frac{1}{2}\rho V^2$, it is appropriate to define in Fung's equations the constant $K \equiv \frac{1}{2}\rho S(2\pi) \rightarrow K \equiv \frac{1}{2}\rho S C_{L\alpha}$. Thus, the motion-dependent and motion-independent aerodynamic resultant lift and nose-up moment are written as:

$$F(t) = \bar{q} S C_{L\alpha} \left(\theta - \frac{\dot{y} - d\dot{\theta}}{V} \right) + F_G(t) = K(V^2 \theta - V \dot{y} + dV \dot{\theta}) + F_G(t) \quad (\text{P16.11-2})$$

$$M(t) = -\bar{q} S c \frac{\pi c}{8} \frac{\dot{\theta}}{V} + M_G(t) = -K \frac{\pi/8}{C_{L\alpha}} c^2 V \dot{\theta} + M_G(t)$$

(a) Substitute Eqs. (P16.11-2) into Eq. (P16.11-1), then transpose the motion-dependent terms from the right-hand side to the left-hand side so that the damping and stiffness matrices in (P16.11-1) become more general; for example, the structural-plus-aerodynamic stiffness matrix becomes $\begin{bmatrix} k_y & -KV^2 \\ 0 & k_\theta - eKV^2 \end{bmatrix}$. Now you have a set of equations that, in principle, can be solved for DOFs $y(t)$ and $\theta(t)$ by Laplace transformation. Assume null initial conditions, $y(0) = 0$ and $\theta(0) = 0$, and assume that $F_G(t)$ and $M_G(t)$ are Laplace transformable functions, then express the Laplace-transformed equations of motion in the following form, writing explicit quadratic (in s) polynomials for the four $M_{ij}(s; V)$ elements of the left-hand side coefficient matrix:

$$\begin{bmatrix} M_{11}(s; V) & M_{12}(s; V) \\ M_{21}(s; V) & M_{22}(s; V) \end{bmatrix} \begin{bmatrix} Y(s) \\ \Theta(s) \end{bmatrix} \equiv [\mathbf{M}(s; V)] \begin{bmatrix} Y(s) \\ \Theta(s) \end{bmatrix} = \begin{bmatrix} L[F_G(t)] \\ L[M_G(t)] + eL[F_G(t)] \end{bmatrix} \quad (\text{P16.11-3})$$

The matrix solution of Eq. (P16.11-3) can be written as

$$\begin{bmatrix} Y(s) \\ \Theta(s) \end{bmatrix} = [\mathbf{TF}(s; V)] \begin{bmatrix} L[F_G(t)] \\ L[M_G(t)] + eL[F_G(t)] \end{bmatrix} \quad (\text{P16.11-4})$$

where the 2×2 coefficient matrix $[\mathbf{TF}(s; V)] = [\mathbf{M}(s; V)]^{-1}$ is the multiple-input-multiple-output (MIMO) *transfer-function matrix* relating two outputs, $Y(s)$ and $\Theta(s)$, to two inputs, $L[F_G(t)]$ and $(L[M_G(t)] + eL[F_G(t)])$; however, it is clear that each element of matrix $[\mathbf{TF}(s; V)]$ is itself a single-input-single-output (SISO) transfer function. Use Eqs. (12-10)-(12-12) to write an equation for $[\mathbf{TF}(s; V)]$ in terms of the four $M_{ij}(s; V)$ elements.

Note, in particular, that the denominator of each of the SISO transfer functions, $TF_{ij}(s;V)$, is the determinant $\det[\mathbf{M}(s;V)] = M_{11}(s;V) \times M_{22}(s;V) - M_{21}(s;V) \times M_{12}(s;V)$. By the logic of Section 16-1, therefore, the quartic (in p) polynomial equation, $\det[\mathbf{M}(p;V)] = 0$, is the general characteristic equation of the system, and its four roots $p_i(V)$ at each free-stream airspeed V determine both the character of unforced time response (*e.g.*, exponential, oscillatory, *etc.*) and the system stability or instability at that particular airspeed.

(b) In this part, you will use the equations of part (a) to calculate and plot the loci of roots, as wind-tunnel freestream airspeed V varies, using numerical parameters that were selected to represent the research project of a Brazilian group, DeMarqui, *et al.*, 2005 and 2006. The parameters of the typical-section airfoil and the wind-tunnel atmosphere are:

$$\text{Mass } m = 18.0 \text{ kg}$$

$$\text{Rotational inertia about mass center } C: J_C = 0.219 \text{ kg-m}^2; \text{ so } J_{EA} = J_C + mr^2$$

$$\text{Offset of mass center } C \text{ forward of elastic axis } EA: r = 5 \text{ mm} = 0.005 \text{ m}$$

$$\text{Stiffness constant of vertical-translation spring: } k_y = 1,110 \text{ N/m}$$

$$\text{Stiffness constant of pitch-rotation spring: } k_\theta = 49.8 \text{ N-m/radian}$$

$$\text{Viscous-damping constant of vertical-translation spring: } c_y = 0.0107 \text{ sec} \times k_y$$

$$\text{Viscous-damping constant of pitch-rotation spring: } c_\theta = 0.00318 \text{ sec} \times k_\theta$$

$$\text{Planform: chord } c = 0.45 \text{ m; span} = 0.80 \text{ m; so, area } S = c \times \text{span} = 0.36 \text{ m}^2$$

$$\text{Offset of } \frac{1}{4}\text{-chord aerodynamic center } AC \text{ forward of elastic axis } EA: e = c/4$$

$$\text{Offset of } \frac{3}{4}\text{-chord dynamic-pitch point } D \text{ aft of elastic axis } EA: d = c/4$$

$$\text{Standard air density at 800-m average altitude of Sao Paulo, Brazil: } \rho = 1.1337 \text{ kg/m}^3$$

$$\text{Lift-curve slope for this low-aspect-ratio airfoil: } C_{L\alpha} = 2.64 \text{ per radian}$$

The most significant single result that you seek is the wind-tunnel freestream airspeed V_F at which the typical section experiences aeroelastic flutter. The *flutter airspeed* V_F is that value of V at which the dominant time response of the typical section is a pure sinusoid; for lower airspeeds, $0 \leq V < V_F$, the dominant response is stable positively damped oscillation; but for higher airspeeds, $V > V_F$, the dominant response is unstable exponentially expanding oscillation. Begin the numerical analysis by using Eq. (11-18) to calculate the *aeroelastic divergence airspeed* V_D in m/sec; because usually $V_D > V_F$, this value of V_D will suggest to you the range of airspeeds, $0 \leq V < V_D$, over which you should calculate the loci of roots in order to determine V_F . Use MATLAB's `conv` and `root` operations to calculate, print out, and plot the loci of roots of characteristic equation $M_{11}(p;V) \times M_{22}(p;V) - M_{21}(p;V) \times M_{12}(p;V) = 0$. You might find useful the form of MATLAB script M-file `MATLABdemo164.m` that produced Figs. 16-7 and 16-8 in Section 16-5. In this problem, freestream velocity V plays the same role that control gain parameter Λ plays in `MATLABdemo164.m`.

Chapter 17 Introduction to system stability: frequency-response criteria

© 2016 by William L. Hallauer, Jr.

Frequency-response concepts have been discussed extensively in many previous chapters, most notably in Chapters 4 and 10 relative to methods of calculation and the physical characteristics of frequency response in stable systems. In this chapter, we consider methods using frequency response for assessing the stability of systems.

To examine the stability of a closed-loop control system, we examine in particular the frequency response of the associated open-loop system, for which the transfer function $OLTF(s) = G(s) \times H(s)$ was described in Section 16-6. The open-loop system itself is usually manageable, not unstable, even though its closed-loop version might be unstable. Therefore, the frequency-response function $OLFRF(\omega) \equiv OLTF(j\omega) = G(j\omega) \times H(j\omega)$ can typically be measured on actual hardware, even if there is no good mathematical model for the system. The reason for measuring and/or computing $OLFRF(\omega)$ is that it provides metrics of the absolute and relative stability of the closed-loop system. In other words, to determine the stability of the closed-loop system, it might not be necessary to close the loop with real hardware, possibly risking damage and/or injury.

Recall that root-locus analysis is based on the characteristic equation $1 + G(s) \times H(s) = 0$, or $G(s) \times H(s) = -1$; obviously, the right-hand-side number -1 is important to the closed-loop poles and to closed-loop system stability. Similarly, the number -1 is also highly significant when we evaluate stability using open-loop frequency response $G(j\omega) \times H(j\omega)$.

17-1 Gain margins, phase margins, and Bode diagrams

In order to describe and illustrate the most basic form of frequency-response stability analysis, we consider again a familiar system from Chapter 16: the rotor position-feedback control system with a 1st order low-pass filter in the feedback branch, for which the functional diagram is Fig. 16-2 and the block diagram is Fig 16-3. We have already studied this system to determine absolute stability by Routh's criteria in Section 16-3, and relative stability by calculating loci of roots and by applying the root-locus method in Sections 16-5 and 16-6. Knowing the stability characteristics in advance will guide us in interpreting the frequency-response analysis.

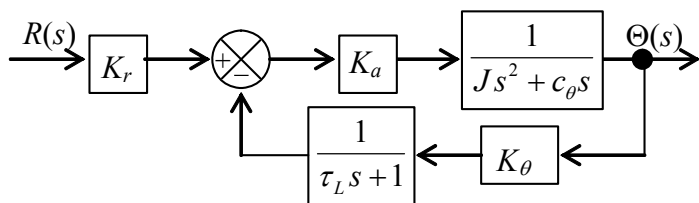


Figure 16-3 (repeated)

The branch transfer functions for the loop in Fig. 16-3 are

$$G(s) = \frac{K_a}{J s^2 + c_\theta s} \quad \text{and} \quad H(s) = \frac{K_\theta}{\tau_L s + 1} \quad (17-1)$$

The closed-loop transfer function is $CLTF(s) = G(s)/[1 + G(s)H(s)]$; the denominator of $CLTF(s)$ in this form for the system of Fig. 16-3 is

$$\begin{aligned} 1 + G(s)H(s) &= 1 + \frac{K_a}{J s^2 + c_\theta s} \times \frac{K_\theta}{\tau_L s + 1} = 1 + \frac{K_a K_\theta}{J} \frac{1/\tau_L}{s(s + c_\theta/J)(s + 1/\tau_L)} \\ &\equiv 1 + \Lambda \frac{\omega_b}{s(s + c_\theta/J)(s + \omega_b)} \equiv 1 + OLT(s) \end{aligned} \quad (17-2)$$

where $\Lambda \equiv K_a K_\theta / J$ is the control parameter, which we now call *gain*. We evaluate the stability of the closed-loop system as Λ ranges from 0 to $+\infty$. The system constants from Chapter 16 are $\omega_b \equiv 1/\tau_L = 300$ rad/sec and $c_\theta/J = 100$ sec $^{-1}$. In Section 16-5, we solved the characteristic equation of the closed-loop system, $1 + G(s)H(s) = 0$.¹ We know from the loci of roots calculated for this system that, with gain Λ positive and increasing, there is a particular value of Λ for which the oscillatory loci of roots intersect the $\text{Im}[s]$ axis; for this value of Λ , the oscillatory time response is purely sinusoidal and periodic, without any exponential envelope. Let's define that intersection as the point of oscillatory *neutral stability* and denote the value of Λ there as Λ_{ns} (the same as Λ_{ub} in Section 16-5). Accordingly, let's denote the oscillatory frequency at that point as ω_{ns} (the same as ω_d in Section 16-5). We determined in Chapter 16 that $\Lambda_{ns} = (c_\theta/J) \times (c_\theta/J + \omega_b) = 40,000$ sec $^{-2}$ and $\omega_{ns} = \sqrt{(c_\theta/J)\omega_b} = 173.2$ rad/sec, and that the closed-loop system is exponentially stable for $0 < \Lambda < \Lambda_{ns}$, but unstable for $\Lambda > \Lambda_{ns}$.

The loci of roots are defined by the characteristic equation:

$$1 + G(s)H(s) \equiv 1 + OLT(s) = 0 \quad (17-3)$$

Therefore, at the point of neutral stability, with $\Lambda = \Lambda_{ns}$ and $s = j\omega_{ns}$, we have

$$1 + OLT(j\omega_{ns}) = 0 \Rightarrow OLT(j\omega_{ns}) = -1 = 1 \times \exp[j(\pm\pi, \pm 3\pi, \dots)]$$

$$OLT(j\omega_{ns}) = |OLT(j\omega_{ns})| \exp[j\angle OLT(j\omega_{ns})] = 1 \times \exp[j(\pm\pi, \pm 3\pi, \dots)]$$

Equating magnitude ratios and phase angles in the last equation gives for $\Lambda = \Lambda_{ns}$:

$$|OLT(j\omega_{ns})| = 1 \quad \text{and} \quad \angle OLT(j\omega_{ns}) = (\pm\pi, \pm 3\pi, \dots) \quad (17-4)$$

Equations (17-4) correspond physically, for $\omega = \omega_{ns}$, to the frequency-response test depicted in Fig. 17-1 (a modification of Fig. 16-2) on the next page. For steady-state

¹ We use the Laplace complex variable s in this chapter because it is traditional for treatment of frequency-response theory to use s , instead of complex variable p (for $s = p$, a solution of the characteristic equation, *i.e.*, a pole of the closed-loop transfer function) that we used in Sections 16-3 through 16-6.

sinusoidal electrical-signal excitation $e_{in}(t) = E_{in} \sin \omega_{ns} t$ of the open-loop system at the neutral-stability frequency of the closed-loop system, $\omega = \omega_{ns}$, the magnitude ratio of the open-loop frequency response is exactly 1 and the output electrical signal is exactly out of phase with the input signal, meaning $e_{out}(t) = -E_{in} \sin \omega_{ns} t$.

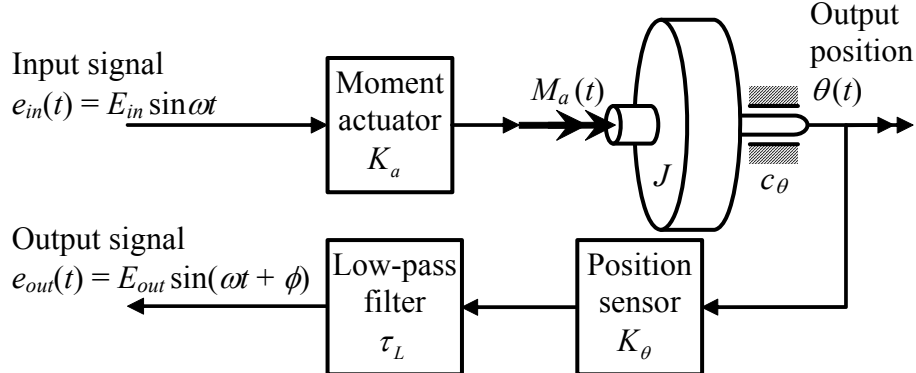


Figure 17-1 Functional diagram of frequency-response testing of the open-loop portion of Figs. 16-2 and 16-3

The observation that, for $\Lambda = \Lambda_{ns}$, output $e_{out}(t) = -E_{in} \sin \omega_{ns} t$ in response to input $e_{in}(t) = E_{in} \sin \omega_{ns} t$ provides motivation for conducting steady-state-sinusoidal tests on the open-loop system over a band of frequencies surrounding ω_{ns} , not just ω_{ns} , and for other values of Λ , not just Λ_{ns} , in order determine if this type of testing provides information regarding the stability of the closed-loop system. We can simulate such a test by evaluating numerically the open-loop frequency-response function, from Eq. (17-2):

$$OLFRF(\omega) \equiv OLT(\omega) = \Lambda \frac{\omega_b}{j\omega(j\omega + c_\theta/J)(j\omega + \omega_b)} \quad (17-5)$$

To begin, in order to establish a reference set of results for the neutral-stability value of gain, $\Lambda = \Lambda_{ns}$, we calculate and plot from Eq. (17-5) frequency-response components using the following MATLAB code:

```

>> wb=300;coj=100;wns=sqrt(wb*coj);
>> wbar=logspace(-1,1,100);w=wbar*wns;
>> lm=4e4;olfrf4e4=lm*wb./(j*w.* (j*w+coj).* (j*w+wb));
>> subplot(2,1,1),loglog(wbar,abs(olfrf4e4)),grid
>> faz=atan(imag(olfrf4e4)./real(olfrf4e4))-pi*ones(1,length(w));
>> subplot(2,1,2),semilogx(wbar,faz*180/pi),grid

```

Figure 17-2 (next page) includes the graphical results from these MATLAB operations. For now, we focus on just the plots of the polar components, magnitude ratio and phase angle, for $\Lambda = \Lambda_{ns} = 40,000 \text{ sec}^{-2}$; the additional annotations on the phase plot for “PM” at other values of Λ will be explained in due course. If we were testing the real hardware of Fig. 17-1, rather than just numerically simulating a test, then the magnitude ratio would be the measured quantity E_{out}/E_{in} as frequency ω is varied, and the phase angle ϕ would be calculated from measurements by the method presented in Section 4-4.

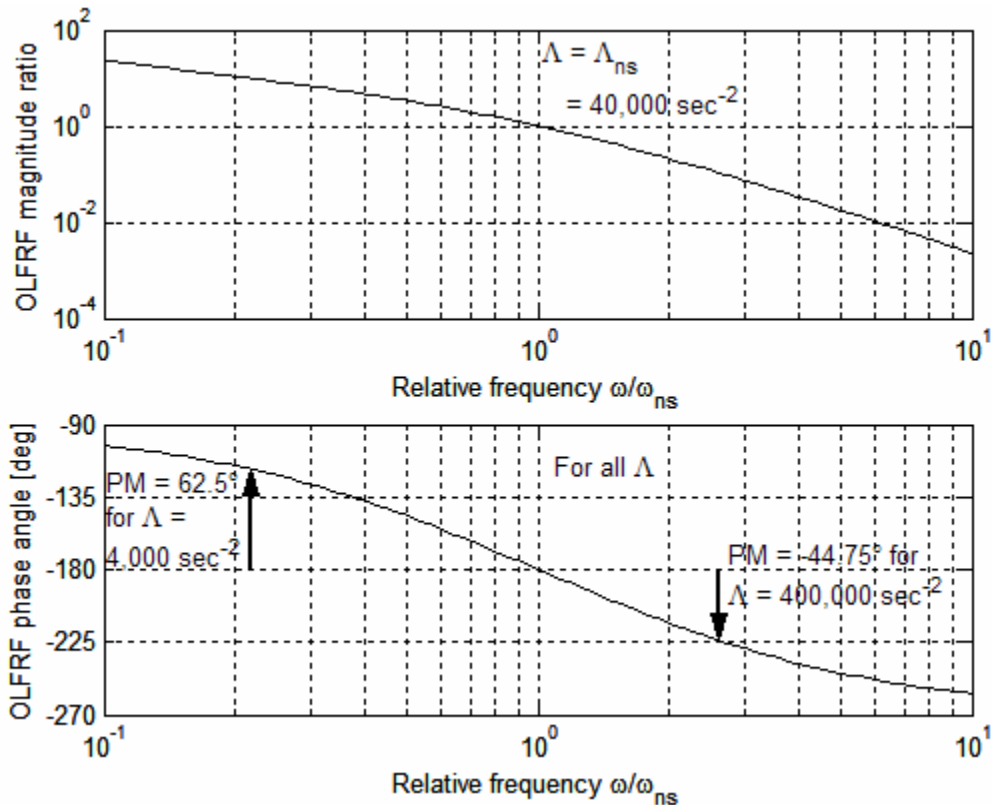


Figure 17-2 Modified Bode diagram, Eq. (17-5), frequency response for $\Lambda = \Lambda_{ns} = 40,000 \text{ sec}^{-2}$ of the open-loop system in Fig. 17-1

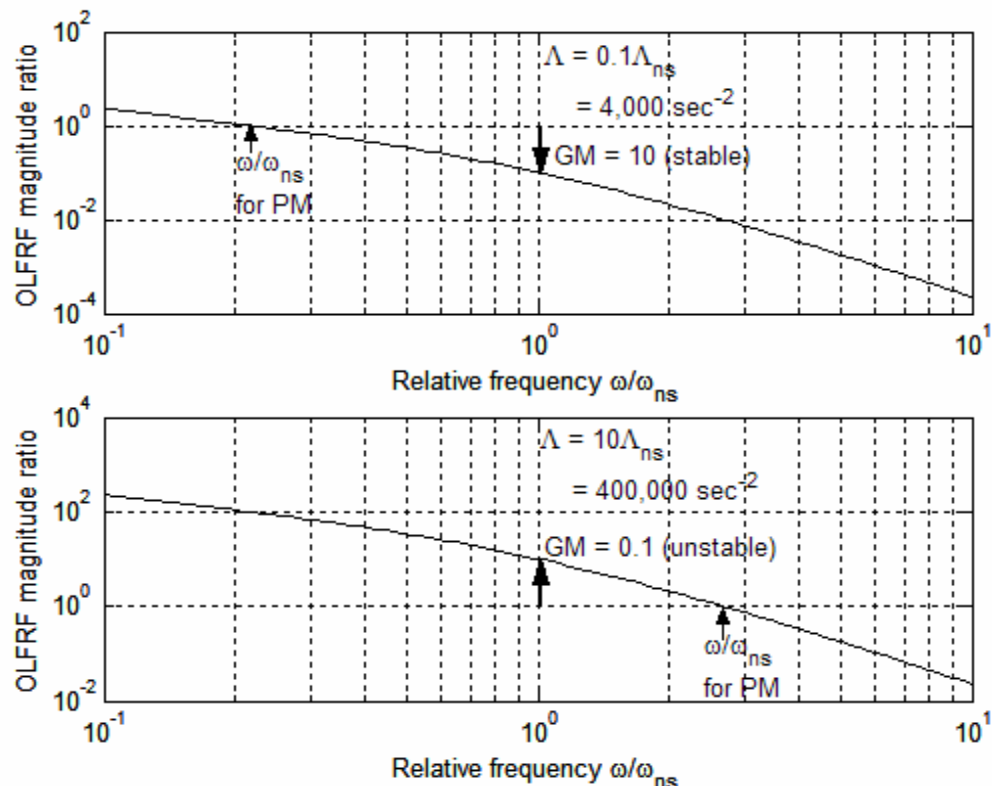


Figure 17-3 Magnitude ratios, Eq. (17-5) for $\Lambda = 4,000$ and $400,000 \text{ sec}^{-2}$

The upper plot of Fig. 17-2 shows that, for $\Lambda = \Lambda_{ns}$, magnitude ratio $|OLFRF|$ varies smoothly from greater than 10 at $\omega = 0.1\omega_{ns}$, through the previously determined value of 1 at $\omega = \omega_{ns}$, down to less than 0.01 at $\omega = 10\omega_{ns}$. The lower plot shows that phase angle $\angle OLFRF$ is a lag ranging from more than -90° at $\omega = 0.1\omega_{ns}$, through the previously determined phase of -180° at $\omega = \omega_{ns}$, down to a lag approaching -270° at $\omega = 10\omega_{ns}$. We have from Eq. 17-4 for $\Lambda = \Lambda_{ns}$, $\angle OLFRF(\omega_{ns}) = (\pm\pi, \pm 3\pi, \dots)$, which is ambiguous regarding the multiple and sign of π that is appropriate; the phase plot of Fig. 17-2 removes the ambiguity, at least for this system: clearly, $\angle OLFRF(\omega_{ns}) = -\pi$ rad.²

With Fig. 17-2 for $\Lambda = \Lambda_{ns}$ as the reference open-loop frequency response representing the neutrally stable closed-loop system, we can now compute simulated open-loop frequency responses for other values of Λ , specifically, those for which the closed-loop system is oscillatory and either exponentially stable or unstable. With the following MATLAB code, we calculate and plot on Fig. 17-3 (on the previous page) the magnitude-ratio (only) frequency-response graphs for the gain $\Lambda = 0.1\Lambda_{ns} = 4,000 \text{ sec}^{-2}$, for which we know the closed-loop system is stable, and for the gain $\Lambda = 10\Lambda_{ns} = 400,000 \text{ sec}^{-2}$, for which we know the closed-loop system is unstable:

```
>> wb=300;coj=100;wd=sqrt(wb*coj);
>> wbar=logspace(-1,1,100);w=wbar*wd;
>> lm=4e3;olfrf4e3=lm*wb./(j*w.*(j*w+coj).* (j*w+wb));
>> lm=4e5;olfrf4e5=lm*wb./(j*w.*(j*w+coj).* (j*w+wb));
>> subplot(2,1,1),loglog(wbar,abs(olfrf4e3)),grid
>> subplot(2,1,2),loglog(wbar,abs(olfrf4e5)),grid
```

If we were to calculate the phase angles for any value of Λ , we would find them to be identical to those on the phase-angle graph for $\Lambda = \Lambda_{ns}$ of Fig. 17-2, which is the reason for not repeating the phase-angle calculations. (The theory behind this feature of open-loop phase angle, and also the variation of open-loop magnitude for different values of Λ , will be presented at the end of this section.)

By comparing the open-loop magnitude-ratio graphs of Figs. 17-2 and 17-3, we observe the magnitudes for the closed-loop stable case $\Lambda = 0.1\Lambda_{ns}$ to be less than those for neutral stability, $\Lambda = \Lambda_{ns}$, and the magnitudes for the unstable case $\Lambda = 10\Lambda_{ns}$ to be greater. We conclude from this that open-loop magnitudes less than or greater than those for neutral stability are an indication of closed-loop absolute stability. If we were to calculate the open-loop magnitude ratios for other values between $0.1\Lambda_{ns}$ and $10\Lambda_{ns}$, we

² The line of MATLAB code that calculates phase requires the angles to be between $-\pi/2$ and $-3\pi/2$ rad, so the argument here appears to be circular. However, if we were to use the more general MATLAB function `angle` in place of that line of code, we would find, in the range of $0.1 \leq \omega/\omega_{ns} < 1.0$, exactly the same lagging phases as are on the phase plot of Fig. 17-2, which does validate the assertion that the appropriate value is $-\pi$ rad. We did not use `angle`, because it is apparently based upon MATLAB's four-quadrant inverse tangent function `atan2`, which returns angle values only between $-\pi$ and $+\pi$ rad. Therefore, on the graph of phase versus ω/ω_{ns} , `angle` would produce an artificial and confusing discontinuous jump in phase from -180° to $+180^\circ$ at $\omega/\omega_{ns} = 1.0$ and, in the range of $1.0 \leq \omega/\omega_{ns} \leq 10$, phase would drop from $+180^\circ$ to a little more than $+90^\circ$.

would find that the variation is monotonic and regular; this suggests that open-loop magnitude can also provide a metric for closed-loop relative stability, *i.e.*, the degree of stability or instability. Indeed, there is a commonly accepted metric called *gain margin* (GM); if we denote the gain margin for a particular value of Λ as $GM(\Lambda)$, then it is defined as the following dimensionless ratio of open-loop magnitudes:

$$GM(\Lambda) \equiv \frac{\left|OLFRF(\omega_{ns})\right|_{\Lambda_{ns}} \text{ at } \angle OLFRF(\omega_{ns})|_{\Lambda_{ns}} = -180^\circ}{\left|OLFRF(\omega)\right|_{\Lambda} \text{ at } \angle OLFRF(\omega)|_{\Lambda} = -180^\circ} \quad (17-6)$$

$$= \frac{1}{\left|OLFRF(\omega)\right|_{\Lambda} \text{ at } \angle OLFRF(\omega)|_{\Lambda} = -180^\circ}$$

In the second form of Eq. (17-6), which is the working definition, we applied the unit magnitude value derived in Eq. (17-4). The condition $\angle OLFRF(\omega)|_{\Lambda} = -180^\circ$ is called, descriptively, a *phase crossover*.

Applying Eq. (17-6) to Figs. 17-2 and 17-3, we calculate these gain margins: $GM(0.1\Lambda_{ns}) = 10$ for the closed-loop stable system; and $GM(10\Lambda_{ns}) = 0.1$ for the unstable system. Clearly, $GM > 1$ implies closed-loop stability and $0 < GM < 1$ implies instability. Expressing GM in terms of its logarithm to the base 10 (denoted “log”) is also of value, since in this form GM is positive for closed-loop stability, zero for neutral stability, and negative for instability. It is traditional in control-system engineering to express GM in *decibels* (dB), in which unit the value of a positive number N is $20 \times \log N$ dB. Accordingly, $GM(0.1\Lambda_{ns}) = +20$ dB for the closed-loop stable case of Fig. 17-3, and $GM(10\Lambda_{ns}) = -20$ dB for the unstable case.

Another open-loop frequency-response metric for closed-loop degree of stability is the *phase margin* (PM). The phase margin for a given value Λ of the control parameter is defined as the lag angle at the frequency for which the magnitude ratio is unity **relative to** the comparable lag angle for the neutral-stability case, $\Lambda = \Lambda_{ns}$:

$$PM(\Lambda) = (\angle OLFRF(\omega)|_{\Lambda} \text{ at } \left|OLFRF(\omega)\right|_{\Lambda} = 1) - (\angle OLFRF(\omega_{ns})|_{\Lambda_{ns}} \text{ at } \left|OLFRF(\omega_{ns})\right|_{\Lambda_{ns}} = 1)$$

From Eq. (17-4) and the phase plot of Fig. 17-2, the reference lag angle is just -180° , so

$$PM(\Lambda) = 180^\circ + (\angle OLFRF(\omega)|_{\Lambda} \text{ at } \left|OLFRF(\omega)\right|_{\Lambda} = 1) \quad (17-7)$$

The condition $\left|OLFRF(\omega)\right|_{\Lambda} = 1$ is called a *gain crossover*. Reading approximately the appropriate phases from the phase plot of Fig. 17-2, we calculate these phase margins: $PM(0.1\Lambda_{ns}) \approx 180^\circ - 120^\circ = +60^\circ$ for the closed-loop stable system, and $PM(10\Lambda_{ns}) \approx 180^\circ - 225^\circ = -45^\circ$ for the unstable system. (See homework Problem 17.2(a) for calculation of the more precise values of PM annotated on Fig. 17-2.) Clearly, $PM > 0^\circ$ implies closed-loop stability and $PM < 0^\circ$ implies instability.

Brogan, 1974, page 25, described succinctly the practical interpretation of these stability margins for an initially stable closed-loop system: “*Gain margin* GM is a measure of additional gain a system can tolerate with no change in phase, while remaining stable. *Phase margin* PM is the additional phase shift that can be tolerated, with no gain change, while remaining stable.”

We have defined and illustrated gain and phase margins for stable and unstable feedback control using the physical system of Figs. 16-2, 16-3, and 17-1. The behavior of this physical system is fairly “common” in the sense that it is stable for gain $\Lambda = 0$ and for low positive values of Λ , but it is unstable for all values of Λ greater than a particular neutral-stability value, Λ_{ns} . For any such common physical system, the open-loop frequency-response metrics of gain margin and phase margin described in this section are valid measures of absolute and relative stability. However, for “uncommon” physical systems, gain margins and phase margins of open-loop frequency response can be ambiguous and difficult to interpret; for example, such an uncommon system might have $PM = +78^\circ$ but $GM = -10$ dB, yet still be closed-loop stable. For such uncommon systems, a more general and involved, but unambiguous, approach to frequency-response analysis is based on the Nyquist stability criterion, which is the subject of Section 17-3.

Now that we know how to calculate open-loop frequency responses in the format of Figs. 17-2 and 17-3 using standard MATLAB commands, it is appropriate that we not have to do so for every problem, but, instead, that we can apply the built-in MATLAB functions `margin` and `bode` to produce more easily the same results. Before calling one of these functions, it is necessary first to define with the `tf` command a MATLAB linear-time-invariant (LTI) transfer-function model. The following, for the gain $\Lambda = 10\Lambda_{ns}$ of the same system as that of Figs. 17-2 and 17-3, shows one of the many ways to do this, along with the MATLAB responses:

```
>> wb=300;coj=100;
>> s=tf('s')

Transfer function:
s

>> lm=4e5;oltf4e5=lm*wb/(s*(s+coj)*(s+wb))

Transfer function:
1.2e008
-----
s^3 + 400 s^2 + 30000 s

>> margin(oltf4e5)
```

This `margin` command produced the *Bode diagram* or *plot* of Fig. 17-4 (next page), which is annotated with the GM and PM for this case, $\Lambda = 10\Lambda_{ns}$, that of the unstable closed-loop system. (The `bode` function itself also produces the Bode diagram, but without calculating and printing the GM and PM.) Note that it was not necessary to specify the frequency band—MATLAB chose an appropriate band. By comparing Fig. 17-4 with

Figs. 17-2 and 17-3, you should observe some differences in format, which is why Fig. 17-2 is labeled a “modified” Bode diagram; but there are no differences in the essential content. A traditional Bode diagram such as Fig. 17.4 plots the frequency-response magnitude ratio (in decibels) versus frequency (in rad/sec or Hz), which is presented on a logarithmic scale in order to accommodate a very wide band.

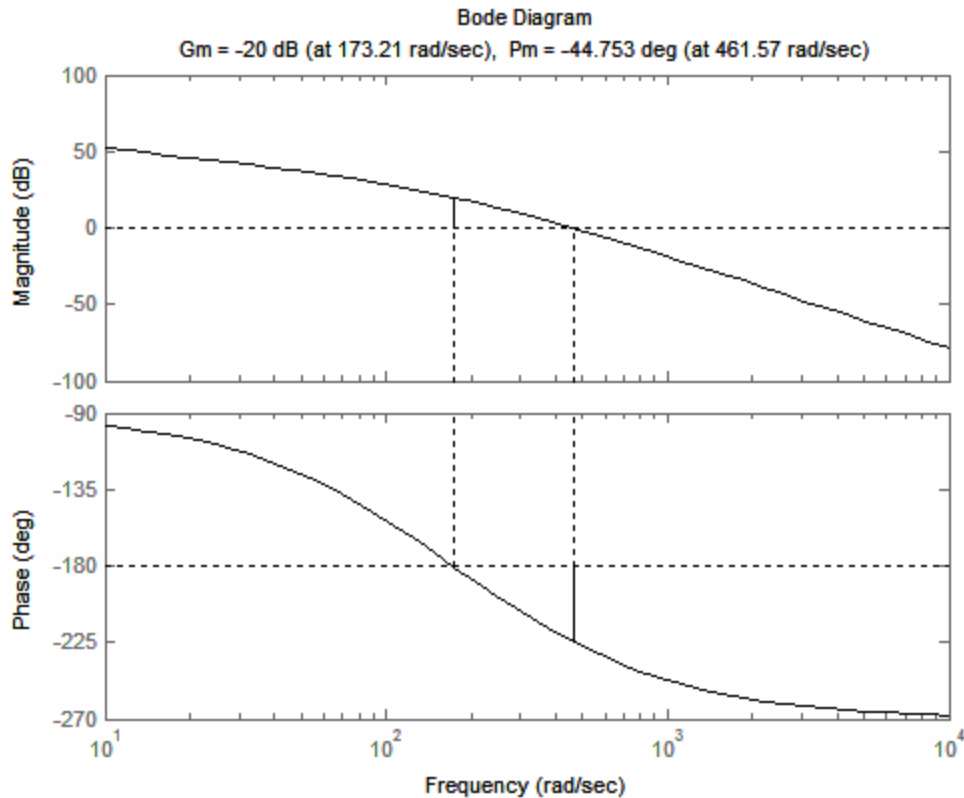


Figure 17-4 MATLAB’s traditional Bode diagram, Eq. (17-5), frequency response for $\Lambda = 10\Lambda_{ns} = 400,000 \text{ sec}^{-2}$ of the open-loop system in Fig. 17-1

To conclude this section, we consider for systems in general how changes in gain Λ influence open-loop frequency responses and their graphical representations on Bode diagrams (and Nyquist diagrams in Section 17-4). We infer from Eqs. (16-61) and (16-62) that an open-loop transfer function can generally be expressed in the form

$$OLTF(s) = \Lambda \times TF_1(s) \quad (17-8)$$

where the *baseline* transfer function $TF_1(s)$ is obviously defined as $OLTF(s)|_{\Lambda=1}$. The associated general frequency-response function is

$$OLFRF(\omega) = \Lambda \times TF_1(j\omega) = \Lambda \times |TF_1(j\omega)| \times \exp[j\angle TF_1(j\omega)] \quad (17-9)$$

Equation (17-9) leads to the following general forms for open-loop frequency-response magnitude ratio (MR) and phase angle ϕ :

$$MR(\omega) = |OLFRF(\omega)| = \Lambda \times |TF_1(j\omega)| \equiv \Lambda \times MR_1(\omega) \quad (17-10)$$

$$\phi(\omega) = \angle TF_1(j\omega) \quad (17-11)$$

Equation (17-11) shows that the variation of phase angle with frequency, $\phi(\omega)$, is the same for all values of gain Λ , as was stated earlier in the context of Figs. 17-2 and 17-3.

In the final form of Eq. (17-10), we define the baseline magnitude ratio (*i.e.*, for unity gain, $\Lambda = 1$) as $MR_1(\omega) \equiv |TF_1(j\omega)|$. It is also informative to express Eq. (17-10) in a logarithmic form, either in logarithm to base 10 as on Figs. 17-2 and 17-3, or in decibels as on a traditional Bode plot such as Fig. 17-4:

$$\log(MR(\omega)) = \log(\Lambda) + \log(MR_1(\omega)) \quad (17-12a)$$

$$20 \times \log(MR(\omega)) \equiv [MR(\omega)](\text{dB}) = [\Lambda](\text{dB}) + [MR_1(\omega)](\text{dB}) \quad (17-12b)$$

We infer from Eqs. (17-10) and (17-12) that the graphical shape of the functional variation with frequency of magnitude ratio $MR(\omega)$ does not change with changes in gain Λ . For modified Bode plots such as Fig. 17-2 and 17-3, given the baseline curve $MR_1(\omega)$, we can find from Eq. (17-12a) the curve for any other gain $\Lambda > 1$ just by adding to the baseline curve the value $\log(\Lambda)$, which moves the entire curve up by the distance $\log(\Lambda)$ along the magnitude-ratio axis. The process of finding curves for different gains Λ from Eq. (17-12b) is easy for a traditional Bode plot such as Fig. 17-4, on which magnitude is plotted in decibels with a linear scale. For example, we can find from Fig. 17-4 the magnitude curve for $\Lambda = 40,000 \text{ sec}^{-2}$ simply by moving downward by 20 dB, *i.e.*, by $20 \times [\log(40,000) - \log(400,000)]$, the magnitude curve for $\Lambda = 400,000 \text{ sec}^{-2}$.

17-2 Nyquist plots

We now depart temporarily from the analysis of stability in order to describe a type of frequency-response graphical representation that has not appeared previously in this book. Such a graph is commonly called, in the language of control-system engineering, a *Nyquist diagram* or *plot*.

We begin the description of Nyquist plots by re-visiting a familiar system from several previous chapters: the standard, positively damped 2nd order system. The ODE of this system for output $x(t)$ in response to input $u(t)$ is $\ddot{x} + 2\zeta\omega_n\dot{x} + \omega_n^2x = \omega_n^2u(t)$ [Eq. (9-13)], and the frequency-response function is

$$FRF(\omega) = \frac{\omega_n^2}{\omega_n^2 - \omega^2 + j2\zeta\omega_n\omega} \quad (10-7, \text{repeated})$$

The previous graphical representation of Eq. (10-7) in this book is Fig. 10-2, a modified Bode diagram displaying the variation with frequency ω of the polar components, magnitude ratio $|FRF(\omega)|$ and phase angle $\phi = \angle FRF(\omega)$. A Nyquist plot, in contrast, displays directly the mathematical rectangular components, in the format $\text{Im}[FRF(\omega)]$ versus $\text{Re}[FRF(\omega)]$, with frequency ω being the implicit independent variable, for which there is no graduated scale without extra annotation or a three-dimensional third axis perpendicular to the complex $FRF(\omega)$ -plane. For example, the following MATLAB commands produce Fig. 17-5, a Nyquist plot of Eq. (10-7) for undamped natural frequency $\omega_n = 2\pi$ rad/sec and damping ratio $\zeta = 0.2$:

```
>> wn=2*pi;zt=0.2;
>> w=wn*logspace(-2,2,400);
>> frf=wn^2./(wn^2-w.^2+j*2*zt*wn*w);
>> plot(real(frf),imag(frf)),grid
```

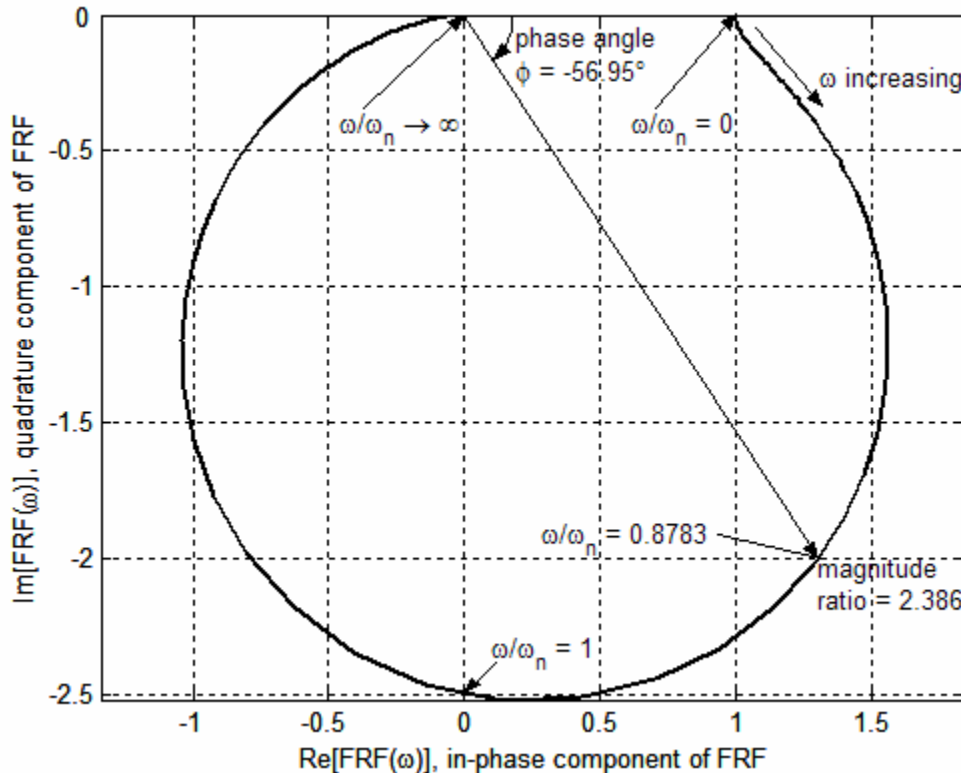


Figure 17-5 Nyquist plot of $FRF(\omega) = \omega_n^2/(\omega_n^2 - \omega^2 + j2\zeta\omega_n\omega)$ for $\omega_n = 2\pi$ rad/sec and $\zeta = 0.2$

Observe on Fig. 17-5 that the abscissa and ordinate axes are labeled both with the mathematical descriptions, $\text{Re}[FRF(\omega)]$ and $\text{Im}[FRF(\omega)]$, and with the corresponding physical descriptions of the response components, respectively: *in-phase* (0° , also known as *coincident*) and *quadrature* (leading by 90°). If you were measuring frequency response experimentally on a damped 2nd order system you might generate the physical information of Fig. 17-5 in the following manner: first, measure the polar components of

response, magnitude ratio $|FRF(\omega)|$ and phase angle $\phi(\omega) = \angle FRF(\omega)$, using the procedure described in Section 17-1 relative to Fig. 17-2, the modified Bode diagram; then, use Eq. (2-5) for converting complex numbers from polar form into rectangular form to calculate $FRF_{in-phase}(\omega) = |FRF(\omega)| \times \cos\phi(\omega)$ and $FRF_{quadrature}(\omega) = |FRF(\omega)| \times \sin\phi(\omega)$. An example of this conversion is illustrated on Fig. 17-5 for $\omega = 0.8783\omega_n$: $1.301 = 2.386 \times \cos(-56.95^\circ)$, and $-2.000 = 2.386 \times \sin(-56.95^\circ)$.

The concept of physical in-phase and quadrature frequency-response components might seem strange. Moreover, their values can be either positive or negative (as Fig. 17-5 shows for the in-phase component), and that might be confusing: if a pure “in-phase” response is negative, then the response is actually 180° out of phase with the excitation; and if a pure “quadrature” response is negative, then the response actually lags the excitation by 90° . In order to provide more clarity, even at the risk of being redundant, we present the following table, which lists multiple-of- 90° values of phase angle ϕ that correspond to particular values or ranges of the in-phase and quadrature components.

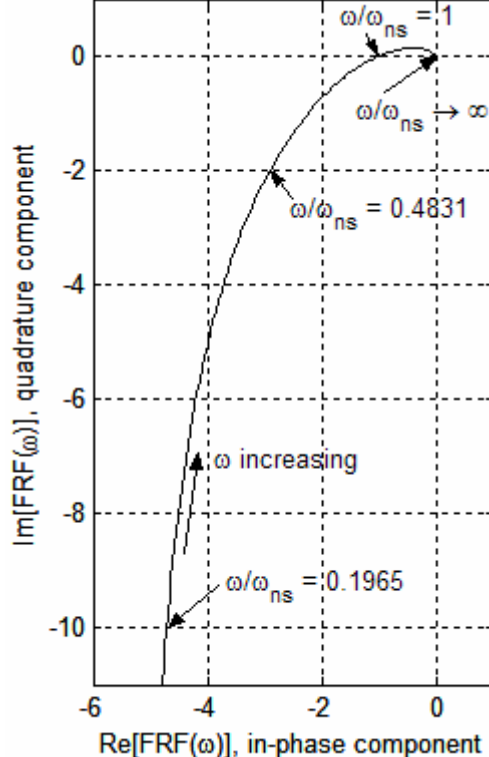
In-phase component	Quadrature component	Phase angle ϕ
> 0	$= 0$	0° and $\mp 360^\circ$
$= 0$	< 0	-90° and $+270^\circ$
< 0	$= 0$	$\mp 180^\circ$
$= 0$	> 0	-270° and $+90^\circ$

It might be instructive also to compare the Nyquist plot of Fig. 17-5 with the corresponding polar components for $\zeta = 0.2$ on the modified Bode plots of Fig. 10.2. On both figures for $\omega \approx 0$, the response is essentially the static value, $FRF(0) = +1 + j0$. As frequency ω increases from $0+$ to ω_n , the magnitude ratio varies (mostly increasing) from $+1$ to $1/(2\zeta) = 2.5$, while the phase angle, a lag, varies from 0° to -90° . At $\omega = \omega_n$, the response is pure negative quadrature, $FRF(\omega_n) = 0 - j2.5$. As ω increases above ω_n , the magnitude ratio decreases monotonically while the phase lags further, with the magnitude ratio approaching zero and the phase approaching -180° as $\omega \rightarrow \infty$.

Frequency response of the standard, positively damped 2nd order system is well behaved, especially for $\omega = 0$, *i.e.*, a non-zero input that is constant in time, for which the system has an unquestionably stable non-zero constant static output. Let’s consider now Nyquist plotting for a contrasting system, an open-loop system that lacks a stable static response, the system of Section 17-1 (also Sections 16-3, 16-5, and 16-6). The clearest indication of a possible difficulty is Eq. (17-5) for $OLFRF(\omega)$, which indicates an infinite response for $\omega = 0$. The mathematical source of this difficulty is the pole of $OLTF(s)$ at the s -plane origin, which is apparent in Eq. (17-2), Fig. 16-9, and elsewhere. The graphical display of frequency response magnitude becoming very large as $\omega \rightarrow 0$ is produced by the following MATLAB commands, which calculate frequency response and produce a Nyquist plot of the same numerical solution as that on Fig. 17-2, for the neutral-stability case $\Lambda = \Lambda_{ns} = 40,000 \text{ sec}^{-2}$:

```
>> wb=300;coj=100;wns=sqrt(wb*coj);
>> wbar=logspace(-1,1,200);w=wbar*wns;
>> lm=4e4;olfrf4e4=lm*wb./(j*w.*(j*w+coj).* (j*w+wb));
>> plot(real(olfrf4e4),imag(olfrf4e4)),grid
```

Figure 17-6 is an annotated portion of the MATLAB graph that displays the noteworthy features of the Nyquist plot. This plot shows that for frequency ω becoming progressively smaller, the negative quadrature component of response becomes progressively larger.



In fact, we can calculate from Eq. 17-5 the asymptotic nature of the variation of open-loop frequency response as $\omega \rightarrow 0$, by applying the method of complex rectangular division described in Section 2-1:

$$\begin{aligned} OLFRF(\omega) &= \frac{\Lambda\omega_b}{j\omega(j\omega + c_\theta/J)(j\omega + \omega_b)} \\ &= \frac{40,000 \times 300}{(j\omega)^3 - (100 + 300)\omega^2 + (100 \times 300)j\omega} \\ &= \frac{1.2 \times 10^7 \times [-400\omega^2 - j(3 \times 10^4\omega - \omega^3)]}{9 \times 10^8\omega^2 + 1 \times 10^5\omega^4 + \omega^6} \end{aligned}$$

Therefore, as $\omega \rightarrow 0$,

$$\begin{aligned} OLFRF(\omega) &\rightarrow \frac{1.2 \times 10^7 \times [-400\omega^2 - j(3 \times 10^4\omega)]}{9 \times 10^8\omega^2} \\ &= -5\cancel{j} - j\frac{400}{\omega} \end{aligned} \quad (17-13)$$

Figure 17-6 Nyquist plot, Eq. (17-5), frequency response for $\Lambda = \Lambda_{ns} = 40,000 \text{ sec}^{-2}$ of the open-loop system in Fig. 17-1, with parameters $\omega_b = 300 \text{ sec}^{-1}$, $c_\theta/J = 100 \text{ sec}^{-1}$, and $\omega_{ns} = \sqrt{(\omega_b \times c_\theta/J)} = 173.2 \text{ rad/sec}$

17-3 The practical effects of an open-loop transfer-function pole at $s = 0 + j0$

The development above demonstrates an important characteristic of an open-loop system with a transfer-function pole at the s -plane origin: frequency response of such a system increases in magnitude progressively as excitation frequency decreases, becoming, in theory, infinitely large for zero frequency. What is the significance of this type of response relative to experimental testing? The question is appropriate since, as asserted in the introduction to this chapter, frequency-response of the open-loop portion of a practical system (actual hardware) can indicate the stability or instability of the corresponding closed-loop system. Figure 17-6 and Eq. (17-13) show clearly that the frequency-response magnitude for very low frequencies of excitation could indeed be impractically

large. This might lead us to assume that, in order to avoid excessive output magnitudes, we would need only to excite the open-loop system at frequencies above some practical lower limit. The discussion in this section will show that this would be a potentially harmful assumption.

What is the nature of response associated with a system's transfer-function pole at the origin of the s -plane? We know that a pole on the $\text{Re}(s)$ axis in the right-half s -plane means the system's time response (to an impulse, for example) is essentially monotonically growing exponential, an instability. (See the discussion of Section 16-4.) Conversely, a pole on the $\text{Re}(s)$ axis in the left-half s -plane means the response is essentially monotonically decaying exponential, a stable response. Can we infer, then, that a pole on the $\text{Re}(s)$ axis at the origin, between the right- and left-half planes, means time response is neither unstable nor stable, but somehow neutral?

Let's try to answer that question, at least for the open-loop system of current interest that motivated this discussion, by deriving the unit-impulse response, $h(t)$. From Eq. (8-35), a system's transfer function is also the Laplace transform of its unit-impulse response; accordingly, Eq. (17-2) gives $L[h(t)] = \Lambda\omega_b/[s(s + c_\theta/J)(s + \omega_b)]$. We could find the complete equation for $h(t)$, but it is easier and equally relevant for this discussion to apply the final-value theorem [Eq. (15-15)] to find the steady-state response [which we can show follows the decay to zero of stable terms whose time functions are $e^{-(c_\theta/J)t}$ and $e^{-\omega_b t}$]: $\lim_{t \rightarrow \infty} h(t) = \lim_{s \rightarrow 0} s \times L[h(t)] = \Lambda J/c_\theta$. This constant-in-time response to an impulse excitation is unusual, since impulse response of a stable system normally decays to zero.

Let's probe further and find the response to a step input, which is a better gauge of stability than impulse response. Equation (8-40) shows that the unit-impulse response of any LTI-SISO system is the time derivative of the unit-step response, $h(t) = dx_H/dt$. Therefore, the unit-step response as $t \rightarrow \infty$ of the open-loop system of current interest must be $\lim_{t \rightarrow \infty} x_H(t) = C + (\Lambda J/c_\theta)t$, C being a constant. This linear-function-of-time response to a constant input can increase monotonically, without bound. This is not an exponential monotonic instability or exponential oscillatory instability of the type we have observed previously; nevertheless, for all practical purposes, it is a genuine form of instability.

We can be even more specific relative to frequency response. With reference to the functional diagram that depicts testing of the open-loop system, Fig. 17-1, suppose that the input signal, in addition to the sinusoidal excitation, has a slight constant voltage offset, E_{off} . (Even with high-pass filtering, it is often nearly impossible to eliminate all such offsets from real circuitry used in experimental testing.) Therefore, with $H(t)$ denoting the Heaviside unit-step function, the complete input signal is:

$$e_{in}(t) = E_{in} \sin \omega t + E_{off} H(t) \quad (17-14)$$

With use of $OLTF(s)$ of Eq. (17-2) and inverse Laplace transformation, we can find an algebraic equation for the response in time to input Eq. (17.14), assuming zero initial conditions. The full equation is quite lengthy. It includes transient-response terms whose time functions are $e^{-(c_\theta/J)t}$ and $e^{-\omega_b t}$, both of which decay quickly to insignificance. If we omit those transient-response terms, then we can express the “steady-state” response in the form (homework Problem 17.7):

$$e_{out}(t) = E_{in} \left(MR(\omega) \times \sin(\omega t + \phi(\omega)) + \frac{\Lambda}{\omega(c_\theta/J)} \right) + E_{off} \frac{\Lambda J}{c_\theta} \left[t - \frac{(c_\theta/J + \omega_b)}{(c_\theta/J)\omega_b} \right] \quad (17-15)$$

Open-loop frequency-response magnitude ratio $MR(\omega)$ and phase angle $\phi(\omega)$ are the quantities defined generally by Eqs. (17-10) and (17-11), respectively, and represented for this specific system, from Eq. (17-5), by the equations:

$$MR(\omega) = \left| \Lambda \frac{\omega_b}{j\omega(j\omega + c_\theta/J)(j\omega + \omega_b)} \right| \quad \text{and} \quad \phi(\omega) = \angle \left(\frac{\omega_b}{j\omega(j\omega + c_\theta/J)(j\omega + \omega_b)} \right)$$

Ideally in experimental sinusoidal testing, there would be only steady-state sinusoidal response. Much less ideally, however, there are in Eq. (17-15) three types of time response: the sinusoidal term, two constant-in-time terms, and a term that increases linearly with time. The constant-in-time terms would be a nuisance, but they could be tolerable, provided they were not so large as to overcome mechanical or electrical limits. However, the unstable linear “drift”, $E_{off}(\Lambda J/c_\theta)t$, would present a serious problem in the testing process. Consider, for example, the numerical solution of Eq. (17-15) for the open-loop system with the ideal frequency response of Figs. (17-2) and (17-6), and for excitation at the neutral-stability frequency, $\omega = \omega_{ns}$. For this case, Figs. (17-2) and (17-6) show that $MR(\omega_{ns}) = 1$ and $\phi(\omega_{ns}) = -180^\circ$. Completing the calculations in Eq. (17-15) with the remaining numerical values gives:

$$e_{out}(t) = E_{in} \left[(-\sin \omega_{ns} t + 2.309) + \frac{E_{off}}{E_{in}} (400t - 5\%) \right] \quad (17-16)$$

Equation (17-16) shows, for example, that if the offset voltage is even a mere 1% of the input sinusoidal magnitude, $E_{off}/E_{in} = 0.01$, then, after only one second of system response, the linear drift increases to four times the sinusoidal-response magnitude; and the linear drift just continues rising inexorably thereafter. Practical sinusoidal testing of this system would be possible only if the offset voltage were almost completely eliminated, in order to prevent, or at least minimize, this unstable drift.

The type of response represented in Eq. (17-15) and illustrated numerically in Eq. (17-16) would pose a formidable challenge for any type of standard experimental testing on any system whose mathematical model has a pole at the origin of the s -plane. This mathematical model represents a general physical deficiency of such a system: the absence of a passive mechanism that tends to restore the system toward a static equilibrium state after the system has been perturbed dynamically. For example, the damped-rotor

plant of our system of current interest, Figs. (16-3) and (17-1), is the prime contributor to the unstable drift; this plant lacks a restoring rotational spring, and so its transfer function, Eq. (16-39), $PTF(s) = 1/[s(J_s + c_\theta)]$, has a pole at the origin.

17-4 The Nyquist stability criterion

Section 17-1 describes how the stability margins of gain (GM) and phase (PM) are defined and displayed on Bode plots. It is informative and it will turn out to be even more general to extract the same stability margins from Nyquist plots of frequency response. To begin this study, we will repeat the Nyquist plot of Fig. 17-6, the closed-loop neutral-stability case, for which $\Lambda = \Lambda_{ns} = 40,000 \text{ sec}^{-2}$ and $\omega_{ns} = 100\sqrt{3} \text{ rad/sec}$, but over a narrower band of excitation frequencies, $100 \leq \omega \leq 1,000 \text{ rad/sec}$, or $1/\sqrt{3} \leq \omega/\omega_{ns} \leq 10/\sqrt{3}$; the intent here is to restrict our attention primarily to frequency response for which the phase lag exceeds about 150° , *i.e.*, for which the frequency-response curve in the OLFRF-plane is somewhat close to the negative real axis. Moreover, we will add to the same graph the Nyquist plots of frequency response for a case of positive closed-loop stability with $\Lambda = \frac{1}{2}\Lambda_{ns} = 20,000 \text{ sec}^{-2}$, and for a case of closed-loop instability with $\Lambda = 2\Lambda_{ns} = 80,000 \text{ sec}^{-2}$. The MATLAB commands follow that calculate [from Eqs. (17-5) and (17-9)] and plot these cases of open-loop frequency-response function, and the resulting Nyquist diagram (after additional editing):

```
>> wb=300;coj=100;w=logspace(2,3,200);
>> olfrf01=wb./(j*w.*(j*w+coj).* (j*w+wb));
>> olfrf20k=20e3*olfrf01;olfrf40k=40e3*olfrf01;olfrf80k=80e3*olfrf01;
>> plot(real(olfrf80k),imag(olfrf80k),real(olfrf40k),imag(olfrf40k),...
real(olfrf20k),imag(olfrf20k)),grid
```

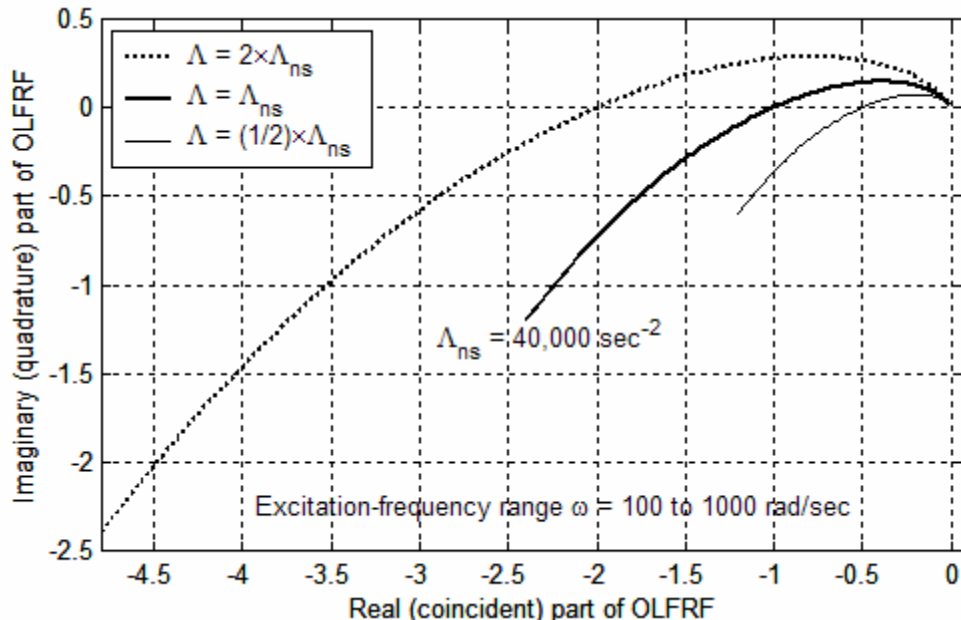


Figure 17-7 Nyquist plots of Eq. (17-5), open-loop frequency-response functions (OLFRF) for $\Lambda = (\frac{1}{2}, 1, \text{ and } 2) \times \Lambda_{ns}$ for the system in Fig. 17-1, with parameters $\omega_b = 300 \text{ sec}^{-1}$, $c_\theta/J = 100 \text{ sec}^{-1}$, and $\omega_{ns} = \sqrt{(\omega_b \times c_\theta/J)} = 173.2 \text{ rad/sec}$

Gain margin and phase margin are present and measurable on Nyquist plots such as those of Fig. 17-7. Gain margin (GM) is defined by Eq. (17-6), from which we find

$$\frac{1}{GM(\Lambda)} = \left| OLFRF(\omega) \right|_{\Lambda} \text{ at } \angle OLFRF(\omega)_{\Lambda} = -180^\circ \quad (17-17)$$

Equation (17-17) is illustrated on Fig. 17-8 for both closed-loop stable and unstable cases. Note that a closed-loop-stable case has $0 < 1/GM_S < 1$ so that $GM_S > 1$, and a closed-loop-unstable case has $1/GM_U > 1$ so that $0 < GM_U < 1$.

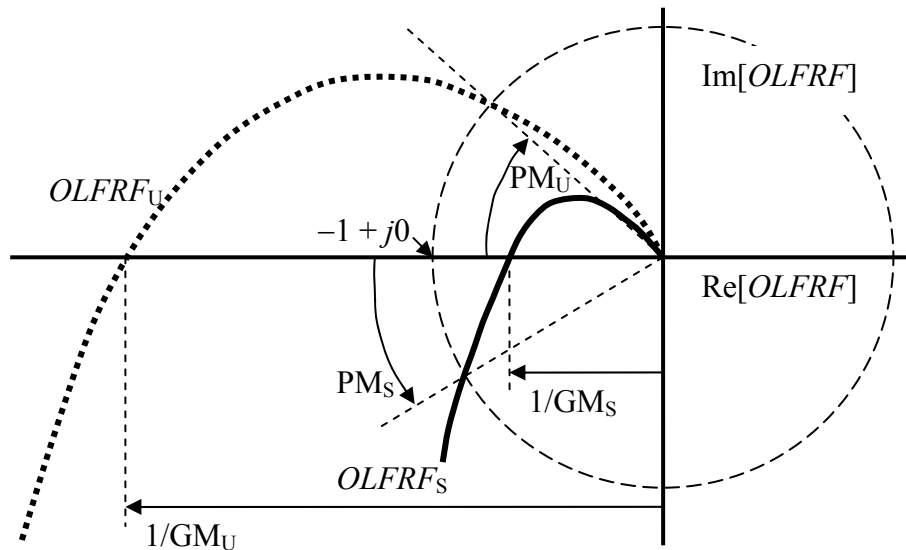


Figure 17-8 Schematic Nyquist plots of open-loop frequency-response functions ($OLFRF$) for closed-loop-stable and –unstable cases

We can measure phase margin directly by drawing on the Nyquist diagram a circle with radius of 1 unit and centered on the origin of the complex $OLFRF$ -plane, so that it passes through the important point $-1 + j0$. Phase margin is defined by

$$PM(\Lambda) = 180^\circ + (\angle OLFRF(\omega)_{\Lambda} \text{ at } |OLFRF(\omega)|_{\Lambda} = 1) \quad (17-7, \text{ repeated})$$

Phase margins are indicated graphically on Fig. 17-8. The positive PM_S for a closed-loop-stable case is the counterclockwise angle from the negative $\text{Re}[OLFRF]$ axis to the intersection of the unit circle with the $OLFRF_S$ curve; conversely, the negative PM_U for a closed-loop-unstable case is the clockwise angle from the negative $\text{Re}[OLFRF]$ axis to the intersection of the unit circle with the $OLFRF_U$ curve.

Note on Fig. 17-8 that the phase-crossover point (phase angle $\phi = -180^\circ$) and the gain-crossover point (magnitude ratio $MR = 1$) of an FRF are clearly evident on a Nyquist plot, perhaps even more naturally than on a Bode diagram. On the other hand, a Bode diagram displays the phase-crossover and gain-crossover frequencies, which are not explicit on a traditional Nyquist plot.

With a little imagination, we infer from the Nyquist plots of Fig. 17-7 that the open-loop system represented in that figure has $GM > 0$ and $PM > 0$ for $0 < \Lambda < \Lambda_{ns}$, and that $GM < 0$ and $PM < 0$ for all values of gain Λ greater than Λ_{ns} ; accordingly, the associated closed-loop system is stable for $0 < \Lambda < \Lambda_{ns}$, and unstable for all values of gain Λ greater than Λ_{ns} . Thus, this physical system (of Figs. 16-2, 16-3, and 17-1) is considered a “common” system, for which gain margin and phase margin provide clear and unambiguous metrics of stability. Let’s consider next an “uncommon” system, for which the determination of stability or instability requires a more detailed examination of the stability margins. Suppose that the open-loop transfer function of a system is³

$$G(s) \times H(s) \equiv OLT(s) = \Lambda \frac{s^2 + 4s + 104}{(s+1)(s^2 + 2s + 26)} = \Lambda \frac{s^2 + 4s + 104}{s^3 + 3s^2 + 28s + 26} \quad (17-18)$$

You should be able to show that the zeros of this transfer function in the complex s -plane are at $(-2 \pm j10)$, and the poles are at $(-1 + j0)$ and $(-1 \pm j5)$.

In order to establish the reference for stability and instability of the closed-loop system corresponding to Eq. (17-18), we determine the loci of roots from the characteristic equation, $1 + GH = 0$, or

$$s^3 + 3s^2 + 28s + 26 + \Lambda(s^2 + 4s + 104) = s^3 + (3 + \Lambda)s^2 + 4(7 + \Lambda)s + 26(1 + 4\Lambda) = 0 \quad (17-19)$$

The following MATLAB commands, adapted from the code that produced Fig. (16-7), calculate and plot the loci of roots:

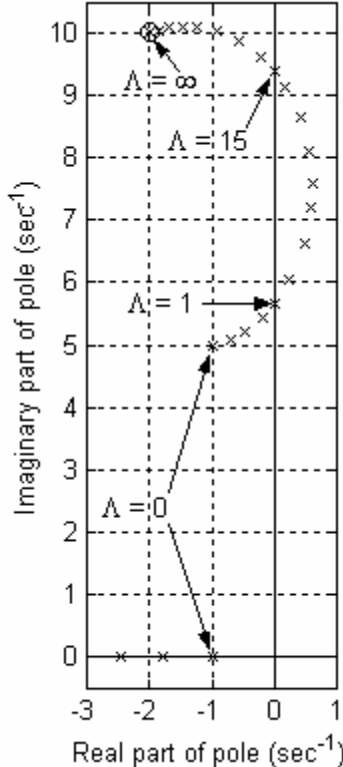
```
Lm=[0 .2 .4 .7 1 1.5 2.5 3.7 4.75 6.5 9 12.5 15 18.5 25 35 50 70 125 250];
Np=length(Lm);
for i=1:Np;
    a2=3+Lm(i);a3=4*(7+Lm(i));a4=26*(1+4*Lm(i));
    p(i,1:3)=roots([1 a2 a3 a4]).';
end
plot(p,'kx'),grid,xlabel('Real part of pole (sec^-^1)')
ylabel('Imaginary part of pole (sec^-^1)')
```

The significant roots of Eq. (17-19) are shown on Fig. 17-9 (next page): the complete locus of oscillatory roots with positive imaginary parts is shown; only the beginning of the locus of real (exponentially stable) roots is shown, since those roots become progressively more negative as gain Λ increases from the initial small values. The oscillatory roots on Fig. 17-9 show that the closed-loop system is stable for $\Lambda = 0$ up to $\Lambda \approx 1$, it is unstable for $\Lambda \approx 1$ up to $\Lambda \approx 15$, and it becomes stable again for Λ greater than ≈ 15 . We regard this closed-loop system as being “uncommon” or unusual because it is stable for small and large values of gain Λ , but unstable for a range of intermediate values.

³ This transfer function was concocted for the purpose of demonstration. It does not represent any specific real physical system, but it has characteristics that are representative of some real systems. Gain Λ has physical units of sec^{-1} , but we will not bother to show units in the following discussion.

If we were to test experimentally the open-loop part of this system in order to determine the stability of the closed-loop system, what would the open-loop frequency responses be for different values of gain Λ ? To simulate that testing, we have from Eq. (17-18), the following equation for the frequency-response function:

$$OLFRF(\omega) \equiv OLTF(j\omega) = \Lambda \frac{104 - \omega^2 + 4 \times j\omega}{(1 + j\omega)(26 - \omega^2 + 2 \times j\omega)} \quad (17-20)$$



Let's begin this study by computing $OLFRF(\omega)$ and displaying it on Nyquist plots for a low value of gain, $\Lambda = 0.7$ (for which the closed-loop system is stable), and for the value corresponding to the transition from stability to instability on Fig. 17-9, which we denote as $\Lambda_{ns1} \approx 1$. The value of Λ_{ns1} is not exactly 1, as Fig. 17-9 might suggest; see homework Problem 17.2(b) for calculation of the more precise value $\Lambda_{ns1} = 0.96438$. The following MATLAB commands calculate and plot the two frequency responses and also, for determining phase margins as shown on Fig. 17-8, an arc of the unit circle centered on the origin of the complex $OLFRF(\omega)$ -plane.

```
>> w=3.4*logspace(0,2,500);
>> olfrf01=(104-w.^2+4*j*w)./((1+j*w).*(26-
w.^2+2*j*w));
>> olfrf007=0.7*olfrf01;
>> plot(real(olfrf007),imag(olfrf007)),grid
>> cirangrad=0.8*pi:0.01:1.2*pi;
>> hold,plot(cos(cirangrad),sin(cirangrad))
Current plot held
>> olfrfnsl=0.96438*olfrf01;
>> plot(real(olfrfnsl),imag(olfrfnsl))
```

Figure 17-9 Loci of roots of Eq. (17-19)

The portions of both Nyquist plots (for $\Lambda = 0.7$ and $\Lambda = \Lambda_{ns1}$) that are closest to the negative $\text{Re}[OLFRF]$ axis are shown on Fig. 17-10 (next page). Observe on Fig. 17-10 the small loops beneath the negative $\text{Re}[OLFRF]$ axis as driving frequency becomes very high: the frequency responses approach zero from below the origin of the complex $OLFRF$ -plane. This is distinctly different from the Nyquist plots of a more “common” open-loop system on Fig. 17-7, which approach the origin from above as frequency becomes very high. Another aspect of the difference between the plots on the two figures is particularly significant: whereas the plots on Fig. 17-7 cross the negative $\text{Re}[OLFRF]$ axis only once as driving frequency ω increases, those on Fig. 17-10 have two phase crossovers, *i.e.*, the phase angle is -180° for two different values of ω . Since on Fig. 17-10 there are two different frequencies at which $\angle OLFRF(\omega)|_\Lambda = -180^\circ$, the definition of gain margin in Eqs. (17-6) and (17-17) is ambiguous: at which, if either, of the phase

crossovers is it appropriate to read the quantity $1/GM$, as shown on Fig. 17-8? Which, if either, of the values calculated from that reading, $GM = (1/GM)^{-1}$ is a legitimate metric of closed-loop stability? Figure 17-10 includes the Nyquist plots for both $\Lambda = 0.7$ and $\Lambda = \Lambda_{ns1}$, the latter of which by definition crosses the negative $\text{Re}[OLFRF]$ axis at the point $-1 + j0$, not far to the left of where the $\Lambda = 0.7$ plot crosses at about $-0.73 + j0$; therefore, it might be that the appropriate value of gain margin for $\Lambda = 0.7$ is found from $1/GM_{0.7} \approx 0.73$, so that $GM_{0.7} \approx 1.37 = 2.7$ dB, a small gain margin indicating that the closed-loop system is just weakly stable. If, on the other hand, we were to calculate gain margin using the other phase crossing, at about $-0.04 + j0$, then that would lead to the exaggerated $GM \approx 25 = 28$ dB, which is obviously a defective metric of stability. Note that the phase margin for $\Lambda = 0.7$, found as shown on Fig. 17-8, is quite clear on Fig. 17-10 and not at all ambiguous like the gain margin: $PM_{0.7} \approx +20^\circ$; this value also indicates a stable, but weakly so, closed-loop system.

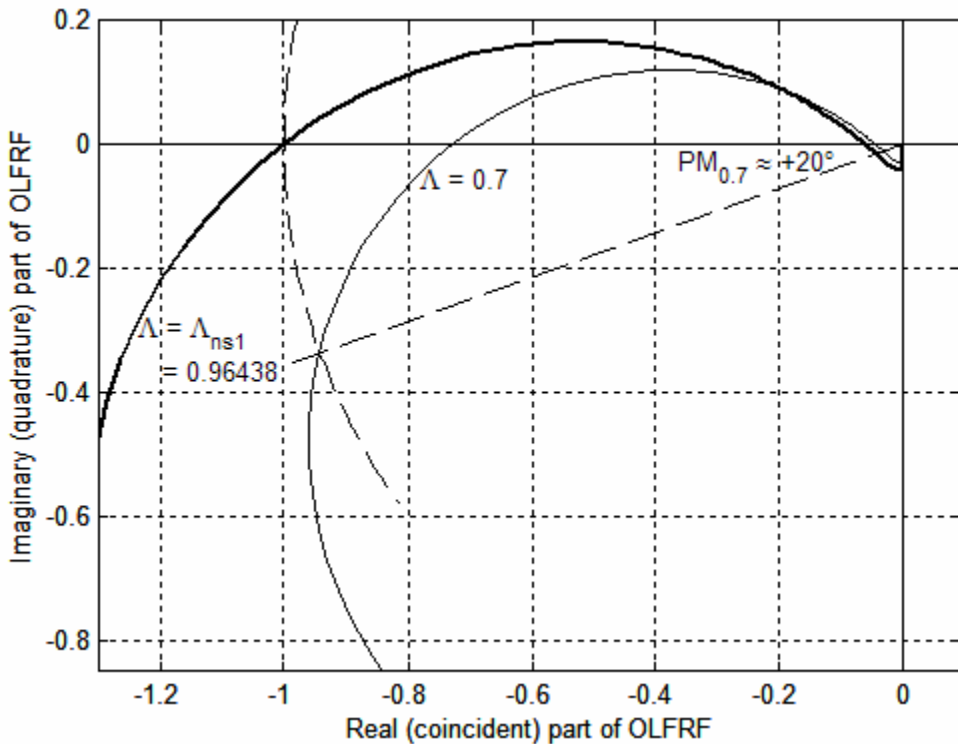


Figure 17-10 Nyquist plots, Eq. (17-20), open-loop frequency-response functions ($OLFRF$) for $\Lambda = 0.7$ and $\Lambda = \Lambda_{ns1} = 0.96438$ in the system of Eq. (17-18)

Let's continue this study by computing $OLFRF(\omega)$ and displaying it as a Nyquist plot for an intermediate value of gain, $\Lambda = 4.75$, for which Fig. 17-9 shows the closed-loop system is unstable. The following MATLAB commands calculate [from Eqs. (17-9) and (17-20)] and plot the frequency response and an arc of the unit circle centered at the origin of the complex $OLFRF(\omega)$ -plane.

```
w=3.4*logspace(0,2,500);
olfrf01=(104-w.^2+4*j*w)./( (1+j*w).* ( 26-w.^2+2*j*w));
>> olfrf0475=4.75*olfrf01;
```

```
>> plot(real(olfrf0475),imag(olfrf0475)),grid
>> cirangrad=0.8*pi:0.01:1.2*pi;
>> hold,plot(cos(cirangrad),sin(cirangrad))
```

The portion of the Nyquist plot for gain $\Lambda = 4.75$ that is closest to the negative $\text{Re}[OLFRF]$ axis is shown on Fig. 17-11. The $\Lambda = \Lambda_{ns1}$ plot of Fig. 17-10 is expanded radially outward on Fig. 17-11 by the factor of $4.75/0.96438 = 4.9254$, so the loop for high frequencies beneath the negative $\text{Re}[OLFRF]$ axis is more prominent than on Fig. 17-10. The frequency-response curve leading into that loop crosses the $\text{Re}[OLFRF]$ axis at about $-0.315 + j0$; if we were to use this phase crossover to calculate gain margin, then we would find $\text{GM} \approx 1/0.315 = 3.175 = 10.0 dB. Moreover, if we apply for this system with $\Lambda = 4.75$ the MATLAB `margin` command to generate a Bode diagram in the same form as Fig. 17-4, then MATLAB annotates that diagram with the values $\text{GM} = 10.007$ dB and $\text{PM} = -23.721^\circ$ (the same as $\text{PM}_{4.75}$ shown approximately on Fig. 17-11). We know from Fig. 17-9 that this case of $\Lambda = 4.75$ is closed-loop unstable. However, the positive gain margin 10 dB suggests positive stability. The negative phase margin indicates, to the contrary, instability. Clearly, the calculation $\text{GM} \approx 1/0.315$ is a defective metric of stability. The other phase crossover, at $-4.9254 + j0$ (beyond the range of Fig. 17-11), might be the appropriate point for calculation of gain margin, since it at least indicates instability, $\text{GM}_{4.75} = 1/4.9254 = 0.20303 = -13.85$ dB.$

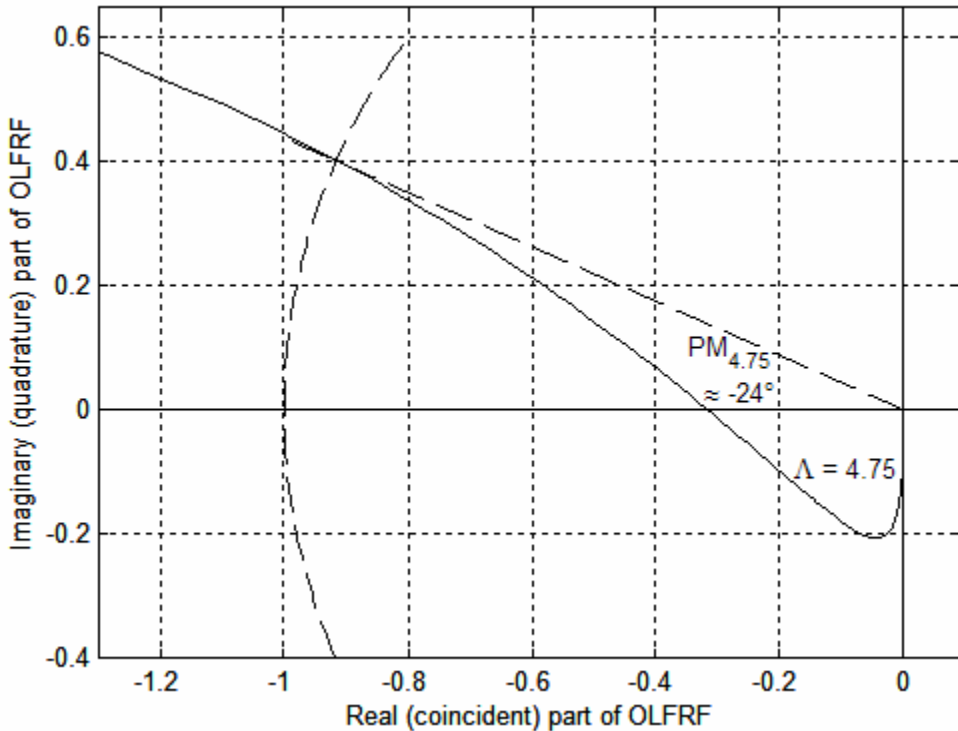


Figure 17-11 Nyquist plot, Eq. (17-20), open-loop frequency-response function ($OLFRF$) for $\Lambda = 4.75$ in the system of Eq. (17-18)

Let's complete this study by computing $OLFRF(\omega)$ and displaying it on Nyquist plots for the value corresponding to the transition from instability back to stability on Fig.

17-9, which we denote as $\Lambda_{ns2} \approx 15$, and for a slightly higher value, $\Lambda = 18.5$, for which the closed-loop system is stable. The value of Λ_{ns2} is not exactly 15, as Fig. 17-9 might suggest; see homework Problem 17.2(b) for calculation of the more precise value $\Lambda_{ns2} = 15.0356$. The portions of both Nyquist plots (for Λ_{ns2} and $\Lambda = 18.5$) that are closest to the negative $\text{Re}[OLFRF]$ axis are shown on Fig. 17-12, which was produced by the MATLAB commands that produced Fig. 17-10, except with gains 18.5 and Λ_{ns2} replacing, respectively, gains 0.7 and Λ_{ns1} .

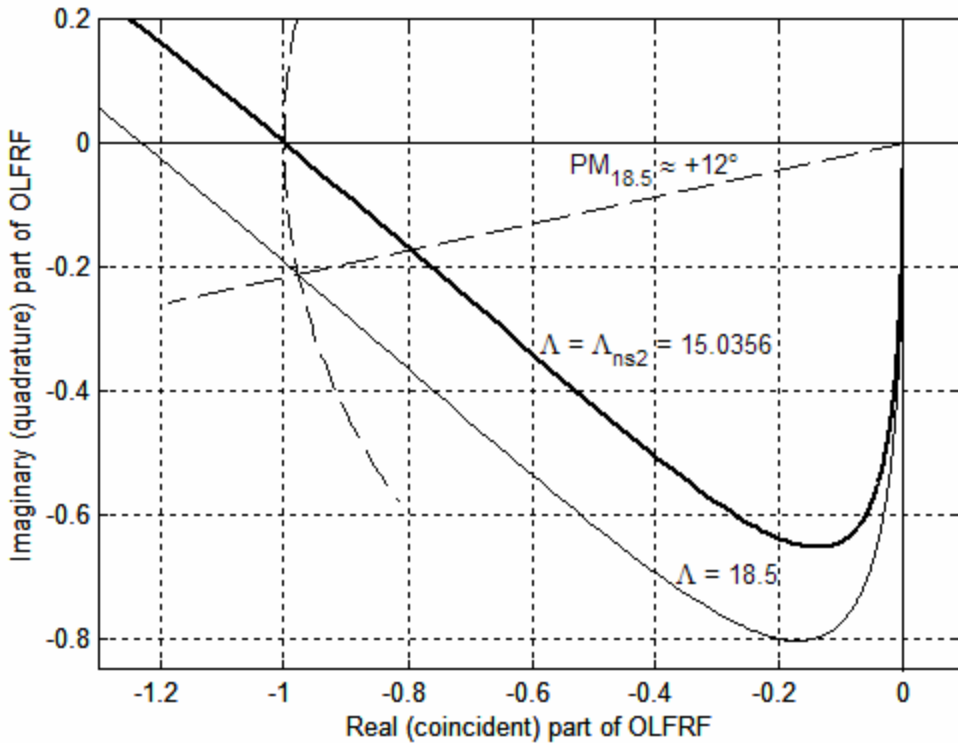


Figure 17-12 Nyquist plots, Eq. (17-20), open-loop frequency-response functions (*OLFRF*) for $\Lambda = \Lambda_{ns2} = 15.0356$ and $\Lambda = 18.5$ in the system of Eq. (17-18)

For gain $\Lambda = 18.5$, there are two phase crossovers: one evident on Fig. 17-12 at $-18.5/15.0356 + j0 = -1.230 + j0$, and the other way beyond the range of Fig. 17-12 at $-18.5/0.96438 + j0 = -19.18 + j0$. We know from Fig. 17-9 that the closed-loop system with $\Lambda = 18.5$ is stable, albeit weakly. However, the gain margin calculated from either of the two phase crossovers suggests instability, showing that both are deceptively defective metrics of stability. On the other hand, the phase margin shown on Fig. 17-12, $PM_{18.5} \approx +12^\circ$, correctly indicates weak stability.

We draw the following conclusions from the discussions above of Figs. 17-9 through 17-12, relative to an “uncommon” system with an open-loop transfer function such as Eq. (17-18): (1) gain margin as defined on Fig. 17-8 can be an ambiguous, unreliable, and even deceptive metric of closed-loop stability; (2) phase margin as defined on Fig. 17-8, on the other hand, is usually an unambiguous and reliable metric, with $PM > 0$ indicating closed-loop stability, and $PM < 0$ indicating closed-loop instability. Con-

clusion (2) regarding phase margin is a form of the *Nyquist stability criterion*, a form that is pertinent to systems such as that of Eq. (17-18); it is not the most general form of the criterion, but it suffices for the scope of this introductory textbook.

Proofs of the general Nyquist stability criterion are based on the theory of complex functions of a complex variable; many textbooks on control theory present such proofs, one of the clearest being that of Franklin, *et al.*, 1991, pages 261-280. This reference shows that the form of stability criterion described above [Conclusion (2)] is not sufficiently general to handle all cases that might arise. For example, the unusual case of an open-loop system that has unstable poles requires the general Nyquist stability criterion. However, the actual hardware of such an open-loop system could not be subjected to frequency-response experimental testing due to its unstable character, so a control-system engineer would find it necessary to analyze a mathematical model of the system. It is likely that the most reliable theoretical analysis of such a model for closed-loop stability would be by calculation of closed-loop loci of roots, not by calculation of open-loop frequency response. Another unusual case that would require the general Nyquist stability criterion is an open-loop system with more than one gain crossover, *i.e.*, a system whose frequency response curve intersects more than once the unit circle shown on Fig. 17-8, thus rendering ambiguous the definition of phase margin.

We conclude this chapter on frequency-response stability criteria by observing that margins of gain and phase are used also as engineering design goals. For example, Brogan, 1974, page 25, wrote “Experience has shown that acceptable transient response will usually require stability margins on the order of $PM > 30^\circ$, $GM > 6 \text{ dB}$.” Franklin, *et al.*, 1991, page 285, wrote “Many engineers think directly in terms of PM in judging whether a control system is adequately stabilized. In using PM this way, a phase margin of 30° is often judged to be the lowest acceptable PM, with values above 30° desirable.”

17-5 Homework problems for Chapter 17

17.1 The subject of this problem is frequency response of an RC band-pass filter circuit. The appropriate transfer function is Eq. (13-5):

$$TF_B(s) = \frac{L[e_o]}{L[e_i]} = \frac{\tau_H s}{(\tau_H s + 1)(\tau_L s + 1)} = \frac{\omega_L s}{(s + \omega_H)(s + \omega_L)}$$

in which $\omega_L \equiv 1/\tau_L$ is the low-pass break frequency and $\omega_H \equiv 1/\tau_H$ is the high-pass break frequency, and for band-pass functioning it is usually specified that $\omega_H \ll \omega_L$.

- (a) This transfer function has (in the s -plane) a zero at the origin and poles at $-\omega_H$ and $-\omega_L$. Consider the case for frequency response: $s = j\omega$, $\omega \geq 0$. Sketch a graph of the s -plane that shows the zero and the poles, and sketch on the graph three complex vectors with tails at the zero and the poles, and heads at an arbitrary point $s = j\omega$ on the positive imaginary axis. Use this graphical construction to derive the frequency-response function in the polar form $FRF(\omega) = MR(\omega) e^{j\phi(\omega)}$, in which you derive explicit formulas for magnitude ratio $MR(\omega)$ and phase angle $\phi(\omega)$. [NOTE: This graphical method of deriving (or calculating) a frequency-response function is somewhat similar to (but simpler than) Evans' general root-locus method described in Section 16-5, with the "locus" in this case being the positive imaginary axis—see, in particular, the unnumbered figure that directly follows Eq. (16-56).] *Partial answer:* $\phi(\omega) = \pi/2 - \tan^{-1}(\omega/\omega_H) - \tan^{-1}(\omega/\omega_L)$ radians
- (b) Let $\omega_H = 5$ rad/sec and $\omega_L = 500$ rad/sec. Adapt the MATLAB code that produced Fig. 17-2 to calculate and print a modified Bode diagram for this particular band-pass filter. Your diagram should show that signals at frequencies between about 10 and 200 rad/sec are passed through this filter with very little amplitude reduction and relatively little phase change, but that signals at frequencies below about 0.5 rad/sec and above about 5,000 rad/sec are effectively "filtered out", removed.

17.2 In these exercises, you will use MATLAB function M-files and the MATLAB command `fzero` to calculate some results that are stated but not explicitly derived in Chapter 17.

- (a) Calculate for at least one of the gains $\Lambda = 4,000 \text{ sec}^{-2}$ and $400,000 \text{ sec}^{-2}$ the more precise value of PM that is annotated on Fig. 17-2. The procedure is based on the definition of $PM(\Lambda)$ in Eq. (17-7), which shows that you need to find the frequency ω_{PM} at which $|OLFRF(\omega)|_\Lambda = 1$, i.e., the gain-crossover frequency. Accordingly, write a function M-file that uses Eq. (17-5) to compute the quantity $|OLFRF(\omega)|_\Lambda - 1$. Then calculate ω_{PM} by calling that function M-file with the `fzero` command, in which you also include an estimate for ω_{PM} that you read from Fig. 17-2. Finally, use Eq. (17-5) again to

calculate $\angle OLFRF(\omega)|_{\Lambda}$ for $\omega = \omega_{PM}$, and substitute that result into Eq. (17-7) to obtain the more precise value of $PM(\Lambda)$.

(b) Calculate for at least one of the neutral-stability points on Fig. 17-9 the more precise value of gain (Λ_{ns1} and/or Λ_{ns2}) that is stated in the text of Section 17-4. The procedure is based on setting to zero the real part of the appropriate root of the characteristic equation, Eq. (17-19). Accordingly, write a function M-file that first determines with the `root` command the three roots of Eq. (17-19), then uses MATLAB flow control features (perhaps a `for` loop containing an `if` loop, or some alternative of your choice) to select the one root of the three that has a positive imaginary part, and finally computes the real part of this root. Then calculate the required Λ_{ns} by calling that function M-file with the `fzero` command, in which you also include an estimate for the Λ_{ns} , which you read from Fig. 17-9. [See homework Problem 16.8(b) for a different method of solution.]

17.3 In this problem, re-visit the system of homework Problem 16.5: it is a damped rotor with position feedback that is 2nd order low-pass-filtered. Use the same component values: $\omega_b = 300$ rad/sec, $c_\theta/J = 100$ sec⁻¹, and $\gamma = 1/\sqrt{2}$. Also as before, denote the varying control-system gain parameter as $\Lambda \equiv K_a K_\theta / J$.

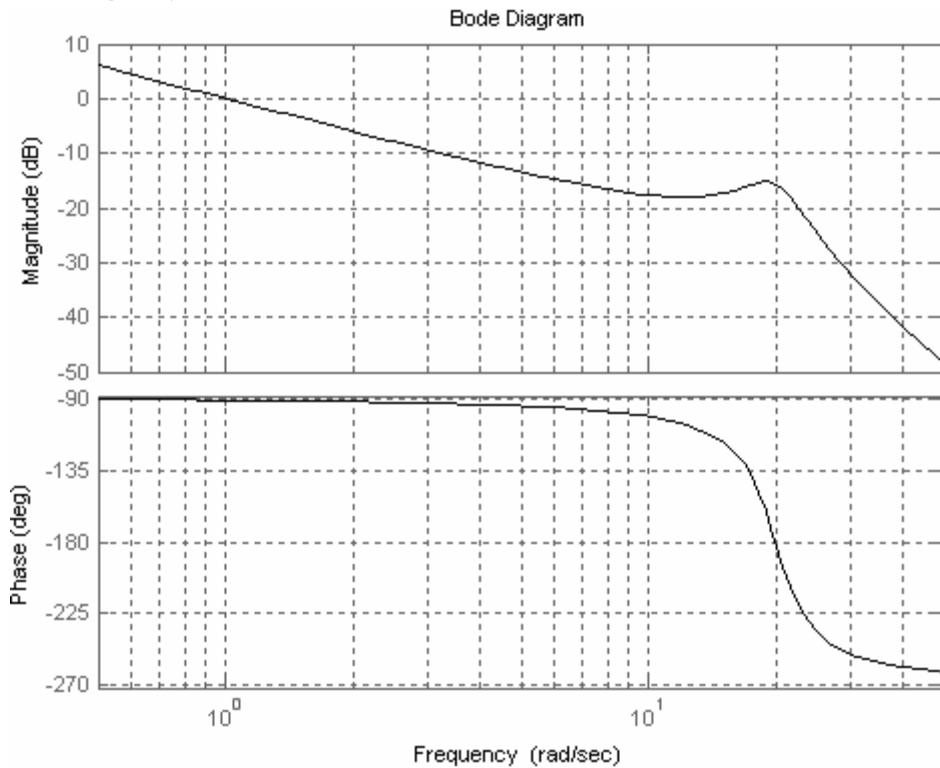
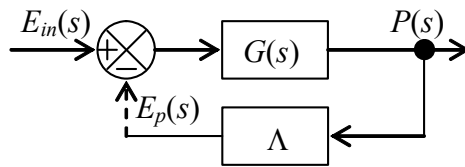
(a) Show that the open-loop transfer function is

$$OLTF(s) \equiv \frac{E_{out}(s)}{E_{in}(s)} = \Lambda \frac{\omega_b^2}{s(s + c_\theta/J)(s^2 + 2\gamma\omega_b s + \omega_b^2)}$$

(b) Homework Problem 16.5(b) showed the following by loci-of-roots analysis for the closed-loop system: (i) $\Lambda \equiv \Lambda_{ns} = 22,000$ sec⁻² is the neutral-stability gain, the upper limit of stability; and (ii) for $\Lambda = 3,400$ sec⁻², the system is stable, with the dominant mode being oscillatory and having damping ratio $\zeta \approx 1/\sqrt{2}$. Your task is to evaluate stability again for $\Lambda = 3,400$ sec⁻² and for $\Lambda = \Lambda_{ns}$, but now using frequency-response criteria. Define the excitation-frequency range of interest to be the band $10 \leq \omega \leq 1000$ rad/sec. First, use appropriate MATLAB commands to calculate the baseline open-loop frequency-response function, *i.e.*, $OLFRF(\omega)$ for $\Lambda = 1$ sec⁻². Now, use MATLAB to calculate and plot on some type (your choice) of Bode diagram the curves of magnitude ratio and phase angle over the defined frequency band, for both $\Lambda = 3,400$ sec⁻² and $\Lambda = \Lambda_{ns}$. Estimate from your Bode diagram the gain margin GM (in both decimal form and dB) and the phase margin PM (in degrees) for both values of Λ .

(c) Use MATLAB's `margin` function to validate the correctness of your estimated stability margins in part (b).

17.4 Suppose that you have an LTI rotary motor with unknown transfer function $G(s)$. The input is a voltage signal $e_{in}(t)$, and the output is shaft speed $\dot{\theta}(t) \equiv p(t)$. You want to control the shaft speed by sensing it with a tachometer, which has variable gain Λ , and feeding the tachometer voltage signal $e_p(t)$ back to the input in the standard form shown on the Laplace block diagram. In order to evaluate the stability of the closed-loop system, you conduct a stepped-sine-sweep frequency-response test on the stable open-loop system, which consists of the motor and the tachometer in series, with the gain set at $\Lambda = 0.4$ volt per rad/sec. Specifically, you drive the open-loop system with sinusoidal input voltage $e_{in}(t) = V_{in} \sin \omega t$ with the frequency increasing in small increments through the range $0.5 \leq \omega \leq 50$ rad/sec, you measure at each sine-dwell frequency the steady-state sinusoidal output voltage $e_p(t) = V_p(\omega) \sin[\omega t + \phi(\omega)]$, and then you plot the results for $V_p(\omega)/V_{in}$ and $\phi(\omega)$, leading to the following diagram:



- Would the closed-loop system be stable with the tachometer gain for which the above data apply, $\Lambda = 0.4$ volt/(rad/sec)? If so, calculate from the diagram above, with as much accuracy as the plots permit, the phase margin PM and gain margin GM of stability. Indicate the graphical representations of your PM and GM on a sketch or photocopy of the diagram.
- Would the closed-loop system be driven unstable by any positive values of tachometer gain, $\Lambda > 0$? If so, estimate those values. Explain your reasoning clearly.

17.5 Figure 17-5 is in the traditional two-dimensional format of a Nyquist plot, *i.e.*, $\text{Im}[FRF(\omega)]$ versus $\text{Re}[FRF(\omega)]$, on which excitation frequency ω is the implicit independent variable. But this format might be considered unsatisfactory for many purposes because it lacks a graduated scale for ω . An enhanced-format Nyquist plot, a three-dimensional plot, can show such a graduated scale of frequency in addition to the scales of the rectangular components, $\text{Re}[FRF(\omega)]$ and $\text{Im}[FRF(\omega)]$. In order to explore that format, run in MATLAB the following alternative version of the commands that produced Fig. 17-5, which applies, in particular, the `plot3` command to plot three-dimensionally:

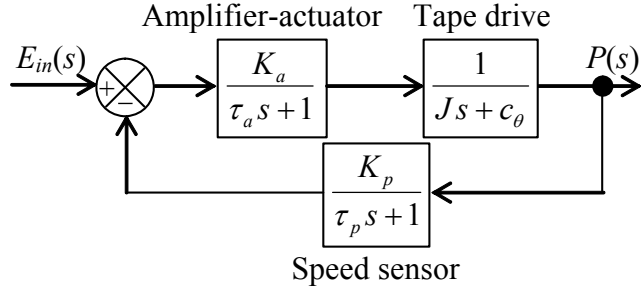
```
>> wn=2*pi;zt=0.2;
>> w=wn*(0:0.05:2.5);
>> frf=wn^2./(wn^2-w.^2+j*2*zt*wn*w);
>> plot3(real(frf),imag(frf),w/wn),grid
>> axis equal
```

These commands should produce a three-dimensional plot on which the $\text{Re}[FRF(\omega)]$ axis (the x -axis) extends from ≈ -1 to $\approx +1.5$, the $\text{Im}[FRF(\omega)]$ axis (the y -axis) extends from 0 to -2.5 , and the ω/ω_n axis (the z -axis) extends from 0 to 2.5. Make a print of the initial plot, which probably will be from the “Default 3-D View” (azimuth = -37.5° , elevation = 30° ; Orthographic, not Perspective). The Reference 3-D View, azimuth = 0° and elevation = 0° , is from $y = -\infty$ looking in exactly the $+y$ direction, so it is a two-dimensional projection of the x - z plane. Azimuth angle is positive rotation (in the sense of the right-hand rule) of the viewpoint about the z axis, relative to the Reference 3-D View; thus, for example, the view azimuth = 90° and elevation = 0° is from $x = +\infty$ looking in exactly the $-x$ direction, a two-dimensional projection of the y - z plane.

Consider two consecutive excitation frequencies in a frequency-response experiment, denoted as ω_i and ω_j , with $\omega_j > \omega_i$ [*e.g.*, two consecutive values in the series represented by the MATLAB command `w=wn*(0:0.05:2.5)`], and denote $\Delta\omega_{ij} = \omega_j - \omega_i$; denote the change from ω_i to ω_j of the in-phase component $\text{Re}[FRF(\omega)]$ as Δx_{ij} , and that of the quadrature component $\text{Im}[FRF(\omega)]$ as Δy_{ij} ; then the line segment between those two points in the $\text{Im}[FRF(\omega)]$ -versus- $\text{Re}[FRF(\omega)]$ plane (*e.g.*, Fig. 17-5, the x - y plane) is $\Delta s_{ij} = \sqrt{\Delta x_{ij}^2 + \Delta y_{ij}^2}$. Engineers who conduct stepped-sine-sweep frequency-response vibration tests on resonant systems (such as that of this problem) consider the rate of change $\Delta s_{ij}/\Delta\omega_{ij}$ to be a physically significant quantity that leads to experimental determination of a system’s natural frequency, ω_n . Describe how your three-dimensional Nyquist plots (from whatever viewpoints are required) demonstrate that $\Delta s_{ij}/\Delta\omega_{ij}$ is maximum at excitation frequencies near ω_n , but is below the maximum at frequencies both above and below ω_n .

17.6 In this problem, re-visit the system of homework Problem 16.7: the Laplace block diagram of the speed-control system of a magnetic-tape drive is shown in the figure on the next page. The operator setting is input voltage signal $e_{in}(t)$, the Laplace transform of which is $E_{in}(s)$. Each major sub-system of the control system functions as a 1st order system. The sub-system consisting of a power amplifier and a torque actuator has vari-

able sensitivity K_a (N-m/V) and time constant $\tau_a = 1.0$ sec. The tape drive has rotational inertia $J = 4.0$ N-m per rad/sec² and lubricated-shaft viscous damping constant $c_\theta = 1.0$ N-m per rad/sec; the output of the tape drive in this application is rotational speed $p(t)$ in rad/sec [with Laplace transform $P(s)$], not rotational position $\theta(t)$. The rotational-speed sensor in the feedback branch has sensitivity $K_p = 1.250$ V per rad/sec; this sensor is sufficiently slow relative to the other sub-systems that we must account for its time constant, $\tau_p = 0.50$ sec.



(a) Defining the control gain parameter as $\Lambda = K_a K_p / (J \tau_a \tau_p)$, with units of sec⁻³, show that the closed-loop transfer function is
$$\frac{P(s)}{E_{in}(s)} = \frac{K_a}{J \tau_a} \frac{s + \tau_p^{-1}}{(s + c_\theta/J)(s + \tau_a^{-1})(s + \tau_p^{-1}) + \Lambda}.$$
 Consider response to a unit-step input, $e_{in}(t) = (1.0 \text{ V})H(t)$. Use the final-value theorem (assuming system stability) to find an equation in terms of the system parameters for the steady-state response, after all transients have decayed, $\lim_{t \rightarrow \infty} p(t)$. Select the value of sensitivity K_a that makes the overall steady-state sensitivity of the control system be 0.750 rad/sec per volt, then calculate gain Λ corresponding to that value of K_a . (*partial solution:* $\Lambda = 7.50 \text{ sec}^{-3}$)

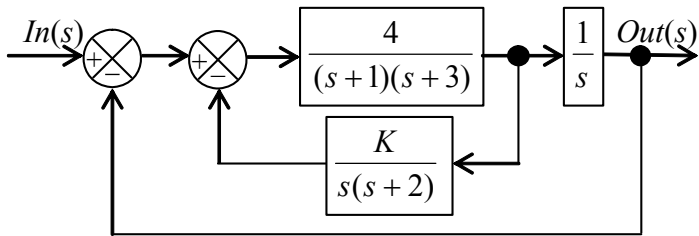
(b) Show that the open-loop frequency-response function can be written as $OLFRF(\omega) = \Lambda \times \frac{1}{(j\omega + c_\theta/J)(j\omega + \tau_a^{-1})(j\omega + \tau_p^{-1})}$. Calculate for the given parameter values the phase-crossover frequency ω_{ns} , i.e., the frequency at which $\angle OLFRF(\omega) = -\pi$ radians = -180° ; this task will require the numerical solution of a transcendental equation, which you might want to accomplish by applying the MATLAB function `fzero` in the manner described in homework Problem 17.2. Next, calculate for the baseline case, $\Lambda = 1 \text{ sec}^{-3}$, the magnitude ratio at phase crossover, $MR_1(\omega_{ns})$, and the corresponding gain margin, GM_1 . (*partial solution:* $GM_1 = 8.4375$)

(c) Now consider the gain determined in part (a), $\Lambda = 7.50 \text{ sec}^{-3}$. Calculate the magnitude ratio at phase crossover, $MR_{7.50}(\omega_{ns})$, and the corresponding gain margin, $GM_{7.50}$. Calculate the phase margin, $PM_{7.50}$, using the equation for $OLFRF(\omega)$ of part (b)—to do this, you will need first to find the gain-crossover frequency ω_1 [$MR_{7.50}(\omega_1) = 1$], which you might want to accomplish by applying again the MATLAB function `fzero` in the manner described in homework Problem 17.2; then you will need to calculate phase angle $\angle OLFRF(\omega_1)$ to use in the definition of phase margin.

(d) To validate your work in the previous parts, produce a diagram showing the Nyquist plots for both values of gain, $\Lambda = 1$ and 7.50 sec^{-3} ; you might wish just to adapt for this

case the MATLAB code that produced Fig. 17-10. What is your assessment, based on the gain and phase margins, of the control system with gain $\Lambda = 7.50 \text{ sec}^{-3}$?

- 17.7** Consider the feedback control system depicted in the Laplace block diagram at right. Assume that units of all constants are consistent, and don't bother to label units.



- (a) Combine the two feedback loops with block-diagram algebra to show that the forward-branch and feedback-branch transfer functions can be written, respectively, as:

$$G(s) = \frac{4}{s(s+1)(s+3)} \text{ and } H(s) = \frac{s + (2 + K)}{s + 2}. \text{ Apply Routh's criteria, as described in}$$

homework Problem 16.9(c), to determine the range of the sensitivity constant K over which the control system is stable.

- (b) Use any method of your choosing to determine the value of K for which the phase margin PM is approximately 35° . Note that the characteristic equation of this system does not have the form of either of Eqs. (16-62): this K does not play the role of Λ in Eqs. (16-62). Therefore, many of the equations developed in Chapter 17, such as Eqs. (17-8)-(17-12), are not applicable in this problem.

- (c) To validate your work in parts (a) and (b), produce a diagram showing the Nyquist plots for two values of K : both that for neutral stability (the upper-bound K for system stability), and that for $PM \approx 35^\circ$; you might wish just to adapt for this case the MATLAB code that produced Fig. 17-10. Explain the features of the Nyquist plots that confirm the correctness of your results in parts (a) and (b), using annotations on the diagram and/or written discussion.

- 17.8** Your task in this problem is to derive, with the assistance of MATLAB's symbolic capabilities, the "steady-state" response Eq. (17-15), which includes the unstable linear drift due to the open-loop transfer function's pole at $s = 0 + j0$. Because the equations that MATLAB produces are long and complicated, it will be advantageous to separate the voltage input function Eq. (17-14) into the following two parts:

$$e_{in1}(t) = E_{in} \sin \omega t \quad \text{and} \quad e_{in2}(t) = E_{off} H(t)$$

For each of these parts individually you will seek the voltage output solution, respectively, $e_{out1}(t)$ and $e_{out2}(t)$, then you will add the two to obtain the total response.

- (a) The Laplace transform of $e_{out1}(t)$, with the use of Eq. (17-2) and Eq. (2-30), is

$$L[e_{out1}(t)] = L[e_{in1}(t)] \times OLT F(s) = E_{in} \frac{\omega}{s^2 + \omega^2} \times \Lambda \frac{\omega_b}{s(s + c_\theta/J)(s + \omega_b)}$$

You might be able to find the inverse transform of this equation in some reference, but it is likely that a more efficient process is to define the equation symbolically in MATLAB and then to use the `ilaplace` command to find the inverse transform. The less appealing aspect of this approach is that MATLAB's initial solution will probably be long and difficult to interpret. To convert the initial solution equation into a more transparent form, use the `simple` and `pretty` commands. You seek the "steady-state" response, so discard (from the equation displayed after use of `pretty`) the transient terms involving the time functions $e^{-(c_\theta/J)t}$ and $e^{-\omega_b t}$. At this point, you should be able to express the solution in the form:

$$\frac{e_{out1}(t)}{E_{in}} = \frac{\Lambda}{\omega(c_\theta/J)} + \Lambda\omega_b \frac{-(c_\theta/J + \omega_b)\sin\omega t + [\omega - (c_\theta/J)\omega_b/\omega]\cos\omega t}{[\omega^2 + (c_\theta/J)^2](\omega^2 + \omega_b^2)}$$

The second right-hand-side term above is clearly a frequency-response term; but it is not yet expressed in the form from which equations for magnitude ratio and phase angle can be written, so you need to convert it into that form. Use the general trigonometric identity $\sin\theta \times \cos\phi + \cos\theta \times \sin\phi = \sin(\theta + \phi)$, and follow the procedure described in Eqs. (4-6)-(4-8), to show that $C\sin\omega t + S\cos\omega t = \sqrt{C^2 + S^2} \sin(\omega t + \phi)$, where $\phi = \tan^{-1}(S/C)$. Use this result to write explicit equations, in terms of c_θ/J and ω_b and ω , for magnitude ratio $MR(\omega)$ and phase angle $\phi(\omega)$. In the remainder of this problem, don't write out again those somewhat lengthy equations; instead, just use the symbols $MR(\omega)$ and $\phi(\omega)$.

(b) Use Eq. (17-2) again and MATLAB's `ilaplace` command in order to solve for output voltage $e_{out2}(t)$ in response to $e_{in2}(t) = E_{off}H(t)$.

(c) Combine the response equations of parts (a) and (b) to write the complete solution $e_{out}(t) = e_{out1}(t) + e_{out2}(t)$, the "steady-state" response Eq. (17-15):

$$e_{out}(t) = E_{in} \left(MR(\omega) \times \sin(\omega t + \phi(\omega)) + \frac{\Lambda}{\omega(c_\theta/J)} \right) + E_{off} \frac{\Lambda J}{c_\theta} \left[t - \frac{(c_\theta/J + \omega_b)}{(c_\theta/J)\omega_b} \right]$$

References

References

The following list includes only books and articles that are cited in this book. These references are arranged alphabetically by the family name of the first author.

Robert K. Adair, *The Physics of Baseball*, 2nd edition, HarperCollins, 1994.

Ferdinand P. Beer and E. Russell Johnston, Jr., *Mechanics of Materials*, 2nd edition, McGraw-Hill, 1992.

Pierre R. Bélanger, *Control Engineering: a Modern Approach*, Saunders College Publishing, 1995.

Robert M. Bennett, “Test Cases for Flutter of the Benchmark Models Rectangular Wings on the Pitch and Plunge Apparatus,” Defense Technical Information Center Compilation Part Notice ADP010713, <http://www.dtic.mil/cgi-bin/GetTRDoc?AD=ADP010713>, October 2000.

Raymond L. Bisplinghoff, Holt Ashley, and Robert L. Halfman, *Aeroelasticity*, Addison-Wesley, 1955; paperback edition published by DoverPublications.com, ISBN 10: 0486691896.

A. R. S. Bramwell, *Helicopter Dynamics*, Edward Arnold (Publishers) Ltd, 1976.

William L. Brogan, *Modern Control Theory*, Quantum Publishers, Inc., 1974.

Robert H. Cannon, Jr., *Dynamics of Physical Systems*, McGraw-Hill, 1967; paperback edition published by DoverPublications.com, ISBN 10: 0486428656.

Robert N. Clark, *Introduction to Automatic Control Systems*, John Wiley & Sons, 1962.

Ray W. Clough and Joseph Penzien, *Dynamics of Structures*, McGraw-Hill, 1974.

Roy R. Craig, Jr., *Structural Dynamics—an Introduction to Computer Methods*, John Wiley & Sons, 1981.

James W. Dally, William F. Riley, and Kenneth G. McConnell, *Instrumentation for Engineering Measurements*, John Wiley & Sons, 1984.

Carlos DeMarqui Jr., E. M. Belo, and F. D. Marques, “A Flutter Suppression Active Controller,” *Proceedings of the Institution of Mechanical Engineers*, Vol. 219, Part G: J. Aerospace Engineering, February 2005, pp. 19-33.

Carlos DeMarqui Jr., D. C. Rebolho, E. M. Belo, and F. D. Marques, “Identification of Flutter Parameters for a Wing Model ,” *Journal of the Brazilian Society of Mechanical*

References

Science & Engineering, <http://www.scielo.br/pdf/jbsmse/v28n3/30571.pdf>, July-September 2006, Vol. XXVIII, No. 3, pp. 339-346.

J. P. Den Hartog, *Mechanical Vibrations*, 4th edition, McGraw-Hill, 1956; paperback edition published by DoverPublications.com, ISBN 10: 0486647854.

Clarence W. de Silva, (editor), *Vibration Damping, Control, and Design*, CRC Press, Taylor & Francis Group, 2007.

J. William Dettmer, *Space Integrated Controls Experiment (SPICE) Program*, Defense Technical Information Center (DTIC) Accession Number ADA297200, Phillips Laboratory PL-TR-95-1035, <http://www.dtic.mil/get-tr-doc/pdf?AD=ADA297200>, May 1995.

Walter R. Evans, *Control-System Dynamics*, McGraw-Hill, 1954.

David J. Ewins, *Modal Testing: Theory and Practice*, Research Studies Press Ltd., 1984.

Neil J. Fergusson and Walter D. Pilkey, "The Dynamic Stiffness Method, a Survey of the Published Literature: Part I: DSM Elements; Part II: Frequency Extraction Methods and Modal Analysis", *Shock and Vibration Technology Review*: Volume 1, Number 7, July 1991, pp. 4-13; Volume 1, Number 8, August 1991, pp. 14-20.

Stanley Fifer, *Analogue Computation: Theory, Techniques and Applications*, in four volumes, McGraw-Hill, 1961.

Gene F. Franklin, J. David Powell, and Abbas Emami-Naeini, *Feedback Control of Dynamic Systems*, 2nd edition, Addison-Wesley, 1991.

Y. C. Fung, *An Introduction to the Theory of Aeroelasticity*, John Wiley & Sons, 1955; and Dover Publications, 1969.

Donald T. Greenwood, *Principles of Dynamics*, Prentice-Hall, 1965.

James E. Gordon, *Structures, or Why Things Don't Fall Down*, Penguin Books, 1978; paperback edition published by DaCapoPress.com, ISBN 0306801515.

David Halliday and Robert Resnick, *Physics for Students of Science and Engineering*, John Wiley & Sons, 1960.

S. B. Hammond, *Electrical Engineering*, McGraw-Hill, 1961.

Russell C. Hibbeler, *Mechanics of Materials*, 3rd edition, Prentice Hall, 1997.

Francis B. Hildebrand, *Advanced Calculus for Applications*, Prentice-Hall, 1962.

References

Paul Horowitz and Winfield Hill, *The Art of Electronics*, Cambridge University Press, 1980.

A. L. Kimball and D. E. Lovell, "Internal Friction in Solids," *Physical Review*, Series 2, Vol. 30, 1927, pp. 948-959.

George Fox Lang, "Analog was not a Computer Trademark!", *Sound and Vibration*, <http://www.SandV.com>, August 2000, pp. 16-25.

Benjamin J. Lazan, *Damping of Materials and Members in Structural Mechanics*, Pergamon Press, 1968.

Augustus E. H. Love, *A Treatise on the Mathematical Theory of Elasticity*, 4th edition, Dover Publications, 1926.

Andy Lightbody, Joe Poyer, and Dick Cole, *The Great Book of Fighter Planes*, Beekman House, 1990.

M. James Lighthill, *Introduction to Fourier Analysis and Generalised Functions*, Cambridge University Press, 1958.

Richard H. MacNeal, *Electric Circuit Analogies for Elastic Structures*, John Wiley & Sons, 1962.

Nuno M. M. Maia and Julio M. M. Silva (editors), *Theoretical and Experimental Modal Analysis*, Research Studies Press Ltd., 1997.

Leonard Meirovitch, *Analytical Methods in Vibrations*, Macmillan, 1967.

Leonard Meirovitch, *Fundamentals of Vibrations*, McGraw-Hill, 2001.

N. O. Myklestad, *Vibration Analysis*, McGraw-Hill, 1944.

Ahid D. Nashif, David I. G. Jones, and John P. Henderson, *Vibration Damping*, John Wiley & Sons, 1985.

Robert C. Nelson, *Flight Stability and Automatic Control*, McGraw-Hill, 1989.

Katsuhiko Ogata, *Modern Control Engineering*, 4th edition, Prentice-Hall, 2001 (or 2002 because there is ambiguity in different listings of the publication date; however, the ISBN is 0-13-060907-2, without ambiguity.)

Katsuhiko Ogata, *System Dynamics*, 3rd edition, Prentice-Hall, 1998.

Gerald R. Peterson, *Basic Analog Computation*, Macmillan, 1967.

References

Thomas P. Sarafin (editor), *Spacecraft Structures and Mechanisms—from Concept to Launch*, Microcosm Press and Kluwer Academic Publishers, 1995.

Joseph E. Shigley and Larry D. Mitchell, *Mechanical Engineering Design*, 4th edition, McGraw-Hill, 1983.

Arnold Sommerfeld, *Mechanics: Lectures on Theoretical Physics, Volume 1*, translated into English from the 4th German edition by Martin O. Stern, Academic Press, 1964.

Stephen P. Timoshenko and Donovan H. Young, *Elements of Strength of Materials*, 4th edition, Van Nostrand, 1962.

Eric E. Ungar, “Compromises: Academia and the Real World,” *Sound and Vibration*, <http://www.SandV.com>, March 1998, p. 5.

Appendix A Table and derivations of Laplace transform pairs

A-1 Table of Laplace transform pairs used in this book¹

General conventions: (1) time t is a real number, $t \geq 0$; (2) Laplace variable s is a complex number with dimension of time⁻¹; (3) n and k are positive, real integers; (4) p and σ are finite constants, with dimension of time⁻¹; (5) t_s is a real, finite constant, with dimension of time; (6) ω is a positive, real, finite constant, with dimension of time⁻¹.

Function of time t , inverse Laplace transform	Function of Laplace variable s , forward Laplace transform	Source and notes
$f(t) = L^{-1}[F(s)]$	$F(s) = L[f(t)]$	General notation, p. 2-6
$f(t)$	$\int_{t=0}^{t=\infty} e^{-st} f(t) dt$, or $\int_{t=0^-}^{t=\infty} e^{-st} f(t) dt$	Definitions: Eq. (2-13), or Eq. (8-12) if $f(t)$ involves $\delta(t)$
$\dot{f}(t)$	$s F(s) - f(0^-)$	Eqs. (2-15b) and (8-21); $t = 0^-$ for ICs precedes all inputs
$\ddot{f}(t)$	$s^2 F(s) - s f(0^-) - \dot{f}(0^-)$	Eq. (2-17), Problem 2.4
$\frac{d^n}{dt^n} f(t)$	$s^n F(s) - s^{n-1} f(0^-) - s^{n-2} \dot{f}(0^-) - \dots - \overset{(n-1)}{f}(0^-)$	Eqs. (2-16) and (8-22), Ogata, 1998, pp. 25-26
$\int_{\tau=-\infty}^{\tau=t \geq 0} f(\tau) d\tau$	$\frac{1}{s} F(s) + \frac{1}{s} \int_{\tau=-\infty}^{\tau=0} f(\tau) d\tau$	Eq. (2-32), derivation in Section A-3; note that $-\infty < t < +\infty$
$\int_{\tau=0}^{\tau=t \geq 0} f(\tau) d\tau$	$\frac{1}{s} F(s)$	Eq. (2-33), derivation in Section A-3
$CI(t) = \int_{\tau=0}^{\tau=t} f_1(\tau) f_2(t-\tau) d\tau$ $= \int_{\tau=0}^{\tau=t} f_1(t-\tau) f_2(\tau) d\tau$	$F_1(s) \times F_2(s)$	Eq. (6-2), convolution integral, derived in Section A-5
$e^{\sigma t} f(t)$	$F(s - \sigma)$	Eq. (9-18); σ is any constant
e^{pt}	$\frac{1}{s - p}$	Eq. (2-14); p is any constant
$\frac{1}{p}(e^{pt} - 1)$	$\frac{1}{s} \frac{1}{s - p}$	Eq. (A-15); p is any constant

¹ Much more extensive tables of Laplace transform pairs are available in many references, for example, Cannon, 1967, Appendix J.

Appendix A Table and derivations of Laplace transform pairs

Function of time t , in- verse Laplace transform	Function of Laplace variable s , forward Laplace transform	Source and notes
$f(t) = L^{-1}[F(s)]$	$F(s) = L[f(t)]$	General notation, p. 2-6
$f(t)$	$\int_{t=0}^{t=\infty} e^{-st} f(t) dt$, or $\int_{t=0^-}^{t=\infty} e^{-st} f(t) dt$	Definitions: Eq. (2-13), or Eq. (8-12) if $f(t)$ involves $\delta(t)$
$\delta(t) \equiv \delta(t - 0)$	1	Eq. (8-13); Dirac delta function of Eq. (8-8)
$H(t - t_s)$	$\frac{e^{-st_s}}{s}$	Eq. (2-28); general unit- step defined in Eq. (2-27)
$H(t)$	$\frac{1}{s}$	Eq. (2-29); Heaviside unit-step function defined in Eq. (2-26)
$f(t - t_s) H(t - t_s)$	$e^{-st_s} F(s)$	Ogata, 1998, p. 18; trans- lated function of time
t	$\frac{1}{s^2}$	Eq. (A-17)
$t e^{\sigma t}$	$\frac{1}{(s - \sigma)^2}$	Eqs. (A-17) and (9-18); σ is any constant
$\sin \omega t$	$\frac{\omega}{s^2 + \omega^2}$	Eq. (2-30); ω is a positive real constant
$\cos \omega t$	$\frac{s}{s^2 + \omega^2}$	Eq. (2-31); ω is a positive real constant
$\frac{1}{\omega^2} (1 - \cos \omega t)$	$\frac{1}{s(s^2 + \omega^2)}$	Eq. (A-16); ω is a positive real constant
$\frac{\omega_n^2}{\omega_d} e^{-\zeta \omega_n t} \sin \omega_d t$	$\frac{\omega_n^2}{(s + \zeta \omega_n)^2 + \omega_d^2}$	Problem 9.12; $ \zeta < 1$, $\omega_d^2 = \omega_n^2 (1 - \zeta^2) > 0$
$1 - e^{-\zeta \omega_n t} \times$ $\left(\cos \omega_d t + \frac{\zeta \omega_n}{\omega_d} \sin \omega_d t \right)$	$\frac{\omega_n^2}{s[(s + \zeta \omega_n)^2 + \omega_d^2]}$	Problem 9.12; $ \zeta < 1$, $\omega_d^2 = \omega_n^2 (1 - \zeta^2) > 0$
$e^{-\zeta \omega_n t} \times$ $(\omega_d \cos \omega_d t - \zeta \omega_n \sin \omega_d t)$	$\frac{s \omega_d}{(s + \zeta \omega_n)^2 + \omega_d^2}$	Problem 9.15; $ \zeta < 1$, $\omega_d^2 = \omega_n^2 (1 - \zeta^2) > 0$
$2 C e^{\sigma t} \cos(\omega t + \angle C)$	$\frac{C}{s - p} + \frac{\bar{C}}{s - \bar{p}}$	Eq. (16-9); C is complex, $p = \sigma + j\omega$, σ and ω are real, $\omega > 0$
$\sum_{k=1}^n \frac{Num(p_k)}{Den'(p_k)} e^{p_k t}$	$\frac{Num(s)}{Den(s)}$	Eq. (A-7), Section A-2 for definitions, derivation, and restrictions

Appendix A Table and derivations of Laplace transform pairs

Function of time t , inverse Laplace transform	Function of Laplace variable s , forward Laplace transform	Source and notes
$f(t) = L^{-1}[F(s)]$	$F(s) = L[f(t)]$	General notation, p. 2-6
$f(t)$	$\int_{t=0}^{t=\infty} e^{-st} f(t) dt$, or $\int_{t=0^-}^{t=\infty} e^{-st} f(t) dt$	Definitions: Eq. (2-13), or Eq. (8-12) if $f(t)$ involves $\delta(t)$
	$\lim_{t \rightarrow 0^+ \text{ from } t > 0} f(t) \equiv f(0^+) = \lim_{s \rightarrow \infty} [s F(s)]$	Initial-value theorem: Eq. (8-20) and Eq. (8-24) in Section 8-6
	$\lim_{t \rightarrow \infty} f(t) = \lim_{s \rightarrow 0} [s F(s)]$	Final-value theorem: Eq. (15-15) and Section 15-3, valid <u>only if</u> $\lim_{t \rightarrow \infty} f(t)$ is a finite, constant value

It is worthy of note that MATLAB's symbolic software, which is introduced in homework Problem 1.6, can sometimes be helpful for finding forward and inverse Laplace transforms by applying, respectively, the `laplace` and `ilaplace` commands. The following are two relatively simple examples that do not appear explicitly in the table of transform pairs. In these examples, MATLAB finds the forward transform $L[\sinh(at)] = a/(s^2 - a^2)$, and the inverse transform $L^{-1}[(s+a)/[(s+a)^2 + \omega^2]] = e^{-at} \cos \omega t$.

```

>> syms s t a w
>> ft=sinh(a*t)

ft =
sinh(a*t)

>> Lft=laplace(ft,t,s)

Lft =
a/(s^2-a^2)

>> pretty(Lft)

          a
          -
          2      2
          s      - a

>> Fs=(s+a)/((s+a)^2+w^2)

Fs =
(s+a)/((s+a)^2+w^2)

>> fFs=ilaplace(Fs,s,t)

fFs =
exp(-a*t)*cos(w*t)

```

Appendix A Table and derivations of Laplace transform pairs

For functions of time t or functions of Laplace variable s that are more complicated than those in the examples above, MATLAB might produce solutions that are correct, but are expressed in an unfamiliar form, or in a long and unwieldy form that must be simplified by human touch in order to become useful.

A-2 Laplace transform of a ratio of two polynomials, with only simple poles

Suppose that we have a Laplace transform as the ratio of two polynomials, from Eq. (2-10):

$$F_n(s) \equiv \frac{Num(s)}{Den(s)} = \frac{b_1 s^m + b_2 s^{m-1} + \dots + b_{m+1}}{a_1 s^n + a_2 s^{n-1} + \dots + a_{n+1}} = \frac{b_1(s - z_1)(s - z_2) \cdots (s - z_m)}{a_1(s - p_1)(s - p_2) \cdots (s - p_n)} \quad (\text{A-1})$$

The results derived in this section are based upon three assumptions: (1) the roots p_k of $Den(s)$, which are the poles of $F_n(s)$, are not repeated (such roots are called *simple* poles); (2) the degree of $Den(s)$ exceeds that of $Num(s)$, $0 \leq m < n$; and (3) none of the zeros of (A-1) equals any of the poles. Under these circumstances, we can expand transform (A-1) into partial fractions, from Eq. (2-24):

$$F_n(s) = \sum_{k=1}^n \frac{C_k}{s - p_k} \quad (\text{A-2})$$

In Eq. (A-2) the residues are given by Eq. (2-25b) as

$$C_k = [(s - p_k) F_n(s)]_{s=p_k} = \left[(s - p_k) \frac{Num(s)}{Den(s)} \right]_{s=p_k}, \quad k = 1, 2, \dots, n \quad (\text{A-3})$$

Let's examine what might be considered the “total denominator” of Eq. (A-3):

$$D_k = \lim_{s \rightarrow p_k} \left[\frac{Den(s)}{(s - p_k)} \right] \quad (\text{A-4})$$

Observe from $Den(s)$ in Eq. (A-1) that D_k in Eq. (A-4) has the indeterminate form 0/0. Since we assume that all zeros of $F_n(s)$ are different from the poles, $Num(p_k)$ in Eq. (A-3) is non-zero and finite. Therefore, D_k must also be non-zero and finite, and we can use l'Hospital's rule to cast Eq. (A-4) into a different form:

$$D_k = \lim_{s \rightarrow p_k} \left[\frac{Den(s)}{(s - p_k)} \right] = \lim_{s \rightarrow p_k} \left[\frac{\frac{d}{ds} Den(s)}{\frac{d}{ds}(s - p_k)} \right] \equiv \left[\frac{d}{ds} Den(s) \right]_{s=p_k} \quad (\text{A-5})$$

Appendix A Table and derivations of Laplace transform pairs

Thus (Hildebrand, 1962, p. 548), residue (A-3) can be expressed alternatively as

$$C_k = \left[(s - p_k) \frac{\text{Num}(s)}{\text{Den}(s)} \right]_{s=p_k} = \left[\frac{\text{Num}(s)}{\frac{d}{ds} \text{Den}(s)} \right]_{s=p_k} \equiv \frac{\text{Num}(p_k)}{\text{Den}'(p_k)} \quad (\text{A-6})$$

Finally (Meirovitch, 1967, p. 532), by substituting Eq. (A-6) back into Eq. (A-2) and then taking the inverse Laplace transform of each term in the summation, we find

$$f(t) = L^{-1}[F_n(s)] = L^{-1}\left[\frac{\text{Num}(s)}{\text{Den}(s)} \right] = \sum_{k=1}^n \frac{\text{Num}(p_k)}{\text{Den}'(p_k)} e^{p_k t}, \quad t \geq 0 \quad (\text{A-7})$$

A-3 Derivation of the Laplace transform of a definite integral

Suppose that a function $f(t)$ has Laplace transform $F(s) = L[f(t)]$, and that we need the transform of the definite integral $\int_{\tau=-\infty}^{\tau=t \geq 0} f(\tau) d\tau$. Note the lower limit of $\tau = -\infty$; we usually consider $f(t)$ only for $t \geq 0$, but occasionally the integral of $f(t)$ over previous time, $t < 0$, is also needed.

$$L\left[\int_{\tau=-\infty}^{\tau=t \geq 0} f(\tau) d\tau \right] = \int_{t=0}^{t=\infty} \left[\int_{\tau=-\infty}^{\tau=t \geq 0} f(\tau) d\tau \right] e^{-st} dt \quad (\text{A-8})$$

Integrating by parts gives

$$L\left[\int_{\tau=-\infty}^{\tau=t \geq 0} f(\tau) d\tau \right] = \left\{ \left[\int_{\tau=-\infty}^{\tau=t \geq 0} f(\tau) d\tau \right] \left(\frac{e^{-st}}{-s} \right) \right\}_{t=0}^{t=\infty} - \left(\frac{1}{-s} \right) \int_{t=0}^{t=\infty} e^{-st} \frac{d}{dt} \left[\int_{\tau=-\infty}^{\tau=t \geq 0} f(\tau) d\tau \right] dt \quad (\text{A-9})$$

The derivative of the definite integral in the second right-hand-side term of Eq. (A-9) is a special case of Leibnitz's rule (Hildebrand, 1962, p. 360):

$$\frac{d}{dt} \left[\int_{\tau=-\infty}^{\tau=t \geq 0} f(\tau) d\tau \right] = f(t) \quad (\text{A-10})$$

With the simple result (A-10), and with evaluation of the limits of the first right-hand-side term, Eq. (A-9) becomes

Appendix A Table and derivations of Laplace transform pairs

$$L\left[\int_{\tau=-\infty}^{\tau=t \geq 0} f(\tau) d\tau\right] = \frac{1}{s} \int_{\tau=-\infty}^{\tau=0} f(\tau) d\tau + \frac{1}{s} \int_{t=0}^{t=\infty} e^{-st} f(t) dt \quad (\text{A-11})$$

Thus, the final form of the required general transform is

$$L\left[\int_{\tau=-\infty}^{\tau=t \geq 0} f(\tau) d\tau\right] = \frac{1}{s} F(s) + \frac{1}{s} \int_{\tau=-\infty}^{\tau=0} f(\tau) d\tau \quad (\text{A-12})$$

For most applications, we have $f(t) = 0$ for $t < 0$, for which the simpler transform is:

$$L\left[\int_{\tau=0}^{\tau=t \geq 0} f(\tau) d\tau\right] = \frac{1}{s} F(s) \quad (\text{A-13})$$

If we regard the integral of $f(t)$ as being the first “negative” derivative (antiderivative), then we see that transform (A-12) is logically consistent with transform (2-15b) for a “positive” derivative, with respect to both power of s and the initial value term.

A-4 Applications of the Laplace transform of a definite integral

A relatively painless method for deriving certain inverse transforms is based upon the inverse transform of Eq. (A-13),

$$L^{-1}\left[\frac{1}{s} F(s)\right] = \int_{\tau=0}^{\tau=t \geq 0} f(\tau) d\tau \quad (\text{A-14})$$

It is necessary to apply carefully the limits of the definite integral, as is illustrated in the following three examples.

$$L^{-1}\left[\frac{1}{s} \frac{1}{s-p}\right] = \int_{\tau=0}^{\tau=t \geq 0} e^{p\tau} d\tau = \frac{1}{p} \int_{\tau=0}^{\tau=t \geq 0} d(e^{p\tau}) = \frac{1}{p} (e^{pt} - 1), t \geq 0 \quad (\text{A-15})$$

$$L^{-1}\left[\frac{1}{s(s^2 + \omega^2)}\right] = \frac{1}{\omega} \int_{\tau=0}^{\tau=t} \sin \omega \tau d\tau = -\frac{1}{\omega^2} \int_{\tau=0}^{\tau=t} d(\cos \omega \tau) = \frac{1}{\omega^2} (1 - \cos \omega t), t \geq 0 \quad (\text{A-16})$$

$$L^{-1}\left[\frac{1}{s} \frac{1}{s}\right] = \int_{\tau=0}^{\tau=t \geq 0} H(\tau) d\tau = \int_{\tau=0}^{\tau=t \geq 0} d\tau = t, t \geq 0 \quad (\text{A-17})$$

Appendix A Table and derivations of Laplace transform pairs

A-5 Derivation of the Laplace transform of the convolution integral

We consider two physically realistic functions of time, $f_1(t)$ and $f_2(t)$, that are zero for all time $t < 0$ and non-zero only for $t \geq 0$. The *convolution integral* is defined to be a definite integral involving $f_1(t)$ and $f_2(t)$ in either of the following forms:

$$CI(t) = \int_{\tau=0}^{\tau=t} f_1(\tau) f_2(t - \tau) d\tau = \int_{\tau=0}^{\tau=t} f_1(t - \tau) f_2(\tau) d\tau \quad (6-1) \text{ repeated}$$

In these definite integrals, τ is the dummy variable of integration, and time t appears both in the upper limit of the integral and in argument $(t - \tau)$ of the integrand.

The Laplace transform $L[CI(t)]$ is called the *convolution transform*. Let's assume that the Laplace transforms of functions $f_1(t)$ and $f_2(t)$ exist: $F_1(s) = L[f_1(t)]$ and $F_2(s) = L[f_2(t)]$. The derivation to follow will show that the product of these two transforms equals the convolution transform:

$$F_1(s) \times F_2(s) = L[CI(t)] = L\left[\int_{\tau=0}^{\tau=t} f_1(\tau) f_2(t - \tau) d\tau\right] \quad (6-2) \text{ repeated}$$

Equation (6-2) is certainly not an intuitively obvious result. The short, formal derivation (Meirovitch, 1967, p. 534 and Ogata, 1998, pp. 43-44) involves interchanging of orders of integration. The first step is to revise the upper limit in the convolution integral since, by definition, $f_2(t - \tau) = 0$ for $t - \tau < 0$, that is, for $\tau > t$:

$$CI(t) = \int_{\tau=0}^{\tau=t} f_1(\tau) f_2(t - \tau) d\tau = \int_{\tau=0}^{\tau=\infty} f_1(\tau) f_2(t - \tau) d\tau$$

Next, use the standard definition of a Laplace transform:

$$L[CI(t)] = L\left[\int_{\tau=0}^{\tau=\infty} f_1(\tau) f_2(t - \tau) d\tau\right] = \int_{t=0}^{t=\infty} e^{-st} \left[\int_{\tau=0}^{\tau=\infty} f_1(\tau) f_2(t - \tau) d\tau \right] dt$$

Now interchange the orders of integration between t and τ , an operation permitted by the assumed convergence of the integrals, and re-arrange the terms within the integrands:

$$L[CI(t)] = \int_{\tau=0}^{\tau=\infty} f_1(\tau) \left[\int_{t=0}^{t=\infty} e^{-st} f_2(t - \tau) dt \right] d\tau$$

In the inner integral, change the integration variable to $\lambda = t - \tau$, so that $t = \tau + \lambda$ and $dt = d\lambda$, since τ is regarded as a constant within this integration:

Appendix A Table and derivations of Laplace transform pairs

$$L[CI(t)] = \int_{\tau=0}^{\tau=\infty} f_1(\tau) d\tau \left[\int_{\lambda=-\tau}^{\lambda=\infty} e^{-s(\tau+\lambda)} f_2(\lambda) d\lambda \right]$$

Now, since $f_2(t) = 0$ for $\lambda < 0$, in the second integral we set the lower limit to zero. Also, again re-arrange terms within the integrands, to find

$$L[CI(t)] = \int_{\tau=0}^{\tau=\infty} e^{-s\tau} f_1(\tau) d\tau \left[\int_{\lambda=0}^{\lambda=\infty} e^{-s\lambda} f_2(\lambda) d\lambda \right] \equiv F_1(s) \times F_2(s)$$

This completes the derivation of the convolution transform, Eq. (6-2).

Appendix B: Notes on work, energy, and power in mechanical systems and electrical circuits

© 2016 by William L. Hallauer, Jr.

B-1 Definitions of work and power

Work is defined for translational motion as the product of a force times a distance through which the force moves. For translation in one dimension, denoted here as x , the differential work of force $f_x(x)$ moving through distance dx at position x is

$$dW = f_x(x) \times dx \quad (\text{B-1})$$

So the work by a spatially varying force moving from position x_1 to position x_2 is

$$W = \int_{x=x_1}^{x=x_2} dW = \int_{x=x_1}^{x=x_2} f_x(x) dx \quad (\text{B-2})$$

with units of lb-ft, lb-inch, or N-m \equiv J (for joule).

The velocity of one-dimensional motion is $v_x = dx/dt \Rightarrow dx = v_x dt$. Therefore, alternative expressions for work are

$$dW = f_x \times v_x dt \Rightarrow W = \int_{t=t_1}^{t=t_2} f_x v_x dt \quad (\text{B-3})$$

This leads to the definition of *power*, the time rate of work:

$$P \equiv \frac{dW}{dt} = f_x \times v_x \quad (\text{B-4})$$

with units of lb-ft/sec, lb-inch/sec, or N-m/sec = J/sec \equiv W (for watt).

For rotation in one dimension, denoted here as θ , the differential work of moment M moving through angle $d\theta$ at position θ is $dW = M \times d\theta$, and the differential work of moment M moving with velocity $\dot{\theta}$ during interval dt is $dW = M \times \dot{\theta} dt$. Therefore, the work of a possibly varying moment between states 1 and 2 can be expressed in either of the two forms:

$$W = \int_{\theta=\theta_1}^{\theta=\theta_2} M d\theta = \int_{t=t_1}^{t=t_2} M \dot{\theta} dt \quad (\text{B-5})$$

Appendix B Notes on work, energy, and power in mechanical systems and electrical circuits

with units of lb-ft, lb-inch, or J. The associated definition of power is

$$P = M \times \dot{\theta} \quad (\text{B-6})$$

with units of lb-ft/sec, hp (for horsepower, 1 hp \equiv 550 lb-ft/sec), lb-inch/sec, or W.

At least some of the work that is done on a real system might be stored in some form of recoverable energy, or work done might be completely dissipated and lost. For all real engineering systems, at least part of the input work that is intentionally done on a system is lost irretrievably, not used for the intended purposes.

B-2 Mechanical work, energy, and power (complementary to Chapter 3)

If a force accelerates in translation a body with mass m , $f_x = m a_x = m \dot{v}_x$, then the work done by f_x is conserved as *kinetic energy* of the body, from Eq. (B-3):

$$W \equiv E_K = \int_{t=t_1}^{t=t_2} f_x v_x dt = \int_{t=t_1}^{t=t_2} m \dot{v}_x v_x dt = \frac{1}{2} m \int_{t=t_1}^{t=t_2} \frac{d}{dt} (v_x^2) dt = \frac{1}{2} m [v_x^2(t_2) - v_x^2(t_1)] \quad (\text{B-7})$$

If a force stretches or compresses a standard ideal linear translational spring (assumed here to have negligible mass), $f_x(x) = k x$, then the work done by f_x is stored as *strain energy* (a form of *potential energy*) within the spring, from Eq. (B-2):

$$W \equiv E_S = \int_{x=x_1}^{x=x_2} f_x(x) dx = \int_{x=x_1}^{x=x_2} k x dx = \frac{1}{2} k (x_2^2 - x_1^2) \quad (\text{B-8})$$

At any instant, therefore, the total mechanical energy present in an ideal mass-spring system, relative to an initially stationary and unstrained state, is

$$E_{Me} = E_K + E_S = \frac{1}{2} m v_x^2 + \frac{1}{2} k x^2 \quad (\text{B-9})$$

In an ideal *conservative* mass-spring system, without any agent of energy augmentation or energy dissipation, E_{Me} remains constant in time, oscillating between the kinetic energy of the mass and the strain energy within the spring.

An ideal translational viscous damper dissipates mechanical energy by exerting a force in opposition to velocity: $f_x = -c v_x = -c \dot{x}$. Thus, from Eq. (B-4), the rate of energy dissipation by the damper is

$$P_c = f_x v_x = -c v_x^2 \quad (\text{B-10})$$

Appendix B Notes on work, energy, and power in mechanical systems and electrical circuits

Suppose that a mass-damper-spring system is initially stationary and unstrained, and that an independent, externally applied force $f_x(t)$ is imposed upon the mass. This force is a *source* of power, $P_f = f_x(t)v_x$. The damper, on the other hand, is a *sink* of mechanical energy. Therefore, total mechanical energy E_{Me} varies in time:

$$\frac{d}{dt}E_{Me} = \frac{d}{dt}\left(\frac{1}{2}mv_x^2 + \frac{1}{2}kx^2\right) = P_c + P_f \Rightarrow mv_x\dot{v}_x + kx\dot{x} = -cv_x^2 + f_x(t)v_x \quad (\text{B-11})$$

Cancelling $v_x = \dot{x}$ out of Eq. (B-11) and re-arranging terms leads to the general ODE of motion for a mass-damper-spring system¹:

$$m\ddot{x} + c\dot{x} + kx = f_x(t) \quad (\text{B-12})$$

The following relations for rotational motion can be derived from the basic definitions in the manner used above for translational motion. If a moment M accelerates a body with rotational inertia J about the axis of rotation, then the work done by M is conserved as *kinetic energy* of the body:

$$W \equiv E_K = \int_{t=t_1}^{t=t_2} M\dot{\theta} dt = \frac{1}{2}J[\dot{\theta}^2(t_2) - \dot{\theta}^2(t_1)] \quad (\text{B-13})$$

If a moment M twists an ideal linear torsion (rotational) spring (assumed here to have negligible rotational inertia) with spring constant k_θ , then the work done by M is stored as *strain energy* within the spring:

$$W \equiv E_S = \int_{\theta=\theta_1}^{\theta=\theta_2} M d\theta = \frac{1}{2}k_\theta(\theta_2^2 - \theta_1^2) \quad (\text{B-14})$$

A rotational viscous damper with constant c_θ dissipates mechanical energy by exerting a moment in opposition to velocity: $M = -c_\theta\dot{\theta}$. Thus, the rate of energy dissipation by the damper is

$$P_c = M\dot{\theta} = -c_\theta\dot{\theta}^2 \quad (\text{B-15})$$

¹ The direct power-balance method giving Eq. (B-11) and leading to ODE of motion (B-12) is also used in this appendix to derive governing ODEs (B-19) and (B-34). Each of these applications is for a one-degree-of-freedom (1-DOF) system, *i.e.*, a system that has only one time-dependent variable. (See Chapters 11 and 12 for more detailed definitions of degrees of freedom and examples of multiple-DOF systems.) Unfortunately, this direct approach fails for systems with more than one DOF, as is observed and illustrated by Cannon, 1967, p. 166. For deriving the governing ODEs of multiple-DOF systems, a more general energy method was developed by Joseph Louis Lagrange (French-Italian mathematician and mechanician, 1736-1813). *Lagrange's equations* are derived and illustrated in detail by most textbooks on classical mechanics and structural dynamics, *e.g.*, Bisplinghoff, *et al.*, 1955; Cannon, 1967; Craig, 1981; Greenwood, 1965; and Meirovitch, 1967 and 2001.

Appendix B Notes on work, energy, and power in mechanical systems and electrical circuits

For our final example of mechanical energy, consider translation in the y direction of a mass m that is within a field of constant *gravitational field strength* g (with SI units newton/kilogram). The force required to sustain the mass without acceleration (either stationary or at constant velocity) against gravity is

$$f_y = mg \quad (\text{B-16})$$

Therefore, the work required to raise the mass without acceleration against gravity is stored conservatively as *gravitational potential energy*:

$$W \equiv E_G = \int_{y=y_1}^{y=y_2} f_y dy = mg(y_2 - y_1) \quad (\text{B-17})$$

For reference in the next section, we define also the *gravitational potential difference*, $g(y_2 - y_1)$. The following is an application of Eq. (B-17). Suppose that we shoot a projectile of mass m straight up against Earth's gravity from surface elevation y_1 , with initial velocity v_1 sufficiently low that g remains essentially constant over the entire trajectory. Let's assume that atmospheric drag is viscous with damping constant c .² Drag force $-cv_y$ dissipates energy, so the total mechanical energy E_{Me} varies in time:

$$\frac{d}{dt} E_{Me} = \frac{d}{dt} \left(\frac{1}{2} m(v_y^2 - v_1^2) + mg(y - y_1) \right) = P_c \Rightarrow m v_y \dot{v}_y + m g \dot{y} = -c v_y^2 \quad (\text{B-18})$$

Canceling out $v_y = \dot{y}$ from Eq. (B-18) and re-arranging terms leads to the 1st order ODE describing projectile velocity:

$$m \dot{v}_y + c v_y = -m g \quad (\text{B-19})$$

B-3 Work, energy, and power in electrical circuits (complementary to Chapter 5)

Electrical fields exist in spaces around and between charged particles or charged objects (Halliday and Resnick, 1960, Chapter 27). The *electrical field strength* \mathcal{E} (with SI units newton/coulomb) at a point in space is analogous in many respects to gravitational field strength g , as in Eq. (B-16). Suppose that an electrical field is oriented in the y direction and is constant. Experimental measurements show that the force required to sustain a particle of charge q_p without acceleration against the electrical field is

$$f_y = q_p \mathcal{E} \quad (\text{B-20})$$

² See homework Problem 1.7 for discussion of this projectile-velocity problem using both the viscous (linear) drag mathematical model and a velocity-squared (nonlinear) drag model.

Appendix B Notes on work, energy, and power in mechanical systems and electrical circuits

(This linear relationship is the basis for definition of \mathcal{E} .) Thus, charge q_p within an electrical field of strength \mathcal{E} is analogous to mass m within a gravitational field of strength g . We see from this analogy that the work required to move the charge without acceleration against the electrical field is stored conservatively as *electrical potential energy*:

$$W \equiv E_E = \int_{y=y_1}^{y=y_2} f_y dy = \int_{y=y_1}^{y=y_2} q_p \mathcal{E} dy = q_p \mathcal{E} (y_2 - y_1) \quad (\text{B-21})$$

It is customary and appropriate in electrical theory and applications to define (in analogy with the gravitational potential difference) the *electrical potential difference* in volts between two points in space as (Halliday and Resnick, 1960, Chapter 29)

$$e_2 - e_1 \equiv \mathcal{E}(y_2 - y_1), \text{ or differentially, } de \equiv \mathcal{E} dy \quad (\text{B-22})$$

With $de \equiv \mathcal{E} dy$ in Eq. (B-21), the work required to move charge q_p , work equal to the electrical potential energy, is expressed in terms of electrical potential difference as

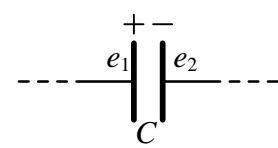
$$W \equiv E_E = \int_{e=e_1}^{e=e_2} q_p de = q_p (e_2 - e_1) \quad (\text{B-23})$$

We infer from Eq. (B-23) the SI unit equivalence: 1 volt = 1 joule/coulomb. Note the sign conventions in Eq. (B-23): work and potential energy are positive if a positive charge, $q_p > 0$, is moved to a higher electric potential, $e_2 > e_1$.

One useful application of Eq. (B-23) for electrical potential energy is to a capacitor within a circuit. Halliday and Resnick, 1960, p. 651, explain the physical process:

... work must be done to separate two equal and opposite charges. This energy is stored in the system and can be recovered if the charges are allowed to come together again. Similarly, a charged capacitor has stored in it an electrical potential energy U equal to the work W required to charge it. This energy can be recovered if the capacitor is allowed to discharge. We can visualize the work of charging by imagining that an external agent pulls electrons from the positive plate and pushes them onto the negative plate, thus bringing about the charge separation; normally the work of charging is done by a battery, at the expense of its store of chemical energy.

To derive an equation for capacitive potential energy, let's suppose that some quantity of positive charge q_+ has already been transferred from the negative plate of an ideal capacitor to the positive plate; the voltage difference between the two plates due to q_+ is expressed in terms of the capacitance C , from Eq. (5-2), as $e_{1+} - e_{2+} = (1/C)q_+$, in



Appendix B Notes on work, energy, and power in mechanical systems and electrical circuits

which e_{1+} is a higher potential than e_{2+} . From Eq. (B-23), the differential work required to transfer an additional differential quantity of positive charge dq_+ from the negative plate to the positive plate is given by

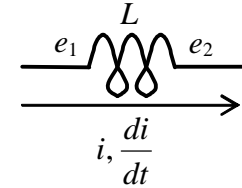
$$dW = dq_+ (e_{1+} - e_{2+}) = \frac{1}{C} q_+ dq_+ \quad (\text{B-24})$$

We integrate Eq. (B-24) to find the total work required to fully charge the ideal capacitor from zero to a quantity q , which also is the total electrical potential energy stored in the capacitor:

$$W = E_E = \int_{q_+=0}^{q_+=q} dW = \frac{1}{C} \int_{q_+=0}^{q_+=q} q_+ dq_+ = \frac{1}{2} \frac{1}{C} q^2 \quad (\text{B-25})$$

Whereas the energy of a capacitor, Eq. (B-25), is stored in an electrical field, that of an inductor is stored in the magnetic field within the inductor's coils; this magnetic field exists as a consequence of the electrical current flowing in the wire (Halliday and Resnick, 1960, Chapter 34). Even though it is magnetic field energy, we can still apply Eq. (B-23) for electrical work to determine an equation for the energy within an inductor (Halliday and Resnick, 1960, Section 36-4). From Eq. (B-23), the differential work required to move a differential quantity of positive charge dq_+ through an ideal inductor is

$$dW = dq_+ (e_{1+} - e_{2+}) \quad (\text{B-26})$$



in which e_{1+} is a higher potential than e_{2+} . This is a conservative process, so the electrical work, which might be done by a battery or some other power source, must be stored as magnetic field energy, E_M . The self-induced electrical potential difference across the inductor is given by Eq. (5-6), $e_{1+} - e_{2+} = L(di_+/dt)$. Also, current and charge are related by $i_+ = dq_+/dt$, so that $dq_+ = i_+ dt$. Therefore, we re-write Eq. (B-26) as

$$dW = dE_M = i_+ dt \times L \frac{di_+}{dt} = L i_+ di_+ \quad (\text{B-27})$$

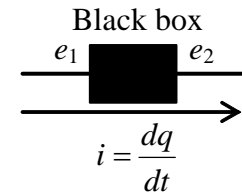
Finally, we integrate Eq. (B-27) to find the total magnetic potential energy stored in the ideal inductor for a quantity of current i :

$$W = E_M = L \int_{i_+=0}^{i_+=i} i_+ di_+ = \frac{1}{2} L i^2 \quad (\text{B-28})$$

Appendix B Notes on work, energy, and power in mechanical systems and electrical circuits

Next, we apply Eq. (B-23) for electrical work once again in order to evaluate power sources and power sinks in electrical circuits (Halliday and Resnick, 1960, Section 31-5). Consider a general component within a circuit, a “black box.”

This might be a passive component such as a resistor, a source of power such as a battery or signal generator, or a device such as a motor that converts electrical energy into another form of energy. For this derivation, let’s consider the upstream terminal of the black box to be at a higher potential than the downstream terminal: $e_1 > e_2$. Suppose that a positive differential charge dq moves through the black box from higher potential to lower potential; Eq. (B-23) shows that there is a reduction of electrical energy: $dW = dE_E = -dq(e_1 - e_2) = -i dt(e_1 - e_2)$. Electrical power also is reduced:



$$P_E = \frac{dW}{dt} = -i(e_1 - e_2) \quad (\text{B-29})$$

Equation (B-29) is an important formula that can be applied usefully for many different black boxes. We shall consider here just two of them. First, suppose that the black box is a resistor with resistance R , for which Eq. (5-1) gives $e_1 - e_2 = iR$; in this case, the downstream terminal is at lower voltage than the upstream terminal, so Eq. (B-29) becomes the following famous formula for the electrical power that is dissipated in heating the resistor:

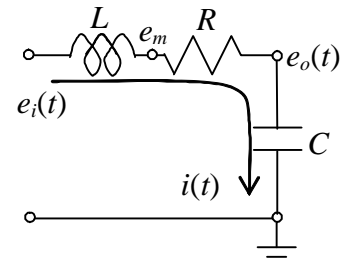
$$P_R = -i^2 R \quad (\text{B-30})$$

Next, suppose that the black box is a source of input voltage $e_i(t)$ (battery or signal generator) for a circuit; in this case, the downstream voltage $e_2 = e_i(t)$ exceeds the upstream voltage (for positive current i), so Eq. (B-29) gives the formula for electrical power introduced into the circuit by the voltage source:

$$P_e = i[e_i(t) - e_1] \quad (\text{B-31})$$

For most, if not all of the relatively simple circuits considered in this book, the upstream terminal of the voltage source is connected to the ground (zero) potential, so that $e_1 \equiv 0$ and the input power is $P_e = i e_i(t)$.

An interesting application of the equations derived in this section is to the powered LRC circuit drawn at right, from the example in Section 9-2. The total stored electromagnetic energy resides in the electrical field of the ideal capacitor and the magnetic field of the ideal inductor:



Appendix B Notes on work, energy, and power in mechanical systems and electrical circuits

$$E_{EM} = E_E + E_M = \frac{1}{2} \frac{1}{C} q^2 + \frac{1}{2} L i^2 \quad (\text{B-32})$$

The signal generator is a source of electrical power, and the resistor is a sink of electrical power, so the total electromagnetic energy varies in time:

$$\frac{d}{dt} E_{EM} = \frac{d}{dt} \left(\frac{1}{2} \frac{1}{C} q^2 + \frac{1}{2} L i^2 \right) = P_R + P_e \Rightarrow L i \frac{di}{dt} + \frac{1}{C} q \frac{dq}{dt} = -i^2 R + i e_i(t) \quad (\text{B-33})$$

Cancelling $i = \dot{q}$ out of Eq. (B-33) and re-arranging terms leads to the general ODE for charge $q(t)$ on the capacitor plates in the *LRC* circuit:

$$L \ddot{q} + R \dot{q} + \frac{1}{C} q = e_i(t) \quad (\text{B-34})$$

Since $q = C e_o$, Eq. (B-34) is essentially the same as that derived from Kirchhoff's voltage law in Section 9-2 for output voltage $e_o(t)$: $\ddot{e}_o + (R/L) \dot{e}_o + (1/LC) e_o = (1/LC) e_i(t)$.

B-4 Analogies between an *m-c-k* mechanical system and an *LRC* electrical circuit

By comparing ODEs (B-12) and (B-34) and the many other mechanical and electromagnetic equations developed in this appendix, we can identify some clearly analogous variable quantities and constants between a forced *m-c-k* mechanical system and a powered *LRC* electrical circuit (Halliday and Resnick, 1960, Section 38-2). The most obvious analogies are listed in the following table.

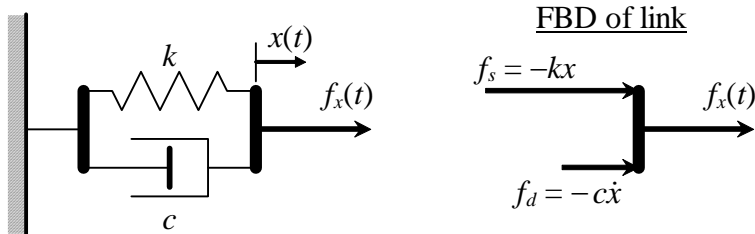
Forced <i>m-c-k</i> mechanical system	Powered <i>LRC</i> electrical circuit
mass m	inductance L
viscous damping constant c	resistance R
stiffness constant k	inverse capacitance $1/C$
position of the mass $x(t)$	charge on the capacitor $q(t)$
velocity of the mass $v_x(t) = \dot{x}(t)$	current through the circuit $i(t) = \dot{q}(t)$
excitation force $f_x(t)$	input voltage $e_i(t)$
kinetic energy $E_K = \frac{1}{2} m v_x^2$	magnetic energy $E_M = \frac{1}{2} L i^2$
strain energy $E_S = \frac{1}{2} k x^2$	electrical energy $E_E = \frac{1}{2} (1/C) q^2$
power dissipation $P_c = -c v_x^2$	power dissipation $P_R = -R i^2$
power input $P_f = f_x(t) v_x$	power input $P_e = e_i(t) i$

The mathematical similarity of an *m-c-k* system to an *LRC* circuit is one of the simpler analogies between physical systems and circuits, and there are many other analogous electrical circuits of greater complexity (Fifer, 1961, Vol. III, Chapter 19; MacNeal, 1962). In fact, during the 1940s and 1950s, methods of *direct analog computation* were

developed extensively for analysis of many physical “prototype” systems with use of electrical circuits. In the introductory chapter of a 1962 book entitled *Electric Circuit Analogies for Elastic Structures*, Richard H. MacNeal wrote (pages 6-7): “The ... direct analog computer is ... a device in which each electrical component (or group of components) is equivalent to a physical component of the prototype system.” MacNeal stated further: “This technique has been frequently used for the solution of problems concerning mechanics and elasticity, the conduction of heat, fluid flow, and electromagnetic waves.” However, during and after the mid-1960s, direct analog computation was completely eclipsed by the rapidly advancing capabilities of digital computers and software written for digital processing. It is an ironic twist of history that MacNeal himself became an innovative pioneer in the development and implementation of the finite-element method for high-precision digital computation of structural behavior.

B-5 Hysteresis and dissipation of mechanical energy by damping

Consider the ideal parallel damper-spring system of Example 3-3, shown again in the figure below, with the damper assumed to be an ideal viscous dashpot. The spring



and dashpot forces acting onto the link are depicted with arrows as positive toward the right so that they have the same polarity as translation $x(t)$. Suppose that $x(t)$ is imposed by some external agent in a steady-state sinusoidal form with frequency ω and constant amplitude X : $x(t) = X \cos \omega t$.

Accordingly, the spring force and viscous-dashpot force are, respectively,

$$f_s(t) = -kx(t) = -kX \cos \omega t \quad \text{and} \quad f_d(t) = -c\dot{x}(t) = c\omega X \sin \omega t$$

Let's examine the relationships between $x(t)$ and the two component forces as the system moves through one complete cycle. These relationships are depicted graphically on Fig. B-1, on which the points labeled 1 represent times $t = 0$ and $2\pi/\omega$ at the beginning and end of the cycle, and the points labeled 2 represent time $t = \pi/\omega$ at the middle of the cycle. On Fig. B-1(a), the loci of spring force f_s and dashpot force f_d are plotted separately versus x . Spring force f_s is exactly out of phase with x , so its locus is simply a straight line. On the other hand, dashpot force f_d lags behind x by $1/4$ of the cyclic period, since $\sin \omega t = \cos(\omega t - \pi/2)$, so that its locus forms a closed loop. A time lag such as this in cyclic motion, of an output quantity (f_d in this case) relative to an input quantity (x in this case), is generally referred to as *hysteresis*, and the locus of the output versus

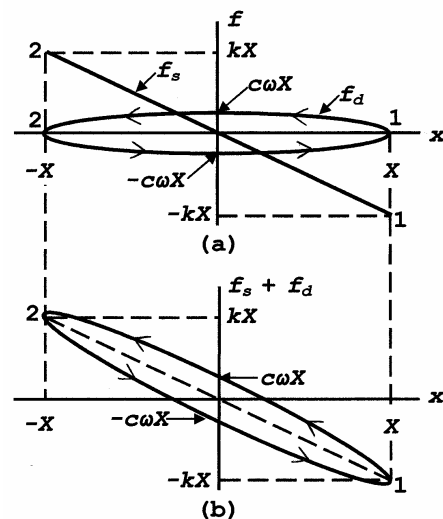


Figure B-1

Appendix B Notes on work, energy, and power in mechanical systems and electrical circuits

the input over a complete cycle is called a hysteresis loop. As shown by the following equation, this particular hysteresis loop has the simple and familiar form of an ellipse, one with semi-major axis X and semi-minor axis $c\omega X$:

$$\frac{x^2}{X^2} + \frac{f_d^2}{(c\omega X)^2} = \frac{(X \cos \omega t)^2}{X^2} + \frac{(c\omega X \sin \omega t)^2}{(c\omega X)^2} = \cos^2 \omega t + \sin^2 \omega t = 1$$

The total area A enclosed within the hysteresis loop is a significant physical quantity, and it is given for the ellipse of Fig. B-1(a) by the following simple formula from plane geometry:

$$A = \pi \times \text{semi-major axis} \times \text{semi-minor axis} = \pi c\omega X^2$$

Let's now derive the work per cycle done by each of the component forces within the damper-spring system. From Eq. (B-2) the work per cycle of viscous-damper force $f_d(t)$ is $\oint f_d dx$, in which the symbol \oint denotes that the integration path covers one complete circuit around the loop, from point 1 to point 2 on the curve of $f_d \geq 0$ of Fig. B-1(a), and then from point 2 back to point 1 on the curve of $f_d \leq 0$:

$$\begin{aligned} W_d &= \oint f_d dx = \overbrace{\int_{x=-X}^{x=+X} f_d dx}^{f_d \geq 0} + \overbrace{\int_{x=-X}^{x=+X} f_d dx}^{f_d \leq 0} = - \overbrace{\int_{x=-X}^{x=+X} f_d dx}^{f_d \geq 0} + \overbrace{\int_{x=-X}^{x=+X} f_d dx}^{f_d \leq 0} \\ &= -\left(\frac{1}{2} A\right) + \left(-\frac{1}{2} A\right) = -A \end{aligned} \quad (\text{B-35})$$

In the second form above for the integral over the path of $f_d \geq 0$, the limits of integration have been reversed, which accounts for the sign change of that entire integral. Therefore, the work per cycle done by the viscous damper is simply the entire area enclosed within the hysteresis loop, $W_d = -\pi c\omega X^2$. Now, having completed carefully the derivation of work per cycle for $f_d(t)$, we can recognize without the necessity of any further mathematical derivation that the work per cycle done by any cyclic force that moves through a cyclic path of translation is simply the area enclosed within the hysteresis loop, even though the loop might not be a simple ellipse such as that for viscous-damper force $f_d(t)$. One immediate application of this general result is that the work per cycle done by spring force $f_s(t)$ is zero, $W_s = 0$; for, as shown on Fig. B-1(a), the path of $f_s(t)$ for x decreasing from point 1 to point 2 is exactly the same as the path for x returning from point 2 back to point 1, so this hysteresis “loop” collapses to a line that encloses zero area. Therefore, the total work per cycle done by the viscous-damper-spring system is the sum

$$W_{d-s} = W_d + W_s = -\pi c\omega X^2 + 0 = -\pi c\omega X^2 \quad (\text{B-36})$$

The polarity of W_{d-s} is negative because the damper-spring system actually dissipates mechanical energy. In a real solid structural component (which is discussed next), the

Appendix B Notes on work, energy, and power in mechanical systems and electrical circuits

dissipated mechanical energy does not disappear, but rather is converted into thermal energy that raises the temperature of the component.

Imagine now that the damper-spring system is a solid, distributed-parameter structural component of some sort, *e.g.*, a metal tensile-test specimen, or a hard rubber pad of the type used to support heavy machines. If we were conducting a cyclic tensile test on this component, we would be able to measure its deformation, comparable to $x(t)$ on Fig. B-1. But the structural component could not be separated into a discrete damper and a discrete spring, so we would be able to measure directly only the total resisting force of the component, comparable to $f_d(t) + f_s(t)$, but not individual damper and spring forces. Therefore, Fig. B-1(b) is more representative than Fig. B-1(a) of actual physical measurements. A thoughtful study of Eq. (B-35) should convince you that, even though the hysteresis loop of Fig. B-1(b) is not a true ellipse, the area that it encloses, and the work per cycle done by the viscous-damper-spring system, is still

$$W_{d-s} \equiv W_\zeta = \oint (f_d + f_s) dx = -\pi c \omega X^2 \quad (\text{B-37})$$

The symbol W_ζ is introduced in Eq. (B-37), with subscript ζ indicating that this particular equation applies for the linear viscous-damping mathematical model, $f_d = -c\dot{x}$, since ζ is the standard symbol for viscous-damping ratio in vibrating systems.

For over a century now, experimental measurements on distributed-parameter structural components have demonstrated that the linear frequency dependence of mechanical-energy dissipation in Eq. (B-37) is unrealistic (Love, 1926, pp. 117-121, Kimball and Lovell, 1927; Ungar, 1998). The subject of damping in solids under loading is very complicated (see books by Lazan, 1967; Nashif, *et al.*, 1985; and de Silva, 2007): different solid materials behave differently, of course, and even the same material usually behaves differently after different time-histories of loading, temperature, exposure to corrosion or chemicals, *etc.* Nevertheless, laboratory measurements with structural metals and elastomers (rubber-like materials), at stresses below yield and fatigue endurance limits, generally show that mechanical-energy dissipation (conversion of mechanical energy into heat energy) is not proportional to excitation frequency, as predicted by the viscous-damping model, but, instead, is much more weakly dependent on frequency. For this reason, engineers have developed an alternative, simple, linear, approximate mathematical model of damping, for which mechanical-energy dissipation is specified to be independent of frequency. Further for this model, the energy dissipation is specified to be proportional to the stiffness of a solid structural component, which is at least plausible physically. Thus, for this alternative model, we replace the term $c \times \omega$ in Eq. (B-37) with the term $k \times \eta$, in which constant of proportionality η is generally called the damping *loss factor*. Accordingly, the work per cycle for this model, denoted as W_η , is written as

$$W_\eta = -\pi k \eta X^2 \quad (\text{B-38})$$

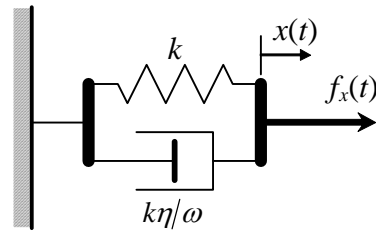
Engineers have used this mathematical model of damping at least since the 1940s (Bisplinghoff, *et al.*, 1955, pp. 558-568), but, unfortunately, there is no standard, recognized

name for it in engineering literature.³ We shall call it the *internal-friction model*, in recognition of the 1927 article entitled “Internal Friction in Solids” by Kimball and Lovell, who reported the first experimental measurements of energy dissipation that is independent (or nearly so) of cyclic frequency.

We derived Eq. (B-38) for damping energy dissipation by replacing $c \times \omega$ in Eq. (B-37) with $k \times \eta$. Next, we need for the internal-friction model a corresponding linear equation for damping force that can be used directly in ODEs of motion, an equation comparable to $f_d = -c\dot{x}$ for the viscous-damping model. Based only upon algebra, if $k \times \eta$ replaces $c \times \omega$, then $k\eta/\omega$ replaces c , and the desired equation is

$$f_d = -(k\eta/\omega)\dot{x} \quad (\text{B-39})$$

Accordingly, the figure at right depicts a damper-spring system for the internal-friction model, and the ODE for this simple system is

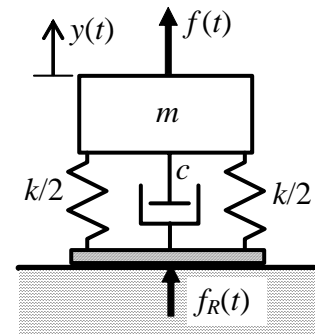


$$(k\eta/\omega)\dot{x} + kx = f_x(t) \quad (\text{B-40})$$

Question: If we want to apply damping force $f_d = -(k\eta/\omega)\dot{x}$ for general motion $x(t)$, we can probably find values for material constants k and η , but what value should we use for ω , since general motion is not necessarily steady-state sinusoidal?

Answer: Damping force $f_d = -(k\eta/\omega)\dot{x}$ is mathematically consistent only for steady-state sinusoidal motion at known frequency ω , so, in general, this equation for internal-friction-model force should be used only in frequency-response derivations and calculations. (However, engineers and physicists occasionally bend the rule a bit and use this model for more general structural motion that consists primarily of lightly damped vibration, by setting ω equal to the dominant natural frequency of the system.)

An interesting and practically relevant application of the internal-friction model of structural damping is to passive *vibration isolation*, which is described in homework Problem 10.13 for the viscous-damping model. The drawing from Problem 10.13 is reproduced at right. A mass m (often a machine that includes unbalanced rotating or translating parts) is supported on elastomeric padding. The padding is modeled as an ideal shock strut (from Example 3-3), with a spring of stiffness constant k and, on the drawing, a viscous damper of constant c ; here we shall consider as well elastomeric padding with the internal-friction damping model, which is more realistic than the viscous-damping model. Dynamic force $f(t)$ is applied to m , by either external or internal agents, and



³ Perhaps the most common name used is “hysteretic damping”, but that name is misleading because every form of solid damping involves hysteresis.

Appendix B Notes on work, energy, and power in mechanical systems and electrical circuits

dynamic reaction force $f_R(t)$ is transmitted through the padding to the supporting structure. The purpose of passive vibration isolation in this form is to protect the supporting structure, with the flexible padding designed so as to minimize the transmitted dynamic force $f_R(t)$.

Part of the assignment in Problem 10.13 is to derive the transfer function $TF(s) = F_R(s)/F(s)$ relating the floor-reaction dynamic force to the excitation force and then to show that the corresponding complex frequency-response function, known as *transmissibility*, is

$$TF(j\omega) \equiv FRF(\omega) \equiv \frac{F_R(\omega)}{F} e^{j\phi(\omega)} = -\frac{1 + j2\zeta\beta}{(1 - \beta^2) + j2\zeta\beta}$$

where $\zeta \equiv c/(2\sqrt{mk})$ and $\beta \equiv \omega/\omega_n = \omega/\sqrt{k/m}$. Therefore, the magnitude of transmissibility, which we denote as $T_\zeta(\omega)$ for the viscous-damping model, is

$$T_\zeta(\omega) \equiv |FRF(\omega)| = \sqrt{\frac{1 + (2\zeta\beta)^2}{(1 - \beta^2)^2 + (2\zeta\beta)^2}} \quad (\text{B-41})$$

For the internal-friction model, the viscous-damping constant c is replaced by the term $k\eta/\omega$, Eq. (B-39). Frequency-response functions that are derived for a mathematical model based upon viscous damping can be converted easily to apply for internal-friction damping, without the necessity of a complete re-derivation. To show this, we write below the mass-damper-spring ODEs for the viscous-damping and internal-friction models and then express these ODEs in terms of ζ , ω_n , and β :

$$\text{Viscous: } m\ddot{y} + c\dot{y} + ky = f(t) \quad \text{Internal friction: } m\ddot{y} + (k\eta/\omega)\dot{y} + ky = f(t)$$

$$\ddot{y} + \frac{c}{m}\dot{y} + \frac{k}{m}y = \frac{f(t)}{m} = \frac{k}{m}\frac{f(t)}{k}$$

$$\ddot{y} + \frac{k}{m}\frac{\eta}{\omega}\dot{y} + \frac{k}{m}y = \frac{f(t)}{m} = \frac{k}{m}\frac{f(t)}{k}$$

$$\ddot{y} + 2\frac{c}{2\sqrt{mk}}\sqrt{\frac{k}{m}}\dot{y} + \omega_n^2 y = \omega_n^2 \frac{f(t)}{k}$$

$$\ddot{y} + \omega_n^2 \frac{\eta}{\omega}\dot{y} + \omega_n^2 y = \omega_n^2 \frac{f(t)}{k}$$

$$\ddot{y} + (2\zeta)\omega_n\dot{y} + \omega_n^2 y = \omega_n^2 \frac{f(t)}{k}$$

$$\ddot{y} + \left(\frac{\eta}{\beta}\right)\omega_n\dot{y} + \omega_n^2 y = \omega_n^2 \frac{f(t)}{k}$$

From the terms in parentheses in the final forms of the two ODEs, we see that replacing 2ζ with η/β , everywhere 2ζ appears in any response equation derived from the viscous-damping ODE, will convert the response equation to apply for internal-friction damping. We note that engineers sometimes carelessly assert that the two types of damping are equivalent if we simply equate 2ζ with η . That assertion is clearly incorrect; for, even if

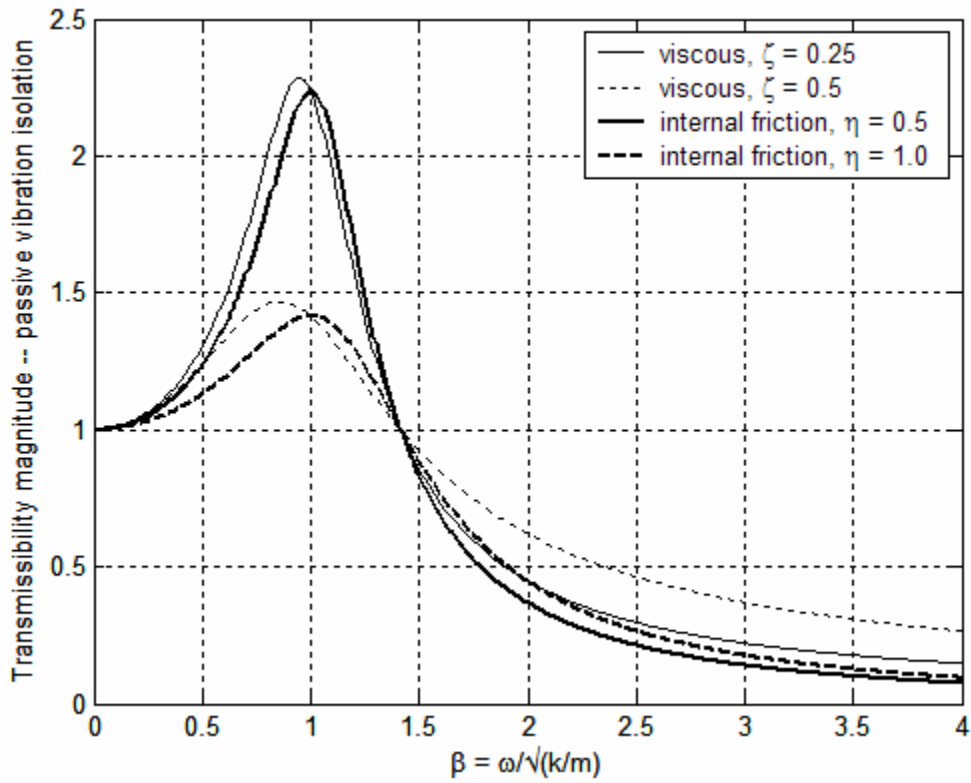
Appendix B Notes on work, energy, and power in mechanical systems and electrical circuits

$2\zeta = \eta$, the only frequency at which frequency-responses of the two different models are certain to be equal is $\omega = \omega_n$, $\beta = 1$.

Using the replacement $2\zeta \rightarrow \eta/\beta$ in Eq. (B-41) for the viscous-damping-model transmissibility $T_\zeta(\omega)$ gives the equation for transmissibility $T_\eta(\omega)$ that is applicable for internal-friction damping:

$$T_\eta(\omega) = T_\zeta(\omega) \Big|_{2\zeta \rightarrow \eta/\beta} = \sqrt{\frac{1 + (2\zeta\beta)^2}{(1 - \beta^2)^2 + (2\zeta\beta)^2}} \Big|_{2\zeta \rightarrow \eta/\beta} = \sqrt{\frac{1 + \eta^2}{(1 - \beta^2)^2 + \eta^2}} \quad (\text{B-42})$$

Equation (B-41) is plotted below for $\zeta = 0.25$ and 0.5 , and Eq. (B-42) is plotted for the two values of η that produce the same transmissibility magnitude at $\beta = 1$ as the corresponding ζ values, namely, $\eta = 0.5$ and 1.0 , respectively. The plotted values, especially those for $\beta > \sqrt{2}$, demonstrate why it is good that the frequency responses of real elastomeric vibration isolators are much closer to the predictions of the internal-friction model than to those of the viscous-damping model (Ungar, 1998).



Index of all Chapters and Appendices

A

abs MATLAB function, 2-3, 4-16
 absolute stability, 16-18, 17-1
 absolute unit system, 3-1
 AC = aerodynamic center, 11-7
 acceleration, 10-13
 acceleration in G 's, 1-19
 accelerometer, 7-17, 9-9, 9-24, 10-13, 10-25, 10-27, 15-4
 actions = forces or moments, 11-2
 active system, 7-1, 16-18
 actuator, dynamics, 15-4
 ..., position, 15-4, 15-19
 adapting standard solutions, 3-7, 7-3, 7-17, 7-19, 7-20, 9-4, 9-5, 9-21, 9-31, 10-21, 11-6, 13-4, 14-11
 added-mass (-inertia) method, 7-22, 12-18
 adjoint matrix, 12-3
 admittance, electrical, 10-11
 ..., mechanical, 10-12
 aerodynamic center (AC) of a wing section, 11-7
 aerodynamics, coefficients, 1-21, 3-8, 11-8, 16-43
 ..., drag, 1-20
 ..., rolling moment, 3-8
 ..., quasi-static, 11-9, 16-42
 aeroelasticity, divergence and flutter, 11-7, 16-41
 aeronautical unit system, 3-1
 aileron, 3-8, 11-9
 air density, 1-21, 3-9, 3-18, 11-8, 16-43
 air-jet thruster, 8-28
 airplane, aileron, 3-8, 11-9
 ..., blowdown moment, 11-9
 ..., Boeing 747, 3-18
 ..., bomb release, 9-28
 ..., brake release, 7-6
 ..., Douglas A-4 Skyhawk, 3-18
 ..., landing contact, 7-9, 7-19
 ..., rolling, 3-8, 9-14
 ..., trimming tab, 11-13
 ..., wing, 3-8, 11-7, 11-9
 airspeed, free-stream, 3-9
 algorithms, numerical, for 1st order ODE, 6-7, 6-12, 8-15, 8-20
 ..., ..., for 2nd order ODE, 8-15, 8-22
 aluminum flat, 7-21
 amp, ampere (A), unit of electrical current, 5-1
 amplification, dynamic, 10-2
 amplifier, inverting, 5-10
 ..., non-inverting, 5-16
 ..., summing inverting, 5-16
 amplitude modulator, 10-15
 analog computation, direct, B-8
 analog computer, electronic, 5-15, 5-17, 7-20, 9-31, 10-31
 analogous systems, 5-6, B-8
 angle MATLAB function, 2-3, 4-16
 angle of a complex number, 2-2
 angle of attack of a wing section, 11-8
 antenna, 7-20
 apparent frequency of beating, 10-16

apparent mass, 10-14
 approximate numerical solutions, 6-8, 8-15, 9-14
 ..., convolution sum, 8-15, 9-14
 ..., recurrence formulas, 6-8, 6-10, 6-12
 arctangent, four-quadrant, 2-2
 argument of a complex number, 2-2
 array multiplication, MATLAB, 1-16, 9-23, 9-27
 arrow, double-headed, 3-4
 artificial spring, 14-7, 15-14
 artificial viscous damper, 12-19, 14-16, 15-15
 asymptotes, loci of roots, 16-32
 ..., low- and high-frequency, 4-7
 atan2 MATLAB function, 2-2
 attitude (vehicle rotational orientation), 14-1, 14-4, 15-19
 automotive vehicle, 11-15, 12-14
 axis equal MATLAB function, 16-28

B

balloon carrying a basket, 7-3, 7-9, 7-18
 band-pass filter, 5-12, 9-21, 9-31, 13-1
 base excitation, 9-23, 10-20, 10-21, 10-25, 12-13, 13-2, 13-4, 14-7
 baseball, 1-20
 baseline, transfer and frequency-response function, 17-8
 battery, electrical, 5-1
 beam, structural, 7-9, 7-22
 beating of vibrating systems, 1-24, 10-14, 10-31
 beating period and frequency, 10-16
 black box, general circuit component, B-7
 block diagram, algebra, 13-2, 14-8, 14-15, 14-18
 ..., closed-loop, 13-2
 ..., junctions, 13-3
 ..., Laplace, 13-1
 ..., open-loop, 13-2
 blowdown moment, 11-9
 Bode diagram, 4-6, 10-11, 17-4, 17-7
 Boeing 747 airplane, 3-18
 branch point junction, 13-3
 branch, feedforward, 14-18
 ..., forward or feedback, 13-2
 break frequency, 4-6
 break-away point, 16-20, 16-24
 break-in point, 16-20, 16-24
 buoyancy force, 7-18

C

cantilever (ideally clamped-free) beam, 7-12, 7-22
 capacitors, circuit components, 5-3
 ..., in parallel, 5-14
 ..., in series, 5-14
 ..., potential energy, B-5
 capsule (re-entry vehicle), 14-3
 Cartesian coordinates x and y , 2-2
 Cartesian xyz axis system, 11-1
 causality of transfer function, 4-12, 15-13, 15-18
 cavity resonator, 7-20

Index of all Chapters and Appendices

- center of mass, 11-1
- characteristic equation, 1st order ODE, 1-7
 - ..., 2nd order ODE, 1-22
 - ..., damped 2nd order system, 9-1
 - ..., free-vibration problem, 12-4, 12-10
 - ..., n^{th} order, 16-2, 16-43
 - ..., polar form, 16-25
- characteristic time, 8-11
- characteristic values, 1st order ODE, 1-7
 - ..., 2nd order ODE, 1-22
- charge, electrical, 5-3, B-4
- circular frequency (radians/second), 1-6, 1-17, 4-8
- clamped beam, non-ideal support, 7-16
- classical control theory, 14-17
- closed loop, 13-2
 - ..., control, 14-6
 - ..., transfer function (CLTF), 13-4, 14-8, 17-2
 - ..., circuit for op-amp, 5-10, 15-2
- CLTF = closed-loop transfer function, 13-4
 - ..., general formulas, 14-9
 - ..., P control, 15-6, 15-14
 - ..., PD control, 15-15
 - ..., PI control, 15-8
 - ..., position + rate feedback, 14-15
 - ..., position feedback, 14-9
- coil of conducting wire, 5-6
- coincident frequency-response component, 17-10
- command, 1-2
 - ..., control, 9-14, 13-4, 14-1, 14-2
- common open-loop system, 17-7, 17-17
- compensator, 16-36
- complementary solution of an ODE, 1-6
- complex, arithmetic, 2-3
 - ..., conjugate, 2-4
 - ..., function $F(s)$, 2-6
 - ..., number $z = x + jy$, 2-1
 - ..., variable $s = \sigma + j\omega$, 2-6
- compliance, dynamic, 10-13
- component of a system, 1-1
- concentrated mass, 7-15
- conjugate of a complex number, 2-4
- conservative system, B-2
- consistent mass, 7-23
- continuity condition, 5-2
- control, actuators and sensors, 15-4
 - ..., $m-c-k$ system by base excitation, 13-4
 - ..., open-loop, 14-2, 14-6
 - ..., output feedback, 14-14
 - ..., P, 15-2, 15-6, 15-14
 - ..., PD, 15-2, 15-13, 15-14
 - ..., PI, 15-2, 15-8
 - ..., PID, 15-1
 - ..., remote (indirect), 14-1
- controller (control processor, filter), 15-1
- control theory, classical and modern, 14-17
- control-moment gyroscope (CMG), 12-13, 14-5
- `conv` MATLAB function, 6-2, 8-19, 8-26, 16-43
- convolution integral, 6-1, 6-3, 6-8, 7-1, 7-3, 9-7, 9-14, 9-21, 9-30
 - ..., Laplace transform of, 6-1, A-7
- convolution sum, 6-2, 8-15, 8-17, 9-14
- coordinates, Cartesian, 11-1
- ..., polar, 11-4
- corner frequency, 4-7
- coulomb, unit of electrical charge, 5-3
- coupled ODEs, 1-12, 3-14, 11-1, 11-11, 13-7
- critical viscous damping constant, 9-1, 10-19, 16-34
- critically damped 2nd order system, 9-2, 9-28
- crossovers, phase and gain, 17-6
- cruise-control system, 15-17
- cyclic frequency (cycles/second), 1-17, 4-8

D

- damped natural frequency, 9-3, 14-20
- damper-spring ($c-k$), parallel system, 3-13, 4-2
 - ..., series system, 3-14, 4-16, 4-17, 5-6, 5-14, 15-3
- damping laws, nonlinear, 3-12
 - structural internal-friction, B-12
 - structural viscous, B-9
- dashpot (mechanical viscous damper), 3-12
- decibel (dB) scale, 4-7, 10-11, 17-6
- definite integral, Laplace transform of, 2-14, A-5
- degrees of freedom (DOFs), 11-2, 11-10, 12-1, 16-41
- density of air, 1-21, 3-9, 3-18, 11-8, 16-43
- departure angles, loci of roots, 16-32
- derivative time constant, 15-1, 15-13, 15-16
- derivative, Laplace transform of, 2-8
- design, control system, 14-21, 15-2, 15-11, 15-16, 15-17, 16-28, 16-36, 17-22
- determinant of a matrix, 12-3
- DFBD = dynamic free-body diagram, 7-7, 11-5, 12-2
- dielectric (insulating) material, 5-3
- differentiator, approximate, 15-13, 15-18
 - ..., exact, 15-18
- digital camera, 7-11
- Dirac delta function, 8-3, 16-40
- direct term of partial-fraction expansion, 2-19, 15-19
- distributed-parameter system, 7-9
- disturbance, 1-2
 - ..., internal or external, 14-3, 14-5
 - ..., response of controlled system, 14-8, 14-18, 14-20, 15-17
- divergence, aeroelastic, 11-7, 16-22, 16-43
- DOF = degree of freedom, 11-2
- dominant modes of response, 16-30, 16-43
- dot notation, 1-2
- Douglas A-4 Skyhawk airplane, 3-18
- `dsolve` MATLAB operation, 1-20, 1-23
- Duhamel integral, 8-15
 - ..., 2nd order ODE with RHS dynamics, 9-30
 - ..., underdamped 2nd order system, 9-14
- dummy variable of integration, 1-4, 6-1
- duration of pulse, 1-6
- dwell, vibration testing, 10-8, 17-25
- Dynamax and Dynamobile, 1-18
- dynamic, behavior, general definition, 1-1
 - ..., flexibility, 10-8, 10-13, 10-31
 - ..., free-body diagram (DFBD), 7-7, 11-5, 12-2
 - ..., pressure, 1-21, 3-8, 11-8, 11-9, 16-43
 - ..., stiffness, 10-8, 10-13, 10-31

Index of all Chapters and Appendices

E

e, the base of natural logarithms, 1-6
 EA = elastic axis of a flexible wing, 11-7
 elastomers, 10-26, B-11, B-12
 electrical, current, 5-1
 ..., field strength, B-4
 ..., potential (voltage), 5-1, B-5
 ..., potential energy, B-5
 electromagnetic force shaker, 10-30
 element of a system, 1-1
 emf (electromotive force), self-induced, 5-6
 energy, dissipation, B-2
 ..., kinetic, B-2
 ..., potential. *See* potential energy
 ..., sinks and sources, 16-18, B-3, B-7
 engineering models, 1-5
 equations of plane motion, 11-1
 error, signal, 14-6
 ..., propagation of, 7-21
 ..., steady-state output, 15-7
 Euler's equation, 2-3
 Evans, Walter R., 16-28
 excitation, general definition, 1-2
 existence of Laplace transforms, 2-10
 exponential, decay, 1st order, 3-6
 ..., envelope, 16-4
 ..., ..., underdamped 2nd order system, 9-8
 ..., rise, 1st order, 3-7
 ..., stability, 16-3
 ..., unit-impulse function, 8-30, 16-5
 ..., unit-step function, 1-23, 8-30, 16-5
 external disturbance, 14-3

F

Faltung, 8-19
 farad (F), unit of electrical capacitance, 5-3
 FBD = free-body diagram, 1-3
 feed across, block diagram, 13-7
 feedback control, 7-1, 13-1, 14-1
 feedback MATLAB function, 15-20
 feedback, block diagram, 13-2, 13-3
 ..., for an op-amp, 5-10
 ..., output, 14-6, 14-11
 ..., unity, 14-10, 14-18, 14-19
 feedforward branch, 14-18
 field strength, electrical, B-4
 ..., gravitational, B-4
 filter, 2nd order low-pass, 10-7, 16-35
 ..., band-pass, 5-12, 9-21, 9-31, 10-10, 13-1
 ..., controller, 15-1
 ..., damper-spring, 3-14, 3-19, 4-8, 4-16, 4-17, 5-6,
 5-14, 14-18
 ..., high-pass, 4-17, 5-12, 5-14
 ..., low-pass, 4-8, 4-16, 5-4, 5-12, 16-13
 ..., RC band-pass, 5-12, 10-10, 13-1
 ..., RC high-pass, 5-12, 5-14
 ..., RC low-pass, 5-4, 5-12
 final-value theorem, application, 15-6, 15-8, 15-16
 ..., derivation, 15-12
 first (1st) order, LTI ODE, 1-2, 1-19

..., system, 1-4
 flat impulse, 8-3
 flat pulse, 6-11, 8-1, 9-32
 flexibility, dynamic, 10-8, 10-13
 ..., static, 10-8
 flutter, aeroelastic, 11-7, 11-10, 16-41
 folding, 8-17
 forced response, 6-3
 ..., approximate numerical, 6-8, 8-15, 9-14
 forcing function, general definition, 1-2
 forward Laplace transform, 2-6
 forward path or branch, 13-2
 Fourier series, 7-14
 four-quadrant arctangent, 4-10
 four-quadrant tangent, 4-4
 fourth (4th) order system, 3-14, 11-11, 13-7
 free vibration, undamped 2nd order system, 7-4, 12-1
 ..., distributed-parameter system, 7-10
 ..., undamped 2-DOF system, 12-2
 ..., undamped 2nd order system, 12-2
 free-body diagram (FBD), 1-3, 3-4, 7-9, 11-14, 11-15
 frequency of sinusoidal signal, circular (radians
 /second), 1-17
 ..., cyclic (cycles/second = Hz), 1-17
 frequency response, 4-1, 10-1, 17-1
 frequency, circular and cyclic, 1-17, 4-8
 frequency, excitation, 10-3
 FRF = frequency-response function, 4-6
 ..., damped 2nd order, 10-2
 ..., general definition, 4-12, 10-11
 ..., general derivation, 4-12
 ..., *m-c-k* system, 4-18, 10-8
 ..., open-loop (OLFRF), 17-1
 ..., RC band-pass filter, 10-10, 10-24
 ..., stable 1st order system, 4-6, 4-10
 ..., stability criteria, 17-1
 ..., undamped 2nd order system, 10-1

G

g, gravitational acceleration, 3-2
 gain, crossover, 17-6, 17-16, 17-22, 17-23
 ..., margin (GM), 17-6, 17-16
 ..., control parameter, 17-2
 ..., proportional, 15-1, 15-16
 general response solution, 1st order system, 6-7
 ..., stable 1st order system, 6-2
 ..., undamped 2nd order system, 7-3
 ..., underdamped 2nd order system, 9-6
 generalized functions, theory, 8-4
 gimbal, 9-5
 graphics, electrical circuits, 5-4
 ..., engineering, 1-10
 gravitational, field strength, B-4
 ..., potential difference, energy, B-4
 ..., unit system, 3-1
 ground voltage, 5-4
 gyroscope, control-moment (CMG), 12-13, 14-5
 ..., rate, 9-4, 9-32, 15-4
 ..., rate-integrating, 9-32, 15-4

Index of all Chapters and Appendices

H

half-amplitude formula, small damping, 9-11
 half-sine pulse, 1-6, 6-4
 hammer strike, 9-19, 9-25, 9-29
 Heaviside unit-step function, 2-12, 3-5
 helicopter rotor blade, 11-3
 henry (H), unit of inductance, 5-6
 higher-order, ODEs, 3-14, 11-1, 12-2
 ..., systems, 12-8, 13-7
 high-frequency asymptote, 4-7
 high-pass filter, 4-17, 5-12, 5-14
 ..., approximate differentiator, 15-13, 15-18
 ..., damper-spring, 3-15, 3-19, 14-18
 homogeneous solution, 1st order ODE, 1-6
 ..., damped 2nd order ODE, 9-1
 ..., undamped 2nd order ODE, 7-4, 12-1
 ..., undamped 2-DOF system, 12-3
 horsepower (hp), traditional unit of power, B-2
 hydroplaning, 1-18
 hyperbolic, cosine and sine, 2-18, 15-10
 ..., functions, 9-8, 9-20
 hysteresis, B-9
 Hz (hertz) = cycles/second, 1-17, 4-1

I

IC = initial condition, 1-4
 ideal, impulse, 8-3
 ..., shock strut, 3-13
 idealized physical model, 1-5
`i laplace` MATLAB function, 17-29, A-3
 imaginary number, 2-1
 impedance, electrical, 10-11
 ..., low output, 5-13
 ..., mechanical, 10-13
 impulse of force, 8-3, 9-19
 impulse response, 8-5, 8-7, 8-9
 ..., ideal vs. real, 8-10
 ..., underdamped 2nd order system, 9-13
 impulse-momentum theorem, 8-3, 14-4
 indeterminate form 0/0, 12-4
 inductor, circuit component, 5-6
 ..., potential energy, B-6
 inertance, 10-13
 inertia matrix, 11-11, 12-2
 inertial, force, 3-12, 3-14
 ..., moment, 11-2
 ..., reference, 11-1
 initial conditions (IC), 1-4
 ..., 2nd order, 1-13
 ..., 2-DOF system, 12-1
 ..., distributed-parameter system, 7-10
 ..., n^{th} order, 16-1
 initial-condition (IC) response, 6-3
 ..., 1st order, 3-5
 ..., 2-DOF system, 12-7
 ..., 3rd order system, 16-15
 ..., distributed-parameter system, 7-10
 ..., n^{th} order, 16-3
 ..., undamped 2nd order system, 7-4
 ..., underdamped 2nd order system, 9-8

initial-value theorem, application, derivation, 8-7
 in-phase, sinusoidal response, 4-6
 ..., motion, 2-DOF IC response, 12-7
 ..., frequency-response component, 17-10
 input resistance, 5-9
 input, general definition, 1-2
 ..., reference for control, 14-2, 14-4
 input-error operations, 14-14, 15-1
 instability, 16-3, 16-6, 16-11, 16-18, 16-20
 ..., by linear drift, 17-14, 17-28
 ..., degree of, 16-20
 integral time constant, 15-1, 15-11
 integrating factor, 6-7
 integration, by parts, 2-7
 ..., approximate, 10-27
 integrator, electronic circuit, 7-20, 9-31
 ..., op-amp circuit, 5-15
 internal disturbance, 14-3
 internal-friction model of structural damping, 10-27, B-12
 inverse Laplace transform, 2-7
 inverse matrix, 12-3
 inverse tangent, four-quadrant, 2-2
 IRF = unit-impulse-response function, 8-13
 ..., 2nd order ODE with RHS dynamics, 9-30
 ..., underdamped 2nd order system, 9-14

J

j = unit imaginary number, 2-1
 joule (J), SI unit of work, B-1
 junction, block diagram, 13-3
 ..., branch point, 13-3
 ..., summing, 13-3

K

KCL = Kirchhoff's current law, 5-2, 5-3
 kilogram force (kg_f), 3-2
 kinetic energy, B-2
 KVL = Kirchhoff's voltage law, 5-7, 5-15

L

l'Hospital's rule, 1-25, A-4
 labor-saving method, partial-fraction expansion, 2-9, 4-14
 Lagrange's equations, B-3
 Laplace block diagram, 13-1
 ..., 2-DOF system, 13-7
 ..., $m\cdot c\cdot k$ system with base excitation, 13-3
 ..., output feedback, 14-8
 ..., stable 1st order system, 13-7
`laplace` MATLAB function, A-3
 Laplace transform, 2-5
 ..., pairs, table of, A-1
 LC electrical circuit, 7-20
 leading-lagging rotation, 11-3
 Leibnitz's rule, A-5
 linear algebraic equations, 12-3
 linear, constant-coefficient ODEs, 1-1

Index of all Chapters and Appendices

- linear, time-invariant (LTI) system, 1-1
linearity of an ODE, 1-2
linearized ODE, 7-3, 7-18
linearly independent functions, 1-7
linear-system theory, 8-13, 8-14
liquid-layer damping, 1-12
loci (or locus) of roots, 16-18, 16-22, 16-31, 17-17
logarithmic decrement, 9-10
loss factor, structural damping, B-11
low-frequency asymptote, 4-7
low-pass filter, 4-8, 4-16, 5-4, 5-12, 16-13
... , damper-spring, 3-15, 15-3
... , 2nd order, 10-7, 16-35
LRC electrical circuit, 5-15, 9-4, 9-29, 10-6, 10-23, B-7
LTI = linear, time-invariant, 1-1, 8-13
lumped-parameter system, 7-9
- M**
- Mach number, 3-9
MacNeal, Richard H., B-9
magnetic field energy, B-6
magnitude of a complex number, 2-2
magnitude ratio, sinusoidal response, 4-5, 17-3
margin MATLAB function, 17-7, 17-24
margins, gain and phase, 17-6
mass center, 11-1
mass, apparent, 10-14
mass, translational inertia, 1-3
mass-damper (*m-c*) system, 1-3
mass-damper-spring (*m-c-k*) system, 1-12, 1-22, 3-13, 7-1, 9-1, 9-18, 10-7, 10-19, 13-2, 13-4, 14-12, 16-21, 16-34, B-3
mass-spring (*m-k*) system, 1-13, 2-18, 7-1, 12-1, 14-7
Mathematica, 1-20
mathematical model, 1-5
MATLAB, 1-1
... , Symbolic Math Toolbox, 1-20, 16-40, A-3
MATLAB functions, operations, *abs*, 2-3, 4-16
 angle, 2-3, 4-16
 array multiplication, 1-16, 9-23, 9-27
 atan2, 2-2
 axis equal, 16-28
 bode, 17-7, 17-24
 conv, 6-2, 8-19, 8-26, 16-43
 dsolve, 1-20, 1-23
 feedback, 15-20
 ilaplace, 17-29, A-3
 laplace, A-3
 margin, 17-7, 17-24
 plot3, 17-26
 pretty, 1-20
 residue, 2-19, 16-16, 16-40
 roots, 12-16, 16-23, 16-43
 series, 15-20
 simple, 1-20
 syms, 1-20, 1-23, A-3
 tf, 15-20, 17-7
 vpa, 16-40
- MATLAB script M-file, 1-9, 1-15, 4-3, 4-16, 10-3, 12-11, 15-10, 16-10, 16-16, 16-23
matrix, notation, 12-3
 ..., equations of motion, 11-11, 12-2, 12-9, 12-13, 12-14, 12-15, 16-41
 ..., 2-DOF mode shapes, 12-6, 12-7
 ..., adjoint of, 12-3
 ..., determinant of, 12-3
 ..., inverse of, 12-3
 ..., positive definite, 11-11, 11-15, 12-2
 ..., zero determinant (singular), 12-3, 16-43
Maxwell's equations of electromagnetism, 5-6
mechanical admittance, 10-31
mechanics of materials, 7-12, 7-23
mho, electrical impedance unit, 10-12
MIMO = multiple-input-multiple-output, 14-17, 16-42
missile, rolling, 3-8
mobility, 10-13
modal analysis, 12-8
mode shapes, 2-DOF system, 12-6
models (engineering, idealized physical, mathematical), 1-5
modern control theory, 14-17
modes of response, 16-25, 16-30
 ..., dominant, 16-25, 16-30, 16-40
modes of vibration, 2-DOF system, 12-6
 ..., distributed-parameter system, 7-14
 ..., *n*th order system, 16-30
mode-shape matrix, 12-7
modulus of a complex number, 2-2
modulus of elasticity (Young's modulus), 7-12
moment of inertia, rotational inertia, 3-3
 ..., area, 7-12
musical instrument, 7-14
- N**
- natural frequencies of vibration, 2-18
 ..., 2-DOF system, 12-5
 ..., distributed-parameter system, 7-14
 ..., damped, 9-3, 14-20
 ..., undamped 2nd order, 1-14, 7-1, 7-5, 14-16, 15-15
natural logarithm, 9-10
negative stiffness, 11-9, 16-22
neutral stability, 17-2
Newton, Isaac, 1-3
Newton's 2nd law, for forces, 1-3, 11-2, 12-2
 ..., for moments, 3-4, 11-2
Newton's 3rd law, 3-14
node (nodal point) of a vibration mode, 12-10
non-homogeneous solution of an ODE, 1-7
nonlinear ODE, 1-2, 1-21
notation, dot, 1-2
 ..., matrix, 12-3
*n*th order ODE, 4-11, 16-1
numerical approximate solutions, 6-8, 8-15, 9-14
 ..., convolution sum, 8-15, 9-14
 ..., recurrence formulas, 6-8, 6-10, 6-12
Nyquist, diagram or plot, 10-11, 17-9
 ..., stability criterion, 17-15, 17-22
 ..., three-dimensional plot, 17-26

Index of all Chapters and Appendices

O

$O(10^5)$, e.g., order-of-magnitude symbol, 5-9
 ocean surface ship, 3-17
 ODE = ordinary differential equation, 1-1
 ..., 1st order, 1-2
 ..., 2nd order, 1-13
 ..., derived from power balance, B-3
 ..., derived from transfer function, 16-7
 ..., nonlinear, 1-2, 1-21
 ..., n^{th} order, 4-11, 16-1
 offset, voltage, 10-27
 ..., P control, 15-7
 ohm (Ω), unit of electrical resistance, 5-1
 Ohm's law, 5-2
 open loop, 13-2
 ..., control, 14-2, 14-6
 ..., frequency-response function (OLFRF), 17-1
 ..., poles and zeros, 16-31
 ..., transfer function (OLTF), 16-31, 17-1
 operational amplifier (op-amp), 5-9
 ..., PI controller, 15-2
 operations, control, input error, 14-14, 15-1
 ..., output, 14-14
 operator setting (reference input), 14-2, 14-4
 optical encoder, 12-17
 ordinary differential equation (ODE), 1-1
 out-of-phase motion, 2-DOF IC response, 12-8
 out-of-phase, sinusoidal response, 4-6
 output, general definition, 1-2
 ..., feedback, 14-6, 14-11
 ..., impedance, 5-13
 ..., operations, 14-14
 overdamped 2nd order system, 9-2, 9-20, 9-31, 14-19, 15-10
 overshoot ratio, underdamped 2nd order, 9-14, 14-20
 overshoot, PI control, 15-11

P

pair, Laplace transform, 2-7
 parallel damper-spring low-pass filter, 4-8
 parallel, electrical components in, 5-3, 5-14
 ..., mechanical components in, 3-13
 parallel-axis theorem, 11-4
 parameter identification, 3-18
 partial-fraction expansion, 2-9, 4-12, 15-5, 16-3, 16-5, 16-40, A-4
 ..., direct term, 15-19
 ..., repeated poles, 16-8
 particular solution of an ODE, 1-7
 passive system, 7-1, 16-18
 peak time, underdamped 2nd order, 9-14, 14-20
 pendulum, simple, 7-2
 pendulum-spring systems, 11-14, 11-15, 12-14
 period, 4-3, 4-8
 ..., of damped vibration, 7-11
 ..., of sinusoidal signal, 1-17
 phase angle, sinusoidal response, 4-5, 17-3
 phase crossover, 17-6, 17-16, 17-18
 phase lead or lag, sinusoidal response, 4-5
 phase margin (PM), 17-6, 17-16

PID = proportional-integral-derivative, 15-1
 piecewise continuous input function, 6-3
 plane motion, general, 11-3
 ..., rotation about a fixed point, 11-3
 plant (controlled object or process), 14-1
 plant transfer function (PTF), 14-2, 15-3
 plausibility check, 1-11, 7-12
 plot3 MATLAB function, 17-26
 pluck testing, 7-10
 pogo stick, 7-19
 polar coordinates r and θ , 2-3, 11-4
 polar form, complex number, 2-3
 ..., characteristic equation, 16-25
 poles, of a complex function, 2-6
 ..., at the s -plane origin, 17-12, 17-28
 ..., of a transfer function, 4-13, 16-2
 ..., repeated, 16-8
 ..., sub-system, 16-25
 polynomial equation, roots, 12-16, 16-3, 16-22
 polynomials, multiplication of, 8-26
 port, of operational amplifier, 5-9
 position feedback, 14-6
 positive definite matrix, 11-11, 11-15, 12-2
 potential energy, electrical, B-5
 ..., gravitational, B-4
 ..., magnetic field, B-6
 ..., of a capacitor, B-5
 ..., of an inductor, B-6
 ..., strain, B-2
 potentiometer = variable resistor, 5-17
 power, B-1
 power-balance method, B-3
 prefixes indicating powers of ten, 3-2
 pretty MATLAB function, 1-20
 proof-mass actuator (PMA), 10-28, 10-29, 12-19, 15-5
 propagation of error, 7-21
 proportional (P) control, 15-2, 15-6, 15-14
 proportional gain, 15-1, 15-16
 proportional-derivative (PD) control, 15-2, 15-13, 15-14, 16-6
 proportional-integral (PI) control, 5-17, 15-2, 15-8
 proportional-integral-derivative (PID) control, 15-1
 proximity (displacement) sensor, 7-10
 pseudo-static response, 1-17, 7-2, 9-4, 9-27, 11-15, 14-7
 PTF \equiv plant transfer function, 14-2
 pulse duration, 1-6
 pulse, flat, 6-11, 9-32
 ..., half-sine, 1-6, 6-4
 ..., ramped exponential, 1-14, 16-5, 16-8
 ..., sawtooth, 6-12
 Pythagoras, theorem of, 16-26

Q

quadratic equation, 2-1, 12-4, 16-12, 16-27
 quadrature frequency-response component, 17-10
 quadrature phase, 10-7
 quality factor Q , 10-6
 quasi-static (quasi-steady) aerodynamics, 11-9, 16-42

Index of all Chapters and Appendices

R

radian, units in calculations, 3-10
 radio, tuning circuit, 10-7
 ramp input, 6-5
 ramped exponential pulse, 1-14, 8-31
 rate feedback, 14-11
 ratio of two polynomials, 2-6, 2-11, 14-10
RC, band-pass filter, 5-12, 9-21, 9-31, 10-10, 13-1
 ..., high-pass filter, 5-12, 5-14
 ..., low-pass filter, 5-4, 5-12
 reactance, capacitive and inductive, 10-12
 reaction wheel, 3-3, 3-17, 6-5, 7-17, 14-5
 reaction-mass actuator (RMA), 10-28, 12-19, 15-5
 reality check, 1-11, 14-5, 15-13, 15-19
 receptance, 10-13
 rectangular form of complex number, 2-2
 recurrence formulas, 6-8, 6-10, 6-12
 re-entry vehicle (capsule), 14-3
 reference input (operator setting), 14-2, 14-4
 relative stability, 16-18, 17-1
 remote (indirect) control, 14-1
 residue MATLAB function, 2-19, 16-16, 16-40
 residues of partial-fraction expansion, 2-9, 16-3, 16-7
 resistance, high input, 5-9
 resistors, electrical circuit components, 5-1
 ..., in parallel, 5-3
 ..., in series, 5-2
 resonance, 10-2, 10-4, 12-13
 response, general definition, 1-1
 resultant of distributed force, 10-26, 11-7
 RHS = right-hand-side, 3-16
 right-hand rule, 3-4
 right-hand-side (RHS) dynamics, 3-16, 3-19, 5-12, 5-14, 6-3, 9-23, 9-30, 10-10, 10-20, 10-21, 10-28, 14-18, 15-9, 15-15
 rigid-body plane motion, 11-1
 rise time, underdamped 2nd order, 9-13, 9-14, 14-20
 ..., PI control, 15-11
 robustness of a control system, 14-6
 roll (bank) angle of a flight vehicle, 3-8
 rolling, airplane or missile, 3-8
 root-locus (Evans') method, 16-28
 roots MATLAB function, 12-16, 16-23, 16-43
 roots of a polynomial equation, 16-3, 16-22, 16-43
 roots, loci (or locus) of, 16-18
 rotation, small, 7-3, 11-5, 11-10
 rotational (moment of) inertia, 3-3, 7-2, 11-2, 11-4
 rotational, damper-spring system, 15-2
 ..., inertia-damper-spring system, 11-5
 ..., inertia-spring system, 7-17, 11-7, 11-13, 12-16
 rotational velocity vector, 11-4
 rotor, 14-1, 15-2
 Routh's stability criteria, 16-12, 16-34, 16-38, 16-40
 rule, for analysis of op-amp circuits, 5-11
 ..., of thumb in control design, 15-17

S

sanity test, 1-11
 sawtooth pulse, 6-12
 second (2nd) area moment, 7-12

second (2nd) order system and ODE, 1-13
 seismic motion sensors, 10-24
 seismometer, 10-25
 self-correcting control system, 14-6
 self-excited systems, 16-19, 16-41
 sensitivity of control, to disturbances, 14-5
 ..., to modeling errors, 14-6
 sequence of length N , 8-16
 series damper-spring, high-pass filter, 4-17
 ..., low-pass filter, 4-16, 5-6
 series MATLAB function, 15-20
 series, electrical components in, 5-2, 5-14
 ..., mechanical components in, 3-14
 settling time, 3-4, 14-20
 ..., 1st order, 3-6, 3-7
 ..., underdamped 2nd order, 9-14
 shaker, mechanical vibration exciter, 10-8, 10-30
 shear building, 7-22
 ..., structural model, 10-30
 shock strut, 3-13, 4-2
 SI unit system, 3-1
 simple MATLAB function, 1-20
 simple pendulum, 7-9
 sink, of energy, 16-18, B-3, B-7
 SISO = single-input-single-output, 4-11, 8-13, 14-8, 16-1, 16-42
 small damping, approximation, 9-10, 9-24, 10-6, 10-7, 10-9
 small damping, half-amplitude formula, 9-11
 small rotation, 7-3, 11-5, 11-10
 snapback testing, 7-10, 12-18
 source, of energy, 16-18, B-3, B-7
 spacecraft, attitude control, 14-3, 16-36
 specifications, step-response, 9-13, 9-14
 speed (rotor velocity), PI control, 15-17
 speed, of control system components, 15-4
 ..., of system response, 15-3, 15-11
 spring, artificial, 14-7, 15-14
 ..., close-wound, 7-7
 ..., linear, 1-12, 3-11
 stability, 4-13, 14-16, 15-16, 16-1, 17-1
 stability, degree of, 16-20
 ..., exponential, 16-3
 ..., general criterion, 16-1, 16-2, 16-6
 ..., Routh's criteria, 16-12
 stable 1st order system, 3-6
 stairstep approximation, 6-9, 8-19
 standard form of ODE, stable 1st order system, 3-6
 ..., damped 2nd order system, 9-3
 ..., any 1st order system, 1-2, 1-19
 ..., undamped 2nd order system, 7-2
 state-space representation of systems, 14-17
 static equilibrium position, 7-7, 11-5
 steady-state output error, offset, 15-7
 steady-state sinusoidal response, 4-1, 4-4, 17-1
 step response, 1st order, 3-5, 3-6
 ..., physical applicability of solutions, 7-6
 ..., overdamped 2nd order, 15-10
 ..., P control, 15-10, 15-14
 ..., PI control, 15-10
 ..., position + rate feedback control, 14-16
 ..., undamped 2nd order system, 7-5, 14-11

Index of all Chapters and Appendices

...., underdamped 2nd order, 9-12, 13-5, 14-12, 15-10
, specifications, underdamped 2nd order, 9-13, 9-14
 step-relaxation (twang) testing, 7-10
 stiffness matrix, 11-12, 12-2
 stiffness, dynamic, 10-13
 ..., negative, 11-9, 16-22
 stimulus, 1-2
 strain energy, B-2
 strength of materials, 7-12
 stroke of a force shaker, 10-30
 structural damping model, internal-friction, B-12
 ..., viscous, B-9
 structural unit system, 3-1
 subcritically damped 2nd order system, 9-3
 sub-system poles, 16-25
 summing junction, 13-3
 supercritically damped 2nd order system, 9-2, 9-20
 superposition, 1-2
 ..., integral, 6-3
 ..., impulse responses, 8-14
 sweep, stepped-sine, 10-8, 17-25, 17-26
 Symbolic Math Toolbox, MATLAB, 1-20, 16-40, A-3
 syms MATLAB operation, 1-20, 1-23, 16-40, A-3
 system ID = system identification, 8-11, 9-18
 ..., aerodynamic coefficients, 3-18
 ..., LRC circuit by FRF, 10-23
 ..., m-c-k system by FRF, 10-9, 10-22, 10-23
 ..., m-c-k system by pulse, 9-18, 9-29
 ..., m-k system by added mass, 7-22
 system, basic definition, 1-1

T

t = time, independent variable, 1-1
 tachometer, 3-17
 ..., control sensor, 15-17
 Taylor power series expansions, 2-3
 terminal velocity, 1-21
 tf MATLAB function, 15-20, 17-7
 TF = transfer function, 4-10, 4-12, 4-19
 third (3rd) order system, 13-7, 16-13, 16-22, 16-31
 three-dimensional Nyquist plot, 17-26
 three-DOFs problem, 11-2
 thruster, on re-entry vehicle, 14-3, 14-5
 time constant, 1st order, 1-23, 3-5
 ..., derivative, 15-1, 15-13, 15-16
 ..., integral, 15-1, 15-11
 ..., underdamped 2nd order system, 9-8, 16-20
 time invariance, 1-2
 time lag, 4-4
 ..., artificial numerical, 6-9, 8-25
 torque motor, 7-17
 transfer function (TF), 4-10, 4-12, 4-19
 ..., base-excited m-c-k system, 13-3
 ..., closed-loop (CLTF), 13-4, 17-2
 ..., damped 2nd order, 10-3
 ..., nth order, 16-2
 ..., open-loop (OLTF), 16-31, 17-1
 ..., plant (PTF), 14-2
 ..., RC band-pass filter, 10-10

transient response, 3-4
 translated (in time) function, 8-29
 transmissibility, 10-27, B-13
 trapezoid rule of approximate integration, 8-6
 trigonometric identity, cosine of sum, 4-4
 trimming tab, airplane, 11-13
 tugboat, 3-17
 tuned-mass damper, 10-29
 twang testing, 7-10, 9-24, 10-29, 11-13, 12-18
 two-degrees-of freedom (2-DOF) systems, 11-10, 11-13, 11-14, 11-15, 12-2, 12-9, 12-13, 13-7
 typical-section, aeroelastic model, 11-7, 11-10, 11-14, 12-9, 16-41

U

u(t) = input quantity, 1-2
 uncommon open-loop system, 17-7, 17-17
 underdamped 2nd order system, 9-3
 undetermined coefficients, method of, 1-7, 1-15, 1-19, 1-22, 1-23, 1-24
 unit imaginary number, 2-1
 unit system, absolute, 3-1
 ..., gravitational, 3-1
 ..., SI, 3-1
 ..., traditional aeronautical, 3-1
 ..., traditional structural, 3-1
 unit vectors, Cartesian coordinates, 11-1
 ..., polar coordinates, 11-4
 unit-impulse function, 8-3, 8-13, 8-30
 unit-impulse-response function, 8-13
 unit-step function, 2-13, 8-13, 8-30
 ..., exponential, 1-23, 8-30, 16-5
 ..., Laplace transform of, 2-13
 unit-step-response function, 8-13
 unity feedback, 14-10, 14-18, 14-19
 unstable, 1st order system, 3-6
 ..., linear drift, 17-14, 17-28
 ..., PD-controlled rotor

V

vpa MATLAB operation, 16-40
 variable resistor (AKA potentiometer, pot), 5-16
 vector operations, 11-1
 velocity (rate) feedback, 14-13
 velocity, terminal, 1-21
 vibration absorber, 12-15
 vibration isolation, 7-18, 10-26, 12-15, B-12
 vibration testing, sinusoidal, 10-8, 17-3, 17-26
 viscous damper, artificial, 14-16, 15-15
 viscous damping constant, 1-3, 1-12, 10-9, 14-20
 ..., critical, 9-1, 10-19, 16-34
 viscous damping law, general linear, 3-12
 viscous damping ratio, 9-1, 9-9, 9-17, 10-3, 10-6, 10-9, 13-4, 14-16, 14-19, 15-15
 voice coil, 5-8
 voltage, 5-1, B-5
 ..., divider, 5-14
 ..., follower, 5-11
 ..., generator, 5-3, B-7

Index of all Chapters and Appendices

W

washboard road, 10-7, 10-21
watt (W), SI unit of power, B-1
wing chord, planform, span, 3-9, 11-8, 16-43
work, B-1, B-5
Wright Flyer, 16-39

X

x Cartesian coordinate, 1-4, 11-1, 12-10
 $x(t)$ = dependent variable, output quantity, 1-1

Y

y Cartesian coordinate, 7-7, 10-21, 11-1, 12-1

Z

$z = x + jy$ complex number, 2-1
 z Cartesian coordinate, 11-1
zeros, of a complex function, 2-6
 ..., of a determinant, 12-3, 16-43
 ..., of a transfer function, 16-2